To My

Parents

and

Grandmother.

Chapter 1: Introduction and Background.

Chapter 2: Photography of Transilluminated Tisssue Using an Image Intensifier.

Chapter 3: Instrumentation.

Chapter 4: Spectrophotometric Monitoring of the Redox State of Cytochrome Oxidase: A Non-invasive Method for the Study of Cerebral Metabolism ?

Chapter 6: In Vivo Reflectance and Transmission Measurements.

Chapter 7: The Construction of an Instrument for Recording Photoplethysmograms and its Preliminary Use.

Chapter 8: Summary and Conclusions.

Chapter 9: Addendum.

Optical Methods for Monitoring Physiological and Biochemical Variables.

Thesis submitted by John Crowe, Green College for the degree of D.Phil., Trinity term, 1986.

Abstract.

The use of optical methods for performing non-invasive physiological and biochemical monitoring has been investigated, with particular emphasis on the application of near-infrared spectrophotometry for following changes in the redox state of cytochrome oxidase.

Initial studies of the gross optical properties of *in vivo* tissue were made using an image intensifier. These demonstrated that some light is transmitted through biological tissues and that such material is very highly scattering.

In order to investigate the feasibiity of non-invasively monitoring changes in the redox state of cytochrome oxidase *in vivo*, spectrophotometric and oxygen measurements were made on solutions containing the pure enzyme and yeast cell suspensions. These demonstrated the high affinity that the enzyme has for oxygen in such preparations. in contrast to the much lower apparent affinities *in vivo* that have been reported. These results were then modelled mathematically. and a possible explanation for this anomaly suggested. Potential problems with applying this method are also presented.

The interest in cytochrome oxidase is due to its importance in oxidative metabolism. However in performing this role it also assists in the prevention of oxidative damage, whose contribution to various disease states in paediatrics is briefly considered.

Two instruments were also constructed, and used, firstly to measure the spectral characteristics of transmitted and reflected light *in vivo*, and secondly to study the cardiac synchronous pulsatile component of this light (commonly referred to as the photoplethysmogram).

Chapter 1: Introduction and Background.

1.1 Introduction.

The aim of the work described in this thesis was to investigate the use of optical methods for performing physiological and biochemical measurements, or more precisely the application of such methods to non-invasive *in vivo* monitoring. This use of optical methods is eminently suited to the care of premature infants who are at risk.

Here, an "optical method" is considered to be any technique where a sample is illuminated with light, and the reflected, scattered or re-radiated light subsequently detected and analysed.

Non-invasive refers to the fact that light is shone onto and detected from the surface of the body, although clearly very few techniques can be truly non-invasive since some form of energy (in this case photons) will usually be required to pass through the tissue under investigation.

In addition to the work concerning the *in vivo* optical characteristics of tissue which is of direct relevance to non-invasive monitoring of all types, the thesis also contains a specific assessment of optically monitoring the redox state of cytochrome oxidase (cytochrome aa_3) *in vivo*. It is claimed that this can yield information regarding oxygen sufficiency at its site of utilization. The technique by which this is achieved amounts to performing *in vivo* near-infrared (near-IR) spectroscopy. To obtain artefact free signals relating to the redox state of cytochrome oxidase then oxygen saturation and changes in blood volume (which are of extreme importance in their own right) must also be monitored in the same way.

The specific interest in near-IR spectroscopy is because of the tremendous potential of the technique for studying cerebral metabolism and haemodynamics in preterm infants, who are known to be predisposed to

varying degrees of brain damage. Such a technique may help in discovering the aetiology of the various problems and also offer a means of monitoring, thus improving the achievable standard of nursing care. Because of the similarities between many optical methods, experience gained from the studies on cytochrome oxidase is likely to be transferable.

This introduction aims to review optical methods which have been proposed, assessed or indeed used. Although the emphasis is placed upon information which is relevant to the remainder of the thesis, other details are given which are indirectly related to the work presented, and are considered to supplement this research. Such details illustrate the widespread current and potential uses of optical methods in biology and medicine. They also demonstrate how many of these methods are fundamentally linked to others in some way, and that much can be learned from studying different yet similar techniques.

Within this introduction firstly the basic physical nature of light and its position in the electro-magnetic (em) spectrum are described (Section 1.2) followed by a synopsis of the fundamental ways in which photons may interact with other matter (Section 1.3).

The most important light absorbing compounds in biological tissues are then introduced (Section 1.4.1) along with a brief explanation of why they possess such properties. This is followed by the gross reflectance and transmission spectra of both excised and in situ tissue (Section 1.4.2), and a brief review of the various theories used to explain light propagation in tissue and to model the above optical characteristics (Section 1.4.3).

This background information is sufficient to give details of proposed or practised optical methods (Section 1.5) with particular emphasis on oximetry since it is probably the most widely used and advanced clinical optical method. Moreover, the principles behind its

use (both experimental and theoretical) are applicable to other methods, such as optically monitoring the redox state of cytochrome oxidase, which rely upon measuring small changes in absorbance.

The various merits and disadvantages of optical methods are briefly given in Section 1.6, followed by an outline of the remainder of the thesis (Section 1.7).

It is felt that many optical techniques (and certainly those for use in a clinical enviroment) are therefore related, and that a review of this nature emphasises these connections and serves as a useful introduction to the field.

1.2 Light and the Electromagnetic Spectrum.

Given the above general description of an "optical method" it becomes necessary to define "light", which is generally accepted to be that region of the electromagnetic (em) spectrum known as the visible region extending from about 400nm to 700nm (roughly $7.5x10^{+14}$ to $4.3x10^{+14}$ Hz), and approximately corresponds to the band used for normal human vision (see ROSOTTI (1983)).

However, for reasons described in Section 1.4.1, the part of the em spectrum which is of interest in this thesis is from about 400nm to 1100nm (ie across the visible and near infra-red (IR) regions), and therefore from hereon the term "light" will be used to cover this region.

1.2.1 Maxwell's Equations and Light.

That light is indeed an em wave first became evident in the 19th century through the work of James Clerk Maxwell. He developed a set of four equations (commonly referred to as "Maxwell's equations") summarising all the then known properties of electric and magnetic fields. For free space these can be manipulated into the following two vector equations which represent six scalar equations, one for each component of the electric, E, and magnetic, B, fields:

$$\nabla^2 \underline{E} = \varepsilon_o \mu_o \frac{d^2 \underline{B}}{dt} \qquad 1.1$$

$$\nabla^2 \underline{B} = \varepsilon_o \mu_o \frac{d^2 \underline{E}}{dt} \qquad 1.2$$

and where ε_o and μ_o are the permitivitty and permeability of free space, and ∇^2 is the Laplacian operator.

These six scalar equations are identical in form to the three-dimensional (3-D) scalar wave equation

$$\nabla^2 \psi = \frac{1}{v^2} \frac{\partial^2 \psi}{\partial t^2} \qquad 1.3$$

where ψ is a scalar quantity and v is the propagation velocity of the wave. Consequently, the scalar equations represented by equations 1.1 and 1.2 describe an em wave travelling through free space with:

$$v = \frac{1}{\sqrt{\varepsilon_o \mu_o}} \qquad 1.4$$

As usual for wave motion, the velocity of the wave is equal to the product of its wavelength, λ , and frequency, ν :

$$v = \nu \lambda \qquad 1.5$$

Using experimental values of ε_o and μ_o, Maxwell used equation 1.4 to determine the theoretical value of the velocity of em waves. This value was in such close agreement with direct measurements of the speed of light that Maxwell was led to conclude that light itself is an em wave.

Maxwell's equations also show that both the electric, E, and magnetic, B, fields must be transverse waves (ie perpendicular to the direction of propagation), which are orthogonal to each other and in phase as represented in Figure 1.1. Furthermore, the amplitudes of the E and B fields are related by c, the speed of light:

$$E_y = c B_x \qquad 1.6$$

with the intensity, I, (that is the flow of em energy per unit area per unit time) given by:

$$I = \varepsilon_o c \langle E^2 \rangle \qquad 1.7$$

where $\langle E^2 \rangle$ is the time averaged value of the square of the E field.

Within free space the speed of light, c, has a constant value of $2.998 \times 10^{+8}$ ms^{-1}, but within an homogeneous dielectric medium of permitivitty, ε , and permeability, μ , it changes to speed v, given by:

$$v = \frac{1}{\sqrt{\varepsilon \mu}} \qquad 1.8$$

In accordance with equation 1.5 the change in speed is caused by a change

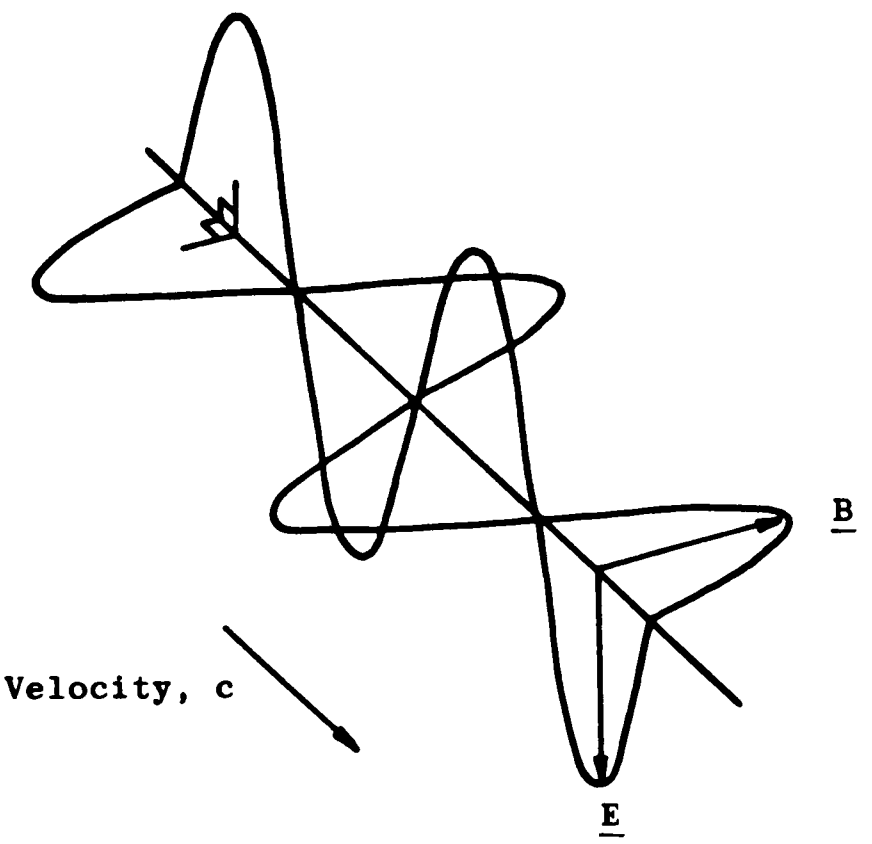

Figure 1.1 Representation of an Electromagnetic wave.

in wavelength of the wave whilst it travels through the medium. The ratio of these two speeds gives the refractive index of the medium, n, as:

$$n = \frac{c}{v} \qquad 1.9$$

If the refractive index is wavelength dependent then this leads to dispersion, the effect which enables a prism to split white light into its component colours.

1.2.2 Quantum Mechanics and Wave-Particle Duality.

The above description of light has been in terms of em waves. However the work of Planck on black body radiation and Einstein on the photoelectric effect led Einstein to suggest that light could also be considered as discrete quanta of energy, or photons, with energy, E, related to the frequency of the light, ν, by Planck's constant, h;

$$E = h \nu \qquad 1.10$$

Returning to Maxwell's equations, they can be used to show that

$$E = p c \qquad 1.11$$

where E and p are respectively the energy and momentum of the em wave. Alternatively the energy of a particle can be expressed by an equation derived from special relativity :

$$E = c (m_o^2 c^2 + p^2)^{\frac{1}{2}} \qquad 1.12$$

where m_o is the rest mass of the particle in question. Equations 1.11 and 1.12 must be equal since a photon can be considered as both a wave and a particle, and thefore the rest mass, m_o, of a photon must be zero.

In addition the total relativistic energy of a particle with velocity, v, is given by;

$$E = \frac{m_o c^2}{(1-v^2/c^2)^{\frac{1}{2}}} \qquad 1.13$$

where $m_o/(1-v^2/c^2)^{\frac{1}{2}}$ is the relativistic mass. The energy of the particle must be finite, which since m_o is zero means that a photon can only exist with velocity c, and that its energy is totally kinetic.

Electromagnetic radiation can therefore be considered as either a wave of velocity c, (in free space), wavelength λ, and frequency ν, or as discrete particles (photons) with no rest mass, and energy $h\nu$, which is totally kinetic.

1.2.3 The Electromagnetic Spectrum.

At the time when Maxwell published his electromagnetic theory, the known band of em radiation extended only from the infra-red (IR) across the visible to the ultra-violet (UV). The em spectrum is now known to extend from radio-frequency (RF) waves of a few Hz to gamma rays with frequencies of the order of 10^{22} Hz as shown in Figure 1.2.

It is perhaps worth reiterating that despite the enormous range of frequencies present in the em spectrum, all types of em radiation are fundamentally identical, that is they are all transverse, orthogonal

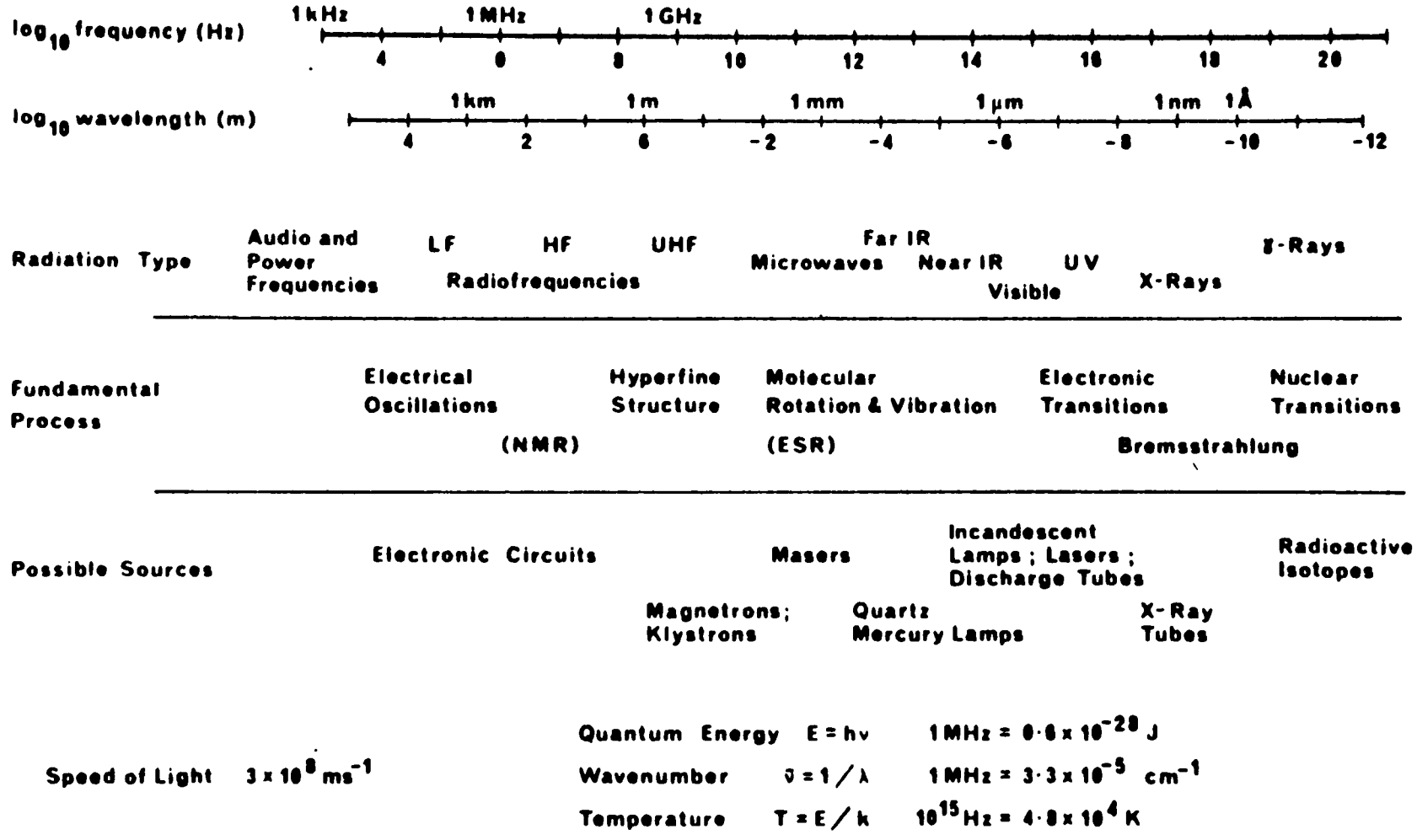

Figure 1.2 The electromagnetic spectrum.

electric and magnetic fields propagating with velocity, c. All that differs is their wavelength and frequency, and therefore energy, as shown by equations 1.5 and 1.10.

One source of em waves is accelerating charges, be it linear acceleration as in a transmitter aerial, or centripetal acceleration as in a cyclotron. The emission of visible light radiation due to the re-arrangement of the outer electrons in atoms and molecules (eg gas discharge tube) is a quantum mechanical process but can also be described in terms of the classical oscillating dipole. How the em spectrum is split into bands is briefly described below.

As shown in Figure 1.2, the em spectrum extends from the very low frequency region (VLF) where the energy of a photon is so small that the quantum nature of radiation is obscured and only a smooth transfer of energy is apparent, through the microwave, far-, intermediate- and near-IR regions, visible and UV to X-ray and γ-rays, where it is difficult to observe any wavelike properties, and detection of single photons is straightforward (as it is within the visible region).

The region of the em spectrum of direct relevance here is the visible part and the edges of the UV and IR. Visible radiation is produced by the re-arrangement of the outer electrons in atoms and molecules which emit at specific wavelengths, and from incandescent (eg tungsten) sources which give broad emission spectra (including near-IR as well).

UV radiation is also produced by electronic transitions but of higher energy than those associated with visible radiation, whilst IR radiation is generally associated with incandescent sources (ie molecular oscillators). Any material will absorb and radiate IR, the spectra of radiation depending in part upon the temperature.

(Textbooks by HECHT and ZAJAC (1974) and EISBERG (1961) were used during the preparation of the above section.)

1.3 The Interaction Between Electromagnetic Radiation and Matter.

If light, or indeed any form of em radiation, is to be used as a probe to investigate or perform measurements upon various samples, then the way in which the E and B fields of the wave interact with the electric and magnetic components of the samples in question is of fundamental importance. The principles behind the interactions are now briefly described, with their implementation into "optical methods" discussed in Section 1.5.

1.3.1 Emission and Absorption Spectroscopy.

In emission spectroscopy a molecule changes from a high energy state, E_1 to a low energy state, E_0 with the excess energy emitted from the molecule as a photon with energy, $h\nu$ (Equation 1.10). That is;

$$E_1 - E_0 = h\nu \qquad 1.14$$

The greater the difference between the two energy states then the greater the energy released and consequently the higher the frequency of the emitted photon.

Conversely in absorption spectroscopy upon absorbing a photon of energy, $h\nu$, from a beam of incident radiation, the molecule then moves to a higher energy state E_1 from its original energy state E_0. The emission and absorption processes are shown diagramatically in Figure 1.3. Equation 1.14 forms the basis for virtually all types of spectroscopy.

As would be expected from equation 1.14, and considering the extent of the em spectrum, there are many branches of spectroscopy covering photons of widely differing energies, all either emitted or absorbed and accompanying changes in the energy state of the atom or molecule.

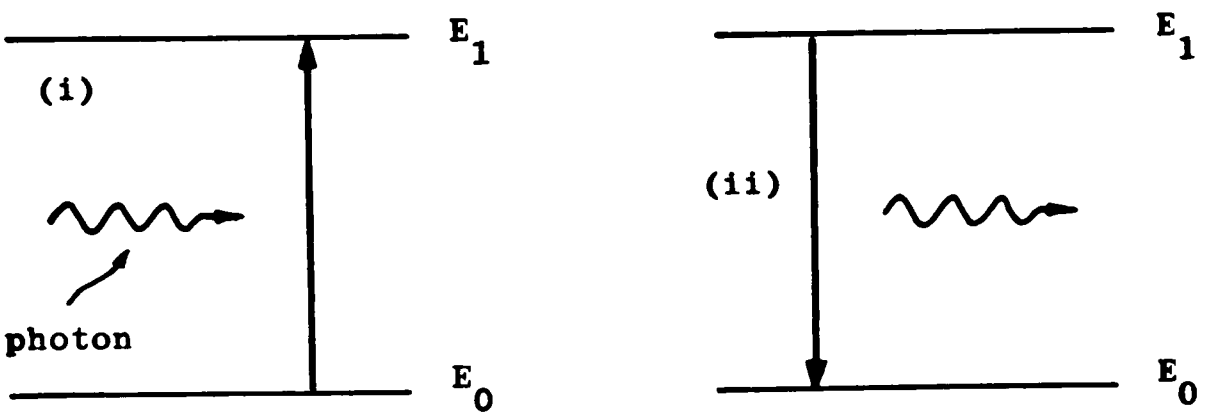

Figure 1.3 Absorption (i) and Emission (ii) Processes.

1.3.1.1 Absorption Spectroscopy.

Once the details (ie shape and magnitude) of the absorption spectra are known for specific compounds (even if not understood theoretically) then they can be used to perform both qualitative and quantitative analysis.

Concerning absorption spectroscopy in the light region of the em spectrum, from Figure 1.2 it can be seen that the fundamental processes involved are given as due to outer electron transitions and molecular vibrations. However, the main class of compounds of interest for biochemical and physiological measurements actually owe their visible absorption spectra to the presence of chromophores. These small groups of molecules (named from Greek for colour bringer) absorb em radiation through the excitation of their particularly mobile electrons (pi elctrons) (see Section 1.4.1).

The majority of naturally occuring coloured pigments and artificial dyes are coloured (ie have characteristic absorption spectra in the visible part of the spectrum) due to the presence of chromphores associated with conjugated long chain or ring structures whose energy levels are of the right separation for the absorption of light photons.

1.3.1.1.1 The Bouguer-Lambert-Beer Law.

An experimental measure of the amount of light absorbed by a given compound is given by the Bouguer-Lambert-Beer Law, (referred to as the Lambert- Beer Law from hereon) which can be written in the form:

$$I = I_o \ 10^{-\alpha Cd} \qquad 1.15$$

where I is the intensity of the transmitted light through a solution of thickness d, concentration C of a substance with absorption coefficient α at the monochromatic wavelength in question, upon illumination by light of intensity I_o. The quantity, (αcd), is generally referred to as the optical density (OD) of the solution at that wavelength. The Lambert-Beer (LB) law is applied within oximetry (see Section 1.5.1).

1.3.1.2 Emission Spectroscopy.

Once the energy of a photon has been absorbed, then this energy is generally simply lost to surrounding molecules, alternatively the excited molecule may take part in some chemical reaction (the field of photochemistry), or the energy can be lost through the re-emission of a photon.

This re-emission can occur through two processes; fluorescence or phosphoresence, which are distinguished by the length of time between excitation and re-emission.

1.3.1.2.1 Fluorescence.

Fluoresence is a short lived emission and therefore disappears as soon as the exciting source is removed. It is basically the reverse process of absorption although fluorescent emissions are always at longer wavelengths than the incident light, because of the loss of some energy within the compound, (meaning the radiative decay is always from the upper energy state's lowest energy level). This is shown in Figure 1.4.

The fluorescent yield is the ratio of photons emitted to the total

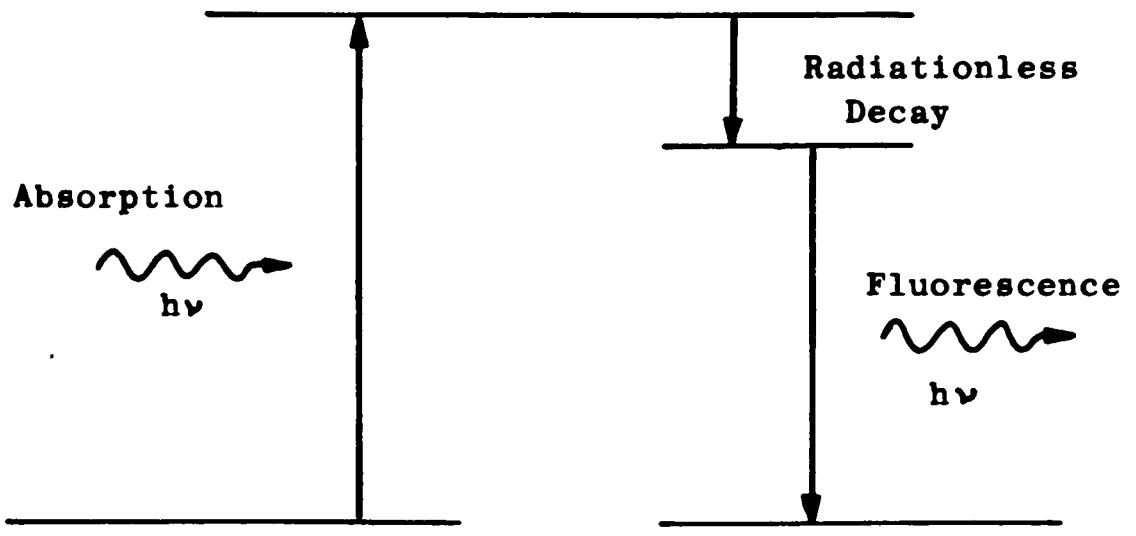

Figure 1.4 Illustration of Fluoresence.

number of photons absorbed. This yield is generally less than one because of the existence of alternative pathways for the absorbed energy to be dissipated along. In this case the fluoresence is said to be quenched.

The intensity of the emitted light decays exponentially, and both these decay times and fluorescent yield, which can be related to the presence of endogeneous or exogeneous quenching agents, can be used to perform fluorescent measurements, (SILVER (1985)).

1.3.1.2.2 Phosphorescence.

Phosphorescence differs from fluorescence in that emission occurs even after the incident radiation has been removed (up to hours afterwards). The cause of the delayed emission is a second excited state which acts as a slowly leaking "reservoir" for the energy absorbed, and so gives the characteristic time delay. Phosphorescence always occurs at longer wavelengths than fluorescence and is not widely used for physiological measurements.

1.3.2 Polarization Studies.

The em wave represented in Figure 1.1 is plane polarized (P) that is its E-field lies in a fixed plane. An alternative polarization state is circular polarization where the E field vector rotates either clockwise (right circularly polarized (R)) or anticlockwise (left circularly polarized (L)) as seen by an observer whom the wave is approaching. The E vector making one complete revolution as the wave passes through one wavelength. (nb Natural light has a rapidly and randomly varying sequence of polarization states).

As earlier described the speed of light through a given medium depends upon the refractive index of the medium, which is usually independent of the direction of the em wave. However, optically active substances (the optical activity being due to the molecular structure) are circularly birefringent, which means they have two distinct refractive indices for left and right circularly polarized light. Since a P-wave can be represented by a superposition of an R- and an L-wave, then upon passing through an optically active medium one wave will travel faster than the other thus emerging sooner and out of phase with the slower wave. The net effect of this is that the resultant P-wave becomes rotated, and so the concentration of optically active solutions can be measured by observing the rotation of a P-wave, which will be proportional to concentration of the solution and path length of the cell used. This is shown diagramatically in Figure 1.5ii.

The extent of rotation will be wavelength dependent due to optical rotatory dispersion (ORD), which is the variation between the refractive index and wavelengh. This variation is generally smooth with wavelength, except at wavelengths where there is a chromophore which results in anomalous ORD. (A similar effect can be observed (anomalous dispersion) in isotropic homogeneous media).

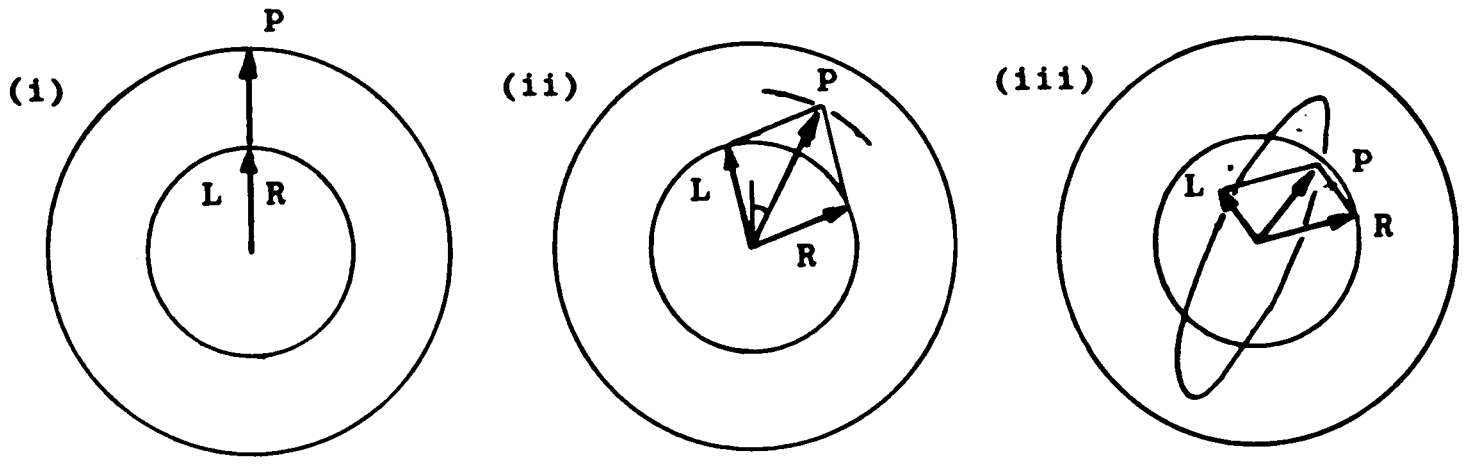

Figure 1.5 Effect on the resultant P-wave after travelling through a: (i) non-optically active medium
(ii) optically active medium
(iii) medium exhibiting circular dichroism.

The optically active substance may also exhibit circular dichroism (CD) (dichroism: 2 colours) meaning the circularly polarized waves will not only travel at different velocities but also be differentially absorbed. Such substances not only rotate the plane of polarization but also cause the wave to become elliptically polarised (see Figure 1.5ii). ORD and CD can be used to study molecular structure (symmetry in particular) and also used for quantitative analysis once the rotatory power of the substance of interest has been found.

1.3.3 Scattering Studies.

When interacting with matter, em radiation can be thought of as causing the constituent electrons to oscillate at the same frequency as the incident radiation, removing energy from the em wave in the process. Re-radiation of part of this energy (due to acceleration of the constituent electrons) is the process known as scattering (which is in fact the fundamental physical process behind reflection, refraction and diffraction).

If the frequency of the re-radiated light is equal to that of the

incident light then the scattered photons cannot have lost any energy (see equation 1.10) and the process is known as elastic or Rayleigh scattering. However, if the emitted photon is of a different frequency then energy must have been either lost or gained during what is then termed inelastic scattering. Raman spectroscopy makes use of inelastic scattering which gives the Stokes and anti-Stokes lines due to the photon's respective loss and gain of energy. These processes are illustrated in Figure 1.6.

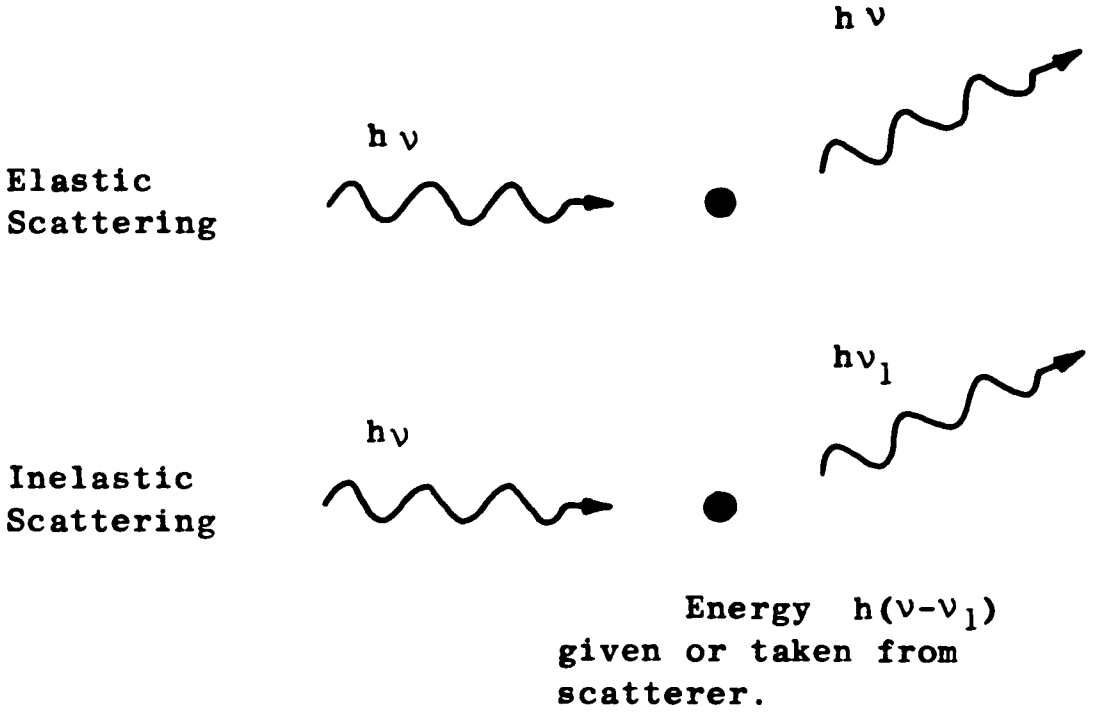

Figure 1.6 Elastic and Inelastic Scattering.

In addition light can undergo quasielastic scattering (QLS: quasielastic light scattering) from macromolecules and cells, in which the frequency of the scattered light undergoes an extremely small shift due to the motion of the scattering particles. If this motion is translational and with constant velocity then the frequency shift is equivalent to the well known Doppler shift and QLS can be used to measure, amongst other things, the particle's velocity.

Unlike Raman scattering the shifts in optical frequency caused by

QLS are too small to be observed spectroscopically and optical mixing (light beating spectroscopy) has to be used. This technique essentially involves mixing two light waves of marginally different frequency at the surface of a photodetector. The resultant E-field is given by the linear superposition of the two waves, but the photodetector output is proportional to the square of the E-field and therfore contains a frequency component (the beat frequency) equal to the frequency difference between the two incident beams. Measurement of the beat frequency therefore gives details of the frequency shift due to QLS.

(Textbooks by the following authors were referred to during the preparation of the above section: ATKINS (1978), CHANG (1971) and HECHT and ZAJAC (1974)).

1.4 The Gross Optical Characteristics of Tissue.

As far as the propagation of light is concerned, tissue is a heterogeneous and turbid medium which strongly absorbs and scatters light. In addition it contains a number of highly absorbing compounds which in conjunction with the scattering leads to very high light attenuation. The strong scattering gives rise to appreciable back-scattering (diffuse reflection) of light, with skin colouring influenced by the action of the highly absorbing compounds.

The gross reflectance and transmission characteristics of tissue which influence the shape of any spectra obtained *in vivo* are outlined in this section. These characteristics are important since any *in vivo* method involves reflecting light from or transmitting light through tissue, they will limit the range of wavelengths available for *in vivo* monitoring to those at which an appreciable level of light is reflected or transmitted.

Indeed, the majority of optical methods involve detecting small fluctuations in detected light intensity due to slight concentration changes of specific compounds, against a gross background absorbance provided at least in part by the same compound.

Below in Section 1.4.1 the chemical structure and characteristics of the compounds largely responsible for the absorption of light by tissue are described, which have been largely determined by experimental studies. As may be expected the predominant absorbing compounds are those whose *in vivo* concentrations it has been attempted to measure.

Following this in Section 1.4.2 the spectra of reflected and transmitted light as known at present are given, with the data drawn from many sources illustrating the wide interest in this field. Literature searches revealed that there is less transmission data available, mainly due to the problems of the low light levels associated with such measurements. The results show the profound influence of the absorbing

compounds described in Section 1.4.1. This data can be compared directly with results presented in Chapter 6.

In Section 1.4.3 the theoretical studies, the majority of which have attempted to model reflection, usually treating the skin as a multilayer structure containing the major absorbing compounds, are described. Although no modelling of this nature was performed, awareness of such work is considered imperative to establish theoretical links with experimental data and so obtain full advantage from the use of optical methods.

1.4.1 Light Absorbing Compounds in Tissue.

The process of light absorption and the importance of chromophores (since light photons are generally of too low energy for ordinary electronic excitation of the electrons in atomic orbitals and too high to be absorbed by molecular vibration) was introduced in Section 1.3.1.1.

Within molecules, the electrons shared by atoms form molecular orbitals with the type of orbital (dependent upon how the atomic orbitals overlap) affecting the molecules physical characteristics. If these orbitals overlap to give a diffuse electron cloud then a pi-orbital is formed. In addition if the molecule is conjugated then the individual pi-orbitals can themselves overlap with the electrons de-localising with a subsequent lowering of their energy.

As with atomic orbitals, their molecular counterparts have various energy levels in which the electrons can exist, or move into upon acquiring more energy (such as after absorbing a photon). The larger the conjugated molecule the more delocalised electrons, and the smaller the gaps between energy levels. Consequently, larger conjugated molecules such as pigment molecules can absorb photons of less energy (ie light photons) than compounds such as benzene which absorbs in the UV.

It is pigment molecules containing delocalised pi-electrons which

are primarily responsible for the absorption of light by most biological compounds. Examples of such molecules are tetrapyrollic compounds and carotenoids, both of which are discussed below.

1.4.1.1 Tetrapyrollic Compounds.

Haemoglobin is contained within the red blood cells and is responsible for transporting oxygen from the lungs to tissue (see Section 4.7.2). It is also (along with melanin) one of the compounds most responsible for tissue colouration. In its oxygenated form haemoglobin appears red (hence the general redness of tissue), turning to blue as oxygen is released (the phenomena upon which oximetry is based). However the gross absorption spectra are similar for the two compounds as shown in Figure 1.7 and these owe their shapes to the fact that haemoglobin is a tetrapyrollic compound.

Tetrapyrolles are basically composed of four pyrolle subunits organised into a ring structure (the porphin ring) which is the parent compound of porphyrin rings, themselves classified depending upon their side chain constituents. Porphyrins are conjugated structures see Figure 1.8, which as described above enables them to absorb light (MILGROM (1984)).

Protoporphyrins are the most abundant of the porphyrins (LEHNINGER (1977) and form quadridentate chelate complexes with various metal ions in which the metal is held by four co-ordination bonds. Of the many possible forms of protoporphyrin only one (protoporphyrin XI), also shown in Figure 1.8, occurs naturally, and this is the tetrapyrollic compound present in haemoglobin, and indeed most of the cytochromes and myoglobin (see below).

In haemoglobin the protoporphyrin exists as a chelate complex with Fe(II) (the heme moiety) with the four ligand groups of the porphyrin forming a square planar complex with the iron, whose remaining two

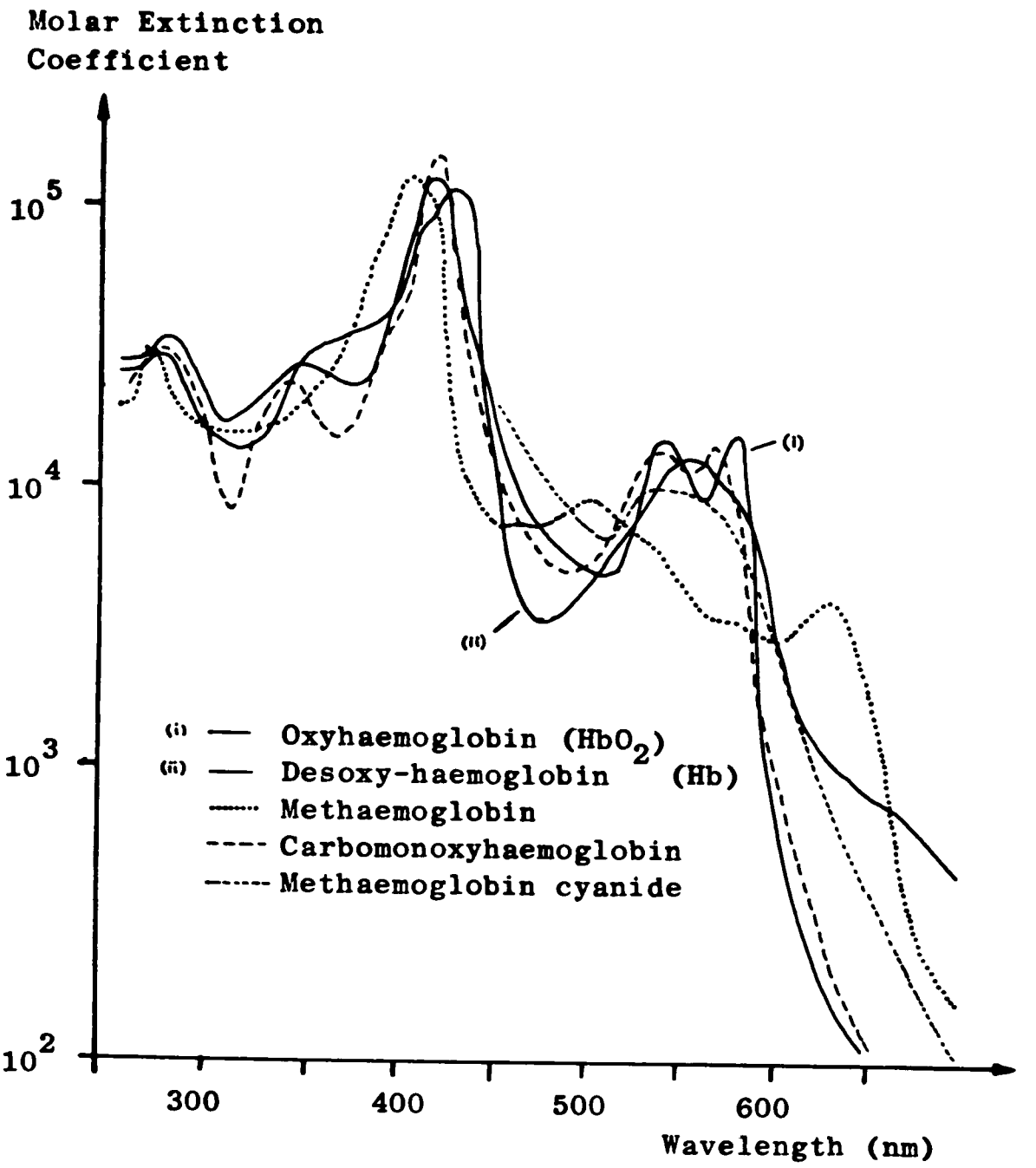

Figure 1.7 Absorption spectra of some haemoglobin derivatives (from (RICHTERICH (1981)).

co-ordination positions (perpendicular to the plane of the ring) can either be occupied (forming oxyhaemoglobin, HbO_2) or unoccupied (haemoglobin, Hb also known as deoxyhaemoglobin) by oxygen.

The haemoglobin molecule consists of four sub-units with each one containing a heme moiety conjugated to a polypeptide. Although the heme moiety gives rise to the gross absorption spectra, the difference spectra between haemoglobin and oxyhaemoglobin is due to conformational changes in the subunits as oxygen becomes bound and released. In addition to binding oxygen, the two spare co-ordination positions of the iron can also be occupied by other ligands such as carbon monoxide, CO, which

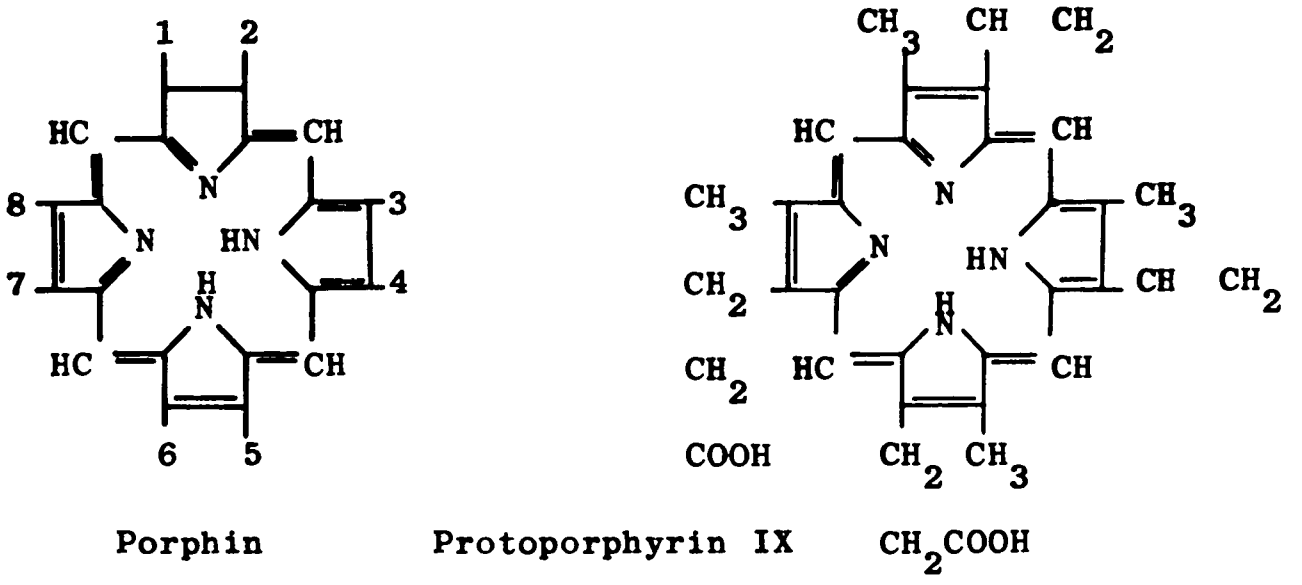

Figure 1.8 Structure of the porphin ring and protoporphyrin IX (from LEHNINGER (1977)).

forms carbomonoxyhaemoglobin. This has a slightly different absorption spectra than either haemoglobin or oxyhaemoglobin (although again grossly similar as shown in Figure 1.7).

Myoglobin (Mb) is also a coloured compound linked with oxygen transport specifically in muscle (see Section 4.7.3), and contains a heme moiety, which gives it both its colour and capacity to carry oxygen. It is particularly abundant in muscles of diving mammals whose dark brown colour is due to its presence. As with haemoglobin the Fe(II) in myoglobin remains in this state as oxygen is bound and released. However, in both haemoglobin and myoglobin it can be converted to Fe(III) (haemin) by the action of oxidizing agents, which itself has a characteristic absorption spectra.

The majority of the cytochromes (Section 4.3) contain protoporphyrin and hence absorb visible light. Unlike haemoglobin and myoglobin in most of the cytochromes both the fifth and sixth co-ordination positions of the iron are occupied and so ligands such as oxygen and CO cannot be bound. (The notable exception is cytochrome oxidase, the terminal enzyme of respiration which normally binds oxygen (Section 4.4.3). Cytochromes

are components of the electron transfer chain, electron transfer being carried out by the iron atom undergoing reversible Fe(II) to Fe(III) transistions. Hence they differ in function from haemoglobin and myoglobin in that they act as electron, as opposed to ligand carriers.

The visible absorption spectra of the cytochromes are similar and distinctive. as shown in Figure 4.8, which should be compared in similarity to that of haemoglobin as both are based on porphyrin. More details are given in Section 4.3.

In addition to the visible absorption spectra due to the heme moiety cytochrome oxidase also has a small broad absorption band in the near-IR due to its containing copper atoms which are also associated with electron transfer. This band is present when the enzyme is oxidised and is of particular significance in the field of non-invasive optical monitoring (Chapter 4). (Note that the cytochromes are only present in sufficient quantity to visibly influence colouration in certain internal organs which have high energy requirements and therfore high cytochrome concentration.)

Another compound which is often responsible for skin colouration is the bile pigment bilirubin. This is a breakdown product of protoporphyrin consisting of an open chain tetrapyrolle containing no metal atom. High concentrations of bilirubin may lead to jaundice in neonates, and measurement of this yellowing of the skin is discussed in Section 1.5.2. The absorption spectra of bilirubin is shown in Figure 1.9, and consists of a broad single absorption peak centred on 460nm. Other bile pigments are of a similar structure to bilirubin and also coloured.

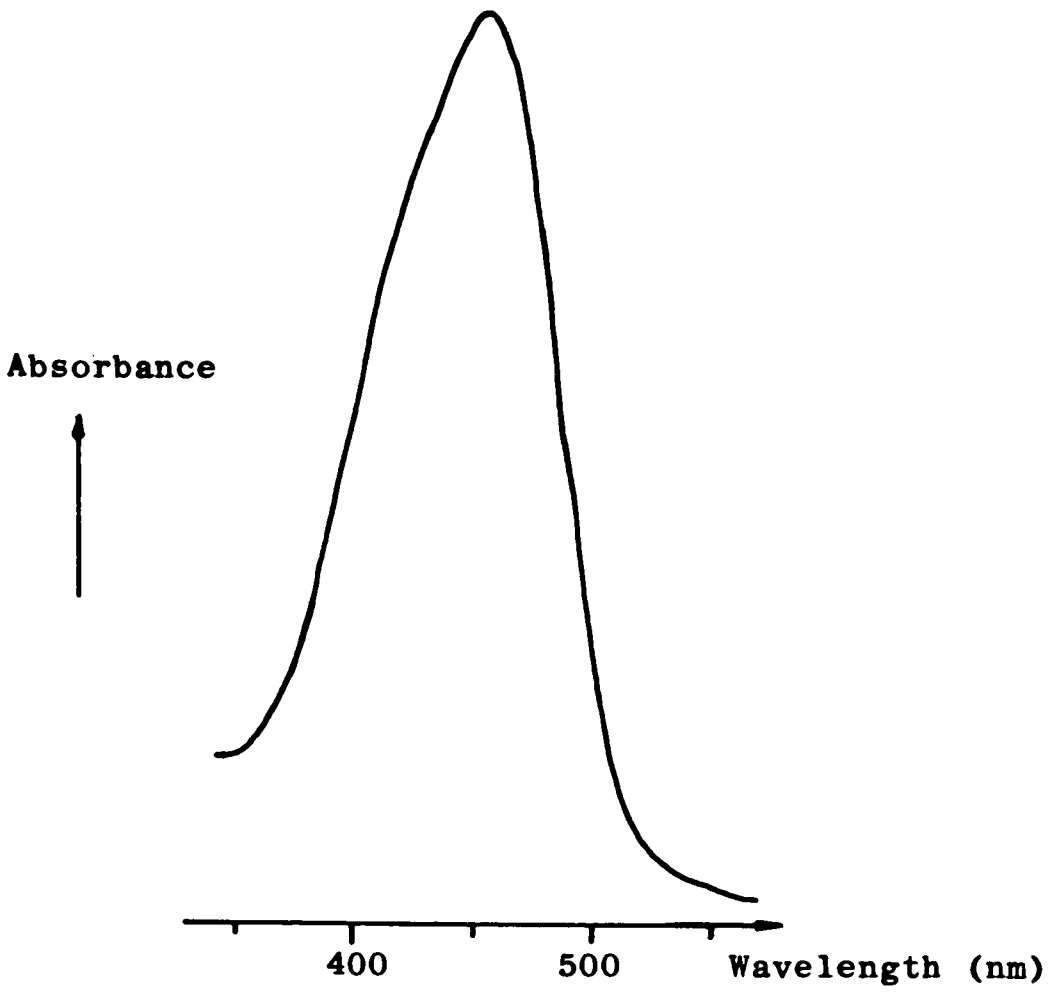

Figure 1.9 Absorbance Spectrum of Bilirubin (from AMAZON (1981)).

1.4.1.2 Non-Tetrapyrollic Light Absorbing Compounds.

Apart from the above tetrapyrollic compounds which influence tissue colouration, at least two other substances also play a part. Namely: melanin and carotene.

Melanin is responsible for the degree of darkness of the skin. It is produced by the polymerisation of the oxidation products of tyrosine and dihydroxyphenol compounds and contains a highly conjugated amorphic polymeric chromophoric backbone (PARRISH (1982). Within the visible spectrum it contains no absorbance maxima or minima but consists of a decreasing absorbance spectrum from the UV to about 1200nm in the near-IR as shown in Figure 1.10. Melanin is produced in the melanosomes, themselves situated in melanocytes, and then transferred to the keratinocytes.

The other compound which contributes to skin colouration, producing

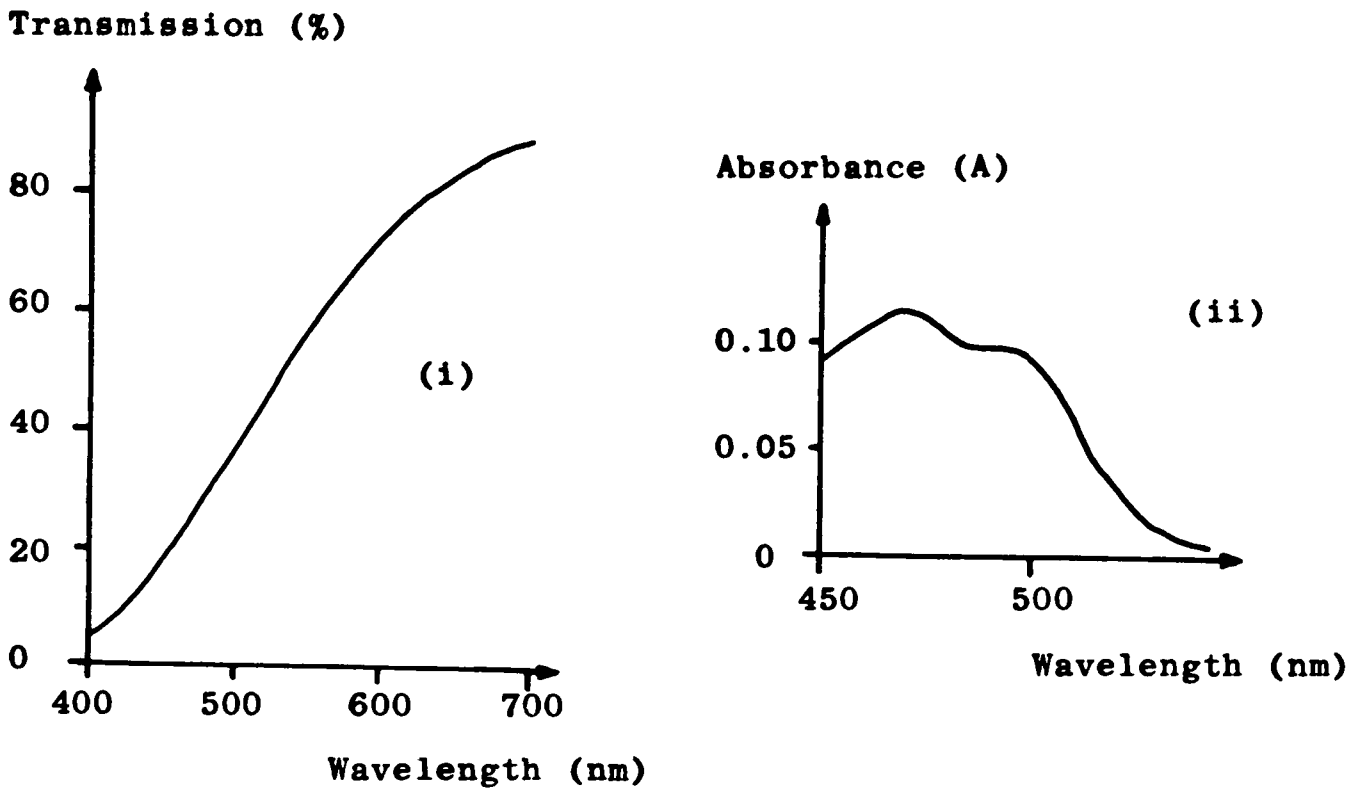

Figure 1.10 (i) Transmission Spectrum of Melanin (from EDWARDS (1939).
(ii) Absorbance Spectrum of Carotene (from FEATHER (1980).

a yellowish tinge is carotene, the precursor of Vitamin A. It belongs to the class of compounds known as terpenes which are constructed of a number of isoprene (2-methyl-1,3 butadiene) sub-units, and is a member of the carotenoids a class of higher terpenes which contain a conjugated backbone. The spectrum is also shown in Figure 1.10. Note the minimum at 480 nm which manifests itself in in vivo reflectance data as a reflectance peak when carotene is present.

The major compounds responsible for skin colouration (ie those absorbing in the visible part of the spectrum) have now been described, however, for completeness it is noted that the UV transmission of the excised epidermis (see below) is strongly influenced by the presence of aromatic amino acid compounds (both free and in proteins) which have the general absorbtion spectrum shown in Figure 1.11.

As with the cytochromes, flavonucleotides (flavoenzymes) which are highly coloured also influence the visible spectral characteristics of certain internal organs. Their absorption spectrum is shown in Figure

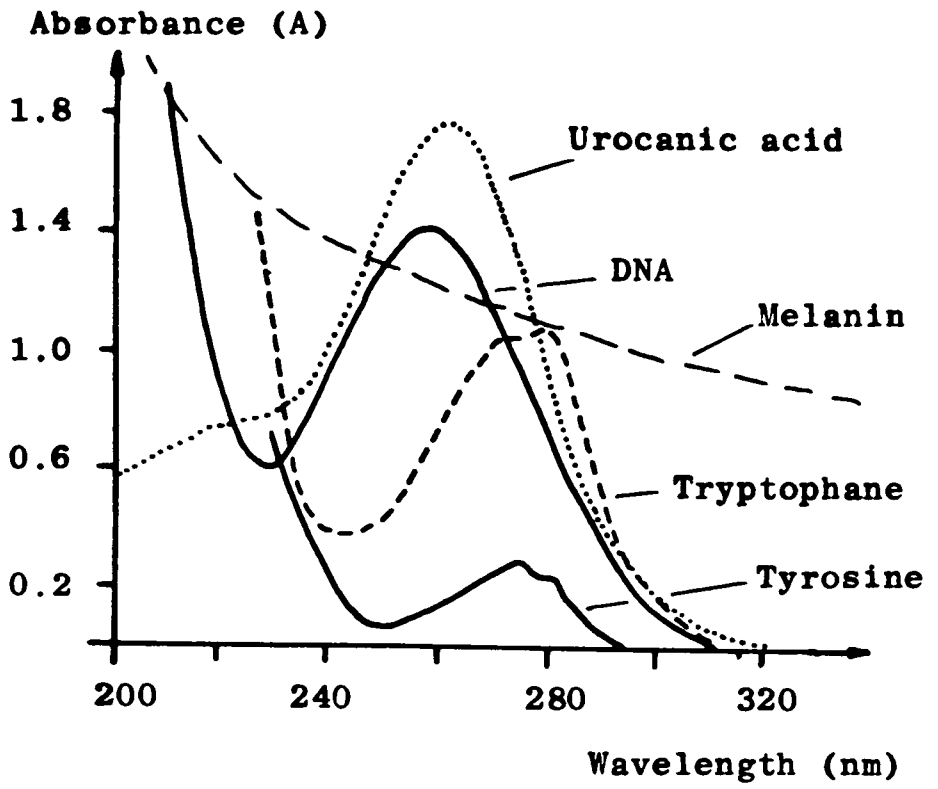

Figure 1.11

UV absorption spectra of the major epidermal chromophores (from PARRISH (1982)).

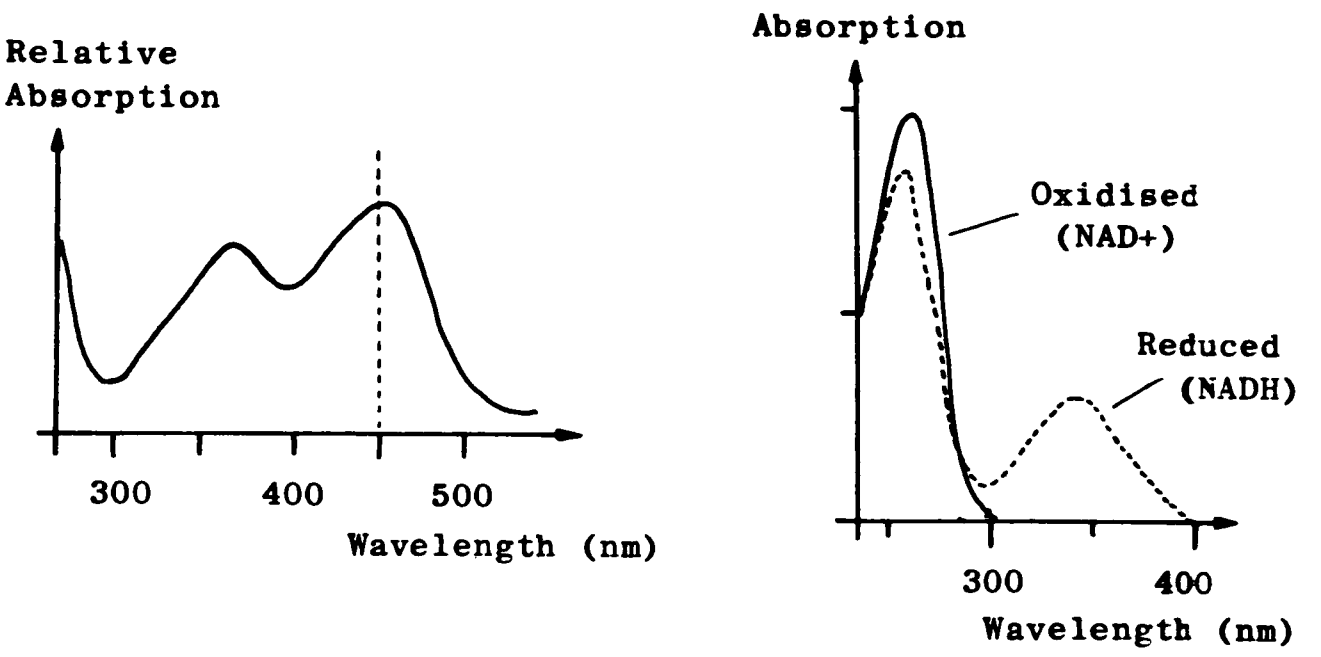

Figure 1.12 The Absorption Spectra of; (i) Flavin nucleotides (Oxidised Form). Reduction causes the 450nm peak to disappear. (from LEHNINGER (1977)).
(ii) NAD+ and NADH

1.12. Other substances containing nucleotides also exhibit UV absorbance, including NADH.

(In the preparation of the above section the textbook by LEHNINGER (1977) was extensively used together with HECHT and ZAJAC (1974), FINAR (1976), ROSOTTI (1985), WILLIAMS and FLEMING (1973) and MURREL (1978)).

1.4.2 Experimental Studies of the Gross Optical Characteristics of Tissue.

Within this section the gross optical characteristics of tissue are given. These are of great importance in the use of any *in vivo* optical method since they dictate the optimum monitoring wavelengths. Many of the results can be directly compared with the results presented in Chapter 6 which complement those given in this section.

It will be seen thatthe most obvious features are the absorbance of light by the compounds in Section 1.4.1. Results from both reflection (Section 1.4.2.1) and transmission measurements (Section 1.4.2.2) are given being further divided into results obtained from whole tissue, intact organs (including those exposed *in situ*) and excised and separated body components. These results illustrate why reflectance measurements for clinical use are generally performed over the range from about 450-700nm and transmission measurements from about 700-1100nm.

(Note that in this context reflection and transmission respectively refer to the light whose intensity is measured leaving the sample in the opposite and same direction as the incident light. Within tissue both types are virtually exclusively due to scattering processes, a point taken up in Section 1.4.3)

The reasons why these measurements have been made (apart from a fundamental interest) are varied. Reflection measurements are useful for determining the level and quality of lighting for photography (STIMSON (1953)), and are also necessary to determine the most appropriate wavelengths for use in the reflectance optical methods (see Section 1.5.1.3.).

Currently however, the bulk of data being published is a result of the growing interest in phototherapy (the use of light for treatment (PARRISH (1982)), including its use in cancer therapy (such as in the activation of hematoporphyrin derivative (HPD), see Section 1.5.10) and

in the use of lasers for treatment and surgery, (see Section 1.5.9) although these measurements are usually only at single wavelength.

Following the experimental data the various theories used to model the optical characteristics of, and light propagation in tissue are reviewed in Section 1.4.3.

1.4.2.1 Reflectance Characteristics.

The spectral properties of light reflected (backscattered) from the skin *in situ* are mainly determined by the absorption spectra of blood (ie haemoglobin and its oxygenation state), melanin and to a lesser extent bilirubin and carotene (all compounds previously introduced in Section 1.4.1). The absorption of incident light by water and fat is also influential further into the near-IR.

(Although the absorption of the incident light appears to be the major factor in determining the spectral properties of reflected light, the scattering of incident light by structures such as collagen (PARRISH (1983)) and melanin granules (DIFFEY (1983)) also play a role (see also ROSOTTI (1983)).

The spectral content of light reflected from a particular region on the surface of the body will therefore largely depend upon the relative concentrations of the above substances at the chosen site, which themselves will vary according to the subjects age, sex, race and the location of the site itself. (Theoretical attempts to describe these spectra are outlined in Section 1.4.3)

Many general reflectance measurements from *in situ* skin have been performed (EDWARDS (1939), STIMSON (1953), JACQUEZ (1955a, 1955b), KUPPENHEIM (1956), FEATHER (1986), TANG (1983), ANDERSON (1980,1981)) with others specifically concerned with reflectance due to a specific compound (HANNEMAN (1978,1979). It is from these that the details for the synopsis given above is drawn.

Typical reflectance spectra over the range 250 to 2600nm are shown in Figure 1.13 with the data drawn from several sources. The two graphs in all but Figure 1.13 (iii) are for negroid and caucasian skin, the difference between them illustrating the effect of the greater amount of melanin in the negroid skin which has the darker appearance. The effect of the absorption by melanin with the magnitude decreasing towards higher wavelengths can be clearly seen (see also the results in Chapter 6).

The influence of haemoglobin on the absorption spectra is evident from the effect of its absorbance peaks at about 420nm (the Soret band), 540 and 580nm, which actually undergo a slight shift upon deoxygenation (see Figure 1.7). The rapidly increasing absorption coefficient of haemoglobin below about 600nm is the main reason why so little light is reflected below this wavelength.

Above 1200nm the two graphs have virtually the same shape, being dominated by the effect of the absorption bands of water one of which is also responsible for the decrease in reflectance at about 970nm. The effects of both this near-IR absorption band and the one due to the presence of fat, are shown in Figure 1.14. These reflectance results arise from studies of the "infrared interactance" as a way of estimating body composition (CONWAY (1984)).

Besides reflectance studies on the surface of the body, measurements on internal organs have also been made by workers such as N.Sato and D.W.Lubbers. The results, from tissues such as liver, kidney, heart or gastric mucosa unsurprisingly, tend to be dominated by the presence of blood. However, if pressure is applied to displace blood near the surface of organs or if the blood is completely drained or replaced then the contribution to the reflectance spectra from the cytochromes and myoglobin in muscle tissue can be seen clearly as illustrated in Figure 1.15.

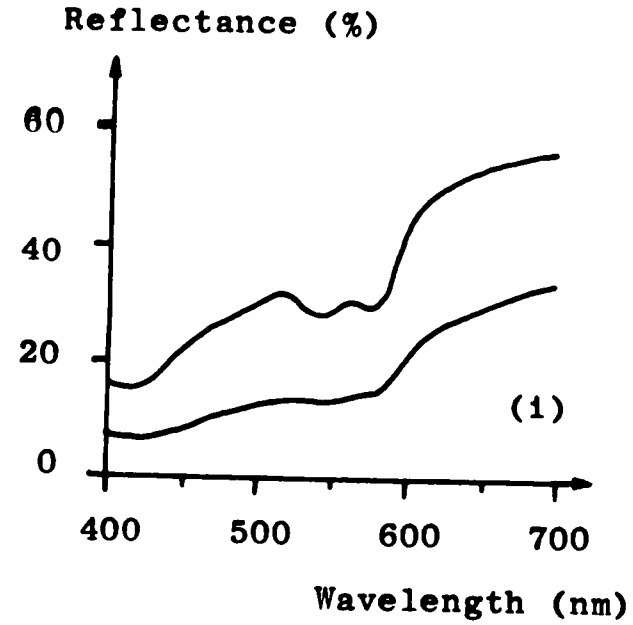

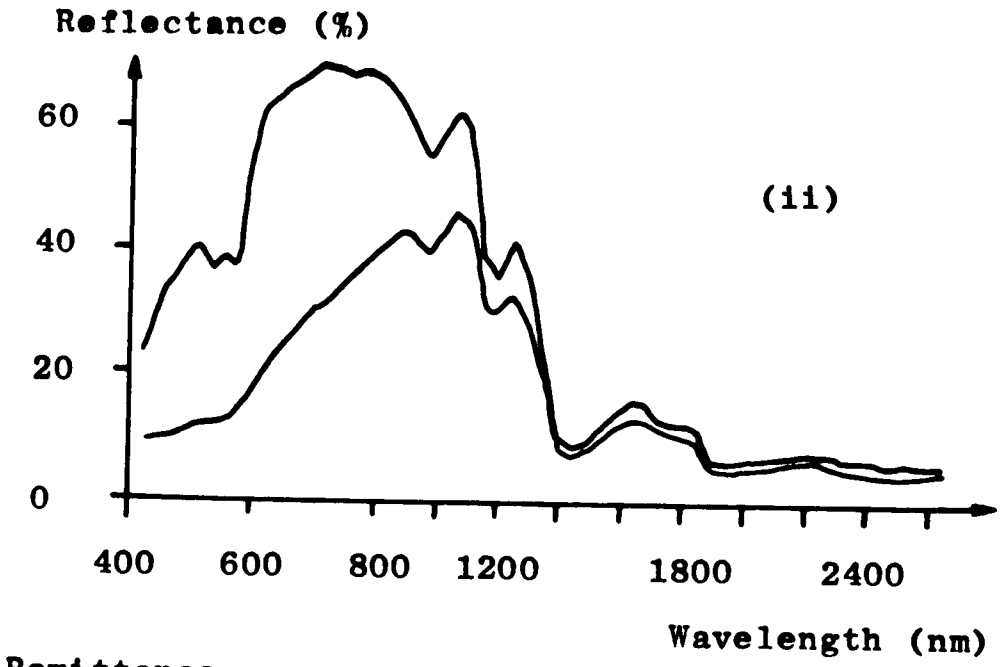

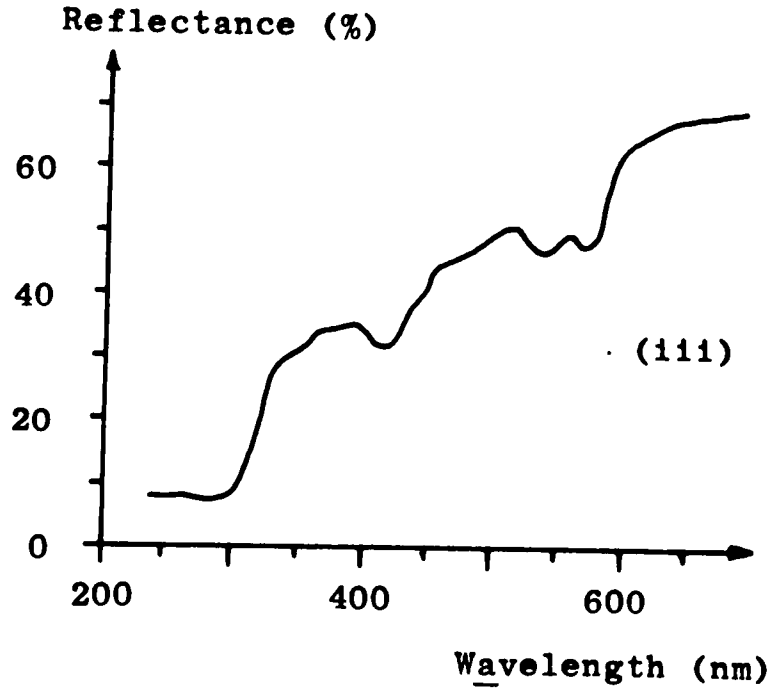

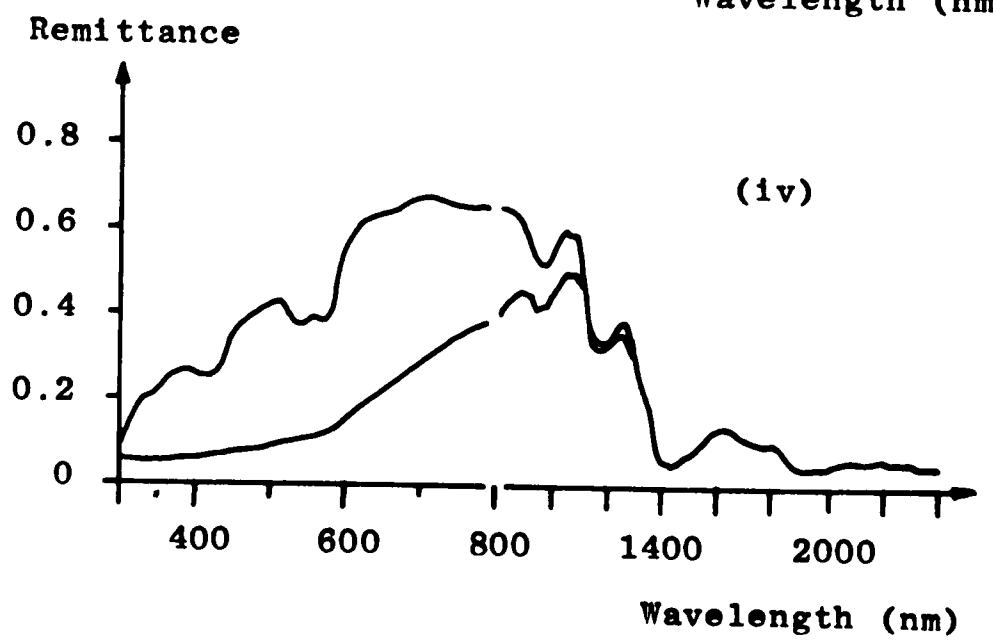

Figure 1.13 Reflectance Spectra from <u>in situ</u> skin. (i) From the palm (from EDWARDS (1939), and from the forearm; (ii) JACQUEZ (1955b), (iii) JACQUEZ (1955a), (iv) ANDERSON (1981) In all figures except (iii) the top and bottom traces are for caucasian and negroid subjects respectively.

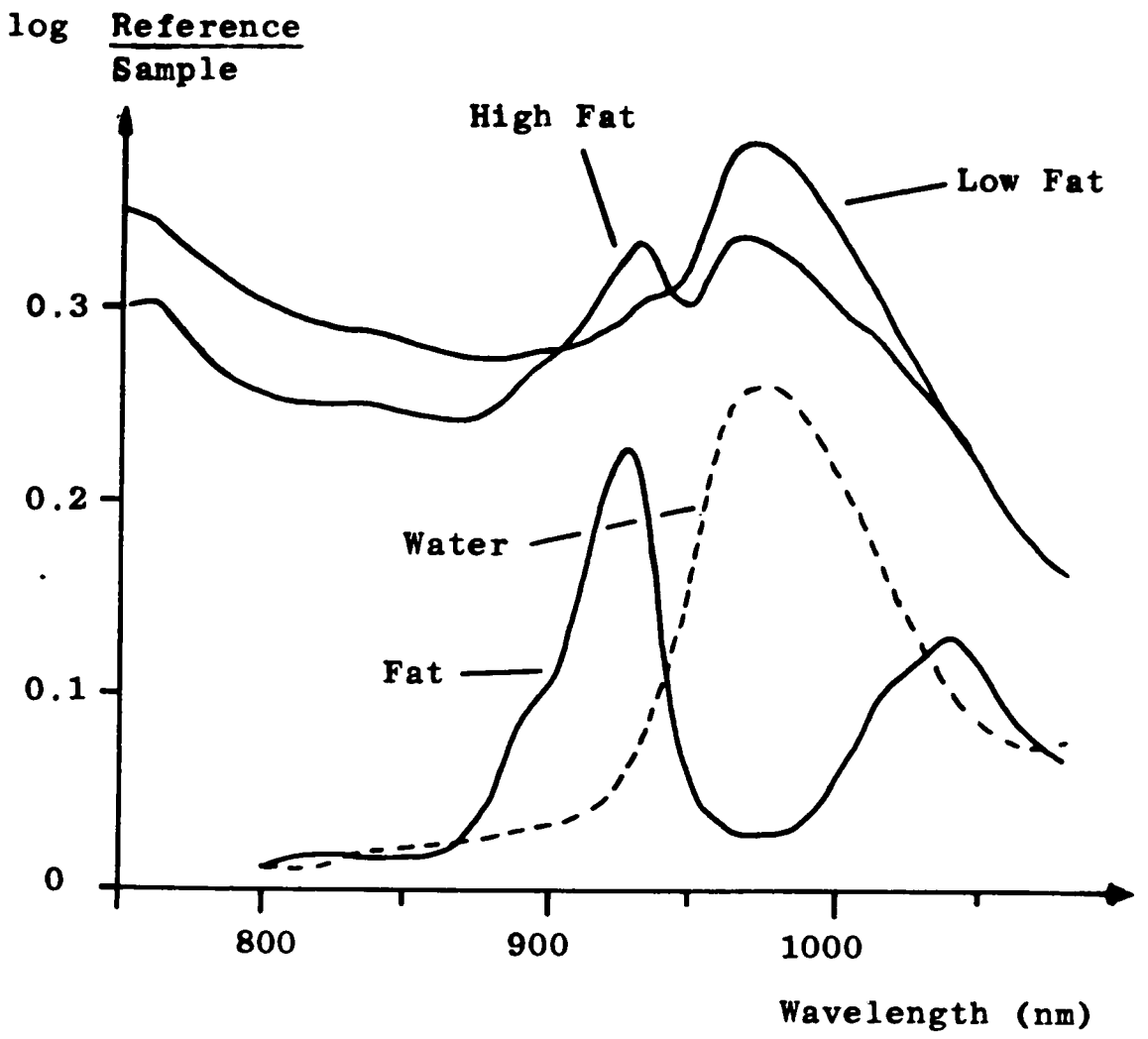

Figure 1.14 Reflectance spectra from triceps of male (low fat) and female (high fat) subjects. Also shown, for reference, are the spectra for distilled water and pure pork fat (from CONWAY (1984)).

1.4.2.2 Transmittance Characteristics.

1.4.2.2.1 Transmission Through Whole Intact Structures.

That light is transmitted through biological tissues, and a dominant feature of this transmission is the absorption due to haemoglobin is readily seen by the emergence of reddish light when a finger or hand is held against a bright light source. However, the fact that a bright source is required also indicates that the transmission is not very high (SMITH (1977).

Similar observations to this simple example of the gross transmission characteristics of whole intact tissue are made in paediatrics (PHILIP (1982)). Intracranial lesions can be diagnosed by

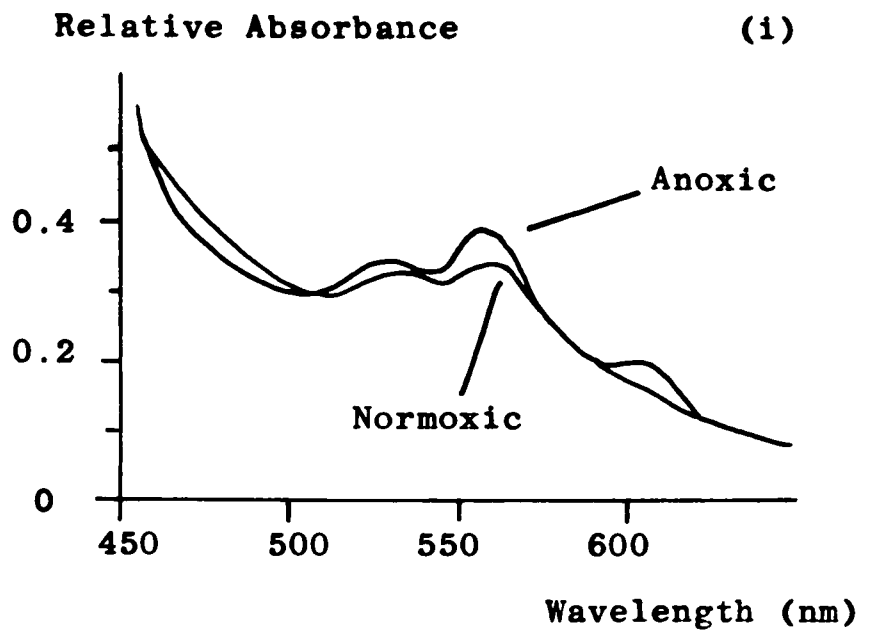

Figure 1.15 Reflectance spectra of (i) blood free perfused rat liver (from SATO (1979b)), and (ii) blood free perfused beating guinea pig heart (from LUBBERS (1983a)).

transillumination (CAMBERN (1961), SWICK (1976)) with a torch being held against the infants skull which then "lights" up. Pneumothoraces can also be found in this manner and veins located for IV injections in the neonatal forearm. Transillumination can also be used to detect the

presence and position of breast tumours (GROS (1972), WATMOUGH (1983)) and it is from such clinical applications that much of the information concerning the spectral transmission characteristics of whole intact tissue is derived.

These characteristics are generally considered to be that virtually no light is transmitted below about 700nm due to the high absorption coefficient of haemoglobin whilst above 1300nm the absorption by water becomes dominant.

This "window" from about 700nm to 1100nm in which light will be relatively well transmitted, is the one in which other transmission measurements are made (as in pulse oximeters described in Section 1.5.1.3) and is extensively referred to by Prof. F. F. Jobsis (see Section 4.8.2) concerning the possibility of monitoring the redox state of cytochrome aa_3 in the brain non-invasively.

However, although such a "window" does exist data concerning the actual transmission spectra of whole intact structures *in situ*, such as the finger, hand, arm or head is scarce, certainly when compared with the abundance of reflectance data (WATMOUGH (1983)). Indeed only the following three *in vivo* transmission spectra were found after extensive literature searches.

The transmission characteristics of the cheek (CARTWRIGHT (1930)) and ear lobe (ELAM (1949)) have been measured and are shown in Figures 1.16 and 1.17 respectively. (The ear lobe data is connected with the *in vivo* determination of blood oxygen saturation using transmission techniques). In addition, and illustrating the scarcity of such results, the "unpublished data" of NORRIS (In SMITH (1977)) shown in Figure 1.18, gives the absorption spectrum of a human hand. This shows the large absorption below about 600nm and the absorption band centred at about 950nm due to water as is probably the smaller peak at 760nm. Measurements of the transmission spectra of whole intact structures are

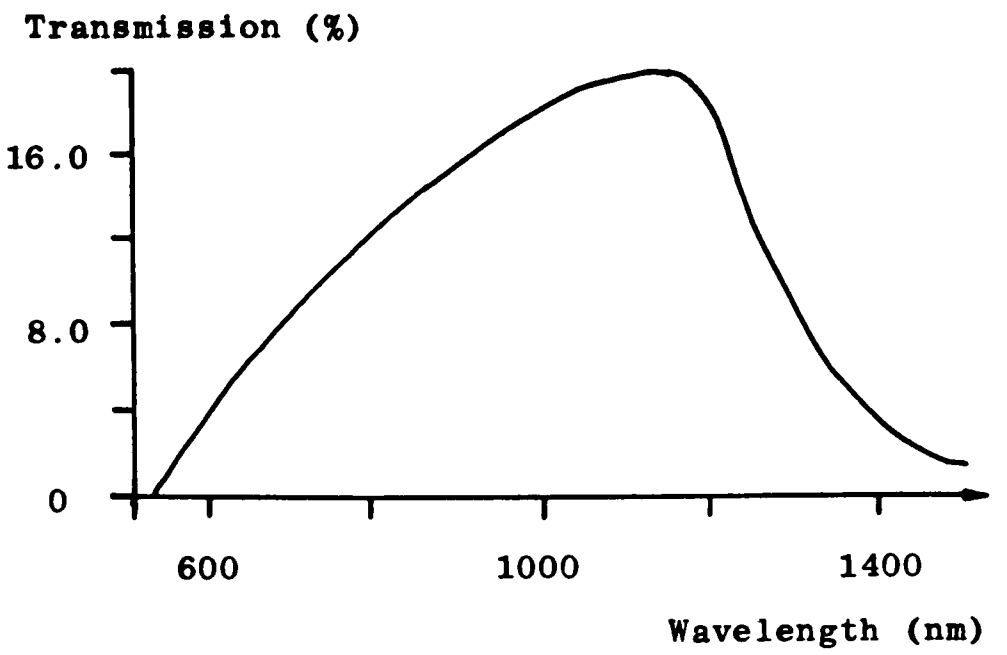

Figure 1.16 Percentage transmission of Infrared through the cheek (from CARTWRIGHT (1930)).

given in Chapter 6, and show similar characteristics.

The reason why so few transmission studies have been performed is that the levels of transmitted light are much smaller and therefore much more difficult to measure than in the reflectance mode. Moreover, considering the difficulty in modelling the optical characteristics of biological samples for a single tissue type which is therfore homogeneous (at least on a macroscopic scale), then attempting to model an arm or the head which consists of several totally different tissues would be a formidable task.

1.4.2.2.2 Transmission Through Excised Organs.

Despite the scarcity of transmission characteristics of whole intact structures, such measurements have been performed on a variety of excised samples. Virtually all the results of this type have been published relatively recently and are concerned with photochaemotherapy and in particular the use of haematoporphyrin derivative (HPD) in the detection

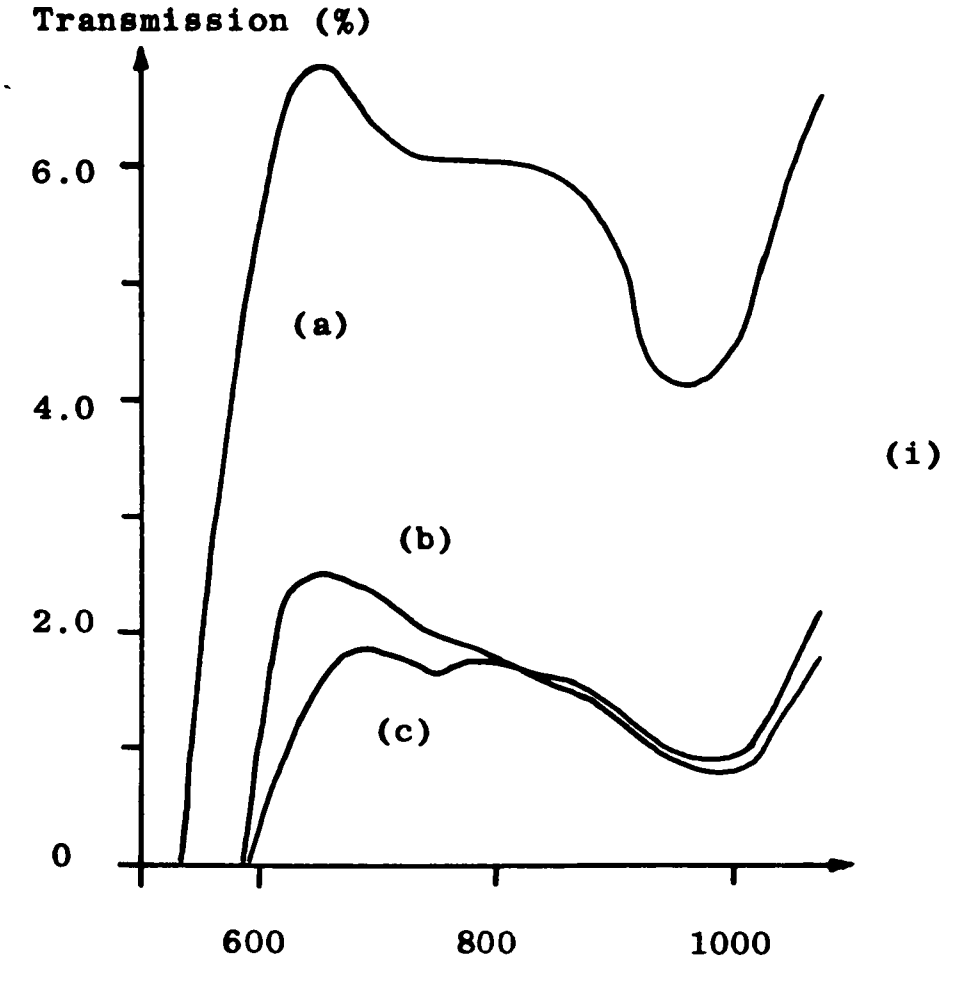

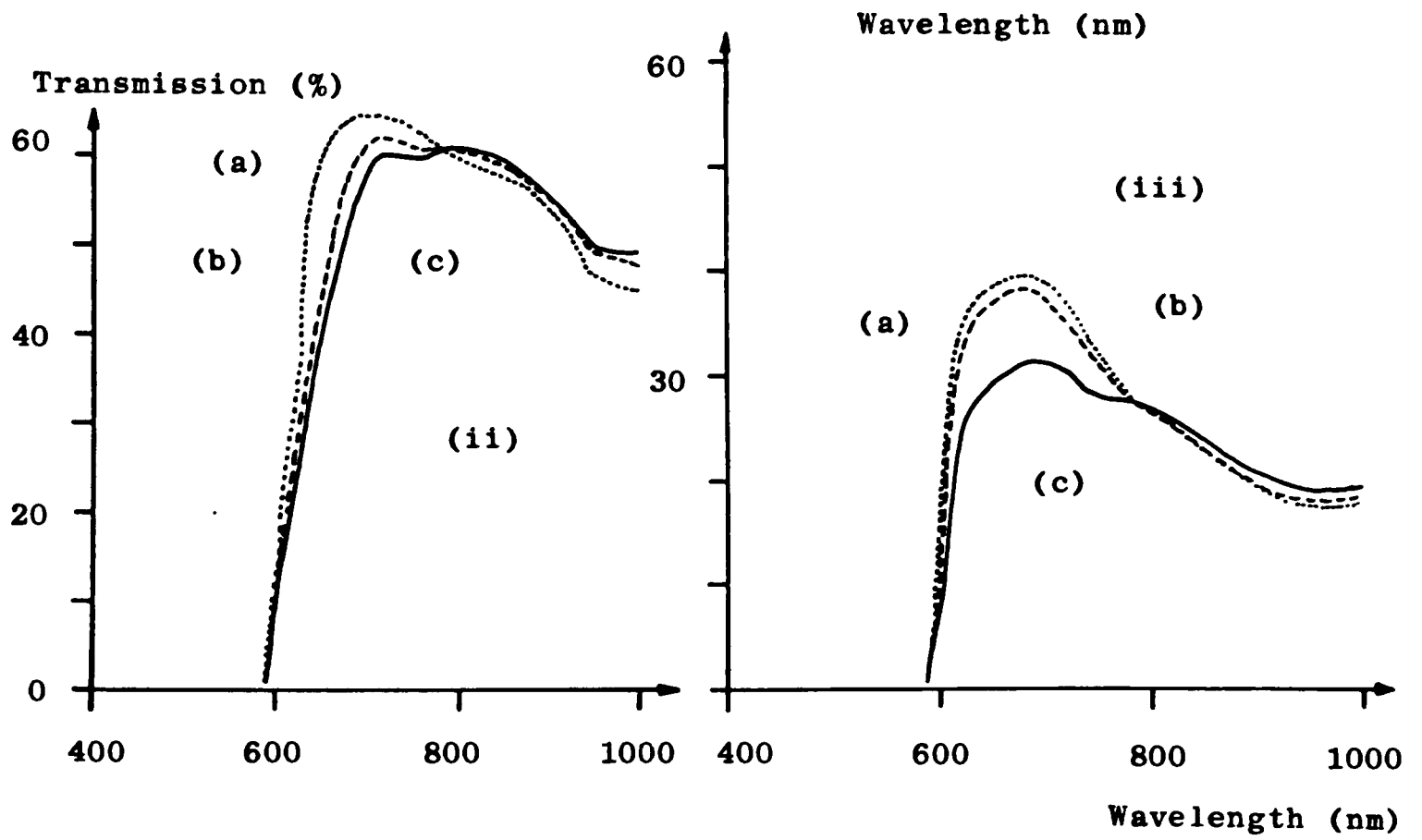

Figure 1.17 Transmission spectra of; (i) cartilaginous helix of adult white male; (a) bloodless, and histamine flushed when breathing (b) 100% and (c) 10% oxygen.
(ii) Heat flushed ear pinna and (iii) histamine flushed ear lobe breathing (a) air, (b) 100% O_2 and (c) 12% O_2 (from ELAM (1949)).

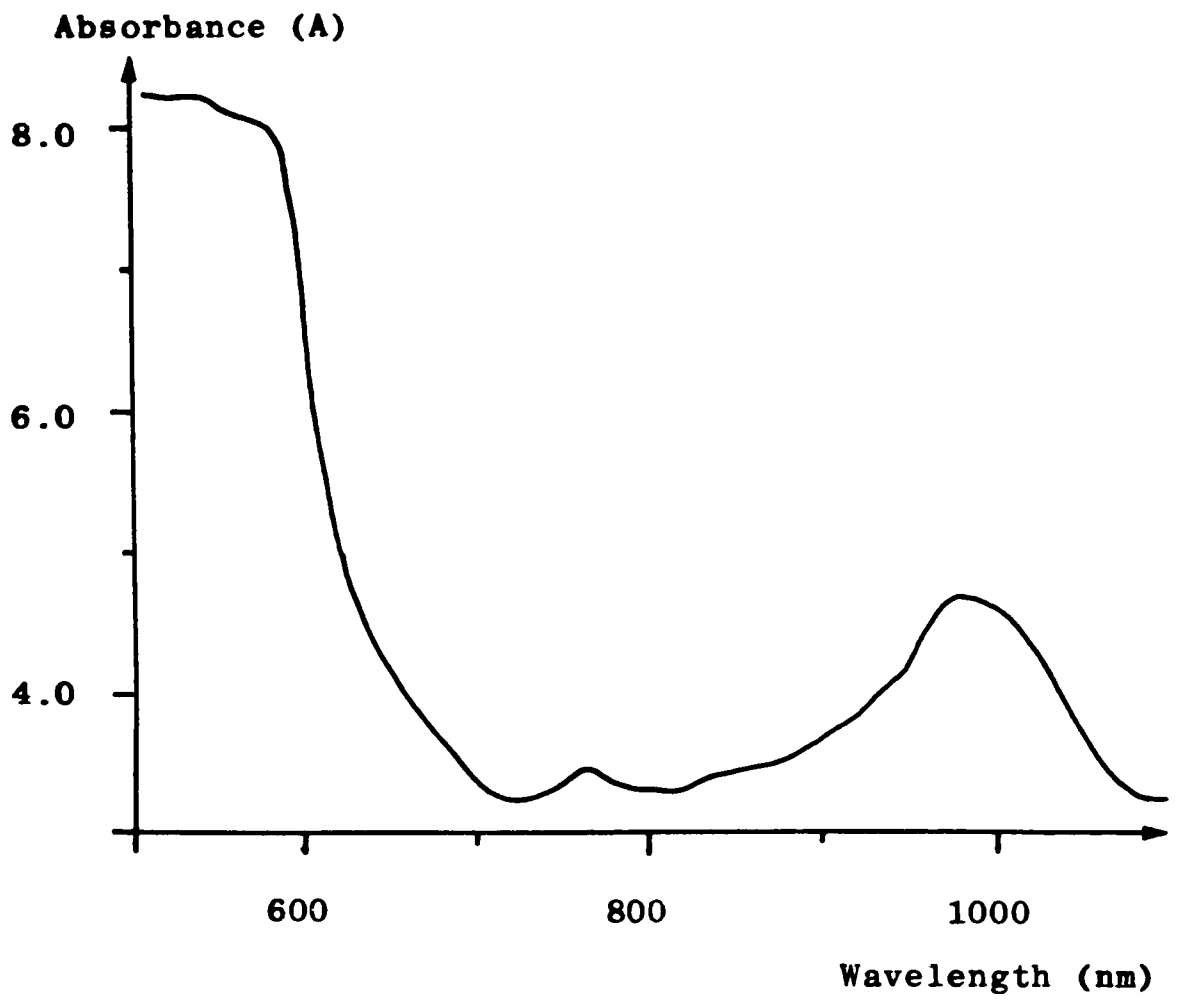

Figure 1.18 Absorption spectrum of a human hand (from NORRIS, unpublished data In SMITH (1979)).

and destruction of malignant growths (DOIRON (1984)).

One approach to studying the optical properties of organs is to use optical fibres to both introduce the light deep into and then detect it from within the sample. With this approach the detecting fibre can be suitably positioned to measure forward, backward or sideways scattered light. Results from these experiments are often quoted in terms of the attenuation coefficient (related to both the absorption and scattering properties, see Section 1.4.3) or the penetration depth (that depth at which the total optical power is reduced to 37 %) which is relevant for dosimetry work. Such figures, at several wavelengths and for a variety of organs from various animals are given by DOIRON (1983).

A similar approach but concentrating on brain tissue has shown that the penetration depth is greater (at all measured wavelengths) in the

adult than in the neonatal brain (SVAASAND (1983a)) which is attributed to the greater degree of myelination. A further study also showed that the penetration depth is longer in human intracranial tumours than in normal brain tissue (SVAASAND (1985)). Both studies are in agreement that the penetration depth increases with wavelength over the measured range from about 600nm to 710nm.

Concerning the actual spectral characteristics of these organs, these have been measured for very thin sections of tissue from 350nm to 1000nm for liver and kidney from various animals (including human) (EICHLER (1977)) with the presence or absence of blood from the sample having a marked effect. Measurements have also been made with the use of fibres on rabbit liver and muscle from 375nm to 825nm (WILSON (1984)), and over the range 400-865nm as ten single wavelength measurements using narrow passband filters through various human structures including the skull (with scalp), chest, abdominal wall and scrotum (WAN (1981b)).

All of these studies show similar findings to their respective counterparts from a comprehensive investigation of the spectral transmission properties over the range 400-1100nm on canine and bovine heart, lung, kidney, liver, adipose and muscle using a scanning spectrophotometer which accepted excised samples of thicknesses from 1.5-16mm(PREUSS (1983), BOLIN (1984)). A selection of the transmission characteristics obtained are shown in Figure 1.19.

The observations which can be made from these studies on the transmission characteristics of specific organs and structures are discussed within the respective papers, however the overall picture which emerges is as follows. In all types of tissue the transmission tends to be higher in the near-IR (from about 600-1100nm) than in the visible (less than 600nm) with a rapid rise in transmission joining the two regions. Within the visible there are also transmission minima usually evident (which often may be due to haemoglobin), and also lesser minima

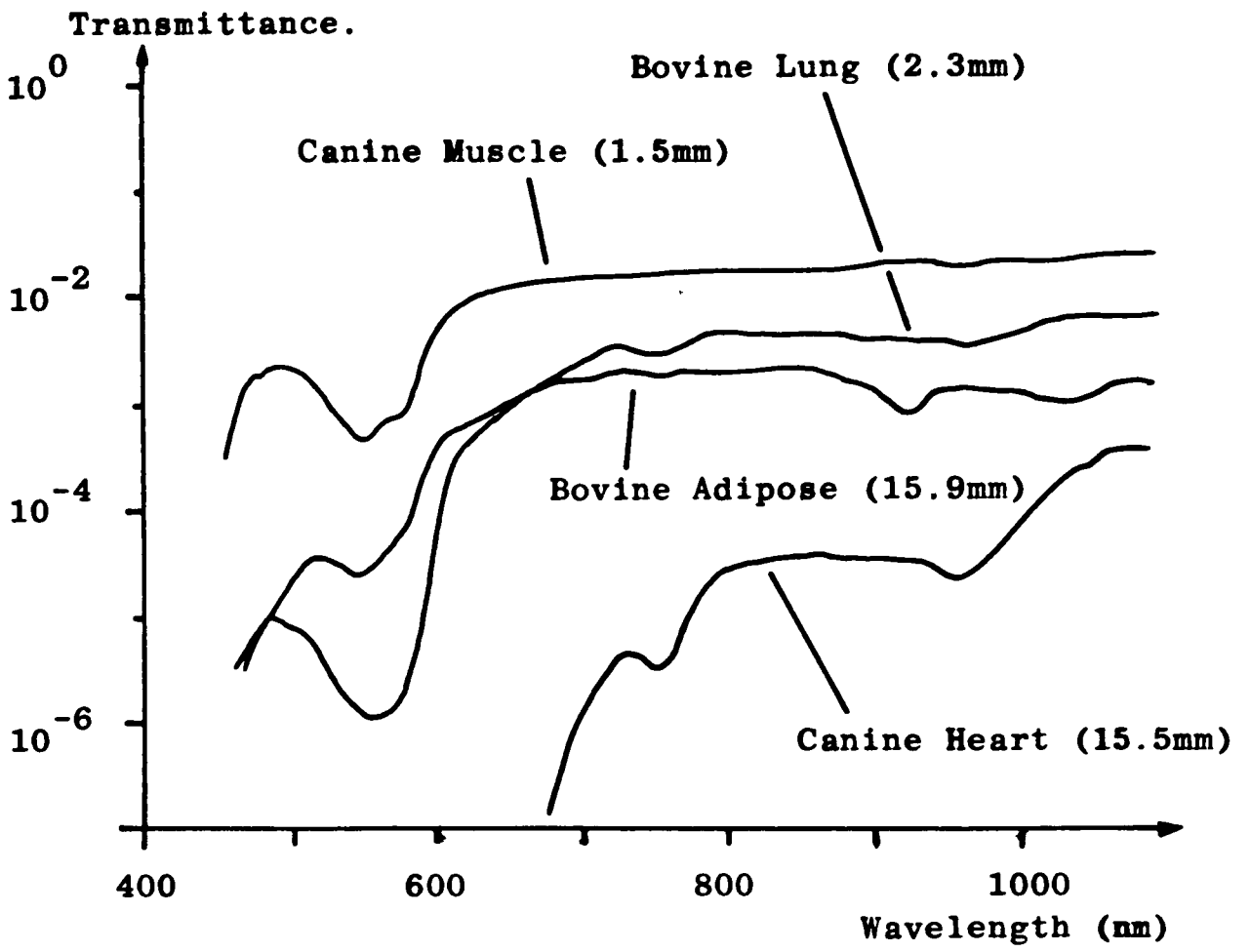

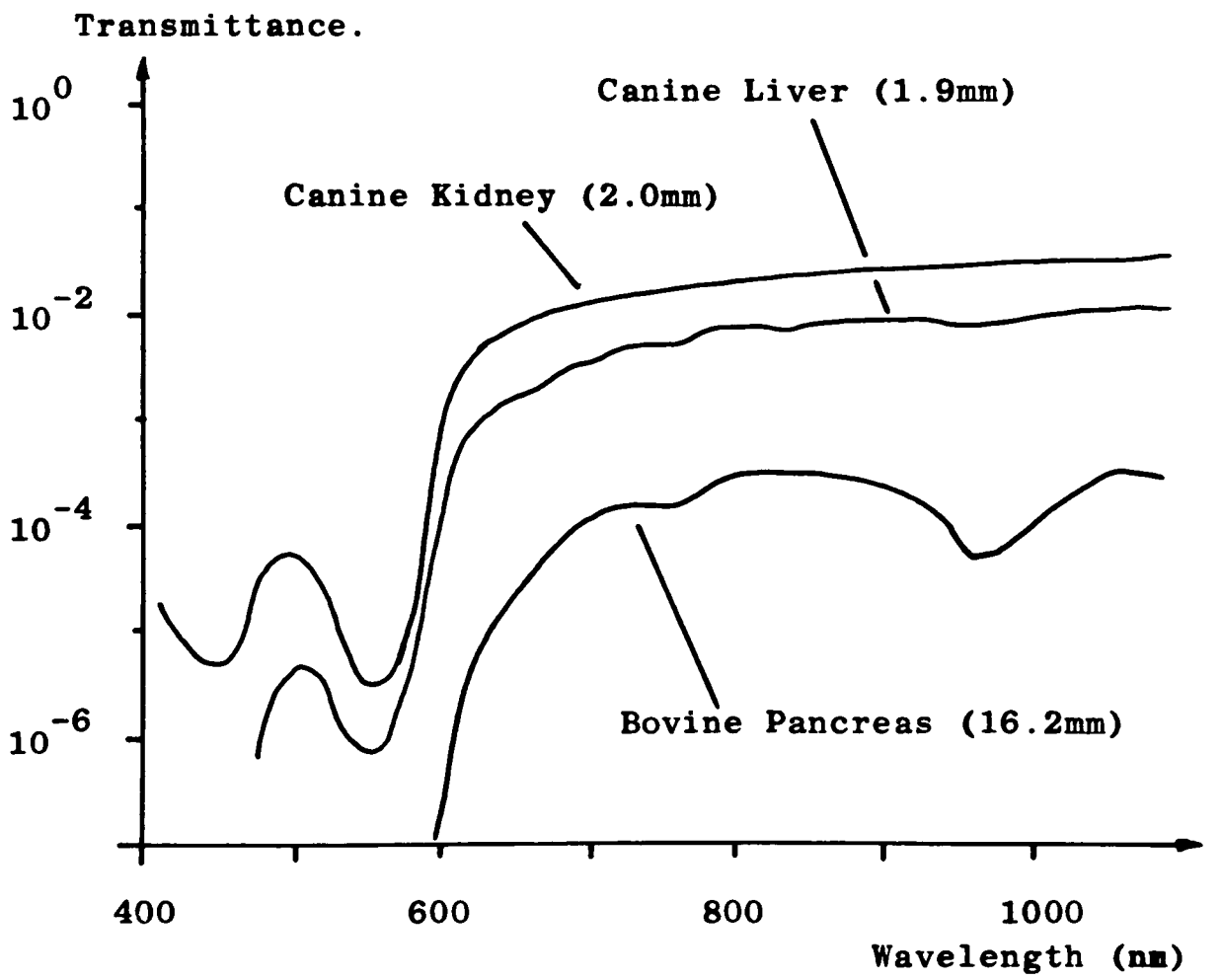

Figure 1.19 Transmission spectra of various samples of excised organs (from BOLIN (1984)).

in the near-IR which are probably due to water and lipids. Despite these similarities between tissue types different tissues do actually possess recognisable transmission characteristics (Figure 1.19) both in shape and attenuation, which is very high (note log scale in this figure).

An important point is that because both transmission and reflectance are fundamentally scattering phenomena then, as with the reflectance spectra, the transmission is heavily influenced by the absorbance spectra of the absorbing compounds present.

Specific measurements of the absorption and scattering properties of various tissues aimed at producing values for use in theoretical modelling of light propagation (WILKSH (1984), MAAREK (1982)) also give some insight into the transmission properties of different organs.

Another field where transmission measurements have been made is in the use of lasers for surgery or treatment. Consequently, the results are only at limited single wavelengths (where lasers are available and used) and concerned with specific tissues, but nonetheless of interest. Such measurements are extensively referred to in reviews of the use of lasers in medicine (see for example McKENZIE (1984)).

1.4.2.2.3 Measurements on Excised Skin.

These types of measurement have again largely been made due to interest in the field of phototherapy. Both transmission and reflection studies have been performed on excised whole skin and samples of separated epidermis and dermis. A schematic diagram of the structure of the skin is shown in Figure 1.20 in the form usually referred to concerning its optical characteristics.

In the UV up to about 300 nm the transmission of the stratum corneum and epidermis is dominated by the presence of aromatic amino acids (especially urocanic acid), nucleic acids and melanin (WAN (1981), ANDERSON (1980,1981), PARRISH (1982), DIFFEY (1983)). Some of these

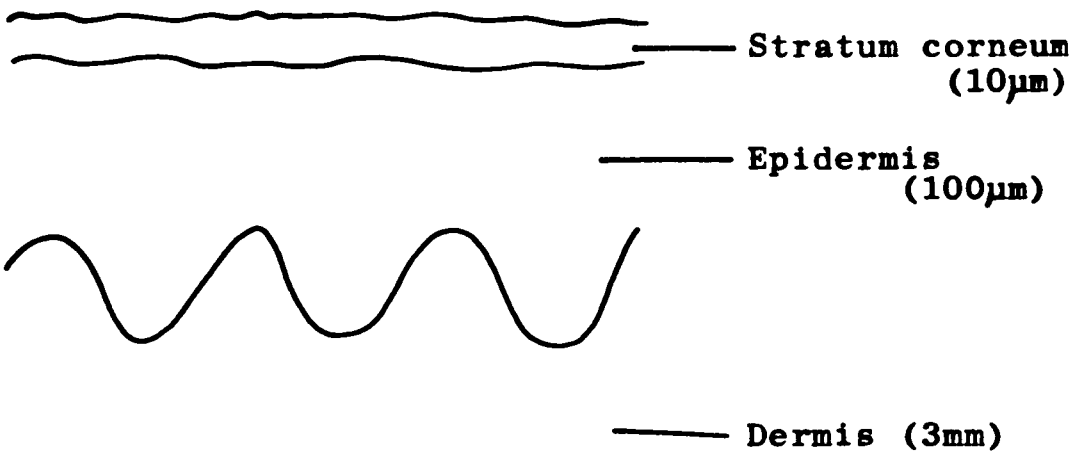

Figure 1.20 Schematic Diagram of the Skin
(from ANDERSON (1981)).

amino acids are also responsible for the autofluorescence of illuminated skin between 330-360nm (ANDERSON (1981)). From 300-800nm the major influence appears to be due to melanin (which continues to absorb, although more weakly, up to about 1100nm). In the near-IR, absorption by water is evident (HARDY (1956)). Transmittance of epidermis from 250-800nm is shown in Figure 1.21. The absorption spectra of melanin, nucleic and aromatic amino acids are given in Figures 1.10 and 1.11 respectively.

The stratum corneum and epidermis do not appear to scatter light very strongly at all (ANDERSON (1981)) an observation borne out by measurements of the reflectance of light from whole skin and the epidermis alone (ANDERSON (1980), hence there is little interest in reflectance measurements.

In contrast the dermis (on which fewer measurements have been made) is strongly light scattering, and *in vivo* contains the blood borne pigments such as haemoglobin and carotene. The transmission and reflectance spectra of human dermis are shown in Figure 1.22. This strong scattering limits the penetration depth (ie the depth of

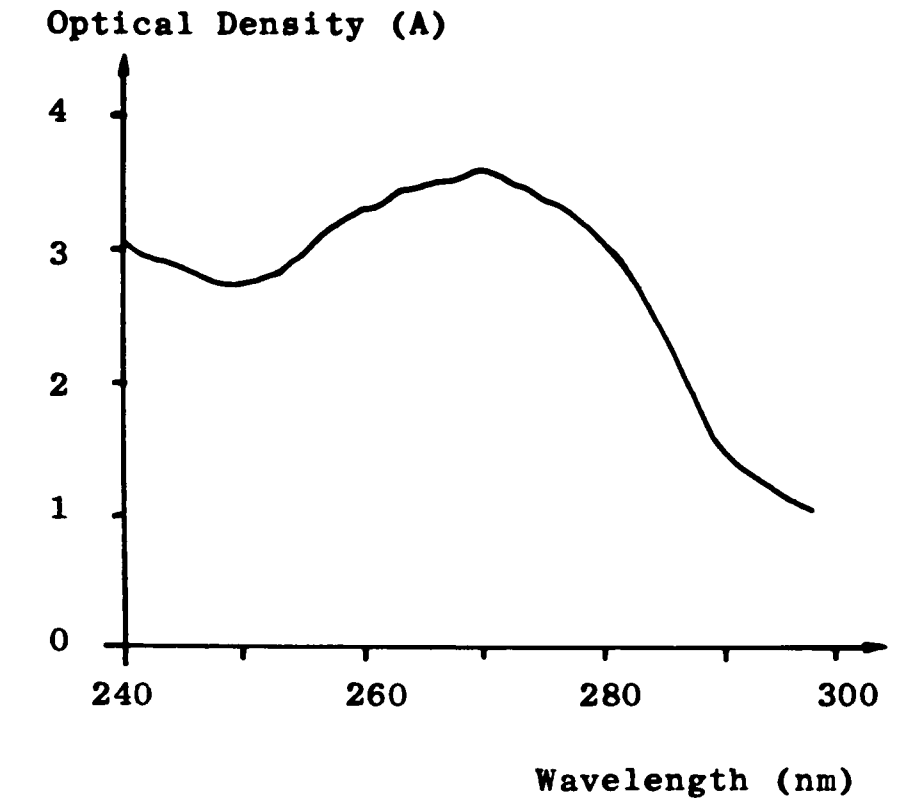

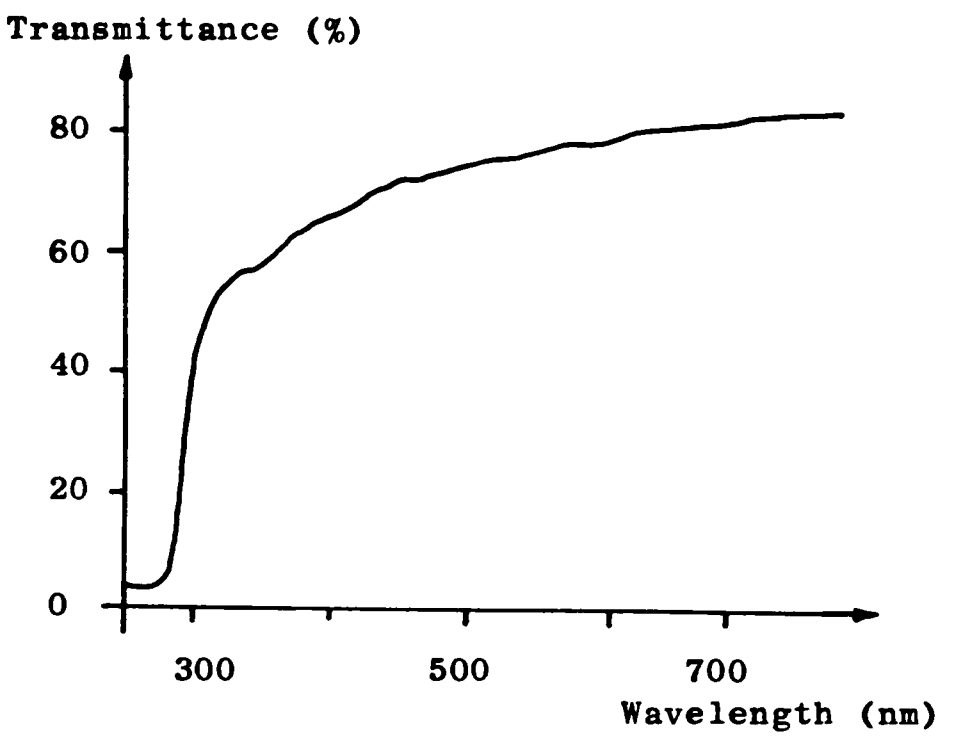

Figure 1.21 (i) Absorbance (from ANDERSON (1981))
(ii) and transmission (from PARRISH (1982)) charactersitics of human epidermis.

penetration of approximately one third of the incident light energy) of light into tissue (ANDERSON (1982), PARRISH (1982), SLINEY and WOLBARSHT (1980)). This differential penetration has in fact been proposed as a means of differentiating between the depth of measurement within the skin in laser doppler and photoplethysmography studies (see Section 1.5.8 and 1.5.4). The variation of penetration depth with wavelength is shown in

Table 1.1. Although these depths are only of the order of micrometres they are the depth at which the intensity is about 37% of the incident level, and do not represent a depth past which no light at the wavelength in question penetrates).

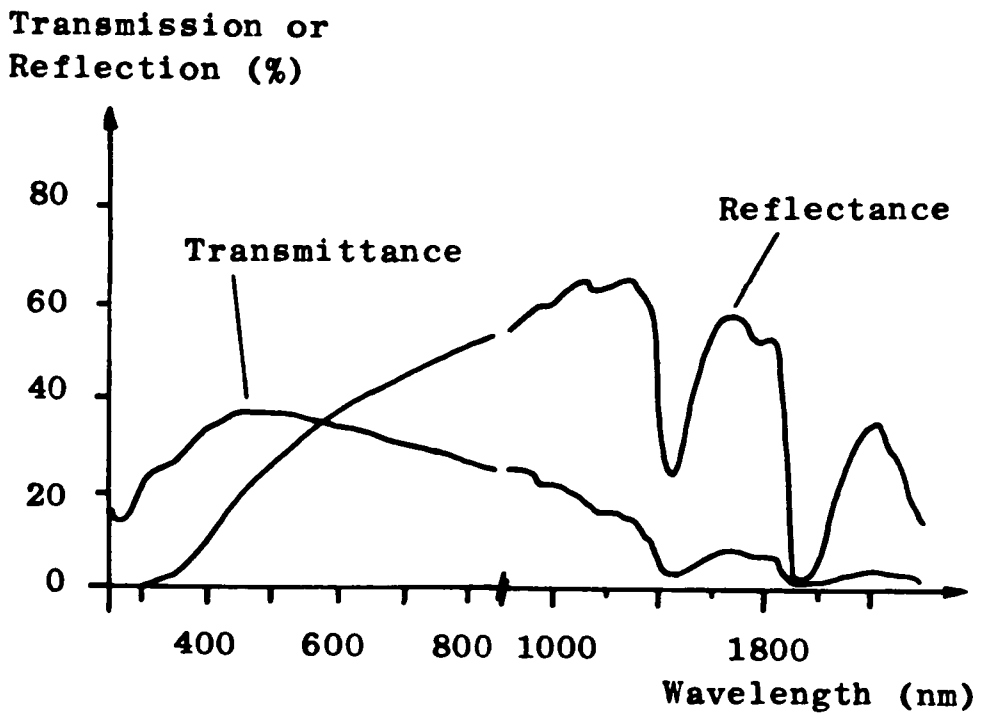

Figure 1.22 Spectral transmittance and reflectance of 200um thick section of human dermis (from ANDERSON (1981)).

Finally, some work has also been performed on the optical characteristics of various tissues within the eye (WEALE (1966), FEUK (1971), FINE (1985)).

Wavelength (nm)	Depth (um)
350	60
400	90
450	150
500	230
600	550
700	750
800	1200

Table 1.1 Penetration of radiation in fair caucasian skin. Approximate depth of penetration is one-third (37%) of the incident energy density.

1.4.3 Theoretical Studies of Light Transmission and Reflection.

1.4.3.1 Introduction.

Within this section a brief review is given of the various attempts to theoretically describe the optical characteristics of biological samples. Such models have been used in a variety of fields: within oximetry (see Section 1.5.1), to model the reflectance and transmission characteristics of skin, to determine the penetration depth of light into tissue during phototherapy and for describing the propagation of photons in biological samples (see Section 1.5.10).

If light (or any other wave) interacts with a system of widely dispersed scattering centres then the outcome can be described by the use of "single scattering" theories such as Rayleigh or Mie theory in which it is assumed that the light encounters only very few particles (BERNE and PECORA (1976), ISHIMARU Part 1 (1978)).

(The scattering described in Section 1.3.3 is basically single scattering with the scattering optical methods in Section 1.5.8 also belonging within this regime).

However, for dense populations of scattering centres, single

scattering theory is inadequate and multiple scattering effects must be taken into account. In such a system the light will now encounter many particles during its passage. Biological samples which are in general inhomogeneous and contain many structure of the order of a wavelength are in this category, and hence multiple scattering effects must be taken into account when considering their optical characteristics.

There are basically two approaches which can be used to model systems in which multiple scattering occurs. Firstly as with single scattering theory an analytical approach, in which single scattering theory, describing the interaction of the wave with the particles, is extended to take into account the effect of the interaction of the other particles (ISHIMARU Part 2 (1978b)). This is generally referred to as multiple scattering theory. Alternatively a "radiative transfer" or "transport" theory approach can be used which effectively deals with the propagation of intensities.

From within these two types of approach several methods have been applied to modelling the optical properties of biological samples; the Kubelka Munk Theory (KMT) and Photon Diffusion Theory (PDT) are both examples of "radiative transfer" theory, whilst Twersky and Mie scattering theory are analytic multiple scattering theories.

1.4.3.2 Multiple Scattering Theory.

The biological material in which virtually all multiple scattering theories have been applied is whole blood. ANDERSON (1965a, 1965b) and LIN (1974) have applied Twersky's and Mie scattering theory respectively whilst KILKSON (1975) has studied the influence of absorption on polarization effects of light scattered from red blood cells, and MULLANEY (1970) the small angle light scattering. In addition, BELMONT (1982) has considered the theory of differential light scattering by chromatin and DIFFEY (1983) used Mie theory in his model of UV optics of

the skin. Most of the above papers are chiefly concerned with the theoretical aspects of the light scattering problem, although some stem from an interest in improving oximetric methods (see Section 1.5.1.2).

Clearly, a rigorous scattering theory approach can be used on suspensions (eg whole blood) but application to actual tissues is extremely difficult. Hence the use of radiative transfer theory, concerned with the propagation of intensities is far more appropriate when modelling the optical characteristics of whole tissue. The use of Radiative Transfer theory in various forms is now described.

1.4.3.3 Radiative Transfer Theory.

In virtually all radiative transfer theory descriptions of light propagation in tissue there are essentially two parameters which are of most significance. These are the scattering and absorption coefficients, and it is relevant to give a broad description of what they represent.

The scattering coefficient is strictly two coefficients associated with the mean free path of a photon (ie the distance between scattering centres) and the direction of scatter. It is therefore this parameter which effects the rate and direction of photon propagation, which is of particular importance in imaging applications and also photoradiation therapy (PRT) (see Section 1.5.10).

The absorption coefficient, as would be expected, is linked to the probability of a photon being absorbed (which in turn can be expressed as an absorbance mean free path) or the amount of energy deposited at each collision. The wavelength dependence of this parameter is related to the spectral characteristics of the sample and hence the absorption spectra of the constituent components. It is of particular importance in determining the energy "deposited" in a region during PRT.

The historical development of the use of theoretical radiative transfer models in oximetry is given briefly during Section 1.5.1. This

is appropriate since this area is where they have been most widely applied (at least until the growth of interest in phototherapy). Actual descriptions and uses of the two most commonly applied radiative transfer models in the field of physiological measurement are now given.

1.4.3.3.1 Kubelka Munk Theory.

The Kubelka Munk approach allows the reflectance and transmission of a single homogeneous absorbing and scattering plane layer to be related to the incident light intensity and scattering and absorption coefficients. The basis of the method is to divide the radiation within the sample into that travelling in the same and opposite directions as the incident light, and then relate the change in these intensities over an incremental thickness to the absorption and scattering coefficients. This is shown in Figure 1.23.

The differential equations obtained can then be solved as appropriate to give relationships concerning the actual properties of interest. (Early use of the KMT was made in the analysis of the colours of powders and paints.)

The theory is rigorously dealt with by KUBELKA (1948, 1954) and ISHIMARU (Chapters 10 and 11; 1978) whilst HECHT (1983) compared this method to other similar approaches, and POLLACK (1979) used KMT as the starting point for considering the theoretical aspects of optical measurements on scattering media for biologiccal applications. Simpler versions of the theory can be found in most of the papers referenced below (especially those dealing with skin reflectance and transmission) which cover the application of KMT to biological systems.

REICHERT (1966) described the use of the KMT in the design of oximeters, whilst LONGINI (1968) and ZDROJKOWSKI (1969) also applied it to oximetry as the starting point for their development of photon diffusion theory (PDT). (KMT leads to expressions for the necessary

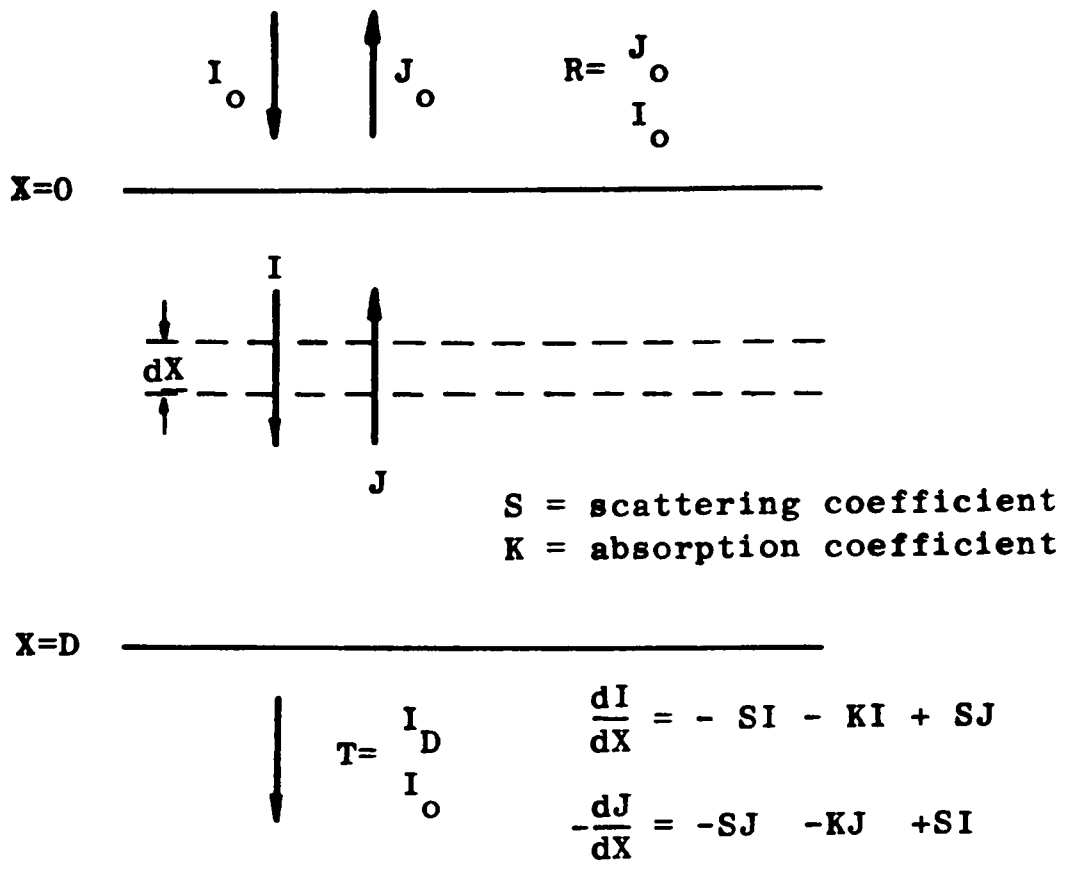

Figure 1.23 The Kubelka-Munk model for radiative transfer (from ANDERSON (1981)).

absorption and scattering coefficients).

Another application of KMT which has found widespread use is in the analysis of the reflectance and transmission of skin both in vivo and in vitro (FEATHER (1980), ANDERSON (1980, 1981), DAWSON (1980), WAN (1981a)). As well as enabling transmission and reflectance characteristics to be predicted such modelling may also allow the concentration of the various absorbing pigments (including haemoglobin and bilirubin) to be quantified using only non-invasive optical measurements. This aim is related to the work of HANNEMAN (1979) and MENDELSON (1983b) who have used forms of the KMT to describe theoretically the in vivo determination of bilirubin concentration and oxygen saturation respectively using reflectance measurements.

The approach adopted when modelling the skin is generally to treat it as a series of plane layers. The intensity of the flux in each layer can then be expressed using KMT (ie by solving the equations shown in

Figure 1.23) whilst the relative transmissions and reflectances of each layer can be related in a manner like that shown in Figure 1.24 (KUBELKA (1954), DAWSON (1980), WAN (1981a), ANDERSON (1981)).

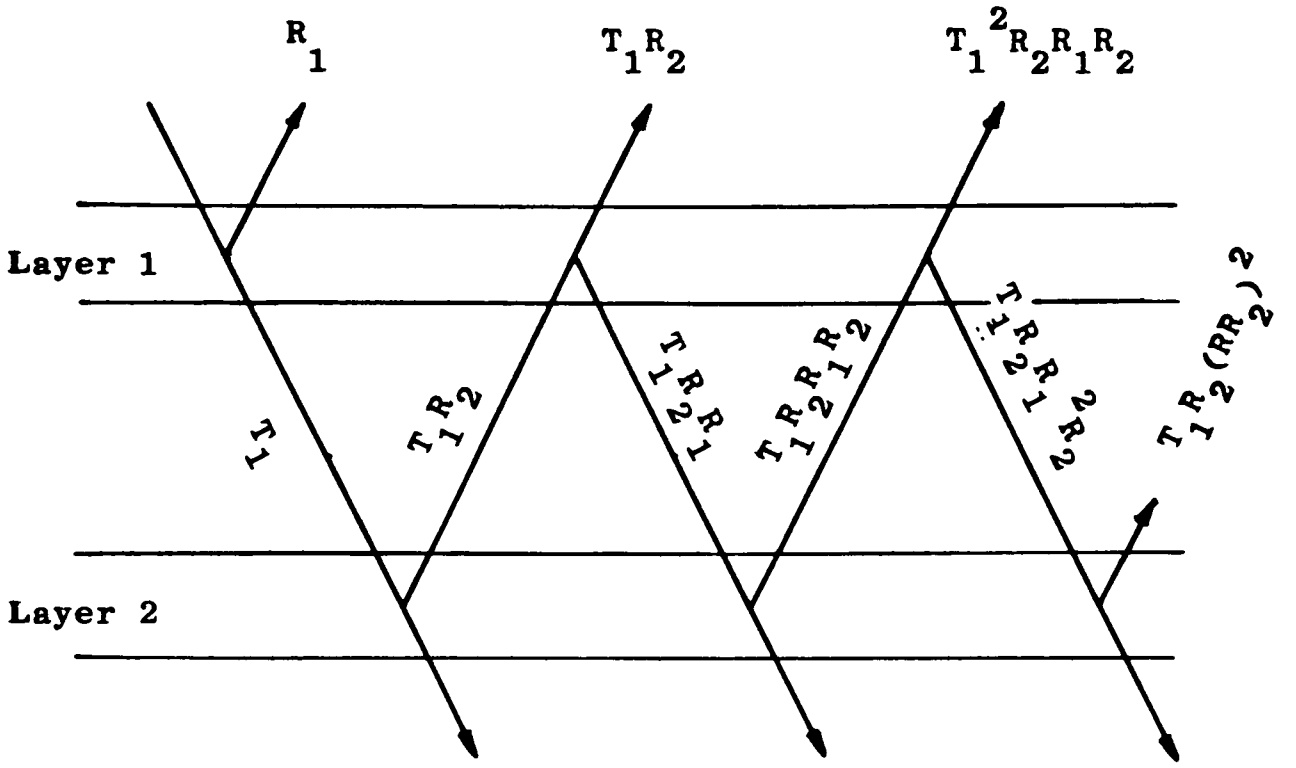

Figure 1.24 Two layered model with corresponding corresponding transmissions and reflections. (R_1, R_2 and T_1, T_2 are the diffuse reflectance and transmittance of layer 1 and layer 2 respectively, from WAN (1981)).

Finally, KMT is also applied in other areas of biological research

where light scattering and absorbing samples are under investigation such as botany (SEYFRIED (1983)).

1.4.3.3.2 Photon Diffusion Theory.

As KMT is an approximate solution to the equations of radiative transfer theory so to is photon diffusion theory (PDT) (ISHIMARU (1978)). In addition KMT and PDT have may common links, illustrated by the work of LONGINI (1968) and ZDROJKOWSKI (1969, 1970) who developed a form of PDT for application to oximetry in which the absorption and scattering coefficients were obtained via KMT. Solutions to the equations they obtained were later given in three dimensions by COHEN (1971, 1972).

JOHNSON (1970) and TAKATINI (1979, 1980, 1978) also used PDT to describe light propagation in blood and in the development of a non-invasive reflectance oximeter respectively. (Takatini's work also includes the use of Twersky's scattering theory to determine the scattering cross sections of red blood cells.)

Within PDT photons are treated as particles which propagate through a medium by a diffusion process with the diffusion determined by the scattering, absorption and diffusion coefficients of the medium. For significant propagation the medium must have a large scattering but small absorption coefficient. The diffusion equation used by the above authors is:

$$D \nabla^2 P - a P = - s P \qquad 1.16$$

and has the form of a typical diffusion equation where D, a and s are the diffusion, absorption and scattering coefficients respectively, and P is the scattered photon density. Hence the diffusion is related to "sources" and "sinks" of photons via the (sP) and (aP) terms. Solutions of this equation for various boundary conditions, away from sources (ie sP = 0) have been obtained (HIRKO (1975), BARBENEL (1979)).

Besides its application in the design of oximeters, PDT has also been used in the field of phototherapy to predict theoretically the dosage received by a region of tissue within the body (SVAASAND (1983a, 1983b) and DOIRION (1983). Again the approach is basically that of solving the radiative transport equations (ISHIMARU (1978)) with a diffusion approximation, which DIFFEY (1983) has also used as a basis for modelling the UV optics of the skin.

As demonstrated by the photon diffusion equation above, the radiative transport equations basically come from considering the conservation of photons. In other words the number diffusing into a volume must equal the number diffusing out except for the effect of "sinks" and "sources" (ie absorbed photons and generated diffusion photons).

1.4.3.4 Other Work.

Concluding this section on the theoretical modelling of light interaction with tissue two other approaches are introduced. The first is Monte Carlo modelling, which is basically a statistical approach in which the absorption and scattering probabilities of the sample (often derived from the models just described) are used to determine the likely paths of a large sample number of photons through the tissue. This method, which is potentially of use in the areas of optical transillumintion imaging and light dosimetry calculations, is described in more detail in Section 1.5.10.

The second alternative approach is one developed by LUBBERS (1973, 1975) as a means of analysing the reflection measurements from tissue, thus enabling oxygen saturation and the redox state of cytochromes to be monitored non-invasively. The method involves considering the tissue as consisting of cuvettes containing solutions at different concentrations. The Lambert-Beer law is then applied to the passage of light through

these cuvettes, with the reflectance dependent upon their configuration.

1.5 Optical Methods for Physiological and Biochemical Measurements.

So far the physical nature of light and the modes in which it interacts with matter have been described together with the gross optical characteristics of tissue, and the major light absorbing compounds in the body.

This section deals with optical methods used for physiological and biochemical measurement. The methods described range from widely used clinical methods, through established research techniques to those which are still in the developmental stage or have been developed but never generally accepted. Both in vivo and in vitro devices are discussed although methods which may ultimately be used for monitoring physiological or biochemical variables non-invasively are of specific interest. The emphasis is placed on the actual principles behind the techniques rather than their clinical importance.

Oximetry is dealt with in most detail (Section 1.5.1) since it has been practised for many years and is considered to be the most advanced and widely used technique. Hence it is an excellent example of an optical method on which much experimental and theoretical work has been performed. Furthermore, other optical methods rely upon measuring small changes in absorbance on a large background attenuation and so have similarities with oximetry. Examples are monitoring the redox state of cytochrome oxidase (Section 1.5.4), studying the photoplethysmogram (PPG) (Section 1.5.6) and other sundry techniques (Section 1.5.3).

For completeness other methods are included which although not strictly relevant, do contribute to the overall subject. This is considered important since it is likely that experience and information gained in one area of optical monitoring may be of use in others.

The techniques in this section are optical as earlier defined, however considering the whole em spectrum, it is perhaps worth noting

that many important and widely used clinical instruments are based on the interaction of em radiation with tissue. For example all X-ray techniques, NMR scanners, the use of microwaves in various applications and thermal imaging.

1.5.1 Oximetry.

Oximetry is defined here as the determination of the oxygen saturation of blood using spectrophotometric methods, whether performed *in vitro* or *in vivo*. It is probably both the most widely used and oldest optical method (see NILSSON (1960)), and that this is so is not surprising considering the influence the optical characteristics of blood has on tissue colour (see Section 1.4.2) and the tremendous physiological significance of oxygen transport and tension within the body (see Chapter 4).

Virtually all oxygen transported around the body is carried in the red cells as oxyhaemoglobin, which is haemoglobin with oxygen bound to it. Oximetry is based upon the existence of a slight difference in the absorption spectra of these two compounds (due to conformational changes in the protein as oxygen becomes bound and unbound) as shown in Figure 1.25 with spectrophotometric analysis used to calculate the relative proportions of haemoglobin and oxyhaemoglobin. This is commonly expressed as oxygen saturation SO_2 given by:

$$SO_2 = \frac{[HbO_2]}{[HbO_2] + [Hb]} \qquad 1.17$$

where the square brackets denote concentration. (Percentage oxygen saturation (pos) is given by $SO_2 x100$).

Oxygen saturation, is alinearly related to the partial pressure of oxygen, pO_2 via the sigmoidal oxygen dissociation curve which governs the take up and release of oxygen from the lungs and to tissue respectively, in a controlled manner. This is described in more detail in Section 4.7 with other physiological aspects of the importance of monitoring tissue oxygen levels also discussed in this chapter. The oxygen dissociation curve is shown in Figure 1.26 and illustrates the fact that SO_2/pO_2 is a more sensitive indicator of changes in arterial oxygenation at low/high pO_2's.

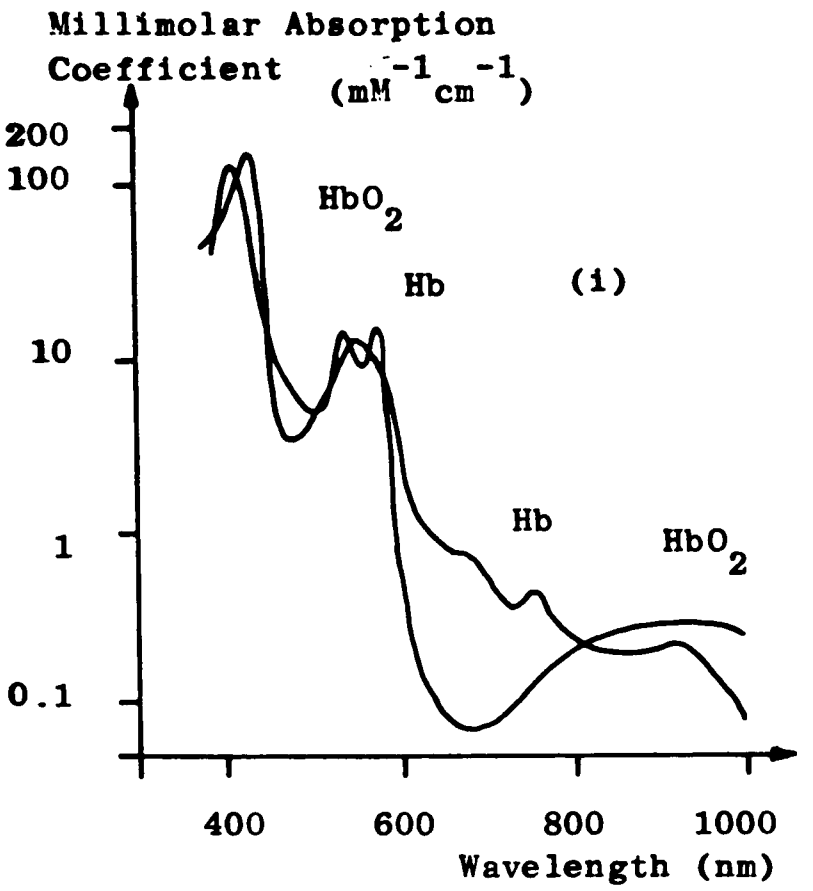

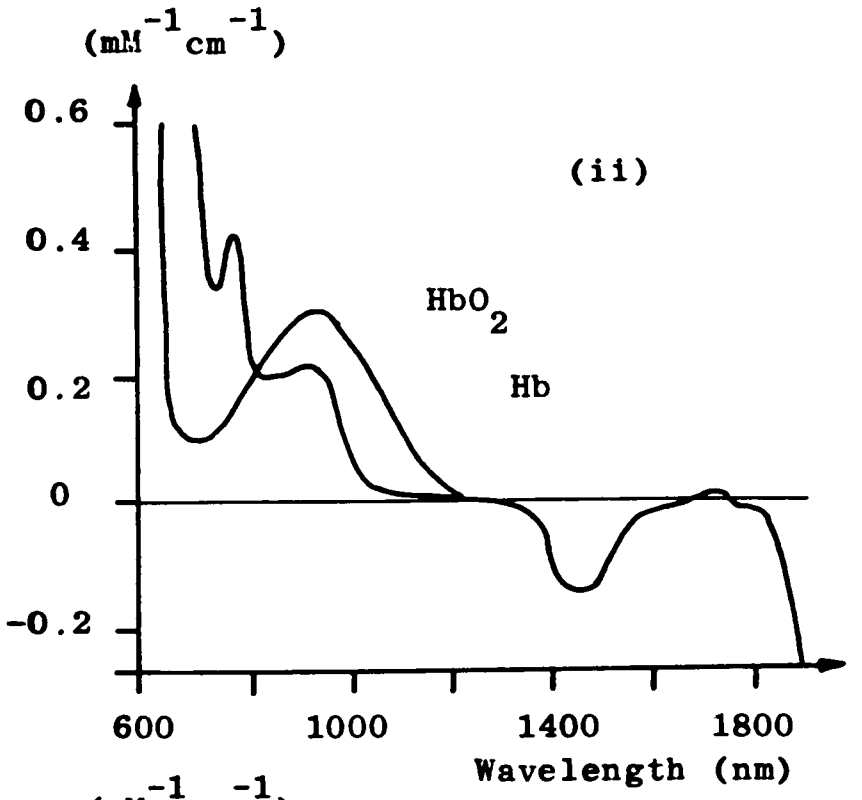

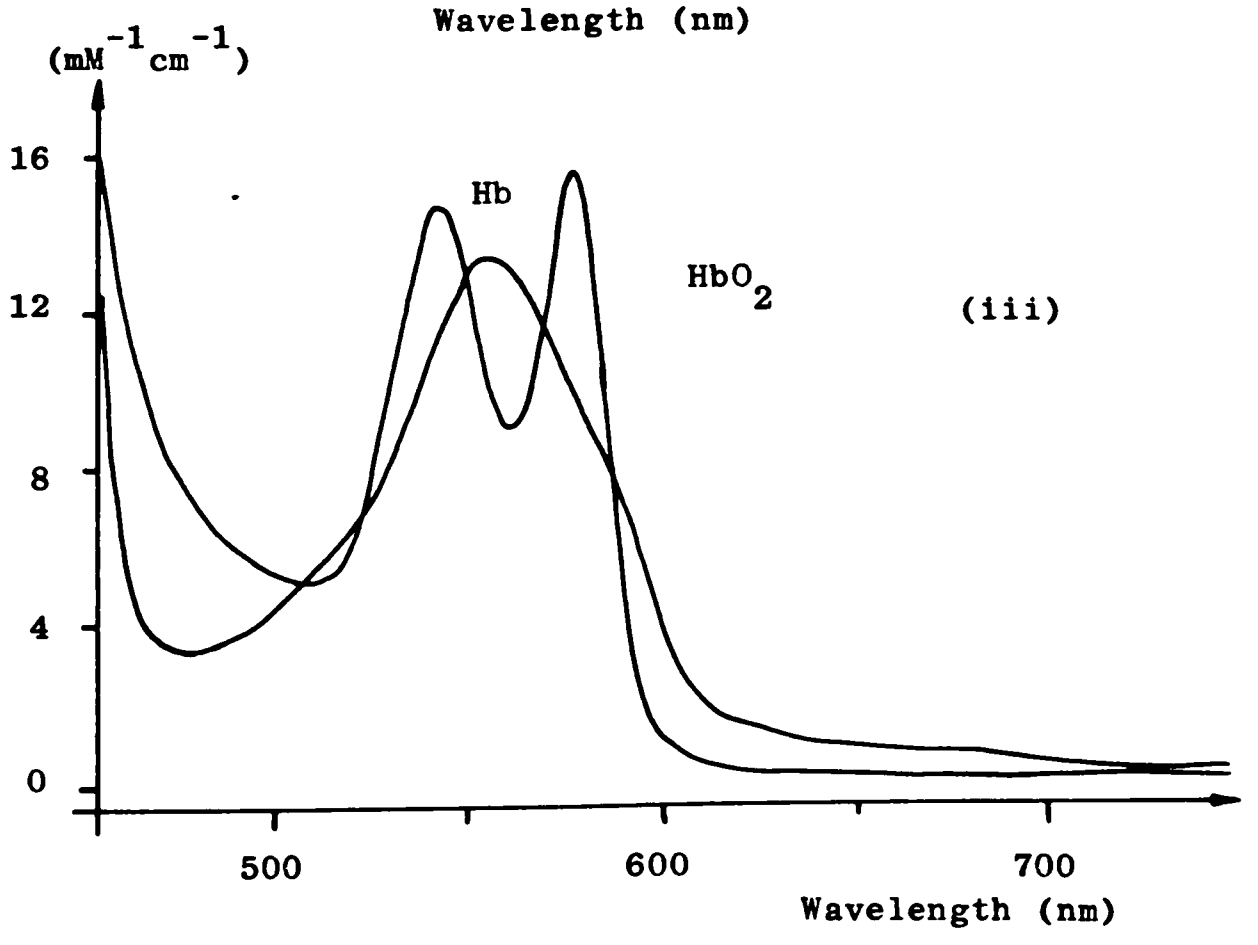

Figure 1.25
The absorption spectra of haemoglonbin (Hb) and oxyhaemoglobin (HbO_2),
(from:
(i) YOSHIYA (1983)
(ii) BARLOW (1962)
(iii) ZIJLSTRA (1983))

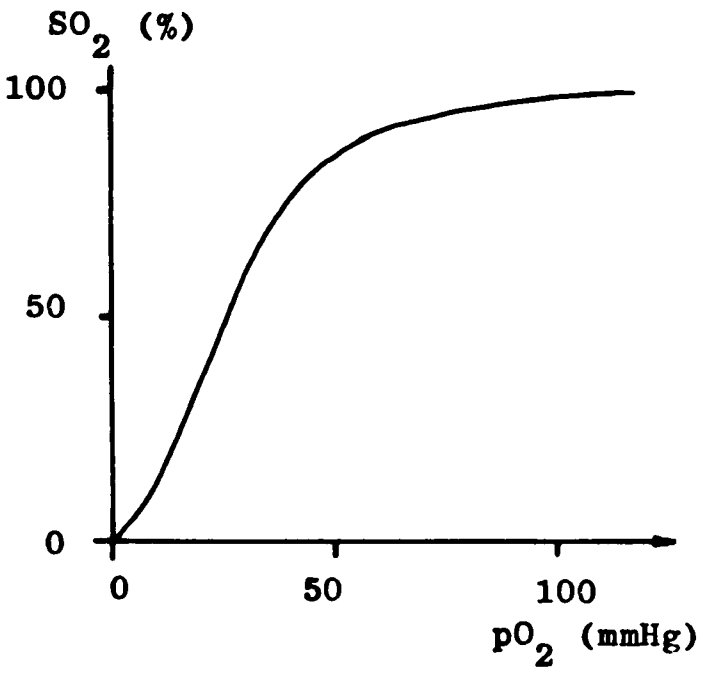

Figure 1.26 Oxygen dissociation curve for haemoglobin (from YOSHIYA (1983)).

The early developments of oximetry have been reviewed by ZILJSTRA (1953), NILSSON (1960) and JANSSEN (1972) with YOSHIYA (1983) covering most of the subsequent significant advances since the earlier reviews. Here the evaluation of oxygen saturation is dealt with in five sections:-

In vitro measurements on:

(1) Haemolysed blood samples, where the Lambert-Beer law can be correctly applied.

(2) Non-haemolysed (whole) blood samples in both transmission and reflection modes, where scattering as well as absorption should strictly be taken into account.

In vivo measurements:

(3) In transmission mode through tissue such as fingers and ear lobes and pinnae, where the scattering is large but the use of the Lambert-Beer law appears adequate.

(4) In reflection mode from whole blood in major vessels using catheterization, which is wholly dependent on back scattering.

(5) Reflection from tissue, which is again dependent on back scattering and for which theories incorporating scattering would appear necessary.

It should be noted that in addition to haemoglobin and oxyhaemoglobin there are several other haemoglobin derivatives, all with distinctive spectra (such as carbomonoxyhaemoglobin (see Figure 1.7)), and therefore lending themselves to quantitative analysis using extensions of the spectroscopic methods outlined below (MALENFANT (1979)). Such analysis is of potential use in applications such as the treatment of victims of pollution from toxic fumes.

However the majority of oximeters operate under the assumption that haemoglobin only exists as either haemoglobin or oxyhaemoglobin. which can lead to problems in obtaining accurate measurements from some oximeters.

1.5.1.1 In vitro Measurements of Oxygen Saturation on Haemolysed Samples.

Haemolysed blood samples ideally contain no cell wall debris or any other scattering material and so give a clear solution which will transmit light according to the Lambert-Beer law (equation 1.15).

If the only absorbing substances in the solution are haemoglobin and oxyhaemoglobin then at wavelength λ_1 the optical density A_1 will be given (from the Lambert-Beer law) by;

$$A_1 = l\,(\,a[HbO_2] + b[Hb]\,) \qquad 1.18$$

where a and b are the absorption coefficients for oxyhaemoglobin and haemoglobin respectively at λ_1 nm, and l is the depth of the solution. (nb $A_1 = \ln I_o/I$ where Io is the incident light on the solution and I the amount of light transmitted).

With a total haemoglobin content of the solution of C, then;

$$C = [HbO_2] + [Hb] \qquad 1.19$$

and the oxygen saturation as defined in equation 1.17 is given by;

$$SO_2 = \frac{A_1 - C1b}{C1-(a-b)} \qquad 1.20$$

The disadvantage of this one wavelength technique is that even for a given apparatus where a, b and l would be known, C is still variable since it will be dependent upon the haematocrit of the blood sample (density of red cells) before haemolysis. Therefore in addition to measuring, A_1, the optical density, the total haemoglobin content, C, must also be found before the oxygen saturation can be determined.

Alternatively, if two wavelengths are used then in addition to calculating A_1 from the measurements of $Io(\lambda_1)$ and $I(\lambda_1)$ a corresponding equation can be obtained at another wavelength, relating the optical density at this wavelength, A_2, to the concentrations of oxyhaemoglobin and haemoglobin by the absorption coefficients at the second wavelength, c and d.

$$A_2 = l\ (c\ [HbO_2] + d\ [Hb]) \qquad 1.21$$

Equations 1.18 and 1.21 can be manipulated to give the saturation as;

$$SO_2 = \frac{A_1\ c - A_2\ a}{A_1\ (c-d) + A_2\ (b-a)} \qquad 1.22$$

which gives an absolute value of oxygen saturation in terms of the measured optical densities at the two wavelengths with no values of other parameters such as cuvette depth, l, or total haemoglobin and oxyhaemoglobin concentration, C, required.

This is because there are in effct two unknowns; oxygen saturation and the combined term (Cl), and two equations.

(Note that the (Cl) term cannot be split by taking a third absorbance measurement at another wavelength. Linked to this is the fact that using two wavelengths, neither haemoglobin or oxyhaemoglobin can be found without l being measured since there are two equations but three

unknowns, even taking a measurement at a third wavelength will not help since the three equations will be linearly related. However, oxygen saturation can be found using only two wavelengths since it involves taking a ratio of two of the variables and hence cancelling the third). The use of the Lambert-Beer law for multiwavelength measurements is taken up again in Section 4.10. (For more details of the above calculations see (for example) ZILJSTRA (1953), GORDY (1957), NILSSON (1960), YOSHIYA (1983)).

Any two wavelengths can be used to determine oxygen saturation, as long as the two forms of haemoglobin have different absorption coefficients for at least one of the wavelengths. In practice one wavelength is usually chosen with the absorption coefficients the same for both haemoglobin and oxyhaemoglobin, (ie an isobestic point), so that equation 1.22 then reduces to the simpler form of;

$$SO_2 = \frac{A_1\ c\ -\ A_2\ a}{A_1\ (c-d)} \qquad 1.23$$

$$= \frac{K_1\ A_2\ +\ K_2}{K_1}$$

From Figure 1.25 it can be seen that several isobestic points exist. The actual choice of both wavelengths is a matter of compromise. The ideal wavelength will have a low overall absorption coefficient for both haemoglobin and oxyhaemoglobin, but a large difference between them, so that a high light signal can be obtained through the cuvette which will also vary dramatically depending upon the oxygenation state. As may be expected these two requirements are conflicting.

In practice wavelengths around the 520-600nm structure in the absorption spectra have been used for oximetric measurements in cuvettes (ZILJSTRA (1953)), although the region from 600-800nm appears to have been generally preferred (YOSHIYA (1983)) due to the lower overall

absorption coefficient. In the latter region (and for most oximetric measurements in practice) 805nm has become the almost standard isobestic point, whilst around 660nm gives a large variation in absorbance for the two forms of haemoglobin (MOOK (1969)). Few, if any, oximeters have been made which operate below about 500nm, that is on the Soret band. The question of which wavelength range to use is considered as appropriate in the following sections.

The above type of derivation can be applied not only to oximetry but to any spectrophotometric analysis of multicomponent samples in clear solution. Furthermore, an extension of this method (ie the application of the LB law) is used in the majority of in vivo transmission oximeters, despite the total lack of allowance for scattering (see Section 1.5.1.3).

1.5.1.2 In vitro Measurement of Oxygen Saturation on Whole Blood.

Non-haemolysed blood is a turbid medium due to the presence of suspended erythrocytes and other particulate matter which means that light is not only transmitted through a sample, but also reflected (back-scattered). Hence both transmission and reflection measurements can be performed, although because of the scattering, in addition to the absorption, the transmission of light through whole blood does not strictly obey the Lambert-Beer law.

Oxygen saturation measurements have been made on whole blood in both reflection (RODRIGO (1953), POLAYNI (1960), WARE (1960)) and transmission (ANDERSON (1965)) modes, the latter aided in part by the fact that at constant cuvette depth and hematocrit there is a linear relatioship between oxygen saturation and the log of light transmission (KRAMER (1950), ANDERSON (1965)). However, variations in hematocrit and cuvette depth definitely do not affect transmission according to the Lambert-Beer law, and this difficulty in obtaining reliable oxygen saturation measurements from whole blood is reviewed by SUTTERER (1967). It has

also resulted in many studies aimed at producing both theoretical and empirical relationships which adequately describe the reflection and transmission of light from whole blood samples, as parameters such as hematocrit and oxygen saturation are varied.

Concerning the wavelength range of the oximeters used on whole blood in vitro all of the papers referred to above use light in the region 600-805nm (the latter wavelength as an isobestic).

Basically two types of theoretical approach have been used to explain the experimental results of optical measurements on whole blood. One is the application of radiative transfer theory and its amendments, (Section 1.4.3.3), and the other the more rigorous analytical approach of multiple scattering theory which is effectively an extension of single scattering theory (Section 1.4.3.2).

RODRIGO (1965) applied Schuster's radiative transfer theory to the problem of single wavelength reflection measurements, which was later extended by POLAYNI (1953) to two wavelengths in a manner similar to that described in the previous section for transmission measurements on haemolysed samples. REICHERT (1966) continued the radiative transfer theory approach and applied it in the form of the Kubelka-Munk theory (KMT) (Section 1.4.3.3.1). The KMT is only applicable to parallel planes (ie it is essentially a one dimensional model), however another approach of the radiative transfer theory is in the form of Photon Diffusion Theory (PDT) (also described in Section 1.4.3.3.2) which can be applied in three dimensions.

The practical and theoretical aspects of the application of PDT to oximetry has been discussed by several authors (LONGINI (1968), ZDROJKOWSKI (1969, 1970)) and JOHNSON (1970a) who has also performed an experimental study into the propagation of near-IR light in blood (JOHNSON (1970b)). Since these early papers on the use of PDT the solution of the equations involved for different boundary conditions have

been considered by many workers (HIRKO (1975), BARBENEL (1979)). Radiative transfer theory has also been applied to the design of catheter and tissue reflection oximeters and its use is therefore referred to again in Sections 1.5.1.4 and 1.5.1.5.

Twersky's multiple scattering theory is a more rigorous analytical approach to the problem of light scattering from red blood cells but has been used by LOEWINGER (1964) and ANDERSON (1967).

Finally, although not strictly concerned with oximetry but of potential interest is work of both a practical and theoretical nature which has been performed on the scattering properties of blood corpuscles (LOTHIAN (1956), NIWA (1982), REYNOLDS (1983)).

1.5.1.3 In vivo Measurement of Oxygen Saturation by Transmission.

Measurement on either haemolysed or whole blood clearly measures the oxygen saturation of the haemoglobin within the sample which is presumably a constant value throughout the cuvette. However, with measurements on whole tissue where there is no defined cuvette, the questions arise as to both where the oxygen saturation is being monitored (eg in the arterial, venous or intratissular blood) and to what should the oxygen saturation be, since it is the oxygen content of arterial blood that is usually considered clinically and then more usually its pO_2 rather than its oxygen saturation. These points are briefly mentioned by NILSSON (1960) and YOSHIYA (1983), and discussed in more detail in Chapter 4 in conjunction with the possibilities of monitoring the redox state of cytochrome oxidase which ostensibly gives an indication of the oxygen tension at its site of utilization.

Early developments in the field of in vivo transmission oximetry are again covered by ZILJSTRA (1953) and NILSSON (1960), in which the means of performing oxygen saturation measurements at a variety of sites are described. The following four techniques are described in some detail as

they are considered to have made a significant contribution, and also illustrate important points in the overall context of optical physiological measurements, including monitoring the redox state of cytochrome oxidase.

1.5.1.3.1 The Wood Oximeter.

This device is based upon the application of the Lambert-Beer law with the ear acting as a cuvette. The major problem with this technique is to obtain quantitative measurements without some form of calibration such as breathing 100% oxygen. This can be achieved if a baseline transmission level can be found, with multiwavelength analysis then performed on another transmission level either above or below the baseline.

In the Wood's oximeter (WOOD (1949)) the ear was compressed until it became bloodless, with the level of light passing through the bloodless tissue then used as the baseline. Consequently when the ear became fully arterialised the light could be considered to pass through both the bloodless tissue component and the arterial blood, with the difference between the two transmitted intensities then used to calcualate oxygen saturation as outlined below. (Note that the method assumes that the blood in the ear is arterial blood, and so arterial and not venous or some oxygen saturation averaged over the circulatory system (ie arteries, capillaries and veins) is measured. (This "averaged" oxygen saturation will be referred to as the tissular oxygen saturation hereon).

Referring to Figure 1.27, the absorbance, A, (optical density (OD)) of the bloodless ear is given by ;

$$A = \log \frac{I_o}{I} \qquad 1.24$$

where I_o is the light incident on the ear and I the amount transmitted by the bloodless component.

Upon releasing the compression, blood flows back into the ear, and

the transmitted intensity drops to I', with total absorbance then given by:

$$A' = \log \frac{I_o}{I'} \qquad 1.25$$

Assuming that the increase in absorbance, ΔA is due to an arterial blood component and that the bloodless tissue component has remained constant, then the absorbance by the arterial blood is given as;

$$\Delta A = A' - A = \log \frac{I}{I'} = l\,(a\,[HbO] + b\,[Hb]) \qquad 1.26$$

where the notation is the same as in equation 1.18. This is shown diagrammatically in Figure 1.27.

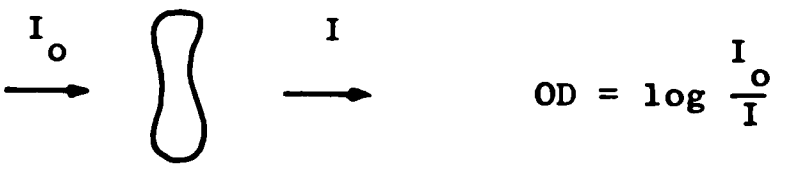

Figure 1.27 Diagrammatic Representation of Wood's ear oximeter.

Since equation 1.26 was obtained solely from the Lambert-Beer law, then by measuring the absorbance in the same way at another wavelength the oxygen saturation can be found in an identical manner as in Section 1.5.1.1 for a clear solution of haemoglobin. Equation 1.22 therefore gives the oxygen saturation in terms of two absorbances or equation 1.23 if an isobestic point is used. This was the case with the Wood's oximeter which used broad band "red" and "near-IR" (isobestic of about

805nm) wavelengths. This theory could be applied to any wavelengths although the low transmission below about 650nm means virtually all transmission techniques are above this wavelength.

In this in vivo application the path length, l, cannot be measured due to the intense scattering, but as before it cancels if two wavelengths are used and it is assumed that the two pathlengths are the same.

The above approach to in vivo transmission oximetry is reasonably successful, which may seem somewhat surprising considering that in optical terms tissue does not even closely approximate a clear solution, and therefore the Lambert-Beer law should not strictly apply. However, it may be connected with the findings that for fixed hematocrit and cuvette depths reasonable results can be obtained from in vitro transmission oximetry using the Lambert-Beer law (KRAMER (1951), ANDERSON (1965)).

The Wood oximeter is also described by ZILJSTRA (1953), NILSSON (1960) and YOSHIYA (1983), as are other in vivo transmission studies including one which relies upon calibration procedures (SEKELJ (1951)) rather than establishing a baseline.

In summary the Wood's oximeter had problems such as the difficulty in rendering the ear completely bloodless, the fact that the compression of the ear is likely to change its optical characteristics and that the blood within the ear may not be truly representative of arterial blood due, for instance, to circulatory disturbances. (This last point being a problem for all in vivo oximeters which operate upon the peripheral circulation). However, the approach adopted resulted in a significant contribution to in vivo optical monitoring, demonstrated by the current success of pulse oximeters which operate in a fundamentally similar way (see later on in this section).

Other work involving monitoring oxygen saturation in vivo using

transmission techniques, but deep in the brain, has been performed by F F Jobsis and his colleagues, with the theory again based upon the Lambert-Beer law. Oxygen saturation is basically monitored to correct for artifacts due to changes in absorbance whilst studying the redox state of cytochrome oxidase. This is described in Section 1.5.5 and in depth in Chapter 4.

1.5.1.3.2 The Hewlett Packard Oximeter.

In the mid 1970's the Hewlett Packard oximeter was introduced (MERRICK (1976), YOSHIYA (1983)) with the theory behind its operation again based upon the Lambert-Beer law. In contrast to establishing a baseline transmission value and subsequently assuming that only the presence of blood comprising solely of haemoglobin and oxyhaemoglobin perturbs this level, (as in Wood's device), the Hewlett Packard oximeter considers the ear as a cuvette containg several absorbing components.

By measuring the optical density (OD) of the ear at a sufficient number of wavelengths, a set of simultaneous equations can be set up which describe the OD at each wavelength in terms of the concentration of the number of absorbing substances (ie an equation of the same form as 1.18, only for more compounds, at each wavelength). Since two of the absorbing substances will be oxyhaemoglobin and haemoglobin then oxygen saturation can be found. This approach is similar to that adopted in section 1.5.1.1 except that more than two simultaneous equations are used, as more unknowns (absorbing compounds) are taken into account. Again the optical path length term is unknown but cancels out since a ratio of two concentrations is used to give oxygen saturation.

The set of simultaneous equations is solved using Kramer's method so that the concentration, C, of any one of the absorbing compounds can be expressed as;

$$c = \frac{\Sigma A_n F_n}{\det K} \qquad 1.27$$

where A_λ is the optical density of the ear at wavelength, λ ; F_λ is related to the absorption coefficients of the compounds at the wavelengths used, and det K is the determinant of the matrix given by the absorption coefficients.

Using the concentrations of haemoglobin and oxyhaemoglobin given by this equation, then after some manipulation the oxygen saturation can be expressed as;

$$SO_2 = \frac{K_o + K_n A_n}{M_o + M_n A_n} \qquad 1.28$$

where K_o and M_o allow for constant absorption components and K_λ and M_λ are terms related to the absorption coefficients of the absorbing substances. A_λ is the absorption at wavelength, λ.

Values for K_λ and M_λ were found by measuring the oxygen saturation in 22 volunteers by conventional means, taking 750 data points and determining the values of A_λ and B_λ giving the best fit between the oxygen saturation measured conventionally and using this method. These constants were then permanently stored in computer memory and used for all future calculations. The actual Hewlett Packard oximeter operates on the ear pinna and uses eight wavelengths selected by interference filters mounted on a rotating wheel. Optical fibres are used to "pipe" the light to and from the ear. One advantage of this instrument is its relative insensitivity to transducer movement, a constant problem when performing physiological optical measurements.

1.5.1.3.3 Pulse Oximeters.

Light transmitted through the finger consists of a constant ("DC") level plus a cardiac synchronous ("AC") pulsatile component generally referred to as the photoplethysmogram (PPG) (which is discussed in more detail in Section 1.5.4 and Chapter 7). Of interest in this section is the analysis of these "AC" and "DC" components, that enables the oxygen

saturation of the pulsatile arterial blood responsible for the "AC" signal to be found. This is now generally referred to as pulse oximetry. Commercially available pulse oximeters tend to operate either on the ear or finger.

The basis of pulse oximetry is very similar to that of Wood's oximeter. The largest value of transmitted light, I, is used as a baseline (the "DC" component) with the decrease in transmitted light to level I' (due to the pulsatile ("AC") component) then considered to be totally due to the influx of arterial blood (YOSHIYA (1980, 1983), KONISHI (1976). Analysis of the difference between these light levels allows the oxygen saturation to be found. The similarity between this and the Wood's device can be seen by comparing Figures 1.27 and 1.28.

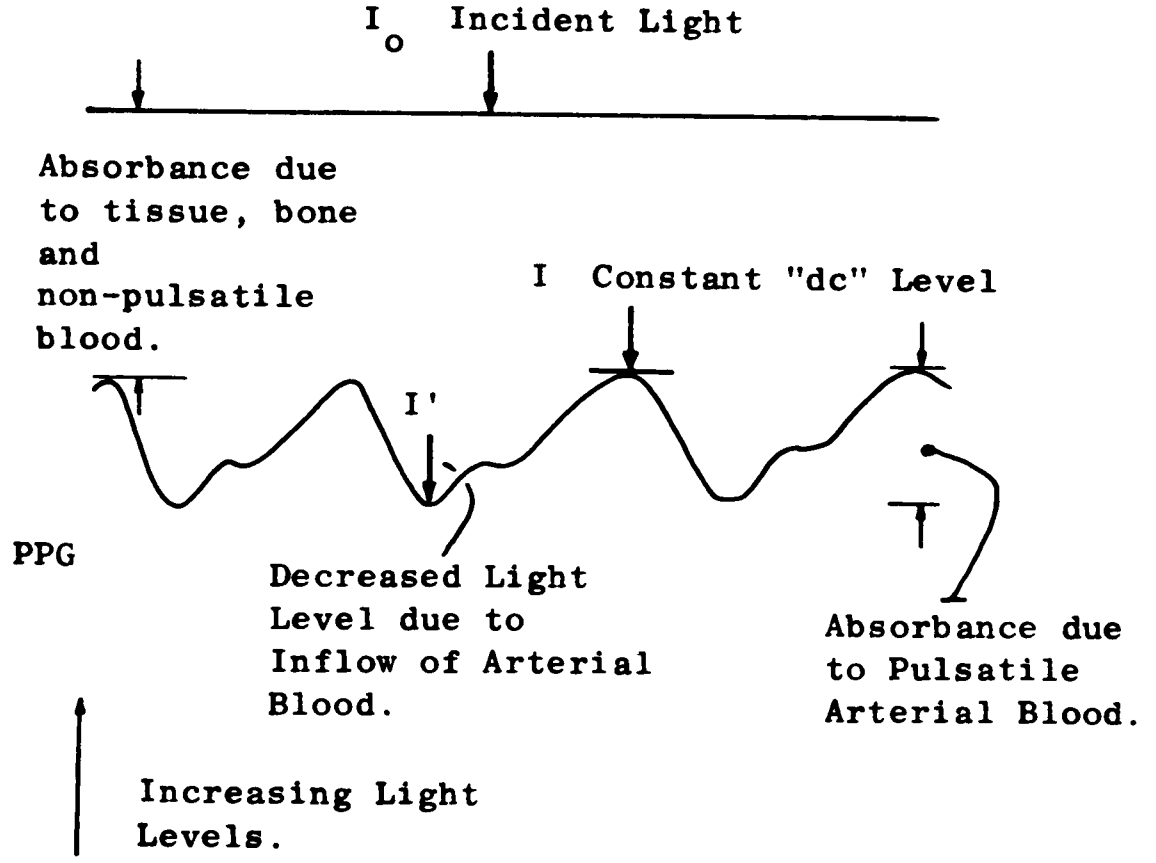

Figure 1.28 Schematic Diagram of the Operation of a Pulse Oximeter.

From Figure 1.28 and comparison with the description of the Wood's oximeter above it can be seen that the OD of the arterial blood is given by equation 1.26 and so use of two wavelengths again allows the oxygen

saturation of this blood to be found and expressed by equation 1.22, or 1.23 if an isobestic point is used. Wavelengths used in this oximeter (manufactured by Minolta) are 650 and 805nm.

In constrast to the Wood's oximeter where the baseline transmission measurement on the bloodless ear was constant this is not the case with pulse oximetry since a continuous measurement of oxygen saturation is being made and therefore the overall transmission of light (the "DC" level) may indeed change, thus altering the baseline. This may lead to errors and is overcome in the Minolta device by using the differential of the absorbance at the two measuring wavelengths (KONISHI (1976)).

Again the Lambert-Beer law appears adequate, although an amendment to how oxygen saturation is calculated has recently been proposed which apparently allows for scattering using the Kubelka-Munk theory. Effectively the square of the optical densities rather than the OD's themselves are used (SHIMADA (1984)).

In addition to the Minolta instrument there is the commercially available Biox pulse oximeter (Ohmeda BOC Health Care) which works on a slightly different principle (WILBER (1983)). The significant difference between these two machines is that whereas the Minolta device uses the (negative) optical density, log (I'/I) (ie log (AC+DC/DC)) of the arterial blood, the Biox instrument uses (I-I'/I) (ie AC/DC), which is in fact the first order approximation of the former term.

This approximation reflects a slightly different means of processing. The Minolta instrument effectively uses the top and bottom of succesive pulses as the light intensities from which the OD is calculated, whereas the Biox instrument continuously samples the PPG (at a rate much faster than the pulse rate) and simply uses successive samples to continually calculate the oxygen saturation. Hence between each sample only a small change in the blood will have occurred, and so a first order approximation is sufficient. (The oxygen saturation of the

incremental amount of blood responsible for the change in blood volume is effectively calculated).

The Biox instrument also has very good resistance to movement artefacts, due to signal processing that weights the calculated oxygen saturation depending upon pulse height and the way in which the oxygen saturation is displayed and updated (WILBER (1983). It uses wavelengths of 660 and 940nm.

Pulse oximeters are intended to measure arterial oxygen saturation since the spectrophotometric measurement should ideally only be made on the pulsating arterial blood solely responsible for the PPG. Whether this is likely to be completely true is discussed in Chapter 7, with the clinical implications of the actual measurements of oxygen saturation covered in Chapter 4. A review of pulse oximetry from a clinical viewpoint together with a clinical evaluation of the method are given by YELDERMAN (1983).

Other potential problems with pulse oximeters exist due to assumptions that the path length is the same for the two wavelengths (ie scattering is the same), that there is no significant change in the depth of tissue with pulsation, and that oxygen consumption by the fingertips is not sufficient to cause significant change in oxygen saturation (see YOSHIYA (1983) and Chapters 4 and 7 for more details).

1.5.1.3.4 Modified Lambert Beer Law.

In Section 1.5.1.2 the problem of measuring oxygen saturation in whole blood due to scattering was outlined, together with references to the application of Twersky's scattering theory as a solution. A combination of the Lambert-Beer law and Twersky's theory has been used (PITTMAN (1975a, 1975b) to develop a technique for monitoring oxygen saturation in the microvasculature (microcapillaries with flowing red blood cells and on microvessels in the hamster cheek pouch) using

transmission spectrophotometry in which the scattering effects are compensated for.

Basically the Lambert-Beer law is used but with the addition of an extra term, S, for scattering. Absorbance, A, is given by:

$$A = \alpha C d + S \qquad 1.29$$

using the same terms as in Equation 1.15, which produces an equation of similar form to that obtained from Twersky's scattering theory.

Use of three wavelengths (two isobestic) enables oxygen saturation to be found whilst also compensating for scattering. This method has been successfully used in microdensitometry (DULING (1983)), using wavelengths at 546 and 520nm (isobestics) and 555nm (measuring), and although developed by PITTMAN (1975a) exclusively for transmission work has also been used in reflection mode on the retinal vessels (DELORI (1982)).

1.5.1.4 In vivo Reflection Measurements on Whole Blood Using Catheterization.

Oxygen saturation can be found *in vitro* from the light backscattered from whole blood as described in Section 1.5.1.2. The same technique can also be applied *in vivo* on the blood in major vessels, or indeed the heart using catheterization, to enable the light to be piped into the body with optical fibres (POLAYNI (1962)). Alternatively solid state devices can be mounted on the end of a catheter (JOHNSON (1971)) which is then inserted.

As with other spectroscopic mehods of oxygen saturation determination two wavelengths are used (one being an isobestic) which in this technique also allows corrections to be made for artefacts such as those due to pulsation of the blood and changes in hematocrit.

Oxygen saturation is given by the following relation:

$$SO_2 = \frac{A\,R_{ir} - B}{R_r} \qquad 1.30$$

where A and B are constants and R is the intensity of the reflection at an IR (ir) and a red (r) wavelength. The formula has been established experimentally and explained theoretically including using an extension of RODRIGO'S (1953) application of Schuster's radiative transfer theory (POLAYNI (1960, 1962, 1972), ENSON (1962)).

PDT as described in Section 1.5.1.2 can also be applied to the design of in vivo catheter oximetrs (eg ZDROJKOWSKI (1970) from POLAYNI (1962)) whilst LIN (1974) uses Mie scattering theory. Further details and thoughts on the method are given by MOOK (1968), JOHNSON (1974) and PAYNE and HILL (Chaps 23-25, 1975) the latter also including a description of the clinical use of the device (see also GAMBLE (1965) and WILKINSON (1979)). JANNSEN (1972) also contributed to the field by describing how careful arrangement of the fibre ends could be used to overcome artifactual problems, while HAASE (1980) describes an in vivo catheter oximeter also capable of monitoring blood pressure and pulse rate.

In addition to monitoring oxygen saturation the technique can also be used for dye dilution studies used to monitor cardiac output. Here a bolus of dye is introduced into the circulation and its progress and dispersion then monitored spectroscopically (SUTTERER (1972), POLAYNI (1972)). The same type of studies can also be performed non-invasively using transmission measurements on the ear (eg JANSSEN (1972)).

1.5.1.5 In vivo Reflection Measurements from Tissue.

Early attempts at monitoring oxygen saturation using skin reflectance measurements are reviewed by ZILJSTRA (1953), NILSSON (1960), YOSHIYA (1983), TAKATINI (1978). The early devices such as Brinkman's haemoreflector only used one wavelength (although later extended to two)

and suffered from lack of suitable instrumentation, both in terms of light emitters, detectors and for signal processing.

In the early 1970's COHEN (1972) produced a skin reflectance oximeter using light emitting diodes, however the problem with such devices is in producing quantitative rather than qualitative relationships with oxygen saturation. Since this time a group at Case Western Reserve University (Cleveland, USA) have made several efforts to produce such a device. LAING (1975) describes measurements on choroidal tissue whilst CHEUNG (1977) developed a five wavelength device for use on the skin surface, with TAKATINI (1979, 1980, 1978) extending this work and introducing a theoretical analysis in 3-D using PDT. The group have also applied KMT to the problem (MENDELSON (1983a)).

The above reflectance devices all use steady ("DC") levels of light reflected from tissue for analysis, but the same group have also suggested using the pulsatile component of the reflected light to determine oxygen saturation (MENDELSON (1983b, 1983c)). This would appear to be related to the pulse oximeters described in Section 1.5.1.3. However, in the reflection device only the pulsatile component of the signal is used to calculate the oxygen saturation, which has been found to be proportional to the ratio of the magnitude of the pulsatile component of light reflected from the finger at two wavelengths.

This type of relationship is of similar form to that used to calculate the oxygen saturation in catheter oximeters (equation 1.30, Section 1.5.1.4) except that in these the whole level of reflected light is used. In addition there is a significant difference between the two types of device in that an increase in the oxygen saturation is related to an increase in theIR/R signal ratio for the catheter oximeter but a decrease in this signal ratio for the skin reflectance device. This represents a fundamental difference in the operation of the two instruments which is discussed in Chapter 7, where a possible explanation

of the reflectance results is given.

Other reflection measurements of oxygen saturation have been performed by SATO (1981) and D.W. LUBBERS and colleagues (LUBBERS (1973,1975), FRANK (1984)) Both workers take complete spectral scans of the tissue and analyse the way in which they vary with changing physiological status, and have extensively used these methods to study not only the oxygen saturation but also the redox states of the cytochromes (see Section 4.8).

Much of Lubbers work in the area of oxygen saturation monitoring involves the use of his qualitative analysis which involve "transferring" the in vitro spectra into that obtained in vivo using the method briefly described in Section 1.4.3.4.

1.5.2 Bilirubinometry.

Bilirubinometry is the measurement of serum bilirubin levels using skin reflectance. One reason for the interest in this technique is its application to paediatrics since neonates are often unable to conjugate and excrete bilirubin (a breakdown product of protoporphyrin) which consequently accumulates in the circulation and tissues. Measurement of these levels of serum bilirubin is important because excessive amounts can lead to severe central nervous system damage (referred to as kernicterus).

Because of its structure (see Section 1.4.1) bilirubin is light absorbing (LEE (1976), AMAZON (1981)) and therefore its concentration can be measured spectrophotometrically, which indeed can, and is, performed on blood samples. The absorbance spectrum was shown in Figure 1.9.

The presence of bilirubin can be seen *in vivo* as a yellowish tinge to the skin, known as jaundice, a condition which was generally diagnosed visually, often with the aid of "tinctometers" and other colour matching devices. Since jaundice is visibly detectable then clearly it should be possible to develop an instrument to perform this task. This is the other reason for the interest in bilirubinometry since like oximetry it is an optical method which has been proven to be clinically applicable with a commercial instrument available. Lessons learnt from its development may be applied to other similar techniques.

In the development of a bilirubinometer HANNEMAN (1978) used a spectrophotometer with fibre-optic probe to measure neonatal skin reflectance spectra over the range 400-750nm, (such spectra actually depend chiefly on tissue and not serum bilirubin levels and these two may differ significantly). The spectra were then analysed empirically in 5nm bands to determine the best fit between the reflectance data and serum levels measured conventionally. Use of data from five of the 5nm "bins" gave the best fit, with two of these associated with the bilirubin

associated with the bilirubin absorption spectra and the other three considered to be correction factors for artefacts such as absorption by haemoglobin, despite the attempts to overcome this problem by applying pressure to displace surface blood.

The idea of producing an optical instrument for monitoring serum bilirubin levels was taken up by YAMANOUCHI (1980, 1983) and a commercial device ultimately produced by the Minolta company. It is a two wavelength device shown in Figure 1.29. The probe end is placed on the neonate's skin and gently pressed which displaces surface blood and then causes a flashlamp to discharge. The intensities of reflected light at the two wavelengths are used to determine serum bilirubin levels with the theoretical basis derived from the Lambert-Beer law (YAMANOUCHI (1983)).

An alternative attempt to theoretically describe bilirubinometry was made by HANNEMAN (1979) using the Kubelka Munk theory, and is described in a paper concerned with the interference of skin colour on the method. This is potentially a major problem and many of the clinical assessments of the Minolta transcutaneous bilirubinometer have addressed themselves to the effect of widely varying skin colours particularly as only two measuring wavelengths are used (HANNEMAN (1982), HEGYI (1981a)).

In conclusion, the relatively recent development of a transcutaneous bilirubinometer can serve as a model concerning the clinical use of optical methods in general. The initial empirical observations which seemed to suggest such a technique was feasible, was followed by spectrophotometric measurements, then the development of mathematical models to describe and analyse the reflectance spectra, and finally the production of a commercial instrument. This was subsequently thoroughly tested with investigations to determine its possible shortcomings (ie interference of other skin pigments), its use as a monitor for other studies (the spread of dermal icterus (HEGYI (1981b))) and finally the question of what the actual device is measuring (ie what do the figures

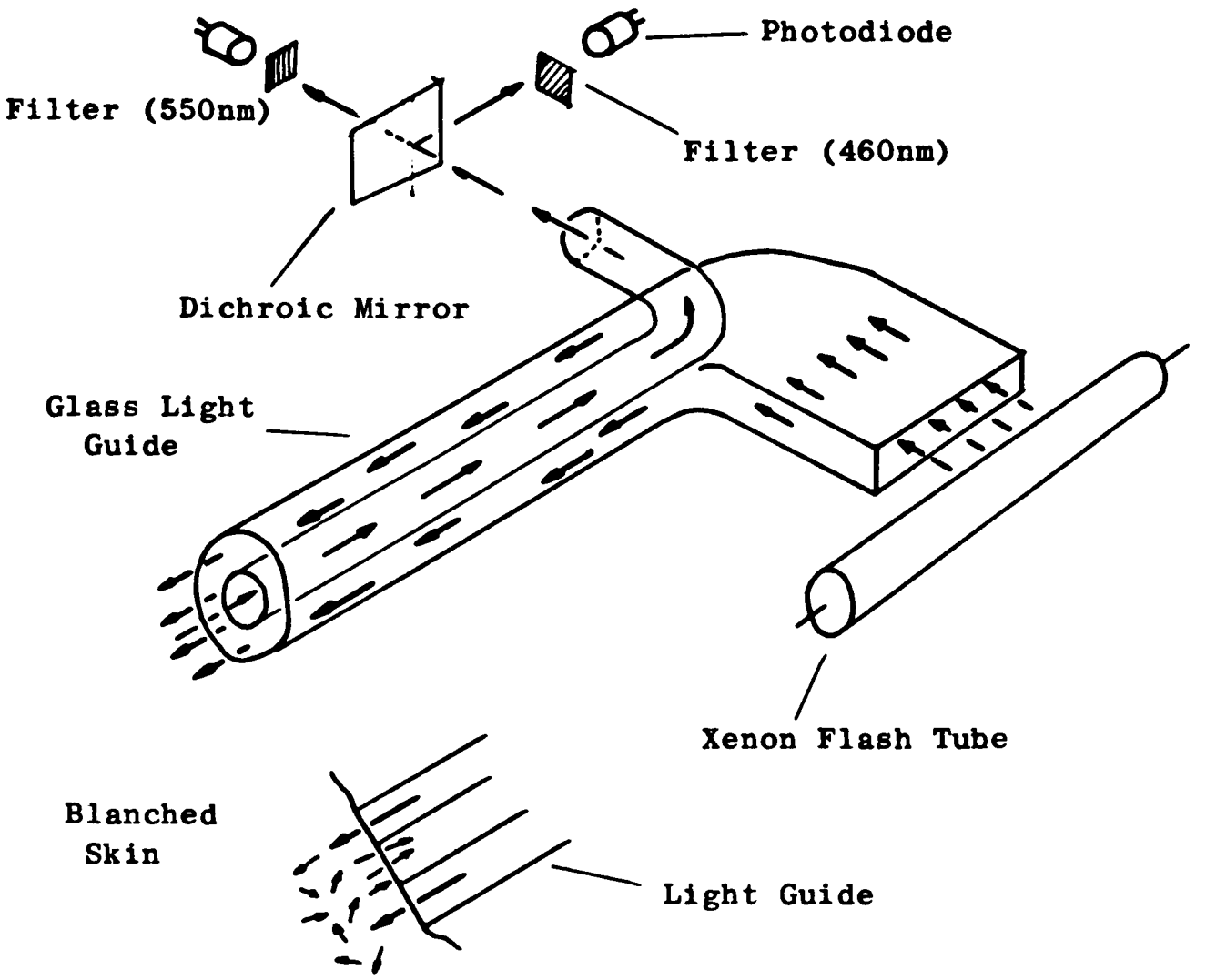

Figure 1.29 Schematic illustration of the transcutaneous bilirubinomter (from YAMANOUCHI (1980)).

mean) and how they should be used clinically. In addition there is the evidence that although optical methods may be thought of as being non-invasive, they clearly are not because of the effectiveness of the incident light from either sunlight or a phototherapy unit in assisting in the breakdown of bilirubin (McDONAGH (1980)). Considering future developments (ENGEL (1982)) to the bilirubinometer perhaps a multi wavelength version would assist in removing any remaining artefacts.

1.5.3 Sundry Optical Reflectance Methods.

Oximetry and bilirubinometry are probably the two most obvious examples of the use of reflectance spectra to perform *in vivo* clinical measurements. However, other reflectance methods have been suggested and these are described in this section, which is concluded with transillumination techniques that are already used.

Firstly it is perhaps worth noting that in the broadest sense the most widely used optical reflectance method is that of judging a person's general state of health by their "colour". For this reason the actual standard (spectral properties and intensity) of lighting in hospitals and surgeries is actually quite important. Dermatologists often rely upon visual assessment of skin colour, when examining the reddening of the skin after allergic tests have been performed by fixing the allergen in contact with the skin for a prolonged length of time.

What amounts to being simply the redness of the skin has been extensively studied by the reflectance from various sites on the body and under different conditions of a HeNe laser (SINGH (1981, 1982), CHITRA (1983)). It was found that reflectance varied with skin pigmentation, blood flow, composition of tissues and difference in density and hydration.

AFROMOWITZ (1979, 1983) has used the reflectance levels of green, red and near-IR light to assess the degree of skin damage caused by burns. It is suggested that the change in reflectance is associated with changes in the structure of skin proteins caused by heat and that such measurements could help in determing the viability of burnt skin or if plastic surgery is required. The earlier this decision is taken then the greater the likely success of the operation, which must be weighed against the chance of the burnt skin recovering.

The results in Figure 1.14 indicate the feasibility of measuring water and fat content *in vivo* using near-IR reflectance ("interactance",

CONWAY (1984)). It has already been suggested it may be possible to monitor pH and electrolyte status from their effect on the water absorption band, whilst this and the haemoglobin band could enable haematocrit to be determined (M.D.W (1986)). Clearly the area of the near-IR reflectance, where there are no large absorbing compounds could become an important region for non-invasive in vivo monitoring.

Reflectance measurements have also been performed on the eardrum (HEEKE (1982), throat (OHYOMA (1982) and gums (GEISER (1982) and used to assess neonatal maturity (KRAUSS (1976)). Finally, for completeness, studies to measure the translucent properties of the skin (HARGENS (1980)) and also its refractive index (PUGLIESE (1980)), both in vivo, should also be mentioned.

Although primarily dealing with reflectance methods, this section is an appropriate place to describe several clinically used transillumination methods. The location of breast tumours using transillumination, known as diaphonography, (WATMOUGH (1983)) has been investigated, although the problems of scattering discussed in Section 1.4.3 compromise definition and restrict the thickness of the sample, meaning the breast must usually be gently compressed before being studied. A new instrument using two wavelengths (one in the near-IR) to compensate for scattering has been reported (M.D.W (1986)) but as yet there appears to be no clinical evaluation of it. In a review of all methods used for breast imaging, KOPANS (1984) states "transillumination techniques should be considered experimental". He also says that there is no well documented evidence that the technique at present has a role to play in scanning, although in the future with suitable sources, detectors and processing an instrument capable of performing this role may be produced.

Within neonatal paediatrics transillumination finds several uses (PHILIP (1982)), partly due to the thinner sections of tissue which are

dealt with. They include the detection of hydrocephalus where the application of a torch to the side of the head causes the fluid filled skull to "light" up (SWICK (1976)), for the location of arteries and veins in the arm for administering injections and in the diagnosis of pneumothoraces.

1.5.4 Measurement of the Redox State of Cytochrome oxidase.

A relatively new technique which is considered extensively in Chapter 4 is monitoring the redox state of the terminal enzyme of the mammalian respiratory chain, cytochrome oxidase (cyt aa_3). This can apparently give information about oxygen sufficiency at an intracellular level (or viewed in other terms about metabobolic rate).

The method is similar to oximetry in that it requires a small absorbance change to be monitored on top of a large background attenuation. The interest is in using this technique non-invasively which means it is a redox state dependent absorbance band in the near-IR that the enzyme posses, upon which measurements are made.

To monitor cytochrome oxidase redox state non-invasively both oxygen saturation and changes in blood volume must also be monitored due to their potential interference thus there are strong links between this technique and oximetry. The method is extensively covered in Chapter 4.

1.5.5 Fluorescence Measurements.

Fluorescence (and phosphorescence) measurements (see Section 1.3.1.2) may involve either monitoring the fluorescent yield or the effect of quenching agents on the decay time (lifetime) of the fluorescence. Consequently the technique can be applied to monitor the state or concentration of either fluorescing compounds or quenching agents, which themselves may be either endogenous or exogenous.

Before spectrophotometric measurements of the redox state of cytochrome oxidase (previous section) were performed the rate of cellular metabolism was monitored using fluorescent measurements of nicotinamide adenine dinucleotide (NADH). NADH is the component which feeds electrons into the respiratory chain, also by alternately accepting / donating electrons and thus changing its redox state (see Chapter 4). Since it fluoresces over the range 450-480nm when reduced (NADH), but does not when oxidised (NAD+) then its redox state can be monitored by fluorescence measurements (the absorption spectra was given in Figure 1.12).

A review of monitoring brain NADH redox state using this technique is given by MAYVESKY (1984), whilst RENAULT (1982) describes a laser fluorimeter for performing such measurments to study cardiac metabolism. He has also considered the use of double beam fluorimetry to try and overcome the constant problem with optical methods of interference due to blood (RENAULT (1984)), which was previously addressed by KRAMER (1979) who considered the problem of movement, hemodynamic (blood volume) and oximetric (changes in oxygen saturation) artefacts when monitoring fluorescence from the cerebral cortex. An instrument for monitoring both spectrophotometric changes (eg hemoproteins) and fluorescence (eg flavins and NADH) is described by HASSINEN (1982). Due to the links between this technique and monitoring the redox state of cytochrome oxidase certain aspects will be considered in more detail in Chapter 4.

The uses of non-naturally occuring fluorescent compounds include the introduction of pyrenebutyric acid (PBA) which enables oxygen concentration to be monitored since the latter is a powerful quenching agent and therefore the degree of quenching gives an indication of oxygen concentration (MITNICK and JOBSIS (1976)). Another such compound is fluoroscein which is widely used in opthamology to study variables such as the rate of transport of fluid within the transparent structures of the eye (JONES (1979), and also look for micro-ulcers in the eye (SILVER (1985)).

Haematoporphyrin derivative (HPD) can also be introduced into the body where it is taken up preferentially by tumour cells. Since it fluoresces from about 620-690nm when excited by light of around 405nm it can be used to detect such cells (KINSEY (1980)). (In addition its activation by HeNe light (628 nm) leads to the production of free radicals and subsequent destruction of these cells). A variety of fluorescent compounds are also widely used in the construction of fibre optic sensors (see Section 1.5.10).

1.5.6 Photoplethysmography.

Photoplethysmography has been extensively reviewed (CHALLONER (1976)) with the field split into "DC" and "AC" photoplethysmography, the latter being involved with the study of the cardiac synchronous component of reflected or transmitted light from various sites on the body.

As part of the research for this thesis an instrument was constructed to enable the "AC" photoplethysmogram (the PPG) to be studied and so the topic is extensively covered in Chapter 7. Suffice to say that in its various forms the technique has been used to study skin blood flow (the most common use), pulse wave transit time and myocardial

contractility.

1.5.7 Glucose Measurement.

The previous six techniques (except fluorimetry) have relied upon monitoring small changes in the attenuation of reflected or transmitted light *in vivo*, and therefore have much in common with the work described in later chapters. Some of the remaining methods in this section rely upon different modes of interaction of light with matter or have less directly in common with the remainder of the thesis, and therefore are included for completeness since they may in some way eventually prove useful to techniques such as *in vivo* near-IR spectroscopy.

Several optical methods for measuring glucose concentration *in vivo* have been proposed, in addition to those already used *in vitro*, and it therefore seems pertinent to consider this topic in a section of its own. The reason for monitoring glucose concentration is because of its use in the care and control of diabetes mellitus, a metabolic disorder due to disturbance of the normal insulin mechanism. A consequence of diabetes is wildly and widely fluctuating blood glucose levels, the stabilization of which (at present by administering insulin) is the aim of treatment. Hence the need to monitor blood glucose concentrations, which can be found from blood samples but do not then provide a continuous glucose profile.

The optical methods described below could all provide continuous measurements and therefore be used to obtain complete profiles of daily glucose concentration, or even as the sensor in a closed loop insulin dispensing system. This would enable tighter glucose control and hence better treatment than is possible using either injections or even a continuous infusion pump.

Three properties of glucose solutions enable their concentration to be monitored optically; their IR spectra and the fact that their optical activity and refractive index are concentration dependent.

1.5.7.1 IR Spectrophotometry.

With the arrival of lasers operating in the IR the spectroscopic analysis of biological samples became possible as the high power outputs available were sufficient to overcome the large attenuation by such samples due to the presence of water.

Consequently IR laser spectroscopy could be applied to the measurement of physiologically important substances. Moreover, use of attenuated total reflectance (ATR) spectroscopy, in which an ATR prism is placed on the surface of the skin, apparently enables IR spectroscopy to be performed non-invasively, with the measurement being made on the boundary layer of the skin due to interaction with the evanescent wave (KAISER (1979), ARAI (1985)). The ATR technique also places less thermal load on the sample. Glucose is one of the substances whose concentration it has been suggested may be measured non-invasively in this manner, with a CO_2 laser operating at about 9000-10000nm as the source (KAISER (1979)).

1.5.7.2 Polarimetry.

Measuring the optical rotatory power of sugar solutions is a standard way of determining concentrations in vitro, and it has been proposed that the same technique may also be applied in vivo using the aqueous humour within the eye as the "sample" (RABINOVITCH (1982), MARCH (1982)). The proposal was to attach a solid state laser diode and detector to a scleral contact lens which could be placed on the eye with the glucose concentration of the aqueous humour then measured. The inclusion of a telemetry system was also suggested to provide feedback

from the sensor to an insulin pump.

Apart from the obvious engineering problems to be overcome there are also the questions of the selectivity of such polarimetric measurements, due to the presence in the aqueous humour of other optically active substances, and the sensitivity of the method, which have both been considered (GOUGH (1982), RABINOVITCH (1982)).

An alternative strategy for measuring the concentration of blood glucose using polarimetry is simply to use part of the body relatively transparent to light, such as the ear lobe, as the "sample cell" (MULLER (1979)). This approach is progressing with apparently successful results (MULLER, Private Communication) despite the fact that it might be expected that the plane polarization state of the incident beam would be lost due to multiple scattering as the light propagates through the sample in question.

1.5.7.3 Refractive Index Changes.

Along with the optical activity of sugar solutions being dependent upon concentration so is their refractive index. Hence the amount of light coupled at a glass/glucose solution interface into the liquid will be dependent upon their relative refractive indices, and so variations in the amount of coupled light can be used to monitor the refractive index of the solution and so its concentration. Such a technique, in which the amount of light lost from an optical fibre surrounded by a glucose solution is used to measure concentration, has been demonstrated in vitro (ROSS (1985)).

Finally colourimetric methods are used as standard practice to monitor urine glucose content by dipsticks whose colour is dependent upon glucose concentration (due to the composition of their coating).

1.5.8 Scattering Studies.

The underlying physical principles of scattering studies were outlined in Section 1.3.3. Virtually all such studies (BERNE (1976)) are performed *in vitro* on widely dispersed systems such as macromolecules, and so single scattering theories (see Section 1.4.3.1) can be used to describe the nature of the scattering.

The most popular technique for investigating biological samples is quasielastic light scattering (QLS) using light beating spectroscopy (CUMMINS (1970)) to detect the small (about a few kHz) shifts in frequency of the scattered light. QLS can be used to measure directly the dynamic properties (eg translational and rotational diffusion coefficients) of macromolecules in solution, and to study the molecular weights of large molecules and viruses, aggregation and polydispersity. The technique has been extensively reported and reviewed (PECORA (1972), BLOOMFIELD (1981), McCONNELL (1981), SATELLE (1982)).

Scattering studies have also been suggested as a means of determining pH since this affects the shape of erythrocytes (REYNOLDS (1983b)), of caterogizing microparticles and biological cells (KAYE 1982)) and also for measuring the refractive index of cells (ie refractive index matching (BARER (1954)).

All of the above are *in vitro* techniques, however one application of QLS has found widespread use *in vivo*, namely laser Doppler velocimetry (LDV) which can be used to measure the velocity of moving particles and was initially used *in vivo* in much the same way to determine the velocity of blood cells in arteries (TANAKA (1974)).

Since then LDV has been applied transcutaneously using a HeNe laser used to illuminate the skin surface through an optical fibre, with Doppler shifted light scattered from the red blood cells then detected at the surface of a photodetector by beating the light with a non-Doppler shifted beam . It is in this form (NILSSON (1980)) that LDV has been

widely used in both clinical and research applications (COCHRANE (1986)).

There is continuing interest in this area concerning the use of different types of sources, at different wavelengths and the precise contribution of Doppler shifted light to the overall signal (DE MUL (1984), GUSH (1984), BOGGETT (1985)).

1.5.9 The Use of Lasers.

The use of lasers in itself is not strictly an "optical method" in the context of this thesis, since no light is necessarily detected. However, due to their now widespread use both in the biological sciences and in a clinical enviroment the inclusion of this section is considered appropriate.

Lasers emit coherent, polarised and highly monochromatic and (usually) collimated light which if required can often have extremely high intensity. They are available over most of the visible and near-IR spectrum and often available in either pulsed or continuous wave (cw) mode.

Typical clinical uses of lasers include opthamology for a variety of purposes (eg fixing detached retinas), dermatology (eg removal of portwine birthmarks and tattoos), surgery (carbon dioxide lasers (10.6 um) used as scalpels and phototherapy (eg activation of HPD to produce free radicals to destroy cancer cells by HeNe laser (628 nm)). A further description of the use of lasers in the biological sciences and medicine can be found in the following reviews (ARNDT (1983), ANDERS (1982), LETOKHOV (1985), McKENZIE (1984)).

There are also now commercially available instruments containing HeNe lasers and GaAlAs laser diodes available which can apparently be used for theraputic purposes. (Ormed, Italy; CBL Optronics, Italy;

Felas Medical Lasers, W. Germany; Acetec, France).

Some laser devices for dermatological applications aim to make specific use of wavelengths at the maximum absorbances of haemoglobin and tattoo pigments for the removal of port wine stains and tattoos respectively. Quite whether such specific wavelength ranges are required is brought into question by the application of a technically much simpler (and cheaper) device which can remove tattoos extremely effectively (COLVER (1985), (1986)). The instrument consists of a tungsten halogen (broad band) lamp, gold coated reflector and quartz rod to guide light to the skin, with a sapphire tip to transmit the light but conduct surface heat from the skin after application of the light.

The "Infra-Red Coagulator" (MBB-AT Technologie, Munich, W. Germany) as it is named, was designed for the thermal coagulation of blood in operations such as liver transplants, however its application to dermatology, with its demonstrated ability to remove tattos effectively is considered particularly interesting.

1.5.10 Monte Carlo Methods.

When the absorption and/or scattering coefficients of biological tissues are known then it may be possible to calculate the reflectance or transmittance characteristics of these samples by using one of the theoretical methods such as Photon Diffusion Theory (PDT), the Kubelka Munk theory (KMT) or the Lambert-Beer law, which have been described above (Section 1.4.3).

These techniques are however limited to the specific uses for which they have tended to be developed and even between them by no means offer a complete description of light propagation in biological samples. Indeed for non-homogenous tissues in which both scattering and absorption

are equally important they are far from adequate.

An alternative means of calculating the optical characteristics of biological samples is to use a Monte-Carlo model. With this method the experimentally derived probabilities for photon absorption and scattering are used to predict the likely course of individual photons entering the sample. By considering a large number of such individual photons and averaging their collective fates an approximation of the overall characteristics of the sample can be estimated. Such a technique is basically statistical, hence the name.

The Monte Carlo method was first developed to study neutron scattering and a general description of the technique is given by McCRACKEN (1955). It has since been applied to many problems otherwise too complex to solve and in the last few years has been used to study the propagation of light through tissue. (Other Monte Carlo models are extensively used to solve problems in other fields).

The method has been used (MAAREK (1982, 1984)) for this purpose, to model the propagation of light through various biological samples including blood. The parameters used in this work were the cumulative probability distributions for the mean free paths of the distance travelled by a photon before its next scattering event, and the direction in which the mean free path will be. Also the absorption probability coefficient to determine whether or not a photon will be absorbed at any one collision is required. The values used were either found by experiment, or derived from the work of ZDROJKOWSKI (1970) (see Section 1.4.3.3).

In addition to calculating the reflectance and transmittance properties of the samples the Monte-Carlo method has also been used by this group to model the propagation of ultrashort light pulses through tissue (with respect to time). Their results have been used in conjunction with their own experimental evidence (JARRY (1984)) to

consider the possibilities of imaging thick biological samples with light using a collimated light source and the spatial and / or temporal (hence the need to model pulse propagation) discrimination of emergent photons (MAAREK (1985b)).

Their interest in imaging stems from work they are also performing similar to that of Jobsis (see Chapter 4) on monitoring the redox state of cytochromes. If the two areas of work could be connected then it may be possible to obtain images showing regions of high or low oxygen saturation, (via cytochrome oxidase redox state, and changes in blood volume.

The Monte-Carlo method has also been independently used to model the absorption and flux distribution of light in tissue (WILSON (1983, 1985)) in order to help determine appropriate dosage in photoradiation therapy (PRT). This topic has been studied both experimentally and theoretically (SVAASAND (1983)) but such theoretical treatment has primarily been concerned with the situation where either scattering or absorption are dominant. The Monte-Carlo technique allows both scattering and absorption processes to contribute equally to the optical properties of tissue.

This application of the Monte Carlo method is fundamentally similar to that described above, although it is chiefly concerned with modelling the energy distribution of the light within the tissue due to absorption processes, which calls for a slightly different approach.

In summary it is clear that the theoretical models of the optical characteristics of biological samples (such as KM theory, PDT and the Lambert-Beer law) described earlier in the introduction have certain limitations. This is largely due to the complex nature of the interaction of light with tissue. However, an alternative means of theoretically determining these characteristics may be to apply the Monte-Carlo method for which the absorption and scattering coefficients

of the tissue must be known.

A major limitation of the method at present is the lack of widely available data giving the values of these coefficients, and therefore also the associated question of how similar these constants are from sample to sample.

1.5.11 Photography.

Photography, undoubtedly an optical method, essentially consists of the recording of intensity variations (possibly with spectral filtering) with spatial discrimination.

Within clinical medicine straightforward photography is often used to record the physical status of parts of a patient's anatomy. Here the reflectance characteristics of skin are important since certain aspects may need to be enhanced by choice of flashlamp "colour" or the use of spectral filters.

As distinct from recording normally visible features from a patient, infrared photography as it is known (or near-IR using the terminology of this thesis since the film is sensitive in the visible and near-IR ranges to about 900nm and is used in conjunction with a high pass filter thus blocking light below about 700nm) enables normally non-visible structures, most noticeably the pattern of the venous system, to be seen. The general use of IR photography is covered in KODAK (1977).

It has been considered as a means of studying the female breast vasculature as an aid in cancer diagnosis (ROSENBLOOM (1953)), and also to study the postprandial intensification of venous pattern (GIBSON (1961, 1964)). The reason the veins (which appear darker) are visible is because they absorb even more light than the rest of the tissue surface which tends to reflect light in this region relatively strongly (see Figure 1.13).

The application of IR photography demonstrates the difference

between this type of measurement and that described in Section 1.4.2, namely that the spatial variation of spectral information is obtained rather than simply the spectral details themselves. With this in mind perhaps photography of the skin over narrow spectral ranges (ie a study of spatial and spectral characteristics of skin reflectance) would reveal previouly unnoticed insights into the anatomy at and just below the skin surface.

Considering photographyas a combination of intensity and spatial optical measurements then other techniques also fall into this category. Flying spot methods (similar in operation to a television) have been used to obtain spatial information of oxygen saturation and fluorescence.

Measurements of retinal venous blood oxygen saturation in humans have also been made using photographs taken with pairs of filters (red and green, and red and near-IR) (HICKHAM (1963)). In addition photographic methods have been used to study the cutaneous microrelief (CORCUFF (1982)) and skin surface texture (MARSHALL (1982)).

1.5.12 Optical Fibre Sensors.

This type of device offers great potential for monitoring both in industry and medicine, since the "sensor" is relatively inert and requires no electrical connections overcoming many safety and "noise" problems. The term optical fibre sensor is used here to imply that there is a "sensor" on the end of a fibre (or fibre bundle), although it is sometimes used to also refer to catheter oximeters (Section 1.5.1.4).

Fibre sensors can broadly be split into two types; physical and chemical. Physical sensors which are reviewed by PETERSON (1984) can be used to monitor the variables: temperature, pressure and even radiation, whilst a variety of chemical sensors reviewed again by PETERSON (1984), NYLANDER (1985), TROMBERG (1984) have been constructed.

The chemical sensors generally operate by measuring either the

reflectance or fluoresence from the reagent in the "sensor", which will be dependent upon the quantity to be measured, with light shone down onto and then reflected back from the "sensor" itself. In such sensors the optical design is relatively straightforward and it is the chemical and physical design and construction of the "sensor" cell which requires most effort to obtain reliable, accurate and a stable senors with fast response times.

Operating in a slightly different manner are sensors which rely upon the compound to be measured interacting with the treated surface of an unclad fibre and thus affecting the total internal reflectance (not unlike the refractive index glucose sensor, Section 1.5.7.3). This technique is now being used to measure antibody concentraion since fibres can be coated with the appropriate antigen with subsequent binding affecting the optical characteristics at the fibre boundary. (NYALANDER (1982, 1983)).

1.6 Advantages and Disadvantages of Optical Methods for in vivo Monitoring.

One of the major advantages of optical methods for in vivo monitoring is their non-invasive nature (except for the passage of photons as noted in the Introduction). Another is the option of using fibre optic bundles (see Section 3.2.4) to "pipe" light to and from the surface of the body, which not only leads to a versatile device in terms of measurement site, but also has the advantages, of electrical isolation and em noise immunity. A similar degree of versatility can be obtained by the use of small semiconductor electro-optic devices.

Further advantages of non-invasive in vivo optical techniques are that they do not suffer from the inherent degredation or contamination problems which electrochemical or enzyme based sensors are prone to. Their component costs are also not prohibitively high.

Although not strictly an advantage, the continued development of novel and improved semiconductor devices (such as laser diodes and photodiode arrays) is likely to enhance the performance of existing optical methods The transfer of techniques from areas of the analytical chemistry and biochemistry to in vivo optical applications is also likely to have a similar effect.

As far as the disadvantages of in vivo optical methods are concerned they share the common problem with other types of sensor of specificity of measurement due to interference from other compounds. There are also potential problems from the unwanted detection of ambient light which may require the use of appropriate light source modulation and signal processing and/or shrouding of the area under investigation. In addition reflectance measurements in particular are prone to movement artefacts, usually due to small changes in detector-sample-source geometry.

A difficulty with optical methods, as seen from Section 1.4.3, is in describing theoretically their precise behaviour. This can lead to

problems concerning the ideal processing of the detected signals, and may also complicate transducer design.

Finally, there is the safety of optical methods to consider as with these techniques photons must pass through the body. Although it is unlikely that sources capable of causing gross tissue damage would be used, those sources actually employed in in vivo monitors could lead to severe eye damage through inadvertent use (SLINEY (1980)). This is particularily so with near-IR sources whose outputs are not visible.

In addition there is the possible effect of physiological and biochemical changes being produced by low level light irradiation (GREGUSS (1984), ROCHKIND (1986)). This has in fact lead to several companies producing therapeutic laser systems using HeNe continuous wave (cw) lasers (which apparently also produce shape changes and haemolysis in erythrocytes (SINGH (1984))), and pulsed GaAlAs laser diodes (904nm) (see Section 1.5.9). These instruments are claimed to be suitable for a wide range of uses and treatments.

That photochemical effects can be produced by such irradiation is shown by the use of phototherapy for the treatment of neonates suffering from jaundice, and the known daily rhythm of certain mammalian hormone productions (TAMARKIN (1985)).

In conclusion optical methods are considered to be particularily applicable to non-invasive in vivo monitoring, although the possibility of the necessary irradiation producing (albeit probably small) biochemical and physiological effects should be borne in mind.

1.7 Brief Description of Thesis Contents.

In Chapter 2, studies performed with a low light level camera are described, their purpose being to investigate the overall light transmission and reflectance characteristics of tissue.

This is followed, in Chapter 3, by a description of the instrumentation used to perform the experiments presented in the thesis, including the microcomputer controlled scanning spectrophotometer which was constructed.

Chapter 4 deals with the feasibility of monitoring the redox state of cytochrome oxidase non-invasively. It contains the results of experiments performed on purified cytochrome oxidase and yeast cells, and a description of these results in terms of a mathematical model. This is then used as a basis of a possible explanation for the apparent lowering of the affinity of cytochrome oxidase for oxygen in vivo.

Chapter 5 is a consequence of the preceding chapter. It addresses the possibility that the disease states which the type of monitoring described in Chapter 4 may help to prevent, are in fact due to oxidative damage, the rate of which can be enhanced or decreased by several factors.

In Chapter 6 the results of *in vivo* reflection and transmission measurements, made with the scanning spectrophotometer are presented, and discussed.

An instrument capable of recording and producing traces of the PPG from different sites and using different wavelength light is described in Chapter 7. Preliminary results obtained using this instrument and the conclusions drawn from them are also presented.

A summary of the whole thesis is given in Chapter 8.

Chapter 2: Photography of Transilluminated Tissues Using an Image Intensifier.

2.1 Introduction and Aims.

That some light is transmitted through tissue can readily be seen by looking at the hand, finger or ear pinna against a light source. This fact was covered in Section 1.4.2.2 including a description of the gross transmittance of biological samples.

Considering the above it was felt that by using a sufficiently sensitive camera it should be possible to photograph the light emerging from tissue during transillumination. Such photographs would give information concerning the position and intensity of emergent light simultaneously as distinct from simply intensity information provided by studies such as those in Chapter 6. With the anatomy of the photographed tissues known, the photographs could be analysed in an attempt to interpret which structures had significantly affected the course of the light through the sample. The effect of wavelength on the photographs could be examined by the use of appropriate spectral filters. In addition the intense backscattering of light from tissue could also be photographed.

These studies are particularily pertinent to the use of *in vivo* optical methods, since the primary requirement of any such technique is to be able to shine light into the tissue and then detect it after either transmission or backscattering ("reflection").

2.2 The Image Intensifier and Other Equipment Used.

2.2.1 Intensifier and Camera.

To obtain sufficient sensitivity to detect the low levels of light emerging from the body an image intensifier was required. The device used was a Hamamatsu "Night Viewer" (Model C1525) which can be used for viewing at extremely low light levels (eg starlight) and has a gain of 40,000. A photograph of the basic device (without camera attached) is shown in Figure 2.1 with a schematic diagram in Figure 2.2.

Figure 2.1 Photograph of the Hamamatsu C1525 "Night Viewer".

The central component of the "Night Viewer" is the image intensifier, onto whose photocathode an image of the object being viewed is focussed by the objective lens (a standard SLR camera lens). The light impinging on the photocathode causes electrons to be ejected which are then focussed, forming an image dependent upon electron density, onto the microchannel plate. Here they are multiplied and emerge to fall

upon a phosphor screen to be converted back to an optical image of many times greater intensity. This image is either viewed using a magnifying lens or photographed with a 35mm camera body.

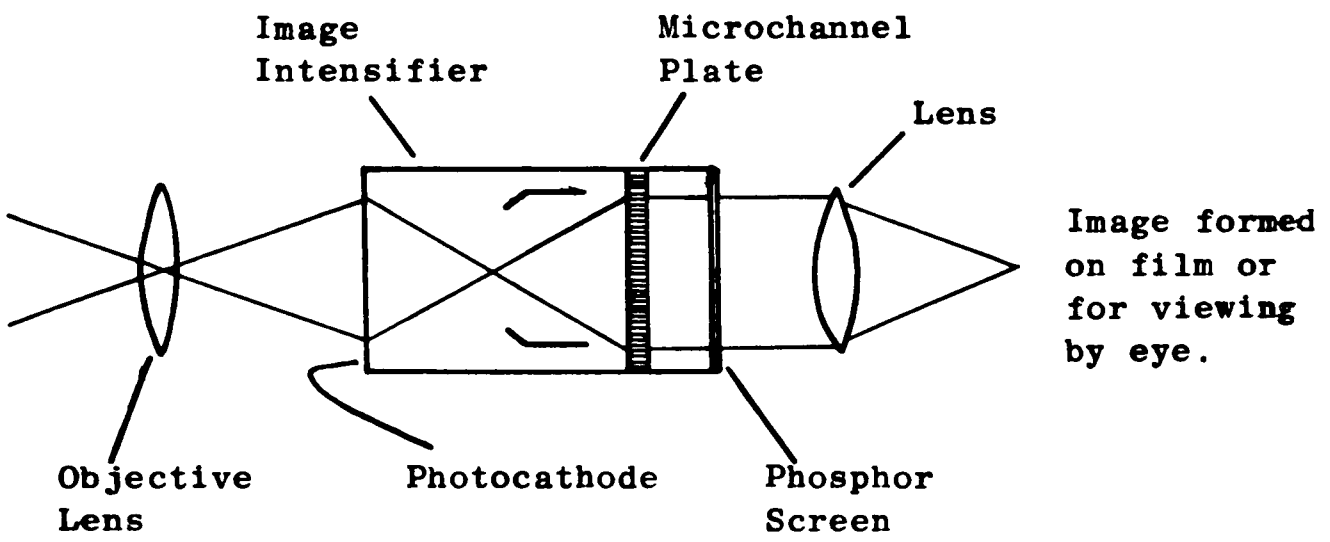

Figure 2.2 Schematic diagram of Night Viewer.

The instrument is battery powered and entirely portable. The spectral range of the image intensifier is limited by the spectral response of the photocathode which is from 300-900nm peaking at 600nm, so covering the range of interest, namely the visible and the majority of the near-IR. The phosphor screen has a peak emission of 560nm (and so the image appears green regardless of the incident light's wavelength).

As far as these experiments were concerned an undesirable feature of the "Night Viewer" was its "auto gain" function, which as the name suggests constantly adjusts the gain in an attempt to keep the image produced at a constant intensity in spite of changes in illumination level. The problem with this is that quantitative measurements cannot be made since if less light enters the device then the gain will automatically be increased (although a "brightness" control is provided

which does give some control over the intensity of the final image).

In all the studies a Nikon 50mm f 1.7 objective lens and Cninon CX 35mm camera body were used. All photographs were taken on Ilford HP5 (400 ASA rated film).

2.2.2 Optical Filters

The image intensifier detects any light within its spectral range and therefore for spectral selectivity optical filters are required. Two types of filter were used; the standard photographic 50x50mm square gelatin type (Ilford and Kodak) and 1" diameter round interference filters (Ealing) (See Section 3.2.2). The absorbance spectra of the band pass and the high pass gelatin filters used are given in the results section. Details of the narrow band pass (about 10nm FWHM) interference filters can be found in Section 3.2.2.1. A 50x50mm filter holder (Kodak) that clamps onto the objective lens was used to hold the gelatin filters with an adaptor made to accomodate the interference filters.

A diagram of the image intensifier with lens, filter holder and camera body attached is shown in Figure 2.3. To fix the camera body in place, the eyepiece had to be removed, an adaptor screwed in its place and a sliding collar (made by Mr P.J.Goddard), attached to the camera body, then placed over this adaptor. This was held in place (once an image in focus was obtained) by three small screws.

2.2.3 Light Sources.

Three types of light source were used; a clinical high intensity source "piped" through a large (about 6mm diameter) optical fibre bundle, a tungsten halogen lamp and a standard 60W bulb.

The tungsten halogen lamp (150W rating) was part of a redundant

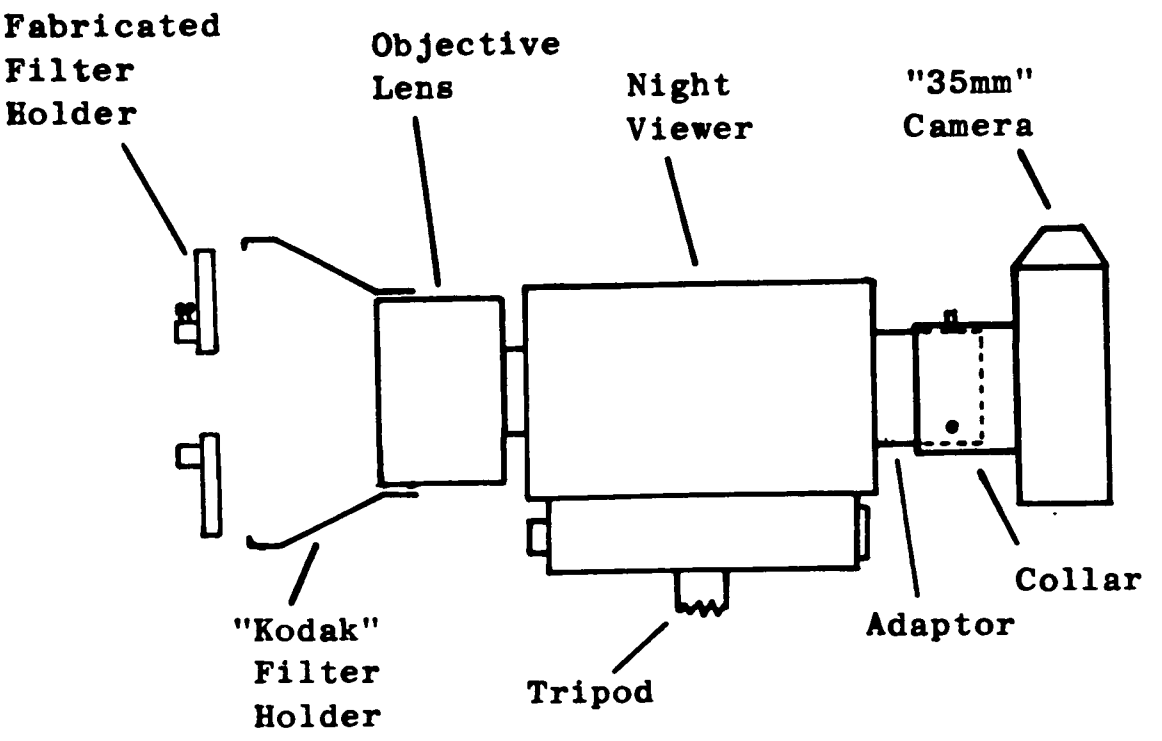

Figure 2.3 Diagram of Image Intensifier with "35mm" camera body and filter holder attached.

piece of equipment which limited its accessibility and hence versatility, with only a small fraction of the total emitted light available. This is described in detail in Section 3.2.1. and as used here provided collimated light from a 25mm diameter aperture. (see also Figure 2.5) The 60W bulb was used in an "anglepoise" lamp as described in Section 2.3.3.

2.3 Results.

2.3.1 Basic Transillumination and Basic Scattering with the Clinical Optical Fibre Bundle (White Light) Source.

Representative photographs taken with the "Night Viewer" and using the high intensity clinical white light source with the fibre bundle are shown in Figure 2.4.

All of these and the following studies, had to be performed in total darkness since any ambient light falling on the subject would have been much greater than the amount of transmitted light. A variety of camera shutter speeds and apertures were used, chosen as appropriate after taking the intensity of the observed image in the viewfinder into consideration.

Figures 2.4a and 2.4b show light emerging from the rear of the hand, with the source held against the front surface. for a dark skinned and caucasian subject respectively. Figure 2.4c shows the light transmitted through the back of the wrist of the same caucasian subject with the source pushed firmly into the tissue opposite. In Figures 2.4d and 2.4e the backscattered light from a dark skinned forearm and the inside of the leg of a caucasian subject are shown. (The fibre optic bundle is visible in both pictures).

These photographs basically demonstrate that some light is transmitted through the hand, and also intensely backscattered from tissue. Since a broad band source and detector were used, no conclusions can be drawn concerning the wavelengths at which the scattering and transmission occurs. However, from the work described in Section 1.4.2.2 and Chapter 6, and since the emerging light appeared red it is likely that the "light" in the photographs is mainly above about 600nm.

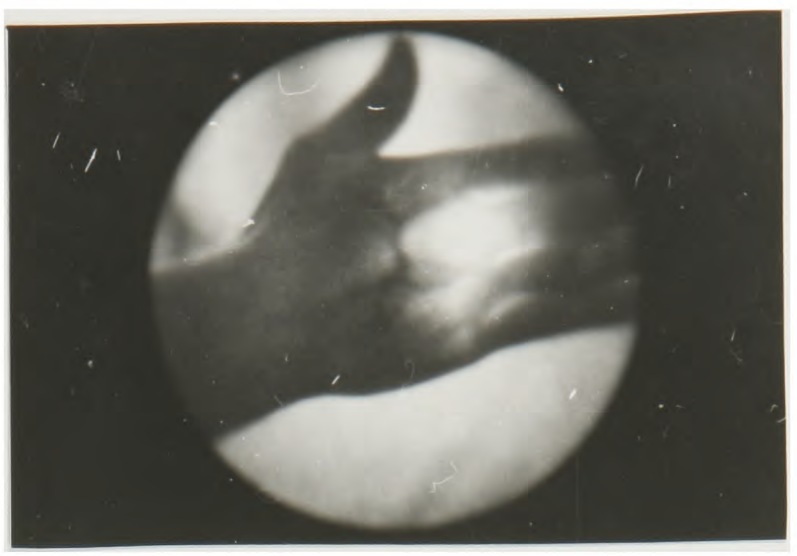

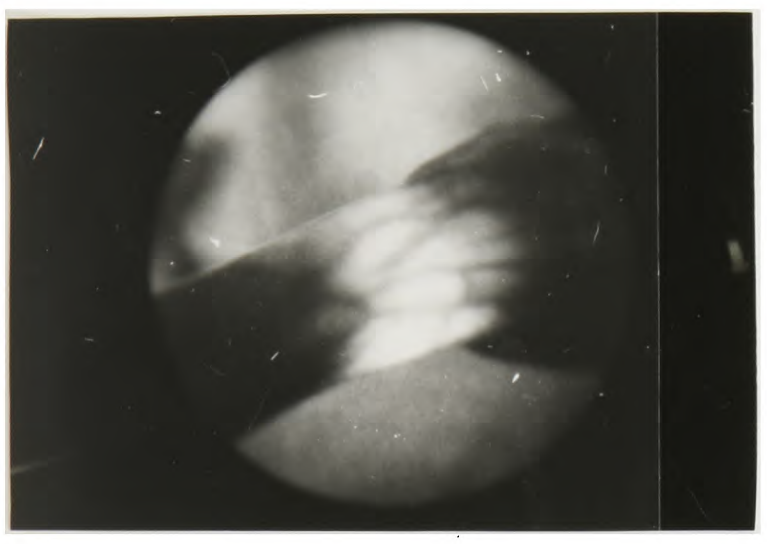

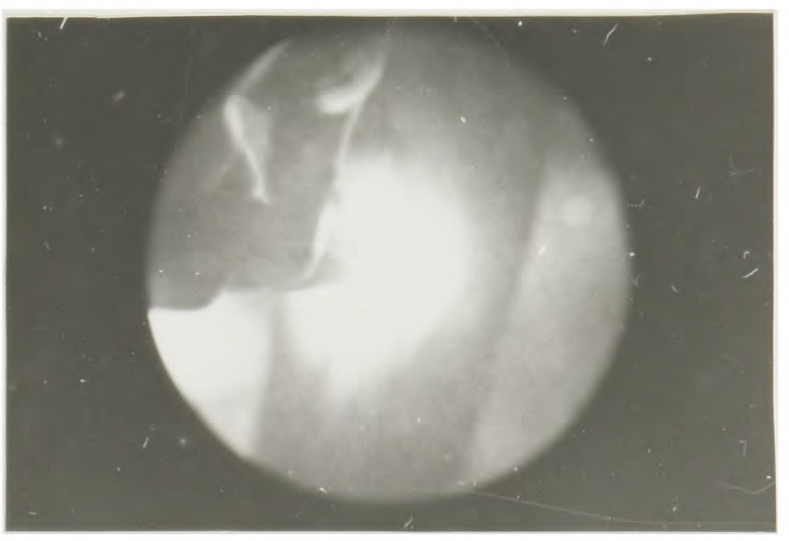

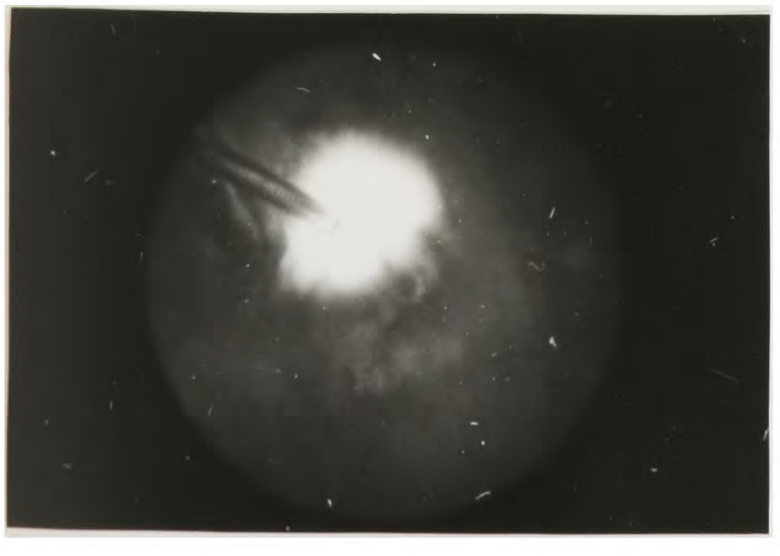

Figure 2.4 Photographs of transmitted and back-scattered light. (See text for details).

The only noticeable visible structures are those veins which are close to the surface, there being no evidence of the bones within the hands. The reason the bones, or no other anatomical features save the venous system, are visible is primarily because tissue is highly scattering (evidenced by Figures 2.4d and 2.4e). Therefore it effectively acts as a diffuser so that the image produced is akin to having a diffuse source placed against the outer layers of the tissue containing the venous system. Since the bones appear to have no large effect on the image produced it seems likely that at least over part of the wavelength range used bone attenuates light no more strongly than other biological tissues. To arrive at a full explanation of these type of photographs both the scattering and absorption characteristics of the constituent components are required.

2.3.2 Transillumination of the Hand

The intention of the studies described in this section were to investigate the wavelength dependence of the transillumination of the hand. Three subjects took part, a male and female caucasian and a dark skinned male.

The tungsten halogen light source was used with the front of the left hand held tightly against the 25mm aperture as shown in the diagram in Figure 2.5. With the "Night Viewer", photographs were taken of light emerging from the back of the hand with the wavelength region selected by filter. No image was visible with the interference filters, because their narrow pass band, and smaller physical size restricted too much light so the gelatin filters were used.

After these studies had been completed, upon obtaining the absorbance spectra of these filters from the scanning spectrophotometer

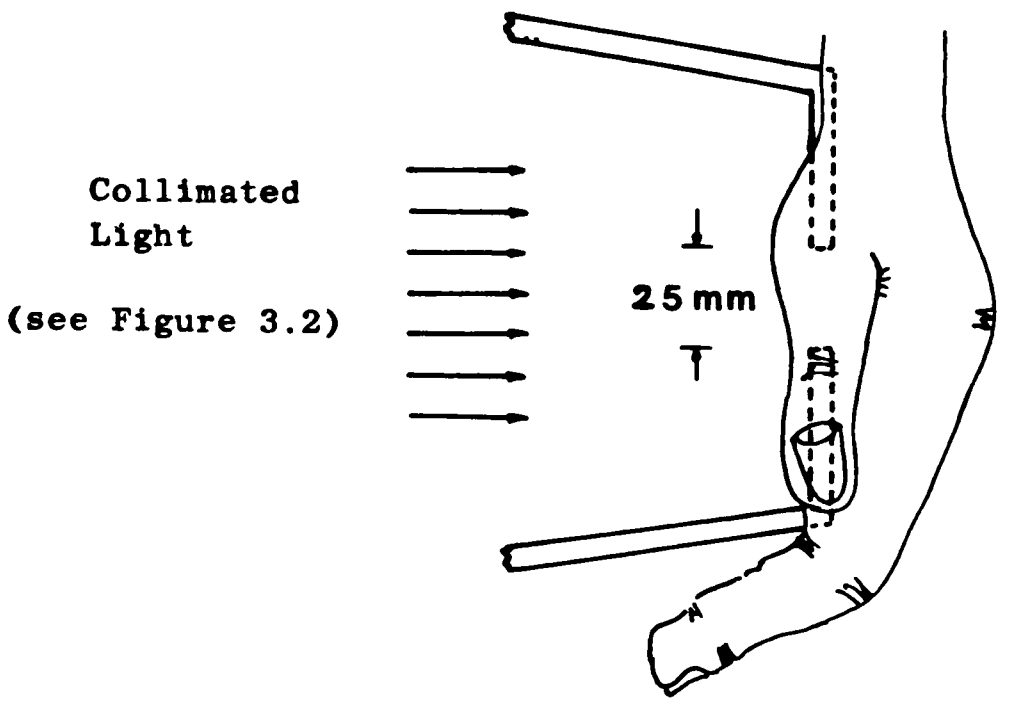

Figure 2.5 Schematic diagram of the arrangement used for transillumination studies of the hand.

described in Section 3.5 it was discovered that these filters actually transmit light in their stated pass band in the visible and then begin transmitting again in the near-IR. This is shown in Figure 2.6 where the spectra of all the gelatin filters used are given. This characteristic was not shown in the data sheets for the filters actually used (Ilford) although it is in another manufacturer's (Kodak) data sheets for similar filters.

The consequence of this is that in all of the photographs obtained a contribution will have been made by near-IR light, with the proportions of the selected wavelength range to near-IR dependent upon the spectral characteristics of the lamp, filter and responsivity of the photocathode in the "Night Viewer". Hence few firm conclusions concerning the wavelength dependence of transillumination can be made, although the following results are still considered of interest, whilst an indication of those wavelengths chiefly involved in transillumination can be

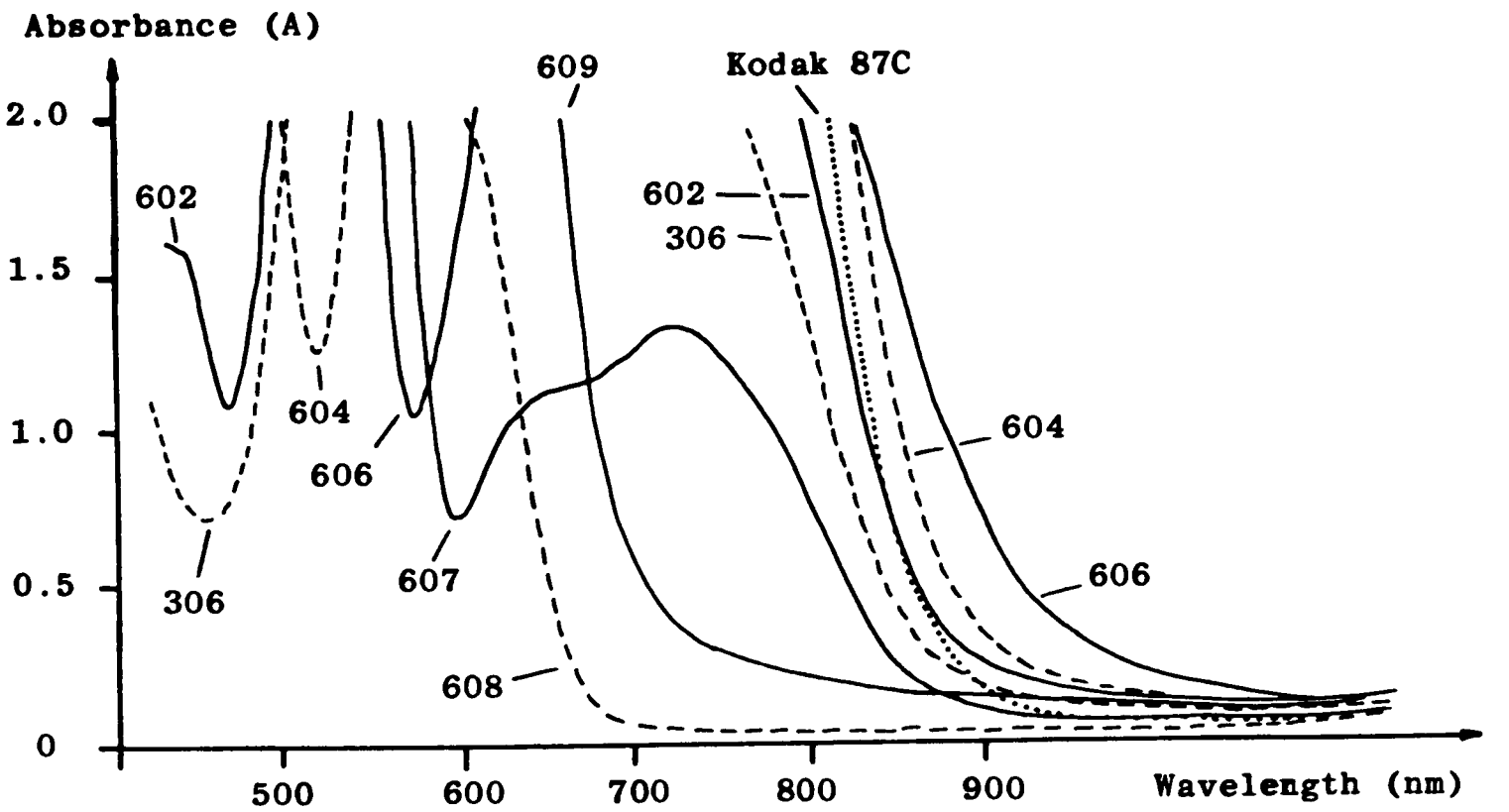

Figure 2.6 The spectral characteristics of the gelatin filters used, obtained using the spectrophotometer described in Section 3.5. (All filters supplied by Ilford unless otherwise stated).

obtained from the results in Chapter 6.

Figure 2.7a is a photograph taken with the back of the female caucasian's hand held against the 25mm diameter collimated source (the only one shown in this mode) with no filter used. The same subject's hand with the palm towards the source is shown in Figure 2.7b with an Ilford 604 filter used, with the corresponding photograph for the male caucasian subject in Figure 2.7c. When the front of the hand is photographed no venous pattern is visible whereas with the back of the hand distinctive patterns for the two subjects can be seen. This observation, that individuals at least to some degree each have their own distinct venous pattern is shown again in Figure 2.7d which is the photograph of the back of the dark skinned subject's hand taken with an Ilford 807 filter.

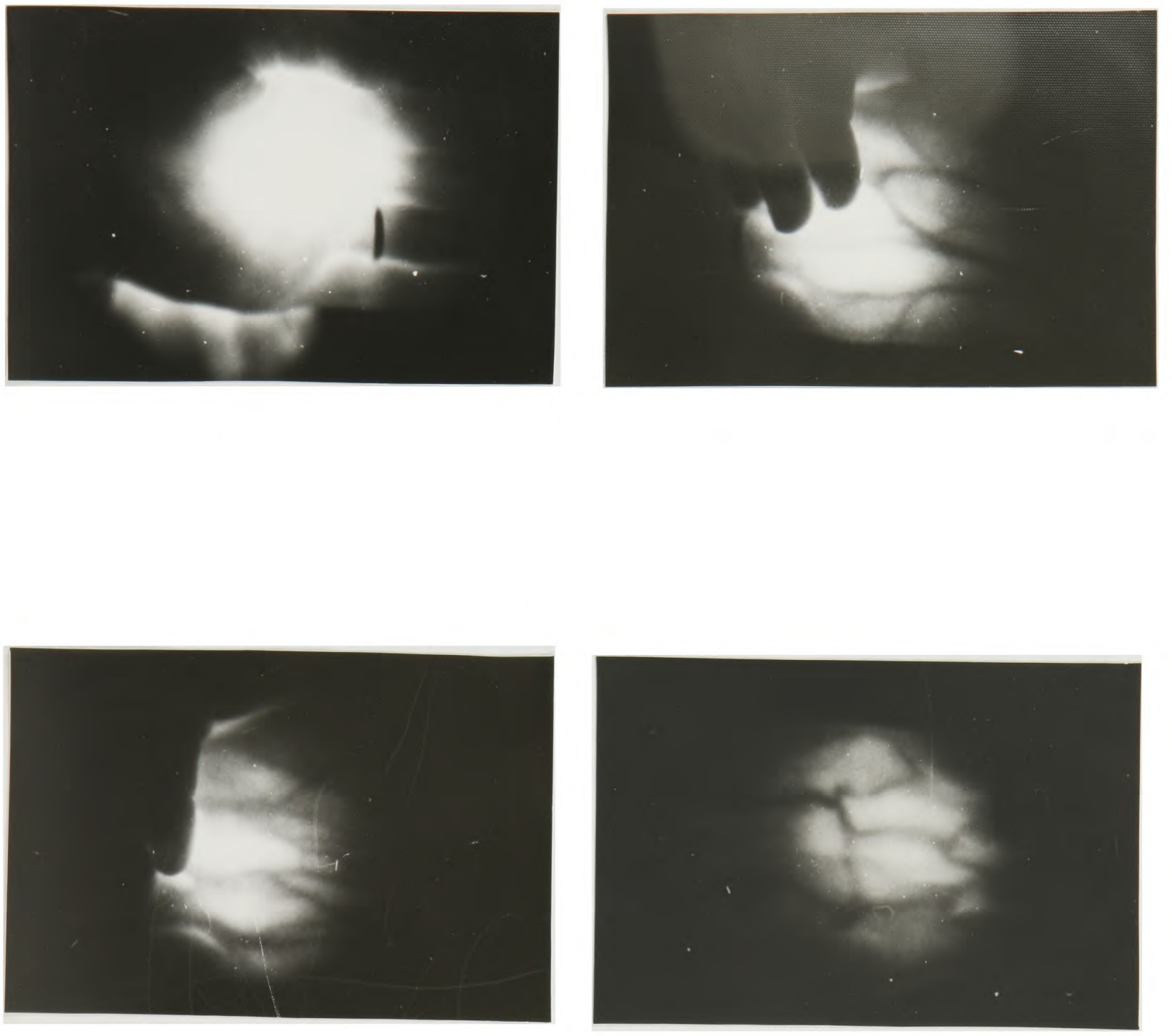

Figure 2.7 Transillumination of the human hand showing the distinctive venous pattern for different subjects.

The remaining pictures shown in Figure 2.8 are all of the dark

skinned subject taken with Ilford 306,607,608,609 and Kodak 87C filters respectively. The last three are all long wavelength pass filters with the cutoff progressing further into the near-IR. Comparison of the photographs is difficult since in addition to the problem described above there is also the effect of the "auto gain" control described above.

The only firm conclusion to be drawn from these studies is that light is transmitted through the hand and the only structures which are readily visible by photography with no form of "optical processing" (see the discussion section), are the veins. These can also be seen by direct photography (ie by the standard reflectance of ambient light) using near-IR film as described in Section 1.5.11. In conclusion, these studies serve as a useful introduction to this area and, as described in the discussion section, with a slightly different type of image intensifier many informative studies could be performed using a similar approach.

2.3.3 Transillumination Studies of Bacon.

As described in the Introduction an advantage of photography for optical measurements is that spatially resolved intensity measurements are obtained, and so the transmission characteristics of the different areas of a heterogeneous sample can be obtained in a single go. The following photographs are of transilluminated slices of bacon taken at different wavelengths in an attempt to see if there were any obvious variations in the transmission characteristics of the different components of the bacon.

The studies were performed by placing a sheet of perspex on top of a sheet of paper (which acted as a diffuser) on an upturned anglepoise lamp. Two slices of bacon were then arranged on the perspex,

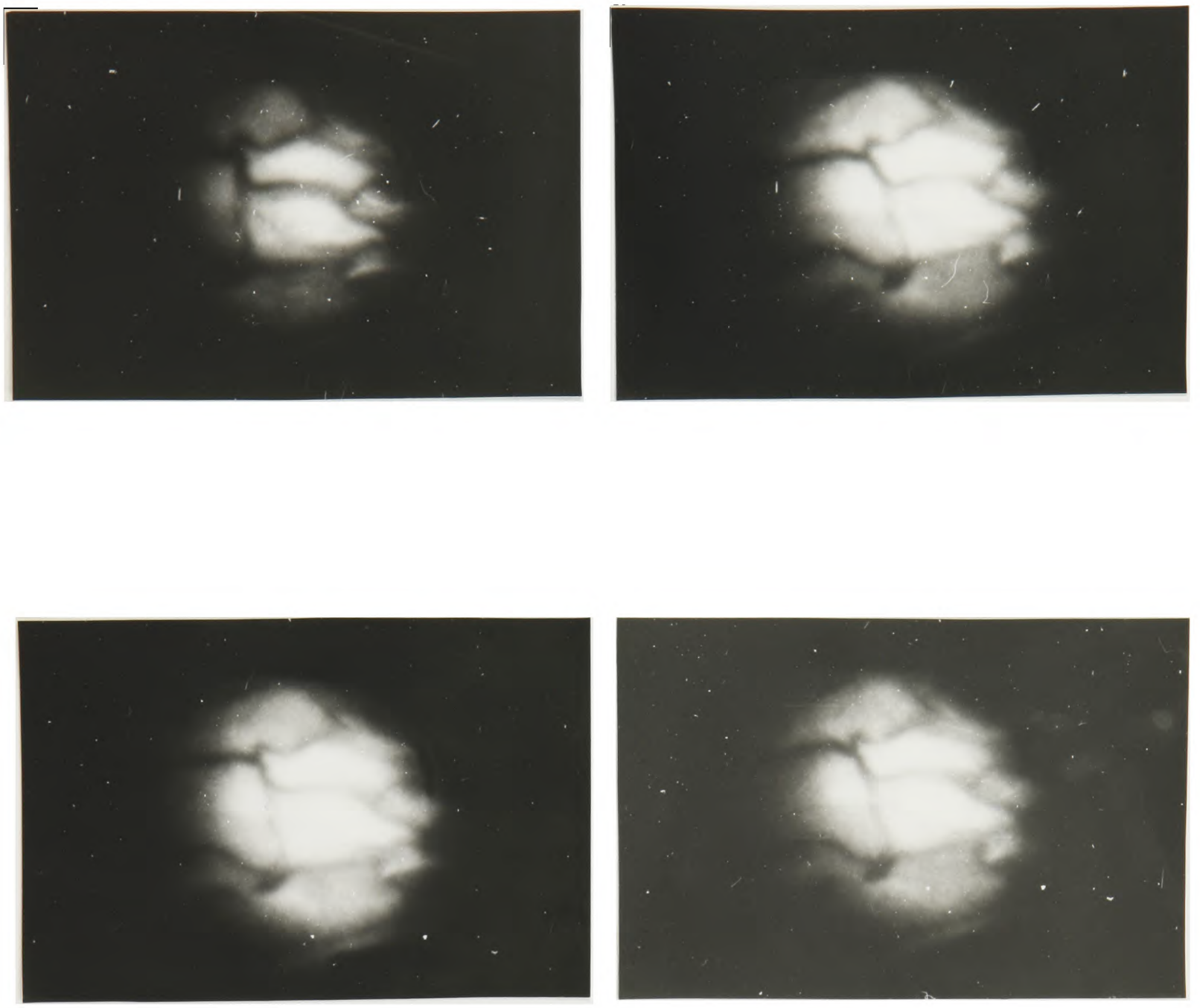

Figure 2.8 Transillumination of the dark skinned subject's hand using Ilford (a) 306, (b) 607, (c) 608, (d) 609 and (e) Kodak 87C filters respectively.

overlapping in the middle so no light would shine directly through, and

masked by sheets of aluminium This arrangement is shown in Figure 2.9. Two scalpel blades were placed below the bacon to try and assess if the sharpness of the image after the light had scattered through the sample was wavelength dependent to any great extent. For comparison two blades were also placed on top.

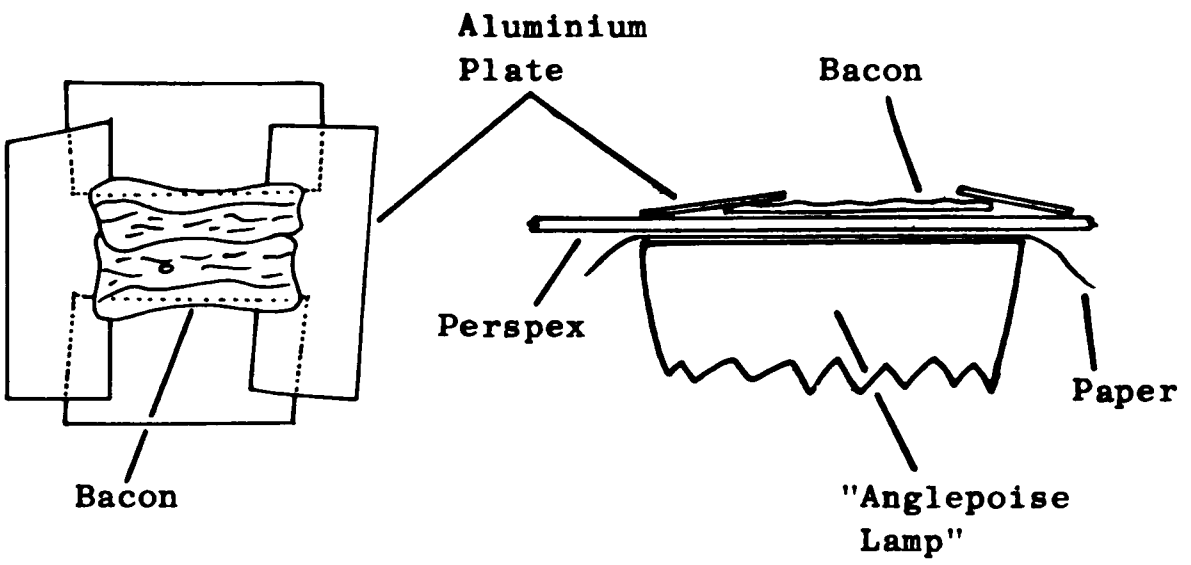

Figure 2.9 Schematic diagram of the arrangement used for transillumination studies of bacon.

The photographs taken with the "Night Viewer", with interference filters transmitting at 550,600,620 and 830nm, are shown in Figure 2.10a to 2.10d respectively. the blades below the sample are on the left. The action of the "auto gain" control again hampers comparison of the photographs, but even so distinctions between them can be seen. These are that at the three lower wavelengths the contrast between the single (at the top of the pictures) and the double layers of bacon (in the centre of the pictures) is greater than the one taken in the near-IR. In addition there appears to be a proportionally greater attenuation of near-IR by the fat (the bottom left corner in Figure 2.10a) than at the visible wavelengths.

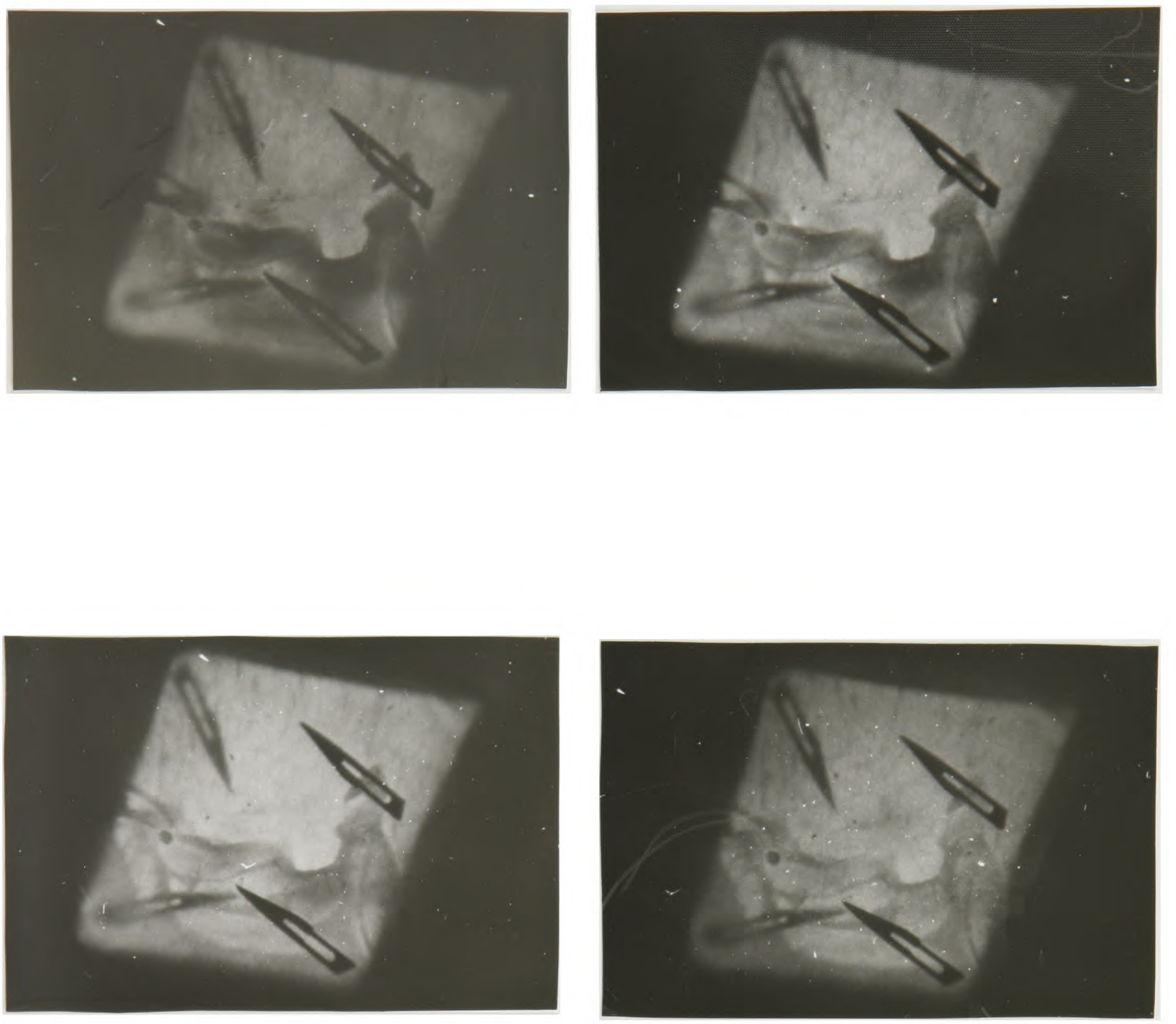

Figure 2.10 Transillumination of bacon with wavelength selection by interference filter at: a) 550, b) 600, c) 620, and d) 830nm respectively.

These photographs were taken with the "Night Viewer" because of the

limited light available due to the use of the interference filters. However with the gelatin filters the image intensifier was not required and so an SLR camera (Chinon CX) with its own lens (Chinon 52mm f1.7) was adequate. This also overcame the problem of the near-IR transmission of the gelatin filters since Ilford HP5 is not sensitive in this region (as is the photocathode of the "Night Viewer").

In Figure 2.11a the standard photograph of the bacon used in the studies with the gelatin filters used (different from that above) is shown to give a guide to the lean and fat regions. The pictures in Figures 2.11b to 2.11e are of the transilluminated sample using Ilford 602,604,606 and 608 filters respectively, whose transmission bands are at increasing wavelength in the visible range (see Figure 2.6).

Again the contrast between the double and single layers of bacon is more noticable at the shorter wavelengths. This is not surprising since the lean bacon has a pink colour and so must be transmiting the longer visible wavelengths more easily, whilst it is also known that there is much less attenuation by biological samples in the near-IR than in the visible.

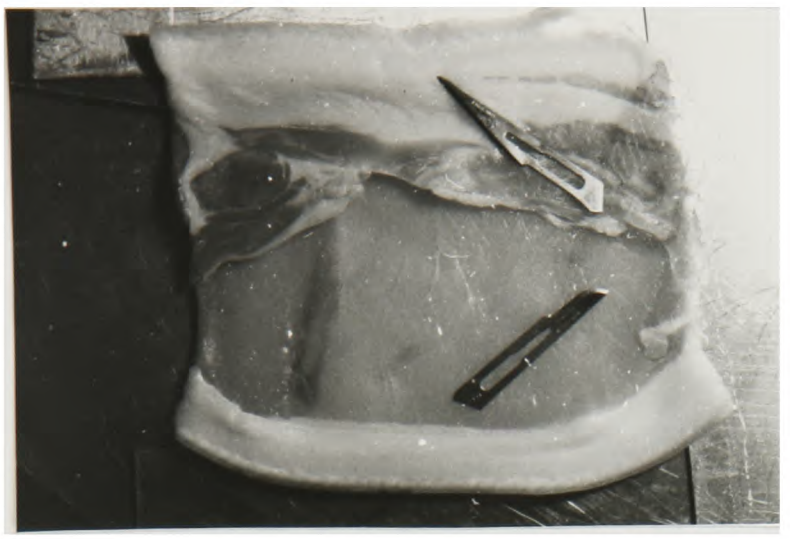

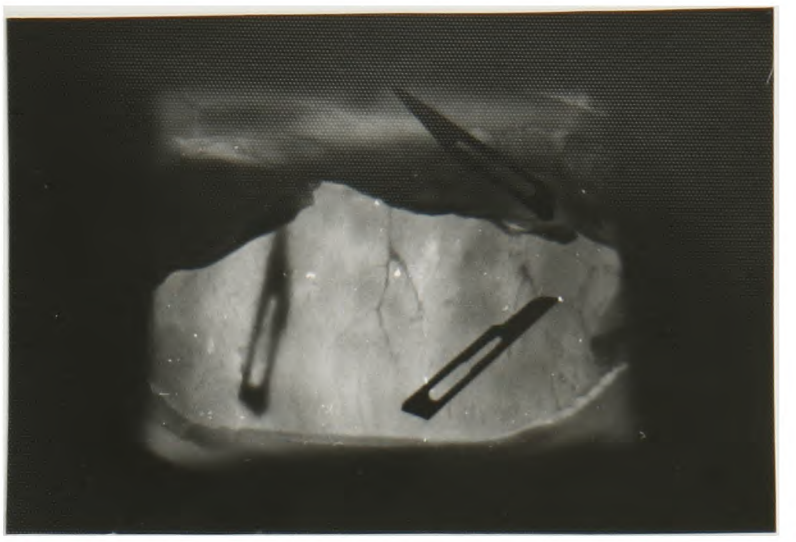

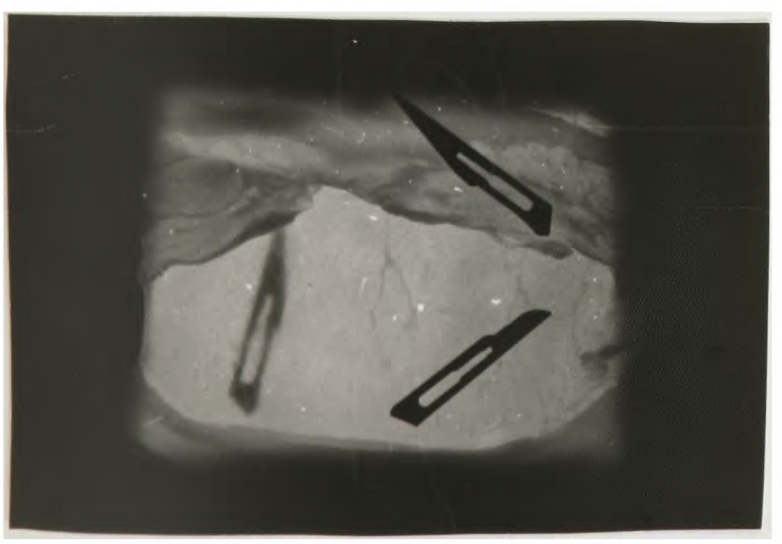

Figure 2.11 Photographs taken with a standard 35mm camera of the sample, and in transillumination mode using gelatin Ilford filters as stated in the text.

2.4 Discussion of Results.

The preliminary investigations described above served as a useful introduction to studying the gross spectral properties of tissue. Clearly light is transmitted to some extent through such samples and also very strongly scattered.

The results from the studies on the bacon seem to indicate that, as expected from previous work (see Section 1.4.2.2), the transmission characteristics are dependent upon wavelength. They also demonstrate the benefits of "photographic" type measurements where intensity measurements are simultaneously spatially resolved.

Further work of the same nature would be of interest, although an alternative image intensifier system than the "Night Viewer" (which was only on loan for several weeks) without the automatic gain control would be needed so that quantitative measurements could be made. A more sensitive system would also be advantageous so that even lower light levels could be recorded, allowing thicker sections of tissue to be examined. (Such instruments are available often using for example, computer controlled averaging and charge coupled device type detectors).

With such an image intensification system a thorough series of transillumination studies similar to those above could be performed using either interference filters or a monochromator for narrow pass band selection. In this way variations in both transmission levels and any characteristics due to the anatomy, could be investigated with respect to wavelength on suitable parts of the body (eg hands, arms, feet, legs). Studies could also be made on excised tissue and organs to gain information concerning the absorbance and scattering characteristics of such samples. Finally variations in transmission (and reflectance)

patterns with respect to incident beam geometry could be examined. As well as being of fundamental interest, the data obtained from these experiments may also be of direct use in fields such as diaphonography which already employ these type of observations.

A further application of such a system would be to obtain standard (ie with surface illumination) photographs at specific wavelengths. It is well known (see Section 1.5.11) that near-IR photographs show up the venous system very well due to the decrease in reflectance of tissue containing blood vessels (because of the absorbance by haemoglobin). It is possible that other anatomical features may manifest themselves in photographs taken over narrow wavelength bands in other regions of the spectrum.

Such a study may even contribute to the work involving the use of different wavelength light for studying the arterial system at different depths (GILTVEDT (1984)) (due to the dependence of penetration depth upon wavelength), since from these results one may expect the relative clarity of vessels at different depths to be wavelength dependent.

2.5 Further Studies

In addition to the suggestions for future studies given above which are simply extensions of the work presented here the following additional investigation would also be possible using an image intensification system. However, the limited availability of the "Night Viewer" meant that this was not attempted.

One of the main areas of this thesis is involved with investigating the feasibility of non-invasively monitoring the redox state of cytochrome oxidase in the neonatal brain (see Chapter 4). For such measurements light must be shone into the brain and detected upon emerging from the skull. One question concerning this operation is the optimum position to illuminate the skull, and with what beam geometry, and where it is best to detect the emerging light (if any), and whether a single or array of detectors is preferable.

Potentially these problems could be solved by the use of an image intensifier and suitable light source, (which would have to be suitably shrouded to prevent direct illumination of the outer surface of the head). For the same reasons the measurements would have to be made in a darkened room or with a safelight used, chosen with regard to the measuring wavelength at any time.

Selection of wavelength would be by filters. To prevent any possibility of injury due to heating by near-IR light, exposure times would need to be kept short or if visible wavelengths were being used, near-IR blocking (ie heat absorbing) filters employed. (This type of filter used in conjunction with the gelatin filters would overcome the problems described in Section 2.3.2).

Obvious studies would be to investigate if use of the areas not

covered by the skull such as the fontanelles and midline sutures would aid the introduction and detection of light.

Chapter Three: Instrumentation.

3.1 Introduction.

To peform any type of optical measurement or indeed any type of spectroscopic investigation in other regions of the em spectrum, what is required is a source (to illuminate the sample), and a detector (to monitor the resultant signal). In addition some limitation on the spectral bandwidth will usually be required so that a means of wavelength selection will be necessary somewhere between the source and detector. There may also be a need for polarizers.

To construct an actual optical instrument these basic elements must be linked together using optical components such as lenses, mirrors and optical fibres, along with control and processing sections to actually run the instrument and convert the signals obtained from the detector(s) into meaningful results.

This chapter describes the instrumentation used to perform the experiments described in this thesis. This includes both constituent optical components and complete spectrophotometers. In Section 3.2 the sources, detectors and means of wavelength selection used are given, followed in Section 3.3 by the actual detection circuits. In Section 3.4 the various standard spectrophotometer configurations are given, which is of importance concerning the monitoring of the redox state of cytochrome oxidase described in Chapter 4. together with details of the commercially available spectrophotometers used. Finally in Section 3.5. details of the computer based scanning spectrophotometer which was constructed and subsequently used for the studies in Chapter 6 are given.

3.2 Optical Components.

3.2.1 Light Sources.

Light sources can be divided into two categories: incandescent and luminescent, depending upon whether the emission is due to a thermal or non-thermal process.

3.2.1.1 Tungsten Halogen Lamp.

In virtually all of the studies described a 12V 150W tungsten halogen lamp was used. This is an incandescent source, the emission produced by the thermal effect of a current passing through a tungsten filament. The typical spectral output of such a lamp is shown in Figure 3.1.

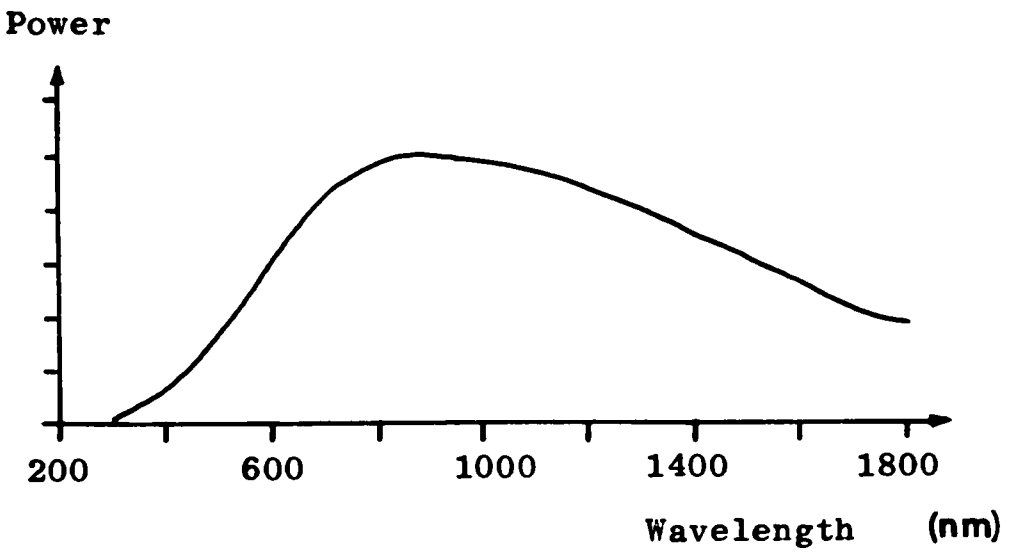

Figure 3.1 Spectral output of a tungsten halogen lamp.

This lamp was part of a redundant piece of equipment (a Joyce-Loebl, thin layer chromatogram scanner) which was taken over for this project. The physical layout is shown in Figure 3.2. The light from the (uncooled) lamp passes through an aperture, separated from the lamp by a chopper wheel, and then through a collimator.

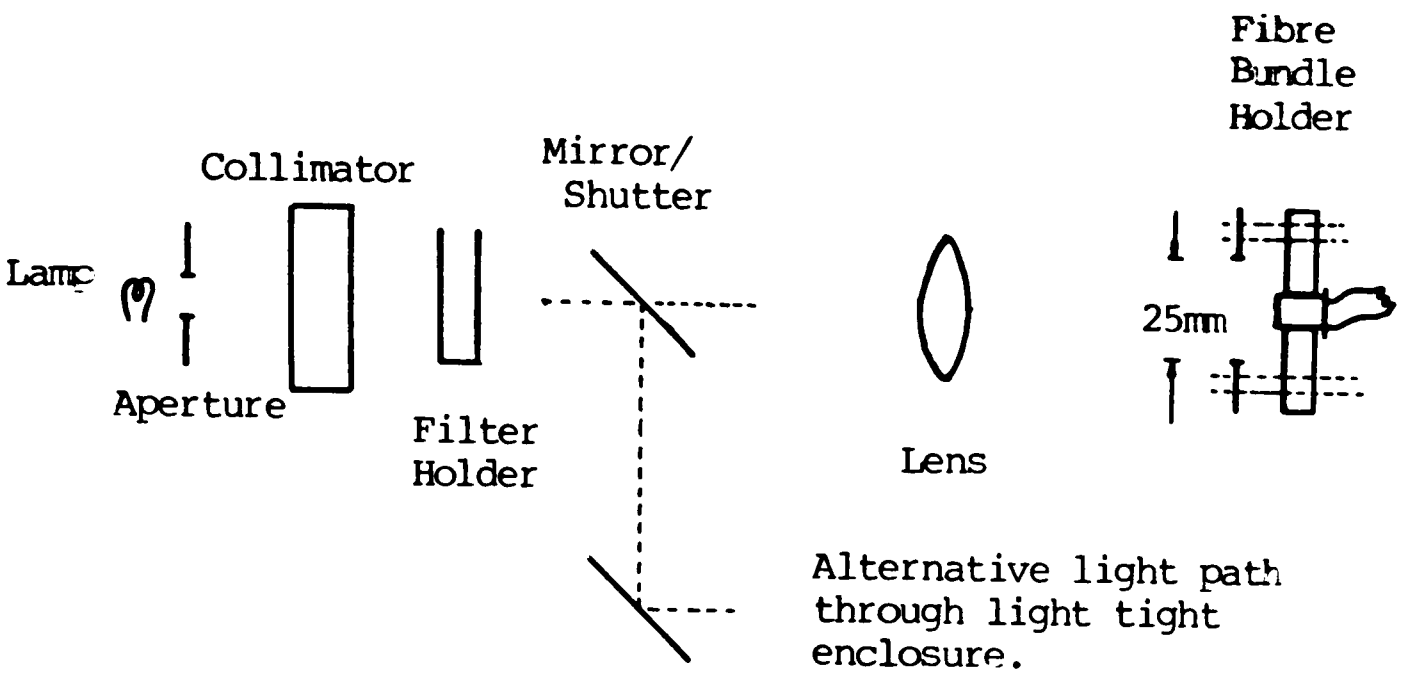

Figure 3.2 Schematic diagram of the tungsten halogen light source and its housing.

The collimated light then takes one of two paths. Either it can be directed (by a sliding mirror) through two right angles to emerge parallel to and below the original beam in a "light tight" enclosure where a modified cuvette holder could be located (see Section 4.6.6). Alternatively the collimated light simply travels in a straight line and through a further aperture of about 25mm diameter, (as used for the studies in the last chapter). Another option with this light path is for a convex lens to be used to focus the light onto the end of an optical fibre (see Section 3.2.4) for which mounts were constructed (see Figure 3.2), thus providing a "piped" light source.

Apart from its basic availability, advantages of this source were the fact that it was easily modified to suit most demands and included a chopper wheel which could be used with the lock-in amplifier (see Section 3.3.2). A slot for filter holders into which the interference filters could be fitted was also present whilst the sliding mirror could be used

to "switch" the source on and off.

The major disadvantage with the source and assembly, (although it is more of a potential disadvantage than one which was realised), is that the absence of a reflector behind the lamp and the small size of the aperture between the lamp and collimator means that a relatively small proportion of the total light output is being used. However, the only study where more light would have been an advantage were the in vivo transmission meaurements, and even then the advantages of higher incident and therefore larger detected intensities would have to be balanced against the problems of an increased thermal load on the sample.

Initially the internal AC power supply was used to drive the lamp but this produced a slight fluctuation in intensity at twice the frequency of the supply, and so was rectified for DC operation. However, eventually a separate DC power supply (Solartron, maximum capactiy 15V 10A) was used which gave an adequate stable lamp voltage and therefore intensity.

Since quartz halogen lamps are widely used in slide and film projectors they are relatively cheap and readily available (even including built in reflectors). Therefore they are ideal visible- near-IR light sources. Alternative broad band incandescent sources are flashlamps which have been used to good effect by YAMANOUCHI (1980) in the bilirubinometer.

3.3.1.2 Laser Diodes.

In Section 4.1 what were considered to be two approaches to adopt in investigating the possibility of optically monitoring the redox state of cytochrome oxidase in vivo and non-invasively are described. One approach involved building a scanning spectrophotometer (described in

Section 3.5) whilst the other was to construct a near-IR spectrophotometer for use in vivo, and operating at 3 or 4 wavelengths. In line with other workers (FOX (1982), COPE (1985)) ideal light sources for this latter type of instrument were felt to be laser diodes. These are luminescent devices which operate in a similar manner to light emitting diodes but have cleaved and polished surfaces to produce a lasing cavity, and therefore have much narrower bandwidths. As they are semiconductor devices they are small, robust, and need no cooling. They also give a high intensity output, and so are ideal for use in what is ultimately intended to be a portable piece of equipment for use in a clinical enviroment.

The suitable type of laser diode for this application are those which operate in a pulsed mode giving intensities of about 10W over 200ns, pulsed at a repetition rate of the order of 1kHz. The major disadvantage of this type of source is that they are at present only available over a limited wavelength range and that their cost increases dramatically as closer tolerance on the required wavelength is specified.

Some preliminary work on constructing laser diode drive circuits was performed. The type used involved charging and then rapidly discharging a capacitor through the laser diode via a thyristor. This side of the project was taken over by Mr Y.A.B.D. Wickramasinghe, who has built a prototype near-IR spectrophotomer which has been used to perform some basic studies (see Appendix A).

3.2.2 Wavelength Selection.

If a broad band source is used then for any spectral analysis some kind of wavelength selection device is necessary. Interference filters,

gelatin filters and a grating (within a monochromator) were used for various experiments as stated in the text.

3.2.2.1 Interference Filters.

Filters are essentially of two types, those which preferentially absorb energy over certain parts of the spectrum and those which reinforce the transmission of light over a given bandwidth.

Interference filters fall into this second category, and are constructed with a layered structure so that of the light incident on the filter some is transmitted at high levels due to constructive interference whilst the remainder is largely reflected. As the majority of the non-transmitted light is largely reflected interference filters suffer less from thermal loading problems.

Various types of interference filter (eg low/high pass, broad/narow band pass) are available. The type used here were narrow band pass filters with full width half maximum (FWHM) bandwidths of about 10nm and maximum transmission of about 50%. They are 1" diameter, and nine were obtained with peak transmission wavelengths at 440. 550, 590. 605. 620. 760. 810. 830. 840 and 905nm (Ealing Optics, UK).

The transmission spectra of two of these are shown in Figure 3.3. These are the specifications as supplied by the manufacturer, and at the actual wavelengths are within 2-3nm of those specified. These filters coupled with the white light source produce quasi-monochromatic light suitable for the kind of studies described here.

3.2.2.2 Gelatin Filters.

Absorbance type filters are gernerally available in glass or gelatin, and here it was the latter type that were used. The peak

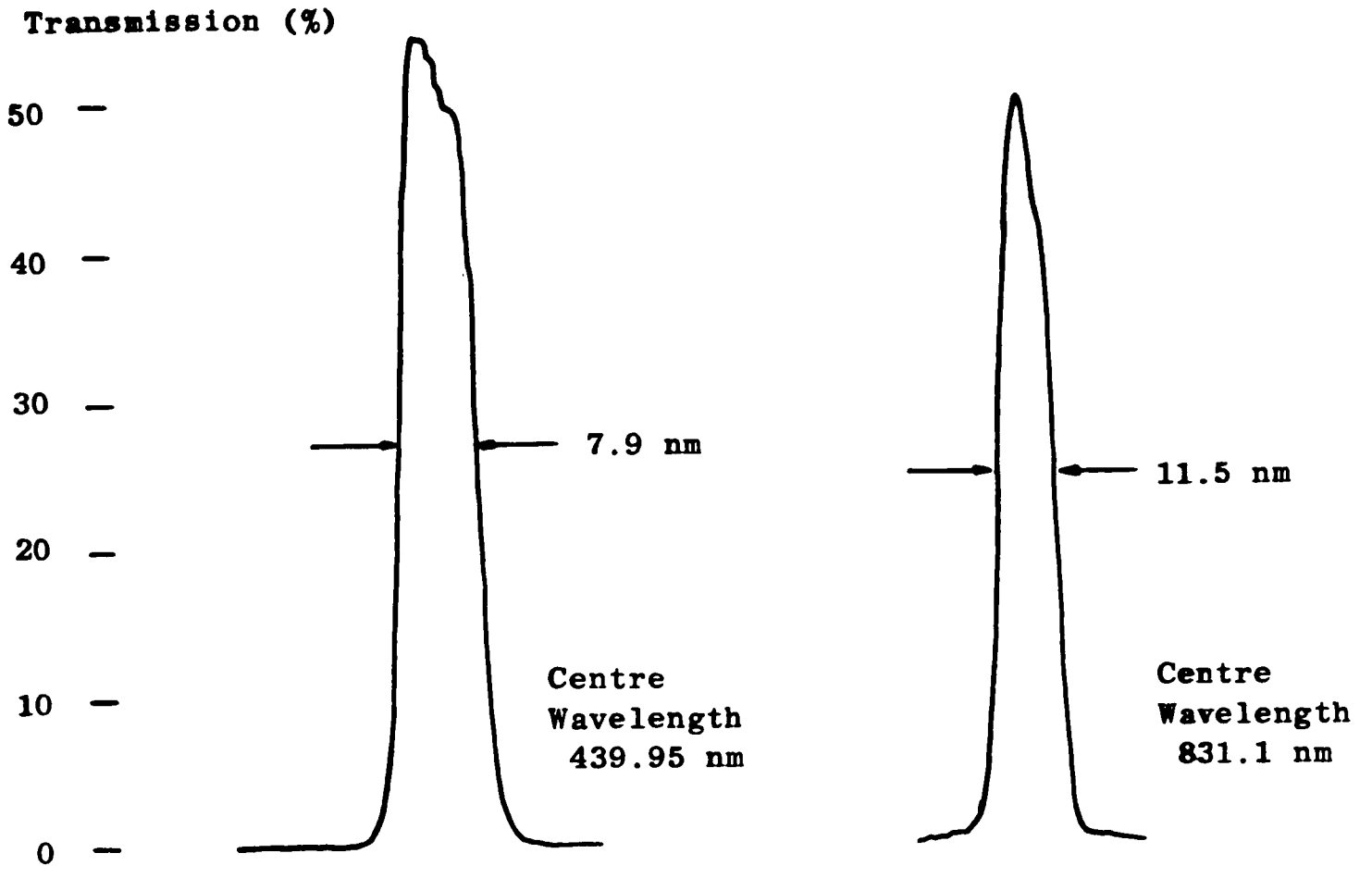

Figure 3.3 Transmission spectra of 440nm and 830nm interference filters used (from supplier's (Ealing Optics, UK) data).

transmission for these absorbance filters are quite low and because they rely upon preferential absorption they can suffer from thermal loading problems (buckling and melting in the worst instance).

A variety of gelatin filters were used (Ilford and Kodak). all 50mm x 50mm square and which fitted into a filter holder (Kodak). Details of this and where appropriate the transmission spectra of the filters are given in Chapter 2.

A potential problem with this type of filter, as discussed in Chapter 2, is that from the supplied data they are shown to have a certain pass band in the visible and then block into the near-IR to the limits of the given graph. However, in practice they may begin to transmit again slightly further into the near-IR, which although of no

consequence in photography (for which these filters are primarily provided), since standard photographic film is not sensitive in this region, for many photodetectors means that in addition to the chosen pass band, near-IR light will also be detected.

3.2.2.3 Rofin Spectralyser.

Whereas filters transmit fixed regions of the spectrum, gratings diffract broad band light into its constituent components by selective interference, thus allowing any wavelength to be chosen. Both reflection and transmission gratings are available for use over the various regions of the em spectrum.

Gratings are the central component in monochromators which are devices that allow a very narrow band of the em spectrum to be selected for use. The actual bandwidth and spectral quality of light emerging from a monochromator depends upon the properties of the grating and geometry and quality of the optics of the monochromator as a whole. Bandwidth is usually selected by varying the output slit width, which simply amounts to taking a larger sample of the diffracted and diverging spectrum.

The Rofin Spectralyser 6000 (Rofin-Sinar, UK) is a continuously scanning monochromator, using a blazed diffraction grating in the side-by-side Ebert configuration as its dispersive element, which is continuously rotated so producing a repeatedly swept optical spectrum at the output slit approximately every 95ms, taking about 10ms to scan from approximately 350-1100nm (see Section 3.5.2). The optical bandwidth can be set at 2.5, 5, 10 or 20nm depending upon which slit in the plate provided is clamped across the input and output apertures as shown in Figure 3.4.

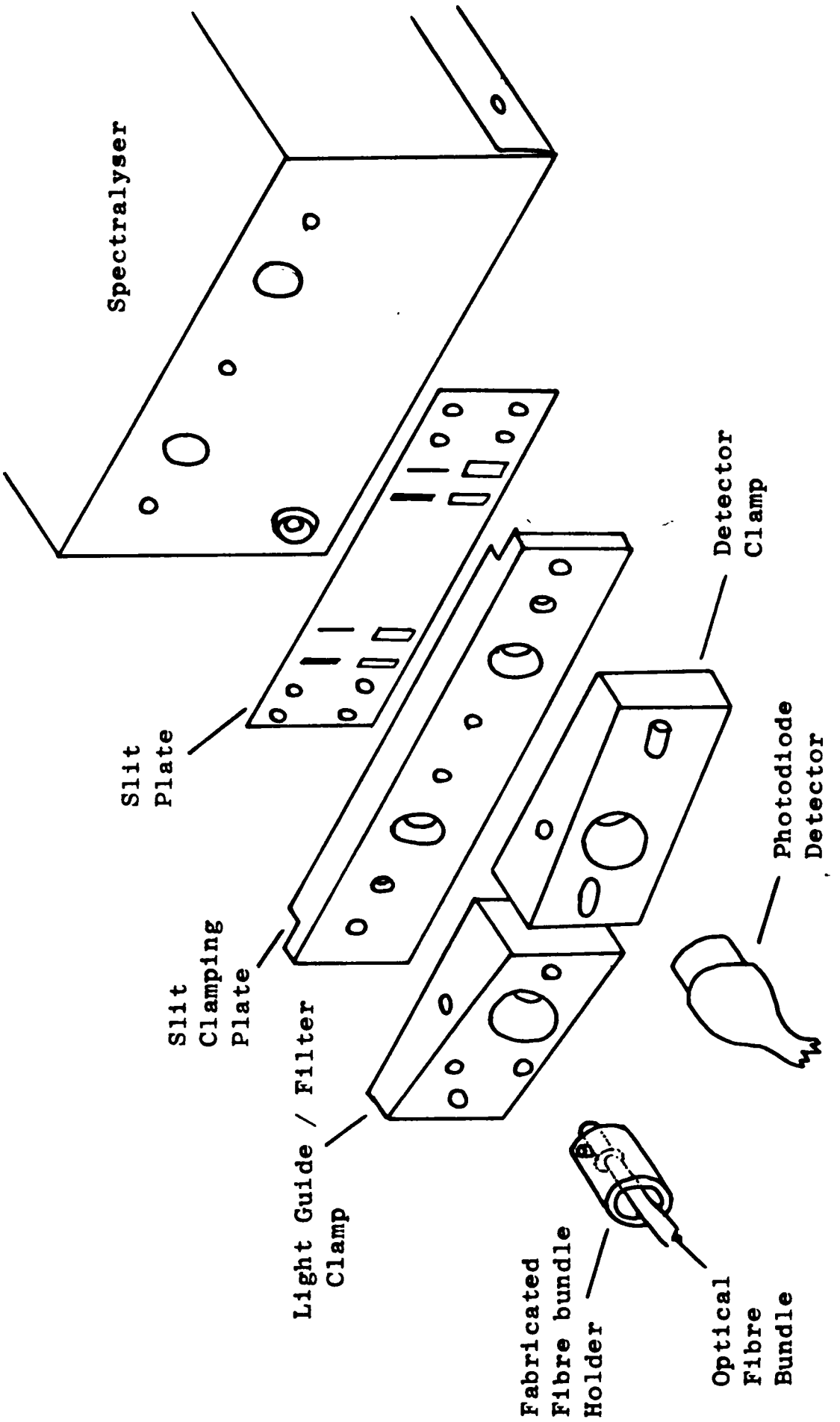

Figure 3.4 Schematic diagram of Spectralyser input, detector and slit plate assembly.

Diffraction grating efficiency varies with wavelength and is also highly dependent upon the polarization state of the incoming light (whether parallel or perpendicular to the grating's grooves). This has a large effect on the "raw" spectra as is discussed in Section 3.5.8.

The Spectralyser does not automatically remove second order spectra, meaning that a source with a spectral peak at λnm will also produce a (much smaller) peak at 2λnm. This can lead to confusion when using broadband spectra since the different order spectra overlap, and can lead to erroneous conclusions (see Section 4.6.5 for instance). The problem can be overcome by using appropriate blocking filters as described in Section 3.5.2.

3.2.3 Detectors.

An optical raditation detector is by definition a device in which optical radiation produces a measurable effect. The many varieties of detector available, their properties and use are extensively covered by BUDDE (1983). The types used in the experiments described in this thesis were photodiodes and a photomultiplier tube (PMT).

3.2.3.1 Photodiodes.

Photodiodes are semiconductor detectors which are generally less sensitive than PMTs but smaller, more robust and cheaper. The operation of semiconductor devices is dependent upon changes in their electrical properties, caused by electron-hole pair creation by incoming photons.

Three types of photodiode were used in the course of these studies, a BPX 65 (RS 304-346), a large area photodiode (RS 303-674) (both from RS Components) and one suppied with the spectralyser (Part No. 6002. Rofin-

Sinar). The spectral responses of the first two are shown in Figure 3.5. the photodiode supplied by Rofin was rectangular shaped to match the slit for optimum performance, with an active area of 2.9mm^2. It is stated that it covers the 300-1100nm range. Details of the detection circuits used are given in Section 3.3, with the Spectralyser's photodiode's input fed into the instruments own internal transimpedance amplifier.

Other types of semiconductor devices which are suitable for this type of work are phototransistors, of which very small versions are made and currently used in various photoplethysmographic applications, and avalanche photodiodes which are much more sensitive than photodiodes but also correspondingly more expensive and requiring a high bias voltage.

In addition to these single detectors, through semiconductor technology, arrays of photodetectors are becoming available in the form of photodiode arrays and charge coupled devices. Such devices may prove very useful for "parallel" processing of light from gratings (as already used in diode array specrophotometers) or in performing intensity and spatially resolved measurements (ie a form of photography). It is likely that continuing advances in electro-optical semiconductor components will be increasingly taken advantage of to the benefit of biomedical instrumentation.

3.2.3.2 Photomultiplier Tube.

PMTs are photoemissive devices whose operation begins through photons striking a photocathode and liberating electrons by the photoelectric effect. These electrons are then accelerated through a high electric field, set up by the dynode system, so striking the dynodes causing secondary emission that continues down the chain resulting in an

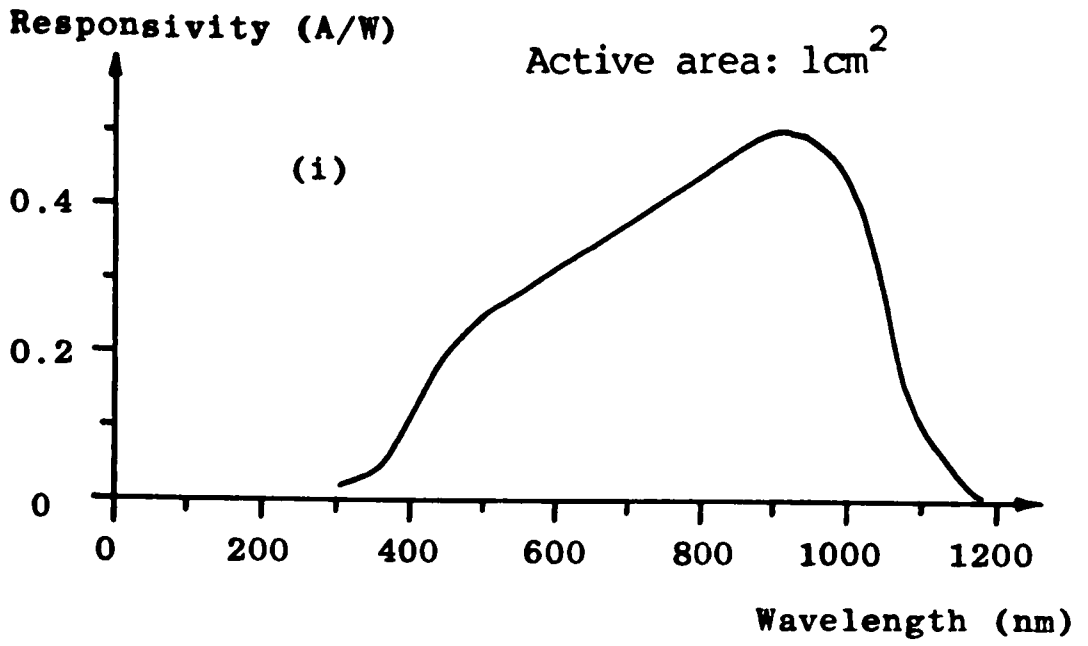

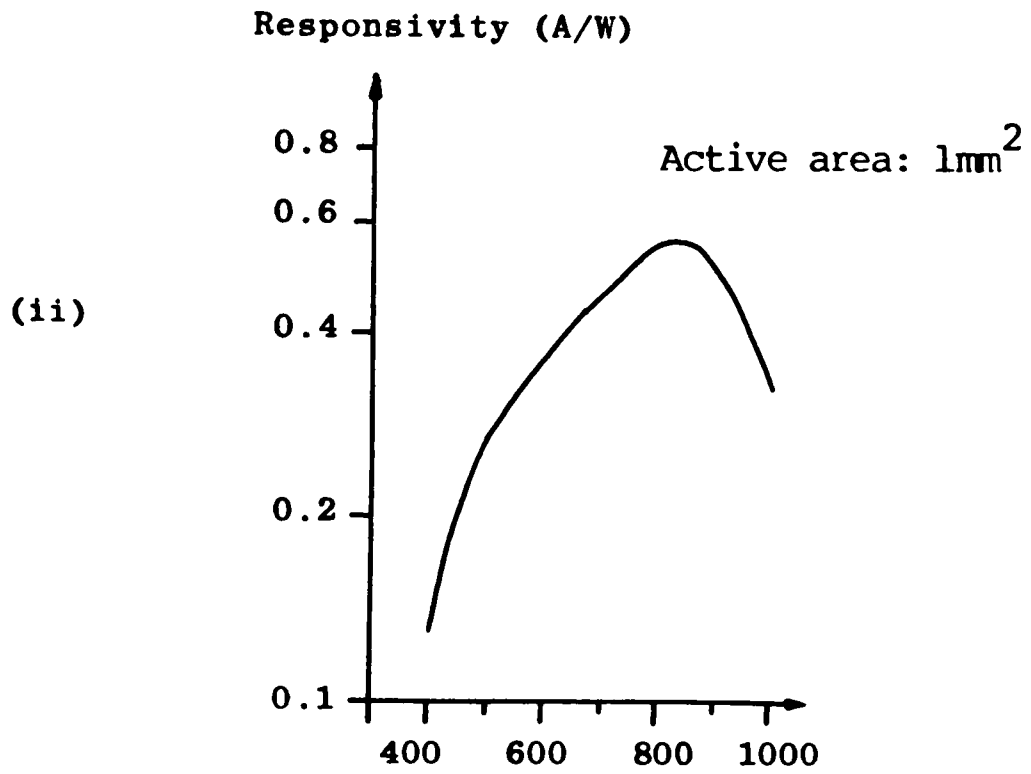

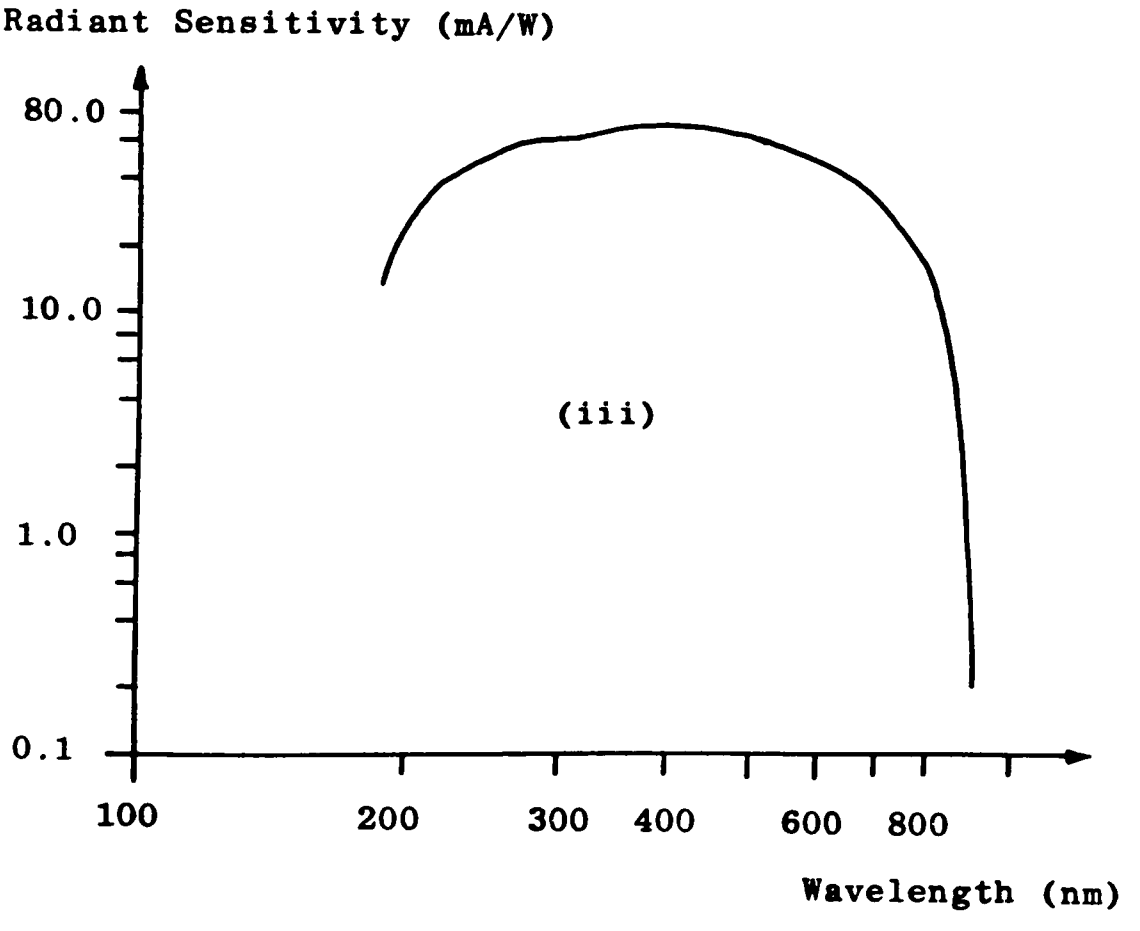

Figure 3.5 Spectral response curves of:

(i) Large area photodiode (RS 303-674)
(ii) BPX 65 (RS 304-346)
(iii) Hamamatsu R928 PMT cathode

enormous increase in the number of electrons, which are collected at the anode to produce the anode current. PMTs vary in their dynode design and physical construction with the spectral response dictated by the transmission properties of the window and principally the spectral sensitivity of the photocathode. (The "Night Viewer" used in Chapter 2 is also a photoemissive device).

The PMT used here was a Hamamatsu R928, with a Hamamatsu C1309 power supply (a DC-DC converter to provide the high-tension (HT) supply for the PMT). The PMT was located in a Hamamatsu socket and placed in a modified photomultiplier housing from a redundant piece of apparatus, which could be directly fixed to the Spectralyser or accept fibre bundles (see Figure 3.12).

The spectral response of this PMT is shown in Figure 3.5(iii), which can be seen to fall away rapidly in the near-IR (as the energy contained by individual photons becomes less).

The detection circuit used is described in Section 3.3.3.

3.2.4 Optical Fibre Bundles.

The preceding sections have dealt with the basic optical components necessary for performing optical measurements. In any spectrophotometer these components must be linked together, which is usually achieved with mirors and lenses, although optical fibre bundles can also be used.

By virtue of total internal reflection, optical fibres enable light coupled in at one end to be transferred along their length. A variety of forms of optical fibres exist depending, for example, upon the material from which they are constructed, the nature of their cladding and their size. They are finding widespread use in an ever increasing

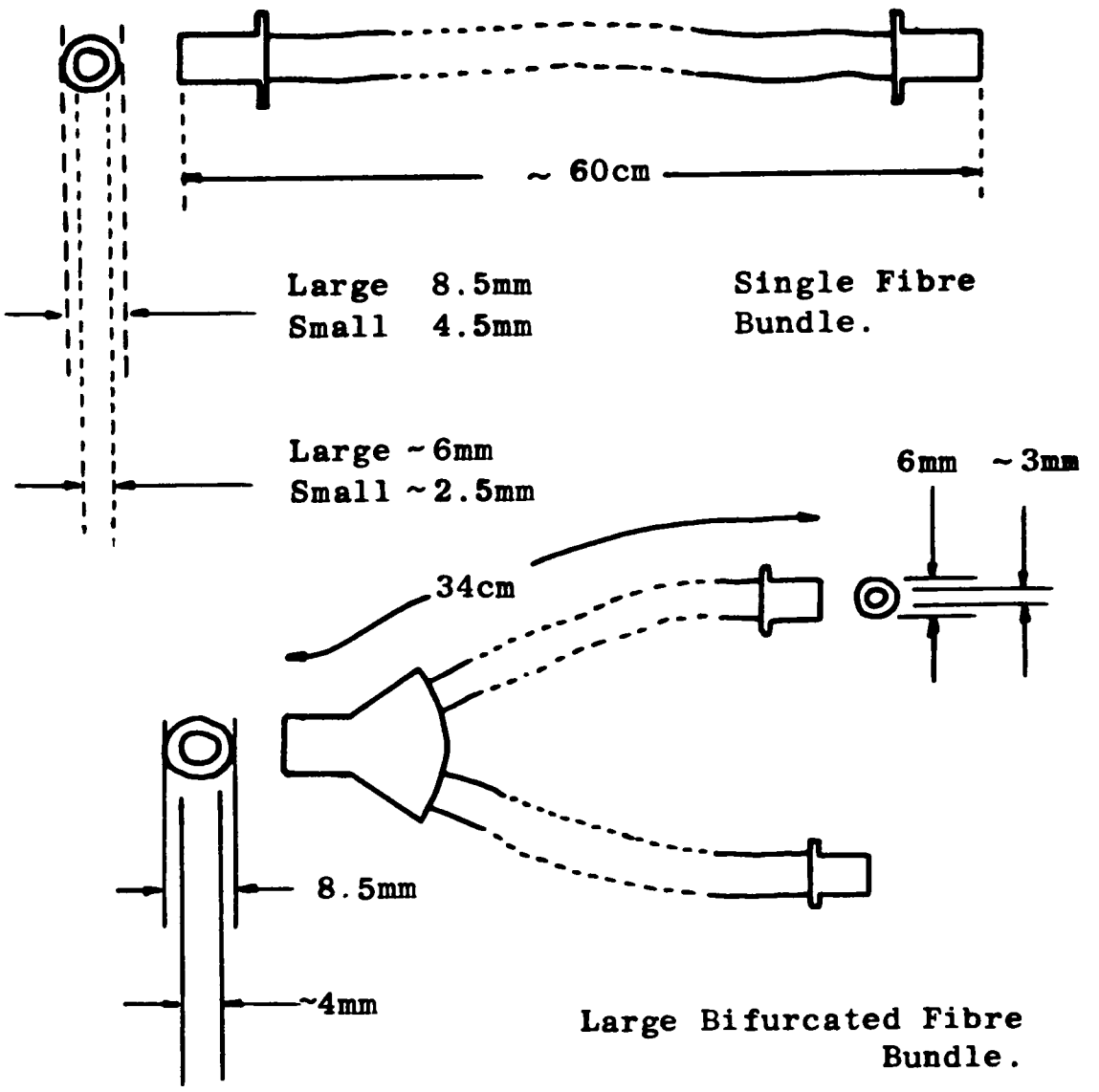

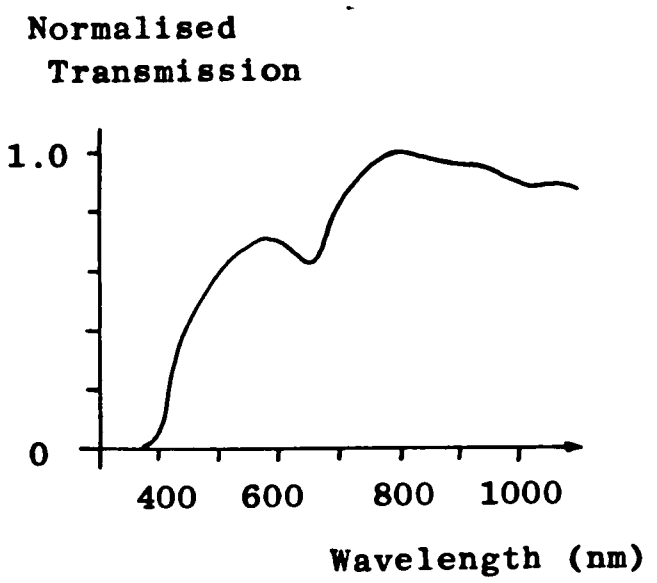

Transmission spectra of fibre bundles (from TBL fibre optics group Ltd. data sheet).

Figure 3.6 Details of the physical dimensions and transmission characteristics of the optical fibre bundles used.

number of areas, and were used here, for their most basic application of

simply "piping" light from one region to another, in the form of optical fibre bundles.

These bundles consist of a large number of glass optical fibres packed together in a single outer cover, and terminated by metal ferrules. Those used here were incoherent (ie not capable of transmitting an image as the individual fibre positions at the two ends of the bundle are not related). They are available with different shaped end terminations and as single cables, or in bifurcated form where the bundle is split into two, enabling two sources, or detectors, to be coupled to the same basic bundle.

All of the bundles used (supplied by TBL Optical Fibres Group and Eurotec Optical Fibres) were terminated in round ferrules and single cables of 2.5mm and 6.0mm active diameters were used of approximate length 50cm. A large bifurcated glass fibre bundle was also used for reflectance measurements which had an active single end of approximately 4mm diameter, with all the fibres randomly mixed and then split into two bundles with active diameters of approximately 3mm. Details of these physical dimensions and the transmission spectra for these fibres are shown in Figure 3.6.

All of these bundles had a plastic covering whilst the larger ones were also metal clad for protection. The latter caused some initial problems with mains pick-up at the photodetector whilst during sensitive measurements it was discovered that the black plastic covering alone was not always sufficient to prevent ambient light entering the sides of the bundles.

In addition to the glass fibre bundles used in the majority of experiments, a bifurcated polymer bundle was also constructed using 0.5mm

polymer fibre. A total of 10 fibres were used and then split into 4 and 6. The fibres were terminated by glueing into plastic tubes and then cleaving using a sharp scalpel, with the loose fibres covered with plastic sleeving.

The fundamental parameter of optical fibres is their acceptance angle which is the maximum angle to the normal at the end of the fibre at which light is incident on the fibre to be coupled in (due to the total internal reflection at the sides). This means a cone of light is accepted into the fibre whilst for the same reason a cone of light also emerges.

This divergence of the emitted beam is one of the main disadvantages of fibres together with their less than total transmission which can be quite significant. The divergence and acceptance angle can cause problems during optical measurements. However, such problems are usually offset by the versatility that fibre bundles give a spectrophotometer with regard to both the position and nature of samples which can be studied.

3.3 Photodetector Circuits and Other Instrumentation.

3.3.1 Introduction.

All of the photodetector circuits used consisted of an operational amplifier (op-amp) used as a current-to-voltage converter. In this configuration the detector sees no load because of the virtual earth at the negative input of the photodetector, whilst because of the "infinite" impedance of the op-amp's inputs all of the photocurrent generated passes through the feedback resistor, to produce the output voltage. This is shown in Figure 3.7.

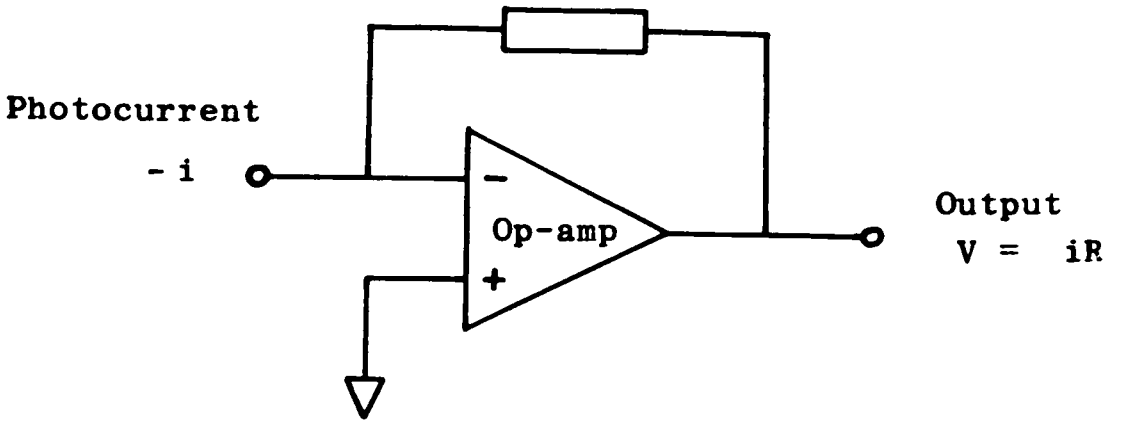

Figure 3.7 Operational amplifier used as a current-to-voltage (I-V) converter.

The actual circuits used are shown below, together with the additional electronics for offsetting and AC-coupling signals as required. Also described is the basic operation of a lock-in amplifier used in the kinetic studies of cytochrome oxidase, and the oxygen measurement cell also used in these and other experiments, for monitoring oxygen consumption.

3.3.2 Instrumentation for the Kinetic Studies of Cytochrome Oxidase.

These experiments are described in Section 4.6.6.3, and required both the oxygen content and absorbance of a solution containing cytochrome oxidase to be monitored simultaneously. In the past this has been achieved using a normal cuvette and miniature vibrating oxygen electrode (CHANCE (1954)), in contrast here an oxygen cell's large sample chamber was used as a "cuvette" with a spectrophotometer effectively built around it.

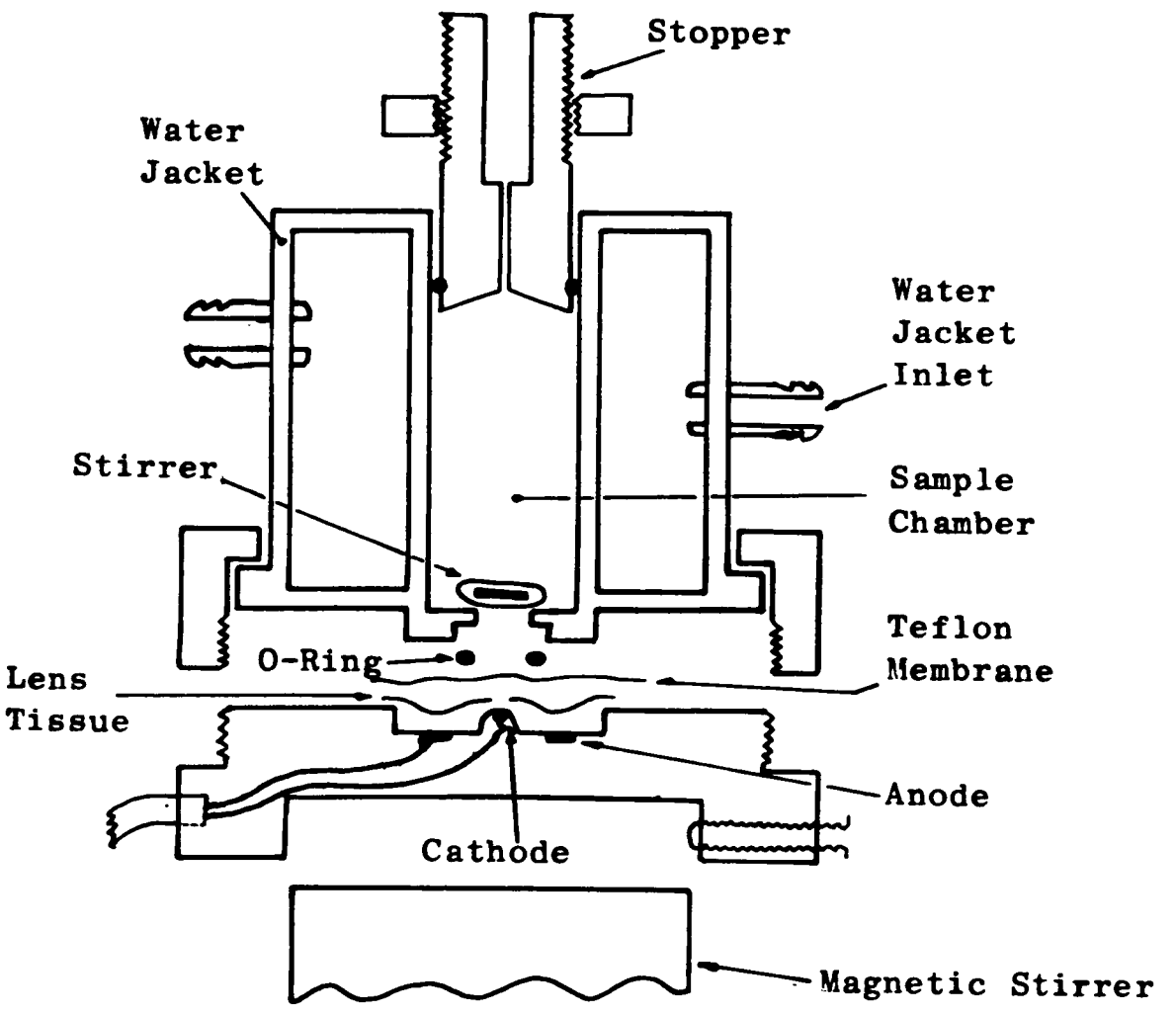

Figure 3.8 Schematic diagram of oxygen measurement cell.

A schematic diagram of the oxygen electrode (Rank Bros) used is shown in Figure 3.8. It consists of a sample chamber of about 5ml

capacity in which the solution whose oxygen content is to be measured is placed. This is closed to the air by a tight fitting stopper with a small hole in the centre that allows it to be placed in intimate contact with the sample and also the introduction of additional small volumes of solutions.

The oxygen electrode itself consists of a platinum cathode polarised at -600mV with respect to a Ag/AgCl reference electrode. The polarisation voltage is provided from an instrument previously constructed within the Bioengineering Unit. Oxygen permeable, teflon, membrane was used with an electrolyte of saturated KCl. These were held in place by an O-ring which is compressed into position when the whole oxygen electrode is assembled.

Oxygen is measured by its reduction at the platinum cathode, in the standard Clark cell configuration. Calibration is performed by equilibrating the sample with room air, and then using a small amount of sodium dithionite ($Na_2S_2O_4$) to remove all oxygen to give a zero reading. The sample is stirred by a magnetic stirrer (Rank Bros.), which is necessary to prevent depletion effects within the solution, and can be held at a steady temperature by means of the water jacket.

To enable the changes in absorbance of the sample to be monitored in addition to its partial oxygen pressure (pO_2) what amounted to a spectrophotometer was built around the sample chamber. An assembly was made housing a large area photodiode and its associated circuitry and including a fibre bundle mounting position, which can all be clamped onto the oxygen cell as shown in Figure 3.9. Light from the tungsten halogen source can be "piped" to the sample cell via a fibre bundle pressed against the water jacket. The light is then detected by the photodiode on the opposite side of the cell, directly in front of which is a holder

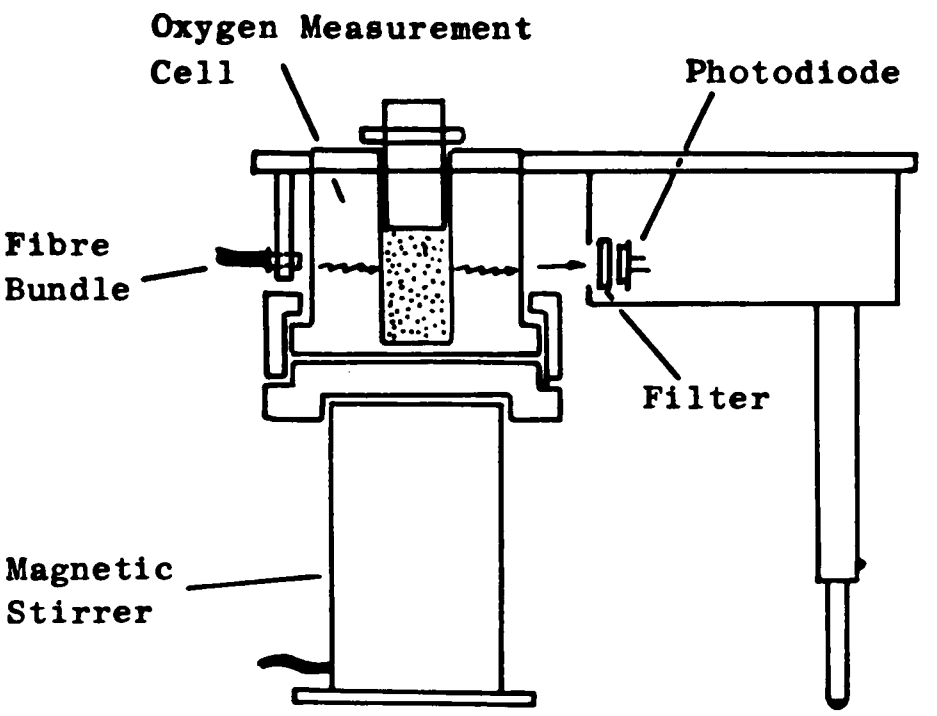

Figure 3.9 Schematic diagram of the spectrophotometer built around the oxygen measurement cell.

for an interference filter for wavelength selection.

R and C combinations:

1) 10kΩ + 1nF
2) 100kΩ + 1nF
3) 180kΩ
4) 270kΩ

Large area
Photodiode
RS 303-674

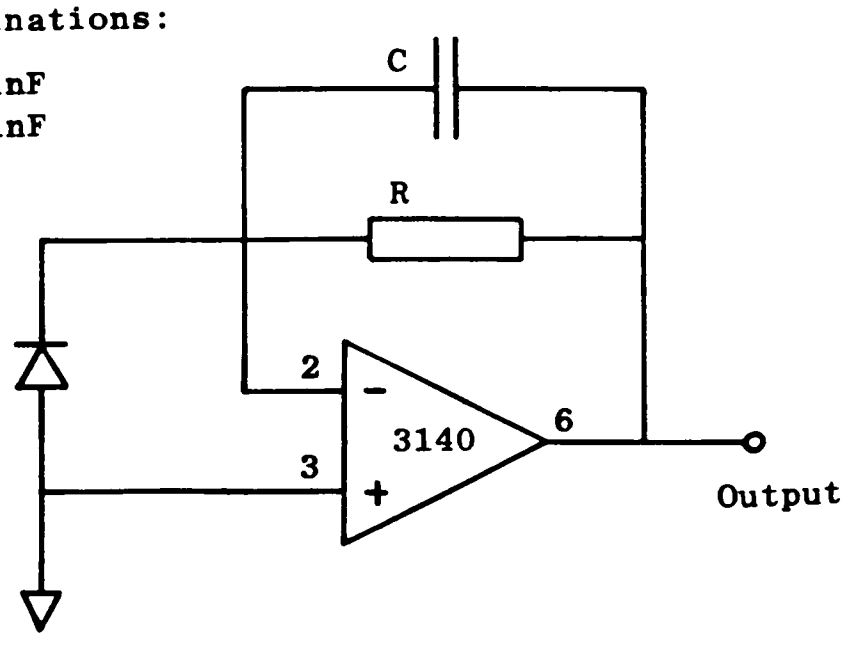

Figure 3.10 Circuit used with the large area photodiode.

This arrangement is not ideal since the light diverges from the

bundle and has to pass through the water jacket, the stirred sample and back through the water jacket before being detected. (This is the reason a large area detector was chosen to enable as much light as possible to be collected). All of these serve to introduce noise into the optical signal but despite this the overall performance was adequate. The photodiode was used in photoamperic mode (zero volts bias) in the circuit shown in Figure 3.10. The four combinations of feedback components allowed different gains to be chosen.

The experiments using this apparatus were not performed in the dark and so a lock-in amplifier (Brookdeal, 9412) was used to overcome the problem of changes in ambient light level affecting the measured intensity level. A lock-in amplifier essentially consists of a phase sensitive detector (PSD) and a low pass filter and produces an output solely dependent upon that component in the detected light level which is of the same frequency and in phase with a reference signal.

The light piped to the oxygen cell was chopped (by the chopper wheel) at 50Hz with the detected signal then fed to the lock-in amplifier. The required reference signal was taken from another photodiode (BPX 65) which detected a portion of the light from the chopper wheel before coupling into the fibre bundle. Use of the lock-in amplifier enabled all studies with this apparatus to be performed in ambient light.

3.3.3 Photomultiplier Detection Circuit.

The PMT detection circuit is shown in Figure 3.11. The anode is connected to the I-V converter via a miniature BNC connector with the circuitry enclosed in a metal box. The PMT's housing was adapted from a

PMT housing from a redundant piece of equipment. It was constructed so that it could either be bolted to the Spectralyser or accept the two sizes of optical fibres. This is shown in Figure 3.12. The I-V converter was operated from a single supply to decrease noise with the op-amp offset adjusted to give an output of zero volts when no light was present. Various values of feedback capacitor could be selected (via a rotary switch) to affect the frequency response and so the capability of the circuit to filter high frequency noise. The feedback resistor used was either 1MΩ or 100MΩ, and with this value known the output voltage was always kept at a level in line with the maximum anode current limit allowed of 100uA for 30 secs.

The high voltage supply to the PMT was supplied from a DC-to-DC converter (Hamamatsu C1309) giving an operating voltage of approximately 1kV.

3.3.3.1 Offset Circuit for Yeast Experiments.

For the experiments described in Section 4.6.6, the PMT was used with the output taken to the circuit shown in Figure 3.13. This enabled the PMT output to be offset to zero volts so it could then be observed on a sensitive scale on the chart recorder as required to see the small changes in absorbance being monitored. After the offset stage an additional op-amp inverts the signal (back to the same polarity as the input) and could be used to obtain additional gain.

The actual DC level from the PMT (ie as input to this offset circuit) was also monitored to ensure the PMT was not operating above its limit, and to enable an "absorbance" change from the yeast cells to be calculated upon going from an oxidised to a reduced state.

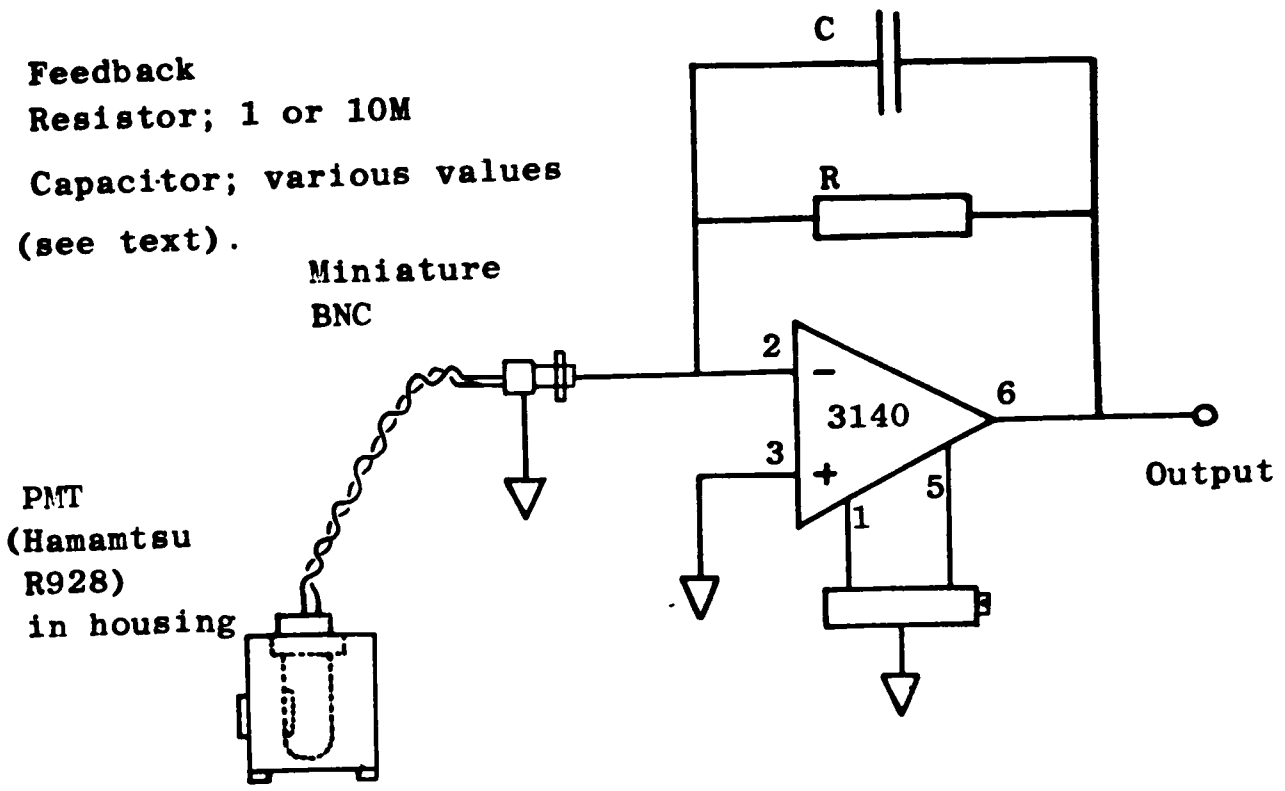

Figure 3.11 Circuit used to obtain an output voltage from the PMT.

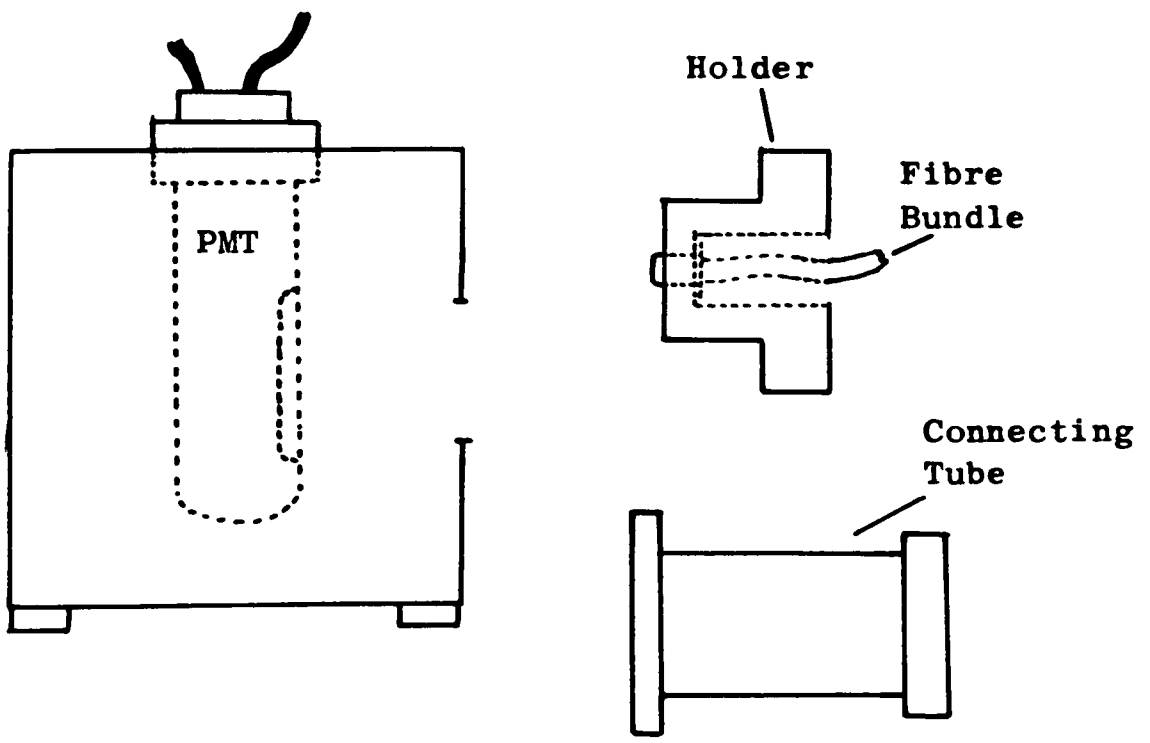

Figure 3.12 Fabricated PMT housing, fibre bundle holder and connecting tube for use with the Spectralyser

3.3.3.2 Photoplethysmography Using the PMT.

To enable photoplethysmograms (PPGs) detected with the PMT to be compatible with the instrument described in Section 7, the. circuit in Figure 3.14 was used.

This simply AC-couples the PPG through the capacitor and resistor and then amplifies it 100 times by means of a non-inverting amplifier.

3.3.4 Photoplethysmography Using a Photodiode.

The majority of PPGs were recorded using a photodiode. As described in Chapter 7 it was intended to do this without any filtering (ie AC coupling) and so an offset circuit was used to back off the "DC" light level. This left the PPG centred on zero volts where it could then be amplified without saturating any circuitry. This circuit is shown in Figure 3.15.

In the event, AC coupling was required (see Chapter 7) so a simple CR filter was used on the output of the above, consisting of a 3.3μF capacitor and various values of resistor as described in Chapter 7.

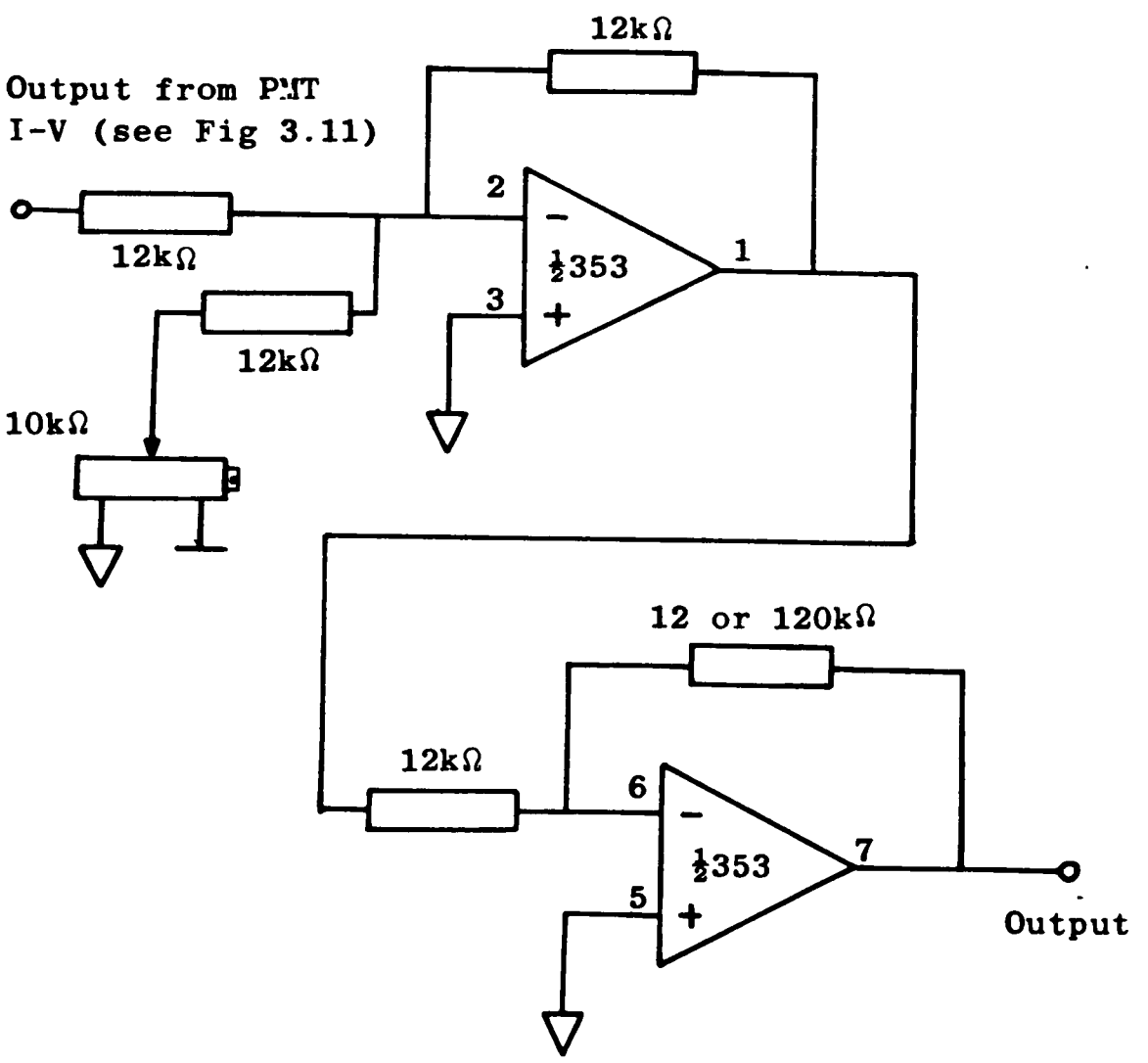

Figure 3.13 Circuit for the offset and amplification of the output from the PMT I-V converter.

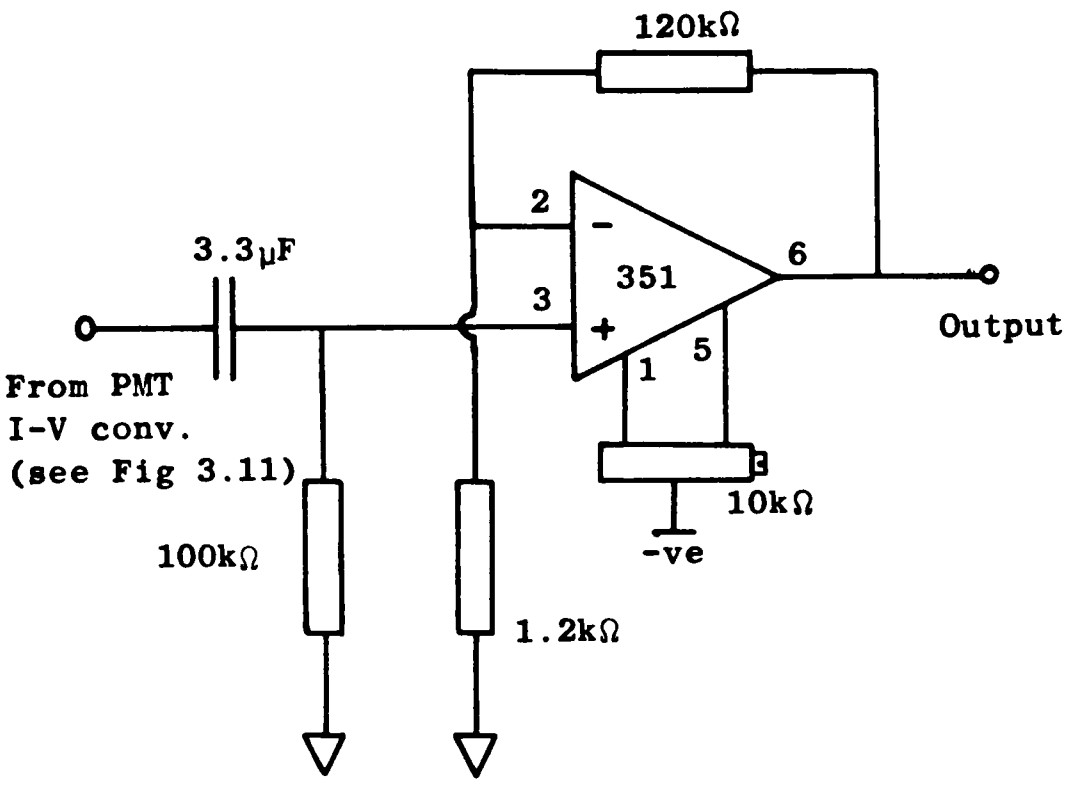

Figure 3.14 Circuit used for rerding photoplethysmograms detected with the PMT.

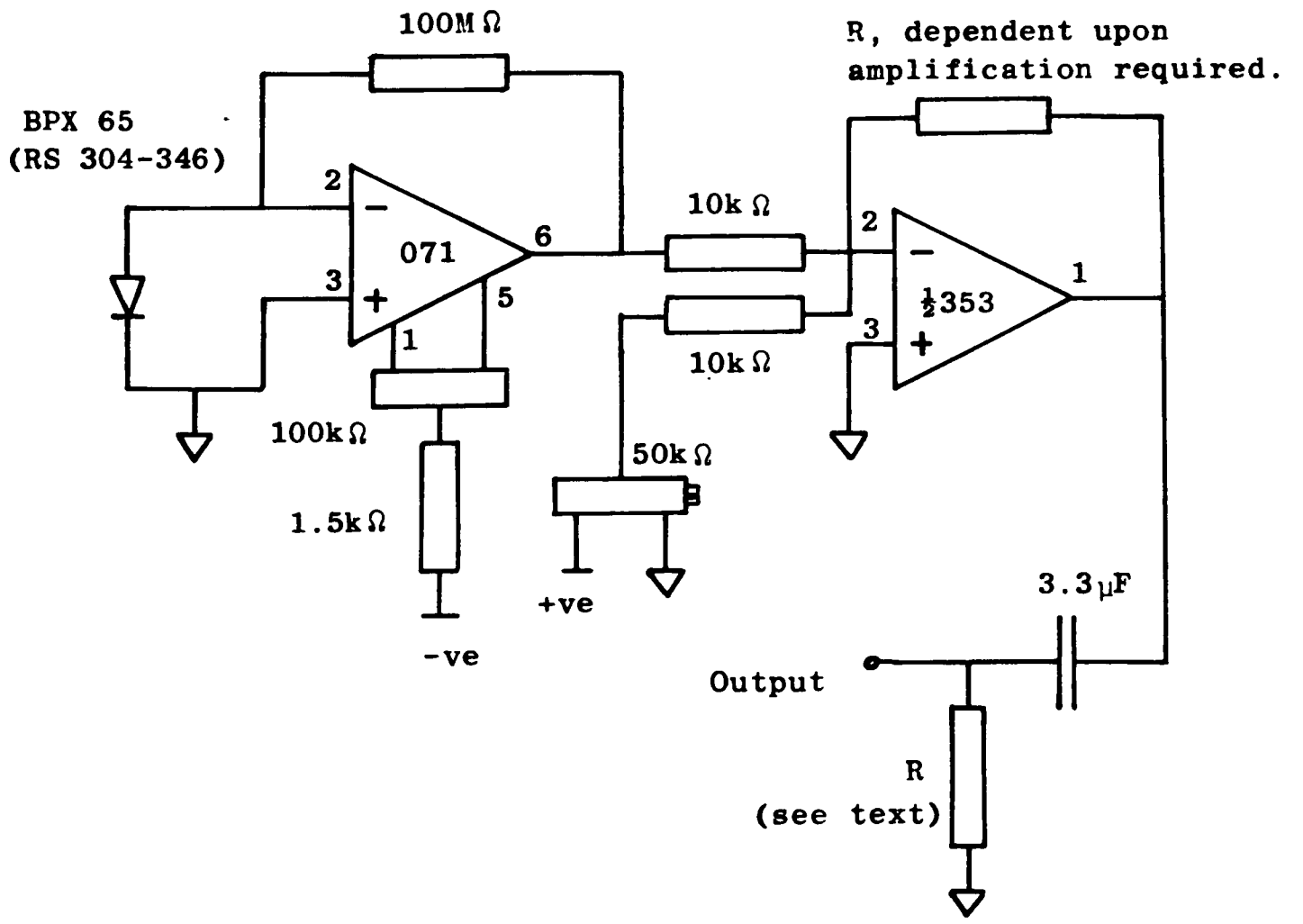

Figure 3.15 Circuit used for recording PPGs with a BPX 65 photodiode. It includes I-V converter, DC offset stage and CR filter.

3.4 Spectrophotometer Configuration.

3.4.1 Introduction.

Commercially available UV-visible spectrophotometers which generally use standard 1cm path length cuvettes are usually operated in one of three possible configurations, namely: single beam, split beam or dual beam mode. Three different spectrophotometers were used to obtain the results in Chapter 4 which covered all of these three configurations. The differences between them are now described, with details of the actual spectrophotometers used given in Section 3.4.5. Further reference to this analysis of spectrophotometer operation is made elsewhere in the thesis.

The three configurations can themselves be used in either of two ways. This is in a scanning mode, in which the variation of absorbance with wavelength is recorded, or a kinetic mode where the variation of absorbance at a fixed wavelength is studied with respect to time.

3.4.2 Single Beam Spectrophotometer.

This is the simplest type of instrument, with a light beam of intensity, I_o, shone onto the cuvette, the transmitted intensity, I, measured and the absorbance then given by the Lambert-Beer law (Equation 1.15). This process is illustrated in Figure 3.16. In this configuration the total absorbance of the sample plus cuvette (which is usually negligible) is measured. If the wavelength is gradually changed then an absorbance spectra of the sample can be obtained, whereas if there is some reaction taking place within the cuvette affecting the content's absorbance then this can be recored, at a fixed wavelengtn, versus time.

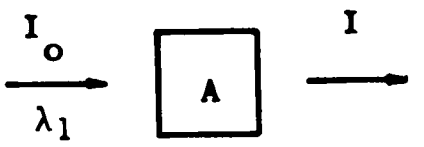

Single Beam

From the Lambert-Beer law the absorbance, A, of the sample is given by:

$$A = \log \frac{I_o}{I}$$

Figure 3.16 Schematic diagram of single beam spectrophotometer operation.

3.4.3 Split Beam Spectrophotometer.

In the split beam mode two cuvettes are used. One containing the "sample" and the other the "reference", (which will often simply be the solvent used in the "sample" cuvette).

In this mode the absorbance of the "reference" cuvette is subtracted from that of the "sample" cuvette. This ideally leaves only the absorbance due to the sample itself, since any absorbance cue to the likes of the cuvette or solvent will have been accomodated for, as illustrated in Figure 3.17. The same incident light beam is used for the two cuvettes and is normally rapidly switched between them.

It is this mode of operation that is classically used to obtain difference spectra of compounds in reduced and oxidised states. Samples in the two states are placed in the two cuvettes and the difference in absorption between them then measured.

(Although a split beam instrument effectively operates in the manner

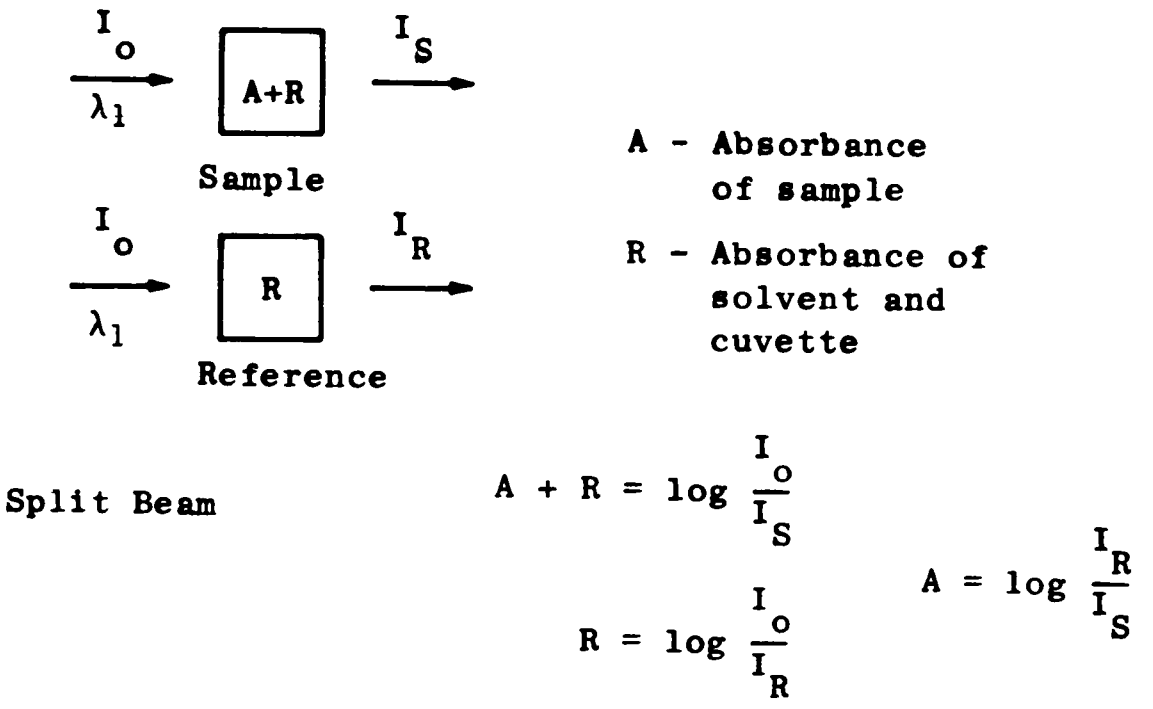

Figure 3.17 Schematic diagram of split beam spectrophotometer operation.

shown in Figure 3.17, in practice a commercial instrument may not calculate the absorbance directly by taking the logarithm of the ratio of the two intensities as shown).

3.4.4 Dual Wavelength Spectrophotometer.

3.4.4.1 Kinetic Mode.

The dual wavelength spectrophotometer only uses one cuvette but two incident light beams at different wavelengths, which are alternately shone onto the cuvette. This type of instrument was developed by CHANCE (1951c) to enable small changes in absorbance to be monitored kinetically on top of a large background attenuation due to absorbance and/or scattering. (The work of B.Chance is described in more detail in Section 4.5).

For very sensitive measurements this technique has the advantage over the split beam method, which theoretically can "remove" large background absorbances. This is because it is performed on a single

cuvette and therefore does not suffer from problems liable from mismatches in optical characteristics between the components in the "sample" and "reference" cuvettes which should, but often will not be identical. Since only one sample is used then the reference beam must be at a different wavelength than the measuring beam, hence dual wavelength.

Measurements on small changes in absorbance on top of a very large apparent absorbance can be made by using only using one beam and "bucking out" the large absorbance (in Chance's terminology, CHANCE (1954)), as done in the experiments described in Section 4.6.6. However, the advantage of the dual beam method is that it not only enables a large background absorbance to be efficiently subtracted but also allows non-specific changes in absorbance with time (ie variations not due to the event being monitored) to be compensated for. Basically any non-specific background attenuation monitored at the reference wavelength is removed from the absorbance measured by the sample beam, as illustrated in Figure 3.18.

Ideally an isobestic point is chosen for the reference wavelength so the change being monitored only affects the absorbance at the measuring wavelength (that is absorbance, X, at wavelength, λ_2, in the figure), and that also the non-specific change is assumed to be the same at both wavelengths (ie M=N).

The technique was originally practised by alternately shining the two beams onto the cuvette and monitoring the amplitude of the resultant square wave signal from the detector. By adjusting the incident light levels at the commencement of a study the levels of transmitted light at the two wavelengths could be equalised, so reducing the amplitude of the square wave to zero. Any non-specific changes would then ideally have

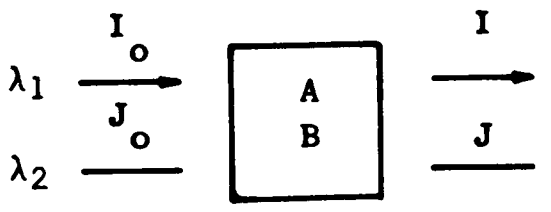

Before Change

Dual Beam

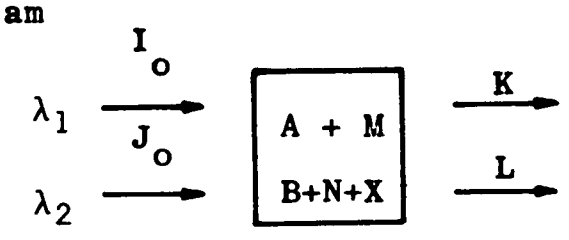

After Change

Background Absorbance at;

$$\lambda_1 : A = \log \frac{I_o}{I} \quad (1)$$

$$\lambda_2 : B = \log \frac{J_o}{J} \quad (2)$$

Non-specific change at λ_1 is M, and at λ_2 is N.

The small change to be monitored is X and only occurs at λ_2

$$A + M = \log \frac{I_o}{K} \quad (3)$$

$$B + N + X = \log \frac{J_o}{L} \quad (4)$$

From (1)+(3): $M = \log \frac{I}{K}$

(2)+(4): $N + X = \log \frac{J}{L}$

But assuming that M = N then:

$$X = \log \frac{J}{L} . \frac{K}{I} .$$

All of this holds if the Lambert-Beer law applies.

Note; If I and J are adjusted to be equal then: $X = \log \frac{K}{L}$

Figure 3.18 Schematic diagram of dual beam spectrophotometer operation.

no effect on this amplitude whilst the change in absorbance being monitored would only affect the measured intensity at one wavelength, so causing a square wave to again be output, with its amplitude indicative of the absorbance change.

This method is considered further in Section 4.10, since is is essentially this technique that was used for many of the *in vivo* non-invasive studies of the redox state of cytochrome oxidase.

3.4.4.2 Scanning Mode.

In dual beam scanning mode a single cuvette is again used with two time shared beams of different wavelengths. During scanning only the measuring beam is scanned whilst the reference remains at a fixed wavelength. Dual wavelength scanning is normally used to correct for artefacts due to scattering and consequently is only satisfactory over a relatively narow wavelength range (75nm on the Aminco DW2) since the scattering properties at the measuring and reference wavelengths should ideally be equal.

Scanning dual wavelength spectrophotometry could be used to follow how the spectrum of a turbid reaction mix varies with time, or to obtain a pseudo-difference spectrum of a sample for which the preparation of "matched" sample and reference cuvettes may be very difficult.

3.4.5 Commercial Spectrophotometers Used.

Three commercially available spectrophotometers were used to obtain the results presented in this thesis.

Philips SP6-550.

This is a single beam spectrophotometer which operates out to 1000nm, but has no automatic scanning facilities. Therefore both "scanning" and "split beam" operations had to be performed manually. with absorbances noted and then plotted for the former. and two sets of readings taken down and subtracted for the latter.

Pye Unicam SP8000.

This is a split beam scanning spectrophotometer with plotting

facilities which operates up to 700nm.

Aminco DW2.

This is an extremely versatile instrument on which the studies on yeast cells were performed. It can be operated in either split or dual beam modes, has a plotting facility and goes out to 900nm. Both modes can be used for either scanning or kinetic operation. A schematic diagram of this instrument is shown in Figure 3.19.

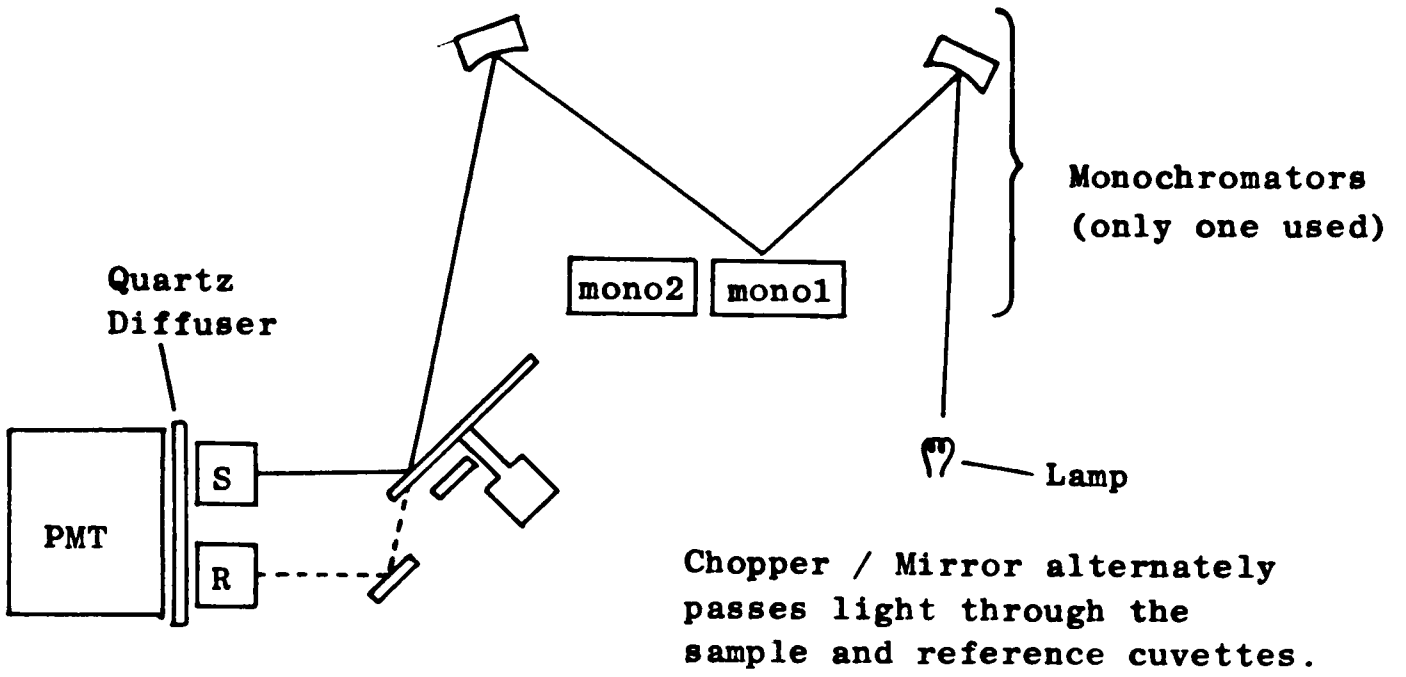

(i) Split Beam Mode

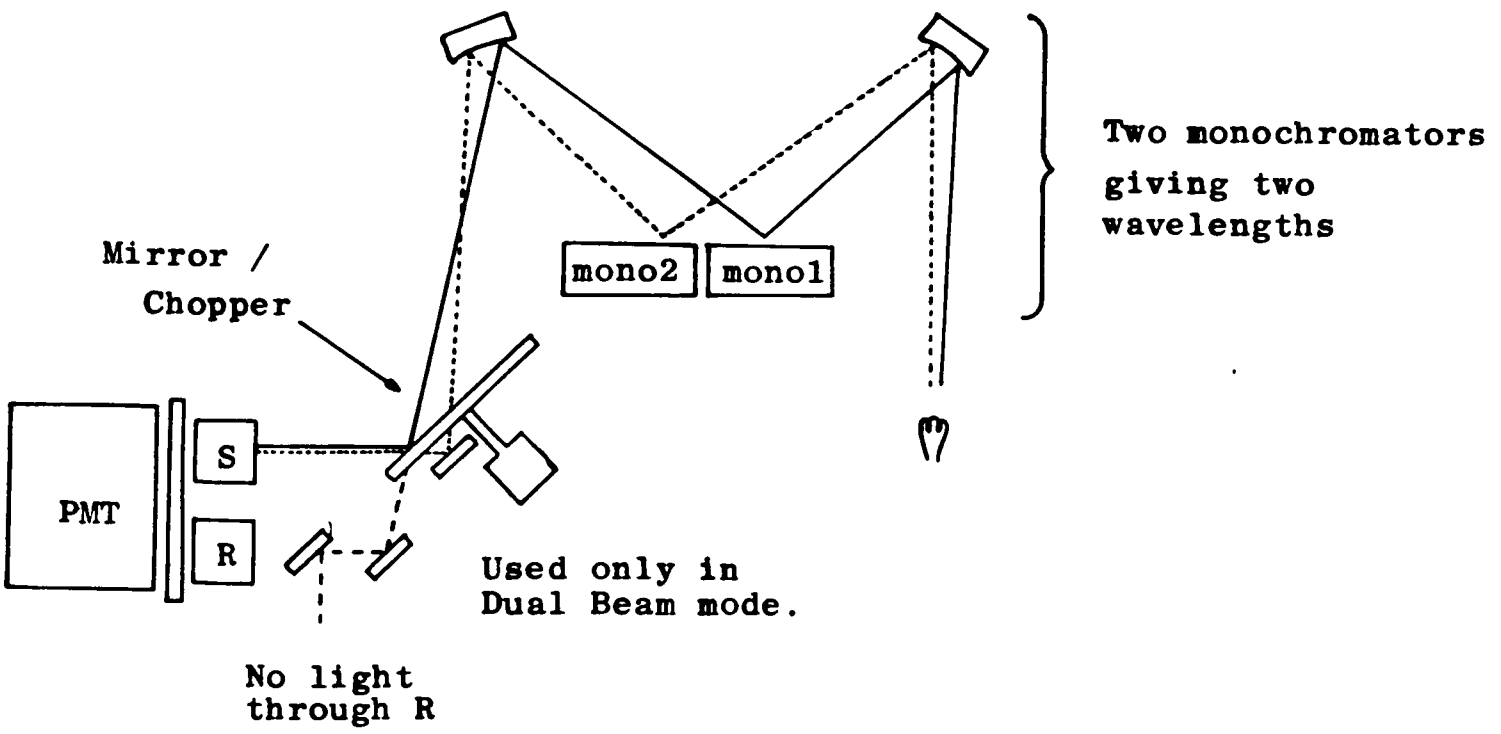

(ii) Dual Beam Mode

Figure 3.19 Schematic diagram of Aminco DW2 spectrophotometer layout as used in (i) split beam and (ii) dual beam modes.

3.5 Computer Based Scanning Spectrophotometer.

3.5.1 Introduction.

3.5.1.1 Requirements.

In order to carry out spectrophotometric studies at multiple wavelengths a scanning spectrophotometer was required. These are commercially available (and in fact examples of such were used as described above) but they are limited in that spectral scans can usually only be run on relatively clear solutions in cuvettes, although attachments (such as dual position cuvette holders (as in the Aminco DW2) and integrating spheres) are often available which also enable turbid solutions to be studied. However this type of attachment not only leads to an increase in versatility but also in cost of any such spectrophotometer.

Specifically the needs were for a scanning spectrophotometer capable of remote measurement in both "reflectance" and "transmission" modes. Such measurements can be made using optical fibre bundles to "pipe" light to and from the sample, but machines offering this facility tend to be even more expensive. It was therefore decided to attempt to construct a reliable scanning spectrophotometer, with optical fibre connections from the source and to the detector.

3.5.1.2 Basic Description of the Constructed Instrument.

Since a broadband light source, photodetectors and optical fibre bundles were already available then only a scanning monochromator was actually required to construct a simple scanning instrument. A suitable monochromator, available at a relatively low cost, is the Rofin Spectralyser 6000, in its basic form (Rofin-Sinar, UK), which essentially consists of a continuously rotating diffraction grating with appropriately

positioned input and output slits in its optical assembly (see Sections 3.2.2.3 and 3.5.2.3).

The Spectralyser is designed to display optical spectra (on an oscilloscope). A trigger pulse is provided which enables the output from the photodetector (coupled to the Spectralyser's output slit) to be displayed on an oscilloscope, so that the spectral distribution of light entering the monochromator can be analysed.

However. in this simple form the scanning spectrophotometer has several serious limitations. The traces seen on the oscilloscope will not only depend upon the spectral properties of the light from the sample under observation, but also upon the light source's spectral output. variations in the efficiency of the monochromator with wavelength and the detector's spectral response. These all serve to make interpretation and analysis of the displayed spectra extremely difficult, particularly as no hard copy output is readily available. In addition. in this form only light of sufficient intensity to enable the output from the photodetector to be clearly displayed on the oscilloscope can be analysed.

These limitations were overcome by using a TMS990 microcomputer (Texas Instruments. (TI)) to sample and process the signals from the photodetector attached to the Spectralyser. together with a HP7475 plotter (Hewlett Packard) to provide hard copy output.

The way the instrument operates is that the trigger pulse from the spectralyser and output from the photodetector are input to the TMS990 via a RTI-1241-R 12-bit analogue-to-digital (A/D) converter (Analog Devices). The trigger pulse is used to synchronise sampling and averaging of the photodetector output. thereby improving the signal-to-noise ratio (S/N) and allowing light to be analysed which would not produce a clear trace on an

oscilloscope.

Once averaged the digitised spectra are stored in memory, from where they can be either retrieved singly to produce hard copy output of the same type of "raw" plot observed on the oscilloscope. or used in pairs to produce "absorbance" or "transmittance" plots using one spectra as a reference. The signal processing required to produce the latter type of plots gives a trace which is theoretically solely dependent upon the optical characteristics of the sample (ie not dependent upon parameters such as the detector's spectral response). "Difference" plots of two spectra can also be obtained.

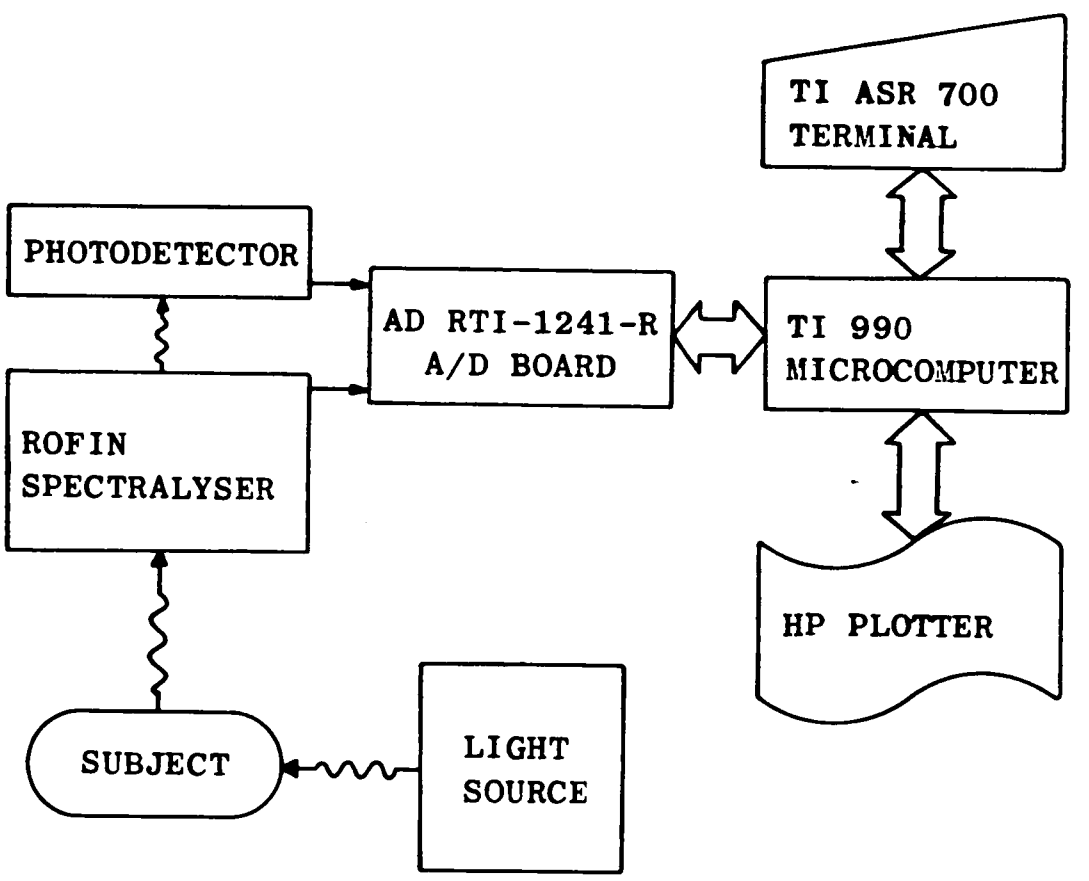

Figure 3.20 Block diagram of the computer controlled scanning spectrophotometer.

The instrument is operated by input via an ASR700 teletype terminal (TI) which also provides prompts and other pertinent information. A block diagram of the microcomputer based scanning spectrophotometer is shown in

Figure 3.20.

The spectrophotometer can be used in two modes: single spectra operation, where one spectra at a time is averaged and stored, or multi-spectra operation which allows many spectra to be taken (each one consisting of a number of averaged and stored spectral scans) at specified time intervals. When used on the same sample, multi-spectra operation can be used to perform kinetic studies.

3.5.2 Spectrophotometer Hardware.

3.5.2.1 Light Source.

The light source used for all studies was the tungsten halogen source as described in Section 3.2.1.1. Various optical fibre bundles (see Section 3.2.4) were used to take light from this source to the sample.

3.5.2.2 Wavelength Selection Mechanism: Rofin Spectralyser.

The Rofin Specralyser. which this instrument is based upon was described in Section 3.2.2.3. It provides a swept optical spectrum from 350-1100nm over 10ms and repeated about every 95ms, and a trigger pulse synchronised to the beginning of each spectra (as shown in Figure 3.21. Hence the output spectra can be observed on an oscilloscope.

The spectralyser must be calibrated before use to determine the relation between the time elapsed after the trigger pulse and the wavelength of the light incident on the output slit. This is because changing the bandwidth (and hence slit width) may result in lateral displacement of the slits centre in relation to the output aperture. hence recalibration is necessary after each such adjustment. This is achieved using a white light source and several interference filters to provide reference wavelengths, although any spectrally distinctive source will suffice.

Because second order spectra are not automatically removed then blocking filters should be used to stop all light below λ nm from entering the monochromator so that no second order effects will be seen up to 2λnm, leaving the wavelength range from λ- 2λnm free for unambiguous use. Two filters (OG395 and OG570. Rofin-Sinar)) with sharp transmittance cut-offs below approximately 395nm and 570nm respectively allow such use within the

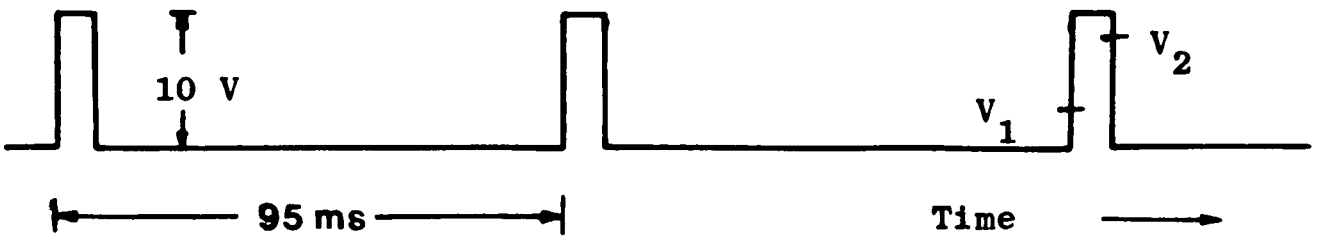

Trigger output from Spectralyser.

Output from photodetector.

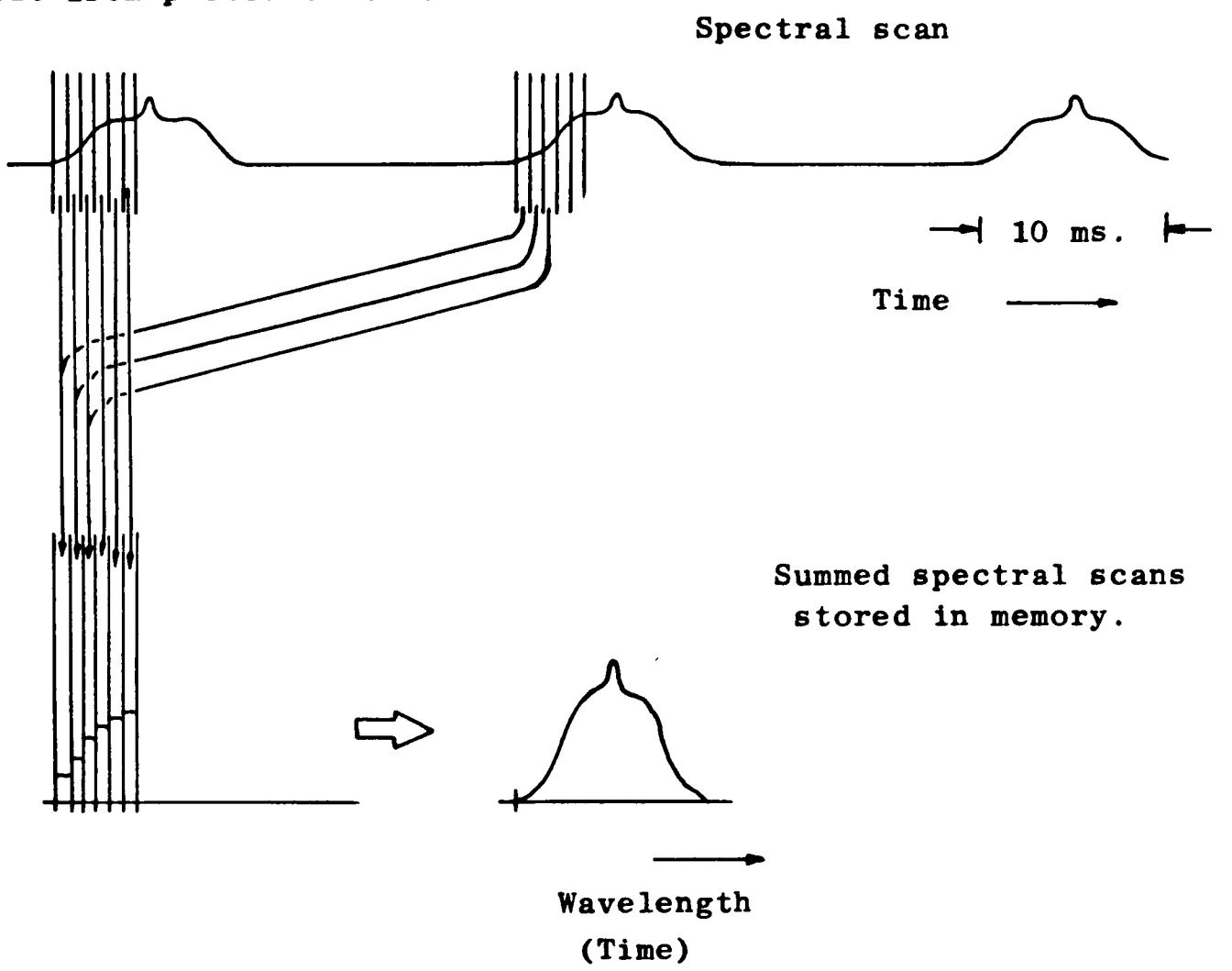

Figure 3.21 Ideal outputs from the Spectralyser trigger channel and photodetector.

Corresponding samples from consecutive spectral scans are summed to produce the summed output spectrum.

approximate spectral ranges of 375-700nm and 570-1100nm.

The Spectralyser's electronics consist of the DC motor for rotating

the grating and associated drive circuitry, a trigger pulse generator and a high gain transimpendance amplifier for use with the photodiode detector.

3.5.2.3 Photodetectors.

Two types of detector were used with the Spectralyser. The photodiode supplied by Rofin and the PMT (see Section 3.2.3). The photodiode was located in a housing specifically to fit into the Spectralyser with the output then going into the transimpedance amplifier housed within the Spectralyser via a BNC connector. as shown in Figure 3.4.

The PMT was mounted in a PMT housing from a redundant piece of equipment which was extensively modified to fit onto the Spectralyser over the output slit at the appropriate angle and distance, this was shown in Figure 3.12.

3.5.2.4 Optical Fibre Bundles.

These were used to "pipe" light from the source to the sample, and from the sample to the Spectralyser and required the fabrication of "collars" to go over the bundle terminations to ensure a good fit into the Spectralyser. (see Figure 3.4)

3.5.3 Instrument Operation and Software Overview.

The trigger pulse and photodetector outputs were input to the TMS990 via channels 0 and 1 of the A/D converter, which was configured to accept voltages from 0 to 10 volts. The programme which controls the overall operation of the spectrophotometer was written in POWER BASIC (TI) with assembly language routines used for the realtime sampling of the photodetector output and trigger pulse. The programme is held on cassette and must therefore be loaded from the ASR700 terminal before use. The BASIC and assembly language programmes are given in Appendices B and C respectively. The spectrophotometer is controlled from inputs to the ASR700's conventional keyboard, with prompts and other relevant information also printed out on this device.

When using the spectrophotometer the user must choose either single-spectra or multi-spectra operation which are described in Sections 3.5.5 and 3.5.7 respectively. (The choice can be reversed at a later stage from within the programme). Depending upon which mode is chosen one of two segments in the main programme is entered. Both of these segments then access the same subroutines which control and run the instrument. The overall structure of the programme is shown in Figure 3.22.

With reference to Figure 3.22 sampling of the required number of spectral scans for averaging any one spectra is carried out by Subroutine A which is described in Section 3.5.4. The four types of graphical output (raw, transmittance, absorbance, difference) are obtained using the Subroutines B, C, D, E. These four routines in turn use Subroutines I, J, K. Three additional (Subroutines F, G, H) enable the format of the graphical output to be changed. The operations of all of these routines affecting graphical output is described in Section 3.5.6.

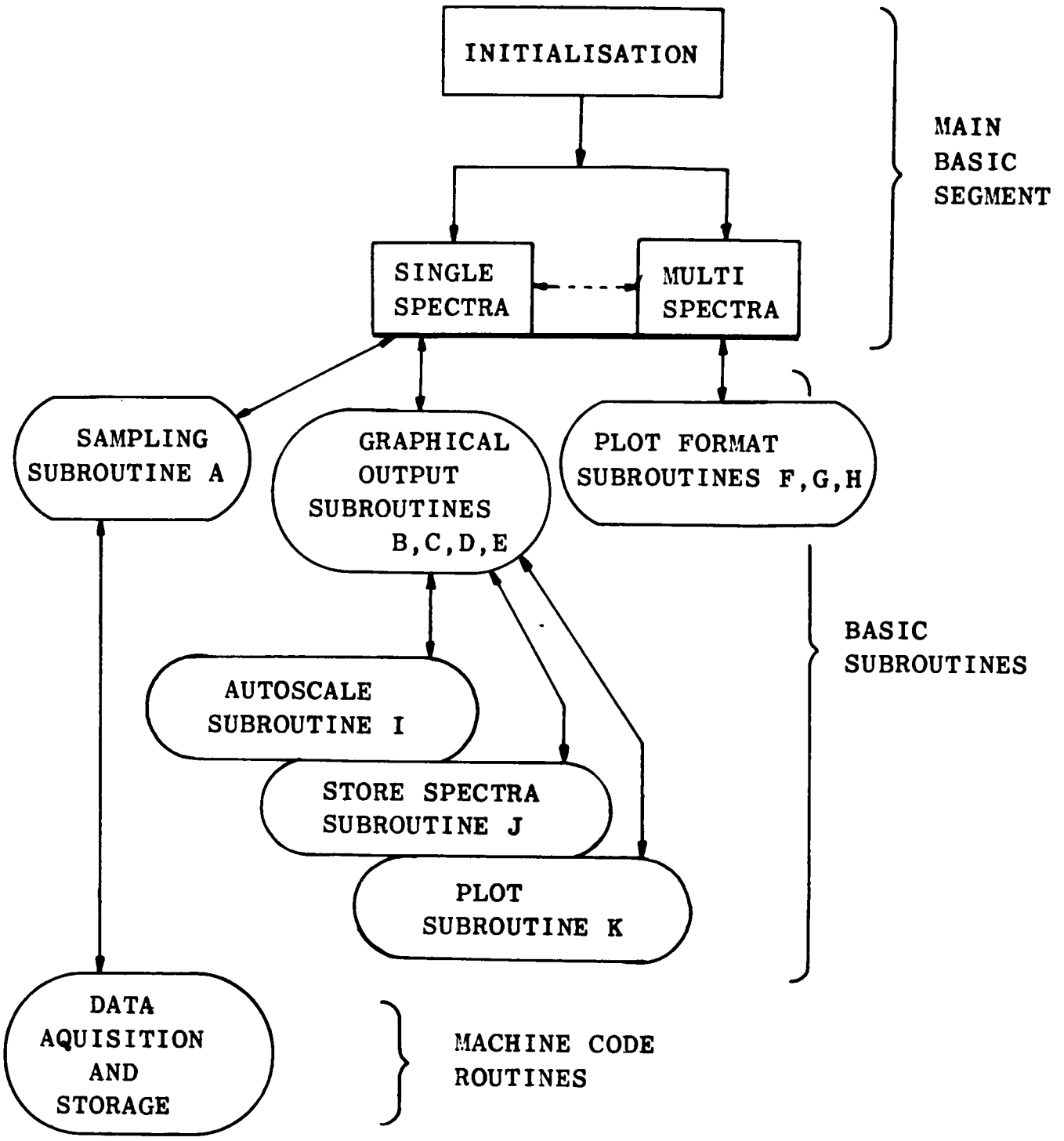

Figure 3.22 Overall structure of the programme which operates the spectrophotometer.

3.5.4 Sampling Subroutines.

When used with an oscilloscope the negative edge of the Spectralyser's igger pulse is used to initiate the beam sweep with the output from the otodetector (coupled to the Spectralyser) displayed on the vertical axis. is procedure displays the optical spectra on the screen, updating about

every 95ms and with each spectral scan lasting about 10ms. Typical output of these two signals was shown in Figure 3.21.

The whole operation of this microcomputer-based scanning spectrophotometer relies upon the sampling, summation (for subsequent averaging) and storage of the spectral scans which can then be processed and plotted. As with oscilloscope based operation it is the negative edge of the trigger pulse which initiates this sampling.

The data acquisition and storage is accomplished by the sampling routines described below which upon detection of the negative edge of the trigger pulse, sample the spectral scan and sum corresponding samples from consecutive spectra (related by the elapsed time from the negative edge) as illustrated in Figure 3.21. Once the required number of spectral scans have been sampled and summed then the values are stored in memory (the memory map as used is shown in Appendix D) together with the number of spectral scans sampled. The data can then be used for Processing and plotting.

3.5.4.1 BASIC Sampling Routine (Subroutine A).

The flow diagram for the BASIC sampling routine is shown in Figure 3.23. For multi spectral operation the number of spectral scans to be sampled and summed will already have been specified (see Section 3.5.7) for single-spectra operation the required number must be given. Following this, identification of the spectra about to be sampled is given, the "bell" warns that sampling is imminent and the assembly language data acquisition routine is called. After the assembly language routine is complete the time is recorded (for annotation of graphical output) and the programme returns to the main segment.

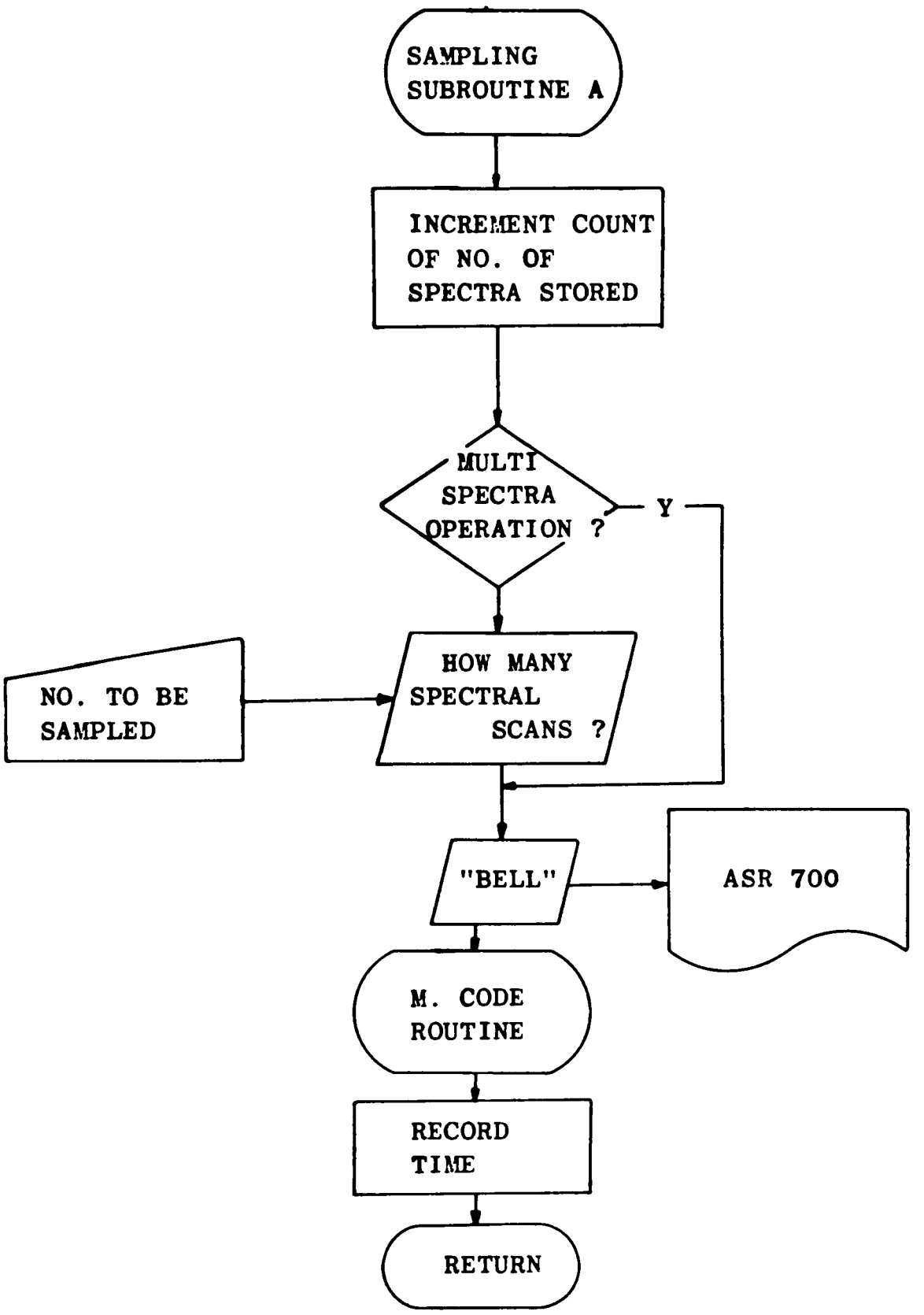

Figure 3.23 BASIC sampling subroutine, which calls the machine code data acquisition and storage routine.

3.5.4.2 Assembly Language Data Acquisition Routine.

The sampling, summation and storage of data is performed by this

machine code routine which consists of three segments.

1) Detection of the trigger pulse's negative edge.

2) Sampling and summation of samples from the required number of spectral scans.

3) Data storage.

These are described in detail below with the flow diagram shown in Figure 3.24.

3.5.4.2.1 Negative Edge Detection.

The output from the trigger pulse generator is sampled approximately every 30μs with these values then used in the negative edge detection algorithm. The principle behind the algorithm is firstly to detect the trigger pulse and then its negative edge.

A positive/negative edge can simply be detected by the signal under observation going above/below some threshold value. Hence the presence of a positive pulse can be detected by its positive edge going above threshold value V1. with its negative edge signified by the signal falling to below V2. This algorithm is shown in Figure 3.24 with typical levels of V1 and V2 illustrated in Figure 3.21. Once a negative edge has been detected then the programme passes onto the actual data acquisition routine.

3.5.4.2.2 Sampling and Summation of Phototdetector Output.

After the trigger pulse's negative edge has been detected then the spectral scan from the photodetector output is sampled 200 times, at intervals of approximately 42μs timed using a software timing loop. This is the fastest rate at which the A/D board can be operated without error in view of its samples from previous spectral scans as shown in Figure 3.21.

This method of summing a sampled signal in time "bins" is a standard

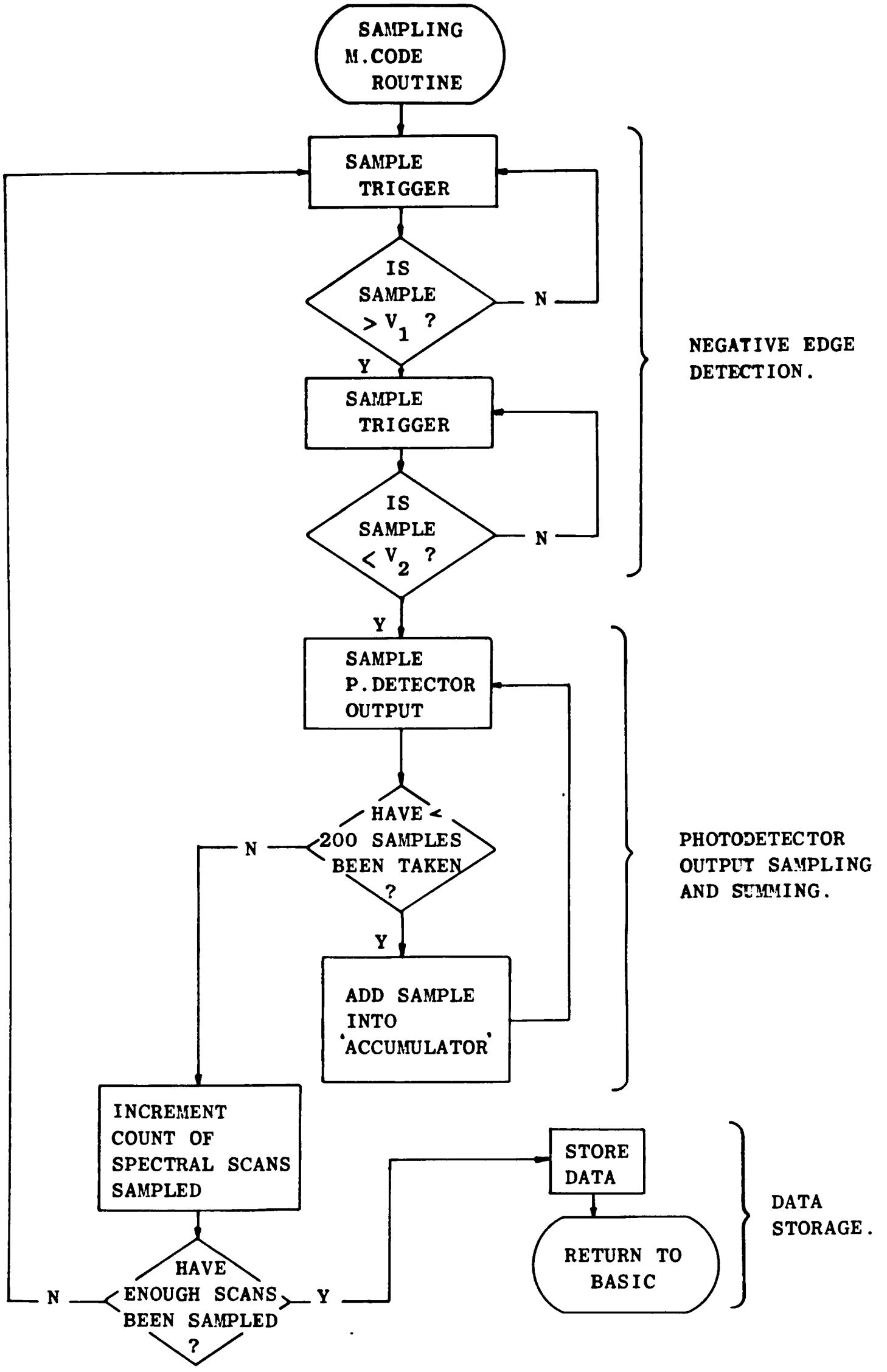

Figure 3.24 Flow diagram of the machine code routine which samples and sums the photodetector output, synchronized to the negative edge of the trigger, and then stores the summed values.

means of averaging noisy signals to achieve a greater S/N ratio as the

random noise adds at a slower rate than the underlying signal.

The total sampling time is about 8.5 ms during which time the Spectralyser will have scanned from approximately 350 to 1100nm). Resolution (in terms of sampling rate) is therefore about 4.5 nm. Once 200 samples have been taken and summed then the programme moves onto the final segment.

3.5.4.2.3 Control and Data Storage.

Following data acquisition, the number of spectral scans which have been sampled is incremented by one and compared to the number requested. If equal then the summed values are stored in memory together with the number of spectral scans sampled (for subsequent processing), and the programme returns to the BASIC subroutine. Otherwise the programme returns to the negative edge detection algorithm and repeats the above cycle until sufficient spectral scans have been sampled.

3.5.5 Single Spectra Operation of the Spectrophotometer.

In single-spectra operation the instrument is capable of sampling and storing up to 17 different spectra. (limited by the available memory). These can then be used to produce graphical output using the routines described in Section 3.5.6. The flow diagram in Figure 3.25 shows the initialisation sequence of the spectrophotometer programme, and subsequent single spectra operation.

Upon running the programme the time, date and spectral range must be entered. The spectral range refers to the extent of the spectra which will be output graphically, not the actual range sampled (200 samples are always taken), and is specified by sample number not wavelength, due to the calibration problems described in Section 3.5.2.2. Three ranges are initially available giving graphical output over the ranges: 1-60. 31-170. or 61-200 samples, although the facility to select any spectral range is available as described in Section 3.5.6.

The user must then choose either single or multi-spectra operation. In single-spectra mode (Figure 3.25) the sampling routine (Section 3.5.4) is called, and the first spectra sampled and stored. The programme then reaches Node 1. one of two points in the programme where the user must select the next operation.

3.5.5.1 User Choice of Programme Operation.

Node S1: "Plot or Sample?"

Choices of the next operation are as follows.

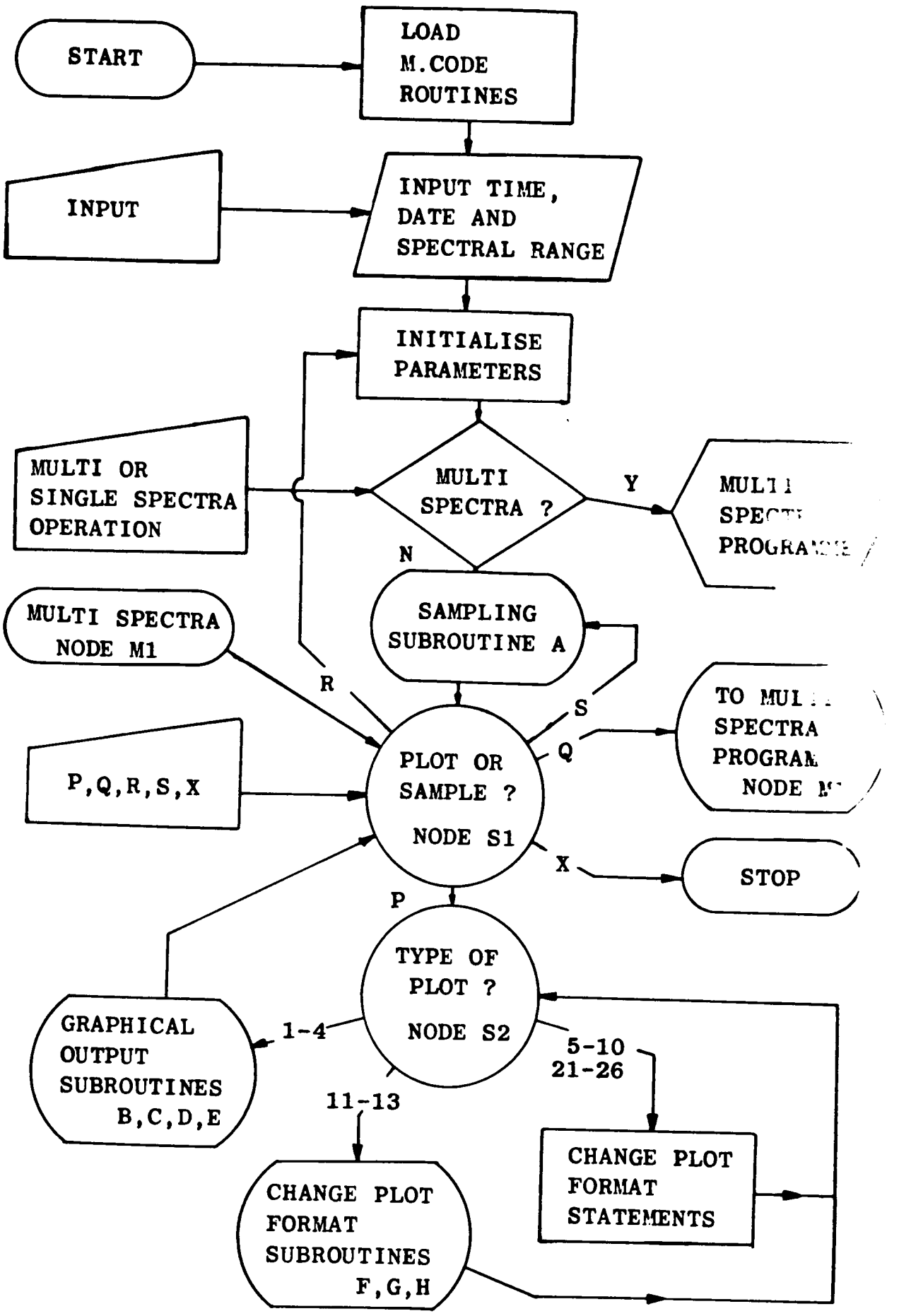

Figure 3.25 Flow diagram of the spectrophotometer programme showing the initialization sequence and single spectra operation.

P Obtain graphical output (goes to Node S2)

Q Obtain graphical output using multi-spectra routine.

R Restart (All previous spectra deleted).

S Sample another spectra.

X End programme.

Node S2: "Type of Plot?"

Node S2 is reached when graphical output is required, and allows the user to select one of the four types of plot available, or change the plot format. The available options are shown in Figure 3.26 and described in more detail in the following section.

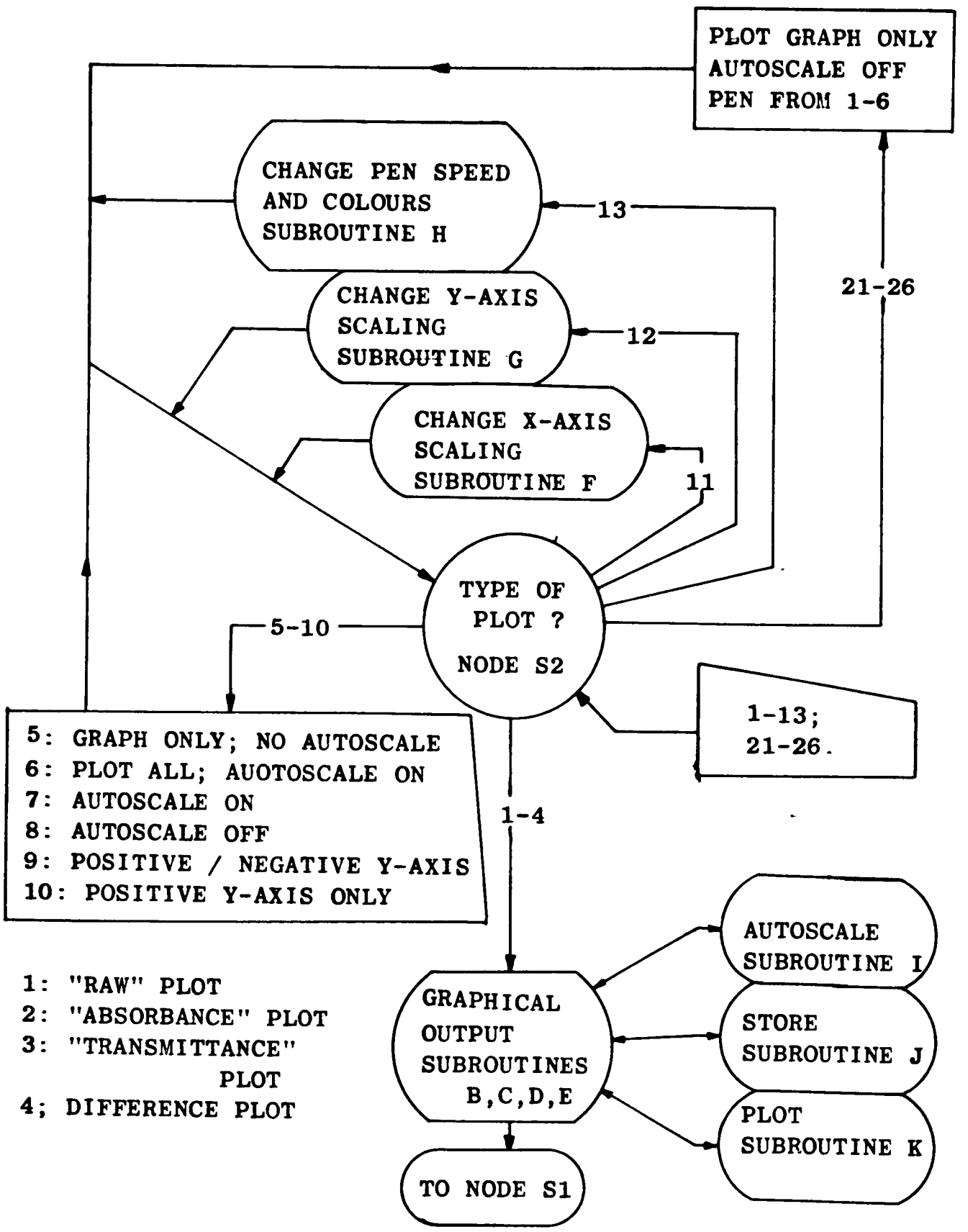

Figure 3.26 Available options for graphical output at Node S2.

3.5.6 Graphical Output Routines.

3.5.6.1 Introduction

Four types of graphical output are available and are selected by the input of a number from 1 to 4 which selects the type of plot as follows:

1) "Raw" plot

2) "Absorbance" plot

3) "Transmittace" plot

4) "Difference" plot

All plots are automatically annotated with time, date and other relevant information with the option for further copies available.

3.5.6.1 "Raw" Plot. (Subroutine B).

This plot simply gives the spectral scan as it would be observed on an oscilloscope, with the exception that the signal-to-noise ratio (S/N) of the plot will be increased, as usually more than one spectral scan will have been sampled and averaged. The ordinate represents the output from the photodetector and the abscissa, wavelength (ie sample number).

3.5.6.2 "Absorbance" Plot. (Subroutine C).

With the "raw" type of plot the trace obtained will be dependent upon the spectral characteristics of the source, detector and all conecting optics in addition to those of the sample which are actually under investigation.

This problem is overcome by normalising the spectra obtained from the specimen with a reference spectra obtained with the specimen absent (ie of the light source only). Essentially corresponding samples from the two spectra are used to calculate an "absorbance" which is then plotted. Since this involves taking the log of the ratio of the samples (as in calculating any absorbance (see Equation 1.15)) then all unwanted

characteristics such as those of the source, detector and connecting optics are cancelled out giving a value solely related to the "absorbance" of the specimen. This is fundamentally split beam operation as described in Section 3.4.3.

This method of processing allows any variations in spectral charactristics between two specimens to be determined, since any similarities in absorbance, will simply be subtracted. This feature is used in Chapter 6.

The inverted commas around "absorbance" are used since a plot can be obtained in "reflectance" mode or from a highly turbid sample in "transmittance" mode with attenuation not only due to absorbance, and therfore not in strict compliance with the Lambert-Beer law. The ordinate represents "absorbance" given by:

$$A = \log \frac{\text{Reference Level}}{\text{Signal Level}} \qquad 3.1$$

Negative "absorbances" can be accommodated which may be required for kinetic experiments when transmitted or reflected light may actually increase.

3.5.6.3 "Transmittance" Plot; (Subroutine D).

The "transmittance" plot again involves normalising the samples representing the spectra obtained from a specimen with those from a reference spectra and so fundamentally offers the same advantages of independence from unwanted effects. The difference between this and the "absorbance" plot is in the processing, with the ordinate representing "transmittance" given by:

$$T = \frac{S}{R} \times 100 \qquad 3.2$$

The inverted commas indicate that the "transmittance" may actually be calculated from reflectance data, and so the term "transmittance" refers only to the type of processing, which calculates the value for the samples from the signal spectrum as a percentage of the reference.

In kinetic studies where both increases and decreases in the "transmitted" light are likely to occur, the transmittance is plotted as a percentage change, ΔT in "transmittance":

$$\Delta T = 100 \left[\frac{S}{R} - 1 \right] \qquad 3.3$$

3.5.6.4 "Difference" Plot; (Subroutine E).

This type of plot can be used to monitor for small changes in light level transmitted or reflected by a sample. The difference is calculated simply as one signal minus another and therefore no normalisation takes place.

3.5.6.5 Subroutines called from the Plot Routines; (Subroutines J-K).

For all types of plot the user must input the identification numbers of the signal (and for all except the "raw" plot) reference spectra. In addition for all except the "raw" plot an identification number of where the resultant calculated spectra is to be stored must be given. ("0" if no storage required). The stored spectra can subsequently either be plot on different axes using the "raw" type plot, or the difference spectra of two such stored spectra can be found. The storage facility is implemented by the storage routine (Subroutine J).

For any plot automatic scaling of the ordinate axis is available if required using the "Autoscale" routine (Subroutine I). The actual plotting of graphical output is carried out by the "Plot" routine

(Subroutine K) which consists of plot instructions to the HP7475 plotter written in Hewlett Packard Graphics Language (HPGL).

3.5.6.6 Additional Plot Format Facilities; (including Subroutines F-H)

The format of graphical output can be changed in various ways through responses of 11,12 or 13 at Node S2 (Figure 3.26). Subroutine F allows the graph to be plot over any spectral range required, whilst Subroutine G enables any desired ordinate scaling to be chosen if the "Autoscale" facility is inadequate for any reason. Subroutine H allows any pen speed and separate colours to be selected for the frame, labels and axis.

From Figure 3.26 it can be seen that in addition the options exist for only a graph to be plot (Response 5) (no frames, no axes) allowing over-plotting, using different colours if required (Responses 21-26). This facility can be reversed when necessary (Response 6). The "Autoscale" facility can be turned on and off as required (Responses 7, 8) and either a totally positive or positive/negative ordinate axis chosen (Responses 9, 10) which may be necessary for applications, where the light level at different wavelengths may either increase or decrease.

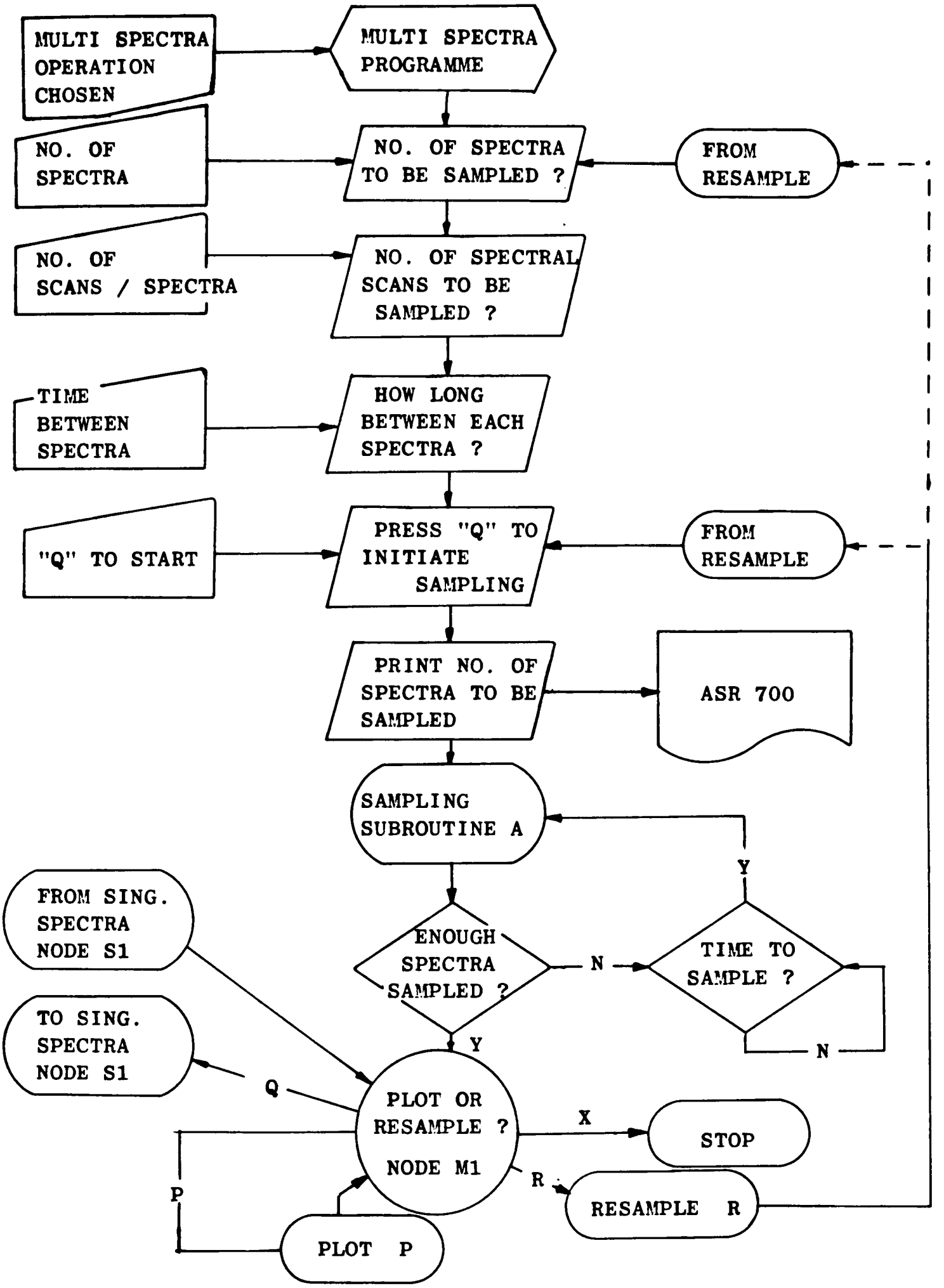

Figure 3.27 Flow diagram for multispectra operation of the spectrophotometer.

3.5.7 Multispectra Operation.

The preceding description has been of single spectra operation, multi-spectra operation (see Figure 3.22) is now considered with the flow diagram for this shown in Figure 3.27.

For multi-spectra operation the total number of spectra to be studied, the number of spectral scans to be sampled, summed and stored for each of these spectra. and finally the time interval between commencement of sampling each spectra must all be given. as can be seen in Figure 3.27. Once these parameters have been given, the key "Q" must be pressed to initiate the sampling sequence, upon which the sampling routine (Subroutine A; see Section 3.5.4) is called.

When each spectra has been sampled and stored a check is made to see if the required number of spectra have been sampled. If not then the programme cycles in a loop until the desired time interval between each spectra has elapsed, upon which the sampling routine is called again. Timing is performed using an internal BASIC timing function which generates an interrupt every 40ms. When enough spectra have been sampled the programme reaches Node M1 which is one of two points where the next operation must be chosen (similar to single spectra operation).

3.5.7.1 User Choice of Programme Operation.

Node M1: "Plot or Resample?"

Choices of the next operation are as follows (see Figure 3.27).

P Obtain graphical output (Goes to Node M2). See below

Q Go to single-spectra operation, entering at Node S1.

R Resample (see Figure 3.29).

X Stop.

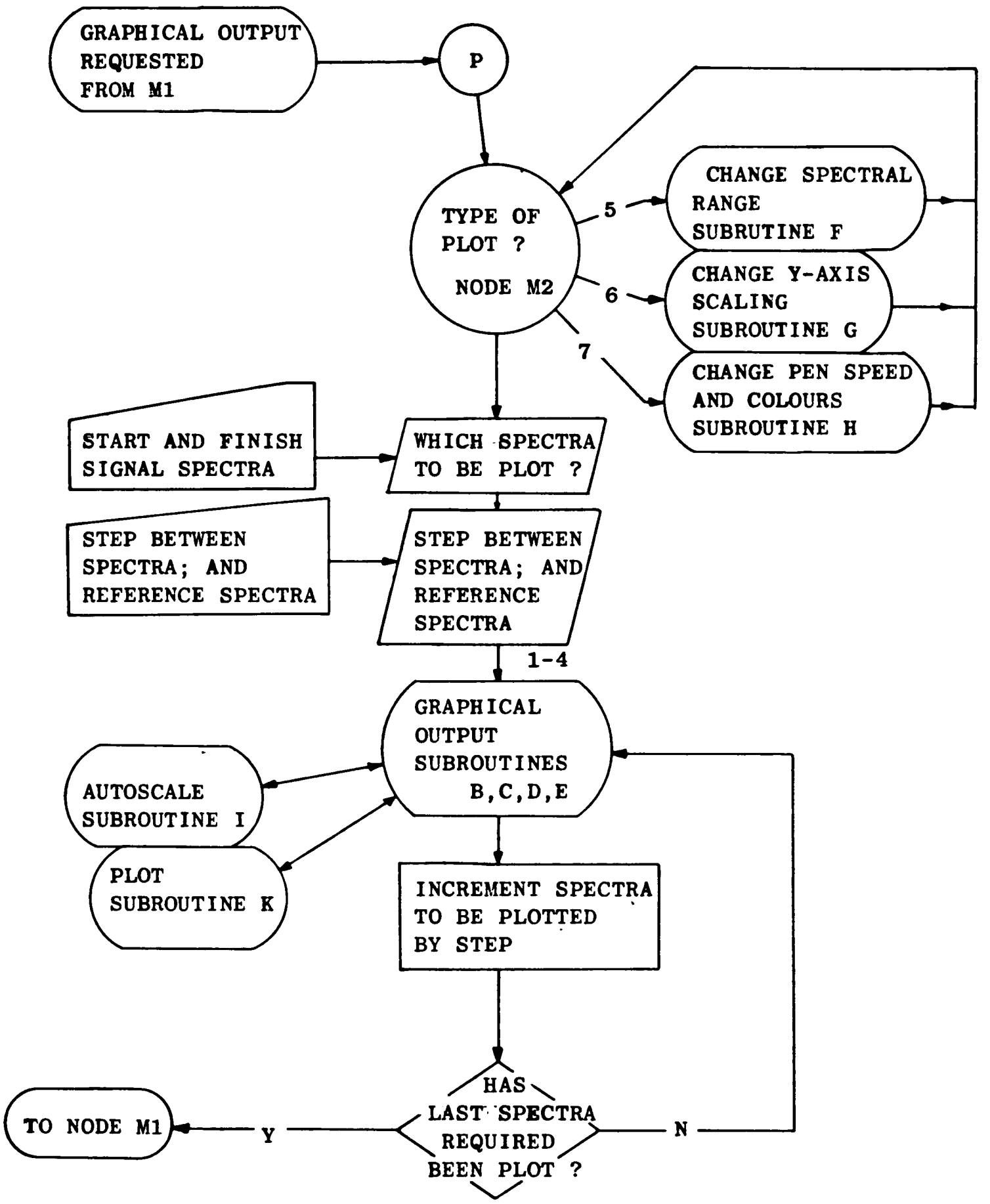

Figure 3.28 Options available to the user at Node M2 during multispectra operation.

Node M2; "Type of Plot?"

Node M2 is reached when grahical output is requested at Node M1. The same types of spectra can be plot as described in Section 3.5.6 for single spectra operation. with similar facilities available (through the same subroutines) for altering the plot format.

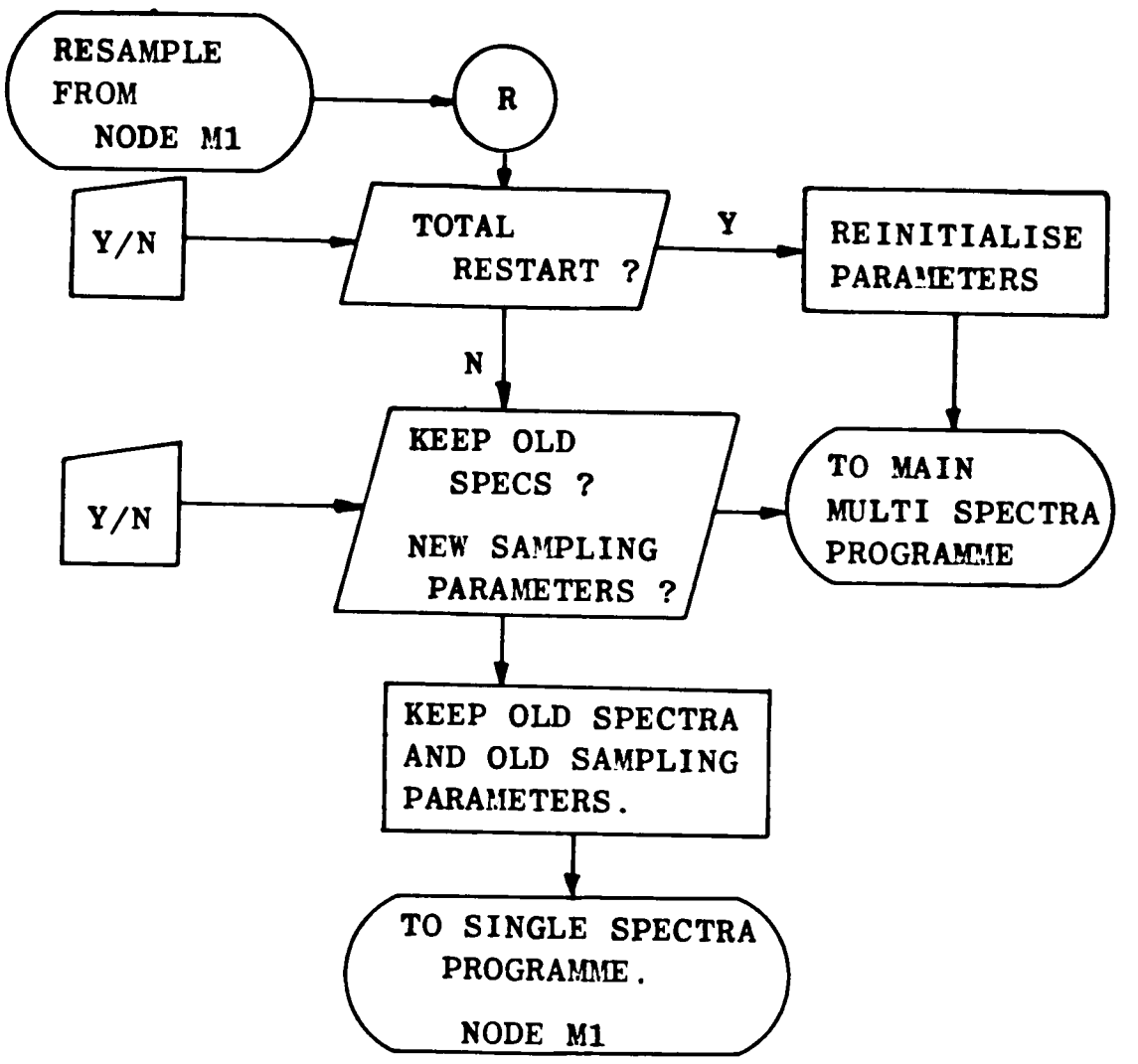

Figure 3.29 User options for resampling during multispectra operation.

To augment the multi-spectra sampling, multi-spectra plotting is possible. The range of spectra to be plot must be given (identified by their storage positions) and then the spectra which is to act as reference, and the steps between spectra to be plotted (if every one is not required), entered. This is illustrated in Figure 3.28.

3.5.8 Performance of the Scanning Spectrophotometer.

200 samples are taken from the output from the photodetector connected to the Spectralyser during each spectral scan which lasts about 8.5ms (see Figure 3.21). Thus the sampling time of aproximately 42μs gives a resolution (in terms of sampling) of about 4.5nm, since the region scanned is approximately 350-1250nm.

As described above any spectrum obtained can be averaged over many spectral scans. The averaging limit is only restricted in that the summed values before averaging must be less than 80V, a limit imposed by the resolution of the microcomputer.

The photodiode and PMT used with the Spectralyser allow a wavelength range from about 400-1100nm to be covered with the lower and upper limits chiefly restricted by the tungsten halogen lamps spectral output and the photodiode's performance respectively. The "raw" spectra obtained using the tungsten halogen lamp and two types of detector are shown in Figure 3.30. These spectra's shapes arise from a combination of the spectral properties of the source, the characteristics of the optical components (eg fibre bundles and diffraction grating) and the detector's responsivity. Since the only difference between the two traces is the use of the different detectors, their effect is clearly evident.

The small distinct peak in both spectra is caused by the greater diffraction grating efficiency for light polarized perpendicular rather than parallel to the grating's grooves. Its efficiency is also wavelength dependent and therefore will have some bearing on the shape of any spectra. (The use of optical fibre bundles, as suggested in the manual, renders the system insensitive to changes in polarization state).

All of the 200 samples taken during each spectral scan are used

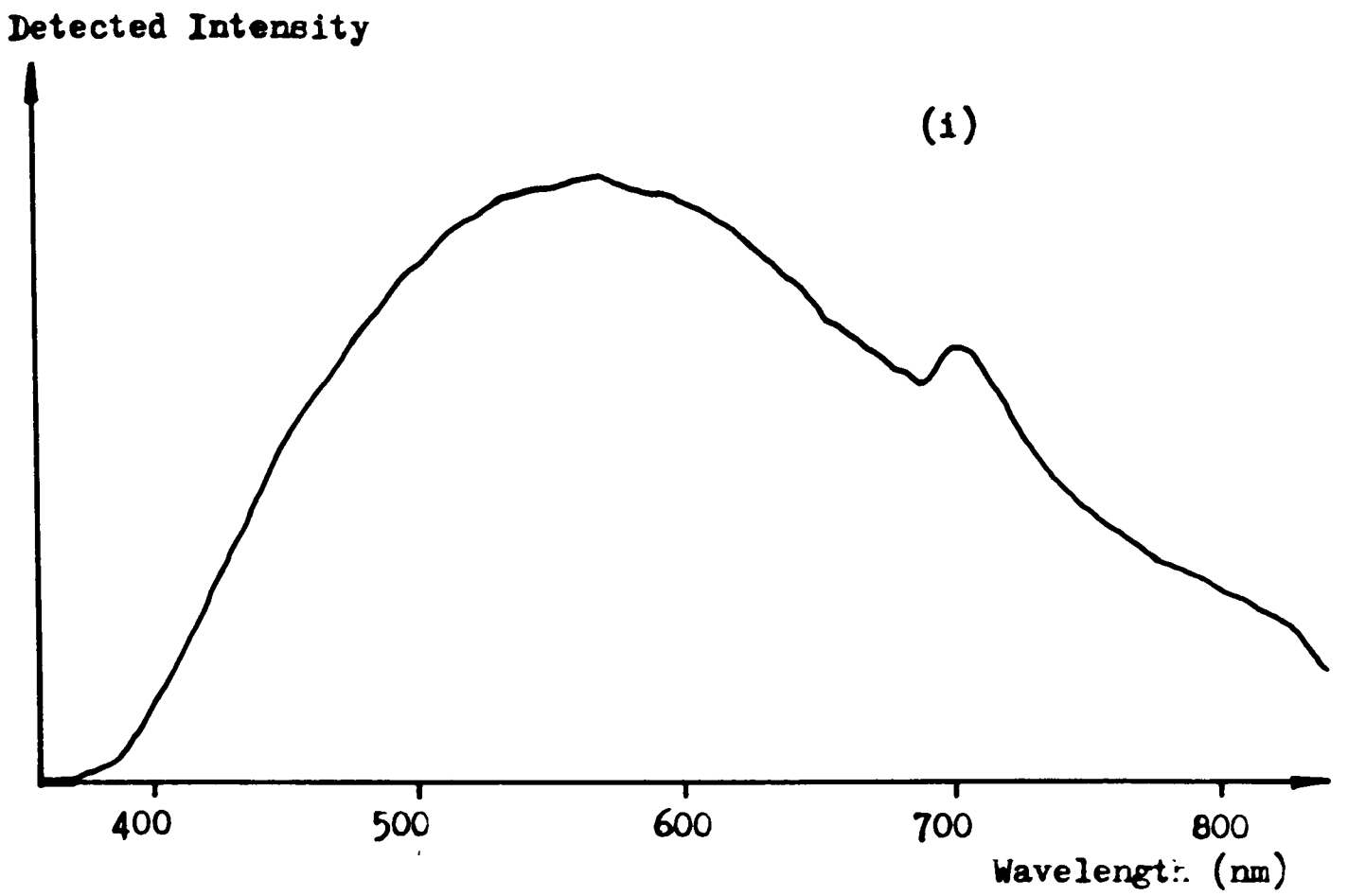

Figure 3.30 "Raw" spectra obtained from the scanning spectrophotometer using the tungsten halogen lamp, and with detection by: i) PMT and ii) photodiode.

during any subsequent processing, with wavelength range selection only

taking effect at the plotting stage. The actual choice of this range is not by wavelength. but rather sample number. This is because to change the slit width of the Spectralyser (for greater resolution or simply to increase light throughput), the slit plate must be removed and reclamped into position. This means the relative timing between the trigger pulse and any wavelength (determined by the angle of the rotating grating) is likely to change due to the lateral displacement of the slits upon reclamping. (Slight variation in detector alignment with respect to the slit may have a similar effect). Consequently upon using the Spectralyser after a change of slit width or detector, it is necessary to recalibrate the output at known wavelengths. This was achieved using interference filters.

In Figure 3.31 is a copy of an absorbance trace produced by the scanning spectrophotometer (from two "raw" traces). This demonstrates typical graphical output and the anotation provided on each trace.

Four slit widths of 2.5, 5, 10 and 20nm are available. The 5nm slit was used whenever possible although for certain in vivo studies, the 10 and 20nm slits were needed simply to obtain large enough intensities of light for detection.

The effect of slit width on resolution although evident is not as great as that due to the selection of the feedback capacitor in the PMT detection circuit. Normally an appropriate value for the feedback resistor would be chosen, with several values of feedback capacitor then available via a rotary switch. The capacitor simply reduces the high frequency response of the photodetector circuit and so produces a smoother output from the I-V converter. However, because the time axis is representative of wavelength this filtering affects the spectral resolution. This was evident by observing the effect of different

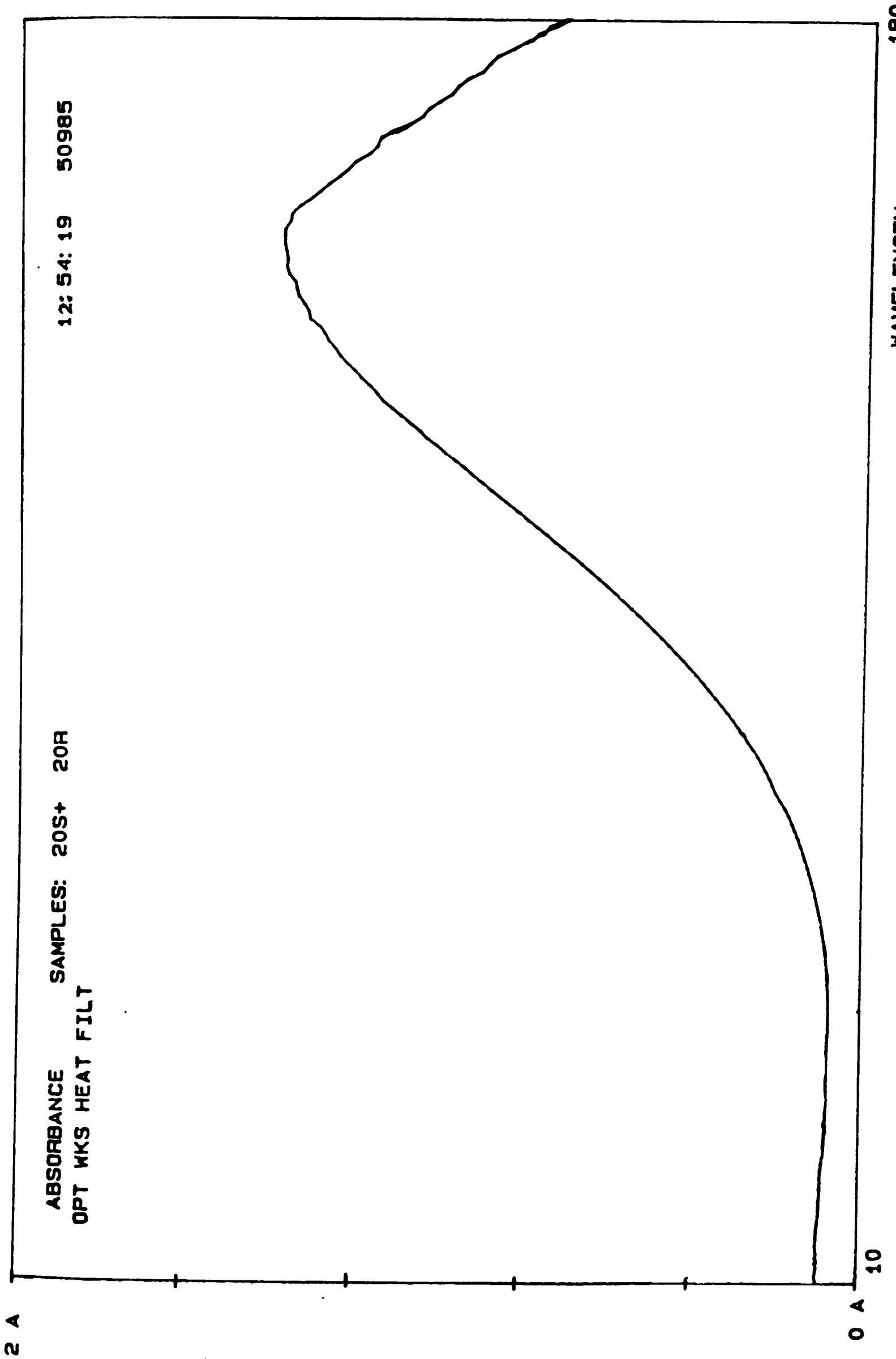

Figure 3.31 The absorbance spectrum of a heat absorbing filter shown as an example of the graphical output from the scanning spectrophotometer.

capacitor values on the spectrum obtained from light transmitted through

an interference filter. (The larger the value the "broader" the transmission peak obtained).

Consequently, there is a compromise between using a large capacitor, and obtaining a smoothed trace with the spectral details observable on an oscilloscope and which needs to be averaged only a few times, or a smaller capacitor and obtaining an apparently very noisy trace with no obvious structure observable on the oscilloscope, and which needs averaging maybe several hundred times. (This is particularily so at low detected light levels using the PMT since each spectral scan then appears very noisy and averaging is necessary to resolve any structure).

It has already been stated that the Spectralyser does not automatically remove second order spectra. This could be seen from the spectra obtained from 440 and 550nm interference filters, with the first order peaks at these wavelengths accompanied by the second order peaks at 880 and 1100nm. The importantance of appreciating that second order effects may be observed is demonstrated by the study described in Section 4.6.5.4.

The problem of interference from second order spectra with the Spectralyser was overcome by using two filters (OG395 and OG570, Rofin-Sinar) which only pass light above about 395 and 570nm and so allow the regions from approximately 395-790 and 570-1100nm to be studied. Virtually all of the studies in Chapter 6 were performed twice using these two filters, thus covering the range under investigation and also ensuring no second order artefacts were seen.

To obtain an "absorbance" or "transmittance" (ie percentage of the incident signal detected) spectrum from the instrument then a sample and reference spectrum are required. For reflection measurements, the

reference spectrum was obtained by placing the bifurcated optical fibre end onto a box of white tissues. Since the actual magnitude of the signal obtained was dependent upon how the fibre was exactly positioned in relation to the tissues (and indeed the specimen) then precise quantification of the reflectance was difficult. However, this was not too much of a problem since it was the shape of the spectra which were of particular interest (ie the relative reflectances between wavelengths) rather than actual magnitudes. (Despite this problem the reproducibility between experiments was still not that poor).

For transmission measurements of samples such as filters the instrument was set up with light from the lamp entering the Spectralyser thus producing a suitable output reference trace. The filter was then simply placed in the beam and the sample trace obtained.

For highly absorbing samples, such as a finger, the same arrangement could not be used. This was because such a high incident intensity was required for the light emerging from the sample to be observed, that if viewed directly to obtain a reference it would saturate (or in the case of the PMT even damage) the photodetector.

Consequently in these studies rather than simply removing the sample from between the two fibre bundles so allowing a large amount of light to pass from one to the other, they were either "mismatched" (held a long way apart) so that only a small portion of the light available was detected. This then produced a reference spectrum with ideally the same spectral characteristics as that which would be obtained from the incident light only much smaller in magnitude. Therefore, the absorbance spectra produced using this method of obtaining a reference, have the correct shape but will severely underestimate the actual absorbance by a set amount as illustrated in Figure 3.32.

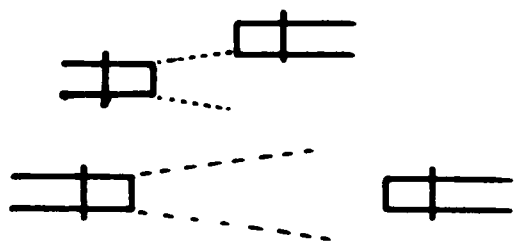

Methods of mismatching to obtain a smaller sized reference signal.

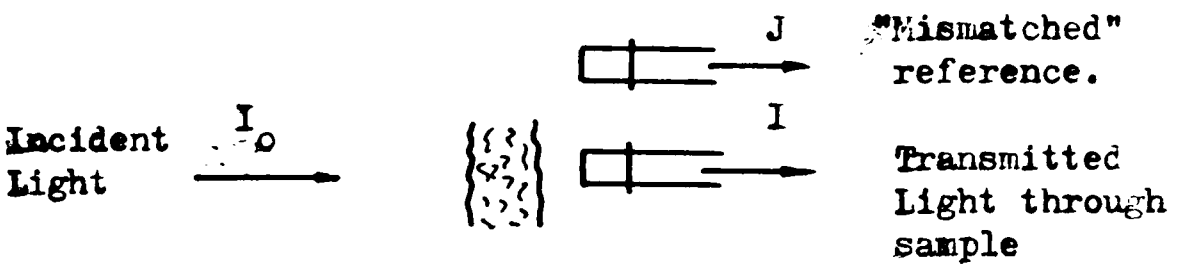

$$\text{Absorbance of sample} = \log \frac{I_o}{I} = \log \frac{I_o}{J} \cdot \frac{J}{I} = A_1 + A_2$$

A_2 = Absorbance of sample calculated using mismatched reference and output by spectrophotometer.

A_1 = the offset absorbance. This can be estimated using the reference spectrum (ie J) and equivalent values for I_o.

These cannot be obtained directly (as I_o is too large) but are found using the spectrum obtained with a N OD neutral density filter, since the intensity I_o is then given by (recorded value) x 10^N, which can be used to find A_1.

Figure 3.32 Diagram showing the "mismatching" of fibre bundles to obtain a reference spectrum, and how the amount that this technique offsets the calculated absorbance can be found.

Also illustrated in this figure is a means of estimating this

additional offset absorbance, although the divergence of light from the fibre bundle and intense scattering of tissue mean this is certainly not a true value, but rather serves only as a guide to the transmitted light intensity to within about an order of magnitude.

A problem with the Spectralyser which was never resolved was made apparent by the small peak due to the polarization effect which was always present. This was that the actual trace observed on the oscilloscope and therefore sampled was very slightly unstable with respect to the trigger pulse (ie the time interval between the trigger pulse and any wavelength showed slight variations with respect to time).

The effect of this was noticeable if the trace shifted between a sample and reference spectrum being taken because then, if for example an "absorbance" trace was produced, a small perturbation in absorbance appeared since the respective peaks in the sample and reference beam were not exactly overlapping.

Although the whole spectrum shifts the effect is only noticeable where the "raw" spectra has a relatively sharp gradient such as at the polarization artefact. (The same effect was also noticed when using polymer fibres because of their relatively large absorbance band in the near-IR). Even though in the flatter regions of the original traces no such effects are noticeable, the shifting must also slightly reduce the resolution of the final spectrum.

It is because of this that, some traces in Chapter 6 show a slight variation in absorbance around 735nm which is the peak produced by the polarization artefact.

The cause of this drifting of the spectral scans could not be found despite various tests, although if the whole instrument (ie lamp,

Spectralyser and detector) was switched on some time prior to use the drifting appeared to be less.

Possible causes are fluctuation in voltage from the DC power supply (perhaps due to mains fluctuations) affecting the quality of light output or jitter in the timing circuit of the Spectralyser which determines the period between the trigger pulse and start of the spectral scan.

Finally, all experiments were performed using optical fibres to "pipe" the light from source to sample and then back to the Spectralyser. Although these confer great flexibility on the instrument they are not the most efficient way of optical coupling. For this reason a few preliminary studies were made, using lenses to focus the light into the Spectralyser to obtain higher signals, but with little success. However, it should be possible to achieve greater inherent efficiency but probably at the expense of flexibility.

Chapter 4: Spectrophotometric Monitoring of the Redox State of Cytochrome Oxidase: A Non-Invasive Method for the Study of Cerebral Metabolism ?

4.1 Introduction.

As the medical care of preterm infants improves, so the survival rate of very low birth weight (VLBW) infants increases. However, such infants are predisposed to suffering from intraventricular haemmorhage (IVH) and cerebral ischaemia, conditions whose aetiology is far from understood. Therefore, an instrument capable of monitoring the preterm infant's cerebral metabolism and hemodynamics could prove to be a major tool in studying the development of the above conditions.

The "Niroscope" (near-IR oxygen sufficiency scope), named by Prof F.F.Jobsis who developed it, is an instrument claimed to be capable of monitoring both cerebral metabolism and haemodynamics. It is basically a near-IR spectrophotometer which is said to monitor the redox state of the terminal enzyme of respiration cytochrome oxidase (cytochrome aa_3) as well as functioning as an oximeter and monitoring changes in blood volume.

This chapter is the result of an investigation into the use of "niroscopy" which is clearly an "optical method" with tremendous potential for application in paediactrics. Because of the similarities between many optical methods, experience gained from these studies is likely to be applicable to other types of optical monitoring.

Following the comprehensive work of Jobsis and colleagues, a "Niroscope" could be built and used immediately to perform measurements. However, for a thorough investigation of the technique it was considered neccesary to begin with experiments on the pure enzyme, gradually moving on to more "complete" and complex organisms (eg yeast cells), to eventually reach non-invasive studies on humans.

This second approach was felt to be particularly important in view of the apparent anomalous behaviour of the enzyme in vivo and the relatively simple signal processing which has been used for what appears to be an exceedingly complex problem (as this may lead to erroneous results due to artefacts). In addition it is not yet totally proven that monitoring the redox state of cytochrome oxidase in vivo actually yields any more clinically useful information than monitoring oxygen saturation (SO_2).

Notwithstanding the above, the construction of a clinically useable instrument is an important aspect of this work, and to this end some prototype laser diode drive circuits were constructed (see Section 3.2.1.2). This side of the project has since been continued by Mr Y.A.B.D. Wickramasinghe, who has constructed a laser diode based near-IR spectrophotometer with which preliminary studies have been performed (see Appendix A).

The need to monitor cerebral metabolism and haemodynamics of sick preterm infants is outlined in Section 4.2, together with a brief review of currently available techniques for this purpose, whose advantages and disadvantages are directly compared with the benefits which an ideal Niroscope should offer. In Section 4.3 the biochemical background to the method is given which explains the neccessity for aerobic rather than anaerobic metabolism in organs with high energy requirements, and the role played by the respiratory chain. The cytochromes within the respiratory chain are dealt with in more detail in Section 4.4, where their action and the spectroscopic properties that enable optical monitoring to be performed are considered.

In Section 4.5 the relationships between the relative redox states of the various members of the respiratory chain are discussed in terms of the efficiency and use of monitoring the redox state of cytochrome oxidase as an indicator of metabolism. Also considered are the basic

kinetics of the reaction between cytochrome oxidase and oxygen which are required to explain the *in vitro* results in the following section. The significance of the apparent change in affinity of the cytochrome oxidase *in vivo* is also introduced. The work of Dr Britton Chance who pioneered the use of spectrophotometric techniques for monitoring the redox states of the respiratory enzymes from which all subsequent methods are effectively derived is then described.

Section 4.6 covers the *in vitro* experiments which were performed on both pure cytochrome oxidase and yeast cells and includes both absorbance and oxygen measurements.

In Section 4.7 the interrelation between haemoglobin, myoglobin and cytochrome oxidase (ie their respective roles in oxygen delivery and utilization) is considered. This is considered necessary before describing the development of the technique of monitoring the redox state of cytochrome oxidase from an *in vitro* to a non-invasive *in vivo* method for studying the redox state of cytochrome oxidase, and oxygen saturation and blood volume in Section 4.8.

Following this in Section 4.9 an appraisal of the application of *in vivo* near-IR spectrophotometry is given including both its potential advantages and problems. The possible lack of appropriate and adequate signal processing is considered further in Section 4.10. whilst, in Section 4.11 the question of the apparent difference in affinities of cytochrome oxidase for oxygen *in vitro* and *in vivo* is addressed. A possible explanation is proposed using physical arguments resulting from the modelling also described in this section, itself a consequence of the results from Section 4.6.

Conclusions concerning the feasibility and use of niroscopy in clinical situations are given in Section 4.12 together with suggestions for further work which may help to answer some of the questions posed in this chapter.

4.2 Current Clinical Perspective.

4.2.1 Introduction.

Cerebral ischaemia and intraventricular haemorrhage (IVH) are two of the main causes of death and disability in preterm infants in the developed countries (PAPE (1979)), with IVH affecting an estimated 40-50% of neonates with a birthweight of 1500g or less (LEVENE (1980)). Certain factors such as hypoxaemia, mechanical ventilation and pneumothorax are known to increase the risk of IVH (PAPE (1979)), possibly due to perturbations in cerebral blood flow (CBF), but apart from prematurity the causes and sequence of events which lead to haemmorhage are largely unknown. However, with IVH uncommon in stillborn babies (HARCKE (1972)), and approximately 80 percent of all recorded IVH's occuring within 72 hours of birth (AHMANN (1980)), the underlying factors appear to be associated with a circulatory and / or respiratory inability to cope with the premature transfer from an intra-uterine to an extra-uterine existence.

At present the diagnosis of IVH and cerebral ischaemia, and the gathering of further information concerning the physiological processes involved, is difficult because of the lack of effective, low-cost instrumentation enabling the continuous, or at least frequent, monitoring of cerebral metabolism and cerebral haemodynamics. A non-invasive near-IR spectrophotometer (Niroscope) may fulfil these requirements.

4.2.2 Current Instrumentation.

The main techniques currently employed or being developed to examine cerebral metabolism, cerebral blood flow, and brain morphology in the diagnosis of brain damage in neonates are:

1) Ultrasound scanning and Doppler measurement of blood flow.

2) X-ray computed tomography.

3) Electrical impedance techniques.

4) Positron emission tomography (PET).

5) Nuclear magnetic resonance (NMR) imaging and Topical 31P-NMR.

4.2.2.1 Ultrasound Scanning.

Although haemmorhage can be detected by ultrasound scanning, cerebral ischaemia cannot unless associated with gross morphological changes. In both instances the fact that detection is possible implies that damage to brain tissue has already occured. Doppler ultrasound methods can be used to measure blood flow.

4.2.2.2 X-ray Computed Tomography.

This technique suffers from the same disadvantage as ultrasound scanning and in addition carries the small but finite risk of causing genetic damage.

4.2.2.3 Electrical Impedance Techniques.

Changes in cerebral haemodynamics can be estimated by these methods, but the cause may be due to fluctuations in a variety of parameters and the technique reveals no direct information concerning cerebral metabolism. Recently this technique has also been applied to the production of impedance images (BARBER (1984)) of the neonatal brain which may be able to detect the presence of IVH.

4.2.2.4 Positron Emission Tomography.

With PET it is possible to measure regional blood volume, CBF and oxygen consumption, and to assess metabolic status. However, the high cost and size of the apparatus plus the requirement of a cyclotron to produce the relatively short lived isotopes, and the ethical consideration of administering positron emitting isotopes to the newborn infant may limit the widespread application of this technique.

4.2.2.5 NMR imaging and Topical 31-P NMR.

Of all the currently available techniques NMR imaging and topical 31-P NMR come closest to the requirements of a true non-invasive metabolic monitor.

The majority of cerebral lesions, including ischaemia and haemmorhage, can be detected by imaging, and topical 31-P NMR allows the simultaneous measurement of adenosine triphosphate (ATP), phosphocreatine, inorganic phosphate and other phospho-compounds together with intracellular pH. However, as with PET there are obstacles to be overcome before NMR instruments can become widely used in clinical practice; namely their size, the need for special housings (to contain an approximate 2 tesla magnetic field in the case of NMR), and cost.

4.2.2.6 "Niroscopy".

In view of the above there is clearly a need for an inexpensive and portable metabolic monitor for use in paediatrics. These requirements may be satisfied by the non-invasive *in vivo* near-IR spectrophotometer being developed by Jobsis and his colleagues at Duke University, NC, USA. This instrument may be used for animal investigations and clinical intensive care applications, including that of premature infants (see Section 4.8). The instrument is said to monitor cerebral metabolism and changes in cerebral blood volume and oxygen saturation.

4.3 Biochemical Background.

4.3.1 ATP and the Transfer of Energy.

In living organisms the energy liberated by the breakdown of foodstuffs is ultimately used for the three basic activities of chemical, mechanical and osmotic work (ie biosynthesis, movement and solute transport). The common intermediary linking the energy yielding to the energy demanding processes is adenosine triphosphate (ATP) which stores the energy released upon the degradation of fuel molecules in its terminal phosphate bond formed by the coupled phosphorylation of adenosine diphosphate (ADP). This energy is subsequently used to drive the processes requiring energy with the ATP breaking back down into ADP and free phosphate (Pi) as it powers the necessary reactions. This is shown in Figure 4.1.

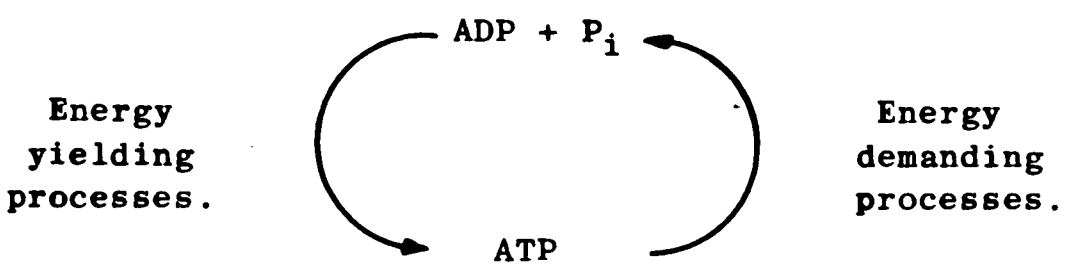

Figure 4.1 The role of ATP: the common intermediary in energy transfer.

The formation of ATP from ADP and free phosphate coupled to the oxidation reactions involved in the breakdown of foodstuffs is essentially what is termed respiration, and can occur either in the absence or presence of oxygen (anaerobic and aerobic respiration respectively).

4.3.2 Glycolysis.

During anaerobic respiration (glycolysis) glucose or other sugars are broken down in a series of reactions catalysed by eleven enzymes present in free form in the cytosol. Despite the absence of oxygen, the series includes oxidation reactions (the glucose being broken down into fragments which oxidize each other), coupled to the synthesis of ATP. The overall reaction for glycolysis is:

$$\underset{\text{(Glucose)}}{C_6H_{12}O_6} + 2\ ADP + 2\ P_i \longrightarrow 2\ CH_3CHOHCOO^- + 2\ ATP + 2\ H_2O \qquad 4.1$$

(Lactate)

So for every molecule of glucose consumed two molecules of ATP are produced (see Figure 4.4).

4.3.3 Oxidative Metabolism.

The lactate generated during glycolysis is produced by the reduction of pyruvate. However, duing oxidative metabolism (aerobic respiration) this pyruvate is further oxidised to carbon dioxide and water, a process which is coupled to the generation of more ATP.

The enzymes responsible for aerobic respiration are situated within the mitochondria, themselves intracellular organelles ovoid in shape and approximately 1-2μm long and 0.5-1μm wide. A diagrammatic representation showing the structure of a mitochondrion is shown in Figure 4.2.

During aerobic respiration the pyruvate is first converted to acetyl-CoA, which is then oxidised by two intimately related pathways. The first, the tricarboxylic acid (TCA) cycle, oxidises acetyl-CoA to carbondioxide reducing nicotinamide adenine dinucleotide (NAD+) to NADH

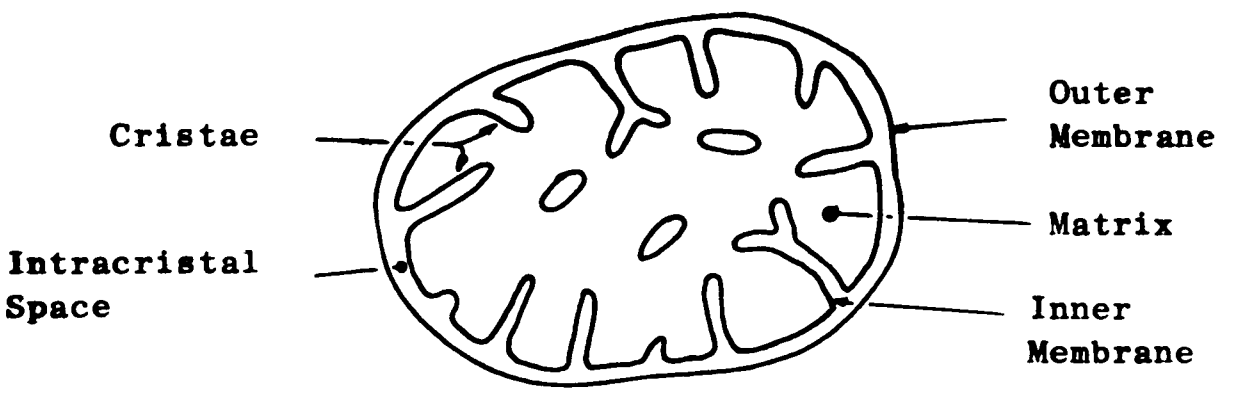

Figure 4.2 Schematic representation of the cross section of mitochondrial structure.

in the process, with the second, the respiratory chain, subsequently reoxidising this NADH back to NAD+ whilst reducing oxygen to water as shown in Figure 4.3. This overall oxidation is coupled to the generation of ATP.

4.3.3.1 Conversion of Pyruvate to Acetyl-CoA.

Pyruvate is enzymatically oxidised to acetyl-CoA according to the reaction:

$$\underset{\text{(Pyruvate)}}{CH_3COCOO^-} + CoA(SH) + NAD+ \longrightarrow \qquad 4.2$$

$$CH_3CO\text{-}SCoA + CO_2 + NADH + H^+$$

(Acetyl CoA)

The acetyl-CoA then feeds into the TCA cycle and the NADH is

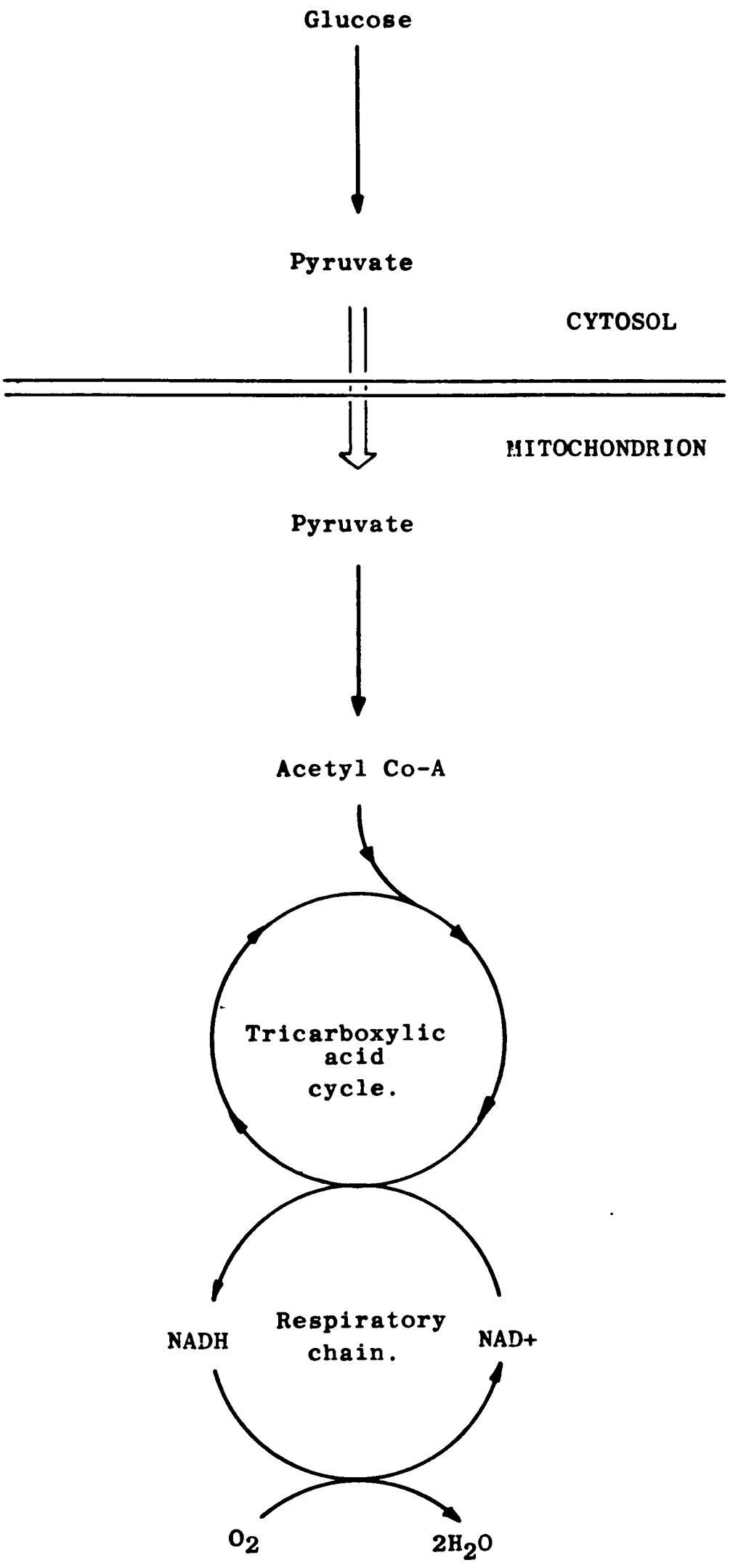

Figure 4.3 The related pathways of oxidative metabolism.

reoxidised by the respiratory chain (see Figure 4.4).

In addition to the formation of acetyl-CoA from carbohydrates (eg glucose) via the glycolytic pathway as summarised in the above reaction, both amino acids and fatty acids can be enzymatically converted to acetyl-CoA and therefore used as an energy source as shown in Figure 4.3.

4.3.3.2 The TCA cycle.

The oxidation of acetyl-CoA to carbondioxide and water is achieved by a cyclic series of eight enzymes, which together with their substrates form the TCA cycle shown in Figure 4.4. The overall reaction is:

$$\underset{\text{(Acetyl-CoA)}}{CH_3CO\text{-}SCoA} + ADP + P_i + 3\ NAD+ + FAD + 2\ H_2O \longrightarrow$$

$$CoA(SH) + ATP + 3\ NADH + FADH_2 + 2\ CO_2 \qquad 4.3$$

The NADH formed being reoxidised by the respiratory chain.

4.3.3.3 The Respiratory Chain.

The respiratory (or electron transport) chain completes the oxidation of acetyl-CoA by reoxidising the NADH formed during the TCA cycle back to NAD+ (and so ensuring the continued operation of the cycle). This is achieved by a sequence of reversible oxidation-reduction reactions which serve to transfer reducing equivalents (electrons or Hydrogen atoms (H)) from NADH and succinate (reaction No.6) to oxygen, producing water. For NADH the overall reaction of the respiratory chain is simply:

$$NADH + H^+ + \tfrac{1}{2}O_2 \longrightarrow NAD+ + H_2O \qquad 4.4$$

GLUCOSE

GLYCOLYSIS

2 ADP + 2P_i

2 ATP

2 NAD+

2 NADH + 2H^+

2 PYRUVATE

CYTOSOL

MITOCHONDRION

2 PYRUVATE

+ CoA(SH)

CO_2

NAD+

NADH + H^+

2 ACETYL CoA

+ H_2O

CoA(SH)

CITRATE

1

OXALOACETATE

NAD

NADH + H^+

MALATE

7

H_2O

FUMARATE

6

$FADH_2$

FAD

SUCCINATE

5

ATP

ADP + P_i

SUCCINYL-CoA

4

CO_2 + NADH + H^+

CoA(SH) + NAD+

-KETOGLUTARATE

3

CO_2

OXALSUCCINATE

3

NAD+

NADH + H^+

ISOCITRATE

2

H_2O

CIS-ACONITATE

2

H_2O

Figure 4.4 The tricarboxylic acid (TCA) cycle.

In addition to forming NAD+ the respiratory chain performs an extremely important second function, which is the coupling of the energy liberated during the oxidation of NADH and succinate to the synthesis of ATP, thus storing the energy in this common intermediate. This process is known as oxidative phosphorylation.

The actual electron transport is carried out by a series of electron carriers which participate in the redox reactions. There are basically three types of these carriers: flavoenzymes, cytochromes (see Section 4.4) and metalloproteins (although some compounds fall into two categories). The difference between the carriers is in their prosthetic groups, which is a heme group for the cytochromes and a metal such as copper for the metalloproteins. In addition NAD+ and coenzyme Q also act as (low molecular weight, ie not associated with a protein) carriers.

The fact that electron transfer from NADH to oxygen occurs over a series of steps means that the energy yielded for each molecule of NADH oxidised can in fact be coupled, at three different sites in the respiratory chain, to the formation of three molecules of ATP thus increasing efficiency. This makes oxidative phosphorylation the most important source of ATP as described in the next section.

The exact components of the respiratory chain and their sequence is still under investigation, with problems existing in isolating the specific components so that they can be studied. A representation of the respiratory chain is shown in Figure 4.5, consisting of four respiratory complexes (a fifth is involved in the actual process of oxidative phosphorylation). These complexes are located in the inner mitochondrial membrane in geometrically specific arrays as shown in Figure 4.6, and are the most important constituents of the respiratory chain. The two other components shown in Figure 4.5, cytochrome c and coenzyme-Q, are "mobile" carriers and shuttle electrons between the complexes.

Each of the four complexes are in effect a miniature respiratory

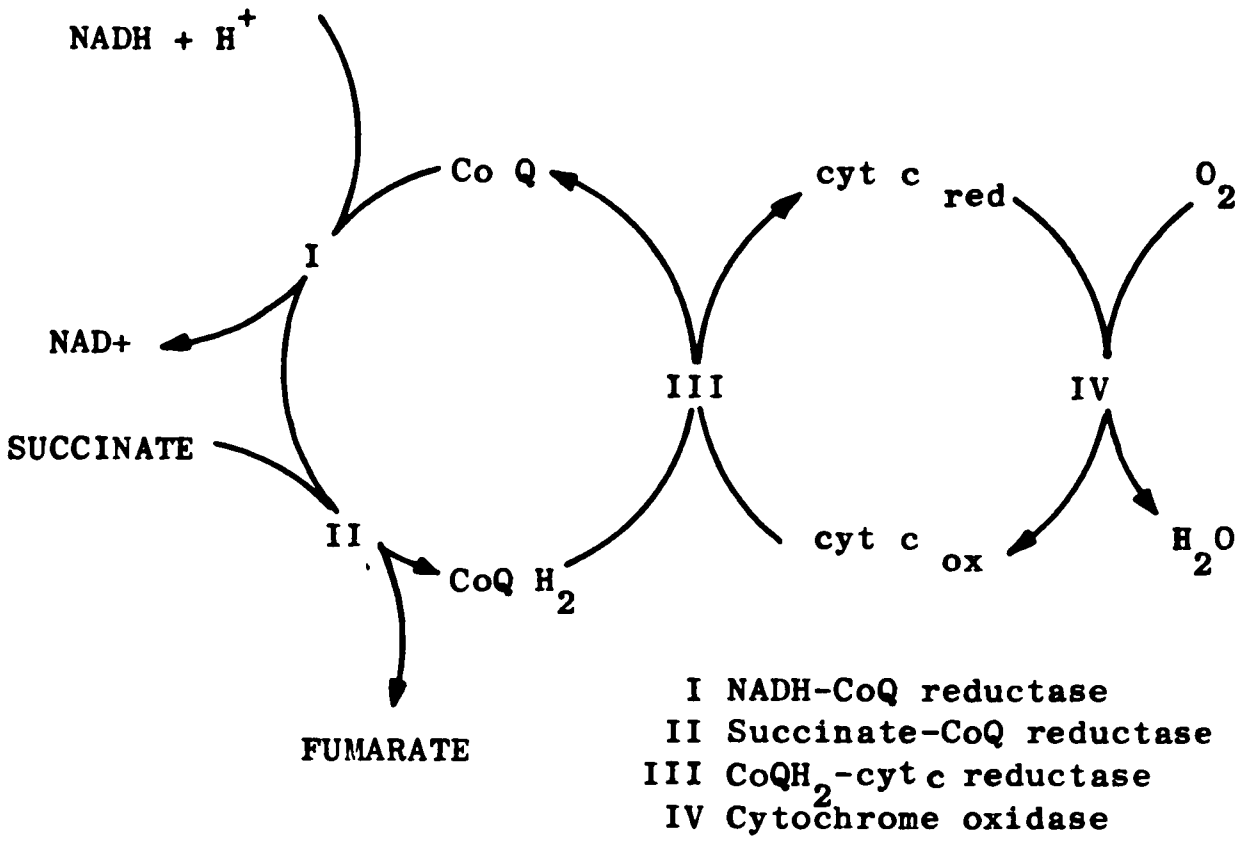

Figure 4.5 A representation of the respiratory chain (from TZAGALOFF (1982)).

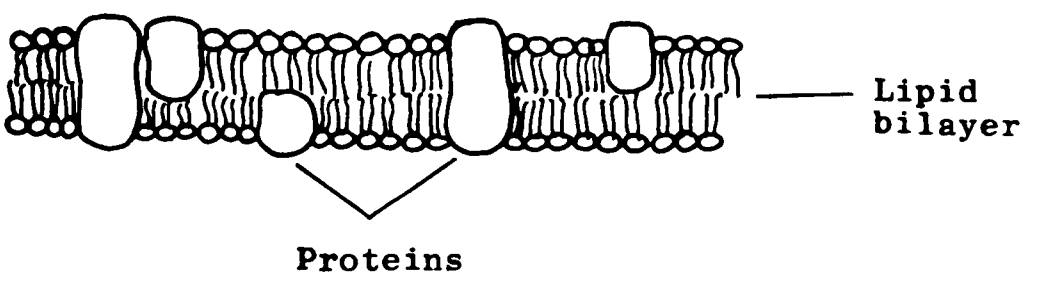

Figure 4.6 Schematic diagram of a biological membrane.

chain in itself, containing several components, the precise nature of

which are not yet fully understood. The known components and their accepted order are shown in Figure 4.7. The sequencing of the components has largely been carried out using spectroscopic techniques (applicable to the cytochromes in particular) and studies of the components redox potentials. The sites of oxidative phosphorylation are also shown in Figure 4.7.

4.3.4 The ATP Yield from Glucose.

During glycolysis two molecules of ATP are produced (see Equation 4.1). If oxygen is present so that the pyruvate can be further oxidised through the TCA cycle and the respiratory chain then this yield is greatly increased.

Two molecules of ATP are produced in the TCA cycle (Figure 4.4) for every molecule of glucose (ie one for every molecule of pyruvate) giving 4 molecules of ATP (including the two from glycolysis) formed by substrate level phosphorylation.

In addition each molecule of NADH formed during the aerobic breakdown of glucose yields 3 molecules of ATP from oxidative phosphorylation coupled to electron transfer in the respiratory chain. The oxidation of one molecule of $FADH_2$ to FAD (succinate to fumarate) by the respiratory chain in contrast is only coupled to the formation of 2 molecules of ATP because of the positioning of the sites of oxidative phosphorylation in relation to the specific electron carriers (see Figure 4.7).

Since for every molecule of glucose aerobically oxidised 2 molecules of NADH are produced during glycolysis, 2 during the formation of acetyl-CoA and 6 during the TCA cycle (see Figure 4.4) this leads to a yield of 34 molecules of ATP produced from one molecule of glucose, when the 4 from the re-oxidation of 2 molecules of $FADH_2$ are also considered.

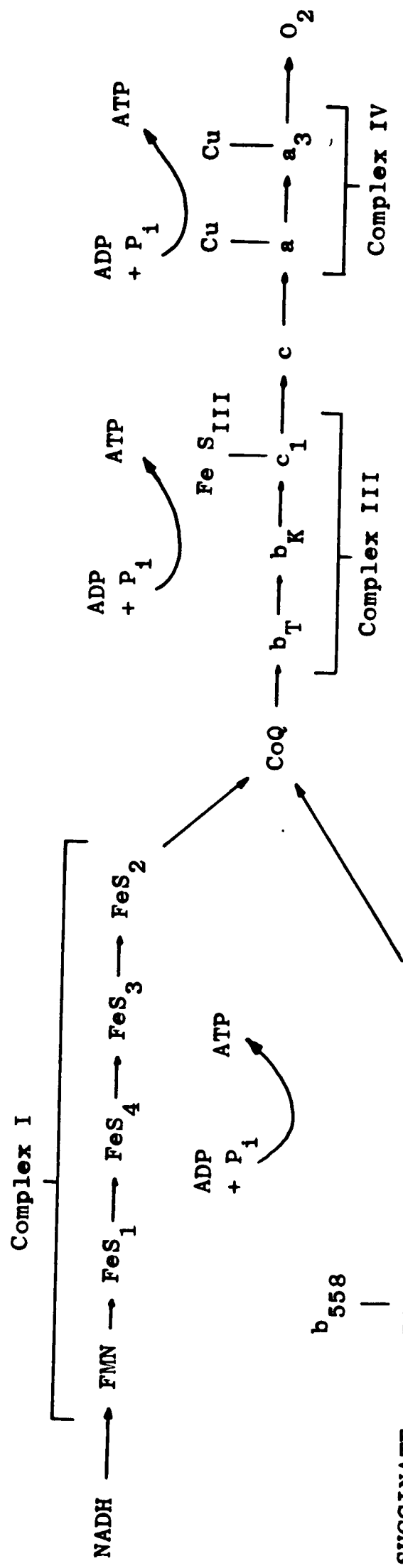

FMN, FAD - flavoenzymes
a,b,c - cytochromes
FeS - iron sulphur centred proteins

Figure 4.7 The Individual Carriers of the Respiratory Chain. The a and a_3 cytochromes are associated with copper metalloproteins, collectively forming Complex IV. (From TZAGALOFF (1982)).

With the 4 molecules of ATP from substrate level phosphorylation this gives an overall yield of 38 molecules of ATP per molecule of glucose from oxidative metabolism compared to the yield of 2 molecules from glycolysis as shown in Table 4.1. (This is the theoretical yield, and it may in practice only be 36).

	moles / mole glucose NADH		ATP	
Glycolysis (see Figure 4.4)			2	← only yield of ATP from anaerobic respiration.
(Glucose → 2 Pyruvates)	2	x3 →	6	
(Pyruvate → 2 Acetyl Co-As)	2	x3 →	6	
TCA cycle			2	
(2 Acetyl Co-As → $4CO_2$)	6	x3 →	18	
$FADH_2$ x 2		x2 →	4	
Total ATP →			38	

Table 4.1 ATP yield during the aerobic oxidation of glucose.

Oxidative metabolism is therefore up to 16 times more efficient than glycolysis at harnessing the energy liberated by the breakdown of foodstuffs. The consequence of this is that organs with high energy requirements are dependent upon oxidative metabolism, except for very short periods of time.

Hence such organs (eg heart, liver, brain, kidneys) are also highly reliant upon an adequate supply of oxygen for their integrity, and so

tend to have high mitochondrial densities and contain relatively large amounts of respiratory chain components including the terminal enzyme of respiration, cytochrome oxidase.

In summary, vital organs tend to have high energy requirements and so must have a functioning respiratory chain, itself requiring an adequate supply of oxygen, to provide plentiful quantities of ATP via oxidative phosphorylation. By monitoring the status of the respiratory chain in these organs it may be possible to gauge their metabolic activity, which is the aim of niroscopy.

4.4 The Cytochromes and Spectroscopy.

4.4.1 Introduction.

Several members of the respiratory chain are cytochromes which are haemoproteins whose active sites are their heme moieties (see Section 1.4.1.1). They were originally discovered by MacMunn in 1866 by virtue of their intense colours and then rediscovered by Keilin in 1925 who named them cytochromes because of their distinctive absorption characteristics (TZAGALOFF (1982)). (The term cytochrome is now used to describe all intracellular hemoproteins with few exceptions, notably haemoglobin and myoglobin). They are classified alphabetically depending upon their prosthetic groups and those in the respiratory chain belong to one of the a, b or c groups. Further classification into subcategories is denoted by subscripts (numerical or alphabetical).

Details of their structure and the differences in types can be found in DIXON (1976) and TZAGALOFF (1982). As noted in Section 1.4.1 whereas haemoglobin and myoglobin are ligand carriers (and so can bind oxygen) with the iron atom in the heme moiety remaining in the same valence state, the cytochromes act as carriers of reducing equivalents which is accomplished by the heme moiety undergoing reversible one electron oxidation-reduction reactions (ferrous $\rightleftharpoons$ ferric) of the iron atom. This leads to the cycling of the cytochrome molecules from an oxidised to a reduced to an oxidised state and so on as it accepts electrons from molecules in a higher energetic state and then passes them on to other less energetic molecules. As described in the preceding section the cytochromes found in the mammalian respiratory chain (see Figure 4.7) play an important function in aerobic respiration.

4.4.2 The Absorbance Spectra of Cytochromes.

Like other tetrapyrollic compounds the cytochromes have characteristic absorbance spectra in the visible part of the spectrum, with the structure in part dependent upon their redox state in a similar manner to that in which the spectrum of haemoglobin is dependent upon whether or not it is carrying oxygen.

Consequently as this latter feature enables oxygen saturation to be monitored spectrophotometrically, so too the redox state of the cytochromes can be studied by the same means. Since the absorbance spectrum will be dependent upon the proportion of oxidised to reduced molecules, ie the redox state.

In the reduced form the cytochromes generally have three distinctive absorption peaks in the visible region refered to as the α , β and γ bands going from high to low wavelengths. (The γ band is also known as the Soret band, and is the largest and broadest of the three). The exact position of the bands, particularly the α and β , is dependent upon cytochrome type, allowing them to be conveniently classified.

The absorption spectra of cytochromes b, c and aa_3 are shown in Figure 4.8, note the similarity between these and those of haemoglobin when oxygenated and deoxygenated which were shown in Figure 1.25.

As mentioned above the α and β bands in the reduced absorption spectra of the cytochromes occur at slightly different wavelengths depending upon the type. This enabled the relative positions of the cytochromes within the respiratory chain to be found using "crossover" experiments (see Section 4.5.4) and also means that in theory the redox states of the different cytochromes within the respiratory chain can be monitored independently and simultaneously.

The significance of these measurements is that the cytochrome's redox state will be in part dependent upon the rate of electron transfer down the respiratory chain (see Section 4.5.2) which itself determines

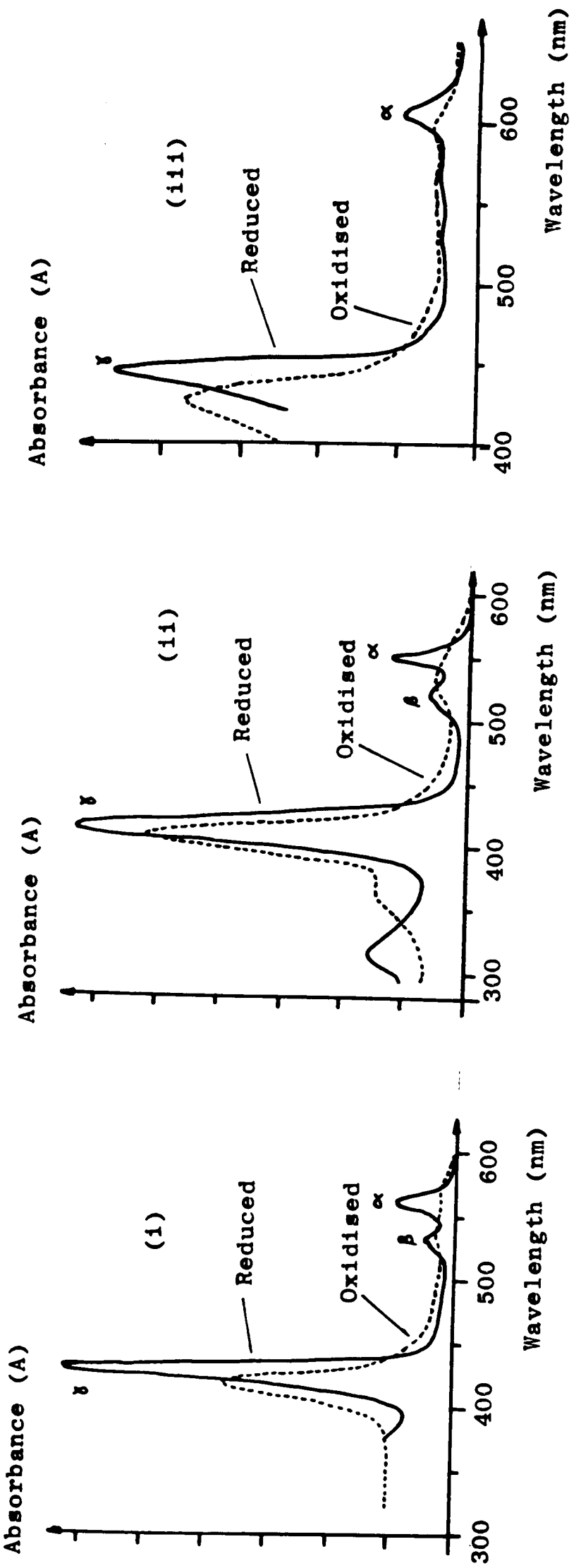

Figure 4.8 The absorption spectra of; (i) cytochrome b
(ii) cytochrome c
(iii) cytochrome oxidase (cytochrome aa_3)

(From TZAGALOFF 1982)

the rate of oxidative phosphorylation. Hence such spectrophotometric monitoring allows an assessment of "metabolic status".

4.4.3 Cytochrome Oxidase.

In the above the cytochromes as a whole have been considered, but of particular interest is cytochrome oxidase (cytochrome aa_3 (E 1.9.3.1)) which was also referred to above as Complex IV and contains both cytochromes a and a_3 (see Figure 4.7). This is the terminal member of the mammalian respiratory chain, and therefore the one which passes reducing equivalents directly to oxygen to form respiratory water. It is because it is the only cytochrome capable of reducing oxygen, becoming oxidised itself in the process, that the redox state of cytochrome oxidase is of particular interest.

ATP can only be produced by oxidative phosphorylation if there are electrons flowing down the respiratory chain, which itself can only occur if there is oxygen available to accept electrons from (reduced) cytochrome oxidase, thus reoxidising it, and so allowing more electrons to be accepted from reduced cytochrome c. This is shown in Figure 4.9. Therefore if a reasonable proportion of cytochrome oxidase molecules are oxidised then electrons will be readily accepted from reduced cytochrome c, and so electron transfer and energy production will proceed uninhibited. However, this is intrinsically linked to oxygen availability (hence "oxygen sufficiency scope") since only oxygen can perform the re-oxidation of reduced cytochrome oxidase. (Note from Figure 4.9 the cyclic nature of these processes, with any one individual cytochrome oxidase molecule continually changing from an oxidised to a reduced state and so on as it donates and then accepts electrons.) By monitoring the redox state of a cytochrome spectrophotometrically the percentage of reduced/oxidised molecules at any instant can be assessed

with this figure reflecting the cytochromes ability to donate/accept electrons.

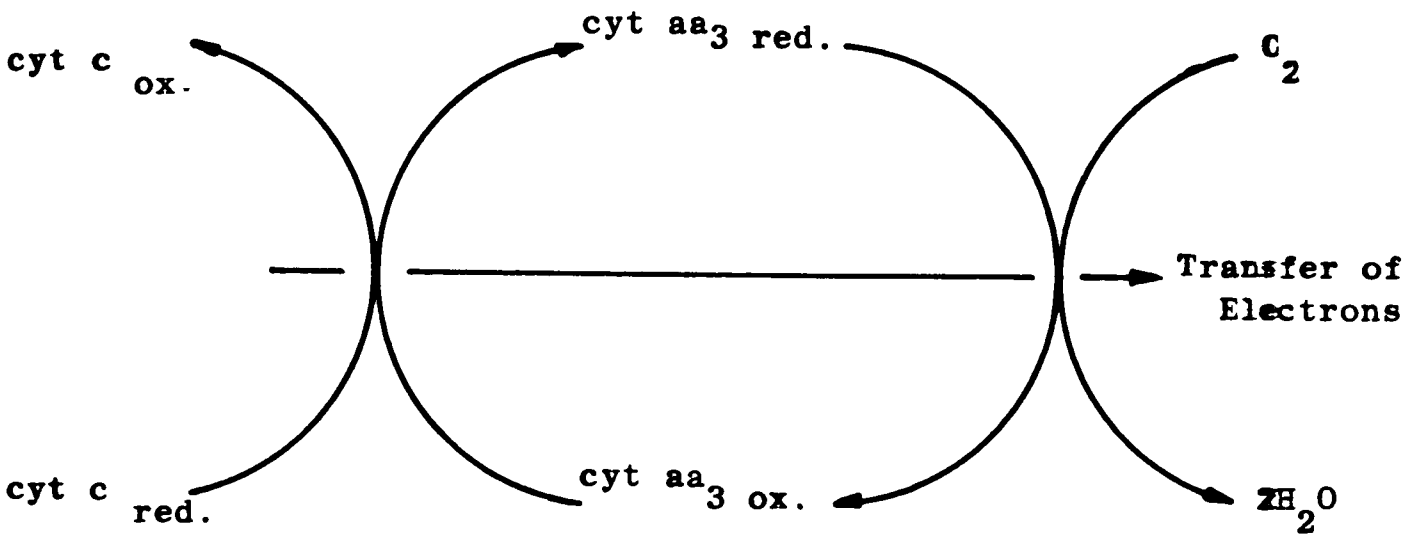

Figure 4.9 The cyclic nature of the reaction between cytochrome oxidase (cyt aa_3) and cytochrome c (reduced) and oxygen.

Cytochrome oxidase differs from the other cytochromes in that it takes part in tetravalent rather than univalent redox reactions. That is it passes four reducing equivalents at a time to oxygen so mediating the reaction:

$$4\,H + O_2 \longrightarrow 2\,H_2O \qquad 4.5$$

It can transfer four electrons because rather than possessing a single heme moiety (with an Fe atom), cytochrome oxidase has two heme moieties (a and a_3) and two copper atoms (see Figure 4.7) which can undergo cuprous ⇌ cupric transitions and so also transfer electrons.

The possession of these two copper atoms is of importance for monitoring the redox state of the enzyme non-invasively. This is because in addition to the visible absorption spectra due to the iron atoms, the

presence of the copper atoms produces a smaller, broader absorption band in the near-IR centred at about 830nm (GRIFFITHS (1961)). This absorption band is also redox state dependent, but in the opposite way to those due to the iron atoms (the absorption is greatest when the molecule is oxidised). This is shown in Figure 4.10, with further spectra given in the experimental results (Section 4.6.3.1).

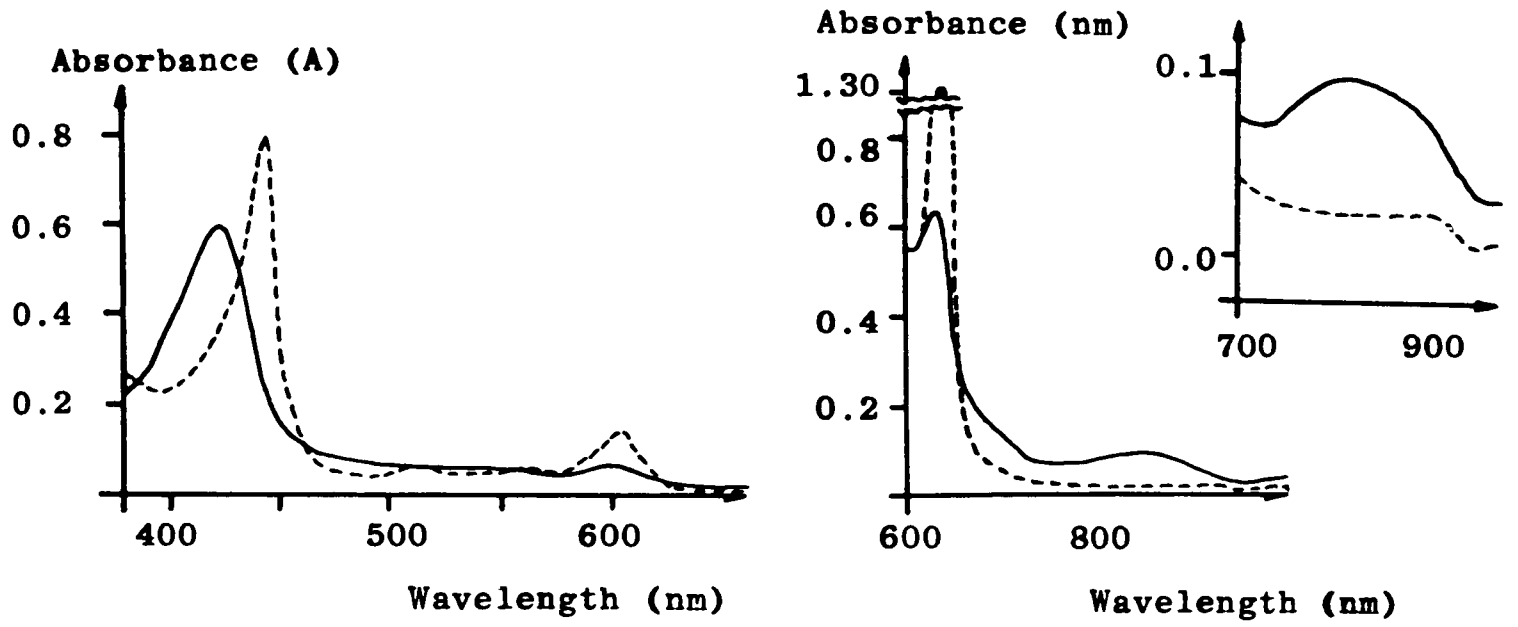

Figure 4.10 Absorption spectra of cytochrome oxidase showing the near-IR absorption band and its size in relation to the visible bands. Oxidised enzyme is drawn with a solid line and reduced enzyme with a dashed line (from GRIFFITHS (1961)).

Why this near-IR band is significant concerning non-invasive monitoring can be seen from the transmission spectra for tissue given in Section 1.4.2.2 and Chapter 6. These show that there is a dramatic decrease in the attenuation of light in the near-IR (chiefly due to the decrease in absorption by haemoglobin), which means that whereas sufficient levels of near-IR light can be shone through tissue to allow spectrophotometric measurements to be made, this is certainly not the case at visible wavelengths.

It was Prof F.F. Jobsis (see Section 4.8) who suggested that the redox state dependent absorption band (at 830nm) and drop in attenuation in the near-IR could be used for non-invasive monitoring of the redox state of cytochrome oxidase in non-surface tissues such as the brain, for

which use of the 605nm absorption band (as is standard practice in other samples), would be technically extremely difficult. This approach has since remained the accepted mode for the non-invasive monitoring of the redox state of cytochrome oxidase, and the associated cerebral haemodynamic variables of changes in blood volume and oxygen saturation.

This exploitation of the near-IR absorption characteristics together with the lower attenuation of tissue in this region of the spectrum is similar to that used in transmission oximeters (see Section 1.5.1.3).

That it is principally due to the large absorption of visible light by haemoglobin that near-IR spectrophotometry is required, means that the redox state of cytochrome oxidase can be monitored using its α band in excised bloodless organs. It also demonstrates the problems of obtaining absorbance measurements, with no artefacts due to interference from other compounds.

The interest in cytochrome oxidase, in this thesis is to monitor its redox state spectrophotometrically, which here is simply considered to exist in two states, either reduced or oxidised, with two corresponding absorption spectra. Enzymatically cytochrome oxidase is assumed to participate in a two substrate (reduced cytochrome c and oxygen) reaction, cycling through the two possible redox states as electrons are transferred from reduced cytochrome c to oxygen as shown in Figure 4.9. In later Sections, this is simplified further and only a one substrate reaction is considered in which cytochrome oxidase effectively consumes oxygen, with excess reduced cytochrome c always present (and so not rate limiting) to re-reduce the cytochrome oxidase.

In reality, the transfer of the four electrons from cytochrome oxidase to oxygen is by no means a simple process, with the cytochrome oxidase (Complex IV in Figure 4.5) consisting of a miniature electron transfer chain in its own right. Indeed, the precise mechanism of electron transfer, roles played by the copper atoms, the absorbance

spectra due to the copper atoms and other features of cytochrome oxidase are still under investigation (TZAGALOFF (1982), HATEFI (1985)).

Finally before describing the processes of monitoring cytochrome oxidase it is pertinent to describe its location and those of the other members of the respiratory chain. This is of importance when considering the relative merits of this technique and oximetry in view of their physically different measurement sites and also the size and scale of intracellular oxygen measurements and gradients.

Cytochrome oxidase is located in close, precise physical proximity to the other components of the respiratory chain in the mitochondrial inner membrane (see Figure 4.2). This precise spatial orientation of the various components (see Figure 4.6) is a likely cause of one of the problems in purifying individual components and then attempting to reconstitute an active system.

The mitochondrial inner membrane is a membrane within the mitochondrion which has cristae that greatly increase the membrane surface area. The mitochondria themselves are cellular organelles which are mainly associated with energy production, and contain not only the members of the respiratory chain but also those of the TCA cycle. As would be expected, those organs and tissues requiring most energy have a higher mitochondrial density and therefore more cytochromes which may be noticable from their distinctive colour.

4.5 The Respiratory Chain Components: Redox State and Kinetics.

4.5.1 Introduction.

In the previous section cytochrome oxidase was introduced as a potentially useful indicator of oxygen sufficiency on the basis that if it is oxidised then oxygen levels are adequate, wheras if it is reduced then they are not.

Here the relationships between the redox states of the respiratory chain components and aerobic respiration are described (Section 4.5.2), which explains in more detail what the redox state of cytochrome oxidase actually represents concerning metabolic status, including its dependence upon oxygen concentration. The relationship between oxygen and cytochrome oxidase is considered in more detail in Section 4.5.3, where the former is treated as an enzyme which consumes the latter.

These sections serve as an introduction to the potential use and shortcomings of using the redox state of cytochrome oxidase as a metabolic indicator, and the information given is relevant to the results presented in Section 4.6.

Much of this work concerning the status of the respiratory chain components' redox states and respiration was performed by Britton Chance and his colleagues. It was he who pioneered the use of spectrophotometric monitoring of redox states and is widely cited by authors who have subsequently used the method. His contribution to the field in terms of the development of instrumentation, investigative techniques and experimental results is briefly described in Section 4.5.4. It was the continued development of this work which finally lead to non-invasively monitoring the redox state of cytochrome oxidase *in vivo*.

4.5.2 The Redox States of the Respiratory Chain Components.

Considering the respiratory chain components (see Figure 4.7), the redox states of the cytochromes (and flavoproteins) can be monitored spectrophotometrically, (and simultaneously) whilst that of the first member of the chain, NADH, can be monitored fluorometrically (see Section 1.5.5). It was this type of study performed by Chance and others (see Section 4.5.4), that led to a more thorough understanding of the structure and function of the respiratory chain as outlined below. This is of significance concerning the relationships between the rate of electron transfer, cytochrome oxidase redox state, and "oxygen sufficiency" and therefore the interpretation of results from a Niroscope.

The order of components in the respiratory chain can be found by measurement of their standard reduction potentials. Those nearest to NADH being more electronegative (and therefore more energetic), and so having a greater tendency to pass electrons on. Alternatively the order of components can be determined spectroscopically since those components closest to the source of electrons are most reduced.

The relevance of the redox state of the various components is that the more reduced/oxidised a component, the greater its ability to donate/accept electrons and so the relative redox states of the members of the respiratory chain are directly linked to electron flow and oxidative phosphorylation.

This situation is shown diagramatically in Figure 4.11, together with an hydraulic analogue. The figure represents a dynamic steady state because although the overall redox state of the individual components remain the same, electrons are continually being transferred along the chain to oxygen, with the individual molecules of any component constantly cycling through being reduced to oxidised and back again. An alternative electrical analogue of the respiratory chain is also shown in

Figure 4.11. This is referred to below and consists of a resistor chain with high and low voltages at the "substrate" and "oxygen" ends respectively, with a high voltage representing a high level of reduction.

The actual redox levels of the respiratory chain components are dependent upon several factors, as is the flow of electrons and rate of ATP production. Complex models describing these relationships have been produced (WILSON (1979), however here a simpler approach is adopted to demonstate potential problems of interpreting the significance of changes in cytochrome oxidase redox state. It is simply assumed that there are three variables which control the overall flow of electrons, which in turn affect the various redox states. These are:

1) The amount of substrate available, which essentially means the quantity of electrons available to flow into the respiratory chain.

2) The amount of ADP present, because in simple terms small levels of ADP present mean high levels of ATP and therefore sufficient energy stored. The significance of this is that ATP production is tightly coupled to electron transfer (ie both proccesses must occur simultaneously), so if no energy is required (little ADP present) there will be no electron flow.

3) The amount of oxygen available to accept the electrons from the terminal member of the respiratory chain, cytochrome oxidase, thus re-oxidising it and so enabling more electrons to be accepted from reduced cytochrome c. (see Figure 4.9)

Hence a lack of any one of: substrate, ADP or oxygen could cause the flow of electrons to decrease (ie they can all have rate limiting effects), whereas if all are present in excess then the rate of electron transfer down the respiratory chain is itself the rate limiting factor.

The way in which respiration (ie electron flow) rate and the redox

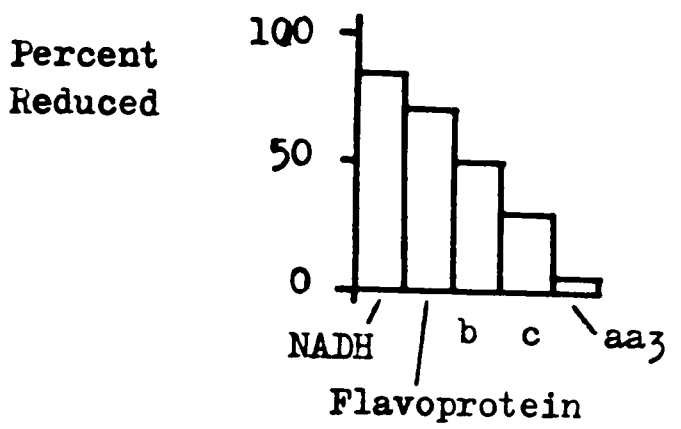

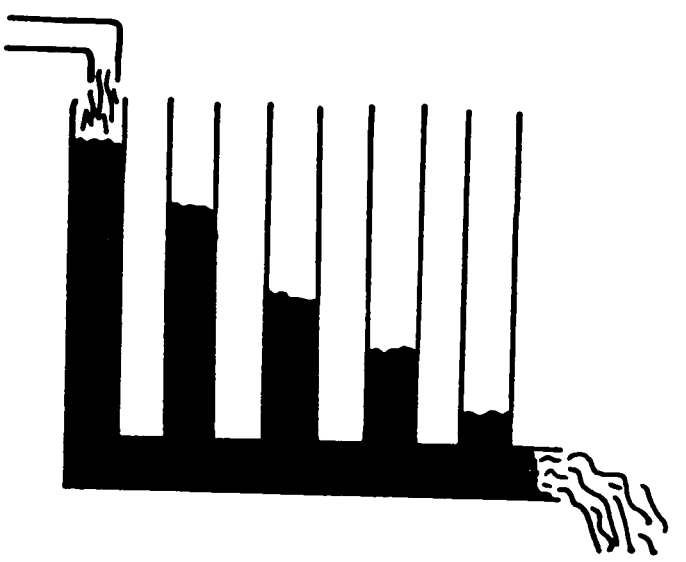

Hydraulic analogue of the respiratory chain.
(Height of fluid is directly related to the level of reduction).

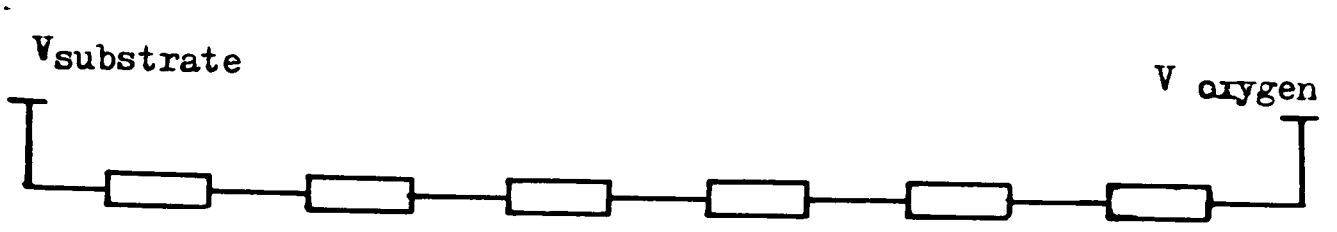

Electrical analogue of the respiratory chain.
(The voltages at the connections between the resistors represent the redox levels of the respiratory chain components).

Figure 4.11 Diagrammatic representation of the redox states of the respiratory chain components, with hydraulic and electronic analogues of this behaviour.

states are influenced by the above three factors (as described below) is summarised in Table 4.2 (from CHANCE (1956)). This shows the steady state percentage reductions of the respiratory chain components for certain respiration "states" (each represented by a number), with those components nearest the substrate always more reduced as was shown by the model in Figure 4.11. The various levels of substrate, ADP and oxygen are given, together with the rate of respiration and nature of the rate limitation.

Considering a mitochondrial suspension, which is a very basic system, where ADP is rate limiting (State 4), then the respiratory rate (equivalent to the flow of electrons) is slow due to tight coupling. However, if ADP is added then the rate increases and the respiration changes to State 3. This increase in respiratory rate affects the steady state reduction levels, with those components near the substrate (NADH) showing a much greater change than those near oxygen. The general decrease in redox levels (ie greater percentage of molecules oxidised) is because of the increased flow of electrons. The exception is cytochrome oxidase whose redox level increases slightly.

The electrical analogue of this situation is to apply a short to the centre of the resistor chain (see Figure 4.11). This causes an increase in current (electron transfer) and "pulls down" the voltages near the high "substrate" voltage.

The change from State 4 to State 3 respiration can be seen experimentally as an increase in the rate of oxygen consumption (as the respiration is higher) after the addition of ADP. The difference in respiration rate in states 3 and 4 is due to the coupling of oxidative phosphorylation to electron transfer. A measure of the "tightness" of this coupling is given by the ratio of oxygen consumption in the two states, known as the respiration control quotient. (The smaller the quotient the tighter the coupling.)

State	Substrate level.	ADP level.	Oxygen level.	Respiration rate.	Steady state percentage reduction of components. NADH	Flavo-protein	cytochrome b	cytochrome c	cytochrome oxidase (aa_3)	Rate limiting substance
2	~ 0	HIGH	> 0	SLOW	0	0	0	0	0	Substrate
3	HIGH	HIGH	> 0	FAST	53	20	16	6	4	Respiratory chain
4	HIGH	LOW	> 0	SLOW	99	40	35	14	0	ADP
5	HIGH	HIGH	0	ZERO	~100	~100	~100	~100	~100	Oxygen

Table 4.2 Metabolic status of mitochondria and the associated oxidation-reduction (redox) levels of the respiratory enzymes (from CHANCE (1956)).

Another group of chemicals which can increase the rate of respiration for an ADP rate limited (State 4) system are uncouplers, so called because they uncouple oxidative phosphorylation. This increases electron flow but does not raise ATP production and only heat is produced.

Considering the other respiration states, in State 2 there is substrate limitation and so no electrons are fed into the respiratory chain. This means all the components are fully oxidised since all electrons will have been transferred along to oxygen whilst no more are entering to re-reduce the components. The electrical analogue of this is of a break in the circuit close to the "substrate" voltage (see Figure 4.11) so that every point in the resistor chain is then at the low "oxygen" voltage.

Conversely in State 5 there is no oxygen present and so no final acceptor of electrons. Therefore electrons fed into the respiratory chain cannot leave, and every component becomes fully reduced. As in State 2, there is no gradual change in redox state along the respiratory chain with all components in this case 100% fully reduced, no flow of electrons taking place and therefore no aerobic respiration.

This is also the case when blockers or inhibitors (such as antimycin, rotenone or cyanide) are used to study respiratory chain function. These substances bind to certain components of the respiratory chain thus preventing them from undergoing reversible redox reactions and passing on electrons. Hence all components on the substrate side of the disabled component become fully reduced whilst those on the oxygen side are fully oxidised. Because of this action, blockers and inhibitors are valuable for studying respiratory function (EPSTEIN (1982), TZAGALOFF (1982)).

The electrical analogue of oxygen limitation and inhibitors in this situation is to break the circuit at the low "oxygen" voltage connection

or at the position analagous to the point of blocking. This causes all points in the circuit to float to the "substrate voltage" on one side of the break and the "oxygen" voltage on the other.

From the above it can be seen that the only time a change in respiration rate is accompanied by a substantial change in the redox state of cytochrome oxidase is when oxygen is rate limiting, since only then does the enzyme become significantly reduced.

However, so far only a total lack of oxygen has been considered which causes the enzyme to go totally reduced, whereas lowered levels of oxygen may also be expected to increase the level of reduction. The electrical analogue of this is to raise the "oxygen" voltage, so increasing the level of reduction of cytochrome oxidase and decreasing the current (ie electron flow). (If the "oxygen" and "substrate" voltages are equal then all points in the resistor chain will be at this voltage, that is fully "reduced").

This is a return to the argument presented in Section 4.4.3, that sufficient oxygen to allow unimpeded electron flow down the respiratory chain, will be accompanied by almost fully oxidised cytochrome oxidase, whereas reduction in the oxygen supply will cause the enzyme to become reduced with the electron flow slowing down and eventually ceasing.

In these simple terms if the enzyme is oxidised then aerobic respiration is occuring and the cells should have sufficient levels of energy, but if the enzyme becomes reduced then the survival of the cells is likely to be compromised as ATP production will have ceased. This is clearly correct to a point since lack of oxygen which is known to eventually lead to serious tissue damage, will cause the reduction of the enzyme. Hence spectrophotometric monitoring of the redox state of cytochrome oxidase should give an indication of intracellular oxygen sufficiency.

However, the purpose of this (and the following) section is to

illustrate that the situation is not quite this straightforward, because although an increased level of reduced cytochrome oxidase is indicative of compromised aerobic respiration through lack of oxygen, normal resting levels (ie very low) of reduced cytochrome oxidase does not guarantee that ATP is being produced. For instance if oxidative phosphorylation is uncoupled then even though cytochrome oxidase is oxidised no ATP is being produced and tissue damage will ensue. Furthermore, if there is substrate limitation or blocking of electron flow from NADH to cytochrome oxidase, the enzyme will again become fully oxidised even though there is no flow of electrons and therefore no respiration.

Fully oxidised cytochrome oxidase is not in itself a guarantee that aerobic respiration is taking place, electrons must be flowing for this, since the enzyme can be fully oxidised (as in the cases above) with no electron flow at all. The high oxidation level must be a dynamic steady state level as referred to above with electrons being continually accepted and passed onto oxygen.

Despite these potential shortcomings the proven use of monitoring cytochrome oxidase in all types of physiological experiment (see Section 4.8) seems to suggest that in normal in vivo circumstances it is oxygen that is commonly the rate limiting factor for respiration and therefore using the redox state of cytochrome oxidase as a "metabolic monitor" is a useful technique.

However, the above must be borne in mind, particularily so, in a clinical situation where the physiological behaviour and responses of intensive care patients, for example, may differ considerably from those of a healthy subject.

At this point it is pertinent to note that cytochrome oxidase is not the only member of the respiratory chain which can be used for metabolic monitoring, since fluorimetric studies of the redox state of NADH are also successfully employed (RENAULT (1982), (1984), MAYEVSKY (1984)).

This is of interest since the two components are at opposite ends of the respiratory chain, and as can be seen from Table 4.2, significant changes in the redox states of the two components occurs under quite different circumstances.

4.5.3 The Kinetics of Cytochrome Oxidase.

In the above section it was described how variations in oxygen concentration will lead to changes in the redox state of cytochrome oxidase. The relationship between the two is now considered, and is of significance concerning the results obtained from monitoring the redox state of cytochrome oxidase *in vitro* and *in vivo*.

In enzymatic terms cytochrome oxidase catalyses the transfer of electrons from reduced cytochrome c to oxygen, and so mediates a two substrate reaction. Consequently both the rates of electron transfer to and from cytochrome oxidase (ie levels of reduced cytochrome c and oxygen) can affect its redox state.

In the treatment here (and in Section 4.11) it is assumed that sufficient reduced cytochrome c is present so that its concentration does not limit the rate of electron transfer. Therefore it is the oxygen concentration that is the rate limiting factor which restricts how fast reduced cytochrome oxidase can donate electrons to become re-oxidised. The reaction being catalysed is essentially that given in Equation 4.5, and so in effect the enzyme is consuming oxygen.

In basic terms the more oxygen consumed then the more oxidised the enzyme, and since the rate of oxygen consumption is dependent upon oxygen concentration, then here is the link between this and redox state. (This relationship is considered in more detail in Section 4.11).

The relationship between the rate of oxygen consumption by cytochrome oxidase, and oxygen concentration is given by the rate

equation for the enzyme (ie cytochrome oxidase) catalysed reaction of the transfer of reducing equivalents to oxygen.

The graphical form of the rate equation which shows the effect of substrate (in this case oxygen) on the rate of an enzyme catalysed reaction with Michaelis-Menten characteristics (DIXON (1976), LEHNINGER (1977)), is shown in Figure 4.12. For a given concentration of enzyme the rate increases gradually with substrate concentration with the reaction reaching its maximum velocity (Vmax), when the enzyme is saturated with substrate. The reaction then proceeds with zeroth order kinetics. An important parameter of this graph is the Km which is the substrate concentration when the reaction rate is half maximal. The Km is linked to the affinity of the enzyme in that an enzyme with a high/low Km has a low/high affinity for its substrate.

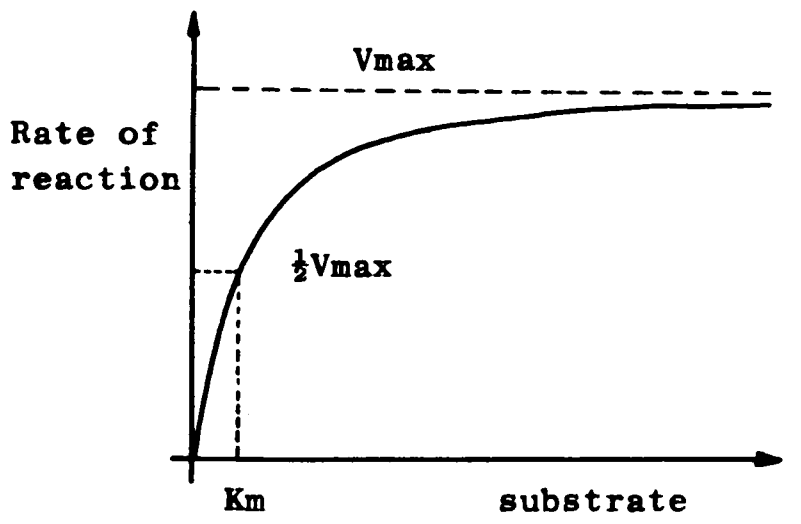

Figure 4.12 Effect of substrate concentration on the rate of an enzyme catalysed reaction.

Considering the kinetics of the consumption of oxygen by cytochrome oxidase the striking feature of the reaction in vitro is the remarkably high affinity of the enzyme for oxygen. The consequence of this is that as long as there is even a small amount of oxygen present the enzyme continues to consume oxygen at the maximum rate (the Km in terms of the

partial pressure of oxygen (pO_2) is less than 1mmHg), only when the pO_2 has virtually fallen to zero does the rate of oxygen consumption decrease, and then extremely quickly. This is shown in Figure 4.13. This feature is demonstrated by the results in Section 4.6, and means that <u>in vitro</u> the redox state of cytochrome oxidase has little scope as an indicator of oxygen concentration since the enzyme will generally be either fully oxidised (down to pO_2 <1mmHg) becoming fully reduced once the pO_2 has virtually reached zero.

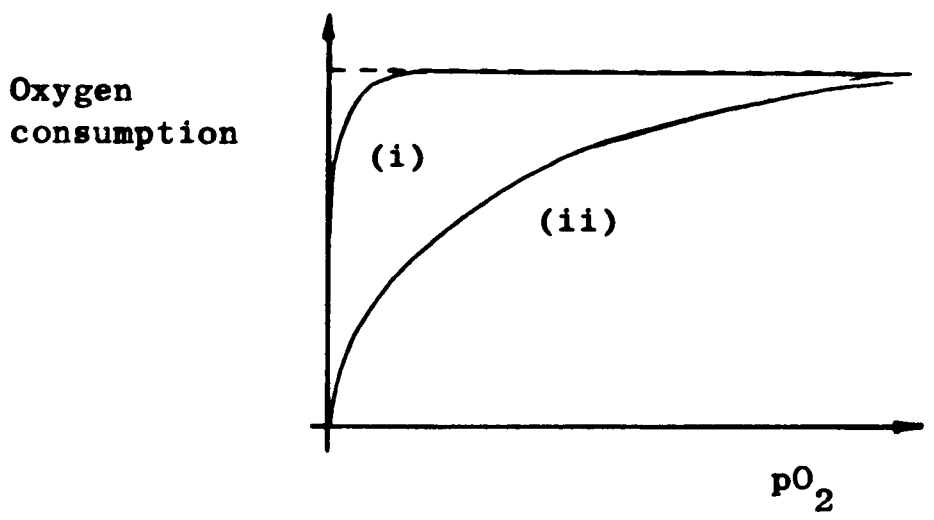

Figure 4.13 Reaction kinetics of cytochrome oxidase with the (i) usual high and (ii) apparently low affinity for oxygen.

If this was also the case <u>in vivo</u> then it may be expected that the only information monitoring cytochrome oxidase would yield would be if tissue was totally anoxic. However, <u>in vivo</u> it has been found that the enzyme appears to have a much larger apparent Km. Consequently at a given pO_2, there will be a much greater percentage of the enzyme present in a reduced form than <u>in vitro</u>, and so variations in redox state will occur over a much larger range of pO_2s (as shown in Figure 4.13). Because of this apparent increase in Km the redox state of cytochrome oxidase may indeed be a potentially useful clinical indicator of oxygen sufficiency, hence the interest in its use for non-invasive <u>in vivo</u>

monitoring.

The question of this apparent difference in affinities of cytochrome oxidase for oxygen *in vitro* and *in vivo* is an interesting problem which has arisen from this work. A possible explanation of how this apparently decreased affinity *in vivo* may occur, based on physical arguments is given in Section 4.11, requiring none of the biochemical based theories which have been proposed, although the actual cause is likely to be due to a combination of several factors.

In summary, *in vitro* cytochrome oxidase has such a high affinity for oxygen that it can almost be considered to be always either fully oxidised or reduced which is demonstrated by the experiments in the next section. However, *in vivo* the enzyme has a much higher Km and a change from fully oxidised to fully reduced enzyme occurs over a much larger range of pO_2s.

4.5.4 The Work of Britton Chance et al.

The information concerning the cytochromes, their absorbance spectra, positions within the respiratory chain and relative redox states described so far represents the findings of many years work by many groups. Britton Chance made a large contribution to this field through the development of instrumentation for performing spectrophotometric measurements on the respiratory chain, and its subsequent use in determining the positions of the cytochromes and their relative redox states and kinetics (see Table 4.2 for instance).

It was his development of dual beam spectrophotometry (see Section 3.4.4) which led to the spectrophotometeric monitoring of small changes in absorption against large background attenuations (as is required for work on the cytochromes in cells). Indeed few of the people involved with monitoring the cytochromes' redox states *in vitro* and then

transferring the method to *in vivo* applications, have not collabarated with Chance at some stage.

His work on the development of spectrophotometric methods is illustrated by a set of three consecutive papers (CHANCE (1951a,b,c)), the final one describing a double (dual) beam apparatus for use on turbid suspensions. The technique used in this instrument is the basis of the dual wavelength measurements made by Jobsis and collegues in their studies of cytochrome oxidase.

The use of this type of instrumentation for biochemical experimentation is described in CHANCE (1952,1954). This work includes the use of simultaneous dual beam and oxygen measurement (using electrochemical methods for oxygen determination), and the recording of difference spectra. (These are the spectra of the difference in absorption between a reduced and oxidised sample).

His future work included extensive studies on the respiratory chain (CHANCE (1956, 1959)), the results of which made extensive contributions to the determination and operation of both it and it's components. Since then he has continued to develop new instrumentation (CHANCE (1970).

In summary the instrumentation developed by Chance for spectrophotometric studies on turbid samples was the forerunner of that used for the *in vivo* studies of cytochrome oxidase. In addition the results obtained with this instrument represent a large contribution to the knowledge of the structure and operation of the respiratory chain, including some of the details given above.

4.6 Experimental Work.

4.6.1 Introduction.

As stated at the beginning of this chapter, the chosen approach to investigate the feasibility and benefits of monitoring the redox state of cytochrome oxidase *in vivo* was to begin by studying the enzyme in its simplest form and then gradually move on to increasingly complex systems. To this end the work presented here was performed on pure cytochrome oxidase and intact yeast cells. The results demonstrate the absorption characteristics and fundamental enzymatic properties of cytochrome oxidase, and led to the development of the mathematical models presented in Section 4.11.

Performing these experiments gave a valuable insight into the problems of making sensitive spectrophotometric measurement on dense multicomponent samples. The work also demonstrated some of the difficulties in working with living biological systems (ie yeast).

In Section 4.6.2 the initial attempts to perform these experiments with proprietary biochemicals are described, with results using purified cytochrome oxidase given in Section 4.6.3. This includes the absorption spectra of purified cytochrome oxidase and kinetic experiments on the enzyme both alone and simultaneously with oxygen measurements.

In Section 4.6.4 the preliminary experiments on yeast and problems encountered are described, whilst the results eventually obtained from yeast cells using a dual beam spectrophotometer are given in Section 4.6.5. Similar experiments to these performed using my own instrumentation are described in Section 4.6.6.

4.6.2 Absorption Spectra of Proprietary Cytochrome c and Cytochrome oxidase

The initial aim was to obtain the absorption spectra of cytochrome oxidase and cytochrome c in their reduced and oxidised forms. This would serve to confirm which wavelengths are likely to be most suitable for redox state monitoring, and also demonstrate the inverse relationship in absorbance at 605 and 830nm of cytochrome oxidase with respect to redox state.

Both cytochromes are commercially available and so this was the source used for the initial experiments.

4.6.2.1 Materials and Methods.

The cytochrome oxidase (C5771) and cytochrome c (C3131) were purchased from Sigma Chemical Co. (both isolated from bovine heart). They were suspended in 0.1M potassium phosphate buffer (pH 7.1) and the absorption spectra obtained from a Pye Unicam SP8000 spectrophotometer (see Section 3.4.5) with buffer in the reference cuvette.

4.6.2.2 Results.

Figure 4.14 shows the absorbance spectra of cytochrome c (60 g in 1.1ml buffer) in its oxidised and reduced forms. The oxidised form refers to the sample simply after its suspension in the buffer, whilst the reduced form was obtained by addition of a small quantity of sodium dithionite. The Soret (γ band) is clearly visible, with a slight shift to higher wavelengths and increase in absorbance upon reduction, as are the α and β bands when the compound is in the reduced form. This spectra can be compared with that in Figure 4.8(ii).

This clear absorbance spectra is a consequence of the relative ease of isolation of cytochrome c from the mitochondria. This is in direct contrast to the difficulty in isolating pure cytochrome oxidase (Complex

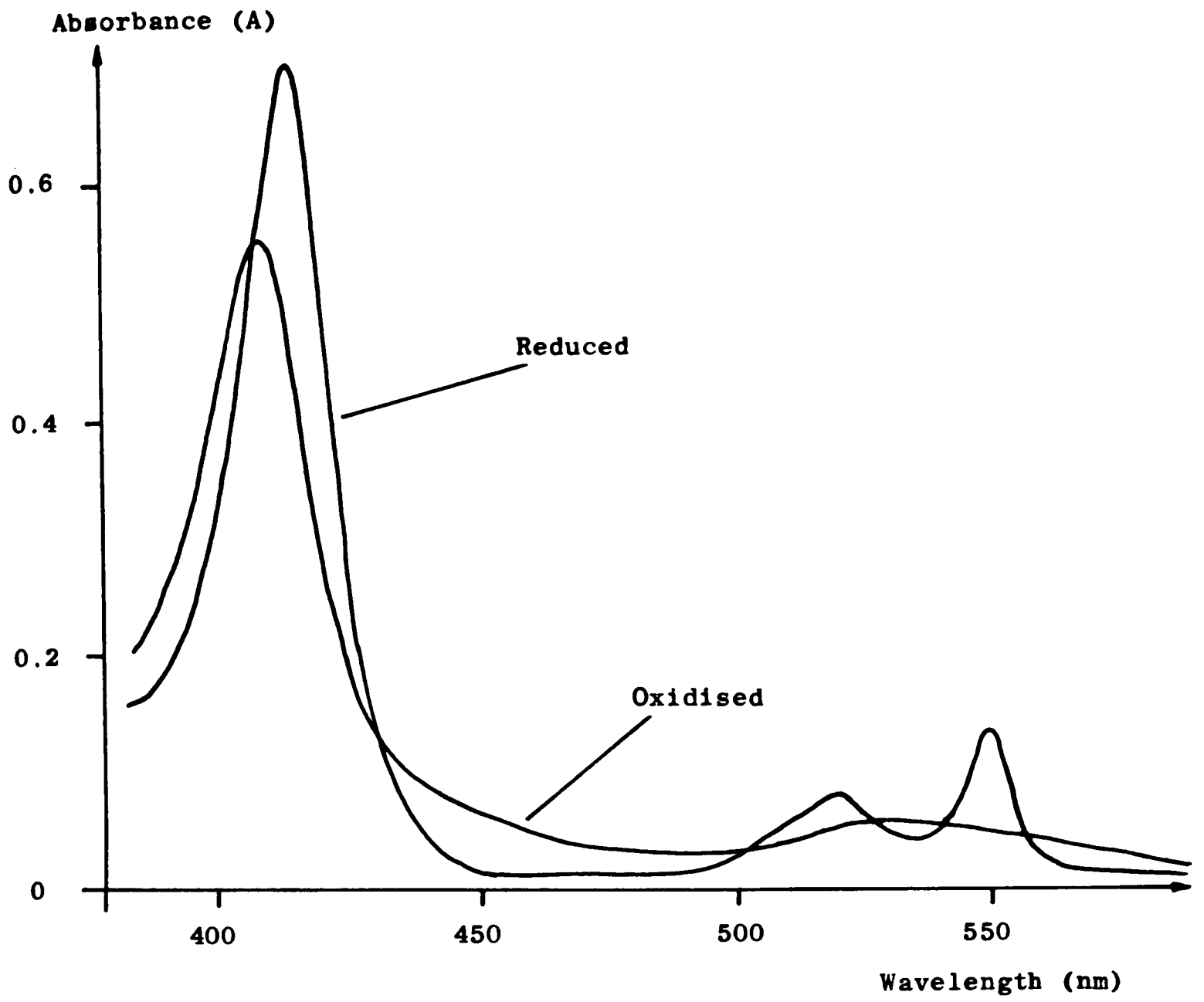

Figure 4.14 The absorption spectra of cytochrome c.

IV), a problem which manifests itself in the absorption spectra with the absorption bands appearing less distinctly on an overall background absorbance. This is shown in Figure 4.15 which is the absorption spectra of cytochrome oxidase (15mg solid (3mg protein) in 1ml buffer), with the oxidised and reduced forms obtained as for cytochrome c. Despite the background absorbance all three visible absorbance bands can be discerned and compared to the absorption spectra shown in Figure 4.8(iii)

The background absorbance and additional peak which appears in the reduced form suggested that although enzymatically the cytochrome oxidase

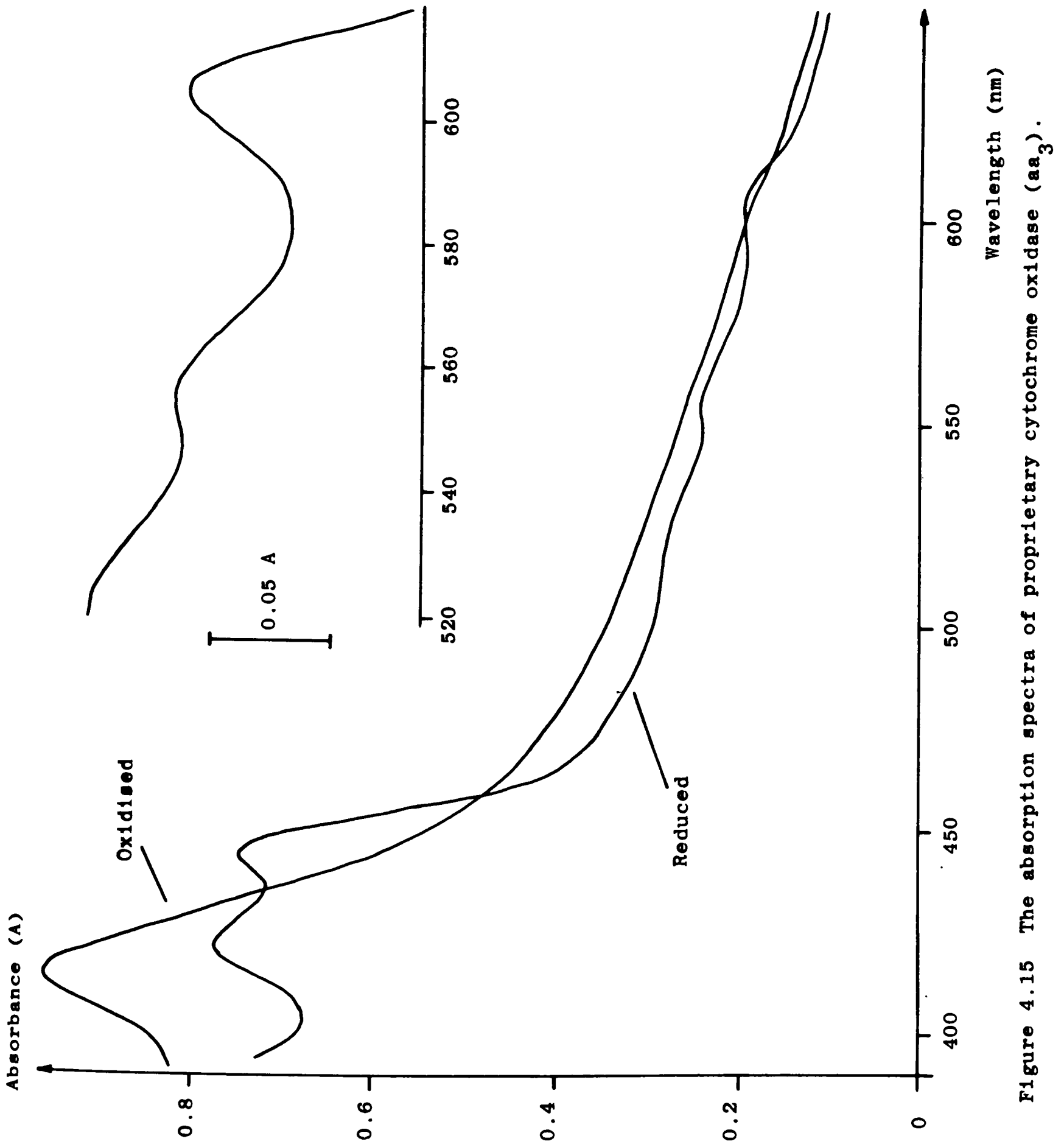

Figure 4.15 The absorption spectra of proprietary cytochrome oxidase (aa_3).

may be pure (ie would catalyse reactions as expected), it contained other compounds rendering it spectroscopically impure. In view of the lack of clarity of the α and β bands and the known relative size of the 830nm absorbtion band it was felt unlikely that this band would be visible in this sample. Runs on a Beckman DU7 spectrophotometer (which operates up to 1000nm) confirmed this, and so it became clear that to perform the intended spectrophometric studies on cytochrome oxidase a purer source of the enzyme was required.

This decision was later reconfirmed during the preliminary yeast studies (Section 4.6.4) when the spectra of the above proprietary cytochrome oxidase was obtained using a Cecil CE598 split beam spectrophotometer. The inset in Figure 4.15 shows the absorption spectra obtained from dithionite reduced cytochrome oxidase (50mg solid suspended in 1.5ml of 0.25M Sucrose, 0.6M Tris-HCl buffer ,pH 8.2) over the range 520-620nm. Despite the clarity of these bands there was no evidence of the 830nm band endorsing the decision to obtain a purer sample of cytochrome oxidase for the near-IR studies.

4.6.3 Experiments Using Purified Cytochrome Oxidase.

Although purer cytochrome oxidase was required, lack of expertise, facilities and time meant that to embark upon attempting to personally purify the enzyme was not a reasonable course of action. However, a literature search revealed that Dr B.Hill and colleagues (University of East Anglia, Norwich) were studying the properties of the enzyme, and they kindly supplied the samples on which the following experiments were performed.

4.6.3.1 The Absorption Spectra of Cytochrome Oxidase.

4.6.3.1.1 Materials and Methods.

Samples were prepared by diluting the cytochrome oxidase as supplied (see Table 4.3 for details) in buffer (0.1M Sodium Phosphate, 0.25% (w/v) Tween 80 (pH 7.4)). The spectra were obtained from a Philips SP6-550 single beam machine with no plotting facility. Therefore "split beam" spectra were obtained manually (see Section 3.4.5) by reading the absorbance of cytochrome oxidase solution and buffer separately over the range required and then subtracting one from the other. Measurements were taken every 10nm except in the regions of particular interest where this was reduced to 5nm.

The region of the spectrum investigated was from 400-1000nm although for concentrations large enough for the 830nm absorption band to be clearly seen the absorbances below about 470nm were greater than the range of the instrument.

4.6.3.1.2 Results.

Figure 4.16 shows the absorption spectra of 44.2μM cytochrome oxidase The oxidised spectra is of the enzyme as supplied after dilution, whilst reduction was achieved by addition of sodium dithionite. The α band at 605nm is extremly distinct, with the 830nm band with its much smaller absorbance, large spread and inverse relationship to the α band with respect to redox state, also clearly visible in this sample.

The 830nm band is shown again in Figure 4.17 with an enlarged absorbance scale for concentrations of 44.2, 75.7 and 99.3μM oxidised cytochrome oxidase. The absorption spectra of the reduced enzyme for 44.2 and 99.3μM solutions are also shown which are notable for their flatness.

The prime interest here is in the absorption bands shown above, however during the course of the kinetic experiments (see below)

The cytochrome oxidase was prepared from bovine heart essentially according to the method of YONETANI (J. Biol. Chem., 235, 845-852).

The concentration was 265μM with the prepatration suspended in 0.1M sodium phosphate pH 7.4, 0.25% Tween-80.

Haem to protein ratio: 7.50 nmoles haem A/ mg protein

Absorbance Ratios.

$$\frac{A^{ox}_{280}}{A^{red}_{443}} = 1.84 \qquad \frac{A^{red}_{443}}{A^{red}_{420}} = 2.37$$

Extinction coefficient for 605-630nm (red-ox) of $27mM^{-1}\ cm^{-1}$

Extinction coefficient for the reduced-oxidise change at 830nm of $-3.20mM^{-1}\ cm^{-1}$

Table 4.3 Details of the purified cytochrome oxidase as supplied by Dr. B. Hill.

absorption spectra of the enzyme showing the relative sizes of the Soret and the other visible bands were obtained from the Pye Unicam SP8000. The absorbance spectra of ferricyanide (an artificial electron acceptor) oxidised and dithionite reduced 4μM cytochrome oxidase are shown in Figure 4.18. All absorption bands are clearly visible, with the structure around approximately 500-600nm shown in greater detail in the inset.

All of the spectra obtained from the purified enzyme can be compared to those in Figure 4.8(iii) to which they are virtually identical.

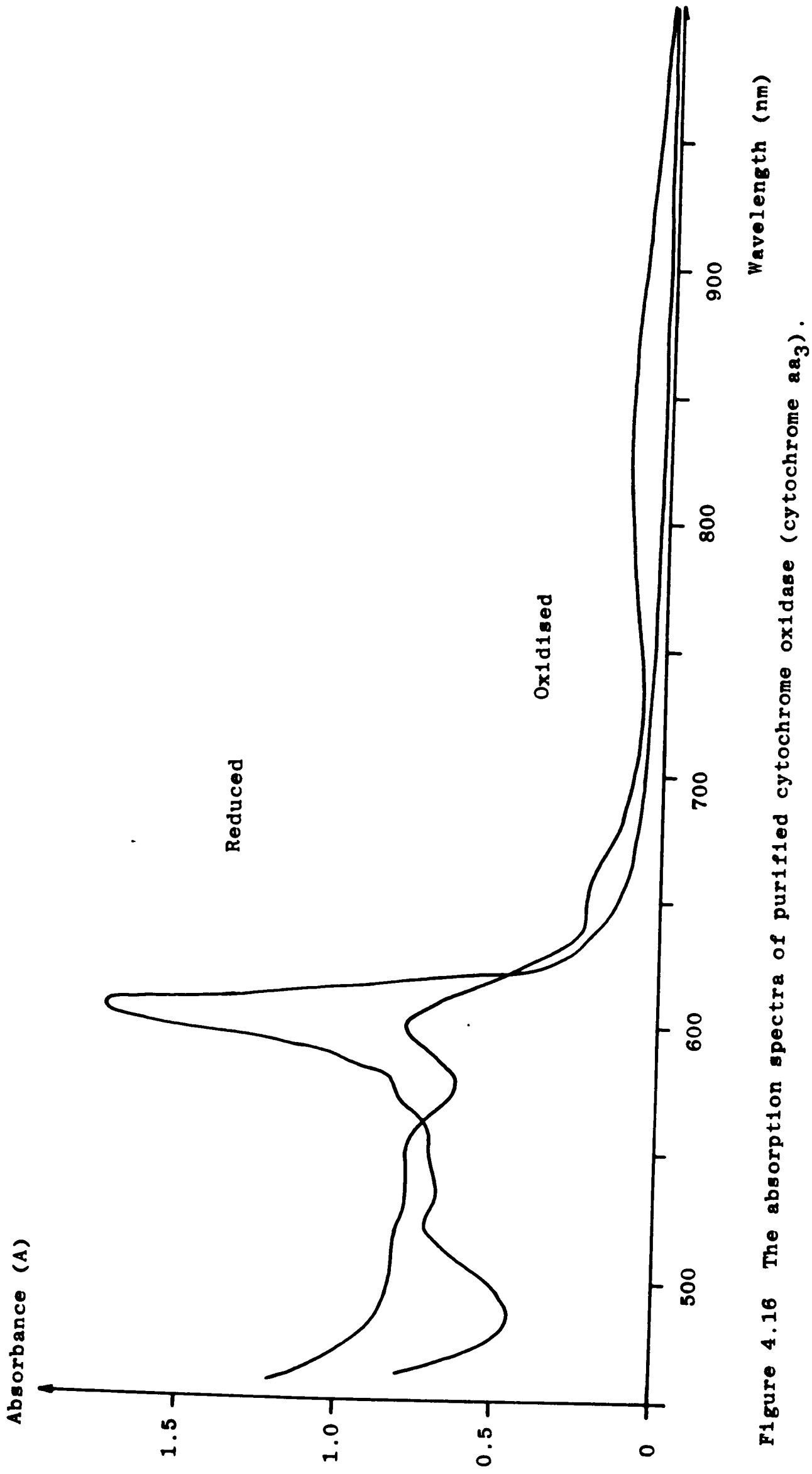

Figure 4.16 The absorption spectra of purified cytochrome oxidase (cytochrome aa_3).

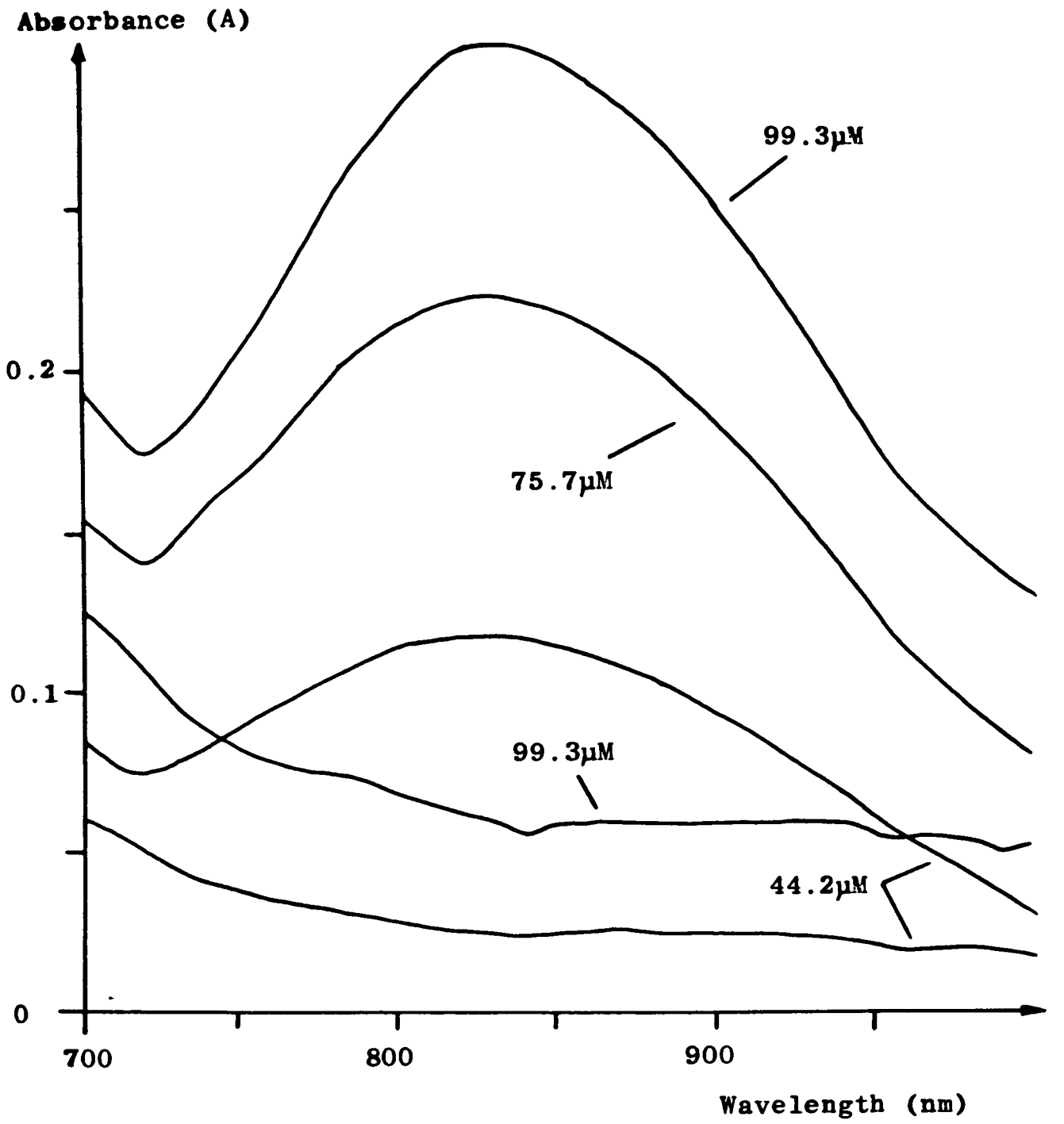

Figure 4.17 The near-IR absorption band of oxidised cytochrome oxidase.

Whilst these spectra show the details of the difference in absorbance of the enzyme in the two redox states, this could also be observed by eye as the solution turned from brown to green upon the addition of sodium dithionite.

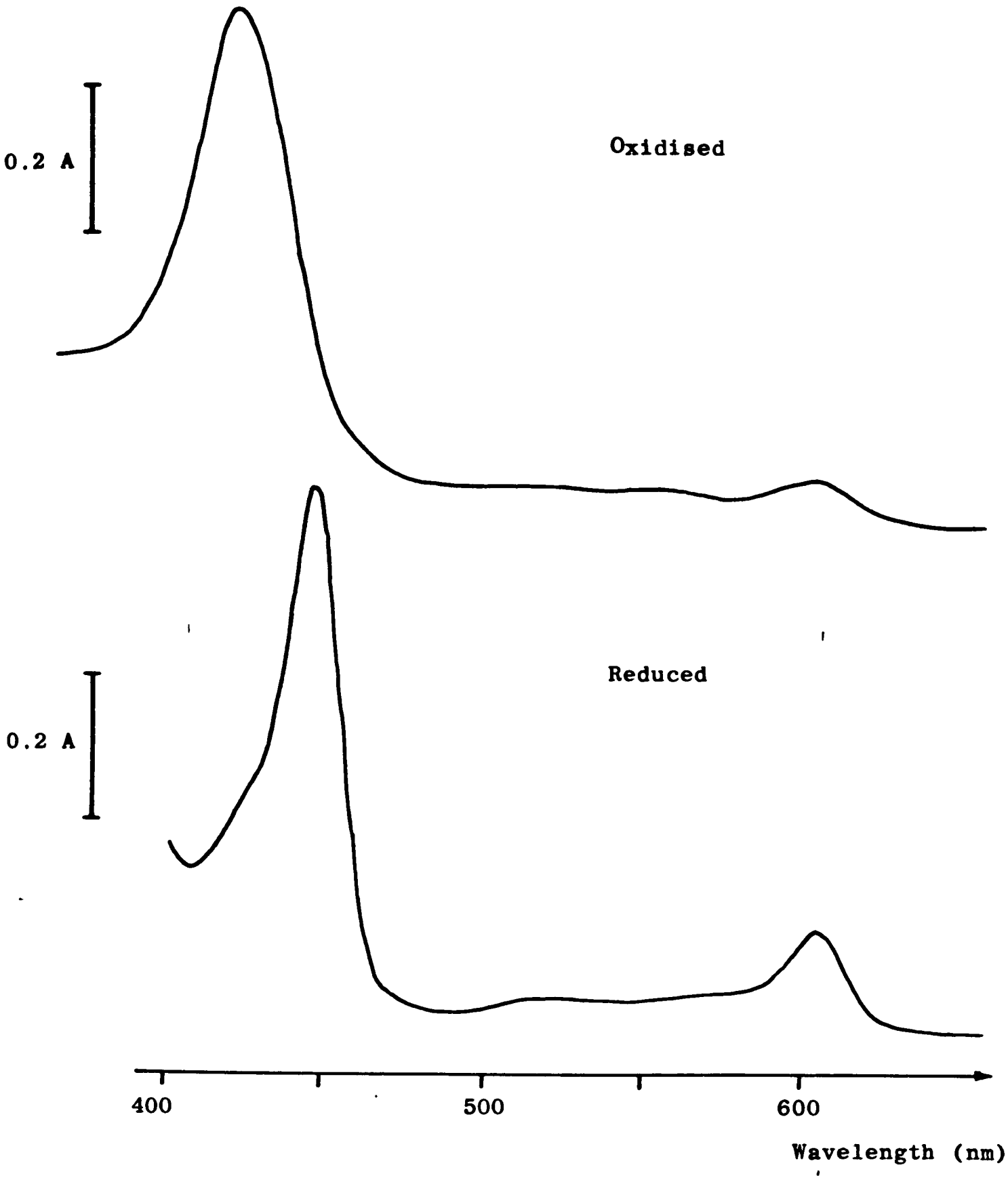

Figure 4.18 The absorption spectra of cytochrome oxidase.

4.6.3.2 Kinetic Studies of Cytochrome Oxidase Using Spectrophotometry

Once the absorption spectra of cytochrome oxidase in its reduced and oxidised forms had been obtained, the next step was to attempt to monitor

the change in absorbance of the enzyme as its redox state altered with time.

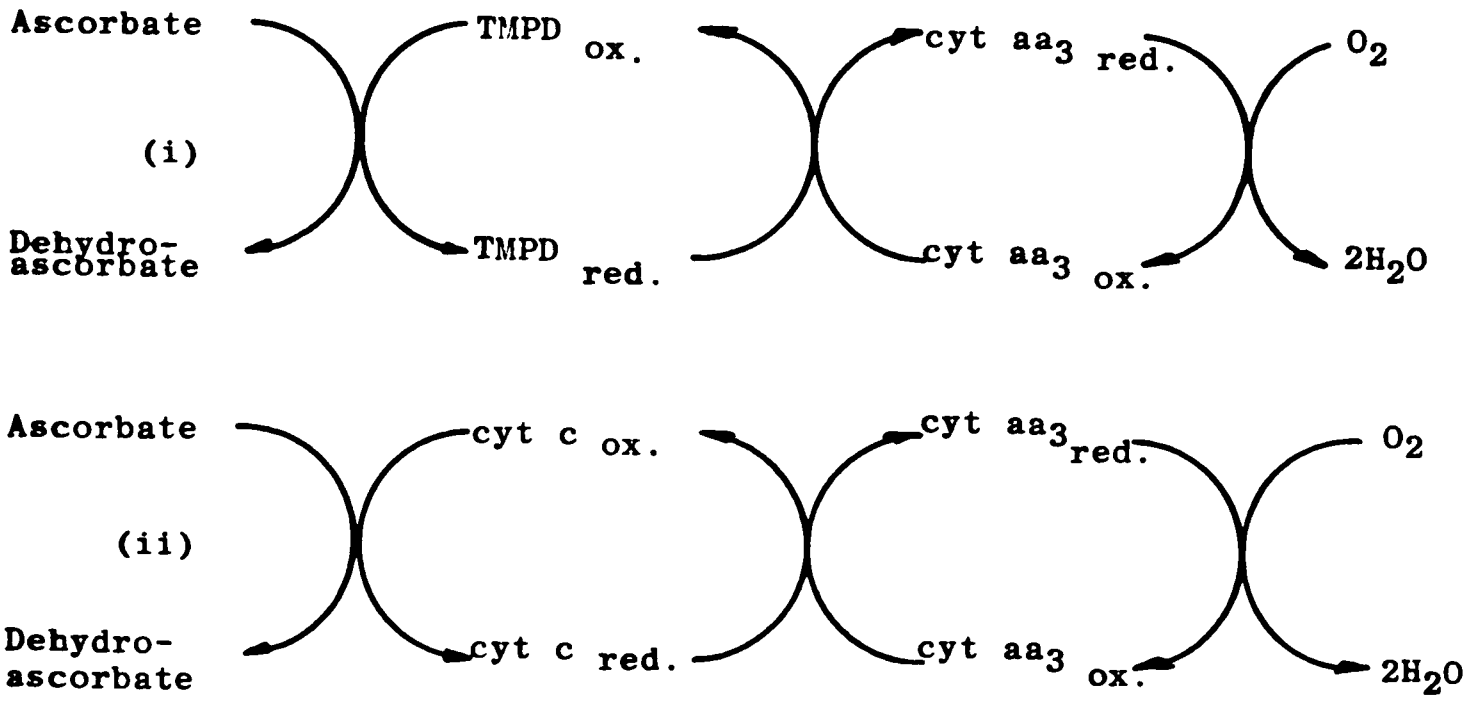

Figure 4.19 The artificial respiratory chains used for the reduction of cytochrome oxidase (cyt aa_3).

The intention in this first series of experiments was to set up a simple artificial respiratory chain to feed electrons to the cytochrome oxidase, so gradually reducing it and causing an increase/decrease in the absorption at 605 nm/830 nm.

Two respiratory chains were used consisting of: 1) sodium ascorbate (L-ascorbic acid), N,N,N',N'-tetramethyl-p-phenyldiamine (TMPD) and cytochrome oxidase and 2) ascorbate, cytochrome c and cytochrome oxidase,

with the second more closely resembling the actual mammalian respiratory chain.

For the ascorbate, TMPD, cytochrome oxidase system the TMPD would give electrons to cytochrome oxidase , becoming oxidised itself but then receive electrons from the ascorbate (present in excess) and hence become re-reduced and ready to feed on more electrons. The same cycling process also takes place in the second system, with both illustrated in Figure 4.19.

In view of the high affinity of cytochrome oxidase for oxygen it was assumed that it would be necessary to block this transfer else the cytochrome oxidase would be constantly feeding electrons at a maximum rate to dissolved oxygen and so no appreciable change in the redox state would be seen. The blocking of electron transfer to oxygen was to be achieved using sodium azide.

4.6.3.2.1 Materials and Methods: TMPD System.

The following materials were used; 265µM cytochrome oxidase as supplied by Dr B. HIll (see Table 4.3), 500mM ascorbate (A7611, Sigma), 6mM TMPD (T7394, Sigma), 156mM sodium azide and buffer solution of 0.1M sodium phosphate containing 0.25% (w/v) Tween-80 (P1754, Sigma) (pH7.4). Recordings of absorption versus time were made by taking the appropriate output from the Philips SP6-550 spectrophotometer to a chart recorder.

4.6.3.2.2 Results: TMPD System.

The top trace in Figure 4.20 shows the change in absorption, at 830nm, with time, of the first artificial respiratory chain system. The cuvette's initial contents were 100µl of cytochrome oxidase and 5ul of azide in 1ml of buffer which had been incubated at room temperature for about 10mins (to enable the azide to bind and therefore inhibit the cytochrome oxidase). Initially 10µl of ascorbate was added. This caused no change in absorbance as the ascorbate cannot directly donate electrons to cytochrome oxidase and so the latter remained in the same redox state. Approximately 45secs later, as indicated, 10µl of TMPD was added which caused an initial drop in absorbance due to the presence of some reduced TMPD, which consequently produced an increase in the proportion of reduced cytochrome oxidase. This transient phase was then followed by a steadying of the redox state, to a relatively stable level until finally there was a rapid decrease in absorbance indicating the enzyme had become fully reduced.

Clearly the expected gradual decrease in absorbance as the enzyme became more reduced, with the transfer of electrons blocked, had not occured. Rather the enzyme was remaining in a (relatively) steady oxidised state by consuming the dissolved oxygen. Only when this oxygen had virtually all been removed, so becoming rate-limiting, did the enzyme become reduced, and then very rapidly due to its low Km.

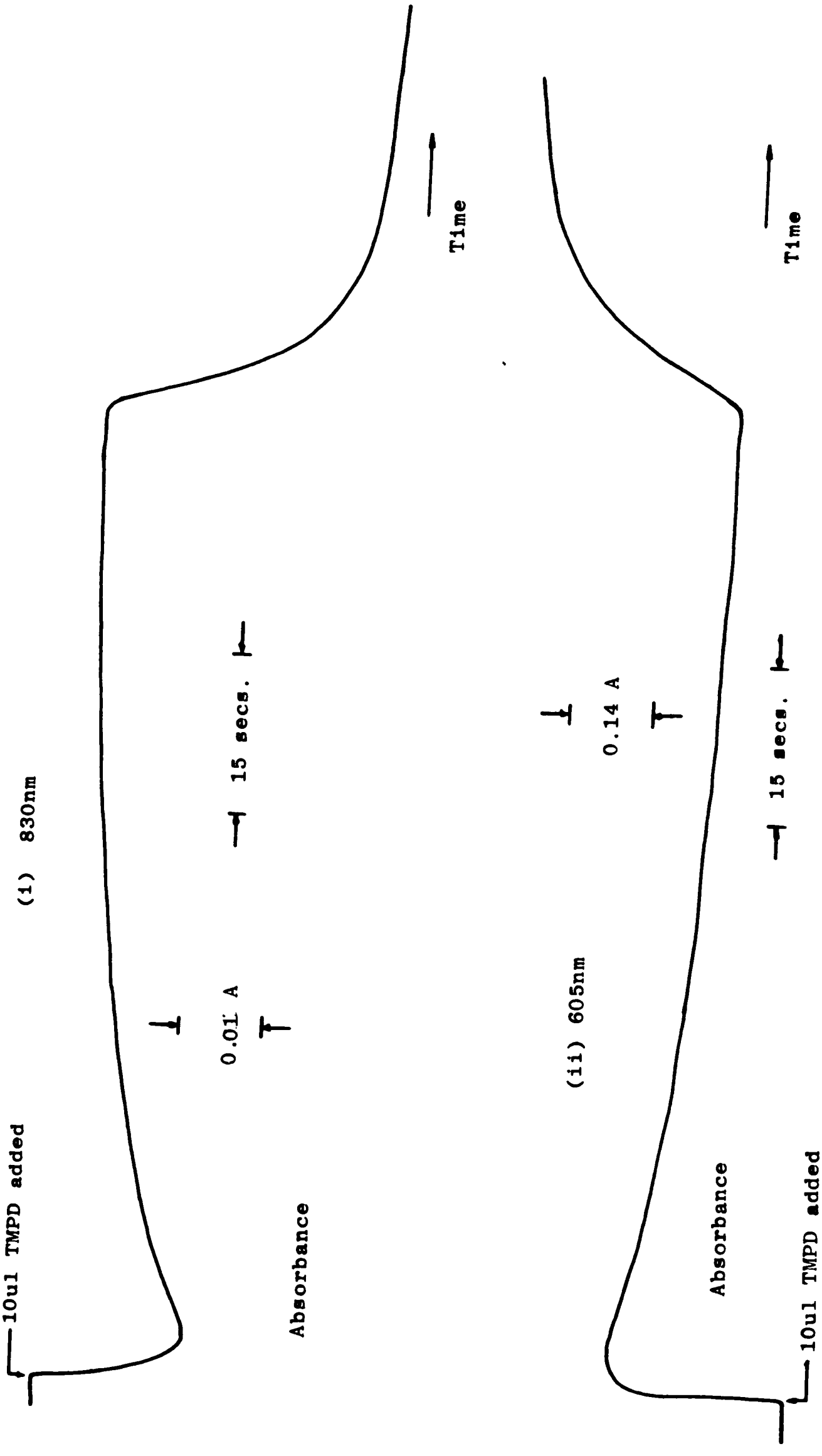

Figure 4.20 Reduction of cytochrome oxidase by TMPD observed at: (1) 830nm and (11) 605nm.

Introducing air into the cuvette caused reoxidation of the sample with again a steady absorbance observed followed by a rapid drop as the oxygen again fell to zero. This confirmed that the azide was not having its required effect. However, as its only purpose was to block the transfer of electrons to oxygen, because it was felt the cytochrome oxidase would otherwise remain permanently oxidised, which was clearly not the case, then this was no problem. The cytochrome oxidase was being reduced because it was consuming oxygen in the cuvette faster than the rate at which it was being replenished from the air (even a stopper was not required to inhibit this). Indeed the traces obtained with the switch from the enzyme being oxidised to reduced due to its consumption of available oxygen are of more interest than the gradual reduction of the inhibited enzyme since they demonstrate the kinetics of the reaction between cytochrome oxidase and oxygen.

The bottom trace in Figure 4.20 shows the same study (with new samples and omitting the azide) performed at 605nm. A similar trace is obtained to that at 830nm except that the reduction of the cytochrome oxidase is accompanied by an increase in absorbance as expected.

Finally in Figure 4.21 to confirm that azide is not required the same solution monitored in Figure 4.20(ii) is shown at 830nm after introducing oxygen to the cuvette with the trace beginning just before the oxygen becomes rate limiting. As expected the trace is of a similar form as the end of the one in Figure 4.20(i).

4.6.3.2.3 Materials and Methods: Cytochrome c System.

These experiments were then repeated using the cytochrome c system for which the materials used were the same except that the TMPD was itself replaced by cytochrome c (C7752 Sigma isolated from horse heart), which was now used to mediate the transfer of electrons from ascorbate to cytochrome oxidase (see Figure 4.19). The experiment was performed by

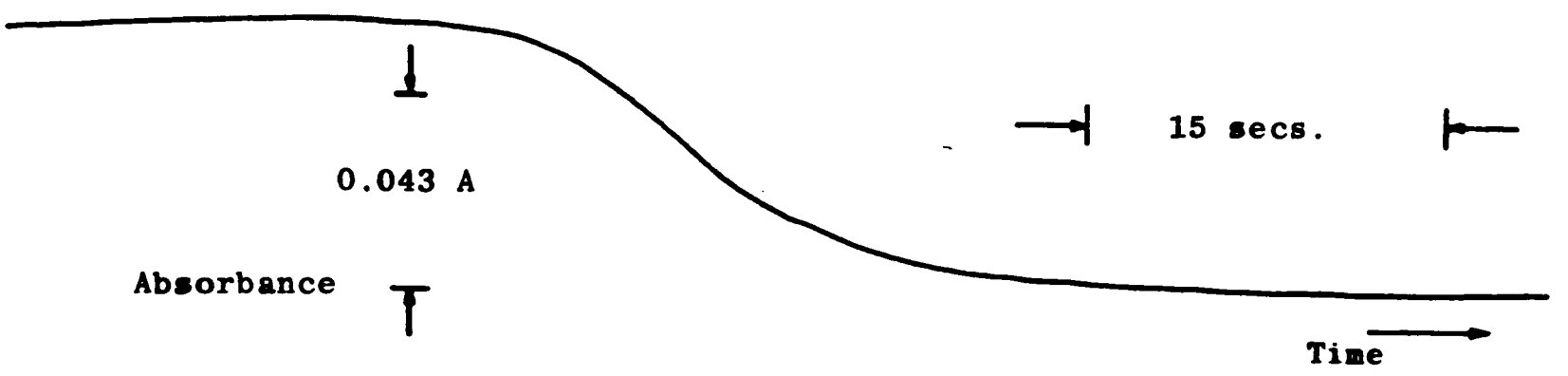

Figure 4.21 Reduction of cytochrome oxidase by TMPD observed at 830nm.

adding a mixture of cytochrome c and ascorbate to a cuvette containing only cytochrome oxidase solution. The cytochrome c/ascorbate mixture was prepared by the addition of 10µl of ascorbate to a cytochrome c solution (2.5mg in 1ml buffer) so causing all of the cytochrome c to go reduced. This reduction was followed by observing the absorbance of the mixture at 550nm (the position of cytochrome c's α band) as shown in Figure 4.22. Ascorbate was present in excess to continually re-reduce cytochrome c after its reaction with cytochrome oxidase.

4.6.3.2.4 Results: Cytochrome c System.

Figure 4.23 shows the reduction of cytochrome oxidase, observed at 605 and 830nm as the oxygen dissolved within the cuvette is finally consumed. In both cases 100µl of the reduced cytochrome c/ascorbate mixture was added to 100µl of cytochrome oxidase in 1ml of buffer followed by a further 10µl of ascorbate added about 100 secs before the start of the traces.

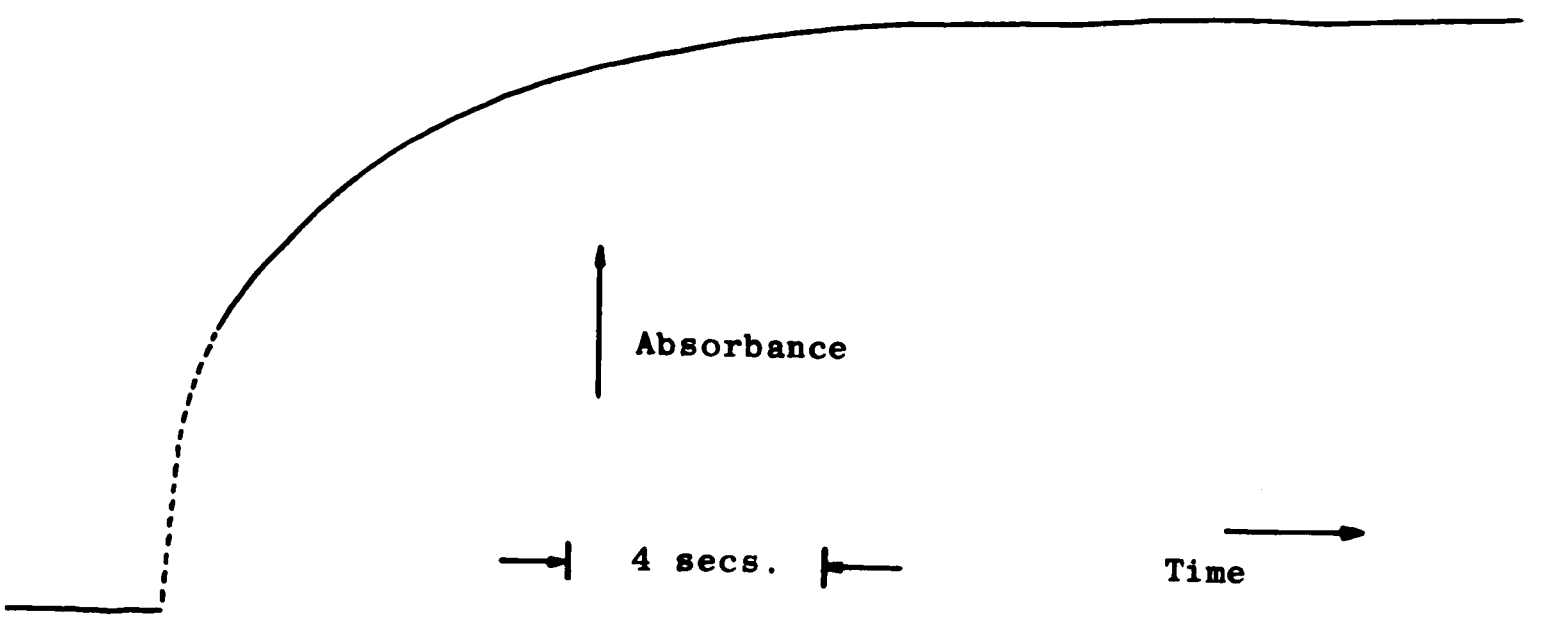

Figure 4.22 Reduction of cytochrome c by ascorbate observed at 550nm.

4.6.3.2.5 Summary.

The above results are of value for several reasons. They show that the absorbance of cytochrome oxidase is related to redox state and the inverse relationship between the absorbances at 605 and 830nm. An interesting experiment would be to repeat these studies using the spectrophotometer described in Chapter 3 (which was constructed after the above experiments). Then the change of the whole absorbance spectra as the enzyme switches from an oxidised to reduced state could be observed.

The results also demonstrate the high affinity of cytochrome oxidase for oxygen, by way of the rapid switch of the enzyme from a "fully" oxidised to reduced state. Referring to the kinetics shown in Figure 4.13, the enzyme consumes the oxygen at a maximum rate, so remaining oxidised until very low oxygen concentrations where the consumption rapidly decreases, and so the enzyme accordingly rapidly becomes reduced.

In these studies redox state is not a particularly good indicatior of oxygen concentration since the change from an oxidised state is so

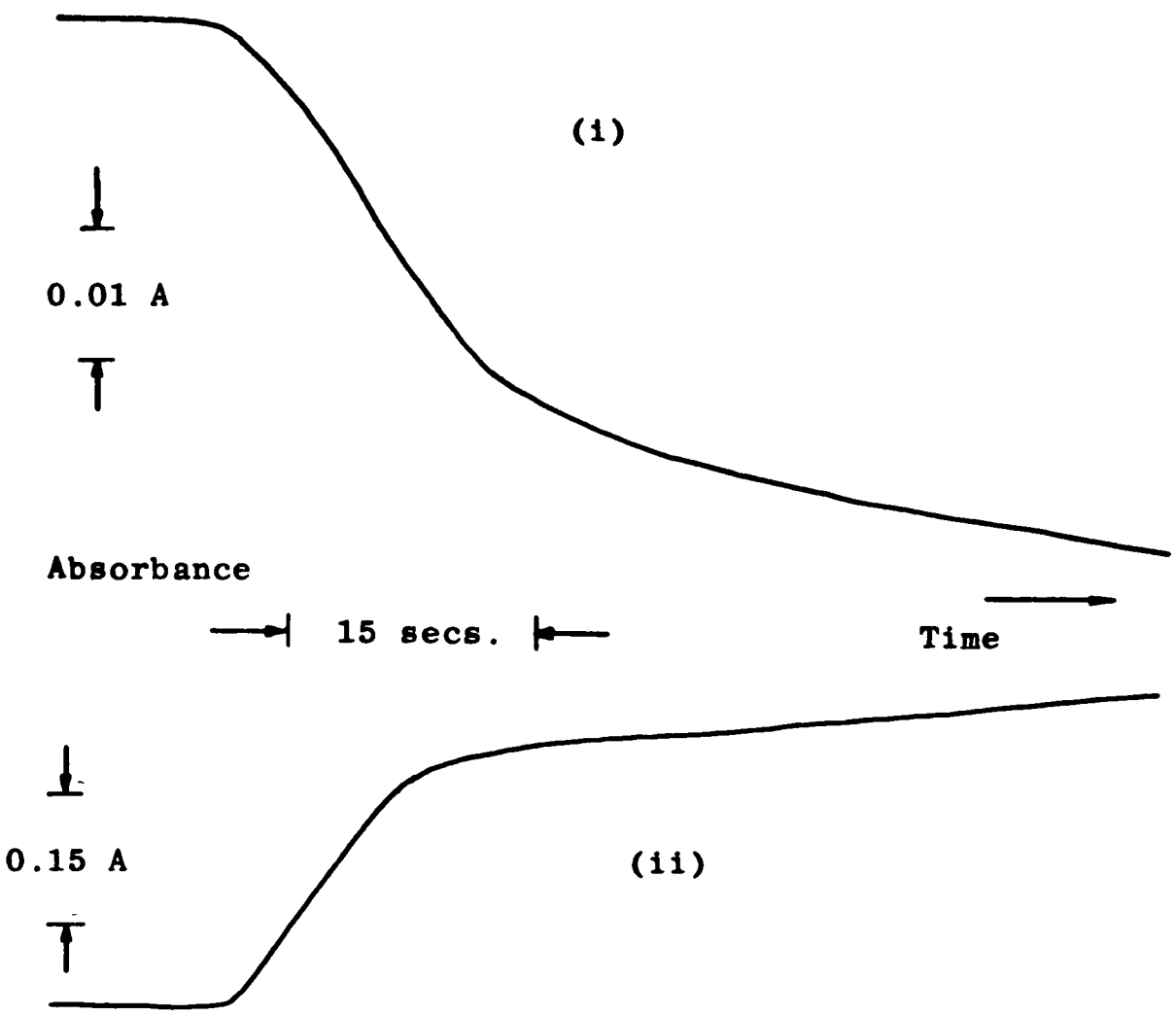

Figure 4.23 Reduction of cytochrome oxidase by cytochrome c observed at: (i) 830nm and (ii) 605nm.

rapid there is little indication of a decrease in oxygen level. Rather the redox state basically reflects whether or not any oxygen is present. This is why the apparent lowering of affinity of the enzyme *in vivo* is important for the technique to be clinically useful.

The relationships between redox state, absorbance, oxygen consumption and oxygen concentration are discussed in detail in Section 4.11, where definite mathematical links between the variables are proposed and used to model the above graphs (and those in the following section). A further model attempts to explain the *in vivo*/*in vitro* affinity anomaly using the observation, that *in vitro* the enzyme can

virtually be considered to be in one of two states, that is either oxidised or reduced.

4.6.3.3 Kinetic Studies of Cytochrome Oxidase: Spectrophotometric and Oxygen Measurements.

Following the above the next set of studies were made to monitor both oxygen partial pressure and absorbance. Results obtained would hopefully confirm the expected relationships between oxygen concentration, oxygen consumption and redox state inferred from the previous experiments. Simultaneous optical and oxygen measurements have been made in the past using microelectrodes within a cuvette (CHANCE (1954). The approach adopted here was to use an oxygen measurement cell, in which the partial pressure of oxygen in the solution placed in the cell was monitored. Initial experiments using such a device, built within the Bioengineering Unit by Mr P.J.Goddard, with the oxygen content and absorbance of similar samples monitored separately using the cell and the SP8000 spectrophotometer proved both unreliable and irreproducible

However all the problems encountered were solved by performing simultaneous oxygen and absorbance measurements using a commercially available oxygen measurement cell (Rank Brothers, Cambridge) with a simple single beam "spectrophotometer" built around it.

4.6.3.3.1 Materials and Methods.

The reduction of cytochrome oxidase in these experiments was achieved using the artificial respiratory chain of ascorbate, TMPD and cytochrome oxidase as described in the last section. Larger volumes of these compounds were needed as the experiments were now performed in the oxygen cell. Stock solutions of approximately 2.7M sodium ascorbate and 30mM TMPD were used to give the required concentrations in the final

mixture volume of 5ml. Cytochrome oxidase was used as supplied whilst the buffer was the same as above.

The oxygen cell was used as the "cuvette" within a spectrophotometer which was built around it as described in Section 3.3.2, where the basic details of the oxygen measurement cell itself are also given. Wavelength selection was by interference filters with filters centred at 600 and 830nm used to study the α and near-IR bands of cytochrome oxidase.

A lock-in amplifier was used to allow studies to be performed under ambient lighting conditions. The absorbance of the solution was not recorded, but rather simply the signal from the photodiode giving the intensity of light detected, therefore an increase in signal corresponded to a decrease in absorbance although the two are not linearly proportional (see Section 3.3.2).

4.6.3.3.2 Results.

The fall in oxygen content and change in light intensity at 600nm passing through a mixture of cytochrome oxidase, 10ul ascorbate and 10µl TMPD in 5ml of buffer is shown in Figure 4.24 for 100 and 200µl quantities of cytochrome oxidase. In both traces there is a linear drop in oxygen content until very low levels are reached. At this time a rapid decrease in light intensity is observed due to the increase in absorbance caused by the reduction of cytochrome oxidase.

In Figure 4.25 the corresponding traces for 300µl quantities of cytochrome oxidase are shown, whilst monitoring the detected light level at 600 and 830nm. These have the same basic form with the reciprocal relationship between the two concerning redox state and absorbance again demonstrated.

It can be seen that as expected the rate of oxygen consumption increases with increasing enzyme concentration. The effect of the smaller change in absorbance at 830nm can be seen by the increased noise

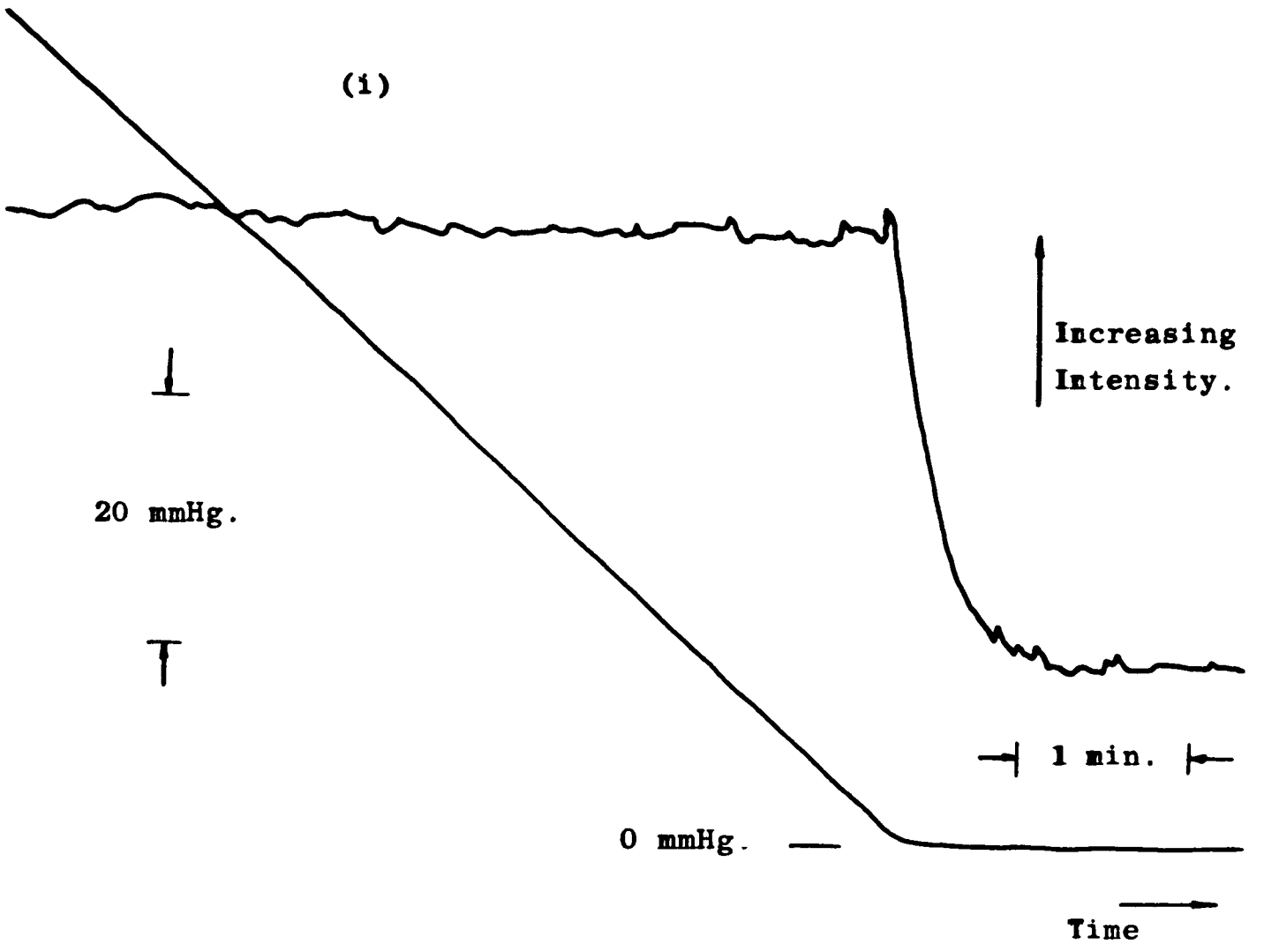

Figure 4.24 Transmitted light intensity (at 600nm), and oxygen content of mixture in the oxygen measurement cell containing: (i) 100µl and (ii) 200µl of cytochrome oxidase.

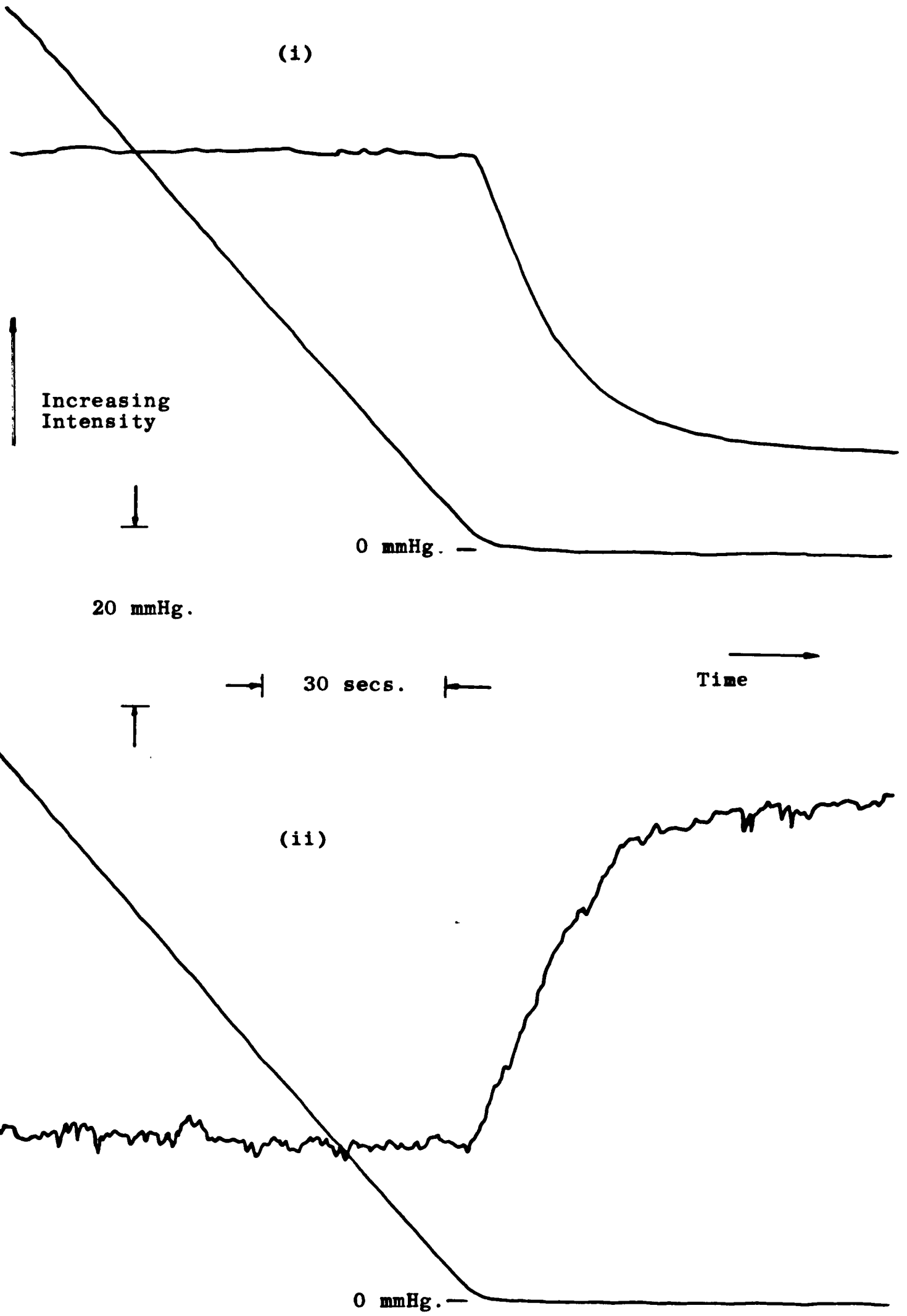

Figure 4.25 Transmitted light intensity at: (i) 600nm and (ii) 830nm, and oxygen content of mixture containing 300ul of cytochrome oxidase.

on the intensity signal due to the increased detector sensitivity

required to monitor the switch in redox state.

During the course of two experiments (once at either wavelength) oxygen consumption decreased, and the solution visibly darkened, although this was only registered as a decrease in transmitted intensity at 600nm. These traces are shown in Figures 4.26 and 4.27.

Although not planned these traces show the effect of the decrease in the ascorbate concentration (since it is not recycled, see Figure 4.19) to such levels that it began to limit the rate of reduction of TMPD. Hence less electrons were transferred from TMPD to cytochrome oxidase to oxygen and so oxygen consumption decreased whilst the TMPD became less reduced. (This is essentially substrate limitation as described in Section 4.5.2). The temporary darkening of the sample is therefore due to a shift in the redox state of TMPD, and once all the oxygen is eventually consumed (albeit at a reduced rate) the cytochrome oxidase finally goes reduced, as does the TMPD and so the intensity level goes to a value determined by the increase in absorbance of cytochrome oxidase and decrease in that of TMPD (see Figure 4.26).

All traces shown in the above sections have been traced from the originals of the intensity, absorbance and oxygen measurement traces. (The latter in particular were noisy which was mainly due to stirrer action and bubbles in the sample and water jacket interfering with the light beam).

4.6.3.3.3 Summary.

The results of these studies confirm that it is a decrease in oxygen concentration to very low levels that finally causes cytochrome oxidase to go reduced whilst before this it is virtually fully oxidised. Together with the rapidity of the change in redox state this shows that cytochrome oxidase has a very high affinity for oxygen, which is also demonstrated by the linear fall in oxygen concentration (ie constant

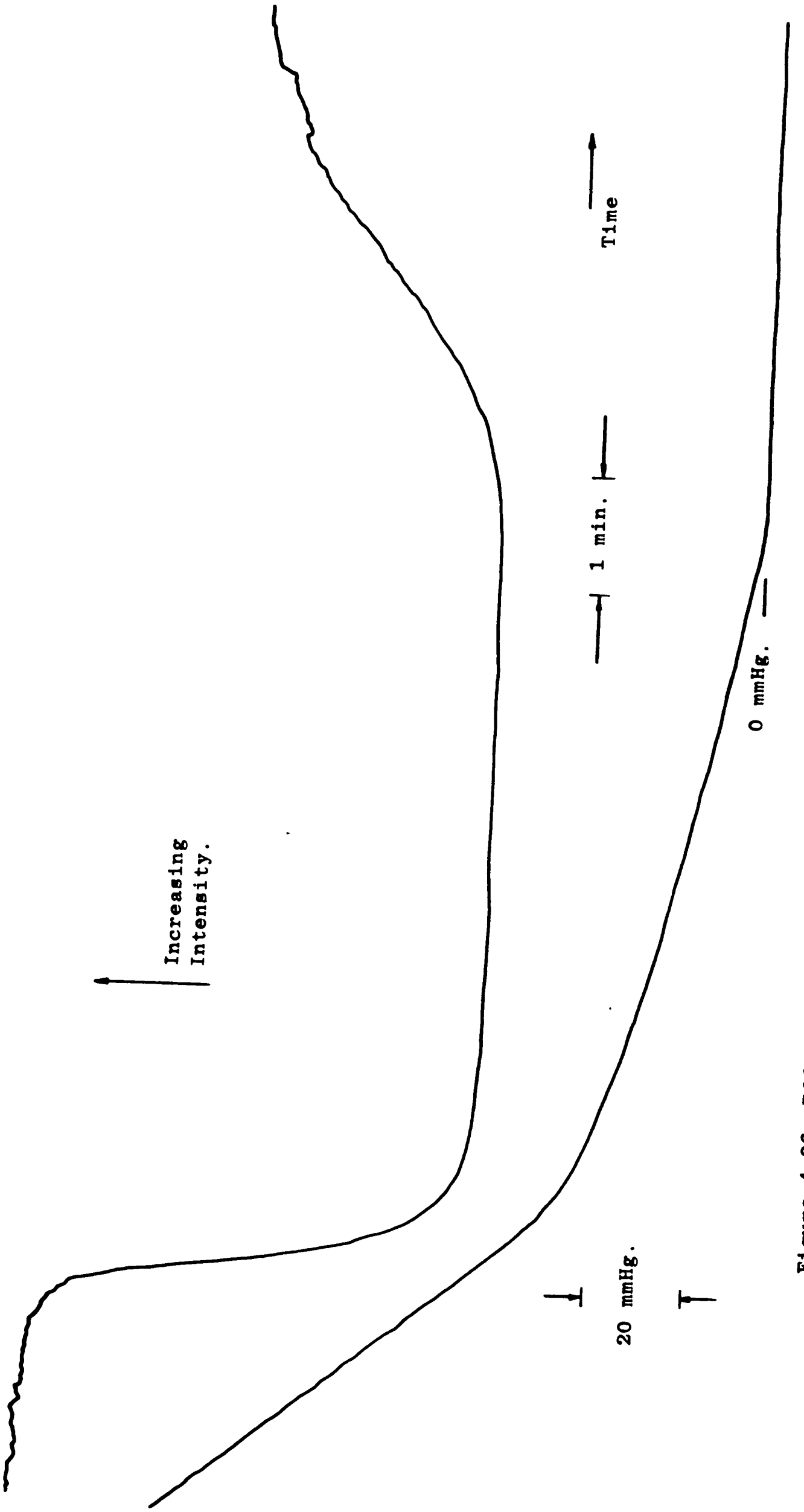

Figure 4.26 Effect of a decrease in ascorbate concentration on transmitted intensity at 600nm, and pO_2 (200ul of cytochrome oxidase in sample).

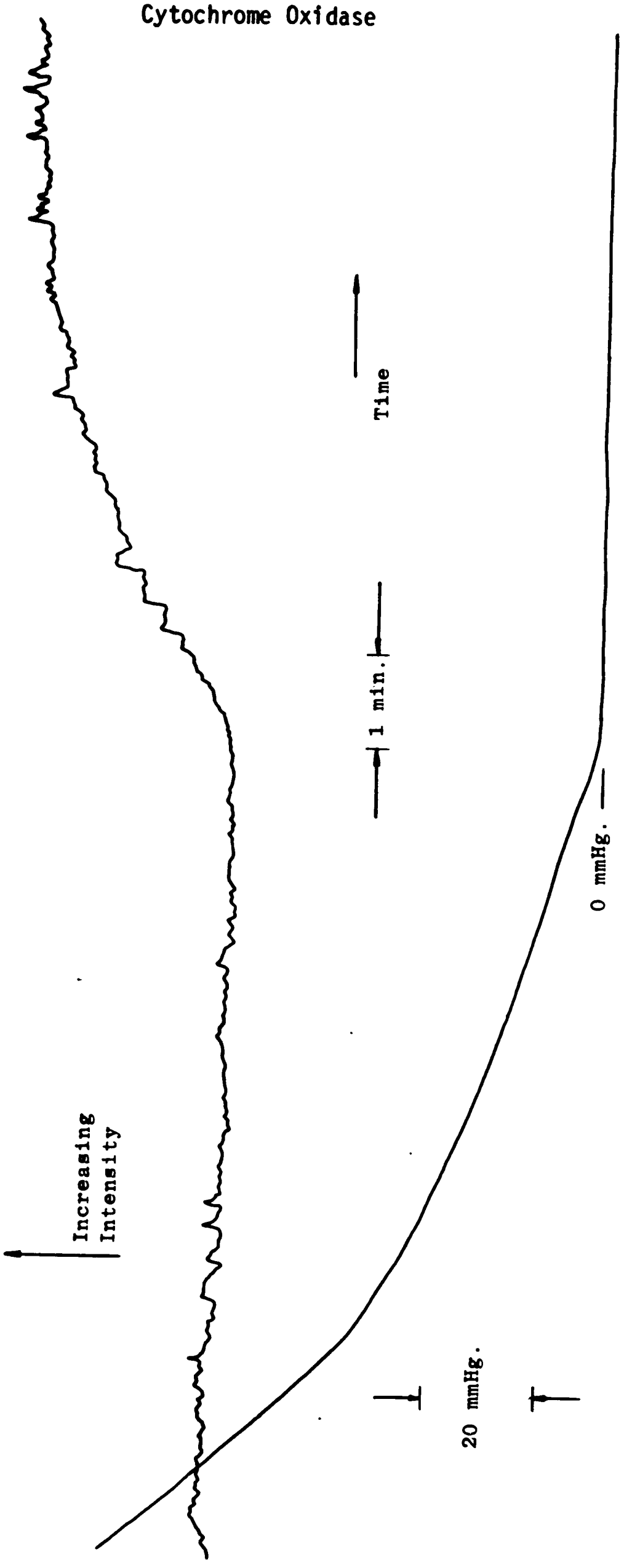

Figure 4.27 Effect of a decrease in ascorbate concentration on transmitted intensity at 830nm and pO_2 (300ul of cytochrome oxidase in sample).

consumption) indicative of a zeroth order reaction, until very low levels

of oxygen (see Figure 4.13). These aspects are considered in more detail in Section 4.11.

The limited accuracy of the oxygen electrode is not considered adequate to place a figure on the Km of the enzyme. However, this is not important since such precise details as this or observations of any differences between the signals obtained at 600 and 830nm was not the aim of these experiments, and it is unlikely the instrumentation was capable of such accuracy.

The results also confirm that absorbance can be used as a monitor of oxygen sufficiency (as the oxygen becomes rate limiting), but that in these in vitro studies it is essentially simply an indicator of whether or not oxygen is present.

The traces which show the effect of ascorbate becoming rate limiting, demonstrate that oxygen consumption is not just dependent upon the concentration of cytochrome oxidase and oxygen but that substrate limitation can play a major part in determining the rate of electron transfer. The trace at 600nm also shows the problem of interference during spectrophotometric measurements as the absorbance of TMPD varies with its redox state thus causing a change in the signal being monitored to represent cytochrome oxidase redox state. Indeed it is likely that in many of the above traces (particularly at 600nm) the changes in absorption and intensity observed as the oxygen concentration approached zero, may in part be due to the shifts in the redox states of cytochrome c or TMPD as the electron flow ceased and all components went to maximally reduced, since no effort was made to correct for these effects.

4.6.4 Preliminary Experiments on Yeast Cells.

4.6.4.1 Introduction.

In line with the proposed plan of work, following the success of experiments on pure cytochrome oxidase the next step was to perform studies on a more complex system. An ideal choice is yeast cells, which were used in some of the original studies of the respiratory chain. Therefore all of the remaining results were obtained from studies using brewer's yeast (Saccharomyces cerevisiae).

The aim was to grow yeast cells and then perform similar spectrophotometric and oxygen measurements on them, to those described above. With an organism such as yeast in addition to cytochrome oxidase other members of the respiratory chain can also be studied. It was expected that spectrophometric measurements would be complicated by large scattering effects and that dual beam spectrophotometry may be required (CHANCE (1951c)), although depending on the cells being studied careful use of single beam instrumentation may suffice (CHANCE (1954)).

Yeast cells can grow either aerobically or anaerobically. In the former case the cells develop the necessary respiratory chain whereas, in the latter the respiratory chain may not be expressed in such quantities since it is not required if all energy is derived anaerobically. Consequently aerobically grown cells would be expected to give good optical signals for studying the respiratory chain wheras this would not be the case for exclusively anaerobically grown cells.

4.6.4.2 Growth of Yeast Cells.

It is imperative to use sterile procedures during cell culture to prevent contamination. This includes sterilisation of all glassware and autoclaving all growth media.

The first step in growing yeast cells was to set up a primary culture. This entailed innoculating a glucose growth media consisting of

D-glucose, yeast extract and required salts from a "stab" (supplied by Dr A.J. Kingsman, Department of Biochemistry, University of Oxford.) This innoculated media was then shaken at 30°C in a shaking water bath. Cell growth was monitored by measuring the absorbance of the culture at 600nm with the cell density then obtained from a previously calibrated graph of cell density versus absorbance. (Cell density for this graph having been determined using a haemocytometer).

After about ten hours secondary cultures were set up. This involved taking cells from the primary culture and innoculating into the secondary media. These either contained glucose (as for the primary) or glycerol. The difference between these is that glycerol can only be metabolised aerobically and so promotes the expression of the respiratory chain wheras glucose can be metabolised anaerobically (glycolysis) and so cells can grow with lower levels of respiratory chain components. Hence a difference in signals from cells grown on glucose and glycerol should be seen with the former therefore serving as a control.

Further control could be obtained by growing the cells either anaerobically or aerobically using tight or loose fitting seals respectively on the culture flasks. Anaerobic glycerol cultures should not grow wheras anaerobic glucose cultures should, not being dependent upon oxidative metabolism. Certainly differences were observed in the growth times using the different culture media, with glycerol cultures taking longer to reach the same cell densities. This is the reason why the primary culture is grown on glucose medium.

4.6.4.3 Experiments using Comercially Available Spectrophotometers.

Once the technique of culturing yeast cells had been learned then spectrophometric studies were attempted. Three commercially available split beam spectrophotometers were used for the initial studies namely: Cecil 558, Cecil 598 and Kontron Uvikon 820. The procedure adopted was

to take two nominally identical samples of cells, oxidise one with ferricyanide and reduce the other with dithionite. The split beam facility of the instruments should then (theoretically) enable a difference spectra to be obtained. Unfortunately, no success at all was had with these studies.

An initial problem was due to the colour of the growth medium and colouration by ferricyanide, but even after repeated washing and resuspension of the cells in buffer, still no difference spectra were obtained. It was felt that the problem may lie in the yeast cells themselves so cultures grown on variations of growth media were used but again with no success. Eventually a series of oxygen consumption measurements (using the Rank oxygen measurement cell) were undertaken to at least confirm that cytochromes were present in the cultured cells.

These studies consisted of monitoring the decrease in oxygen content in glucose and glycerol cultures grown both aerobically and anaerobically, and confirmed that the cultures were consuming oxygen and therefore possessed active respiratory chains. At this stage it was also first noticed that a large proportion of cultures were contaminated (the contaminants may have been contributing to the oxygen consumption) and so various steps were taken to overcome this problem.

The outcome of the studies was that cytochromes seemed to be present in the yeast cells and therefore difference spectra should be obtainable. Since the intense scattering of the cells could have been contributing to the problems, along with the use of a split beam spectrophotometer, (which required very closely "matched" samples), it was decided that further experiments should use a dual wavelength (Aminco DW2) spectrophotometer, which was designed precisely for this kind of study (see Section 3.4.5).

Whilst attempting to grow cells for use on the dual beam machine it was evident that there were still problems of culture contamination. To

ensure that this was not due to inadequate sterile procedure colleagues attempted to grow contaminant free cultures under the same conditions. However they also encountered sterility problems. (A possible cause may have been the hospital enviroment although it is by no means certain). The final solution to these problems was that all further cultures were grown by N.A.Crowe at Dr A.J.Kingsman's Lab, with culture details given in the following section.

4.6.5 Spectrophotometric Studies on Yeast Cells Using a Dual Beam (Aminco DW2) Spectrophotometer.

4.6.5.1 Introduction.

All the cells used for the remaining studies were grown by N.A.Crowe using the following procedure. A primary culture was grown in YPD (2% bacto-peptone, 1% yeast extract, 2% glucose) at 30°C overnight followed by innoculation of a secondary culture in YPG (2% bacto-peptone, 1% yeast extract, 2% glycerol) using cells from the primary culture. This was then grown for approximately 30 hours, after which cells were harvested at 2000g for 10 minutes at room temperature, washed twice with 0.05M phosphate buffer (pH 7.5) and resuspended in the same. Experiments on the cells were performed within 4 hours on an Aminco DW2 dual beam spectrophotometer situated in the Metabolic Research Lab., Oxford University.

Initially attempts to obtain difference spectra in split beam mode (as above) were made, but these again proved unsuccessful. Since no spectrophotometric results had yet been made to show that cytochromes in a functioning respiratory chain were present, it was decided to exploit the full potential of the machine and use the dual beam mode (see Section 3.4.4). Furthermore, rather than fully (and permanently) oxidise and reduce the samples and attempt to obtain difference spectra, kinetic type monitoring would be performed, as on the pure enzyme, with the cuvette contents shaken to ensure oxidation and then observed at appropriate wavelengths to monitor the cytochromes as they became reduced. This should lead to a rapid change in absorbance as the oxygen was finally consumed, which would hopefully be quite distinct from any background noise.

This approach was sucessful and after initially monitoring the Soret bands (since these give the largest and therefore easiest signal to observe), the α bands of cytochromes b,c and aa_3 were monitored using

the wavelengths given in CHANCE (1954) (see below.)

Following this, difference spectra of the respiratory chain from 400-620nm were obtained (in various modes as described below). The same procedure of vigourously shaking the cuvette to aerate the sample thus oxidising the components of the respiratory chain to their steady state values (see Figure 4.11), was used, with fully reduced components obtained once the oxygen within the cuvette was totally consumed. Advantages of this procedure were, no spectroscopic interference from exogenous compounds, and the ability to always return to dual wavelength kinetic measurements to check that the respiratory chain was still functioning and obtain appropriate scaling of experiments in different regions of the spectrum.

4.6.5.2 Kinetic Results.

As described above the successful experiments were kinetic studies using dual wavelength mode. To perform these the sample and reference wavelengths were selected (from CHANCE (1954)), the cuvette then vigoursly shaken to introduce oxygen and the absorbance recorded versus time.

The initial readings were made on the cytochrome oxidase Soret bands (as this gives a large change), followed by recordings of the reduction of cytochrome b, cytochrome c and cytochrome oxidase again, made by following changes in the absorbance of their α bands. An example of the results are shown in Figure 4.28 with the wavelengths used given as sample versus reference wavelength. In all traces reduction was accompanied by a rapid increase in absorbance, the speed indicating that as with the pure enzyme the affinity for oxygen of cytochrome oxidase is very high. The significance of the wavelengths can be seen from Figure 4.8 with the reference ideally being an isobestic point. The reduction of the cytochrome oxidase α band was the technically most difficult to

observe.

To obtain reasonable results using this method there were two conflicting requirements which had to be considered. A high cell density was required to give large changes in absorbance upon the change in redox state, but this then meant that oxygen consumption was also high and could reach such a rate that there was literally insufficient time after aeration to begin recording the sample's absorbance before it became reduced. An additional complication is that the denser the cells the smaller the signal obtained by the photomultiplier in the instrument which could lead to a noiser trace.

The ability of dual beam spectrophotometry to remove non-specific effects is demonstrated by comparing the traces in Figure 4.28 with those in Figure 4.29. These were obtained using split beam mode using either air or reduced cells as the reference (ie effectively single beam mode), and are much noisier. In addition the use of a reference wavelength to reduce interference between compounds can be seen by comparing the traces for cytochrome c (550nm) in both Figures.

4.6.5.3 Difference Spectra.

Having obtained evidence that cytochromes were present in a functioning respiratory chain , the next stage was to attempt to record difference spectra yet again. The standard method is to use reduced and oxidised cells in the sample and reference cuvettes in split beam mode. On the Aminco DW2 this involved placing reduced cells in both positions, manually obtaining a flat baseline, (that is the difference in absorption between the two cuvettes with the cells reduced in both), aerating the reference cuvette and then running reduced versus oxidised difference spectrum.

This procedure was relatively straightforward for the Soret band region but at higher wavelengths manually flattening the baseline was

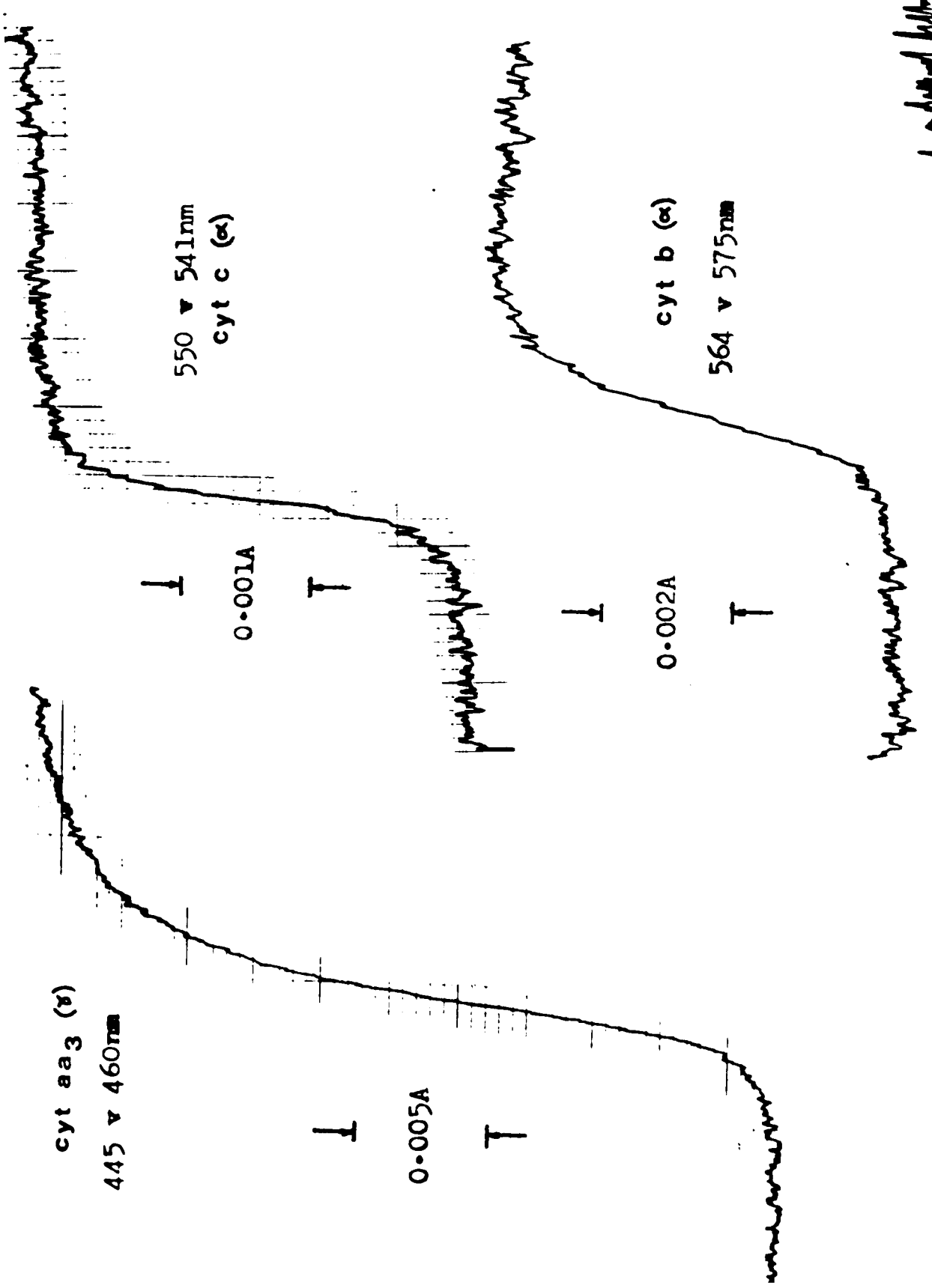

Figure 4.28 Traces obtained using dual beam kinetic mode showing the change in absorbance of the yeast cell suspension due to the cytochromes switching from an oxidised to a reduced state.

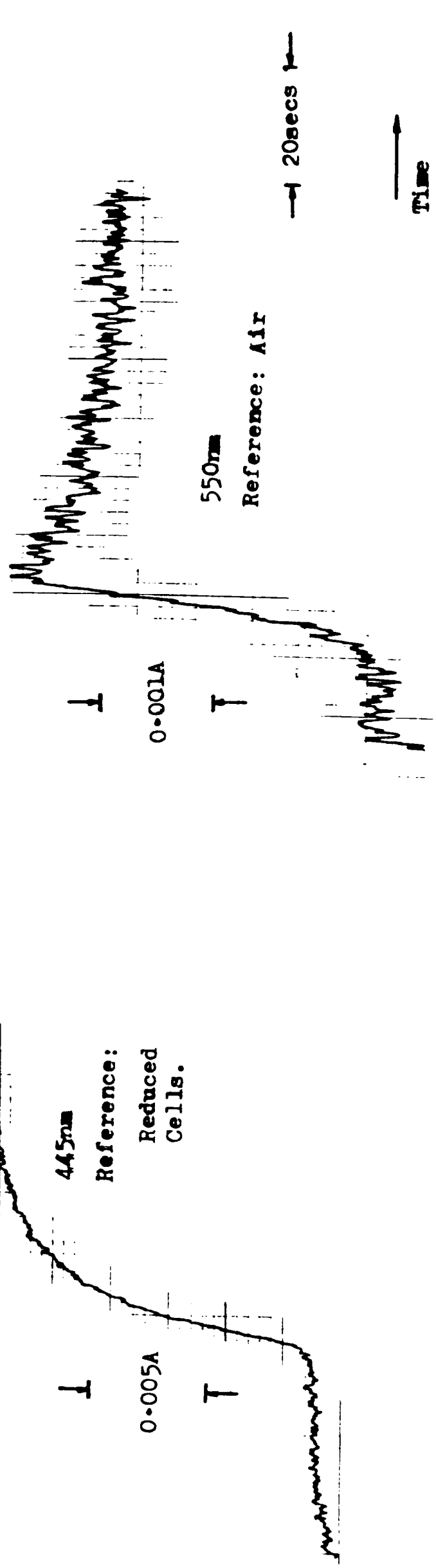

Figure 4.29 Traces obtained using split beam kinetic mode showing the change in absorbance of a yeast cell suspension due to the cytochromes switching from an oxidised to a reduced state.

more difficult. To confirm that difference spectra were being seen in

these regions the split beam mode was used "manually". This involved using the machine simultaneously in both kinetic and scanning modes. Split beam scanning mode was selected so that the X-axis of the recording represented wavelength, but during any one study the monochromator (and recording pen) were kept at one wavelength, and a kinetic study as described in Section 4.6.5.2 was performed. This meant that at any one wavelength a kinetic trace was obtained but with no time base so that a line was obtained with its length representative of the change in absorbance as the cells in the sample cuvette became reduced. Hence a value for the difference in absorbance at that one wavelength could be recorded. By repeating the procedure across the wavelength range covered by the recording a difference spectra consisting of lines could be built up if all kinetic traces were begun with the same baseline starting value.

The "manual" scanning approach was also taken a stage further since over certain ranges even with this technique it proved difficult to obtain difference spectra. When this was so dual beam manual scanning was used which involved setting the machine in dual wavelength scanning mode and then obtaining kinetic traces with no time base giving straight lines as before. Each of these lines corresponded to the difference in absorbance between reduced and oxidised samples measured against the reduced and oxidised sample respectively at the reference wavelength (ideally an isobestic).

Difference spectra were obtained over the range from 400-620nm using all three methods to confirm that the results were genuine since noise free traces in anything other than the Soret region were difficult to obtain. The following traces are representative of the actual results obtained.

In Figure 4.30 the difference spectra using split beam mode from 400-490nm is shown. The peaks are due to the combined Soret bands of

cytochromes b, c and the cytochrome oxidase band at 445nm (see Figure 4.8 for the individual spectra). The effect of the change in redox state of flavoprotein is also visible at 460nm (see Figure 1.12).

Figure 4.31 shows the difference spectra obtained in split beam mode from 490-580nm. The spectra was traced from the actual recording and the state of the baseline demonstrates the difficulty in obtaining something resembling a flat baseline. The two peaks are due to the combined α and β bands of cytochrome b and c (see Figure 4.8). In this and the last trace because one set of cells are oxidised and the other reduced the spectra obtained are not of (totally reduced)-(totally oxidised) cells since the oxidised cells will be in a steady state (see Figure 4.11) so only cytochrome oxidase will be nearly 100% oxidised.

Finally in Figure 4.32 the absorbance due to the cytochrome oxidase α band is shown. This was obtained using dual beam "manual"scanning mode (as described above) with recordings made approximately 2nm apart and the trace then drawn from these. In Figure 4.33 difference spectra obtained by other workers are shown for comparison with those obtained in these experiments.

4.6.5.4 Near-IR Absorption Band.

After, the kinetic and difference spectra due to the cytochromes' haem moieties had been observed, an attempt was made to monitor the reduction of cytochrome oxidase at 830nm. Dual beam kinetic mode with a reference wavelength of 780nm was used with the same procedure as above. Surprisingly, considering the difficulties in observing the 605nm band, results were obtained as shown in Figure 4.34. However, upon attempting to improve the signal by using the switch to remove second order spectra above 600nm, the change in absorbance was no longer seen (see Figure). This showed that the original trace was in fact the second order spectra of the ~ 410nm change in absorbance (see Figure 4.30), and provided a

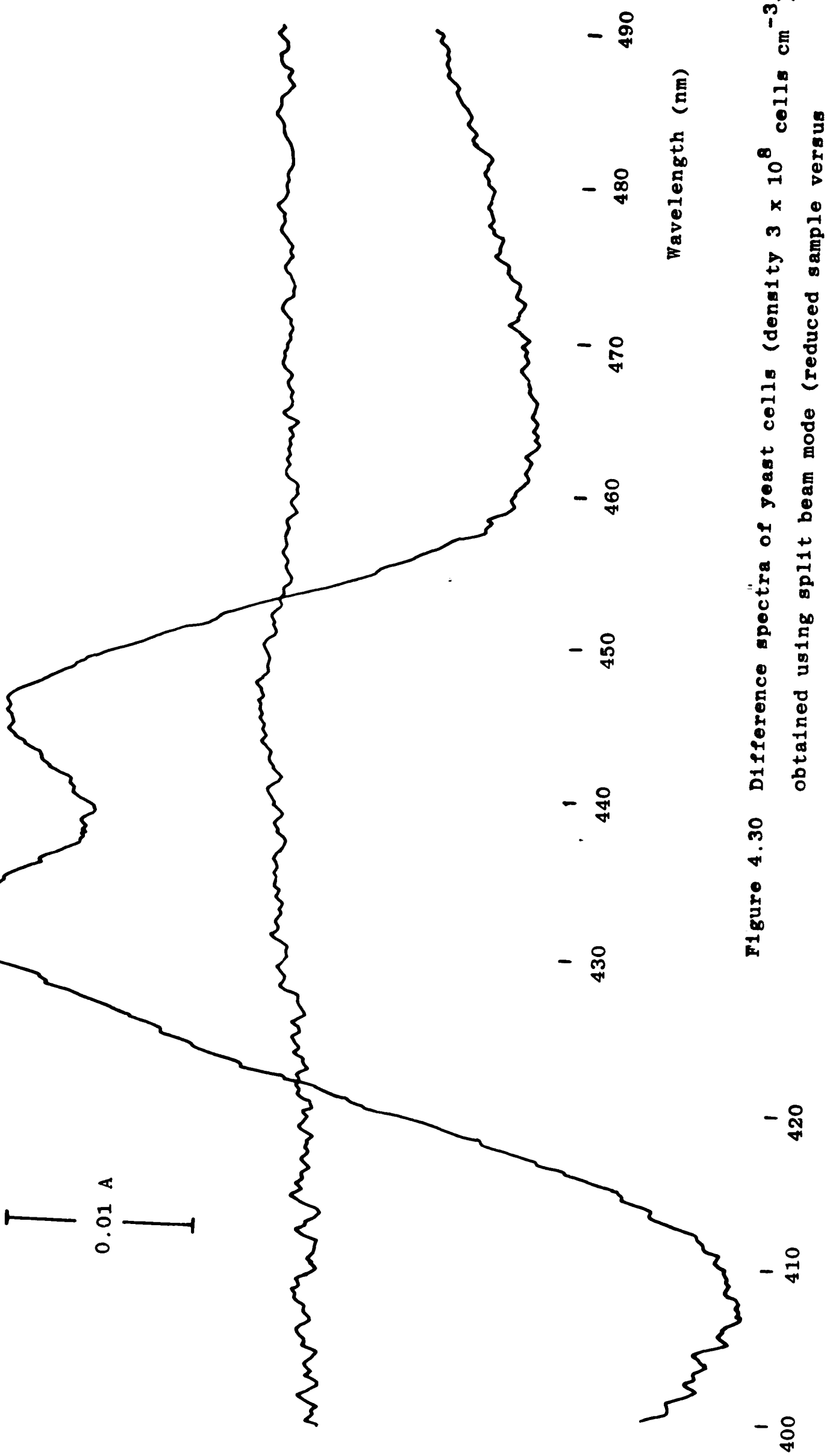

Figure 4.30 Difference spectra of yeast cells (density 3 x 10^8 cells cm^{-3}) obtained using split beam mode (reduced sample versus oxidised reference).

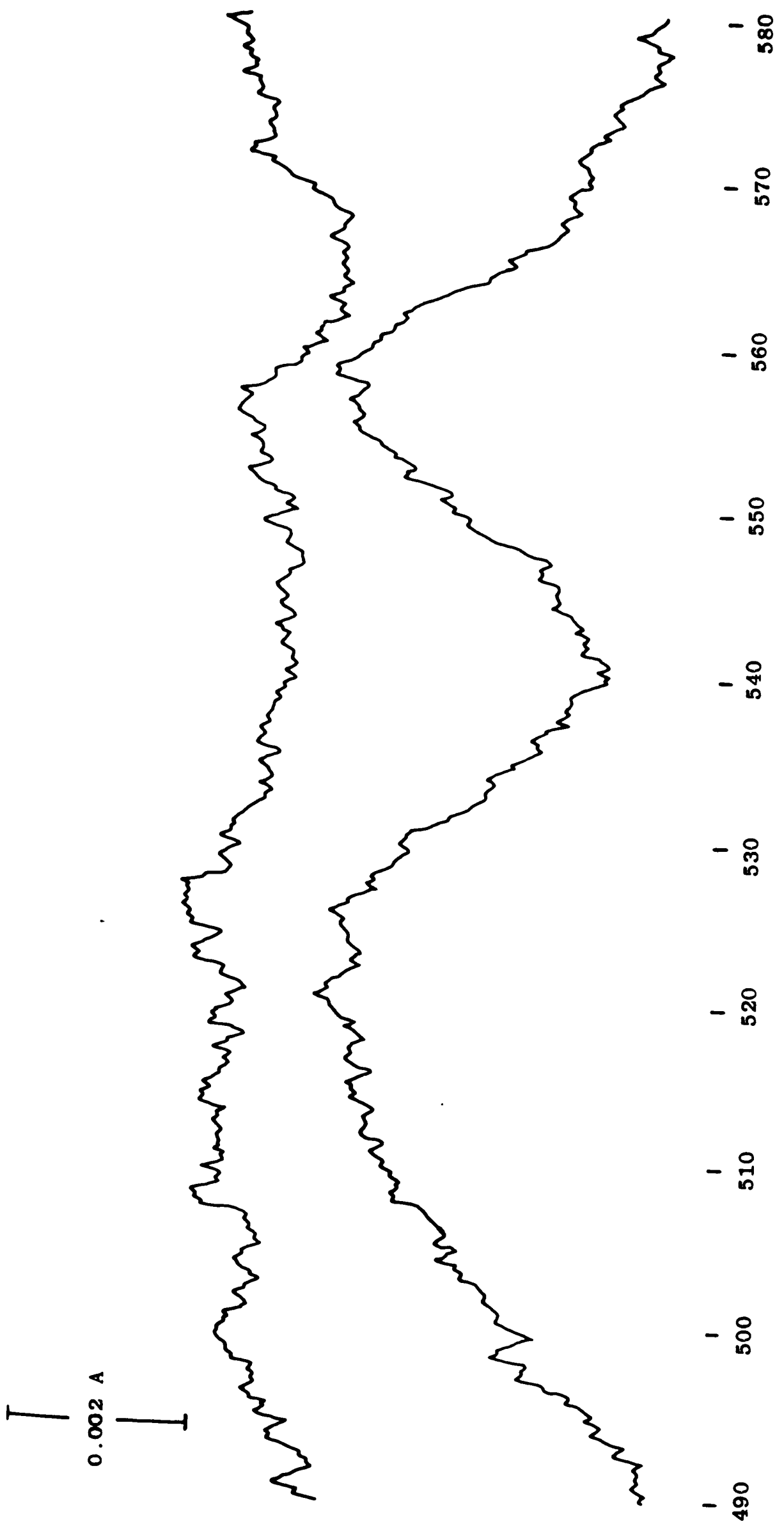

Figure 4.31 Difference spectra of yeast cells (density 1 x 10^8 cells cm^{-3}) obtained using split beam mode. (The actual difference spectra and baseline are shown as recorded, including the overall downward drift of the former).

salutary lesson concerning the use of monochromators for such studies.

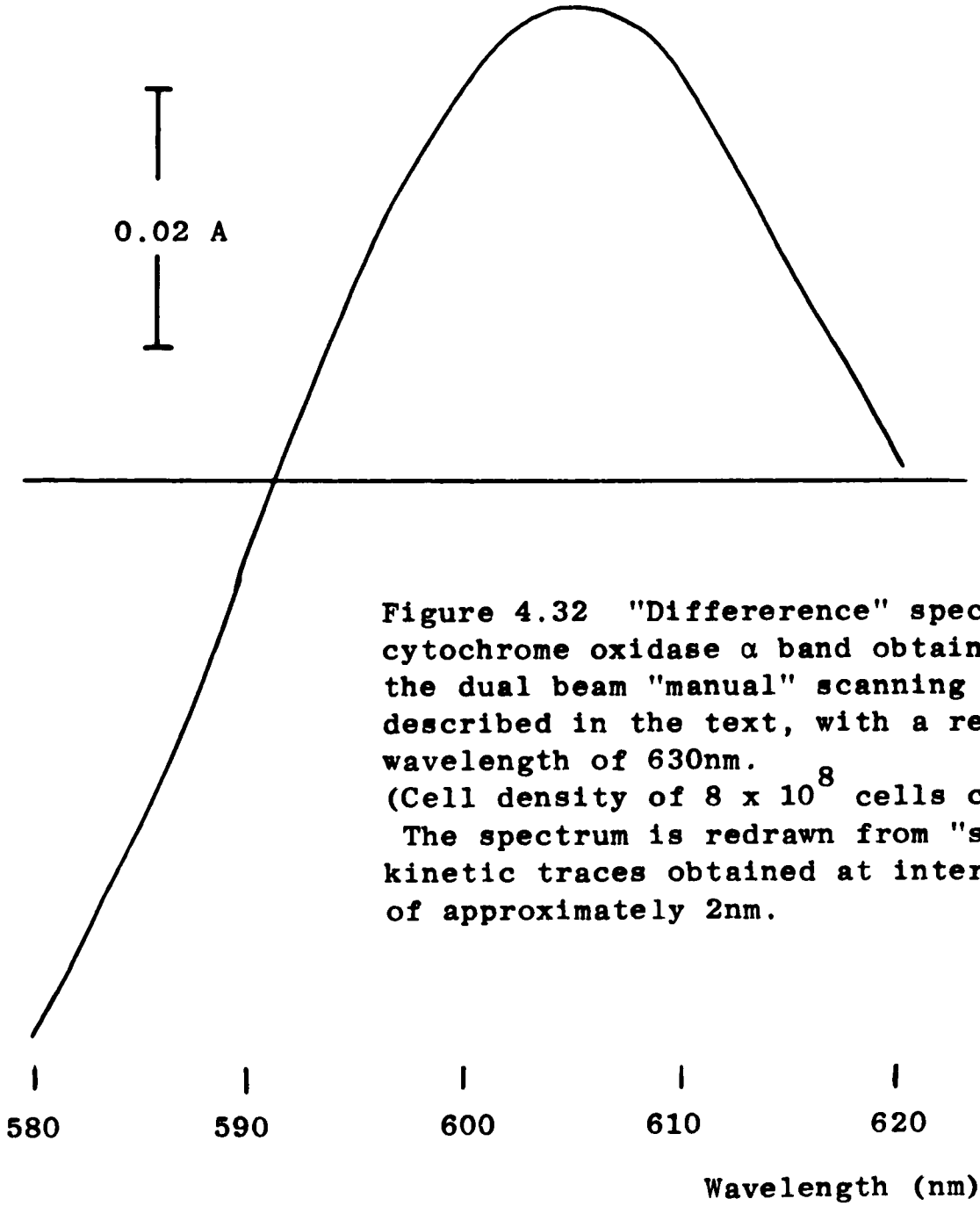

Figure 4.32 "Differerence" spectra of cytochrome oxidase α band obtained using the dual beam "manual" scanning mode as described in the text, with a reference wavelength of 630nm.
(Cell density of 8 x 10^8 cells cm^{-3})
The spectrum is redrawn from "static" kinetic traces obtained at intervals of approximately 2nm.

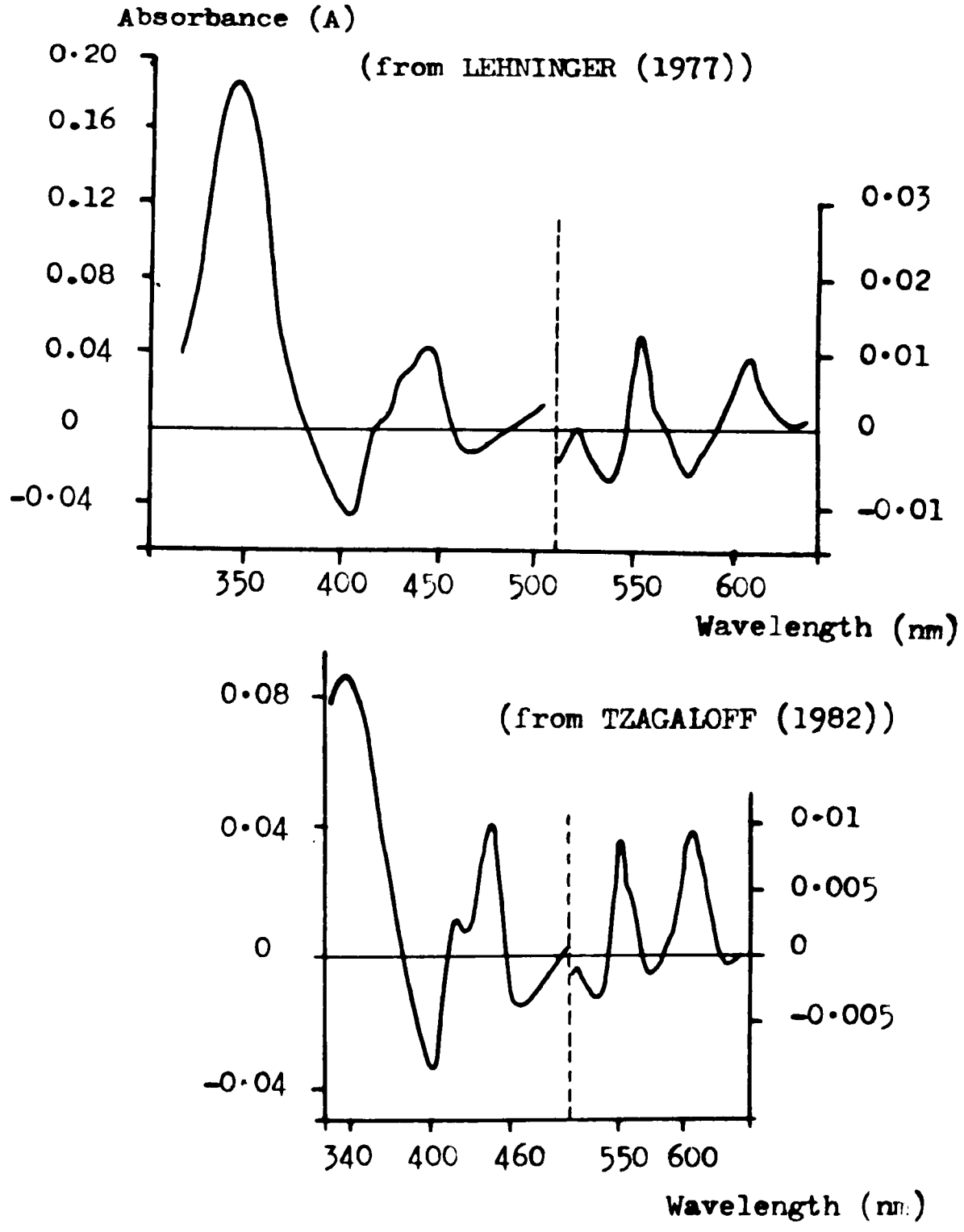

Figure 4.33 Difference spectra

Indeed any near-IR measurements using a monochromator with no second order removal could suffer from the same artefacts.

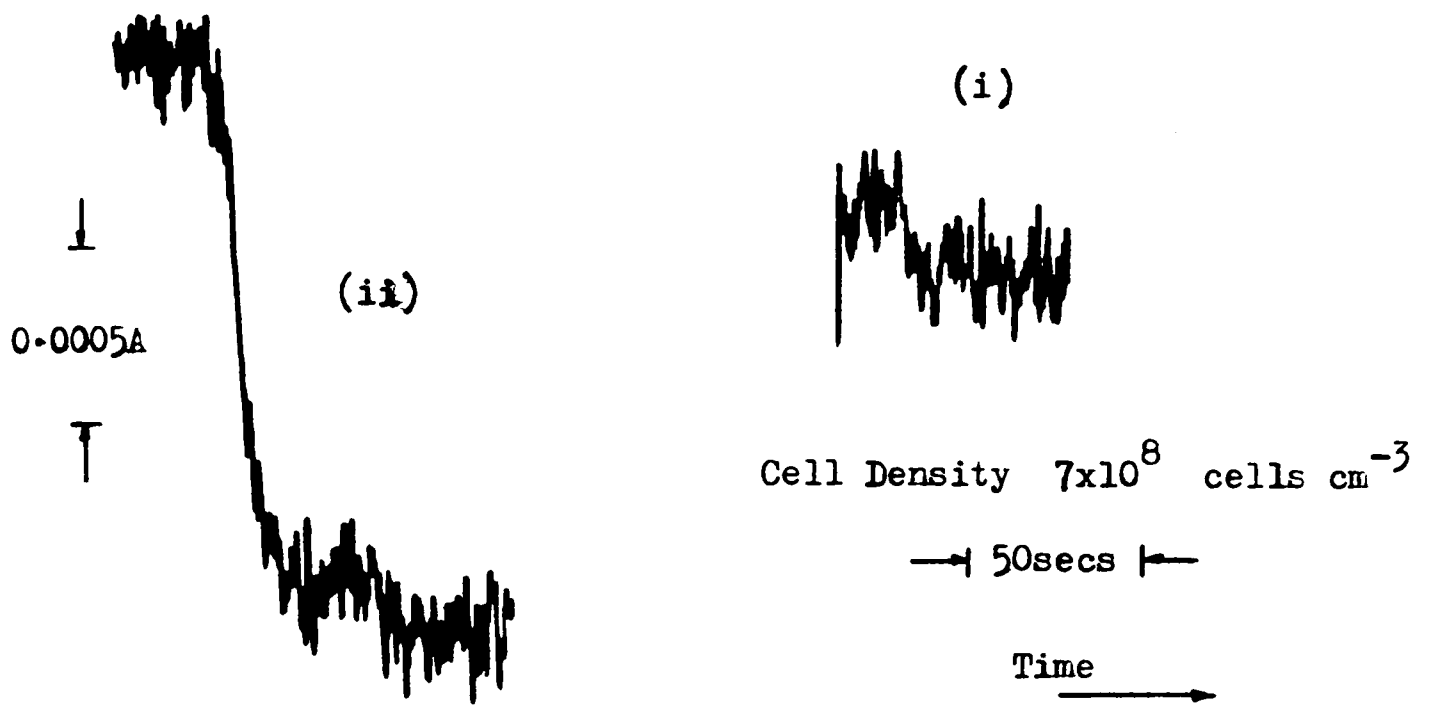

Figure 4.34 Traces obtained using dual beam kinetic mode with wavelengths 825 v. 775nm., both with (i) and without (ii) second order spectrafiltering. The effect seen without filtering is that due to the difference spectra at approximately 410nm. No evidence of the near-IR band was found.

4.6.6 Experiments on Yeast Cells Using Personally Constructed Instrumentation.

This final series of experiments were made after the studies using the dual beam spectrophotometer. The intention was to attempt to repeat these using personally constructed instrumentation, and also make similar spectrophotometric and oxygen measurements on the yeast cells as those made on the pure enzyme.

4.6.6.1 Spectrophotometric Studies.

Both single and multi-wavelength measurements were attempted using interference filters and the Spectralyser respectively. Some success was had with the former although no difference spectra (as was the aim) could be observed using the Spectralyser, because it lacked the required

sensitivity. However, the spectra obtained from fully oxidised and reduced cells with the Spectralyser showed that they possessed no large absorbance bands in the visible and near-IR regions, with the only distinctive band being that due to the water present in the sample. This was expected since the cells appear white, and demonstrates why observing difference spectra from such samples is technically difficult, since they represent very small changes in absorbance on top of a very large background attenuation.

4.6.6.1.1 Materials and Methods.

The white (tungsten halogen) light source was used with interference filters. (440 and 550nm) for wavelength selection. The light was "piped" to a specially constructed cuvette holder to which fibre bundles could be attached with a second bundle taking light from the cuvette to the photomultiplier. (see Section 3.2 for details of the individual components). The cuvette holder was located in a light tight box with the arrangement shown in Figure 4.35.

The photomultiplier detection circuit consisted of a basic I-V converter and then an offset and amplification stage (Section 3.3.3), this enabled the signal from the (aerated) oxidised cells to be backed off to zero volts so that it could then be recorded at sufficient sensitivity to observe the change in redox state once the oxygen had all been consumed. The actual voltage from the detection circuit was also recorded.

The procedure for the studies was to select an appropriate cell density (through initial scaling experiments) to enable a reasonable change in signal to be seen, but also ensure that the cells did not consume the dissolved oxygen too quickly and so make recording of the change practically impossible. The cells were then shaken vigourously, placed in the cuvette holder, the offset circuit used to back off the

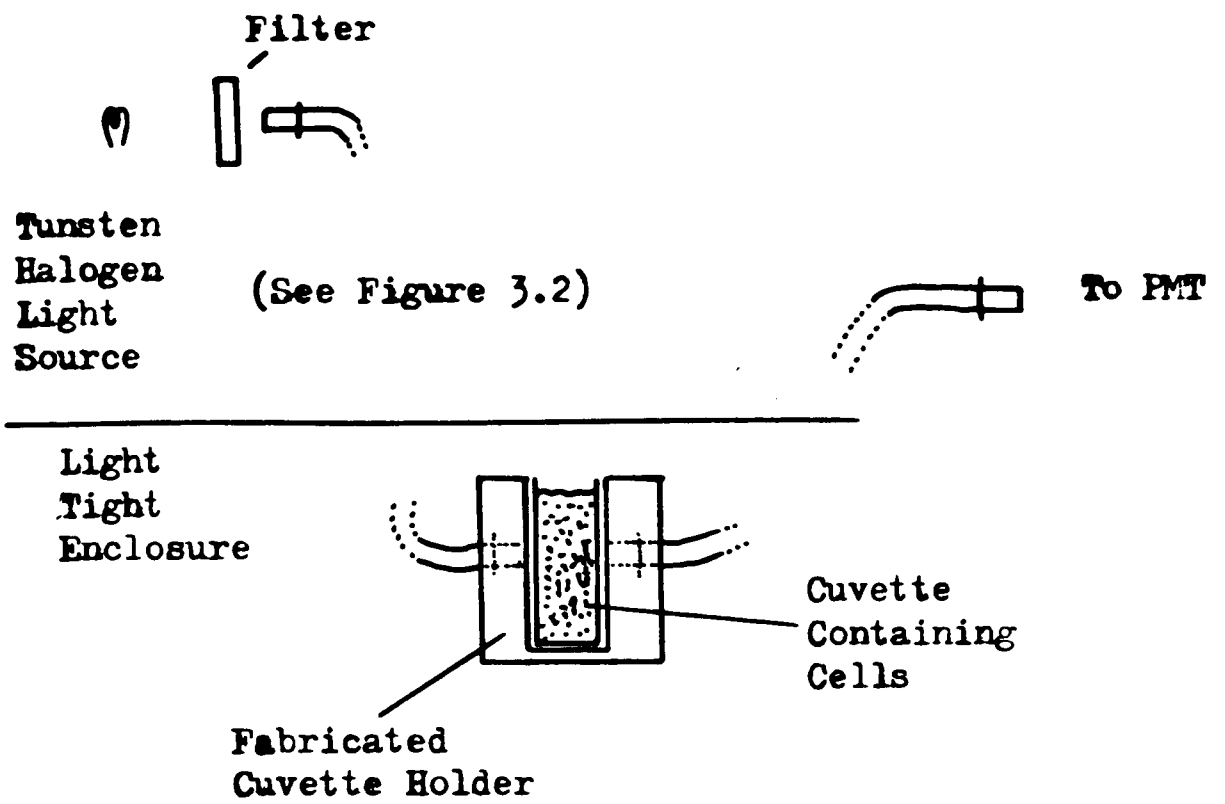

Figure 4.35 Arrangement used for optically monitoring yeast cell suspensions.

signal on the chart recorder to zero volts and the actual voltage from the PMT detection circuit noted. The switch in redox state was then recorded.

The light intensity reaching the cuvette could be controlled by a shutter on the lamp housing. This was used to keep the detected light level at a maximum commensurate without damaging the PMT, under different conditions determined by the sample's cell density and the wavelength used.

4.6.6.1.2 Results.

Traces showing the change in detected light level as the switch in redox state occured were recorded first at 440nm and then as shown in Figure 4.36 at 550nm. However, no such trace could be obtained with the 600nm filter, which is in accordance with the findings from the dual beam machine that the 445 and 605nm bands were respectively the technically easiest and hardest bands to monitor.

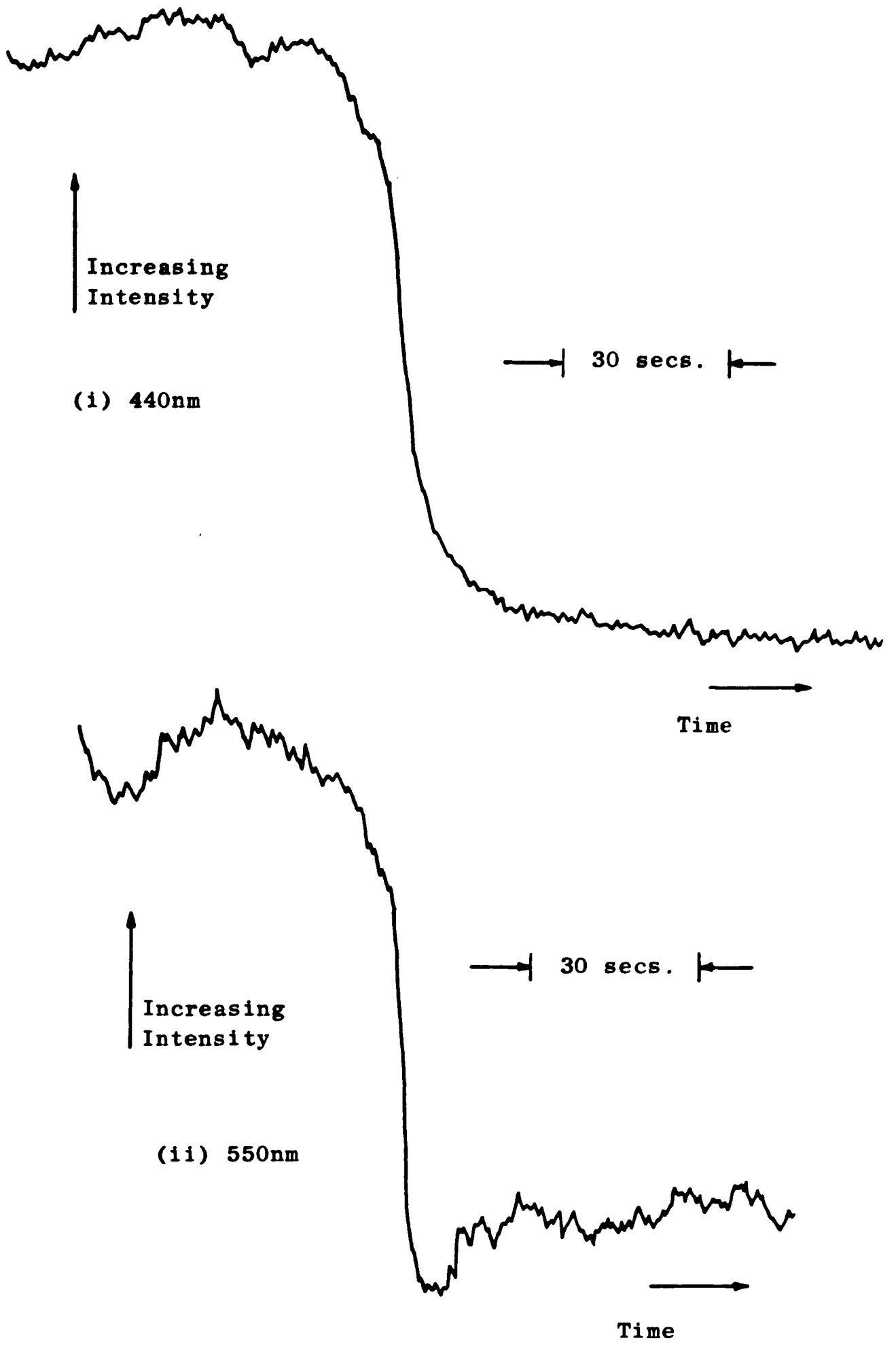

Figure 4.36 Change in transmitted intensity through yeast cells in the cuvette (cell density 8×10^8 cells cm^{-3}), upon the change from an oxidised to a reduced state, at (i) 440nm and (ii) 550nm.
These represent absorbance changes of 0.02A and 0.008A respectively.

4.6.6.2 Spectrophotometric and Oxygen Measurements.

The requirement here was to perform similar studies to those described in Section 4.6.3.3. However, the fact that now a very much smaller change in absorbance was being monitored and the intense scattering of light by the cells meant the previous approach was likely to be unsuccessful, and more intimate contact between source, sample and detector would be required.

The initial attempt to record optical signals from the cells therefore involved the use of a fabricated bifurcated fibre bundle (using polymer fibres, see Section 3.3.4) which could be held in the sample and detect the intensely scattered light. However, when used with the oxygen measurement cell the action of the magnetic stirrer caused tremendous noise problems on the optical signal. Since the stirrer is neccesary to inhibit "depletion effects" occuring within the sample and so enable accurate measurements of oxygen content in the bulk solution to be made, a transmission monitoring mode had to be used as described below.

4.6.6.2.1 Materials and Methods.

The procedure used was the same as that in Section 4.6.6.1, including the use of the same detection circuits. The difference was the use of the oxygen cell to not only measure oxygen content but also as the cuvette for the spectrophotometric measurements. These were made in transmission mode by fitting small fibre bundles through the water jacket inlet and outlet ports so that they were in intimate contact with the actual sample chamber walls. The fact that they were not at the same level (see Figure 3.8) was not important because the cells were so highly scattering. Indeed this could be seen as on shining light into the cells in this manner the whole measurement cell containing the cells appeared to "light up". Aeration of the cells was achieved by bubbling air into

the sample.

To obtain a trace firstly a suitable transmitted light level was selected. The solution was then aerated to an adequate level, by monitoring the oxygen content measured by the electrode on an oscilloscope, to produce a recording of acceptable length (determined by the rate of oxygen consumption). The stopper was then placed in the cuvette and the transmitted light intensity and oxygen content recorded.

To prevent problems from ambient light the experiments were performed in a darkened room with black felt used to cover the measurement cell.

4.6.6.2.2 Results.

The results obtained are summarised in Figure 4.37. They show the intensity and simultaneous oxygen traces obtained at 440, 550 and 600nm corresponding to the reduction of the Soret bands, and the α peaks of cytochrome c and cytochrome oxidase. The latter could not be observed in the earlier experiments using the cuvette and the reason that it was visible in these studies was probably due to the longer path length and was made easier by the fact that the switch in redox state could be correlated to the fall in oxygen tension to virtually zero, so that the actual switch could be distinguished from the noise.

All intensity traces show a rapid switch, like those obtained from the dual beam spectrophotometer, indicative of the high affinity of cytochrome oxidase for oxygen. This is also shown by the linear fall in oxygen consumption to very low levels showing that the enzymes consume oxygen with zeroth order kinetics until these levels.

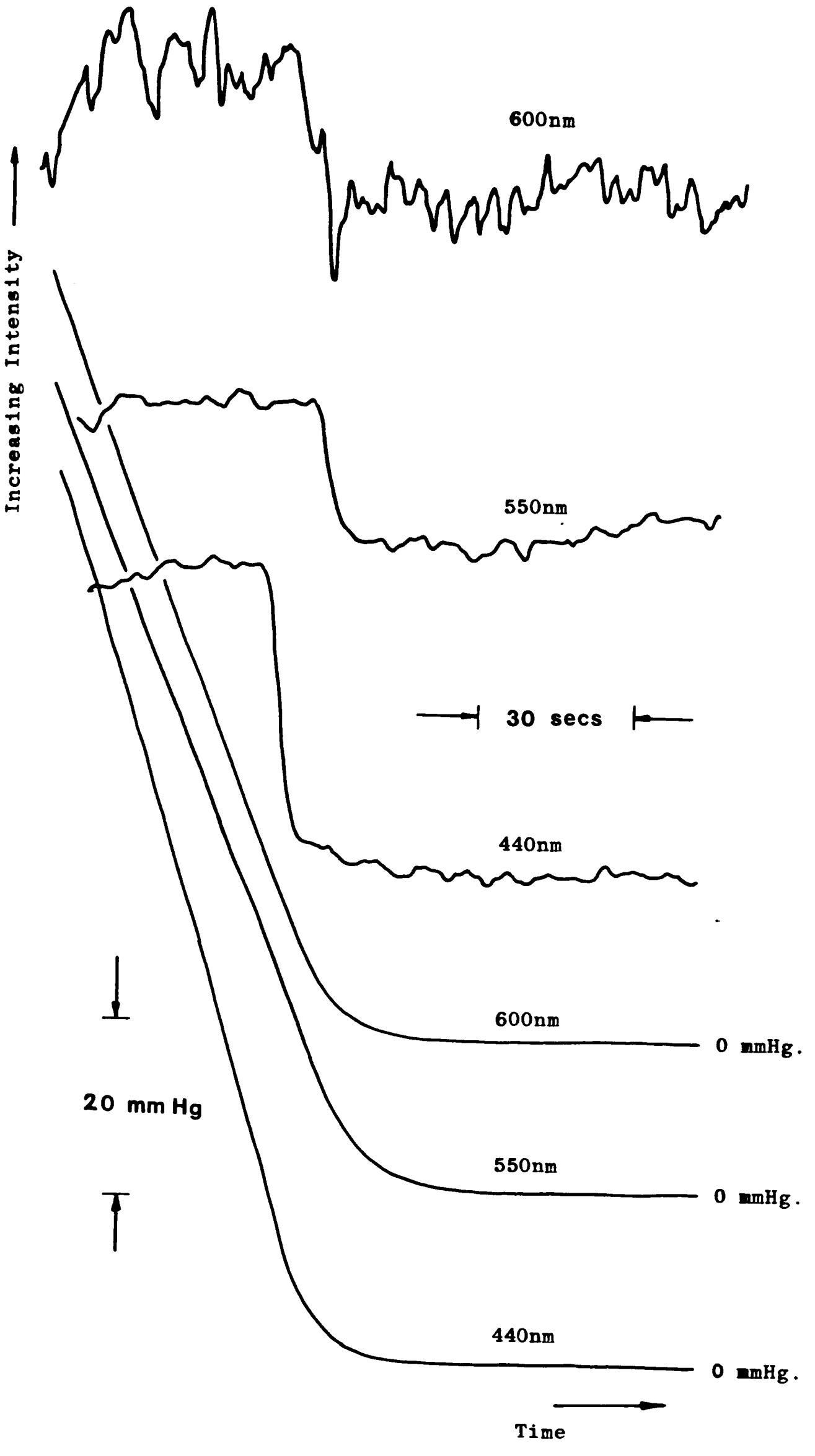

Figure 4.37 Change in intensity transmitted through and pO_2 of a yeast cell suspension (density 1 x 10^9 cell cm^{-3}) monitored at 440, 550 and 600nm. The changes in intensity correspond to absorbance changes of 0.05, 0.02 and 0.005 A respectively.

4.6.7 Summary.

These studies on proprietary enzymes, purified cytochrome oxidase and yeast cells using both commercially available spectrophotometers and personally constructed instrumentation were an invaluable introduction to the field of spectrophotometric monitoring of small changes in absorbance.

The experiments demonstrate that *in vitro* and in yeast cells cytochrome oxidase has a very high affinity for oxygen which results in a linear oxygen consumption in an effectively closed system and rapid changes in absorbance when the oxygen becomes rate limiting and the enzyme goes reduced.

The experiments obtained using the pure enzyme described in Section 4.6.3, provided the basis for the work described in Section 4.11 where these traces are mathematically modelled and a physical argument of why the affinity of cytochrome oxidase is lower *in vivo* is presented.

4.7 Haemoglobin, Myoglobin and Cytochrome Oxidase.

4.7.1 Introduction.

So far within this chapter the use of the redox state of cytochrome oxidase monitored optically as an indicator of "metabolism" or oxygen sufficiency has been discussed. Examples of this have been given in the form of experimental results obtained *in vitro*, together with the fact that *in vivo* the enzyme has a much lower apparent affinity for oxygen which means that it is potentially a useful indicator of oxygen sufficiency over a much wider range.

In the next section a description is given of how optically monitoring the redox state of cytochrome oxidase has been developed from an *in vitro* technique to its eventual application *in vivo*. In the introduction it was described how niroscopy not only enables the redox state of cytochrome oxidase, but also oxygen saturation and haemodynamics to be assessed. This is not simply additional valuable information that is provided, but details that must be known if a signal which is solely representative of cytochrome oxidase redox state (ie with no interference from other compounds) is to be produced.

This highlights the situation that whereas in a yeast cell oxygen diffuses to the mitochondria and the main absorbing substances are the members of the respiratory chain, in a mammalian system the situation is far more complex. Here oxygen is actively transported from the lungs by haemoglobin, (contained in red blood cells), around the body to the microcirculation where it then diffuses to the mitochondria to be used for aerobic respiration (ie consumed by the cytochrome oxidase). In addition in muscle cells, oxygen is "stored" by myoglobin to be released during periods of intense muscle activity.

Therefore, haemoglobin, myoglobin and cytochrome oxidase all play important roles in oxygen transport and utilization. They are also all highly absorbing compounds (see Section 1.4.1) with absorption spectra

dependent upon either whether they are associated with oxygen or redox state, factors which can therefore be determined spectrophotometrically. However, this also means that monitoring any one compound in particular is complicated by the absorbance of the other two.

Hence, in a clinical situation these three substances could all be optically monitored and potentially give information concerning the transportation and utilization of oxygen. The question therefore exists as to which compound it is best to monitor, at what site and under what circumstances. The answers to these problems are by no means simple and no attempt is made to answer them here but they should be appreciated.

4.7.2 Haemoglobin.

Haemoglobin is responsible for carrying virtually all of the oxygen transported by the blood through the circulatory system. As described in Section 1.5.1, the amount of oxygen bound to haemoglobin (the oxygen saturation, SO_2) is primarily determined by the oxygen partial pressure (pO_2) with the two linked via the oxygen dissociation curve (Figure 1.26). This shows that most of the oxygen dissociates from haemoglobin over a relatively small range of oxygen tensions whicn results in the oxygen being offloaded in the areas where it is most required.

A further consequence of the sigmoidal shape of the dissociation curve is that for monitoring the oxygen present in the blood, oxygen saturation is most useful over the range when the dissociation occurs since it then changes markedly with oxygen tension, which is in contrast to the situation at high oxygen tensions where there is (see Figure 1.26) virtually no change in oxygen saturation for large changes in oxygen tension and so its direct measurement (using for example electrochemical devices) is of more value.

Unlike cytochrome oxidase, haemoglobin (ideally) interacts with only one substance, oxygen, and so an individual molecule will either be

oxygenated or deoxygenated changing between the two states by either accepting or giving up oxygen. It does not require a second substrate to change it from one state to the other in the cyclic manner of cytochrome oxidase (see Figure 4.9). In addition, the red blood cells containing haemoglobin are mobile so that by monitoring at a particular site on the body the actual haemoglobin molecules being studied would be constantly changing, whereas for cytochrome oxidase the same molecules would be under observation.

As described in Section 1.5.1 it is usually arterial oxygen saturation which attempts are made to measure (as it is generally arterial oxygen tension). These values give an indication of how effectively the respiratory and circulatory system is functioning, since thay are related to the amount of oxygen being carried by the blood.

In niroscopy where larger and deeper regions of tissue are studied the oxygen saturation is unlikely to be solely calculated from the arterial system, rather a tissular oxygen saturation will be measured, where the term tissular is used to describe a value which is averaged over the whole arterial, capillary and venous system. It is possible that such a measurement would be useful for assessing actual oxygen utilization within the tissues in the same manner as the redox state of cytochrome oxidase a point discussed further below. If this is the case then the site of measurement may become an important factor.

Considering neonatal applications of oximetry the fact that fetal haemoglobin differs from adult haemoglobin the effect this has on the oxygen dissociation curve (which is shifted to the left to enable oxygen transfer across the placenta from maternal to fetal blood to take place) may be significant, particularily if measurements of lower tissular levels of saturation are made.

In addition to oxygen saturation measurements which can be made from haemoglobin, optical monitoring of haemodynamics can also be performed,

from changes in blood volume in the region under observation. Such measurements could be of great use in their own right but one potential pitfall would appear to be in determining the precise extent of the region of tissue being studied.

4.7.3 Myoglobin.

Myoglobin (Mb) consists of a single subunit of haemoglobin (which contains four haem moieties). Consequently it has a similar absorption spectra to haemoglobin and is also capable of binding and releasing oxygen. However, it has a higher affinity for oxygen than haemoglobin with its dissociation curve shifted to the left, and also non-sigmoidal (LEHNINGER (1977)).

Myoglobin is found in muscle cells and its role appears to be primarily to act as a store of oxygen which can be utilized as and when required if the oxygen supply from haemoglobin becomes insufficient. It also appears to play a part in the facilitated diffusion of oxygen. Because it is only present in certain cells and not constantly involved in oxygen transfer its clinical use is somewhat limited. However its presence is important since it is likely to interfere with measurements of either cytochrome oxidase or haemoglobin made on muscle (see Figure 1.15).

4.7.4 Cytochrome Oxidase.

The information concerning oxygen sufficiency available from monitoring cytochrome oxidase *in vivo* has already been extensively discussed, along with the fact that the major difference concerning its use *in vivo* is that the apparent affinity is much higher and so its redox state is indicative of intracellular oxygen sufficiency over a much larger range.

The fact that its redox state is related to intracellular oxygen

tension rather than that in the capillaries would appear to be a reason for monitoring cytochrome oxidase rather than oxygen saturation. However, the fact that the Km for the enzyme is so much higher *in vivo*, does mean that tissular oxygen saturation, (as defined above) and the redox state of cytochrome oxidase monitored in the same region may actually closely parallel each other if oxygen became rate limiting due to a decrease in its level in the microcirculation. Therefore perhaps, monitoring oxygen sufficiency at its site of utilization via the redox state of cytochrome oxidase would be no more advantageous than monitoring tissular oxygen saturation.

4.7.5 Summary.

There are at least three substances *in vivo* whose absorption spectra are intrinsically related to the amount of oxygen in their vicinity. This in turn means that there are three potential indicators of oxygen sufficiency *in vivo*. The intention of this section was to highlight this fact, and to show that in a clinical situation depending upon the site under investigation, the most suitable compound to monitor spectrophotometrically to determine oxygen availability / or sufficiency may not be obvious. Furthermore, the fact that cytochrome oxidase monitors oxygen sufficiency at the site of utilization is often cited as a reason for its potential use, but as noted above, with the apparent lowering of affinity *in vivo*, tissular oxygen saturation measurements may be just as useful (and easier to perform). (In addition changes in blood volume which would also need to be measured along with oxygen saturation measurements, may also provide valuable information). It is considered important to raise these points before describing the development of the technique to a non-invasive clinical tool given in the next section.

4.8 Monitoring the Redox State of Cytochrome Oxidase in vivo.

This section reviews the gradual development of optically monitoring the redox state of cytochrome oxidase from a technique used on isolated cells and mitochondria, to experiments on excised whole organs and exposed in situ organs, to finally non-invasive studies and the clinical use of the method. It is this work that joins the type of in vitro experiments described in Section 4.6, to the use of the technique for non-invasive in vivo monitoring.

As stated in Section 4.5, Britton Chance was the pioneer of the use of this technique and virtually all of the following work has it roots in his early studies. Moreover, the majority of authors cited below have at some stage collaborated with Chance or one of his co-workers, illustrating his influence.

The work is divided into section by authors, the first being Prof F F Jobsis, followed by those workers who were originally associated with him at Duke University and then those with no apparent connection with his group. This is followed by a brief description of the work of groups who have been involved in optical monitoring of haemoglobin and the cytochromes for some time, but largely in reflection mode on exposed organs or the skin surface. Finally the contributions are considered from workers who have entered the field relatively recently, apparently inspired by Jobsis' proposal of a non-invasive metabolic monitor.

The majority of the studies described can be catergorised as being performed in either a "reflection" or "transmission" mode, at 605 nm or 830 nm (visible or near-IR). The enzyme is also usually studied when either maximally oxidised and reduced (eg to obtain difference spectra), or alternatively attempts are made to correlate changes in redox state with various events or corresponding variations in oxygen tension (or inspired oxygen concentration). It is this latter type of study from which estimates of the affinity of cytochrome oxidase for oxygen are

made.

4.8.2 The Work of Jobsis et al.

4.8.2.1 Development of the Technique.

Since it was Prof F.F. Jobsis who first proposed using the 830nm absorption band of cytochrome oxidase for non-invasive monitoring, it is therefore appropriate to begin by considering his work.

Jobsis initial interest in cytochrome oxidase appears to have been primarily concerned with the apparent difference in affinity of the enzyme *in vivo* (MILLS (1970)). In this paper the simultaneous measurement of discharge frequency of the carotid body chemoreceptors (which increases progressively with the decrease of oxygen tension) and the redox state of cytochrome oxidase was made using dual wavelength spectrophotometry on the Soret band. Results suggested that the affinity of cytochrome oxidase was lower *in vivo* (ie it was reduced at oxygen tensions at which it would have been fully oxidised *in vitro*).

In a review paper (JOBSIS (1972)), oxidative metabolism at low oxygen tensions was comprehensively discussed, including results of difference spectra from cat's cerebral cortex (350-605nm) and fluorescence measurements of NADH levels. Within this paper the apparent difference in affinities was emphasised and the possible roles of limited oxygen transport and diffusion in producing this anomaly briefly introduced (see Section 4.11). The observation was also made that monitoring cytochrome oxidase redox state could be a useful indicator of hypoxia, in part due to the reduced apparent affinity.

Jobsis was later involved in a study of the redox state of the respiratory chain enzymes in the silkworm midgut using spectra (430-620nm) obtained in split beam mode and dual beam measurement of the respiratory enzymes (MANDEL (1975)). The role of potassium transport in

particular was considered, which demonstrates that the rate of electron transport is likely to be affected by various biochemical concentrations (in addition to that of ADP as described in Section 4.5.2).

The idea of a "critical pO_2" at which the respiratory chain ceases to function as the cytochrome oxidase finally becomes totally reduced was considered in detail with regard to the cerebral cortex by ROSENTHAL (1976). (The idea of this "critical pO_2" is used in the mathematical modelling in Section 4.11). It discusses the fact that carbondioxide is a powerful vasodilator which may play an important part in increasing the oxidation of cytochrome oxidase. In the study reflectance spectrophotometry was performed on rabbit brain utilizing a surgically implanted plexiglass window in the skull. The redox state of cytochrome oxidase, oxygen saturation and blood volume were all monitored using visible wavelengths (577-605nm) in dual beam (single for the blood volume) mode. Equibestic wavelengths for cytochrome oxidase monitoring were used and the type of processing of the optical signals described in this paper is essentially that which is used for the majority of the following experiments by Jobsis and co-workers (see Section 4.10). Results showed that changes in oxygen saturation were smaller than those in the redox state of cytochrome oxidase suggesting that the latter may be a better indicator of physiological status, whilst also stating that its behaviour is different than in vitro, with a 20% reduction under normal respiratory conditions.

Regarding the affinity of cytochrome oxidase in vivo LAMANNA (1975) also showed, using dual beam wavelength reflection spectrophotometery in the intact cerebral cortex of cats that there was a continuous interdependency of cytochrome oxidase redox state on oxygen availability (measured as the inspired oxygen level).

In 1977 Jobsis published what has become a widely cited paper on reflectance spectrophtometry of cytochrome oxidase on the exposed cat

brain, which thouroughly investigated the feasibility of the technique including an assessment of the problems of interference from haemoglobin (JOBSIS (1977a)). It involved the use of transmission and reflectance spectrophotometry using a split beam spectrophotometer over the range 400-640nm to study both the absolute and difference transmission spectra of haemoglobin, red blood cells and mitochondrial samples. Reflectance spectra were then obtained from intact exposed brain using a scanning spectrophotometer in split beam mode, and finally kinetic measurements using dual and single wavelength methods. This paper is of particular interest due to the comprehensive attempt which was made to quantify measurement of cytochrome oxidase redox state in the presence of haemoglobin.

In the same year Jobsis also published the proposal to use near-IR wavelengths to perform transmission studies of cytochrome oxidase. It was stated that such measurements should allow oxygen suffiency to be determined by monitoring cytochrome oxidase redox state, along with blood volume changes by use of a haemoglobin isobestic point, haemoglobin oxygenation levels and cerebral blood flow (CBF) by using dye dilution techniques monitored optically (JOBSIS (1977b)). (see also COLACINO (1981) for more details of dye dilution techniques).

The evidence for these claims was given (JOBSIS (1977c)) in the form of near-IR difference spectra from cat's heads and dog's heart in situ (and kinetic studies, of the above variables using dual wavelengths). A blood volume increase in the adult human head during hyperventialation was also presented.

A further demonstration of the feasibility of the method was later given in the form of transmission measurements on the human head of cytochrome oxidase and blood volume changes, and also kinetic reflectance studies (JOBSIS (1978)).

In the papers cited above Jobsis had seemingly demonstrated that the

redox state of cytochrome oxidase, oxygen saturation and changes in blood volume could all be monitored non-invasively using near-IR transmission measurements.

This technique and its use up to this stage is summarised in Jobsis (1979a). The majority of the following papers by Jobsis and his colleagues assume that the use of near-IR spectrophotometry for monitoring the above variables is entirely valid, and therefore use it as a reasearch technique. In only a few of the publcations are there comments concerning the apparent change in affinity of the enzyme in vivo and the adequacy of the signal processing used to extract the various signals.

In 1977 Jobsis actually filed for a patent on the use of near-IR spectrophotometery for non-invasive monitoring (JOBSIS (1977d)), granted in 1981). Later patents (JOBSIS (1979, 1981)) granted in 1980 and 1983 respectively, cover the use of the method for "monitoring metabolism in the body organs" and a holder for attaching fibre optic bundles to the head for light delivery and collection. Included in the patents is a comprehensive description of the technique including the wavelengths which it is proposed to use, the relationships between the absorbance coefficients at these wavelengths (eg isobestic, equibestic and contrabestic) and the means of signal processing for the removal of artefacts (see Section 4.10).

4.8.2.2 Use of the Technique.

LAMANNA (1980) used visible wavelengths in the dual wavelength reflection mode (and NADH fluorimetry) to study the temperature coefficients for the oxidative metabolic response to electrical stimulation of the cerebral cortex in both cats and excised toad brains.

SNOW (1981) also used visible dual wavelength spectrophotometry to study cytochrome oxidase redox state in the blood perfused in situ canine

heart. The paper includes a description of the effectiveness of the dual wavelength method in correcting for artefacts, due to changes in either oxygen saturation, or blood volume. There is also a discussion on whether the apparent different affinities may be inherent or are due to anoxic regions of tissue and the possibility that the relation between cytochrome oxidase and oxygen acts as a signal for impending oxygen deficiency. Some scanning spectrophotometry results are also included with the necessary allowance for myoglobin since these studies were performed on muscle.

WIERNSPERGER (1981) used transillumination at near-IR wavelengths to study cytochrome oxidase redox state, and changes in blood volume and oxygen saturation in rat brain after acute reversible common carotid artery occlusion. The monitoring was performed with triple wavelength mode which involves two reflectance wavelengths either side of the necessary wavelength whose intensities are averaged. From the results it was concluded that the technique was satisfactory and can be used to continuously study cerebral metabolism and haemodynamics.

MOOK (1984) also employed near-IR triple wavelength measurements, but in reflectance mode, to monitor cytochrome oxidase redox state and oxygen saturation. Oxygen tension measurements were simultaneously made with electrochemical microelectrodes to assess the correlation between the three.

The continued development of the near-IR technique into a clinically applicable instrument was demonstrated by the studies performed on three adults undergoing general anaesthesia. The instrument used three GaAlAs laser diodes as light sources to monitor cytochrome oxidase redox state and haemoglobin and oxyhaemoglobin levels (FOX (1982)). The admittedly preliminary results showed that cytochrome oxidase was not maximally oxidised at a resting respiratory rate. A further description of the application of niroscopy to anaesthesiology is given in FOX (1983).

In addition to these near-IR studies further use of the method in the visible range was made to determine the effectiveness of using a perfluorocarbon blood substitute for exchange transfusion (SYLVIA (1982)), the recovery of the brain after hypoxic hypotension (PROCTOR (1982)), the sensitivity of the brain to cyanide poisoning and the protective effects against this of antagonists (PIANTADOSI (1983, 1984)).The effect of interference from haemoglobin derivatives was considered in some detail in the latter, as the absorbance spectra of some of the compounds formed by cyanide complexing cause particular problems.

Visible dual wavelength reflection spectrophotometry (KARIMAN (1983)) was also used, simultaneously with oxygen measurements (also made optically using pyrenebutyric acid whose fluorescence is quenched by oxygen), in an attempt to determine the relation between the redox state of cytochrome oxidase and oxygen tension. The relation between the two was found to be quite complex with evidence of hysteresis. The affinity of the enzyme for oxygen was apparently less than in vitro.

The near-IR technique has since been applied to the evaluation of perfluorochemical resucitation after hypoxic hypotension (PROCTOR (1983)), the effect of hypothermia during hypoxic hypotension (PALLADINO (1983)) and as an early indicator of recovery from haemorrhagic shock (KARIMAN (1983)). The latter paper contains a particulaly good description of the processing used.

To investigate the potential application of the near-IR technique to fetal monitoring SEEDS (1984), made such measurements on the exteriorized fetal head. Four wavelengths were used to determine oxygen saturation for both arterial and venous blood, and a strong correlation was found between this and fetal oxygen tension. The method was considered to be of potential benefit for use in the non-invasive assessment of fetal condition during labour.

Niroscopy has since been used in transmission mode on human preterm infants, to obtain details of cytochrome oxidase redox state, and change in blood volume and oxygen saturation (BRAZY (1983)). This paper demonstrates one of the possible uses of the technique in an intensive care application, and many others will certainly follow. An appraisal of the technique of near-IR spectrophotometry applied *in vivo* for non-invasive monitoring is given in Section 4.9.

4.8.3 Studies by Former Colleagues of Jobsis.

The following authors have in general performed studies using the techniques described above.

BALABAN (1981) and EPSTEIN (1982) both performed experiments in the visible range on exposed and isolated perfused rat kidneys respectively. Balaban used reflectance dual beam and scanning measurements, and discusses the interference due to haemoglobin. Amongst his conclusions he proposes that areas of the anaesthetised kidney are locally hypoxic producing the high reduced levels of cytochrome oxidase recorded and states that whether such areas normally exist in unanaesthetised kidney is a question to be resolved. Such areas may be due to a diffusion limited supply of oxygen, and may help explain the apparently lower affinity of cytochrome oxidase for oxygen *in vivo*.

Epstein used dual beam transmission spectroscopy (605nm v 625nm), in isolated perfused rat kidneys and administered respiratory chain blockers to obtain fully oxidised and reduced components of the respiratory chain. Like Balaban he suggests the affinity difference may be due to diffusion limited oxygen supply. Epstein also makes the point that tissue oxygen levels may be kept low under normal physiological conditions quite intentionally to prevent oxidative damage which is more likely to occur at high oxygen tensions. The possible connection between oxidative

damage and disease states in paediatrics is considered in some detail in Chapter 5. The possible effect of locally anoxic areas of tissues producing local areas of reduced cytochrome oxidase, and the apparent affinity of cytochrome oxidase for oxygen is discussed in Section 4.11.

The remainder of the work discussed in this section has been mostly performed at Miami University, Florida. ROSENTHAL (1981) used visible reflection dual beam measurements to study cytochrome oxidase, oxygen saturation and blood volume in exposed rat cerebral cortex in situ to assess the effects of nitrous oxide and pentobarbitol.

KREISMAN (1981) used the same technique, together with oxygen measurements made with microelectrodes. The aim here was to investigate the relationship between cytochrome oxidase redox state and oxygen tension. Cytochrome oxidase was found not to be fully oxidised in these studies, indicative again of an apparently lower affinity for oxygen in vivo, which it is postulated may be due to diffusion limitation.

A paper from the same group describes a similar study made to investigate the comparative oxygenation and mitochondrial redox activity in turtles and rats (SICK (1983)) and includes pO_2 - histograms made in the tissue under study. It was found that the apparent affinity is lower in turtle brain which in this case was linked to the demand for oxygen via biochemical considerations.

A comprehensive discussion of use of cytochrome oxidase redox state for clinical monitoring during recurrent seizures is given by KREISMAN (1983). WIERNSPERGER (1983) has also used near-IR transillumination to monitor cerebral blood volume, oxygen saturation and cytochrome oxidase redox state in rats, to study incomplete cerebral ischaemia, and concluded that under steady state conditions cytochrome oxidase is mainly reduced.

The work of DUCKROW (1982), LAMANNA (1985) and PIKARSKY (1985) demonstrates the continued development of instrumentation for

spectrophotometric measurements of this nature.

4.8.4 The Work of Other Groups.

Sato et al have used computer controlled scanning spectrophotometers to obtain visible reflectance spectra from the gastric mucosa (1979a) and liver surfaces (1979b, 1981a) to study hepatic hemodynamics and oxygen sufficiency and also simply for transcutaneous oxygen monitoring (1981b). (ie reflection oximetry see Section 1.5.1.5). Spectra were taken over the range 400-700nm, stored and subsequently processed.

These results have been used to obtain values for oxygen consumption (from the change in the haemoglobin spectra) and the redox state of the cytochromes. The method used to produce local anoxia is to press the tip of the fibre bundle used onto the organ surface, thus restricting the blood supply which consequently causes all components to become reduced. These studies demonstrate the advantage of observing a region of the spectrum as against using discrete wavelengths since the appearance and disappearance of bands can actually be seen. KOBAYASHI (1979) describes a similar instrument to that of Sato, which was used to study the visible reflection spectra from rat liver.

YAMADA (1981) used dual beam visible reflectance measurements to monitor the redox state of cytochrome oxidase and changes in blood volume via the reference wavelength during and following ischaemia of the cat spinal chord. Amongst the findings was that cytochrome oxidase redox state paralleled decreased oxygenation.

In response to Jobsis's work showing the high resting levels of reduced cytochrome oxidase reduction (ie low affinity for oxygen), BASHFORD (1980) used freeze trapped gerbil brains to measure these levels. Scanning spectrophotometry was performed over 500-650nm on the samples so that cytochrome oxidase and oxygen saturation could be studied

for different amounts of inspired oxygen. It was found that the steady state reduced levels were lower (<20%) than those found by Jobsis (although still higher than in in vitro studies) and that there was no change in these levels until the fraction of inspired oxygen fell below 0.05. This effectively means that cytochrome oxidase behaves in a manner in accordance with what would be expected from in vitro studies. A similar study BASHFORD (1982) came to similar conclusions, and showed that during anoxia cytochrome oxidase only becomes significantly reduced once the oxygen saturation had fallen substantially. However, higher resting levels of reduced cytochrome oxidase than would be expected from in vitro studies were found, and it was suggested that this may be due to either a pool of mitochondria which remained reduced at all levels of oxygenation or another pigment.

D.W. Lubbers and his colleagues have performed extensive visible reflectance spectrophotometric studies of haemoglobin (see Section 1.5.1.5 on reflectance oximetry) and the cytochromes in addition to oxygen tension measurements using microelectrodes. Early work included the use of rapid scanning spectrophotometers to study the variations in absorbance of myoglobin and the cytochromes in the in situ heart, during single heartbeats (FABEL (1965), LUBBERS (1969)).

Visible reflectance spectra from exposed organs have also been used to observe the oxygenation of myoglobin and redox state of the cytochromes, (LUBBERS (1983), FIGULLA (1983), HOFFMAN (1984), HEINRICH (1983)), during various studies. These papers include descriptions of the analysis of the spectra obtained, and this group have used various methods of analysis including the Kubelka-Munk theory and the type described in Section 1.4.3.4. Lubbers has also been involved in work concerning the levels of tissue oxygenation and critical oxygen concentrations required, similar to that discussed by JOBSIS (1972), ROSENTHAL (1976), and these points are discussed further in Section 4.11.

G. Jarry (Universite Paris Val de Marne, France) and his colleagues are interested in the possibility of performing simultaneous spectrophotometric measurements and transillumination imaging of tissue to obtain images of the spectral variation of cytochrome oxidase redox state and tissular oxygen saturation for example. To this end, Monte-Carlo modelling of light propogation through tissue (see Section 1.4.11) and preliminary laser transillumination studies (JARRY (1984) have been undertaken.

Spectrophotometric monitoring of excised rat kidney and heart has also been performed with difference spectra obtained in the visible range (MARZOUKI (1985)) and up to 800nm (JARRY (1985)) (with no significant peaks evident after the cytochrome oxidase α band). In the latter paper dual wavelength mode kinetic studies of cytochrome oxidase and myoglobin were also performed.

4.8.5 Near-IR Studies.

Following Jobsis' demonstration of the potential of niroscopy for non-invasive monitoring several groups have become interested in the application of the technique. This includes D. Delpy and colleagues at University College London, M. Ferrari and I. Giannini in Rome Italy and ourselves within the Bioengineering Unit, Oxford University. D. Delpy's group have used a near-IR spectrophotometer with three laser diodes as the light sources (COPE (1985)). Experiments have been performed on adult human forearm with absorption changes measured after the application of a rapidly inflated cuff. The instrument has also been shown to be capable of making measurements on preterm infants' heads up to diameters of 8.5cm.

At present the system is being modified to use four laser diodes from 775 to 904nm, and animal experiments to obtain appropriate processing algorithms for producing artefact free signals, and further

studies on preterm infants are planned.

The Italian group have performed extensive studies over the range 700-930nm on skeletal muscle and the heads of rats and rabbits, including flurocarbon exchange-transfused animals to overcome problems of haemoglobin interference. Difference spectra from tissue under a variety of conditions have been obtained together with kinetic traces using both dual and single wavelength measurements. (FERRARI (1982,1983), GIANNINI (1982)).

The absorption band centred at 830nm due to oxidised cytochrome oxidase was clearly seen in haemoglobin free animals. They state that their results show that the technique has much to offer, but feel that the required analysis of signals observed is not yet totally understood. They emphasise the potential of near-IR spectrophotometry for low cost intensive care instrumentation, and to this end have performed studies to monitor changes in cytochrome oxidase redox state, oxygen saturation and blood volume in neonates (GIANNINI (1985)).

Our work within the Bioengineering Unit involves that which is presented in this thesis and the development and use of a near-IR spectrophotometer developed by Mr Y.A.B.D. Wickramasinghe as described in Appendix A.

4.8.6 Summary.

The purpose of this section was to describe the development of spectrophotometric monitoring of the redox state of cytochrome oxidase from early invasive visible measurements to non-invasive *in vivo* studies which also give details of oxygen saturation and changes of blood volume in the region being monitored.

Using the information from the papers referred to above and experience obtained from the *in vitro* results in Section 4.6 and *in vivo* measurements presented in Chapters 6 and 7 an appraisal of the use of

this method is given in the following section.

4.9 The Clinical Use of Niroscopy.

In the earlier sections the reasons why the redox state of cytochrome oxidase monitored optically may be an indicator of oxygen sufficiency were given, with the use of the technique then demonstrated by *in vitro* experiments. This was followed by the above description of the development of the method from an *in vitro* research tool to its application in a clinical instrument. An appraisal is now made on the suitability of this method for non-invasive *in vivo* monitoring.

There is little doubt that a fully operational Niroscope providing details of the redox state of cytochrome oxidase, oxygen saturation and changes in blood volume within an organ such as the brain would be of tremendous value. However, before niroscopy becomes a widely accepted technique there are several points concerning both the results obtained and use of the method itself which will require clarification.

Firstly there is the question of the adequacy of the signal processing used. That is whether it is capable of producing a signal which is solely dependent upon the redox state of cytochrome oxidase, with no interference from changes in either oxygen saturation or blood volume, (and indeed capable of giving signals representative of only oxygen saturation and blood volume for the same reasons of spectral interference). The necessary requirements for this, and methods of processing commonly used, are considered, in more detail in Section 4.10.

Secondly there is the anomaly concerning the affinity of cytochrome oxidase for oxygen which besides being of interest in its own right, is also of practical significance concerning the use of the technique. As previously described, it is the apparent lowering of the affinity of cytochrome oxidase *in vivo* which makes the redox state of the enzyme a useful indicator of oxygen sufficiency over a reasonable range of oxygen tensions, with the actual change in affinity affecting the precise relation between the two. Consequently, some knowledge of the change in

apparent affinity would need to be known before using the instrument as a monitor of oxygen sufficiency, or else it would have to be calibrated using simultaneous optical and oxygen measurements. Furthermore, the apparent affinity must remain stable for meaningful results. This is discussed further in Section 4.11 where a possible contributory factor to the apparent increase in the Km of the cytochrome oxidase *in vivo* is given in terms of a physical model.

Connected with the apparent change in affinity is the question of what a perfectly functioning Niroscope should actually be used to monitor. Compounds such as cytochrome oxidase, haemoglobin and myoglobin whose absorbance is dependent upon oxygen concentration are used in studies of the microcirculation and oxygen content in tissue as indicators of these variables. The situation is not that dissimilar with niroscopy where oxygen saturation and the redox state of cytochrome oxidase are monitored to also give details of oxygen availability.

In the studies on the microcirculation the affinities of cytochrome oxidase and haemoglobin are quite different and therefore useful as indicators of oxygen tension over quite different ranges. However, *in vivo* this is not the case, because of the decrease in apparent affinity of cytochrome oxidase.

There appear to be two consequences of this. Firstly if the Km of the enzyme did not increase then there would only be substantially reduced amounts of enzyme present at oxygen levels normally associated with hypoxia, and so the enzyme would not warn of likely impending tissue damage. Secondly, since the Km does increase and therefore its redox state varies over a wide range of oxygen tensions there is the question of whether it actually gives any more useful information than oxygen saturation since its affinity for oxygen has approached that of haemoglobin.

Certainly, since haemoglobin is connected with oxygen transport and

cytochrome oxidase with oxygen utilization there may be occasions when they may react differently, (the level of measurement is also likely to be of importance, since it may play a role in causing the apparent change in affinity as described in detail in Section 4.11). However it would appear that in most circumstances it is likely that in vivo measurements of oxygen saturation and the redox state of cytochrome oxidase would be both related to oxygen tension in a very similar fashion due to the higher Km of cytochrome oxidase in vivo. Therefore the basic question is whether there is more to be gained by monitoring cytochrome oxidase rather than simply oxygen saturation.

(A consequence of this may be the difficulty in assessing the performance of signal processing used since many physiological changes will probably effect the redox state of cytochrome oxidase and oxygen saturation almost simultaneously).

The fact that niroscopy can potentially be used to monitor oxygen saturation and blood volume as well as the redox state of cytochrome oxidase is of relevance to the next point.

This is that although a Niroscope was first used in a clinical enviroment four years ago (FOX (1982)), and a commercially available device was to have become available during the past two years, this has not happened. This tends to suggest that there are certain problems which are delaying the launch of the instrument, with likely problems being related to the points raised above.

However, one would assume, considering the results already obtained, that any problems are related to monitoring the redox state of cytochrome oxidase and not oxygen saturation and blood volume, since the signals resulting from these two variables would presumably be larger than that due to the cytochrome oxidase.

Even if this is the case, a niroscope which would be capable of providing details of tissular oxygen saturation and changes in blood

volume in organs such as the brain non-invasively would be of great value in itself as a clinical and research tool. Indeed, if as suggested above, the cytochrome oxidase and haemoglobin have apparently similar affinities for oxygen in vivo then oxygen saturation and redox state of cytochrome oxidase may well parallel each other anyway, so little information would be lost.

The final point concerning monitoring the redox state of cytochrome oxidase is that in the majority of papers cited in Section 4.8, anaesthetics were used. The importance of this is that many anaesthetics through their effect on the microcirculation, perturb the normal tissular pO_2 levels (SPIEGEL (1986), as measured using microelectrodes to obtain pO_2-histograms. Since the redox state of cytochrome oxidase is dependent upon oxygen sufficiency at this level it is not improbable that this too may be affected by the use of anaesthetics. Clearly this could be of some importance concerning the majority of data where the redox state has been monitored.

(The nature of the pO_2-histogram is an essential part of the model presented in Section 4.11 which attempts to explain the change of affinity of cytochrome oxidase in vivo).

In conclusion, it is considered that in some form niroscopy will have a profound influence on the care of the critically ill, and nowhere more so than in paediatrics. However, exactly which variables prove to be the most useful to monitor is more open to question.

Further reasearch using niroscopy will help provide answers to this and also assist in determining the precise cause of the apparent change in affinity of cytochrome oxidase.

4.10 Signal Processing Requirements to Obtain Artifact Free Traces During Niroscopy.

4.10.1 Introduction.

An essential part of any optical method such as niroscopy, oximetry or bilirubinometry is to take the signals from the photodetectors and use them to calculate the value of the particular variable being monitored. The way in which oxygen saturation is calculated, in the various forms of oximetry, was described in Section 1.5.1, with most results relying upon the application of the Lambert-Beer Law (Equation 1.15) in some form, although this is strictly only applicable for samples which absorb but do not scatter light.

For oximetry, two wavelengths are required because both the oxygen saturation and total concentration of haemoglobin are unknown and can therefore effect the absorbance. (The optical path length is also unknown but is linked in a term together with the total haemoglobin concentration as described in Section 1.5.1.1).

4.10.2 Theoretical requirements.

In Section 1.5.1.1 the spectrophotometric determination of the oxygen saturation of a haemolysed sample using absorption measurements at two wavelengths was described. If a clear solution of both haemoglobin and cytochrome oxidase (with both substances possessing two possible absorption states) is now considered then the absorbance, A, of such a solution in a cuvette of length, l, is given by:

$$A = l(a[HbO_2] + b[Hb] + m[\text{cyt } aa_3(oxi)] + n[\text{cyt } aa_3(red)]) \qquad 4.6$$

where a,b,m,n are the respective absorption coefficients (cf equation 1.18). Assuming the absorption coefficients are known then the equation has five unknown variables, and the problem of finding any of the four concentrations is the same as that which is solved by the Hewlett Packard Oximeter (see Section 1.5.1.3.2).

By taking absorbance measurements at four wavelengths any of the four concentrations could be found in terms of the cuvette depth, l, so that upon calculating the oxygen saturation or redox state (which involves taking a ratio) the term for the cuvette depth cancels out and a value for either would be produced. As was the case with the oximeter the actual values of the four variables cannot be found without measuring l by some means, with a further absorption measurement made at another wavelength being of no help (see Section 1.5.1.1). Therefore to measure either the oxygen saturation or redox state of the cytochrome oxidase of the solution in the cuvette then four absorbance measurements are required.

As with oximetry equation 4.6 can be written in terms of oxygen saturation, S, redox state, R, and total concentration of haemoglobin, C, and cytochrome oxidase, T, as:

$$A = l[C(S(a-b)+b) + T(R(n-m)+m)] \qquad 4.7$$

Written in this form it can be seen why whereas it has been stated that, for solutions of haemoglobin and cytochrome oxidase in a cuvette, measurements at four wavelengths are required, for most of the studies performed in the papers cited in Section 4.8 dual wavelength spectrophotometry was used.

Firstly, in vivo the total concentration of cytochrome oxidase, T, in the volume of tissue under observation will remain constant as long as the source detector geometry is unchanged. This therefore removes one variable, and replaces it with a constant. In addition if an isobestic point for either haemoglobin or cytochrome oxidase is used then at this wavelength the S(a-b) or R(n-m) term will be zero, so simplifying equation 4.7. Alternatively if the haemoglobin absorbance is much larger than that of cytochrome oxidase (or vice versa) then it may be possible for the terms for the compound with the smaller absorbance to be neglected.

However these assumptions are not in themselves sufficient for only two wavelengths to suffice. The further significant fact is that in most of the studies referred to in Section 4.8 the oxygen saturation, blood volume and redox state of cytochrome oxidase were monitored and not measured. That is changes in these variables were observed but their absolute values were not calculated. When values were placed on these variables then this was after some calibration procedure involving, for example, the use of 100% inspired oxygen.

(In the above the same optical path length was assumed for both haemoglobin and cytochrome oxidase. If this is not so then the situation becomes more complex, both in the case of the cuvette and *in vivo*. Furthermore, for either equal or different path lengths, if the absorbance is written in the form of equation 4.6, then it can be seen that as in oximetry the concentration and path length terms are inseperable (by optical measurements) and the effect of an increase in either of these cannot be distinguished from each other.)

Additional problems in performing *in vivo* monitoring may occur since the above is based solely on the Lambert-Beer law. However, although this only strictly applies to non-turbid solutions it has been previously applied to *in vivo* measurements with some success (see Section 1.5).

4.10.3 Dual Beam Spectrophotometry.

The dual wavelength method used by Jobsis and his colleagues is essentially an extension of the dual beam method developed by CHANCE (1951c), and then adapted by YANG (1954) (see Section 4.5.4).

This adaptation involved the use of a feed back signal which controls the gain of the PMT, and which is used to adjust for variations in one variable (eg blood volume) whilst monitoring a second.

The way the dual beam method is used in the majority of studies described in Section 4.8 is as follows. A measurement wavelength is

selected at which there is a large change in absorbance in the compound being monitored between its two possible states, with a reference wavelength chosen to compensate for any changes which may occur in the state of another compound during measurement (ROSENTHAL (1976), JOBSIS (1977a), SNOW (1981), WIERNSPERGER (1981)).

Although only two wavelengths are used and therefore only changes in two variables accounted for, judicious choice of wavelengths allows reasonably artefact free recordings to be obtained, in part due to the reasons given above. (Three wavelengths are also sometimes used with two reference measurements made either side of the sample wavelength, and the average of their intensities then used as the reference signal (WIERNSPERGER (1981)).

Concerning wavelength selection, equibestic and contrabestic wavelengths (JOBSIS (1977d,1979b) are frequently used, where these terms refer to pairs of wavelengths at which the difference in absorbance between the two states of a compound are of the same magnitude but of equal and opposite signs respectively. Such wavelengths assist in compensating for changes in variations in the state of the interfering substance.

In addition to its use for artefact removal dual beam spectrophotometry also posesses the advantage that it compensates for any changes in source intensity or detector response, which may be quite significant when monitoring very small changes in absorbance. It is by using this technique that the redox state of cytochrome oxidase, oxygen saturation and changes in blood volume are often monitored. However, as noted above two wavelength techniques cannot be totally adequate for in vivo measurements on what is a multicomponent sample.

That this is indeed the case was shown by FIGULLA (1984) who compared the abilities of dual beam spectrophotometry and two other methods, to monitor the redox state of cytochrome oxidase and oxygenation

of myoglobin (ie a two component system) in a perfused (haemoglobin free) guinea pig heart. Different results were produced from each of the three different methods and it was concluded that dual beam spectrophotometry can only be applied under special conditions, with an essential requirement being the existence of an isobestic.

Further evidence that dual beam spectrophotometry may at times be inadequate was given by KARIMAN (1985), who subsequently developed a triple wavelength technique. This involves monitoring the redox state of cytochrome oxidase by the absorption at 605nm, use of the other wavelength of the contrabestic pair for haemoglobin which has one wavelength at 605nm and an isobestic wavelength for haemoglobin. The absorption at these three wavelengths were then used with appropriate absorption coefficients for <u>in vivo</u> use in a set of simultaneous equations obtained using the Lambert-Beer law.

4.10.4 Summary.

In conclusion, although the majority of papers cited in Section 4.8 have used dual wavelength spectrophotometry to monitor the redox state of cytochrome oxidase, oxygen saturation and blood volume, consideration of the theoretical requirements, and subsequent publications suggest that such a technique may not always be adequate for artefact removal, and that simultaneous measurements at three or more wavelengths may be necessary.

In addition it is likely that although changes in these variables may be monitored their actual measurement may not be possible due to the points raised above and a similar reason that compression of the ear was necessary in the Wood's oximeter (Section 1.5.1.3.1).

The use of scanning methods such as those used by N.Sato and D.W.Lubbers (see Section 4.8) may prove to be more suitable for processing since the data obtained contains more information, however

this would also increase the complexity of the signal processing required.

4.11 Mathematical Modelling of the Kinetic Behaviour of Cytochrome Oxidase.

4.11.1 Introduction.

The apparently decreased affinity of cytochrome oxidase for oxygen *in vivo*, compared to that *in vitro* is an extremely interesting observation. That is both from a purely enzymatic viewpoint, since the purified enzyme appears to be more efficient than when in a more intact system, and because were the apparent affinity *in vivo* as high as it is *in vitro*, then the usefulness of the redox state of cytochrome oxidase as an indicator of oxygen sufficiency would be severely compromised.

The work in this section arose directly from the results in Section 4.6.3. which show the rapid change in light intensity recorded as the cytochrome oxidase finally consumed all of the dissolved oxygen present in the sample and became reduced. As described in the results, the rapidity of the switch was assumed to be (and is) an indication of the enzyme's extremely low Km. However, from further consideration of these results it became apparent that under certain theoretical conditions (that may not be practically attainable), this assumption is in itself sufficient to demonstrate how the enzyme may appear to have a far higher Km, (ie much lower affinity) than it actually posseses.

Consider a closed cuvette containing oxidised cytochrome oxidase, the trace obtained from monitoring the transmitted intensity at 605nm of the sample, would be of the form shown in Figure 4.37(i), that is similar to the traces in Section 4.6.3. Now imagine a cuvette open to the air, so that oxygen can diffuse into the sample, and in which the intensity is monitored at various levels, as shown in Figure 4.1(ii). A possible situation given the appropriate diffusion coefficient and consumption rates of oxygen in the cuvette, is that the oxygen at the bottom of the cuvette will be totally consumed sooner than the top, where the diminishing levels can be rapidly replenished by oxygen diffusing from

the air. Consequently, the change in the transmitted intensity will occur sooner at the bottom of the cuvette than at the top as shown, but at each level will produce the same basic trace as in the closed cuvette. Now consider, the trace which would be obtained if the total intensity of light transmitted through the cuvette was monitored, by summing the outputs from the individual detectors. This would have the form as shown in the figure of a much slower decrease in light intensity.

The significance of this final trace is that if it was seen in isolation, yet known to have been obtained from a cuvette in which cytochrome oxidase was consuming oxygen, then because of the slower change in the intensity level an obvious assumption would be that for some reason the enzyme had a decreased affinity for oxygen.

This "thought experiment" shows that it is relatively simple to envisage a situation in which, via an optical measurement the Km of cytochrome oxidase is apparently increased. It was therefore natural to consider whether such an effect may be occuring in vivo.

It is worth noting at this stage that the underlying cause of the above apparent change in affinity is due to the fact that the optical measurement is made over a relatively large area (ie on a macroscopic rather than a microscopic scale).

To investigate these ideas further, mathematical modelling of the oxygen content and absorbance of the sample within the cuvette with respect to time was planned to produce rigourous proof of the hypothesis to support the above verbal description.

Since the absorbance of the enzyme is of fundamental importance in this hypothesis, a requirement of this model was to describe the absorbance as a function of oxygen concentration or consumption (themselves linked via the rate equation).

However, since the generally accepted relation between absorbance and pO_2 is simply that in vitro at all but extremely low oxygen tensions

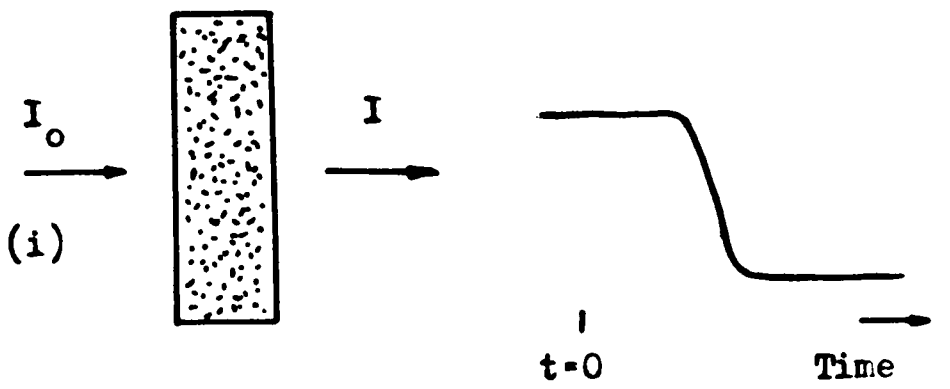

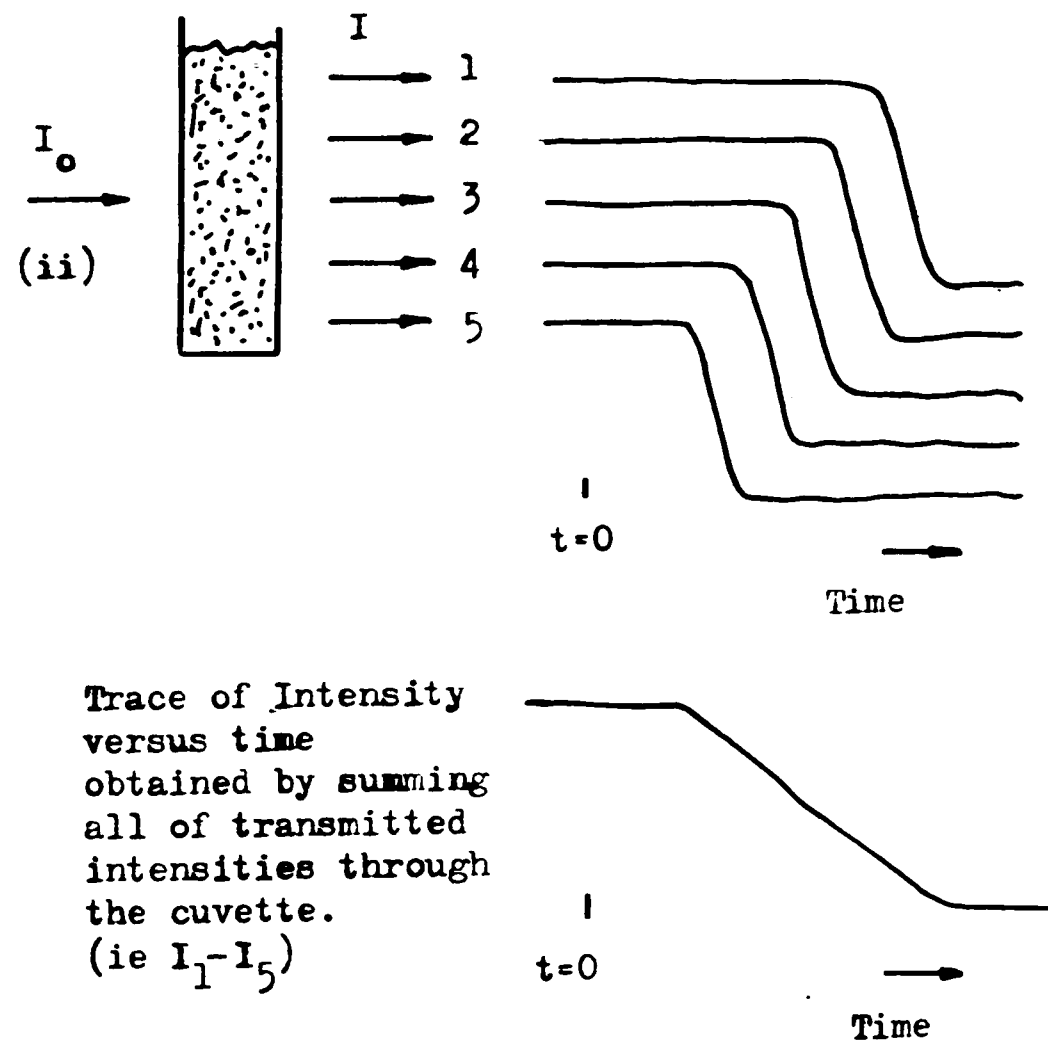

Figure 4.37 Theoretical variations of transmitted intensity versus time for cuvettes containing cytochrome oxidase as a member of an artificial respiratory chain for: i) a closed system and ii) a cuvette open to the air allowing the ingress of oxygen.

the enzyme is fully oxidised due to its high affinity, else it is fully reduced, then the derivation of such an expression and its use in modelling the results in Section 4.6.3 (and predicting results for larger values of Km), was in itself considered a worthwhile aim.

Although such mathematical expressions linking oxygen content, oxygen consumption, and the absorbance and redox state of cytochrome oxidase were obtained and used to model the results obtained in Section 4.6, it became apparent that there were potential problems with using the model to investigate the proposed theory as described below. However, the fundamental idea of an "integration" of the optical signal over a relatively large area was applied in a slightly different but more appropriate form to demonstrate that such an approach is indeed sufficient to explain how the enzyme can retain a high affinity for oxygen on a microscopic level whilst it appears to be much decreased *in vivo* when macroscopic measurements are made (Section 4.11.5).

The results of the model would then be used to find the apparent Km of cytochrome oxidase under different conditions, which amounts to determining the reaction kinetics of the enzyme as can be seen from Figure 4.12.

4.11.2 Reaction Kinetics and Mathematical Modelling of Reactions.

The aim was to produce a mathematical model capable of not only reproducing the results in Section 4.6, in which oxygen diffusion from the air was not considered to exert a major influence (eg a closed system as in Figure 4.37(i)), but also model the pO_2 and absorbance changes at different positions within a cuvette, with diffusion processes as well as oxygen consumption playing a major role (see Figure 4.37(ii)).

The determination of the reaction kinetics of an enzyme is by no means a simple process. As for any chemical reaction the ideal method is to perform a series of experiments with (for what is assumed to be a

single substrate reaction in which the substrate is consumed) a range of initial substrate concentrations covering the range of interest. The initial rate of substrate consumption can then be determined and plotted against substrate concentration to give a graph showing the reaction kinetics such as Figure 4.12.

A significant point concerning this method of determining reaction kinetics is that it is the initial rates of reaction that are used. This may be of importance in an enzyme catalysed reaction where many factors may affect the reaction rate other than the substrate concentration such as a back reaction (which will be dependent upon product concentration) or even inhibition of the enzyme's activity as the concentration of the product rises. In view of this alone the way in which the affinity of cytochrome oxidase for oxygen <u>in vivo</u> has been estimated appears far from ideal. This is because it involves taking simultaneous absorbance measurements (as a guide to the enzyme's redox state) and oxygen measurements (by various means), and then producing a graph showing the reaction kinetics as absorbance versus oxygen content.

In Section 4.5.3 the rate ,v, of a single substrate, S, enzyme catalysed reaction using Michaelis-Menten kinetics was shown in graphical form (Figure 4.12). The equation for this graph is

$$v = \frac{V_m S}{K_m + S} = -\frac{dS}{dt} \qquad 4.8$$

where Vm is the maximum velocity and Km the substrate concentration at which the velocity is half maximal. This equation can be integrated to obtain an analytical expression for the variation of substrate concentration, S, with time as:

$$(S-A) + K_m \ln \frac{S}{A} = -V_m t \qquad 4.9$$

where, A, is the initial concentration. This equation describes how the substrate concentration, S, decreases with time in a single substrate

enzyme catalysed reaction in a closed system with Michaelis Menten kinetics (such as the consumption of oxygen by cytochrome oxidase). Consequently this expression should describe the decrease in oxygen concentration with time seen in the traces in Section 4.6.

The expression is somewhat complicated, although for small values of t then S is approximately equal to A and so S = A-Vmt which is zero order kinetics, showing that the consumption is constant with the oxygen falling linearly as observed. For large values of t then S will be close to zero and the KmlnS/A term begins to reduce the rate at which the oxygen concentration falls, which is also observed.

From recordings of the fall in substrate concentration with time described by equation 4.9, the reaction kinetics could be determined by measuring and plotting against each other both the rate of substrate consumption and concentration from such traces (DIXON (1979)).

However, a problem with this approach is that the kinetics will not then be determined using initial reaction rates and so as described above additional effects may have affected progress of the reaction. For this reason modelling the fall in substrate concentration with only equation 4.8 (as is the case here) may not accurately reproduce experimental results.

Despite these potential problems in the model it was assumed that this equation does describe the rate of oxygen consumption by cytochrome oxidase at any given oxygen concentration, S, at any time, t.

Calculating the fall in pO_2 as oxygen is consumed by cytochrome oxidase was therefore achieved by the numerical (as opposed to analytical) solution of equation 4.8 using finite difference methods (SMITH (1978)). This involved non-dimensionalising the Michaelis Menten equation (4.8) to give:

$$-\frac{ds}{dt'} = \frac{s}{k+s} \qquad 4.10$$

where s = S/A, k = Km/A and t' = (Vm/A)t which is used in its finite difference form as.

$$-\frac{s_{t+1} - s_t}{h} = \frac{s}{k+s} \qquad 4.11$$

Where s_{t+1} is the concentration after the normalised time step h from s_t. (h is equal to $V_m \Delta t / A$ where Δt is the actual time step in secs.)

Consequently, as shown below, the decrease in oxygen content with time in a closed cuvette in which cytochrome oxidase consumes the dissolved oxygen can be modelled. (Before solving the Michaelis-Menten equation in this manner, standard integer order reactions were modelled both numerically and analytically and the results compared to ensure that the numeric solution gave satisfactory results).

What the above shows is that the fall in substrate concentration of a single substrate enzyme catalysed reaction can be mathematically modelled, and that from such a graph (whether experimental or theoretical) the kinetics of the reaction can be determined, albeit perhaps not with total precision since initial reaction rates are not used.

However, here the interest is in using absorbance measurements to determine reaction kinetics and so in the next section an expression linking the absorbance of a sample of cytochrome oxidase to variables such as oxygen concentration and consumption is given. Fitting this into the model should then enable both oxygen and absorbance traces like those presented in Section 4.6 to be produced.

4.11.3 Modelling the Absorbance and Consumption of Oxygen by Cytochrome Oxidase.

Throughout this chapter the link between the redox state of cytochrome oxidase and its absorbance has been evident. Furthermore, as described in Section 4.5.2 since the redox state depends in part on oxygen consumption, which itself depends on oxygen concentration, then the absorbance, redox state, oxygen consumption of the enzyme and oxygen concentration must all be interrelated. The derivation of a mathematical expression for the absorbance of cytochrome oxidise in terms of the other variables is now described.

As shown in Figure 4.9, cytochrome oxidase mediates the transfer of reducing equivalents from cytochrome c to oxygen. The model used here to describe this process assumes the following sequence of events. A cytochrome oxidase molecule accepts an electron from reduced cytochrome c, becomes reduced and then passes it to oxygen and so becomes oxidised. This cyclic sequence is then repeated.

It is further assumed that any cytochrome oxidase molecule has two corresponding levels of absorbance, one for each redox state. This allows the absorbance of an assembly of cytochrome oxidase molecules to be represented mathematically. In a collection of N molecules with number P oxidised, the absorbance, A, will be

$$A = P(m-n) + Nm \qquad 4.12$$

where m and n are the absorbance due to an individual molecule when oxidised and reduced respectively. This shows that the absorbance is linearly related to the number of oxidised molecules.

In the above model any molecule of cytochrome oxidase will be either oxidised or reduced, with the time it remains in either state dependent upon how quickly it either receives electrons from reduced cytochrome c or donates them to oxygen. Consequently in a population of N molecules, at any given time, the number that are oxidised will be equal to the

number that have donated electrons to oxygen, but not yet accepted more electrons from reduced cytochrome c. Therefore an expression for the absorbance of this group of molecules must be related to the rate of production of both the oxidised and reduced forms.

An oxidised molecule is formed every time a reduced cytochrome oxidase molecule donates its four reducing equivalents to oxygen to form two molecules of water, so the rate of formation of oxidised molecules is directly related to oxygen consumption.

As for the rate of production of reduced molecules, that is dependent upon the rate at which reducing equivalents are accepted from reduced cytochrome c. In this model it has been assumed that the cytochrome oxidase is only participating in a single substrate (ie oxygen) reaction because the cytochrome c concentration is considered not to be rate limiting, and so the transfer of electrons takes place with zero order kinetics. Therefore it is assumed that any oxidised cytochrome oxidase molecule will become reduced after a specific time interval of τ secs.

Consequently, at any time T the number of oxidised molecules present will be equal to the number that have become oxidised during the last τ secs and therefore have not yet become reduced again. This principle is shown diagramatically in Figure 4.38.

Hence, the number of oxidised molecules will be given by:

$$\int_{T-\tau}^{T} - \frac{d[O_2]}{dt}\, dt \qquad 4.13$$

which is simply proportional to the amount of oxygen consumed over the time interval τ secs preceding time T.

To actually use this expression to calculate the number of oxidised molecules and so the absorbance a value for τ must be known. However, if τ is small the oxygen consumption can be considered constant over this period and so the number of oxidised molecules can simply be

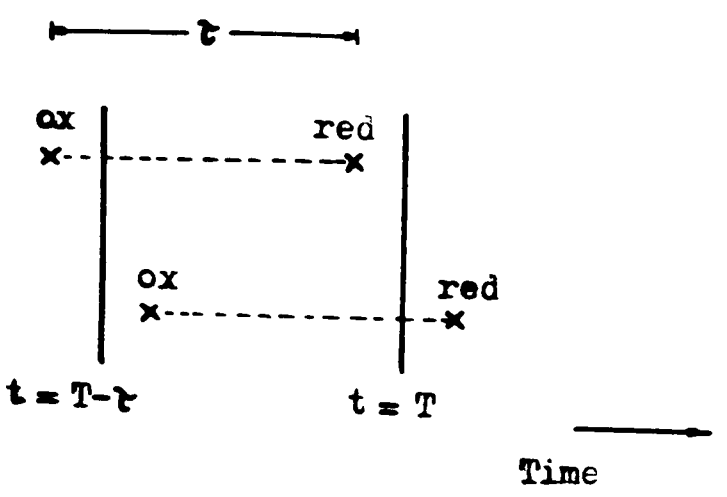

Figure 4.38 Diagram demonstrating the means of estimating the number of oxidised cytochrome oxidase molecules at time T.

expressed as the product of the oxygen consumption at time T, and time interval τ :

$$-\left.\frac{d\,[O_2]}{dt}\right|_{t=T} \times \tau \qquad 4.14$$

which for constant τ shows that the number of oxidised molecules is directly proportional to the oxygen consumption.

The results from Section 4.6 in which the change in transmitted intensity and pO_2 were monitored as cytochrome oxidase consumed the oxygen in what was essentially a closed system can now be modelled. The variation of the pO_2 with time is found using the finite difference methods described above, whilst from equations 4.14 and 4.12 the absorbance is linearly related to the oxygen consumption, and so the latter is actually used as a measure of the absorbance. The programme to implement this model was written in FORTRAN 77 and compiled and run on a mainframe computer, a flow diagram is given in Figure 4.39.

Figure 4.40 shows the (normalised) pO_2 and absorbance traces

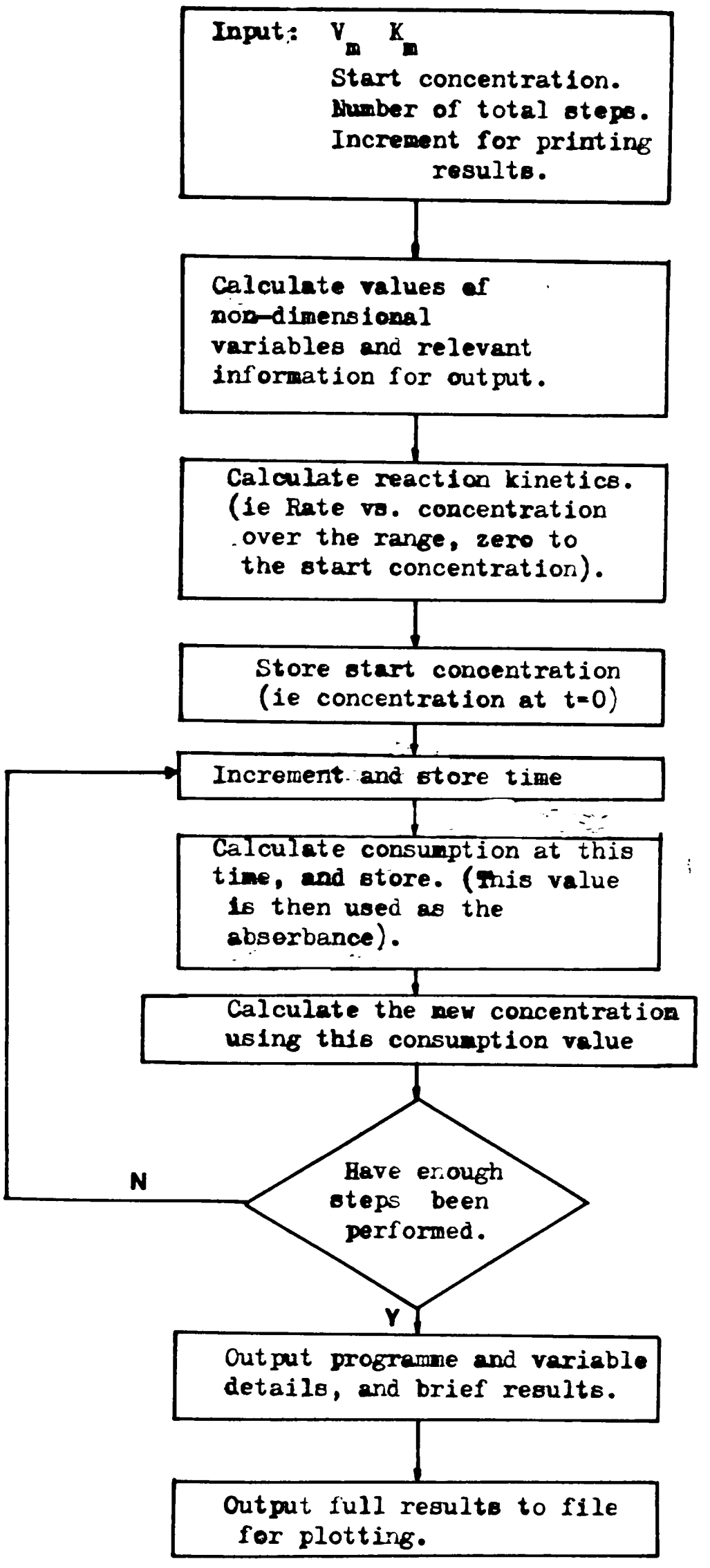

Figure 4.39 Flow diagram of programme for calculating oxygen concentration and consumption with respect to time in a closed system.

obtained for a cuvette with an initial pO_2 of 70mmHg, and containing cytochrome oxidase of sufficient quantity to produce a fall in pO_2 of 0.2 and 0.4mmHg/sec for traces (i) and (ii) respectively, when consuming oxygen at its maximum rate, Vm, and with a Km of 0.1mmHg. (The rates of oxygen consumption are approximately equal to those in Figures 4.24(i) and (ii)). The (normalised) reaction kinetics for the enzyme are shown in Figure 4.41(i).

Also shown in Figure 4.41 are the consumption rates for Kms of 1, 10 and 20mmHg. The effects of these higher Kms on the intensity and pO_2 for a starting concentration of 70mmHg and maximum rate of oxygen consumption equivalent to a fall in pO_2 of 0.2mmHg/sec are shown in Figures 4.42, 4.43 and 4.44 respectively. (Note the time scales are twice those of Figure 4.40). The slower fall in absorbance with increasing Km is expected as discussed in the Introduction to this section.

As noted above the maximal rates of oxygen consumption used to produce these results are similar to those in Figure 4.24 and consequently the traces can be compared. Considering the predicted fall in oxygen the use of Km's of both 0.1 and 1 mmHg produce a linear fall in oxygen concentration (ie zero oreder kinetics) for much of the trace, as was seen in Figure 4.24. Therefore it appears that the model is adequate. At the higher Km's the fall in pO_2 is non-linear as expected, as was the effect of a higher rate of oxygen consumption shown in Figure 4.40.

The absorbance trace in Figure 4.40 demonstrates the rapid change in absorbance (a decrease as the trace is related to the number of oxidised molecules, that is the absorbance at 830nm) seen experimentally, with the chief difference between the results being the fact that whereas in practice the absorbance falls gradually to zero after a large initial change, in the model the absorbance reaches its minimum as soon as the

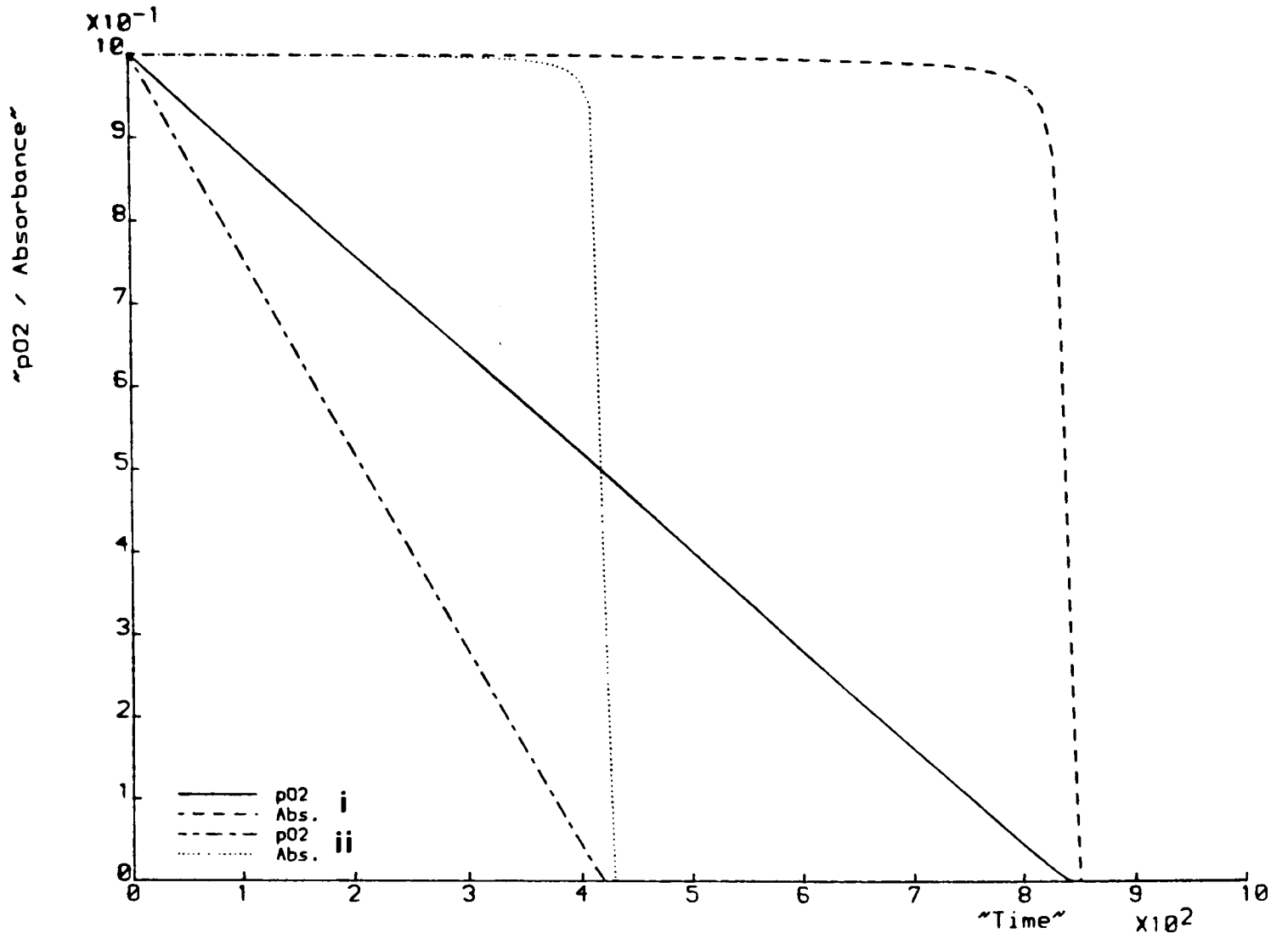

Figure 4.40 Results from mathematical model predicting changes in pO_2 and oxygen consumption (absorbance) with time. (see text for details).

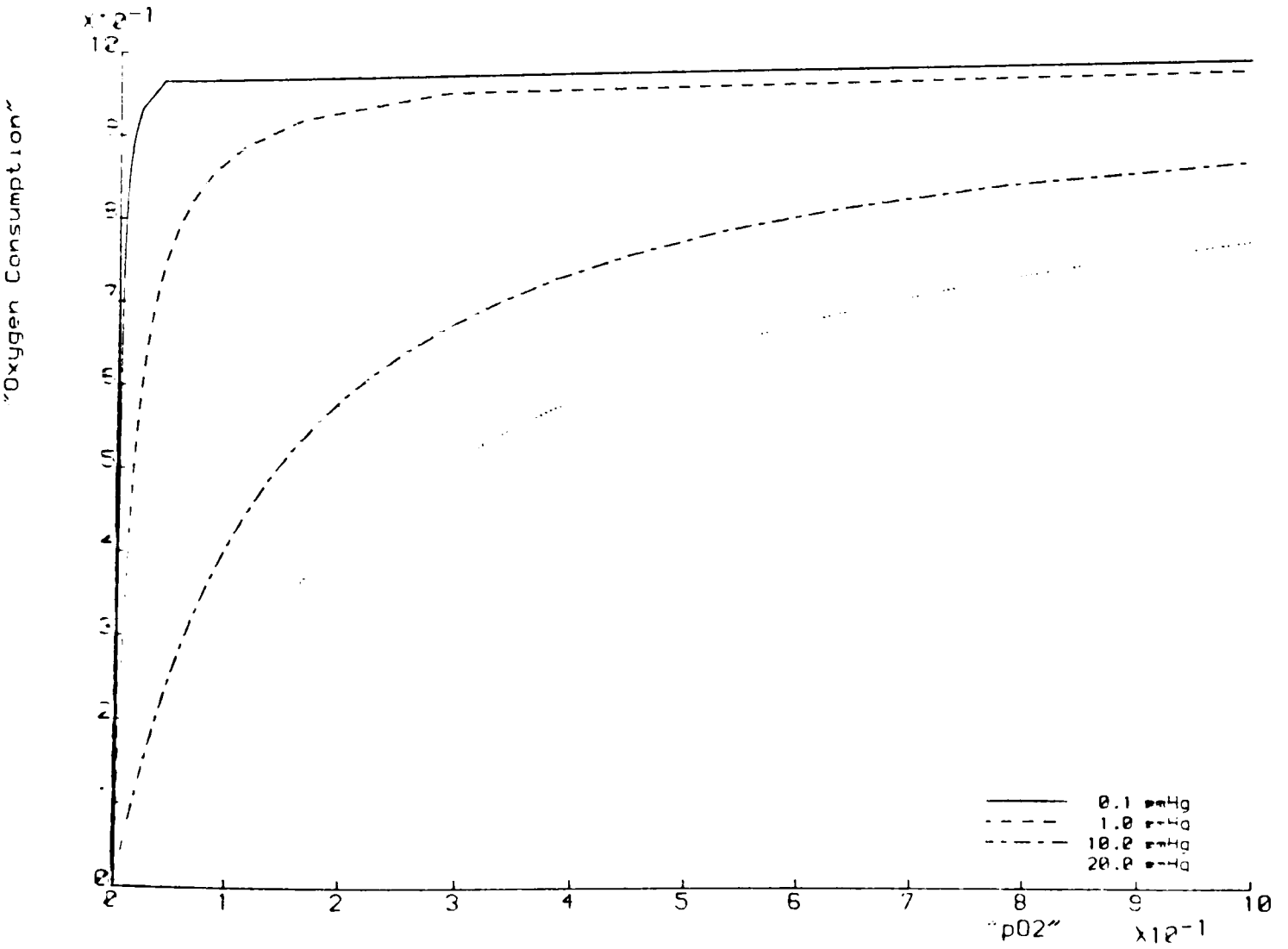

Figure 4.41 Normalised reaction kinetics from mathematical model for four values of K_m and concentrations from 0 to 70mmHg.

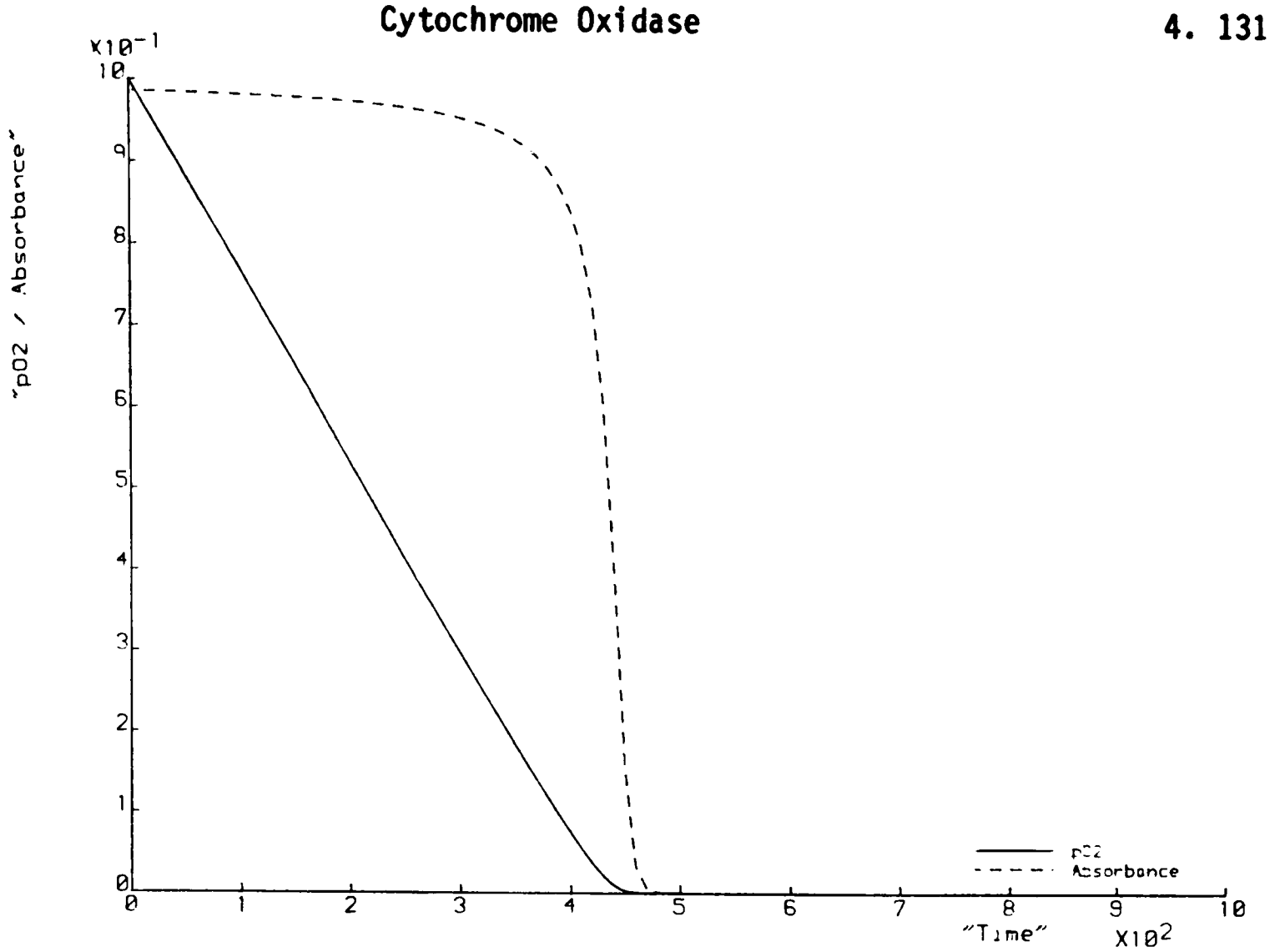

Figure 4.42 Results from mathematical model ($K_m = 1$mmHg).

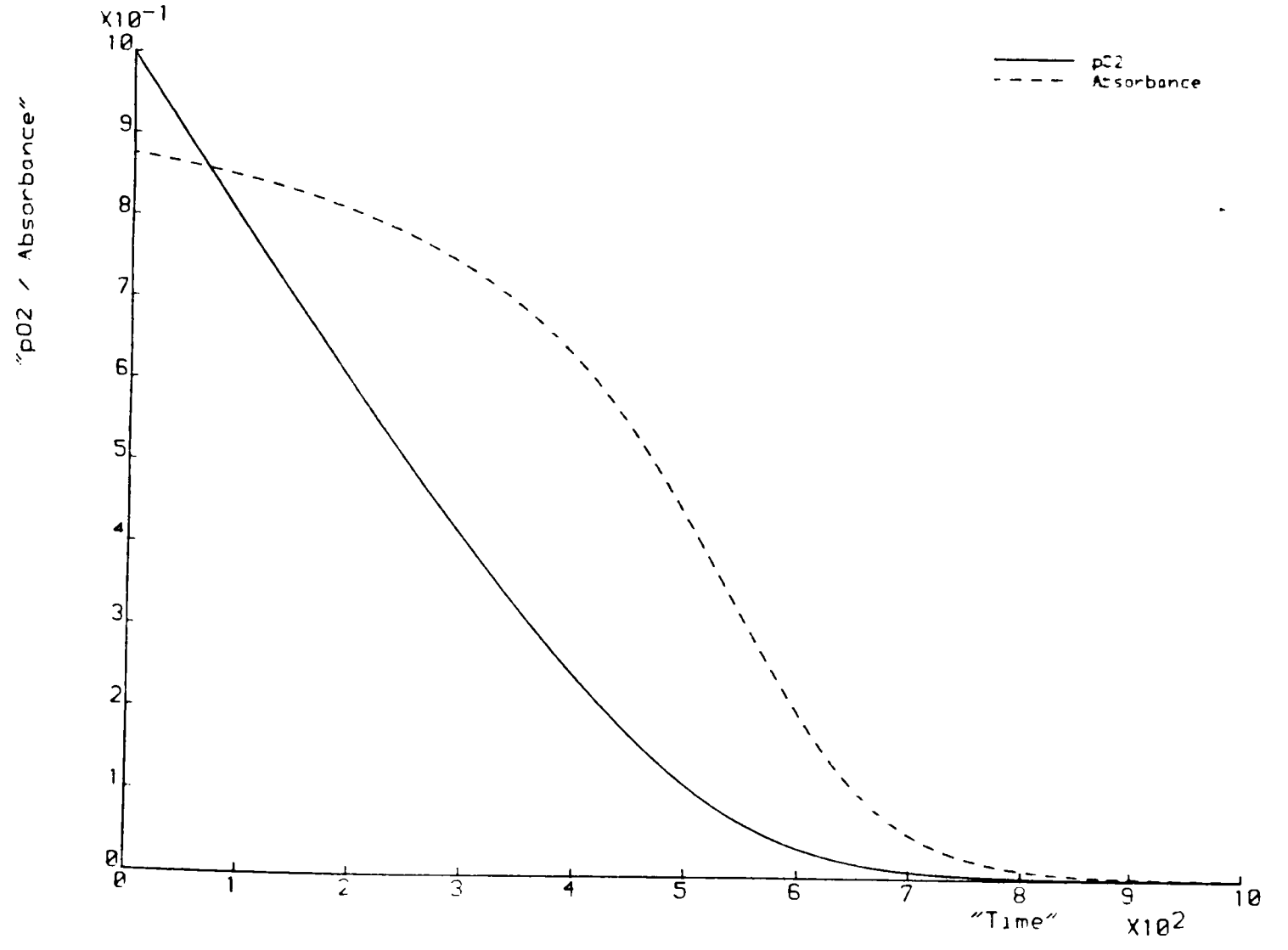

Figure 4.43 Results from mathematical model ($K_m = 10$mmHg).

pO_2 is zero. (This is because the absorbance is proportional to oxygen

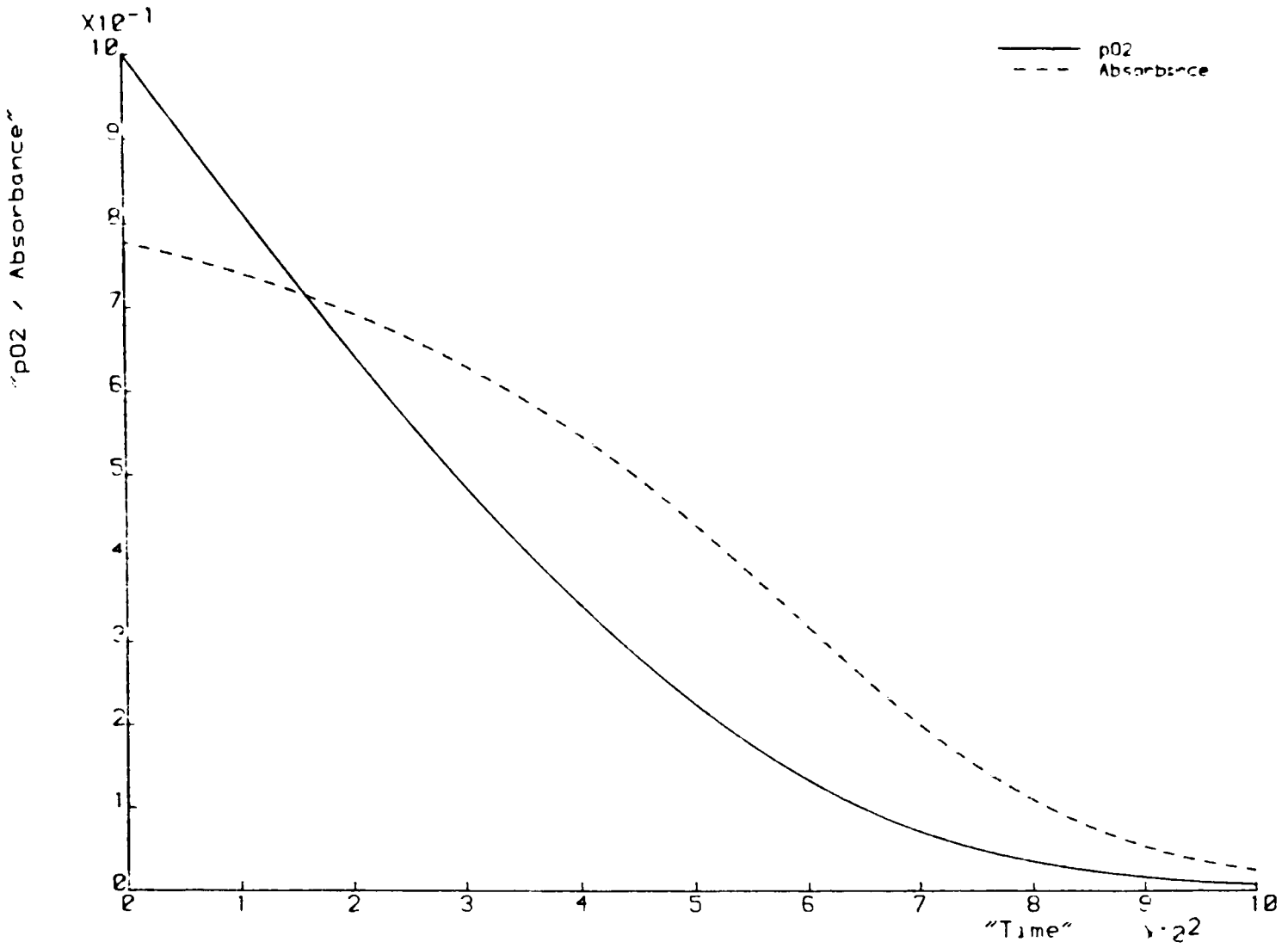

Figure 4.44 Results from mathematical model (K_m = 20mmHg).

consumption, which must be zero if no oxygen is present).

As shown in Figures 4.43 and 4.44 a larger Km produces a more gradual final fall in absorbance but only at the expense of the initial rapid change (and highly non-linear pO_2 traces).

A possible reason for the slower fall observed exprimentally is that under nearly anaerobic conditions the reduction of oxidised cytochrome oxidase occurs at a slower rate (DIXON (1976)). If this is so then at low pO_2s the value of τ in equation 4.13 will increase, and oxidised molecules will remain in this state for longer, so delaying the rapid fall in absorbance.

In conclusion a model to describe the fall in pO_2 and change in absorbance of a closed system in which cytochrome oxidase consumes oxygen has been developed and implemented. A necessity of this was to express the absorbance of a solution of cytochrome oxidase as a function of the other relevant variables. The results obtained are reasonably accurate

and enable the affect of variations in the maximum velocity and Km of the enzyme to be investigated.

However, it should be re-emphasised that as it stands it is a simple model in the way in which it treats both the role and behaviour of cytochrome oxidase in electron transfer, and that no consideration has been made for possible rate limitation effects of changes in the concentration of reduced cytochrome c.

4.11.4 Planned Extension and Use of the Model.

As stated in the Introduction although the production of the above model of a closed system was considered valuable in its own right it was intended to extend said model to allow the initial hypothesis of the averaging of an intensity signal to produce a lower apparent affinity to be investigated.

This could be achieved by allowing for the effect of oxygen diffusing into the cuvette, which means that an additional diffusion term must be added to equatin 4.10, which must then be solved in terms of both cuvette depth and time with the appropriate boundary conditions.

Using such a model it would be possible to find the fall in absorbance at various levels in the cuvette and then average over several levels (see Figure 4.37(ii)). The resultant absorbance trace (ie variation in oxygen consumption) could then be used to estimate what the Km of the cytochrome oxidase would need to be to produce such a trace in a closed system. That is the apparent change in affinity could be estimated.

However, at this stage several problems with this approach were realised. The diffusion of oxygen into the cuvette will itself significantly affect the fall in pO_2 and absorbance traces obtained at each level even before averaging over several levels. Furthermore, this approach uses kinetic results to determine affinity whereas in vivo

simultaneous absorption and oxygen measurements are made for this purpose.

Therefore rather than applying the idea of an integration of optical signals over a relatively large area to explain a change in apparent affinity using results from kinetic studies, this approach was applied to simultaneous measurements which is more applicable to the actual studies in which an apparent change in affinity has been observed.

4.11.5 A Possible Explanation for the Change in Affinity in vivo.

As previously described, the studies which have intimated that the affinity of cytochrome oxidase for oxygen *in vivo* is less than that *in vitro* have involved monitoring simultaneously both the absorbance of the enzyme (as a guide to redox state), an indication of oxygenation by some means (eg microelectrode measurements, fluorescence measurements of pyrenebutyric acid (PBA), or inspired oxygen levels).

In the following the assumption is made that the redox state of cytochrome oxidase is always directly related to pO_2 via equation 4.8. That is, it is the pO_2 alone that determines oxygen consumption and therefore redox state and absorbance. Futhermore it is assumed that the kinetics of the reaction between cytochrome oxidase and oxygen are always the same as *in vitro*.

Consequently if a very small region of tissue is studied then if simultaneous absorbance and pO_2 measurements are made,at the same site for various values of pO_2, and plotted against each other, then the graph produced will be of the *in vivo* reaction kinetics of cytochrome oxidase.

This procedure for determining reaction kinetics is effectively the same as that which is actually used in the studies in Section 4.8. In these the incomplete oxidation of cytochrome oxidase at oxygen tensions significantly greater than zero suggests an apparently lower *in vivo* affinity of cytochrome oxidase. Absorbance versus oxygen content graphs

(which effectively give the kinetics) are also produced which show a corresponding increase in Km.

A potential error in determining reaction kinetics in this manner is simply if the optical and oxygen measurements are made at different sites. For this reason the use of PBA would appear to be the most suitable method of determining pO_2 since both measurements could then be performed using the same optics and therefore on the same region of tissue.

A further assumption is now made that since the Km of cytochrome oxidase is so small than at all pO_2s above some threshold value the enzyme is fully oxidised, whilst below this value it is fully reduced. Hence the absorbance is still solely dependent upon pO_2 but takes one of two values depending upon which side of the threshold level the pO_2 is. This is shown in Figure 4.45.

Using this assumption an explanation for the apparent lowering of affinity can be presented based upon making macroscopic rather then microscopic measurements.

Consider a row of N "cells" whose pO_2s can vary independently and which each contain cytochrome oxidase that behaves as just described, so that each "cell" either has absorbance A, for pO_2s above the threshold level or no absorbance at all. If simultaneous absorbance and oxygen measurements are made on any individual cell, the resultant graph will be of the form shown in Figure 4.45.

If the absorbance of the whole row of cells is measured it would have a value of nA where n is any integer between zero and N, depending upon the individual pO_2 in each cell. Yet, if the pO_2 in all of the cells is the same then the graph produced from absorbance and pO_2 measurements (averaged over all N cells) will again give a graph exhibiting the same kinetics.

However, if the pO_2 is not the same in all cells then the graph

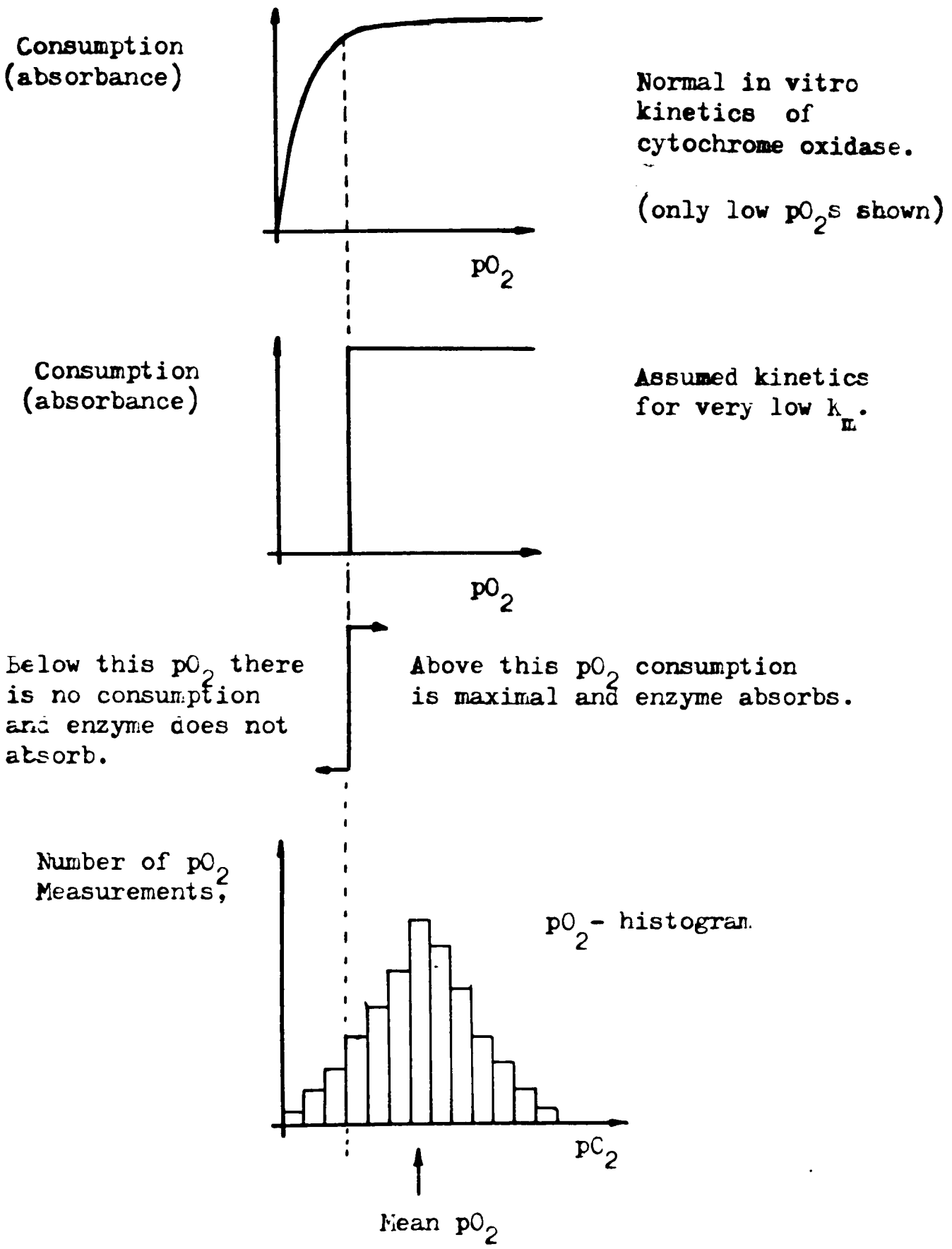

The absorbance is not determined by the mean pO_2 but rather the proportion of readings below/above the threshold pO_2.

Figure 4.45 Diagram of how heterogeneous pO_2 levels in tissue can lead to an apparent change in the affinity of cytochrome oxidase for oxygen. See text for details.

showing the reaction kinetics (and hence Km) produced from the averaged absorbance and pO_2 measurements will be quite different.

Consider the case of a piece of tissue *in vivo* where from measurements using microelectrodes it is known that the pO_2 is not homogeneous, but has a distribution which is generally shown in the form of a pO_2-histogram. Each reading can be assumed to be from a "cell", consequently to obtain the reaction kinetics the mean pO_2 from the histogram must be plotted against the averaged absorbance, which will be proportional to the number of cells with pO_2s above the threshold value. This principle is shown in Figure 4.45.

Clearly at a mean pO_2 just above the threshold value many "cells" will actually have pO_2s below this value and therefore the average absorbance will be considerably less then if all cells had this mean value and were therfore all absorbing.

Therefore although the cytochrome oxidase in each individual cell behaves in exactly the same way as it would *in vitro*, *in vivo* where there is this heterogeneous distribution of pO_2s it appears that this is not so. At a pO_2 where all of the enzyme should be oxidised it is actually partially reduced, which could be interpreted as a lowering of affinity of the enzyme for oxygen. Hence at a microscopic level the enzyme has *in vitro* behaviour whereas at the macroscopic level *in vivo* there is an apparent lowering of affinity.

This effect is solely due to the heterogeneous distribution of pO_2s found *in vivo*, and that a wide range of actual pO_2s will be found either side of the mean value.

From this argument it can be seen how the shape of the pO_2-histogram may be an important parameter in determining the apparent affinity of cytochrome oxidase for oxygen. This may help to explain why SICK (1982) observed apparently different affinities in turtle and rat brains, since the nature of the pO_2-histograms obtained for the two species were

markedly different.

The potential influence of the pO_2-histogram is also one of the reasons why the effect of anaesthetics during studies in which the redox state of cytochrome oxidase is monitored may be significant (see Section 4.9).

This model of why on a macroscopic scale the affinity of cytochrome oxidase appears reduced *in vivo* is in keeping with previous suggestions that this effect is due to diffusion limitation or locally anoxic areas of tissue (BALABAN (1981), EPSTEIN (1982), BASHFORD (1982)).

Similar views on how microcirculatory heterogeneity, may cause cytochrome oxidase to possess an apparently lower affinity *in vivo*, although actually still behaving in an *in vitro* manner, is shared by other workers (HONIG (1981)).

4.12 Summary and Future Work.

In summary, in order to investigate the feasibility of non-invasively monitoring the redox state of cytochrome oxidase in the human brain it was felt that there were two possible, and complimentary courses of action. One involved the construction and use of an instrument that could be used in a clinical enviroment, whilst the other approach would follow a gradual path of studying the use of optical methods for monitoring redox state, beginning with simple systems.

It is the second approach which has been described within this chapter with results presented that were obtained from solutions containing purified cytochrome oxidase and yeast cell suspensions. These experiments provided valuable insight into the behaviour of cytochrome oxidase and the problems involved with monitoring small changes in absorbance against a large background attenuation of light.

The results of these experiments were also modelled mathematically and provided the basis of a physical explanation of why the affinity of cytochrome oxidase for oxygen is decreased *in vivo* compared to *in vitro*. This anomaly is one of the problems considered concerning the clinical application of a Niroscope, another being the adequacy of the signal processing for the removal of artefacts due to non-specific monitoring.

Because of the apparent decrease in the enzyme's affinity it is also possible that monitoring the redox state of cytochrome oxidase would yield little, if any, additional information useful in a clinical enviroment, than an whole organ oximeter. (Such an instrument has essentially the same requirements as a Niroscope).

Considering future work the aim should still be, as stated in the Introduction, to investigate fully the use of optical methods for

monitoring the redox state of cytochrome oxidase (and oxygen saturation and changes in blood volume) in increasingly complex and technically demanding systems.

For each successive system an instrument should be produced which is capable of performing artefact free monitoring of all of the three variables (where relevant), which would involve a thorough study of the signal processing requirements.

To achieve this it is considered that scanning optical measurements would initially be more appropriate than several discrete wavelength measurements, since the greater amount of information would enable more precise analysis of data (eg changes in spectral shape could be observed). In addition such measurements would allow the most suitable discrete wavelengths for monitoring to be selected.

The use of blood substitutes would also prove advantageous in simplifying <u>in vivo</u> measurements of cytochrome oxidase by removing any spectral interference from haemoglobin.

The theory proposed concerning the apparent change in affinity could possibly be tested using PBA so that both cytochrome oxidase redox state and pO_2 measurements would be made on the same area of tissue. If the model is correct then the Km (derived from the two measurements) should appear to approach the lower values found <u>in vitro</u> upon monitoring smaller areas of tissue.

Finally. the use of near-IR measurements to monitor tissue oxygen saturation and changes in blood volume would appear to be a worthwile achievement in itself. Therefore the development of such a clinical instrument prior to the production of a fully operational Niroscope. is

considered of practical significance.

Chapter 5: Oxidative Damage and its Possible Involvement in Disease States in Paediatrics.

5.1 Introduction.

In the preceding chapter the possibilities of monitoring cerebral metabolism and/or haemodynamics *in vivo* were considered in some detail. As outlined in the introduction one reason for the interest in this technique in particular was due to its potential application in paediatrics where it could be used to firstly gain a fuller understanding of the aetiology of cerebral hypoxia and intraventricular haemorrhage (IVH) in preterm infants, and secondly perhaps serve as a monitor to prevent such events.

It was this aim of the prevention of IVH, the pathology of which has been linked to many factors, that led to an interest in suggestions (CHISWICK (1983)) that the underlying cause may be the result of oxidative damage to capillary endothelial membranes of the subepyndymal layer. The collation of results presented here, and taken from the biochemical, and clinical and research paediatric literature appear to produce preliminary evidence to support and strengthen Chiswick's hypothesis. Furthermore, there emerges a strong case for believing that retinopathy of prematurity (ROP) also occurs as a result of damage due to oxygen derived free radicals (KRETZER (1984), HITTNER (1984)).

The intention of this chapter is to show that many disease states in paediatrics, including those which niroscopy may help diagnose and monitor, could have a common underlying cause (ie oxidative damage) (CROWE (1986)). A fuller understanding and appreciation of this cause in itself may lead to a healthier outcome for a significant number of preterm infants.

A further even more direct link between oxidative damage and the preceding chapter is that in tetravalently reducing oxygen to form water, cytochrome oxidase not only donates four reducing equivalents to oxygen, which is a vital step in oxidative metabolism, but also rids the body of wnat is the precursor for extremely toxic substances which are largely responsible for oxidative damage.

This dual requirement of low oxygen tensions to reduce the rate of oxidative damage, and a fully functioning respiratory chain is made possible by the high affinity of cytochrome oxidase for oxygen.

5.2 Free Radicals.

Comprehensive definitions of free radicals can be found elsewhere (FRIDOVITCH (1978), DEL MAESTRO (1980)), suffice to say that a free radical is any atom or molecule with an unpaired electron in its outer orbital. The significance of free radicals is that because of this lone electron's tendency to interact with other electrons to form an electron pair (and so a chemical bond) they are usually highly reactive.

5.3 Molecular Oxygen and Free Radicals.

The complete reduction of molecular oxygen (O_2) to form water involves the addition of four electrons to each O_2 molecule. This is most likely to occur as four sequential one electron reductions (ie along the univalent pathway) which leads to the production of the intermediates: superoxide (O_2^-), hydrogen peroxide (H_2O_2) and hydroxyl radical (OH·) as shown in Figure 5.1.

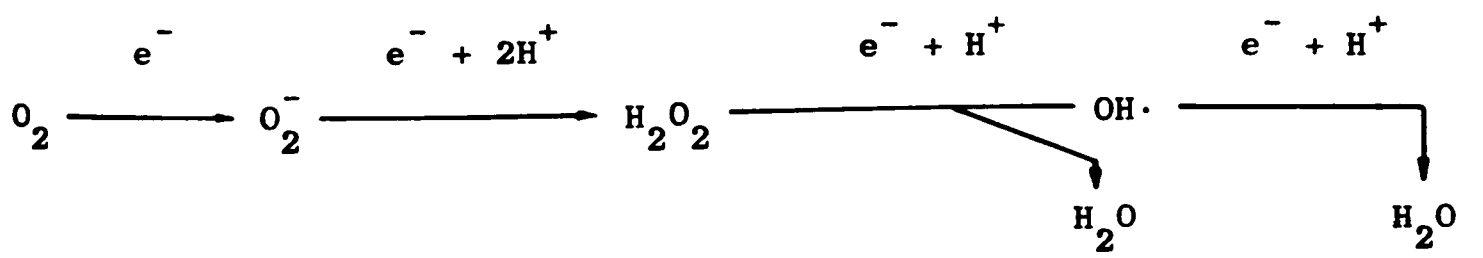

Figure 5.1 The univalent pathway for the reduction of molecular oxygen (from BULKLEY (1983)).

These species are all too highly reactive to be accomodated by living tissue. a problem overcome by enzymatic mechanisms capable of reducing O_2 divalently and tetravalently which considerably restricts its toxicity. It has been suggested (FRIDOVITCH (1978)) that such enzymes were originally evolved for protection against O_2 released during photosynthesis by the first blue-green algae to appear. However, the enzyme now responsible for tetravalently reducing about 98% of the total O_2 reduced in man (McCORD (1982)), and which therefore virtually eliminates the univalent pathway, is cytochrome oxidase which is also intrinsically linked with oxidative metabolism and hence the survival of the typical mammalian cell.

5.4 Protective Mechanisms.

Even though cytochrome oxidase serves to keep intracellular pO_2 very low, free radicals are formed in living cells during oxidative metabolism, with a significant contribution produced by the univalent pathway. The primary defence mechanism against oxidative damage is provided by enzymes that catalytically scavenge the intermediates of univalent oxygen reduction.

Superoxide dismutases (SOD) catalyse the divalent reduction of O_2^- to H_2O_2 whilst peroxidases and catalases divalently reduce H_2O_2 to H_2O as illustrate in Figure 5.2. The removal of superoxide and hydrogen peroxide means that the formation of the highly reactive hydroxyl radical is prohibited. Further protection is afforded by a variety of other substances including: α-tocopherol (Vitamin E), β-carotene, glutathione peroxidase and ascorbic acid (DEL MAESTRO (1980)).

Another important factor in resisting damage is structural integrity (DORMANDY (1983)). For example, disruption of structure in

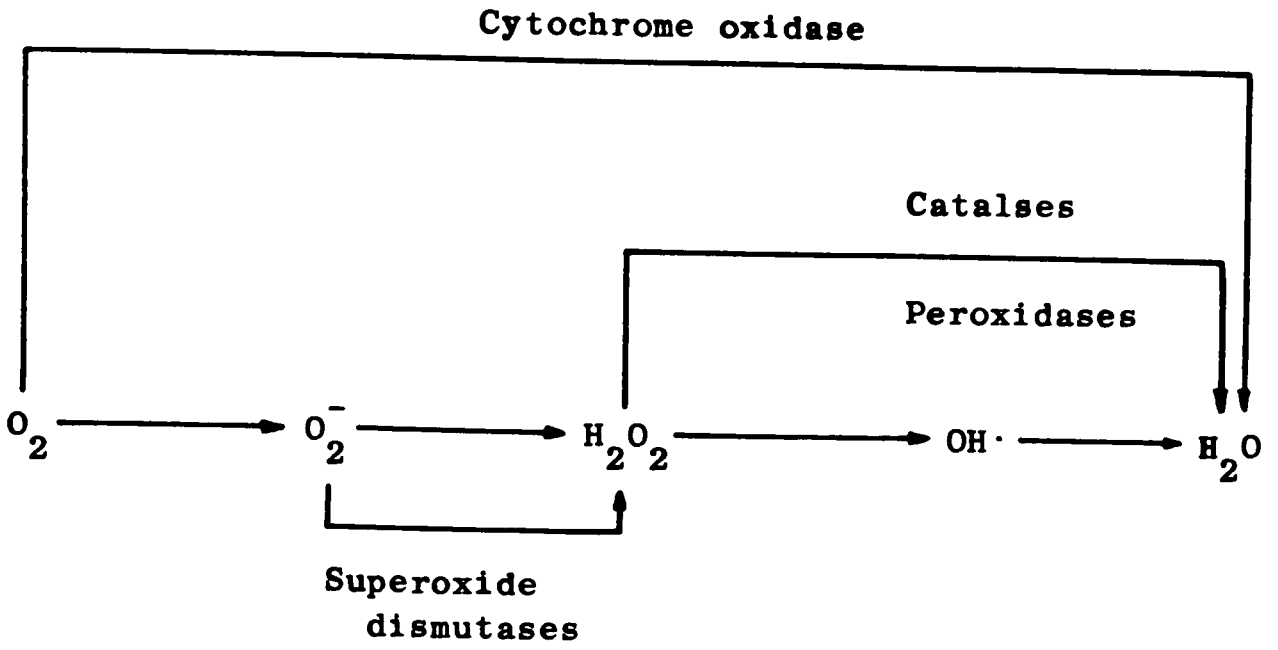

Figure 5.2 Endogenous enzymatic mechanisms for the detoxification of oxygen free radicals generated by the univalent reduction of molecular oxygen (see Figure 5.1) (from BULKLEY (1983)).

polyunsaturated lipids quickly leads to free radical damage (ie rancidification). The antioxidant mechanisms for protecting against this damage are described by BURTON (1984).

A cautious note on the action of free radical scavengers must be added (DORMANDY (1983)). After scavenging the unpaired electron from a free radical, rather than scavenging another electron to produce a pair, the scavenger (with its lone electron) may actually behave as a free radical itself, perhaps being even more reactive than the one originally scavenged. Hence, in a particular organ under specific conditions a substance may act as a free radical scavenger, wheras in a different organ with different conditions, the same substance may actually initiate free radical activity more damaging than that which it was intended to supress.

5.5 Generation of free radicals.

There are many potential means of O_2 free radical generation (DEL MAESTRO (1980), TAYLOR (1982)), and as with the whole field of free radicals this is at present an active area of research. The following methods of generation are generally accepted to be valid and are particularly pertinent in relating oxidative damage to disease states in paediatrics.

Despite the enzymatic divalent and tetravalent reduction of O_2 the univalent pathway still produces a steady flux of free radicals. Hyperoxia. which is known to raise O_2^- production (TAYLOR (1982)), may do so by increasing this leak.

In view of the above it may be expected that low pO_2 levels would reduce oxidative damage. In fact during anoxia this appears to be the case simply due to the complete lack of O_2 (DEL MAESTRO (1980)). However at least two models can explain how hypoxia (which may be caused by ischaemia) can result in an increased free radical load.

Firstly. during hypoxia the scavenging mechanisms may be decreased and mitochondrial function impaired. If so then reperfusion by O_2 will be accompanied by a burst of free radical generation due to the cell's hypoxia- induced inability to cope with the rapid rise in pO_2.

Secondly tissue hypoxia results in the conversion of xanthine dehydrogenase to xanthine oxidase. and the formation of hypoxanthine due to adenosine triphosphate (ATP) catabolism. The addition of O_2 then results in its reaction with hypoxanthine and xanthine oxidase to produce O_2^-. Indeed it has been shown that hypoxanthine and O_2 are more harmful to the neonatal lung than hyperoxia alone (SAUGSTAD (1984)).

Another major source of free radicals is oxidative detoxification, and it is possible that oxidative damage is actually more likely as a result of detoxification than aerobic metabolism (DORMANDY (1983)). However, not all free radicals are unwanted, since they are generated and used by the body's defence system to kill bacteria (BABIOR (1978)).

5.6 Oxidative Damage.

The mechanisms and extent of oxidative damage are still under investigation (eg DEMOPOULOS (1980), McCORD (1982)), but it is clear that lipid peroxidation is a major consequence of free radical action, including damage to the capillary endothelium (GRANGER (1982)), DEMOPOULOS (1980)). It is also likely that free radicals are able to elicit specific responses in the microcirculation (KONTOS (1982)).

5.7 Development Profiles of Antioxidant Enzymes.

If free radicals are formed but not effectively scavenged then oxidative damage will ensue. Such damage could be expected if either more free radicals are generated than the body's defence mechanisms can cope with or if these mechanisms are somehow impaired.

A major influence in the occurence of oxidative damage in preterm infants may be that their antioxidant enzyme systems are not fully developed. This has been shown to be true in both rabbit (FRANK (1984)) and rat (TANSWELL (1984)) lungs with enzyme levels gradually increasing before term. Indeed, this has been suggested as a contributory factor in both bronchopulmonary dysplasia (BPD) and respiratory distress syndrome (RDS) (TANSWELL (1984)).

The incomplete development of these defence systems in the premature infant is in contrast to the neonate's usually increased tolerance to a

hyperoxic enviroment compared to the adult of the same species (KIMURA (1983), TANSWELL (1984)). If these enzymes are not fully developed in the lung then this may be the case in the brain also, although extrapolating data from one organ to another is obviously not entirely valid. Data on antioxidant enzyme levels in the prenatal brain were not found in the literature although increases in levels have been recorded in the postnatal rat brain (MAVELLI (1982)).

In summary, there is no known evidence that the brains of premature infants are lacking in antioxidant enzymes, but research has indicated that this may indeed be the case. If so then the premature infants protection against oxidative damage will be insufficient, and increasingly so with decreasing gestational age.

5.8 Intraventricular Haemorrhage.

IVH is one of the main causes of death and disability in premature infants (PAPE (1979)). Bleeding usually begins in the thin walled capillaries in the highly vascular germinal matrix of the subepyndymal layer of the brain giving a subepyndymal haemmorhage, or if extensive may rupture into the ventricles to give an IVH. Haemorrhage occurs in about 40-50% of premature infants with a birthweight of less than 1500g, and usually within 72 hours of birth (CHISWICK (1983)). The factors normally associated with haemorrhage (eg hypoxaemia. hypercapnoea, mechanical ventilation, pneumothorax (PAPE (1979))) appear to be linked with an inability of the circulatory and/or the respiratory system to cope with a premature transfer from an intra-uterine to an extra-uterine existence.

The protective effects of the antioxidant Vit E against haemorrhage has been reported by CHISWICK (1983) and SPEER (1984), although PHELPS

(1984) found no such evidence. Premature infants have low plasma Vit E levels and Chiswick's study was intended to determine the appropriate dosage of Vit E required to raise the levels to adult values, thus reducing the susceptibility of the red blood cells to haemolysis by H_2O_2. The associated decrease in IVH as Vit E levels were supplemented was found by chance. However. in view of the processes of oxidative damage and the defence mechanisms in premature infants described above these results are perhaps not so surprising.

As a result of his findings that Vit E reduced the incidence of IVH CHISWICK (1983) proposed that oxidative damage to capillary endothelial membranes of the subependymal layer contributes to the pathogenesis of haemorrhage, and that Vit E gives protection. limiting the magnitude of subepyndymal haemorrhage and reducing the risk of IVH. Similarly. SPEER (1984) concluded that Vit E may play an important role in protection against free radical action.

If oxidative damage is responsible for the initial damage to the endothelial cells then the haemorrhage may then be extended by the currently accepted explanations of the cause of IVH. (related to changes in cerebral blood flow and blood gas levels (PAPE (1979)).

In addition to the links between IVH and inadequate antioxidant protection from Vit E, and possibly the antioxidant enzymes, other observations also indicate that IVH may occur as a result of oxidative damage. CHISWICK (1983) noted that IVH is relatively uncommon in stillborn babies, which could be related to the low fetal arterial pO_2 of only about 25mmHg (3.3kPA), and that while acute hypoxia encourages bleeding, chronic hypoxia does not (which can be linked to the amount of free radicals generated). The contribution of hypoxic/ischaemic injury to IVH is also suggested by SPEER (1984), as is the close correlation

with birthweight (and hence prematurity).

SAUGSTAD (1984) speculate that the formation of free radicals from hypoxanthine may be a significant factor in IVH. ROP and necrotising enterocolitis (NEC) in the premature infant, and that this may be related to the large amounts of hypoxanthine present in transfused blood. The possible importance of this source of free radicals in paediatrics is illustrated by the proposed use of hypoxanthine as an indicator of fetal hypoxia.

Protection against oxidative damage in infants weighing less than 1500g is recommended by administering an intramuscular injection of Vit E as soon as possible after birth. with continuing supplementation on the second and fourth days after birth (SPEER (1984)). However. correspondence concerning the use of Vit E for this purpose, has largely centred on its potentially harmful side effects rather than its apparent success in decreasing IVH and the role of antioxidants in general (CROWE (1986)).

5.9 Retinopathy of Prematurity.

Retinopathy of prematurity (ROP) or retrolental fibroplasia (RLF) (the difference between these two terms is not significant in the context of this work), is a blinding disease which inflicts premature infants (SILVERMAN (1980)). In the mid-1950's it was generally accepted that excessive O_2 was the major factor in its occurrence (LUCEY (1984)). This led to the more careful administration of O_2 in neonatal care units which in turn caused an increase in the incidence of brain damage due to lack of O_2. Neonatal care techniques were therefore evolved to provide adequate amounts of O_2 to ensure survival whilst minimising the risks of RLF. LUCEY (1984) states that a growing number of observations indicate

that RLF is a disease of multifactorial origin. However. perhaps the underlying cause is free radical action with all the known and suspected precursors of RLF linked by their ability to promote oxidative damage.

Retinal development consists (KRETZER (1984)) of the migration, canalization and endothelial differentiation of spindle cells (the mesenchymal precursors of the inner retinal capillaries) (KRETZER (1984)). This process normally occurs in utero with its (relatively) low arterial pO_2s. However. relative hyperoxia. which could simply be produced by premature delivery, induces the formation of gap junctions between adjacent spindle cells. These gap junctions change the spindle cells from potential endothelial cells to sites of synthesis and release of angiogenic factors which immediately stops the normal formative process and triggers neovascularisation from existing vessels over the following 8-12 weeks. Thus RLF is not a disease of completed vascularisation as occurs in diabetes mellitus, but rather a pathology of retinal vascular development.

KRETZER (1984) claims the gap junctions are morphologic evidence of O_2 toxicity and that Vit E supplementation to adult physiological levels gives protection to the spindle cells thus supressing gap junction formation and reducing the severity of ROP (KRETZER (1984), HITTNER (1984)). If Kretzer's hypothesis is correct then any increase in free radical generation, lack of antioxidant defence or incomplete retinal development could lead to to ROP. That it is the activated spindle cells which lead to ROP is further shown by the fact that cryoretinopoxy of these cells results in retinal quiescence.

HITTNER (1984) suggest that spindle cells can be activated as a consequence of any factor (eg patent ductus arteriosus, BPD, hyaline membrane disease and apnoea) associated with therapeutic use of O_2, the

amount of O_2 carried in the blood, or factors related to difficult stabilisation of high risk infants.

Further evidence that ROP is caused by oxidative damage to spindle cells is given by considering the conditions known to lead to ROP (LUCEY (1984)): Hypoxia. exchange and replacement transfusions, complications of pregnancy. and sepsis may all lead to increased free radical generation. Prematurity and low levels of Vit E and SOD will reduce the infants antioxidant defence mechanism.

In addition, concerning fullterm infants who contract ROP it has been suggested that their retinal development lags behind that of other organs, whilst infants who are subjected to hyperoxia but do not contract ROP may have complete retinal development and adequate antioxidant protection. The other conditions discussed include several which are concerned with abnormal blood gas levels and circulatory physiology.

In conclusion, since many factors can lead to an increase in the extent of free radical action it appears that ROP is a disease of multifactorial origin, whereas the underlying cause may be due to oxidative damage to the spindle cells. Recommended treatment of premature infants in order to protect against ROP is to raise plasma levels of Vit E to physiological levels (not pharmacological levels which may affect enzymatic processes) (HITTNER (1984)).

5.10 Discussion.

A cautious reaction to the above may be that free radicals appear to be all things to all men, a sentiment echoed by at least one worker in the field (DORMANDY (1983), and illustrated by the list of diseases in which oxidative damage has been implicated (BULKLEY (1983)). Yet what may seem to be anomalous claims that both hypoxia and hyperoxia can

promote free radical formation, and that certain scavengers can have either benificial or deleterious effects can be supported by experiment.

Therefore it is felt that there is enough evidence to provide a strong case for suspecting that oxidative damage may indeed be the root cause of both IVH and ROP (and perhaps other disease states in paediatrics). The clinical conditions known to influence the occurrence of these diseases probably do so by increasing the possibilty of free radical action, and in the case of IVH changes in cerebral blood flow, blood pressure and blood gas levels are likely to lead to extension of haemorrhage beyond the initial oxidative damage. Further work is required to strengthen this case which could include the following. (It is appreciated that considerable planning and co-ordination would be required, as would ethical approval, to perform these studies.)

1) Assay abortion and post-mortem material for the antioxidant enzymes to ascertain their developmental profiles in humans. Studies similar to those of FRANK (1984) may also be performed in brain rather than lung.

2) Attempt to monitor the products of lipid peroxidation such as pentane and ethane (DILLARD (1977)) and malondialdehyde (JOHNSON (1984)) in premature infants and then correlate this with incidence of IVH.

3) Continue studies on the effect of Vit E, and perhaps other protective mechanisms, upon occurence of IVH.

Concerning possible protection against oxidative damage the options are to use antioxidants (DORMANDY (1983), BURTON (1984)), or reduce the concentration of inspired oxygen. The latter approach carries the associated risk of the patient incurring possibly permanent cerebral injury, as has unfortunately happened when attempting to prevent ROP.

Perhaps the ultimate, and most radical solution, would be to replace the premature infant into an enviroment in which it is best adapted to cope. That is some type of artificial womb where blood gas levels can be maintained close to those in utero until organ development has reached term and is ready to cope with breathing relatively high inspired O_2 levels.

Chapter 6: In Vivo Transmission and Reflection Measurements.

6.1 Introduction.

The first type of *in vivo* experiments performed involved monitoring the changes in transmitted light level through fingers and the wrist as venous and arterial occlusions were applied. These were made using both a tungsten halogen lamp and a PMT, with wavelength selection by interference filter, and the laser diode based instrument. Fibre bundles were used to "pipe" light to and from the tissue.

Examples of the results obtained using the laser diode instrument can be found in Appendix A. Similar results were generally found using the broad band based apparatus.

The two most likely explanations for changes in the intensity of transmitted light which are discussed in such studies are alterations in either the amount of blood in the tissue or of the oxygen saturation. It was felt that a means of distinguishing between these two (and other effects such as a dependence of the change in transmitted light levels upon fibre bundle application pressure) was to perform multi-spectral rather than single wavelength studies, ideally monitoring a complete spectrum over a substantial wavelength range, and then observing changes in the spectrum's shape.

In addition, an instrument capable of such measurements, could also be used to measure the basic reflectance and transmission properties of tissue. The requirement for such an instrument was the primary reason for the construction of the scanning spectrophotometer described in Section 3.5.

The results described here were all made with this instrument, and

include both reflectance and transmission spectra obtained from various sites and subjects. Such data is of fundamental interest to *in vivo* optical methods since the overall reflectance and transmission levels indicate in which regions of the spectrum it is feasible to perform measurements, whilst the presence of absorbance bands indicates that the concentrations of the substances responsible for them may perhaps be monitored *in vivo* by a non-invasive optical method.

Kinetic studies of the type performed in the single wavelength studies were also made although only sucessfully in reflectance mode in the visible part of the spectrum, since the machine was not sufficiently sensitive for such studies in the near-IR or in transmission mode.

Although the instrument was not capable of performing all of the intended type of kinetic study, the experience gained from making the measurements described here of the overall reflection and transmission properties at different sites, and the effect of variations in fibre bundle geometry was considered valuable for application to the future design and use of such an instrument.

As the results below demonstrate such non-invasive optical measurements may not only be valuable for monitoring oxygen saturation and the redox state of the cytochromes, which has been the main interest in this thesis, but also for monitoring the water and fat content of tissue (CONWAY (1984)) whilst even the measurement of pH and other physiological variables by the same means has recently been suggested (MDW (1986)).

The results presented below were either performed in reflection or transmission mode and on various sites of the body, with subjects with different skin colouration. By performing all studies with both the PMT

and photodiode, a wavelength range from about 400-1100nm could be investigated. Variations in geometry between source and detector fibre bundles and the skin could also be made. The ability to record spectra and then recall them for subsequent processing enabled sample and reference spectra from either different subjects or different sites to be used so that the difference between them could be directly observed.

6.2 Reflectance Studies.

The following results were all obtained using the large bifurcated fibre bundle, this means there were essentially a great number of minute "sources" and "detectors" in extremely close proximity. Use of this bundle is referred to here as reflectance mode.

Such reflectance spectra were obtained using both the Spectralyser's own photodiode and the PMT. For these studies the non-bifurcated end of the fibre bundle was held in the centre of a holder approximately 25mm in diameter which itself was held on the skin surface by a double sided adhesive disc (as used with transcutaneous oxygen electrodes). This is shown in Figure 6.1(i).

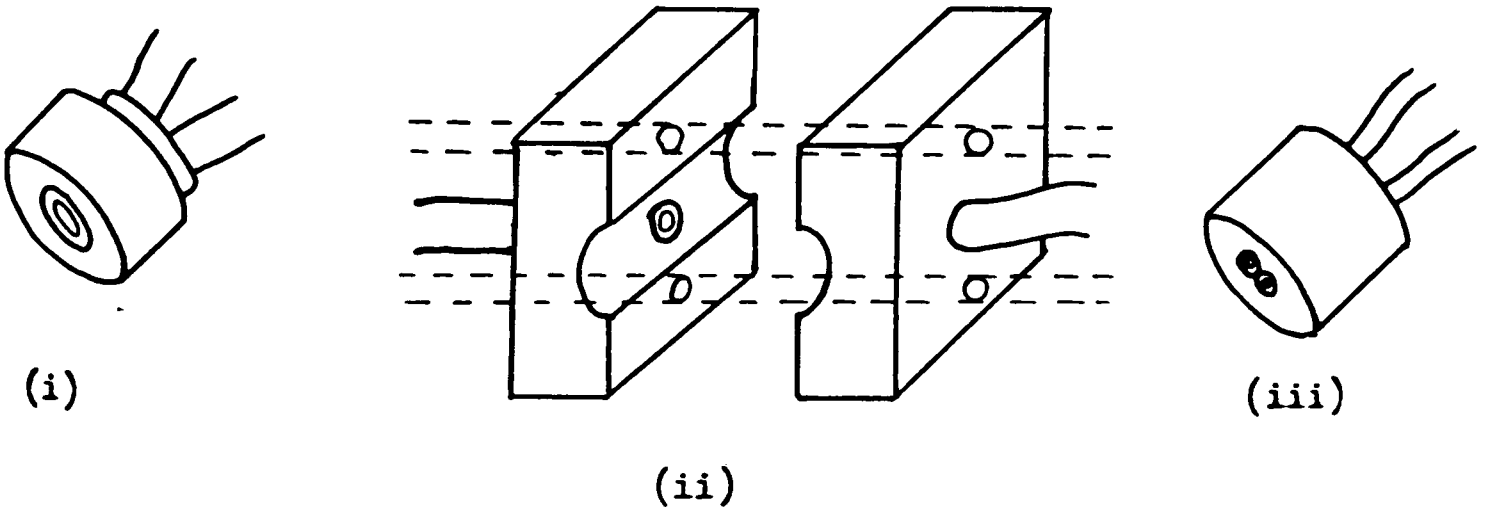

Figure 6.1 Methods of securing fibre bundles to the skin surface for performing: i) reflectance measurements with the large bifurcated fibre, ii) transmission studies and iii) measurements with two small fibres in close proximity.

Light from the broad band source was focussed (see Figure 3.2) onto one of the non-bifurcated ends, whilst the other "piped" light to the Spectralyser. (Optical fibre bundles were used for these purposes in all

of the studies described in this chapter).

For the photodiode measurements two runs were taken, using the two blocking filters (Section 3.5.8) to prevent artefacts from second order spectra.

6.2.1 Results Using the Photodiode.

Figure 6.2 shows the reflectance spectra obtained from the palm of the hand of a caucasian and dark skinned subject over the approximate spectral range of 450-1100nm. A slit width of 5nm was used and the results are from 200 averaged spectral scans. (This figure, as with all traces below has been copied from the original spectra obtained).

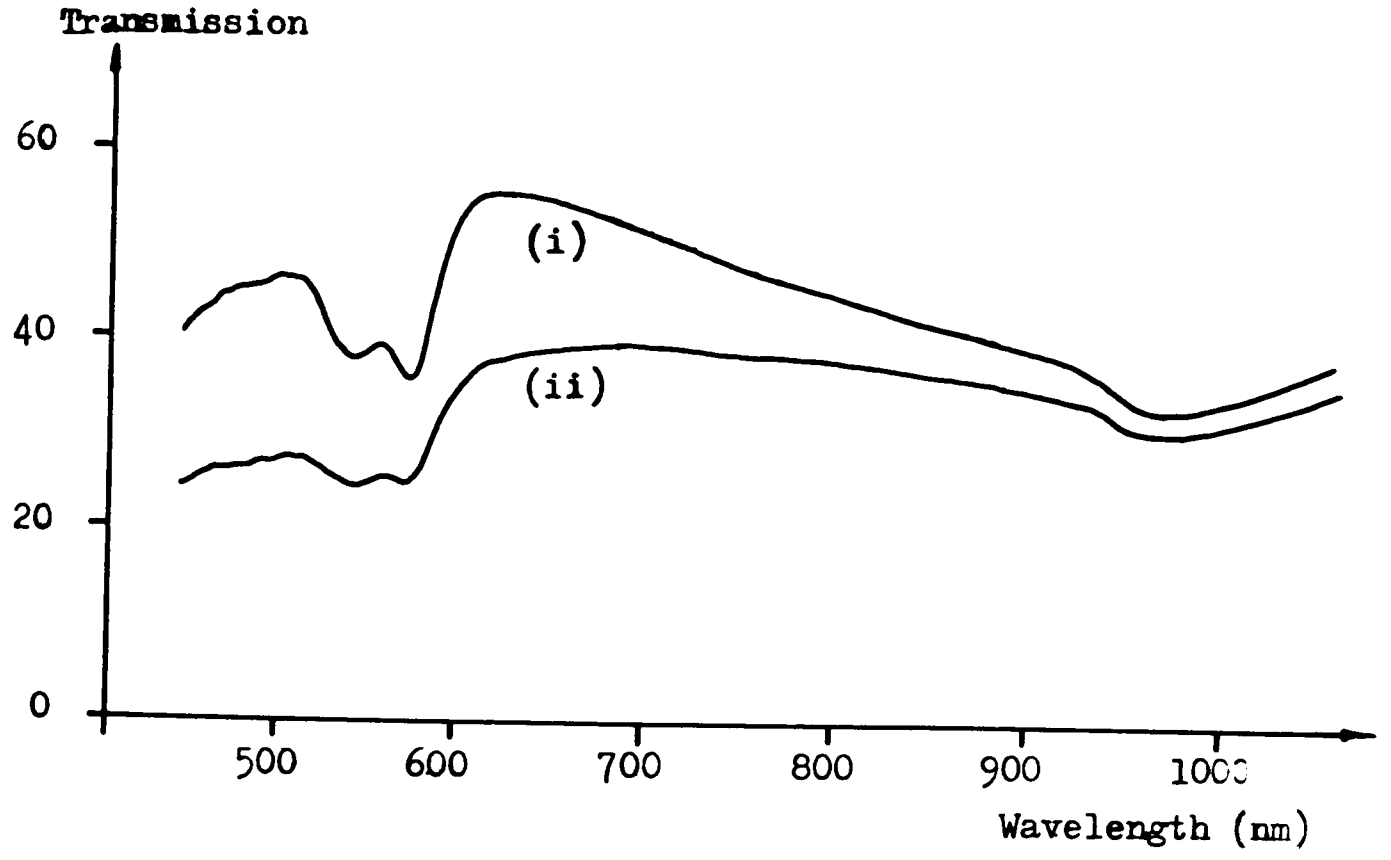

Figure 6.2 Reflectance spectra, as a transmission value (ie a percentage), from the palm of a: i) caucasian and ii) dark skinned subject.

The actual positioning of the fibre is shown in Figure 6.3. The traces are plotted as "transmittance" graphs (see Section 3.5.6), and so represent the percentage of reflected light with respect to a reference. which was the spectrum obtained by placing the fibre bundle on a pile of white Kleenex tissues. This method of obtaining a reference was also used in the reflectance studies described below.

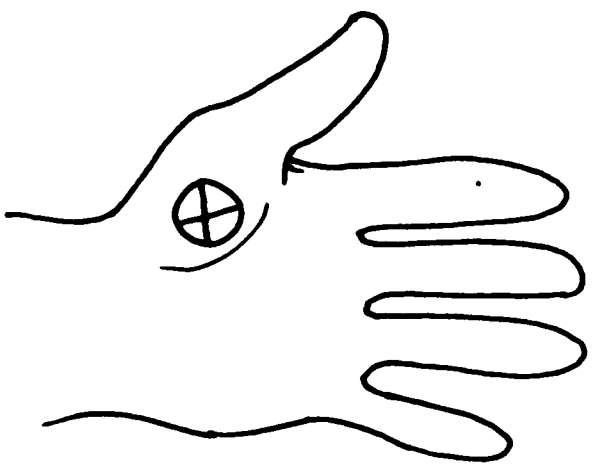

Figure 6.3 Position of the fibre bundle during measurements on the palm.

Although not a perfectly reproducible method of obtaining a reference spectrum (as its amplitude was somewhat dependent upon the precise way in which the bundle was held against the tissues) this procedure was adequate. This was particularly so as the variations in reflectance at different wavelengths or between different specimens were of interest rather than the absolute reflectance values (which in any case will also be partly dependent upon bundle-sample positioning). Use of the tissues to provide a reference assumes they possess no significant spectral characteristics over the range 400-1100nm.

From both spectra in Figure 6.2 the effect of the characteristic absorption by (oxy)haemoglobin can be seen at the lower wavelengths, whilst at approximately 960nm the absorption due to water is evident. There is also a suggestion of absorbance due to carotene.

As expected the spectrum from the dark skinned subject exhibits less reflectance in the visible region although it can be seen that the difference between the two becomes substantially less into the near-IR. These spectra can be compared to those figures in Section 1.4.2.1.

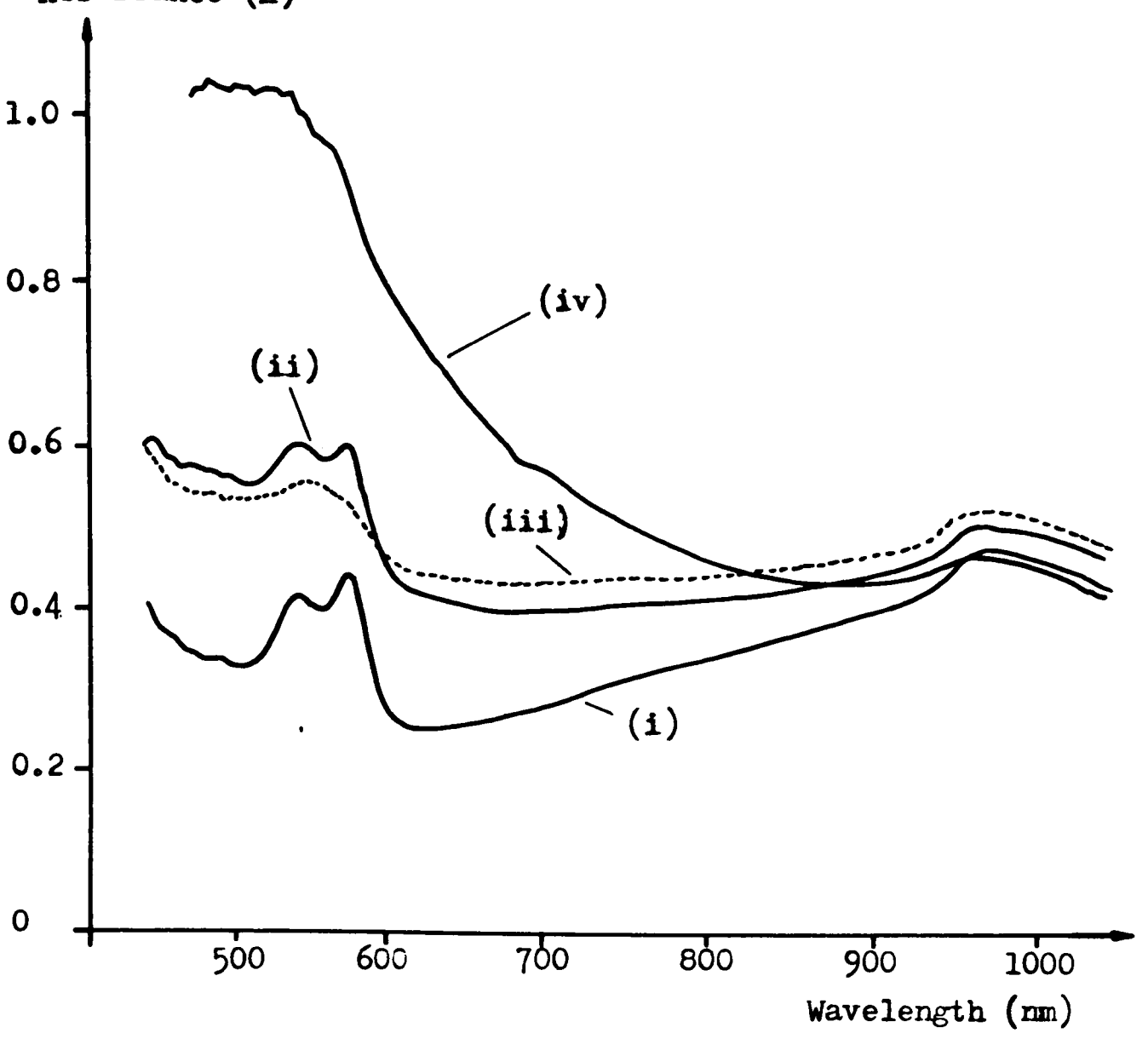

Figure 6.4 Reflectance spectra (as absorbance values) from: the palm of i) a caucasian and ii) a dark skinned subject, iii) as for ii) only with pressure applied, and iv) the back of the back of the dark skinned subject's hand.

In Figures 6.4(i) and 6.4(ii) the "absorbance" traces (see Section 3.5.6) are shown produced using the same data as used in Figure 6.2. The same characteristics can be seen with the caucasian subject absorbing less light in the visible.

In Figure 6.4(iii) the spectra of the palm of the hand of the dark skinned subject is shown with pressure applied to the fibre bundle. The haemoglobin bands have disappeared due to the expulsion of blood and possibly also its deoxygenation which is suggested by the remaining smaller absorbance.

In Figure 6.4(iv) the spectrum obtained from the back of the dark

skinned subject's hand is shown. It can be seen that the back of the hand is much darker than the palm. which is an observation readily made by eye.

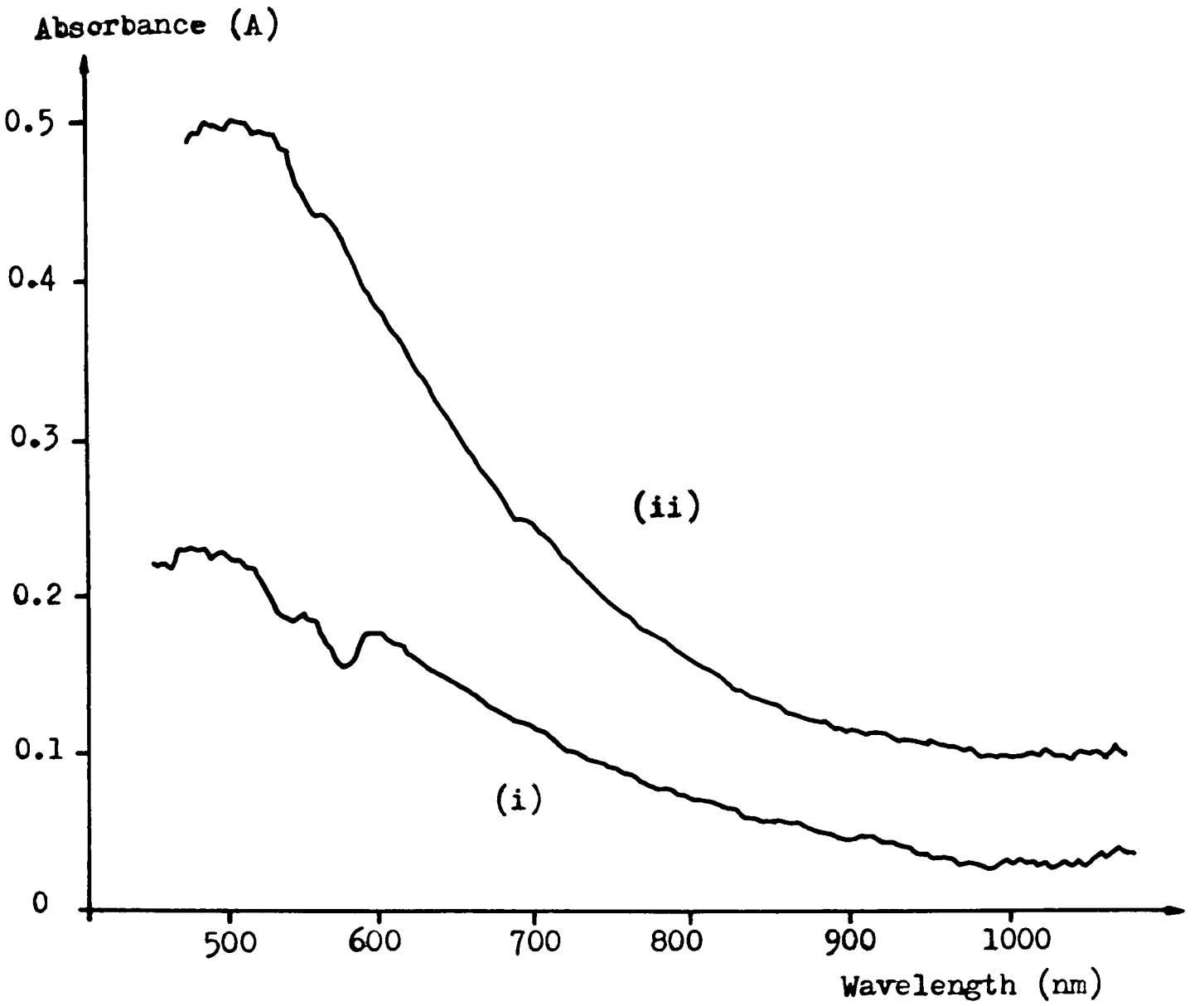

Figure 6.5 Difference in reflectance (as an absorbance) between the reflectance from i) the dark skinned and caucasian subject, and ii) the rear and palm of the dark skinned subject's hand

The difference in the absorbance between the dark skinned and caucasian subject and back and front of the former's hand are shown in Figure 6.5. These traces could be obtained since the scanning spectrophotometer can use any of its stored spectra as either the reference or sample spectra when producing a trace. Consequently these graphs were produced by simply using the sample spectra obtained from the

relevant sites.

The shape of the traces shows the absorption spectra of melanin, which is chiefly resonsible for the absorption difference in both cases and whose absorbance decreases gradually into the near-IR. (In this study a greater absorption by haemoglobin is also evident in the caucasian subject).

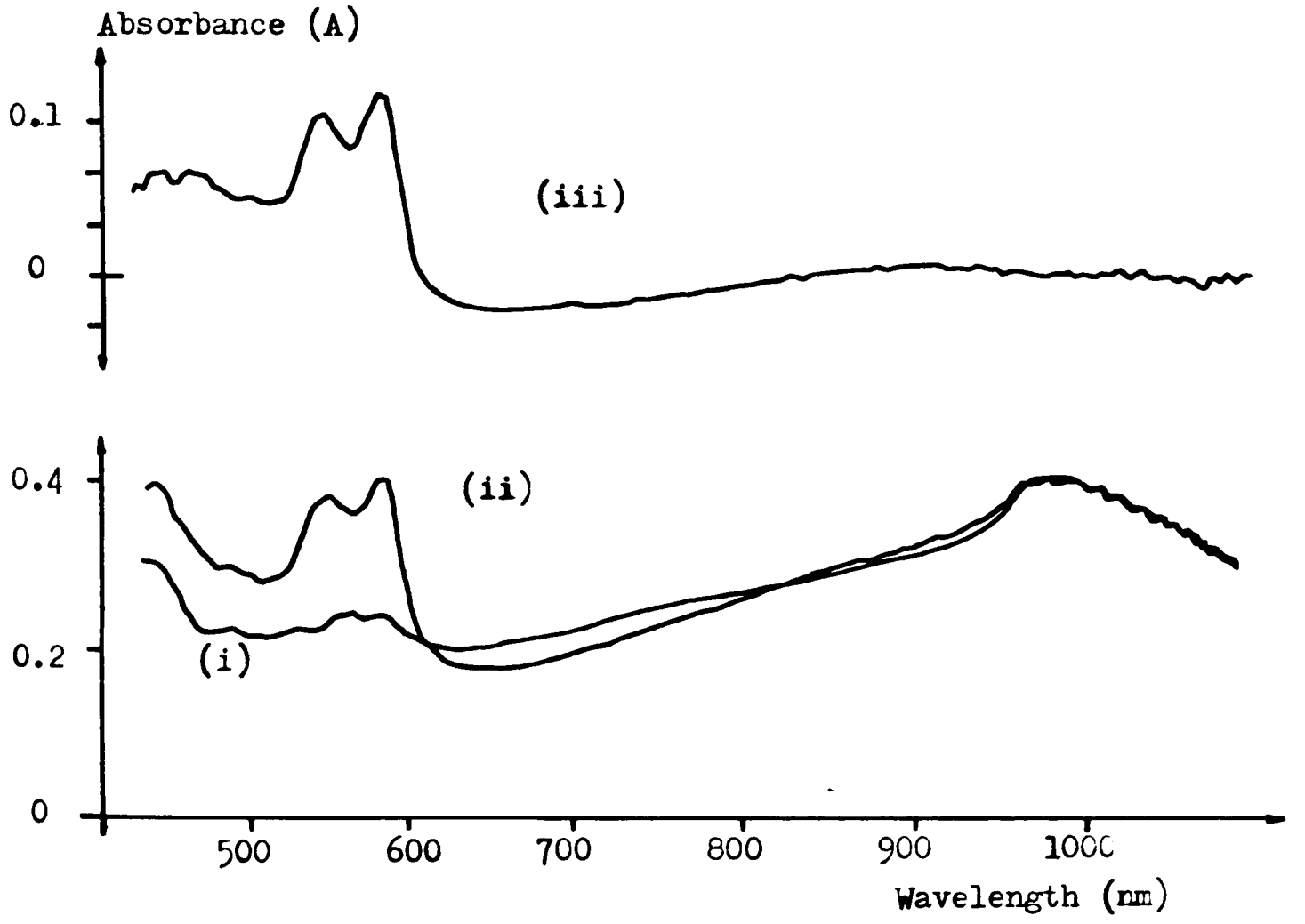

Figure 6.6 Reflectance spectra (as an absorbance) from the thumb of a caucasian subject: i) with and ii) without pressure applied. Trace iii) shows the difference in absorbance between these two.

The final spectra shown, which were obtained with the photodiode, are in Figure 6.6 and are taken from the front of the thumb of a second caucasian subject. (Both the thumb and the palm were found to be good areas from which to obtain spectra with a significant contribution due to the absorbance of haemoglobin).

They show the spectra with and without pressure applied to the fibre bundle, and hence again show the effect of the expulsion of blood and

possible deoxygenation of the same. The absorbance spectra derived from the two signal spectra used to obtain these traces is shown in Figure 6.6(iii), and as expected is largely determined by the absorption spectrum of oxyhaemoglobin.

6.2.2 Results Obtained Using the PMT.

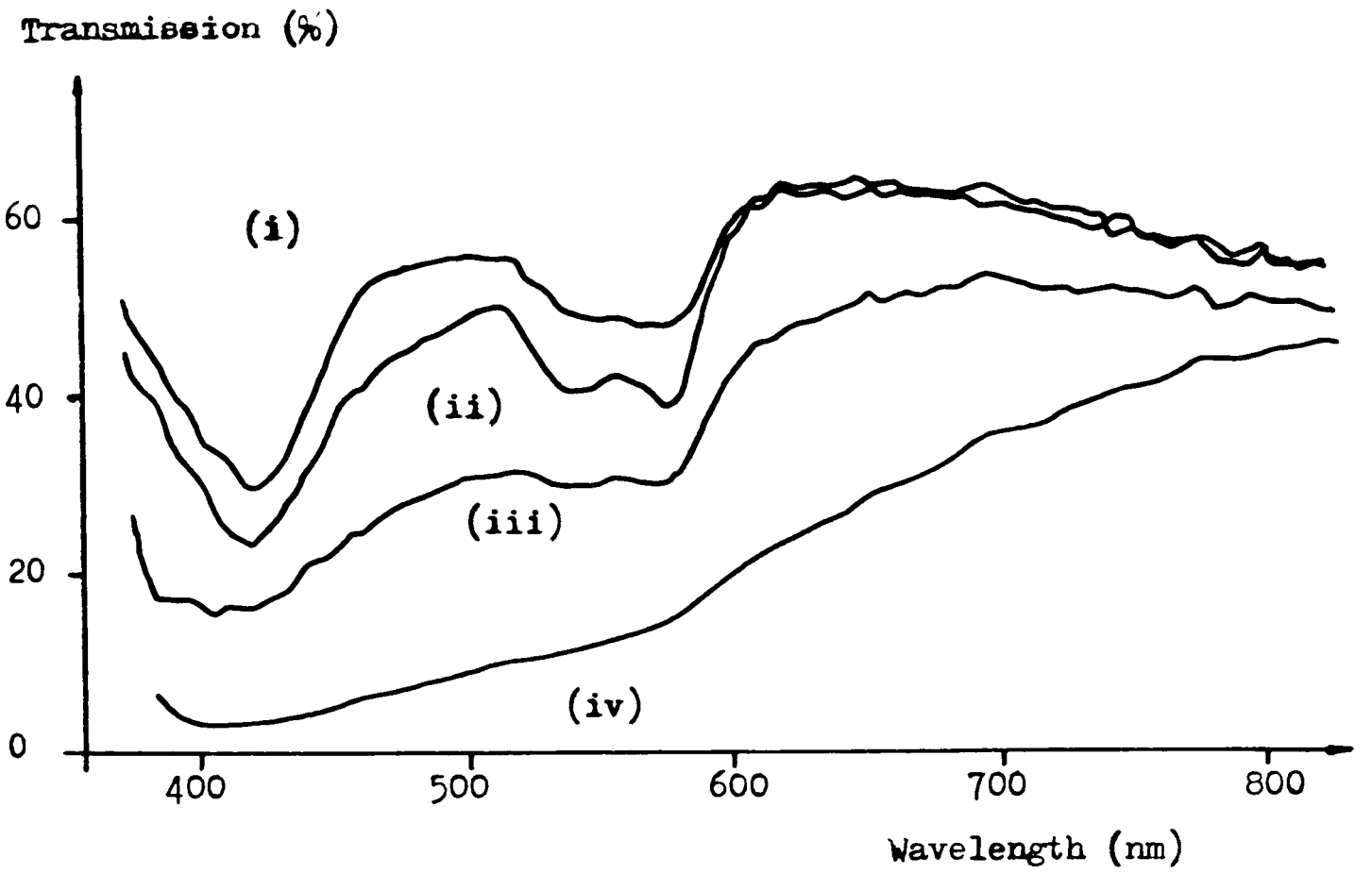

Figure 6.7 Reflectance spectra as a transmission value from the palms of i) and ii) two caucasian subjects, iii) a dark-skinned subject and iv) the back of the latter's hand.

In the results presented in this section the PMT was used with a 100kΩ resistor and 440pF feedback capacitor in its I-V converter. The latter was chosen, as described in Section 3.5.8 to provide adequate high frequency noise rejection but not produce too large an effective spectral bandwidth which would lessen resolution. A bandwidth of 5nm was selected on the Spectralyser. Either 35 or 40 spectral scans were averaged to produce each spectra, with the reference from the tissue paper averaged 20 times.

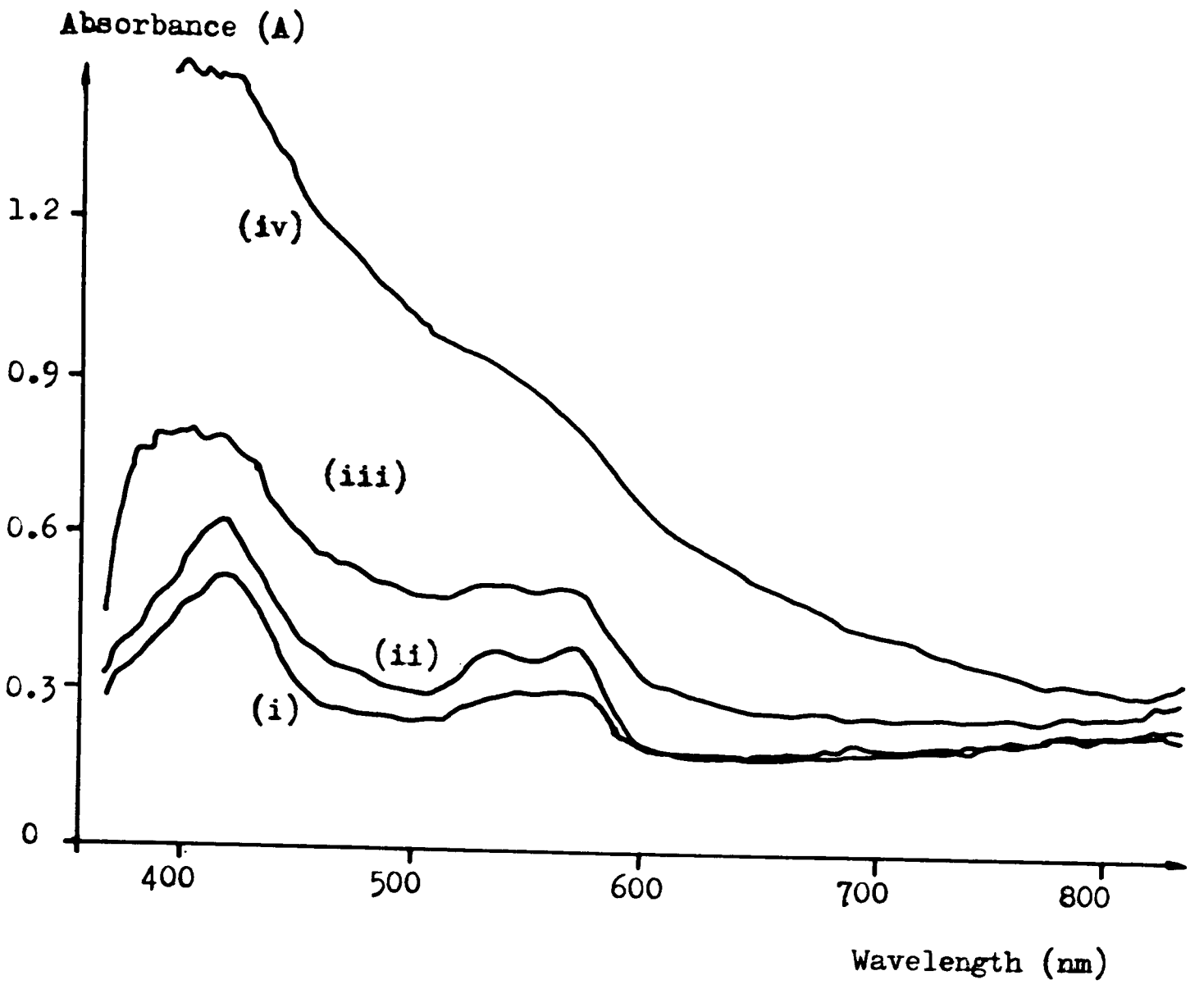

Figure 6.8 Reflectance spectra as for figure 6.7 represented by absorbance

The spectra in Figure 6.7 show the reflectance spectra (as a percentage) from the palms of two caucasian subjects, and the palm and rear of the hand of the dark skinned subject. The traces again show the predominant influences of haemoglobin and melanin on the reflectance charactersitics as in the above photodiode studies.
In addition the higher sensitivity of the PMT in the visible allows the effect of the Soret band of haemoglobin to be seen at approximately 420nm.

The equivalent absorbance spectra are shown in Figure 6.8. with the difference in absorption due to melanin calculated from the dark skinned and caucasian subjects, and the back and front of the dark skinned

Figure 6.9 Difference in absorbance between i) and ii) the dark-skinned and caucasian subjects' hands, and iii) the rear and palm of the former's hand

subjects hand in Figure 6.9.

(In these traces the combined effect of the instability in relative spectral scan position and polarization artefact can be seen).

6.3 Transmission Studies.

In these studies transmission refers to the fact that two large single optical fibre bundles (see Figure 3.6) were used to take light to and from the sample, either the hand or finger. The bundles were held in position using fabricated holders. The one designed for the finger was shown in Figure 6.1(ii) with a similar construction used for the hand.

6.3.1 Results Obtained Using the Photodiode.

In Figure 6.10 the absorbance spectra of the finger of a caucasian and dark skinned subject are shown.

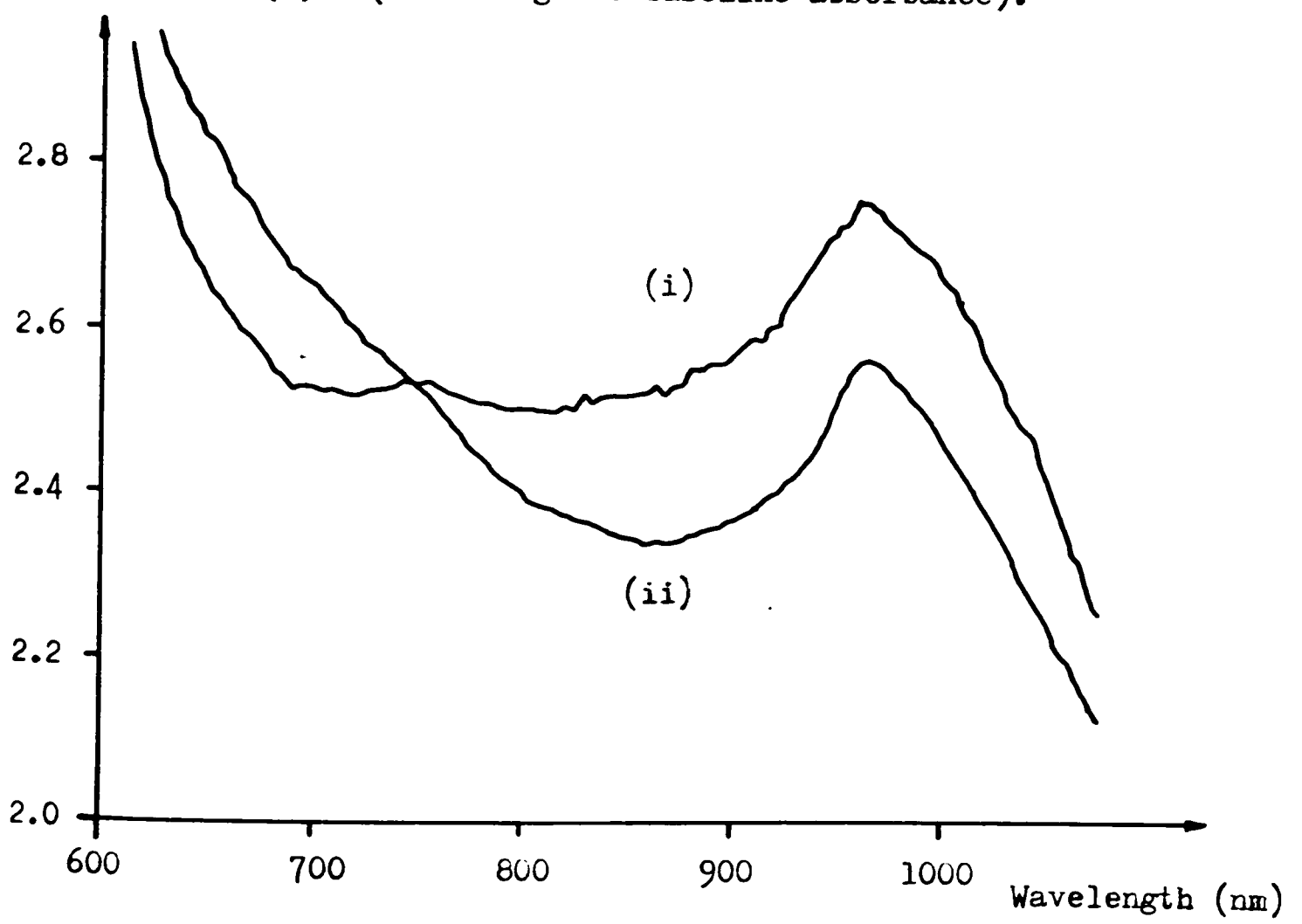

Figure 6.10 Spectral transmission of light through a i) caucasian and ii) dark-skinned subject's finger (as an absorbance)

These traces were produced using a reference spectrum consisting of a

fraction of the actual light incident on the finger as described in Section 3.5.8. A "baseline" absorbance of 0.8A was estimated also using the method described in this section. A slit width of 20nm was necessary for sufficient light throughput for measurements to be made. The sample spectra was averaged over 400 spectral scans.

The results show that the predominant effects (in addition to the large overall attenuation) are the rapid rise in absorbance at around 600nm which is due to the presence of haemoglobin, and the large broad absorption band centred at 960nm due to water. The smaller absorption band due to water at about 760nm can also be seen. (This large rise in absorbance below about 600nm is the reason why light transmitted through tissue appears red).

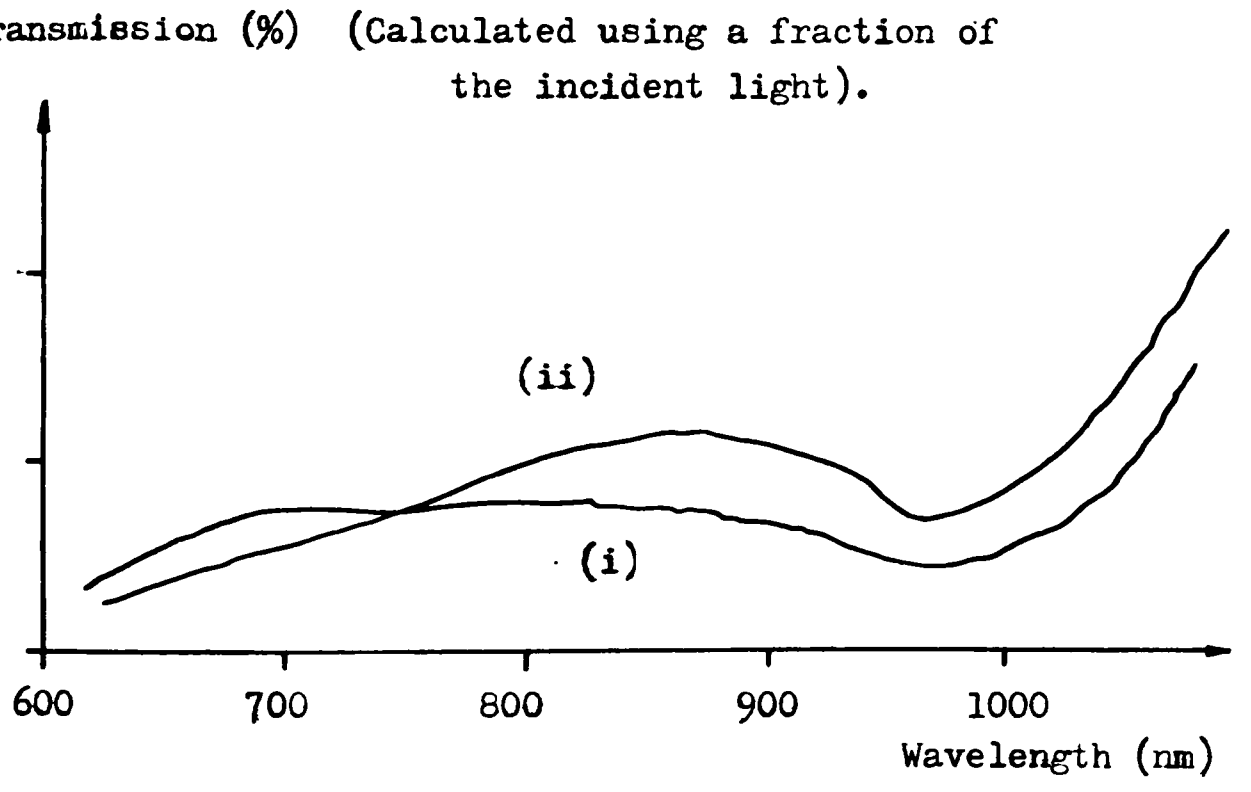

Figure 6.11 As for figure 6.10 only with the transmission represented as a percentage (ie, a transmission plot)

Even in transmission mode the difference between the two traces due to the effect of melanin up to approximately 850nm is still evident. The equivalent transmission spectra are shown in Figure 6.11. (It was

found that the transmission characteristics were partly dependent upon the exact site of measurement on the finger).

In addition to the transmittance studies on the finger measurements were also made on the surface skin of the stomach, pinched between the two large fibres which were held manually.

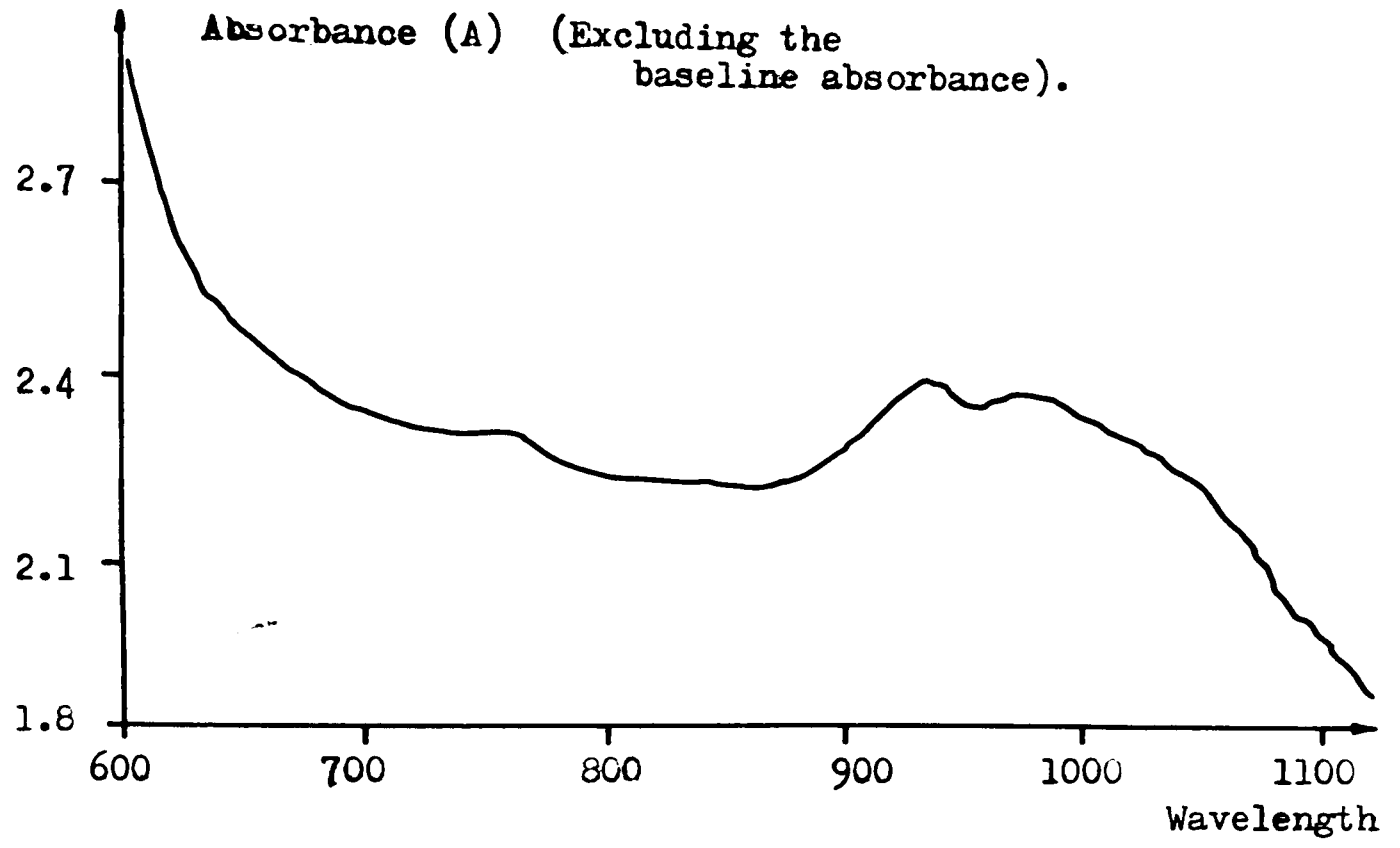

Figure 6.12 Transmission spectrum through the surface skin of a caucasian subject (as an absorbance). The absorption bands due to water and lipid are clearly visible.

The result from a caucasian male subject is shown in Figure 6.12. The trace is similar to those in Figure 6.10 except for the additional absorption band centred at approximately 930nm which is due to the absorbance by lipids (BOLIN (1984), CONWAY (1984)).

The trace was again obtained using a reference as described in Section 3.5.8 with a baseline absorbance of 1.5A calculated.

6.3.2 Results Obtained Using the PMT.

Transmission measurements on the finger with the PMT (using a 100kΩ resistor and 440pF capacitor feedback components) gave similar results to those obtained with the photodiode, showing a sharp rise in attenuation

at about 600nm. No measurements below this wavelength were made although they may be possible with the use of a low pass optical filter with a cutoff at about 600nm, to restrict the much larger transmitted intensities above 600nm from saturating and perhaps damaging the PMT.

With the greater sensitivity of the PMT, studies could also be performed on the hand. These results are particularily interesting since in addition to the expected sharp drop in transmittance below 600nm there is also a large decrease in absorbance at 760nm.

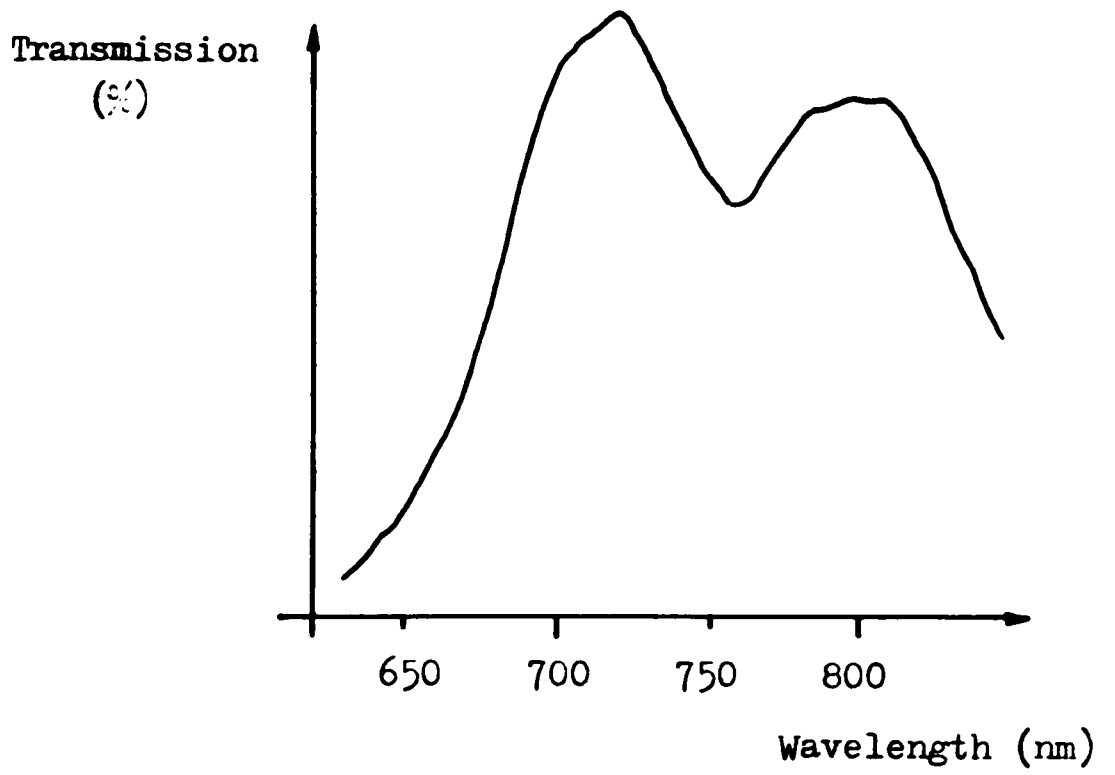

Figure 6.13 Spectral transmission characteristics of the hand (represented as a percentage). The noticeable aspect of this spectrum is the significant decrease in transmission at 760 nm.

A transmission spectra obtained using an arbitary reference (as only the shape of the trace is of interest) is shown in Figure 6.13. (One problem with observing details in this region is its proximity to the polarization artefact).

From the transmission spectra using the photodiode there was evidence of a slight decrease in transmission (increase in absorbance) at 760nm, which was attributed to water. The cause of this much decreased

transmission through the hand (which is disproportionally large considering the relative thicknesses of the finger and the hand) would therefore appear to be due to an increased effect of water, although for what reasons is not yet understood.

Alternatively it is possible that a contribution to the decrease may be due to the presence of deoxyhaemoglobin that also posesses a small absorption peak at 760nm. Whatever the cause of this relative increased absorption (which was apparent in all of the "raw" transmission spectra of the hand), compared to the transmission through the finger it may be of some importance concerning <u>in vivo</u> optical techniques since this region of the spectrum is frequently used.

Many of the results in this section can be directly compared to those in Section 1.4.2.2.

6.4 The Transition from Transmission to Absorbance Measurements.

The above results were described as having been made in either reflection or transmission mode. However, both primarily rely upon a scattering process and the following results demonstrate how as the "source" and "detector" seperation increases there appears to be a transfer from "reflectance" to "transmission" behaviour. This is largely due to an increased dominance in the absorption by blood since with "transmission" the photons must pass through more blood containing tissue whereas in "reflectance" mode photons may be back-scattered largely before such tissues are encountered.

These studies were made using two small fibre optic bundles (see Figure 3.6) mounted in close proximity (approximately 4.5mm separation between the centres) in the holder shown in Figure 6.1(ii). This was held on the skin surface by a double sided adhesive disc.

The reference spectra were obtained by holding the fibre bundle assembly slightly above the white tissues.

6.4.1 Results Obtained Using the Photodiode.

The absorbance spectra obtained from the palm of a caucasian and dark skinned subject, using the photodiode are shown in Figure 6.14. A 20nm slit width had to be used to allow sufficient light through the Spectralyser for detection by the photodiode. 300 samples were taken for each spectra.

The equivalent transmission spectrum obtained from the dark skinned subject's thumb is shown in Figure 6.15.

The results are similar in pattern to those obtained in the transmission mode as detailed in the last section. with common features

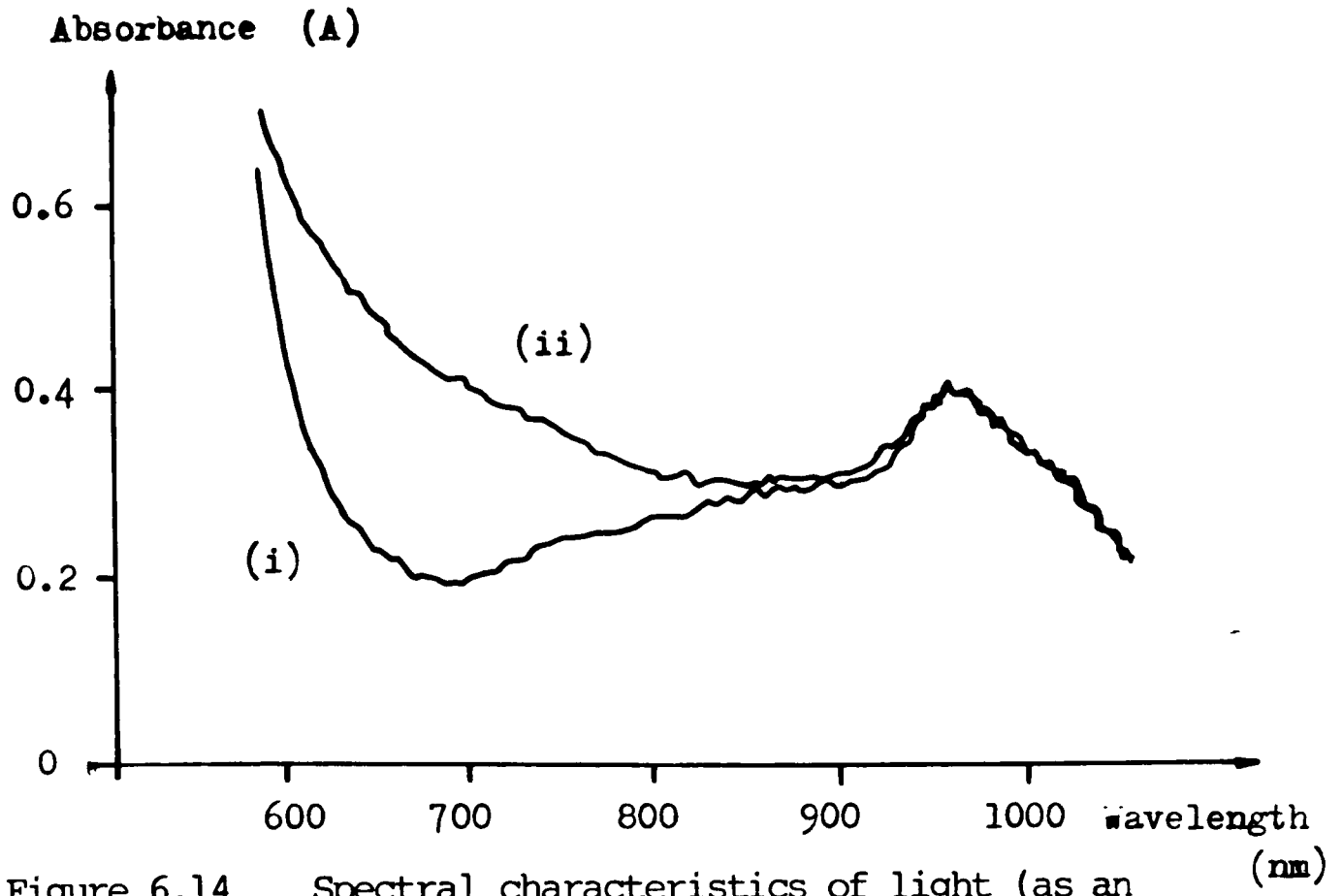

Figure 6.14 Spectral characteristics of light (as an absorbance) recorded from the palm of i) a caucasian and ii) dark-skinned subject's hand, using two small fibre bundles

with the reflectance spectra also apparent. The major difference between these and the reflectance studies is the much greater attenuation of the signal below 600nm. This can be directly attributed to the fact that the photons have to pass through more blood filled tissue.

6.4.2 Results Obtained Using the PMT.

With the increased sensitivity of the PMT measurements could be made below 600nm (using a 5nm slit width and 100kΩ and 440pF feedback components). This demonstrates that there is less attenuation at these wavelengths than in transmission mode as would be expected, and that these studies do indeed give results somewhere between the reflection and transmission measurements.

This is shown in Figures 6.16 and 6.17 which show the spectra obtained from the caucasian subject's thumb with and without pressure applied as "transmittance" and "absorbance" traces respectively (as described in Section 3.5.6). These traces show the step like change in transmission around 600nm and demonstrate the lower end of the in vivo

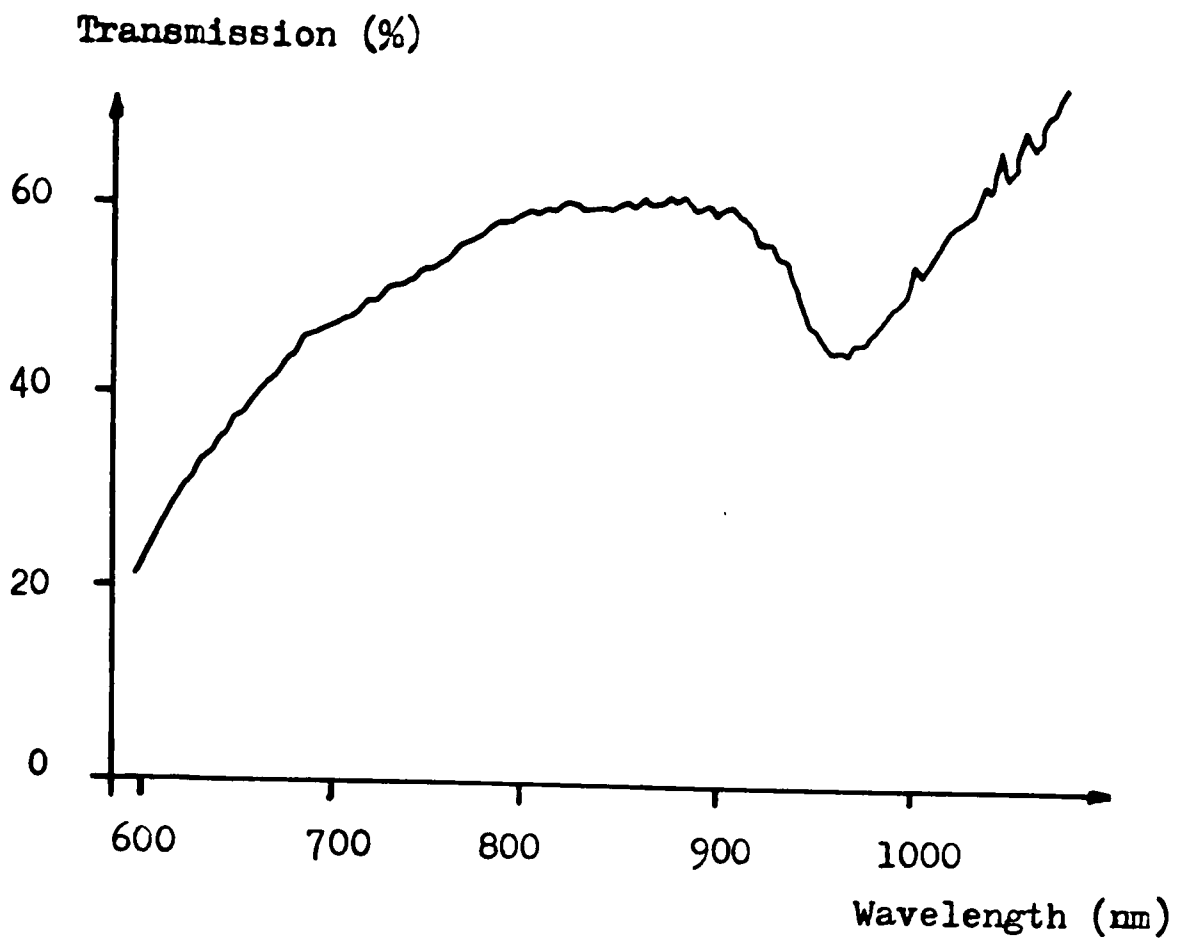

Figure 6.15 Spectrum obtained from the thumb of the dark skinned subject (as a transmission plot), obtained using two small fibre bundles.

transmission "window" that is often referred to in the literature.

These results also show that the source-detector geometry is an important factor concerning the design of the instrumentation for non-invasive <u>in vivo</u> measurements, since this parameter has a strong influence on the size of the signal obtained.

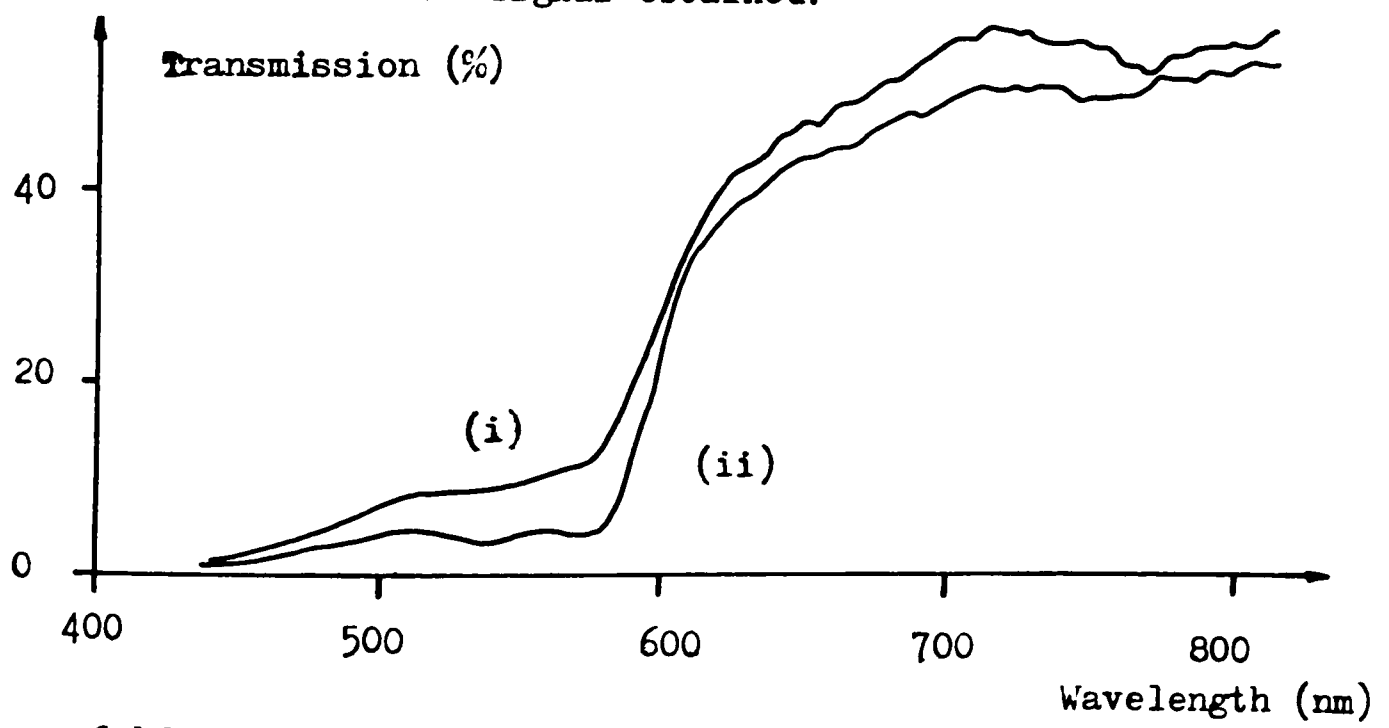

Figure 6.16 Spectra obtained from the thumb of a caucasian subject (as a transmission) using two small fibre bundles: i) with and ii) without pressure applied.

6.5 Kinetic Studies.

All of the studies described above were of steady light levels from the body surface. In this section results from gradually varying light levels measured in reflectance mode (ie with the large bifurcated fibre) are given.

The spectra shown were obtained from the palm of a caucasian subject using the photodiode detector, a slit width of 5nm and taking 200 spectral scans for each measurement.

In this study the fibre was placed on the palm, pressure applied to expel surface blood and a measurement made (Spectrum A). The pressure was then released and the tissue allowed to return to its normal state and a second measurement taken (Spectrum B). An arterial cuff was then applied to the upper arm to halt blood flow in the arm and so cause the haemoglobin to become deoxygenated. During this period a further measurement was taken (Spectrum C). The cuff was then released and a final spectrum recorded (Spectrum D) during the reactive hyperaemic phase.

Ideally these four spectra would be representative of blood free tissue, tissue containing oxyhaemoglobin, tissue containing deoxyhaemoglobin and an increased amount of oxyhaemoglobin. Consequently by using these as the appropriate sample and reference spectra, the traces could be obtained from the spectrophotometer. ("Transmission" type processing was used).

	Sample	Reference
$Hb - HbO_2$ Difference Spectrum	B	C

HbO_2 (due to expulsion of blood)	A	B
HbO_2 (due to increased blood content)	B	D
Hb (from deoxygenation of blood)	A	C

The spectra are shown in Figure 6.18 and are as expected (see Figure 1.25 for comparison). The flattening of the haemoglobin curve may be caused by the presence of both oxyhaemoglobin and deoxyhaemoglobin. Similar results to these were obtained using the PMT and on the forearm as well as the palm.

(The results presented were made using "single spectra" operation, but such studies were performed using the "multi-spectra" option). Attempts to obtain similar results in transmission mode in the near-IR met with no sucess. This was because of the technical limitations of the optical components of the instrument.

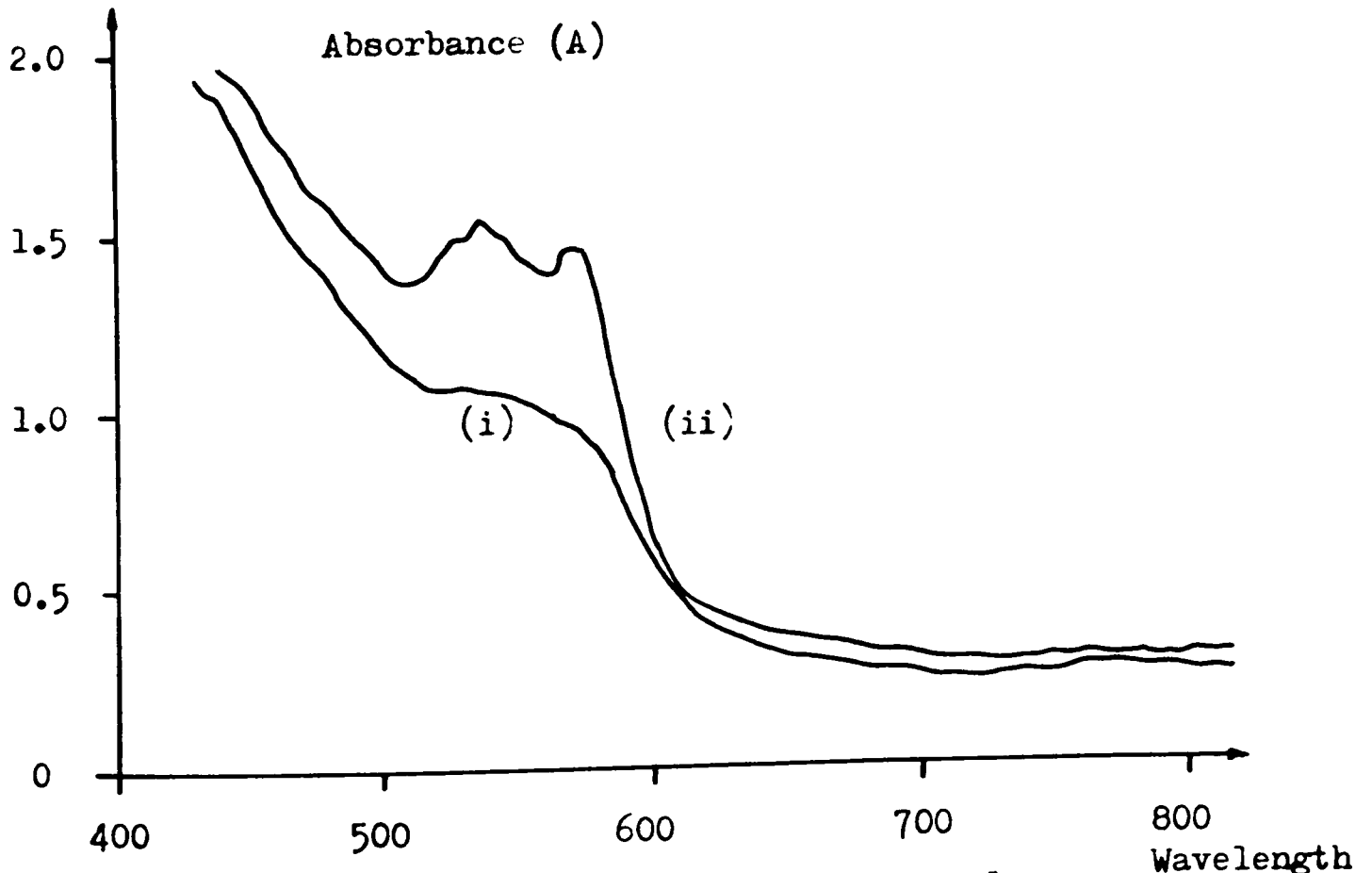

Figure 6.17 As for 6.16 only as an absorbance plot.

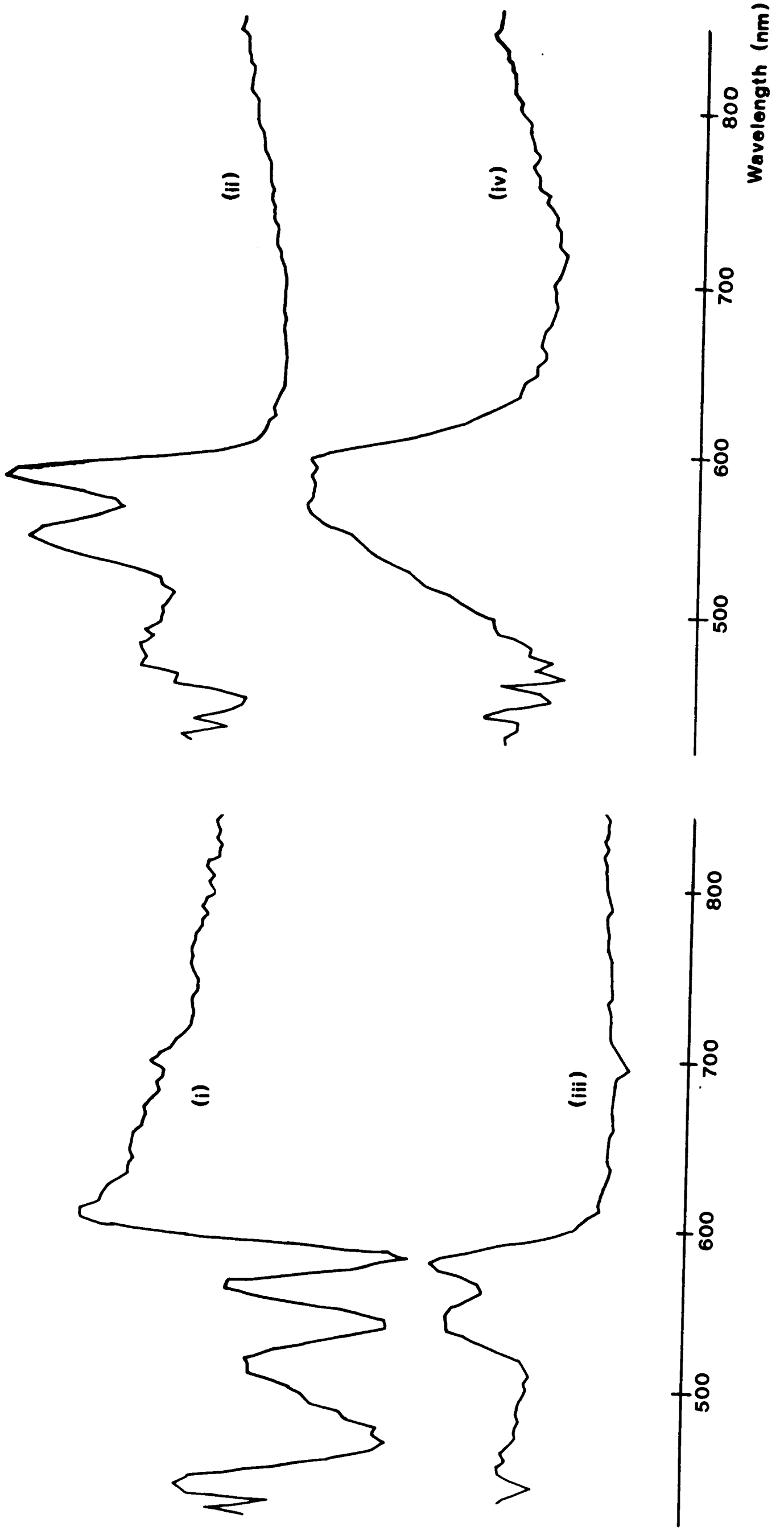

Figure 6.18 Spectra obtained from a kinetic study showing: i) the difference spectrum of haemoglobin, ii) and iii) the spectral characteristics of oxyhaemoglobin derived from the expulsion of blood and reactive hyperaemia respectively, and iv) the spectral characteristics of deoxyhaemoglobin from the use of an arterial cuff.

6.6 Discussion.

The reflectance results presented here are in agreement with previous studies, although the majority of these only cover the visible region to about 700nm, and therefore do not include details of the absorbance by water.

The transmission measurements show that the absorbance of tissue decreases dramatically below approximately 600nm, due to the large increase in the absorption of haemoglobin in this region. These results are of particular interest because there is little published data of the transmission spectra of tissue in vivo.

As described above measurements could be made below 600nm but with the present system a low pass optical filter would be needed to prevent the much larger transmitted intensities above 600nm from damaging the PMT.

The spectrum shown from the stomach demonstrates the absorption by lipids and such measurements may provide a way of measuring the body's fat content (CONWAY (1984). In addition the interaction of the lipid and water absorption bands in the near-IR together with other similar measurements has been sugested as a means of measuring a number of physiological variables (MDW (1986)).

The studies using the two small fibre bundles in close proximity demonstrates that there appears to be a transition from reflectance to transmission type characteristics. This behaviour was also noted in the photoplethysmogram studies described in the next Chapter. The precise nature of this transition is likely to be dependent upon many factors and is of relevance concerning the design of the fibre bundles and their holders for non-invasive measurements.

Whilst performing the above studies a noticeable effect concerning

the fibre bundle taking light from the source is that very little light appeared to enter the skin until the fibre actually touched the surface. This may be associated with the need to couple light into tissue (as with ultrasound studies) and further work into this phenomena may lead to an improvement in the efficiency of such measurements. Studies of the refractive index of skin which are likely to be of relevance have already been performed (PUGLIESE (1980)).

Finally. the present instrument could be linked to a collimated light source and detector assembly to enable collimated transillumination (JARRY (1984)) to be performed over a substantial wavelength range.

An improved instrument could also be constructed (essentially with improved optics) to enable the above studies to be repeated with greater resolution, and also allow transmission kinetic studies in the near-IR.

Chapter 7: The Construction of an Instrument for Recording Photoplethysmograms, and Preliminary Use.

7.1 Introduction.

The reflection and transmission measurements presented in the preceding chapter were either constant or at the very most relatively slowly varying with time. Conversely the work described in this chapter is concerned with studying cardiac synchronous variations in reflected or transmitted light intensity from the body. The now generally accepted term for such a signal is the photoplethysmogram (PPG) with the study of such signals referred to as photoplethysmography. Both terms will be used here with these meanings.

By definition plethysmography is the determination of a change in volume of an organ, limb or part of the body, a clear example being that of monitoring the change in volume of a finger by displacement of fluid from a constant volume chamber surrounding said finger (HAYASHI (1979)). Photoplethysmography therefore implies that these volume changes are measured by optical means, and so is something of a misnomer since the PPG is only partially produced by variations in the volume of the tissue under investigation (which itself will almost exclusively be due to changes in the blood volume). As discussed below, other effects such as reflection from blood vessel walls and variations in erythrocyte orientation with blood flow are also all known to contribute to the PPG.

As stated above in this thesis the PPG is considered to be that signal which is cardiac synchronous. However, it should be noted that blood volume changes may themselves be cardiac synchronous, due to the arterial pulse, or vary much more slowly due to gradual changes in the haemodynamics of the tissue under investigation. For this reason in the

past (CHALLONER(1979)) photoplethysmography has been split and considered separately, into the two areas of "ac" and "dc" photoplethysmography, with "ac" plethysmography being the study of the PPG as defined here. Although not dealt with here and having more in common with the studies in chapter 6, "dc" photoplethysmography has been used as a means of assessing haemodynamics (ie blood flow, volume or pressure, (MUHL(1985), HIGGINS(1986))).

There are many reasons why a thorough study of the PPG is of interest. Having performed the reflection and transmission measurements of tissue given in the last chapter, there was a sense of incompleteness in knowing that on top of these "constant" measurements there was a much smaller cardiac synchronous variation in light intensity. Hence, study of the PPG was a natural extension of this work. In addition it is clear from the literature (see below) that the precise cause and nature of the PPG in both reflection and transmission modes is as yet incompletely understood. Consequently it was felt that if an instrument was constructed to allow the nature of the PPG to be fully analysed, as obtained from different sites on the body, in both modes, under various conditions and at different wavelengths then this would complement the earlier "dc" studies and may lead to a fuller understanding of the origin of the PPG.

The ability to record PPGs at a variety of wavelengths was considered particularily important. This is because it is certain that several phenomena contribute to the production of the PPG, and so if they themselves are wavelength dependent then studying the PPG at a variety of wavelengths may give a guide to how each effects the nature of the PPG.

A further reason for investigating the PPG is its still increasing application in clinical instruments. At different wavelengths the PPG

can apparently give depth specific haemodynamic information (GILTVEDT (1984)) by virtue of the different penetration depths of light with respect to wavelength. (see Section 1.4.2.2), whilst the use of pulse oximeters (see Section1.5.1.3.3) is widespread. Commercially available pulse oximeters essentially rely upon two wavelength analysis of the transmission PPG for their operation, but the feasibility of reflection pulse oximetry has also been shown (MENDELSON (1983b,c)). A possible explanation of why a reflection pulse oximeter gives a measurement of oxygen saturation is given in Section 7.6.5.2.

For the above reasons an instrument capable of averaging and recording the PPG, in both reflectance and transmission modes, from any site was constructed and used to perform preliminary investigations.

The next section briefly describes the developement, use and current views of photoplethysmography followed by the aims of this work in Section 7.3. After this the rationale behind the type of processing of the PPG employed is given in Section 7.4.

In Section 7.5 a description of the microcomputer based instrument and associated electronics can be found with preliminary results obtained presented in Section 7.6. A comprehensive discussion of these together with their implications is given in the final section.

7.2 Previous Use and Current Views of Photoplethysmography

Reports of the application of photoplethysmography began to appear in the 1930's (see review CHALLONER (1979)) although in these early days, as with oximetry, the technique was hampered by the lack of ideally suitable light sources and detectors. Since then D'AGROSA (1967) has studied the "opacity pulse" of individual minute arteries, with URETZKY (1971) describing a method for comparing transmitted and reflected PPGs and MEDGYESI (1973) reviewing the use of photoplethysmography for assessing skin flap circulation

Together with Challoner's review these papers describe the development of the technique to date and show that although the potential clinical use of the PPG, for assessing blood flow in particular, was fully appreciated, so too was the fact that the exact underlying mechanisms responsible for producing the PPG were (and still) are incompletely understood.

However, from the work on "ac" photoplethysmography reviewed by Challoner and further comprehensive *in vitro* and *in vivo* experiments using both reflection and transmission photoplethysmography (WEINMANN (1977), NIJBOER (1981)), several broad conclusions can be drawn concerning the nature of the PPG.

In vivo the transmission PPG is produced by a chiefly absorption process with the incoming arterial pulse causing an increase in blood volume and a corresponding decrease in the transmitted light level (ie the volume and light intensity pulses are in antiphase). Similarily the reflection PPG is also usually in antiphase with the volume pulse, showing that it also is predominantly produced by an absorption process. (Note here the term reflection is used although the light reaches the

detector, as in the transmission mode, by a scattering process.)

However, in both modes other than absorption processes can play a part and these may manifest themselves during <u>in vitro</u> studies. For instance an antiphase transmission PPG can be produced in a rigid (ie a constant volume) tube which cannot therefore be due to changes in volume and is considered to be caused by the effect of erythrocyte orientation (CHALLONER(1979). In addition in-phase reflection PPGs can also be obtained caused either by the reflection and orientation of the red blood cells, or reflection directly from the vessel wall.

A diagrammatic representation of transmission and reflection photoplethysmography (on the finger) is shown in Figure 7.1 together with an example of in phase and antiphase PPGs.

The reflected PPG, in phase with the volume fluctuations can also be obtained <u>in vivo</u> from certain sites and/or under certain physiological conditions. Because it is observed less often it is generally refered to as the "inverted" PPG, with the following theory concerning its origin proposed by NIJBOER (1982) following a rigorous series of studies.

This basically says that if the region of tissue being monitored has a low background attenuation then the incoming arterial pulse will absorb more light so dominating any other effects and producing an antiphase PPG. However, if the overall optical density of the area under investigation increases sufficiently the dominating effect of the arterial pulse, which contributes to the reflection PPG, will be an increased reflection from the arterial wall and red blood cells, and so the PPG will then be in phase (ie "inverted"). In practice "inverted" PPGs are usually obtained from tissue such as the finger after venous engorgement or from the surface of the skin over a large vessel.

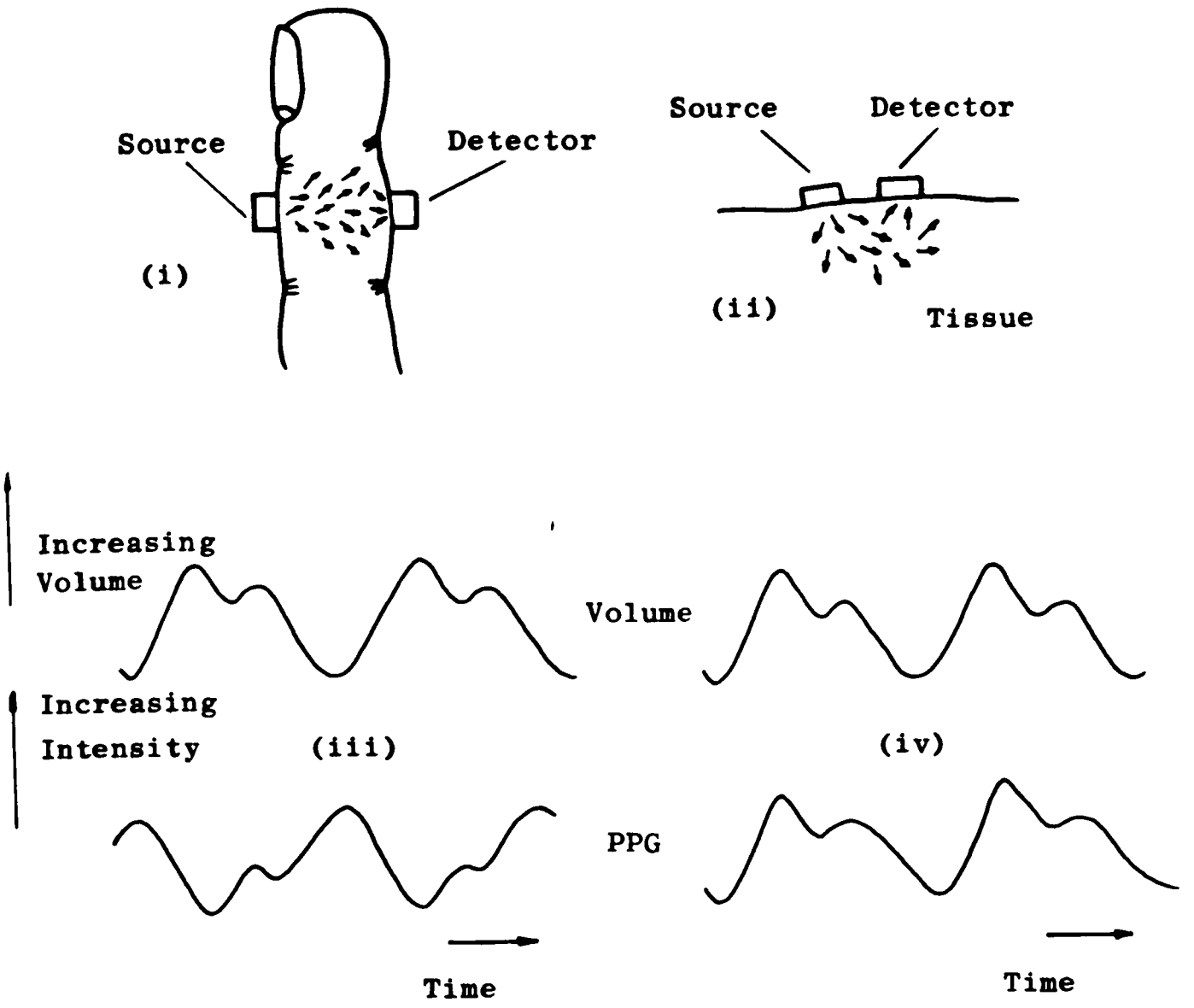

Figure 7.1 Schematic diagram of: i) transmission and
ii) reflection mode photoplethysmography, and
iii) antiphase and iv) in-phase ("inverted") photoplethysmograms.

Other attempts to study and explain the nature of the PPG have also been made. OCHOA (1980) observed that *in vitro* there was an inverse relationship between haematocrit and pulse height, whilst the opposite was true *in vivo*. ROBERTS(1982) used PDT (see Section 1.4.3.3.2) to attempt to explain some aspects of the PPG by considering the optical characteristics of blood in motion. The theory was compared with *in vitro* results on flowing (although not pulsatile) blood.

An example of the clinical use of photoplethysmography is given by

SAMUELOFF(1982) which as with most applications of the technique is concerned with assessing vascular blood flow. Here it is simply the actual presence and size of PPG which is of most interest, but as demonstrated in other areas of Bioengineering there are many ways in which pulses can be parameterised.

One such variable associated with the PPG is the time interval between the R-wave of the ECG (which causes the ventricles to contract and hence eject blood from the heart causing the arterial pulse) and the arrival of the pulse wave at a particular site. This pulse wave transit time (or cutaneous R-pulse interval) is primarily related to, and hence has been used to monitor, blood pressure (OBRIST (1979)) the state of the vasculature (as effected by the sympathetic nervous system, JENNINGS (1983)) and cardiovascular function in neonates (via the myocardial contractility, WAFFARN (1983)). (In addition a standard means of non-invasively monitoring heart rate is by counting the number of PPGs in a given interval).

As stated earlier pulse oximeters using transmission photoplethysmography are now in widespread use (see Section 1.5.1.3.3). In addition reflection pulse oximetry has also been shown to be feasible (MENDELSON (1983b,c)). The preliminary results described later in this chapter raise some interesting points concerning the means of operation of both of these techniques.

Reflection photoplethysmography has also been used, with the knowledge that the penetration depth of light in the skin varies with wavelength to monitor blood flow at different depths, and therefore at different parts of the vasculature (GILTVEDT (1984)). This was achieved by obtaining PPGs at 560nm (green) and 905nm (near-IR) work which promoted a response on the precise nature and meaning of the signals

observed upon changes in blood volume and blood flow (TRAFFORD (1984)), further illustrating the questions still to be answered in this field.

Since photoplethysmography is most often linked with the measurement of blood flow it is not surprising that users of either this technique or laser doppler flowmetry (LDF) (see Section 1.5.8) have reciprical interests in the other method (especially since both are optical techniques).

Workers at Linkoping University, where much research on LDF has been performed, have used similar processing techniques to those used in LDF to perform photoplethysmography. Rather than observing the PPGs direct the power spectral density of the reflected signal over the range 0.1-10kHz was recorded and used. Studies on hands and forearms at 13^{o}C and 42^{o}C using light at 560,630, and 850nm showed that the ratio of total power during cold stress to the total power during heat stresss was much larger at 560nm than the other two wavelengths (TAMURA (1985)). It was concluded, amongst other things, that the choice of wavelength is important in photoplethysmography. The results of this experiment are considered in more detail in Section 7.6.2.

Concerning LDF it is perhaps also worth noting the signals obtained often contain a pulsatile component, and that in addition comparisons of photoplethysmography and LDF have been made elsewhere (FAIRS (1985)).

7.3 Aims

The basic aims of this work were firstly to construct an instrument capable of averaging and producing hard copy output of suitably processed PPGs. These must be able to be obtained in both reflection and transmission modes, from various sites on the body and at different wavelengths. Secondly this instrument was to be used to perform *in vivo* studies (whilst *in vitro* measurements could also be made if required). Such an instrument, capable of producing an "average" PPG under defined conditions (rather than a continuous trace) was intended to make the analysis of data from controlled experiments simlpler to analyse.

As described above, although many investigations into the origin of the PPG have been made, and much learnt, its exact cause is not yet fully understood. The intention was to construct an instrument with which it would, eventually be possible to discover more about the PPG such as the effects of the absorption, "reflection" and orientation of erythrocytes and of the vessel walls. In addition the differences between reflection and transmission photoplethysmography and the borderline between them since both are fundamentally scattering processes could be studied, and also the cause of the variations in signals obtained from different sites (eg diffuse vascular beds and single larger vessels), the effect of physiological conditions and source-detector geometry.

Clearly to investigate all of the above in a single study is not practically possible due to the interrelationship of many of the various effects. Rather several studies were considered which would hopefully give an indication of the precise nature of the PPG, and also have some practical relevance concerning the use of photoplethysmography for clinical monitoring.

The aspect of the PPG which was actually considered to be the most interesting to study was its dependence upon wavelength. Little work appears to have been done on this topic since wavelengths giving relatively large signals (ie in the near-IR) have generally been used. However, as stated in the Introduction this type of study is a natural continuation from Chapter 6, whilst recent results (GILTVEDT (1984), TAMURA (1985)) and the use of photoplethysmography in oximeters, suggests that the wavelength dependency of PPGs has many potential applications in clinical monitoring. On a more fundamental level, any variations in the transmission, reflection and "inverted" PPGs with wavelength may give an insight into the mechanism producing them.

Since optical fibre bundles are used to "pipe" light to and from the skin in this instrument, the effect of transducer geometry is readily investigated, as is the size of the "source" and detector (by using different diameter fibre bundles). Hence, these were areas in which preliminary studies could be made.

Finally, as discussed in the next section, the PPG is usually observed after being AC coupled so that a trace of the PPGs is stable (ie the slowly varying "dc" component is removed). With this instrument the effect of such filtering could be examined.

7.4 Processing the PPG.

There are two distinct aspects to processing the PPG to consider. Firstly the requirement of taking the signal from the photodetector and rendering it suitable for the microcomputer's A/D board, and secondly, the processing required on the signals (PPGs) once averaged and stored in the microcomputer so that a valid comparison between PPGs obtained at different wavelengths can be made.

7.4.1 Analogue Electronics to Provide Input for the A/D Converter.

The signal obtained from the photodetector used for photoplethysmography in any mode consists of a relatively small "ac" component (the PPG) superimposed upon a large "dc" pedestal as shown in Figure 7.2. This can present immediate problems concerning the choice of a photodetector. For instance a PMT, ideal for observing small fluctuations in low intensity light is likely to become saturated by the "dc" bias before the "ac" component even registers an effect.
Ideally a photodetector with very high dynamic range and large sensitivity over all of this range is required. The problems of the choice of detector (and source) is extensively discussed by CHALLONER (1979). The most commonly used detectors are semiconductor based.

Once a suitable detector has been chosen its output, representative of both the "dc" and "ac" photoplethysmograms, must be presented in an appropriate form to the inputs of the A/D converter. For "dc" photoplethysmography there are no problems since only the change in the "dc" pedestal is required. However, with "ac" photoplethysmography because the "ac" fluctuation represents such a small proportion (typically 1-2% CHALLONER (1979), NIJBOER (1981)) of the total signal, then the A/D converter is unlikely to have sufficient resolution to

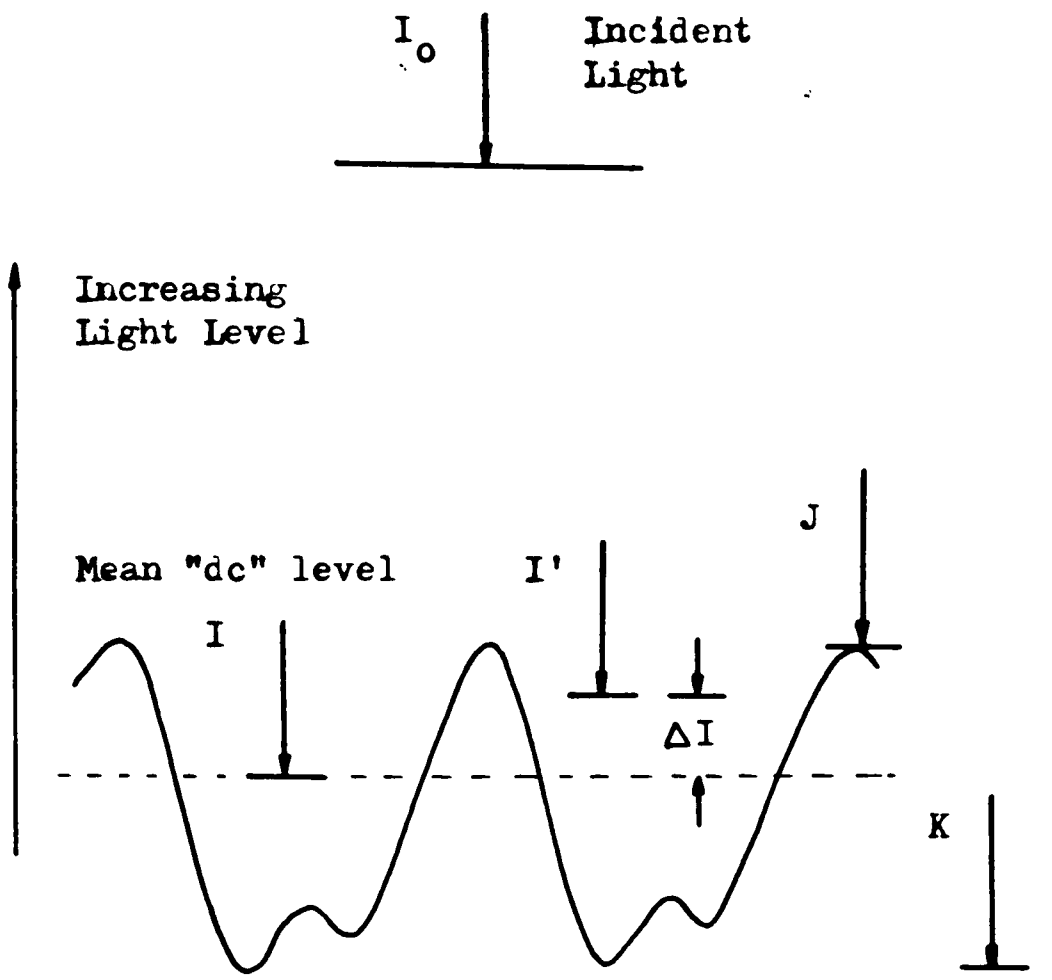

(not to scale)

Figure 7.2 Diagram of light levels obtained during photoplethysmography, and which are referred to in the text.

adequately resolve the "ac" PPG if the whole signal from the

photodetector is used.

The solution is to either AC-couple the photodetector output or offset the DC pedestal. both of which remove the DC bias leaving the "ac" PPG centred on (or about) zero volts. It can then be amplified to a suitable size for the A/D converter.

The PPG is usually studied using AC-coupling (or an equivalent process) to obtain a stable trace with the "dc" plethysmograph (ie the large but gradual changes in the "dc" bias) suitably removed.

Simply offsetting the DC pedestal with an equal but opposite voltage has the disadvantage that it does not remove the drifting of the signal due to changes in the "dc" photoplethysmogram. rather it simply offsets the level about which this drifting occurs. However. the advantage of this approach is that the PPG is left unfiltered, whereas AC coupling (ie use of a high pass filter) may exert some influence on the shape of the PPG, with the "heavier" the DC blocking the greater the likely effect on the PPG, whose fundamental frequency component is only 1-2Hz. Indeed this is one of the areas suggested for investigation in Section 7.3.

7.4.2 Processing the PPG Itself

A typical output from a photodetector used to observe the PPG is shown in Figure 7.2. upon which various levels of light intensity referred to below are marked. In the figure I_o represents the intensity of light incident upon the tissue. and I the "dc" photoplethysmogram. that is the mean level of light detected. The PPG is superimposed upon this mean level and corresponds to the fluctuation in intensity from a maximum J to a minimum K. At any given wavelength (assuming linear response of the photodetector) the output from the detector will be given by the product of these intensities and its responsivity.

After either AC-coupling or offsetting a constant DC pedestal from this output then the resultant signal fed to the A/D converter is that corresponding to the intensities from J to K (ie the "ac" PPG) all offset by an amount so that the level I is represented by zero volts.

The A/D converter is configured to accept bipolar signals and so intensities above/below I are represented by positive/negative voltages. Indeed any intensity, I', will be represented by a voltage V:

$$V = k\,(I'-I) = k\,\Delta I \qquad 7.1$$

where k is the responsivity of the detector and accompanying circuit at the wavelength in question in V/W, and V will be positive or negative depending upon whether I' is either above or below the "dc" photoplethysmogram level.

One plotting option of the instrument constructed is simply to output the "raw" PPG, that is to plot the actual voltages recorded. However. these voltages will depend upon k, which will be wavelength dependent. the optical characteristics of the tissue producing the variations in voltage of both "ac" and "dc" plethysmograms, and I_o the incident intensity since if this increases so too will all detected levels. In addition I_o will be dependent upon the spectral output of the source. Therefore it is not valid to compare "raw" PPGs obtained at different wavelengths since they will not be solely dependent upon the optical characteristics of the tissue.

Similar problems were discussed in Section 3.5.6 concerning the scanning spectrophotometer and this is why only absorbance or transmittance spectra can be reliably used to investigate a sample's spectral properties. Here the same solution is used, which is to normalise the recorded PPGs with respect to an intensity measurement made with the same detection circuit.

The intensity used is the "dc" photoplethysmogram. that is I in Figure 7.2. Using the voltage representing this intensity two types of normalised plots are offered from the instrument. corresponding to the "transmittance" and "absorbance" plots from the spectrophotometer.

The "transmittance" PPG trace effectively plots the variations in intensity producing the PPG out as a percentage change in the intensity of the "dc" photoplethysmogram. At any point on the PPG using this type of processing, the value plot is given by:

$$PPG = \frac{I_o}{I_o}\frac{k'k\,(I'-I)}{k'k\,I} \times 100 \qquad 7.2$$

$$= \frac{\Delta I}{I} \times 100$$

where it is assumed that all intensities used are proportional to the incident intensity I_o by the same amount k' at this wavelength.

Hence by using this method there is no longer any dependence of the calculated PPG upon the source and detector characteristics, which cancel out. and as stated above the PPG is plotted as the percentage change in the "dc" pedestal (ie the mean level of light transmitted or reflected).

An alternative means of presenting the PPG is as an absorbance plot where the increase or decrease in light producing the PPG, is given as an absorbance with respect to the "dc" level where the value of the trace at any point is given by:

$$PPG = -\log\frac{I}{I'} \qquad 7.3$$

(The negative log is taken so that the PPG produced has the same orientation as both the "raw" and "transmittance" PPGs).

Although not ideal these methods of processing at least largely remove the effects of variations in output intensity of the source and detector response with wavelength. This then allows comparison of the properties of the pulsatile component of the overall light level (ie the PPG) at different sites and under different conditions.

7.5 Microprocessor Based Instrument for Averaging, Processing and Displaying Photoplethysmograms.

7.5.1 Introduction.

The instrument described in this section is able to average and produce hard copy graphical output of PPGs after suitable processing as discussed in Section 7.4.2. Fibre bundles and optical filters allow PPGs to be obtained from various sites and at specific wavelengths respectively. Averaging of the PPG is accomplished as PPG sampling is cardiac synchronous.

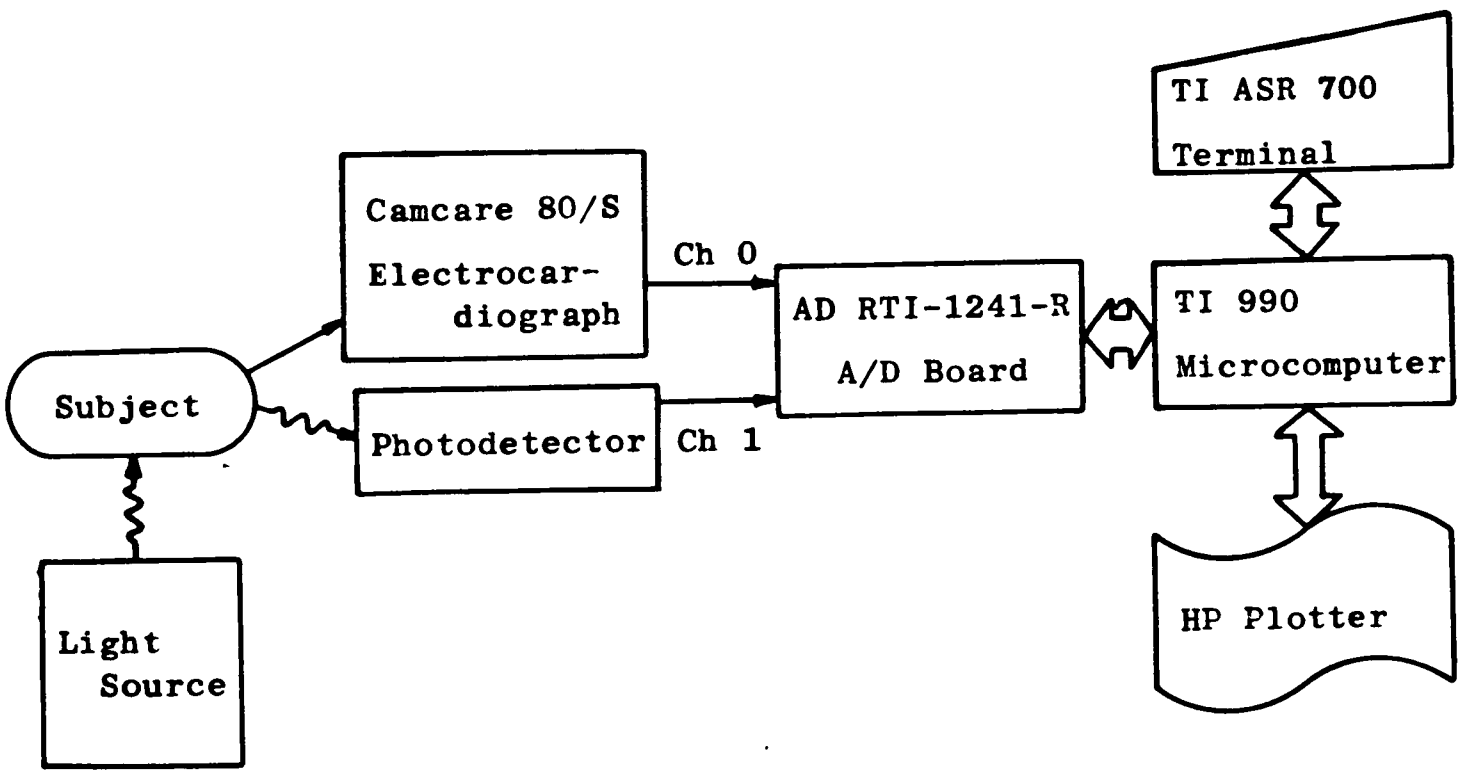

Figure 7.3 Block diagram of the instrumentation used for recording photoplethysmograms.

A block diagram of the instrumentation is shown in Figure 7.3. Signal processing and overall instrument control is performed by the TMS 9900 microcomputer (Texas Instruments (TI)), with user input (and output pertinent to instrument operation) being via the 700 ASR teletype

terminal (TI). Annoted graphical output is produced by the HP7475A plotter (Hewlett Packard).

The analogue inputs. namely the electrocardiogram (ECG) taken from the Fenline 80/S electrocardiograph (Camcare), and the PPG, from the output of the photodetector. are digitised by the RTI-1241-R 12-bit analogue-to-digital (A/D) converter (Analog Devices).

7.5.2 Analogue Inputs.

7.5.2.1 ECG.

The ECG was obtained from a Fenline 80/S (Camcare) electrocardiograph. Since all that was required was an R-wave capable of being detected as described below, two electrodes were sufficient. connected to the centre of the chest and slightly in front of and below the left armpit.

7.5.2.2 Photodetectors.

A BPX 65 photodiode and PMT (see Section 3.2.2) coupled to optical fibre bundles were used to detect the PPG which required amplification and removal of the large "dc" pedestal. The circuits to achieve this were described in Section 3.3. Details of the fibre bundles used are given in the results section.

7.5.3 Programme Structure and General Description.

The programme which operates the instrument was written in Power BASIC (TI) with machine code routines called from the BASIC programme used for data acquisition and storage.

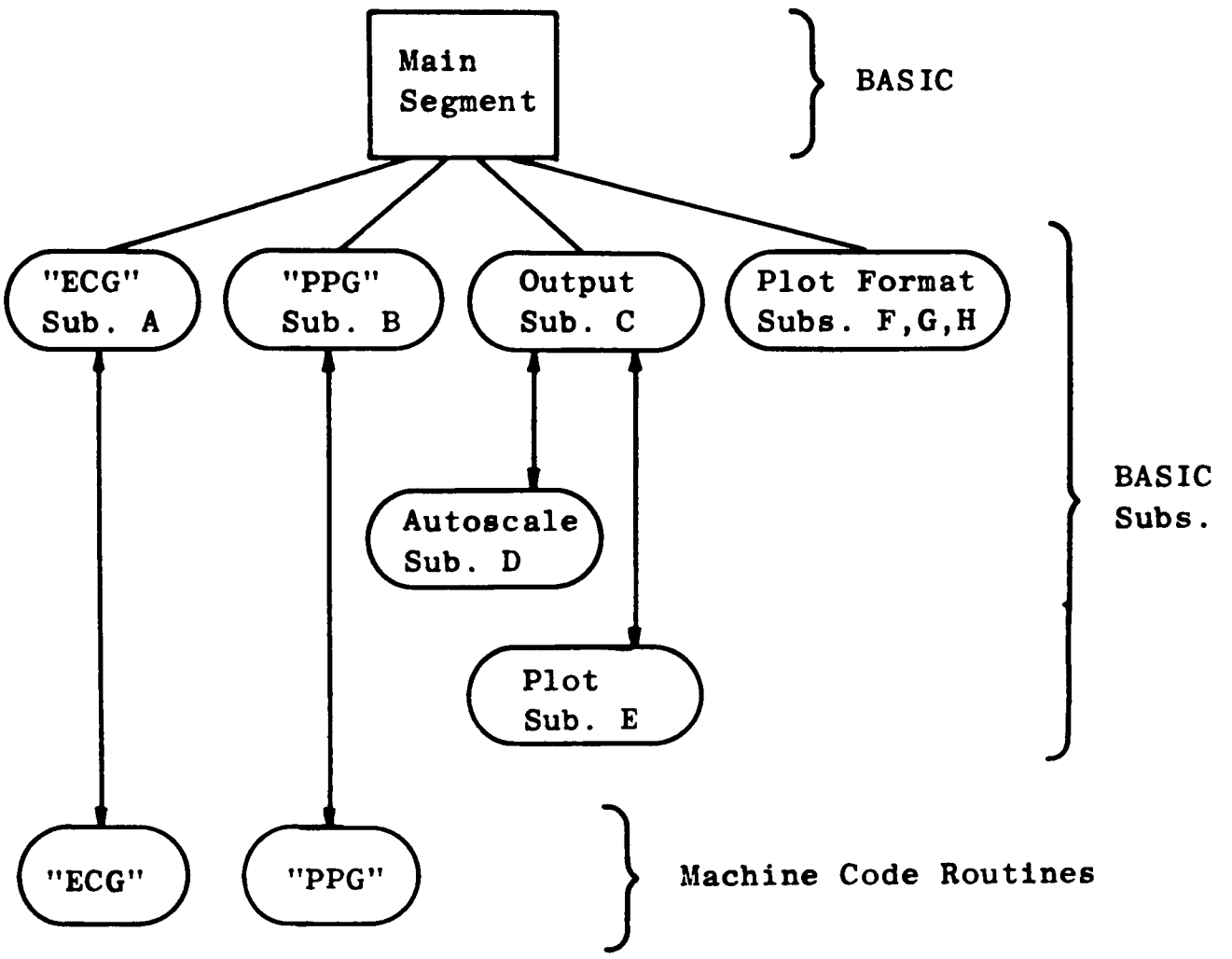

Figure 7.4 Overall structure of the programme.

The programme was held on cassette tape and therefore had to be loaded from the 700 ASR terminal prior to use. The overall structure of the program is shown in Figure 7.4. and the flow diagram in Figure 7.5. (The memory map of the TMS 9900 as used is given in Appendix D). The purpose of the programme is to sample, average and store specific PPGs (ie from a particular site and with a particular optical filter), and then produce processed, annotated graphical output of any stored PPG as required.

Averaging is achieved by summing corresponding samples from

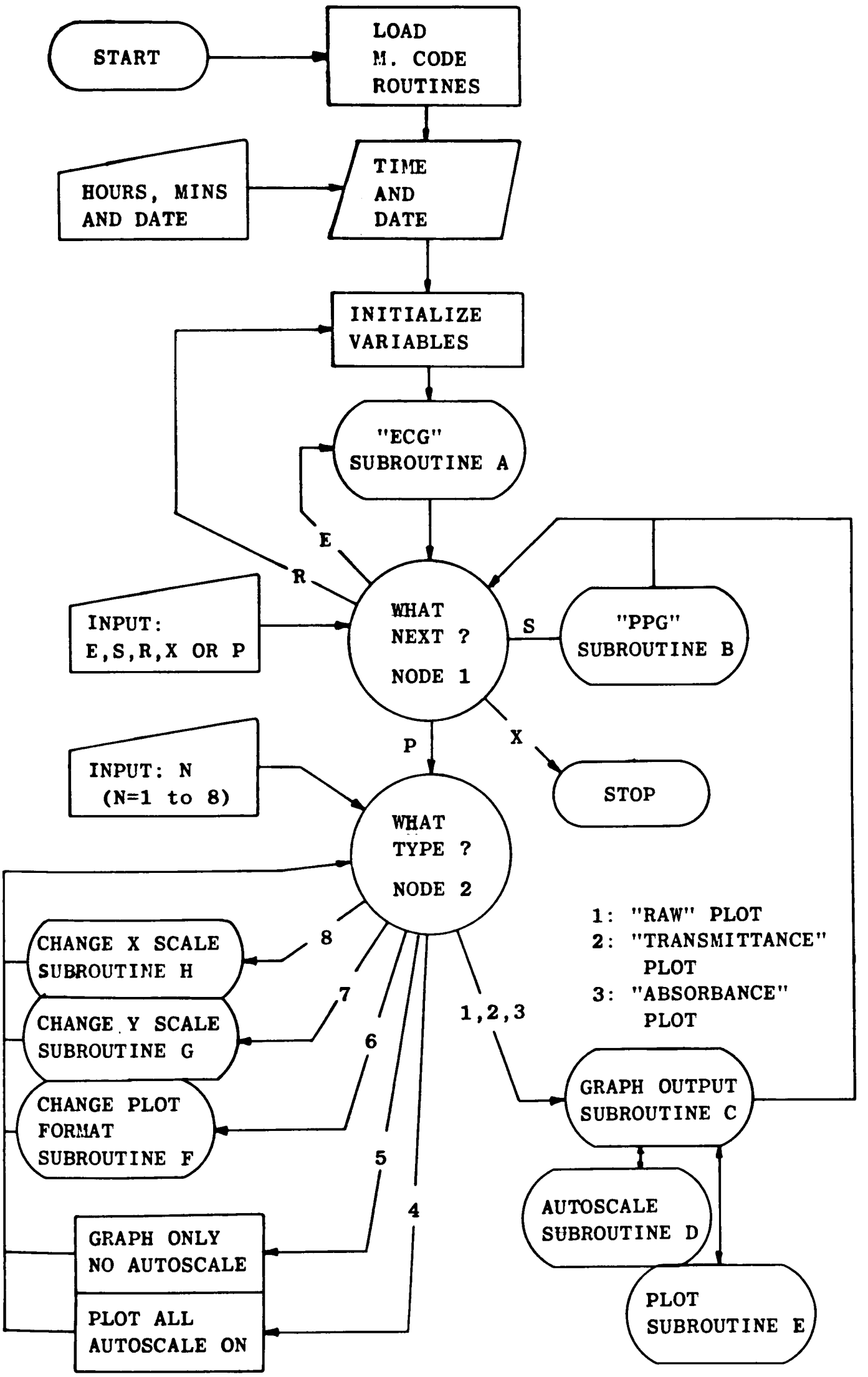

Figure 7.5 Overall flow dagram of the programme.

consecutive PPGs, synchronised to the R-wave peak of the ECG. This is

shown diagramatically in Figure 7.6 and is essentially the same technique used with the scanning spectrophotometer (see Figure 3.21).

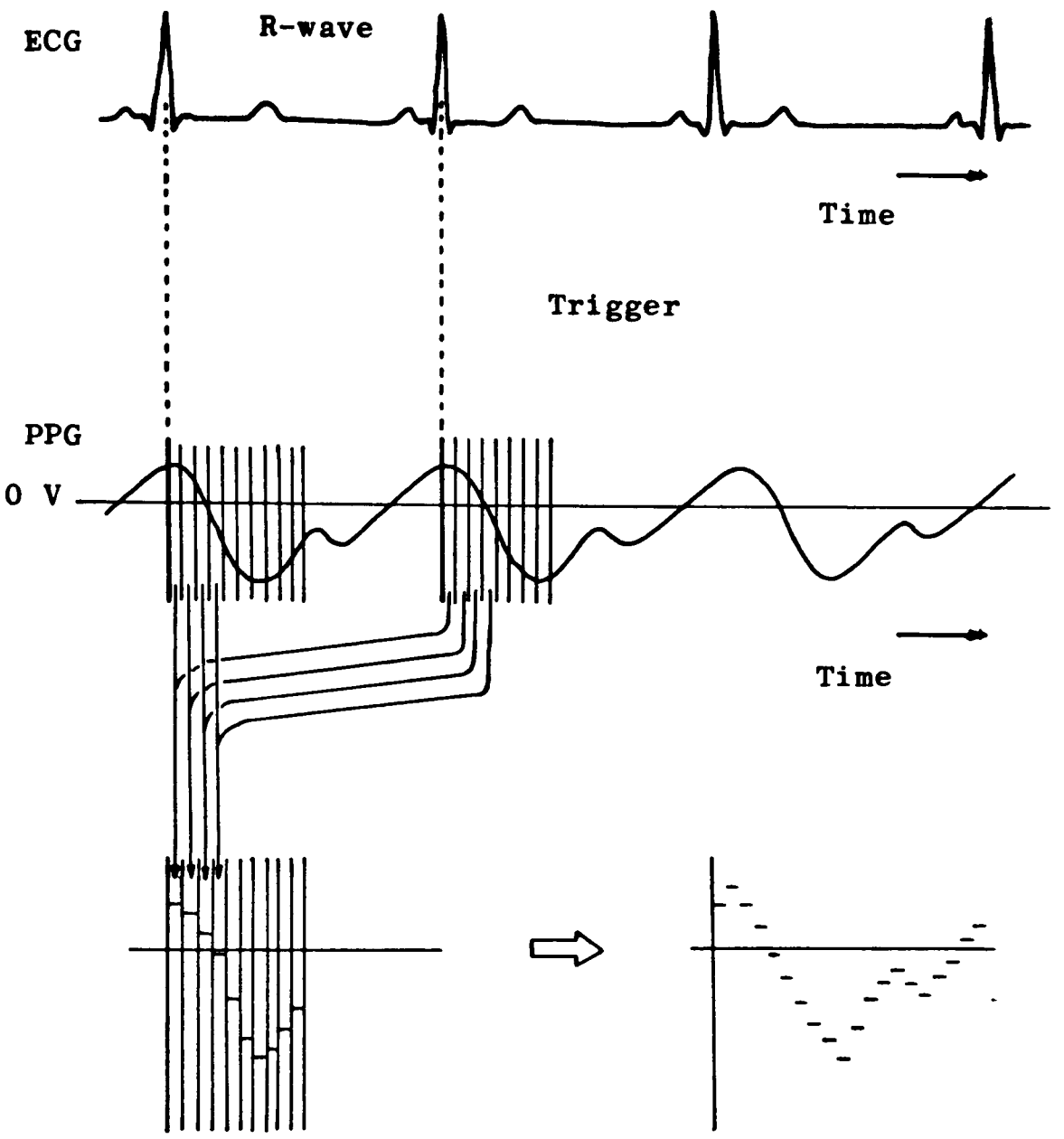

Figure 7.6 Diagram illustrating how the summation of corresponding samples from consecutive PPGs is synchronised to the R-wave of the ECG.

With reference to Figure 7.5 the following is a brief description of the programme which operates the instrument. More details are given in the sections below.

Upon entering the programme the machine code routines are loaded and the date and time requested. The "ECG" subroutine (Subroutine A,

Section 7.5.4) is then called, during which the ECG is continously sampled for a specified period and the minimum and maximum signal levels recorded. These levels are subsequently used in the R-wave peak detection algorithm within the PPG routine.

The first point at which the user must choose the next operation is then reached (Node 1. see Section 7.5.5). From here one possible option is to call the "PPG" subroutine (Subroutine B, see Section 7.5.6), which forms the core of the programme and with the aid of the machine code routine controls the interrupt driven sampling, and the summation and storage of the PPG. Summation of consecutive PPGs is triggerec using an R-wave peak detection algorithm. Available memory allows up to 10 specific sampled and summed PPGs to be stored.

After the "PPG" routine the programme returns to Node 1 again. A further option from here is to select graphical ouput (enter "P") which leads to Node 2 where various options are available as also described in Section 7.5.5. The options concern the choice of output routines (see Section 7.5.7) used to obtain graphical hardcopy output from the HP7475A plotter. The summed values for the required PPG are averaged, processed plotted (see Section 7.4.2) with three types of output are available.

Additional subroutines allow changes to the format of the plots.

7.5.4 "ECG" Subroutines.

The purpose of these subroutines are to continuously sample the ECG for a given period and record its minimum and maximum levels. These two values are then used in the R-wave peak detection algorithm.

7.5.4.1 Interrupts.

PPG sampling is interrupt driven; that is a sample is taken every time an interrupt occurs. The interrupts are issued (on Level 4) at regular intervals timed using an interval timer (TMS 9902 Asyncronous Communication Controller (TI)). Upon detection of an interrupt the timer is reloaded (and hence begins counting down to the next interrupt) and a sample taken.

The interval between interrupts can be set to any value of t ms where:

$$t = (0.064)\ N \qquad 0 < N < 256 \text{ and integer.} \qquad 7.4$$

which gives a range from 64us to 16.32ms.

Interrupts are introduced in this section because the ECG machine code routines also use interrupts to time the required duration of ECG sampling, (not its sampling rate which is maximal). Furthermore, the interrupt interval chosen during the ECG subroutine is the one used for subsequent PPG sampling and hence sets the sampling rate (a new rate can be selected by re-executing the "ECG" subroutine).

7.5.4.2 "ECG" BASIC Subroutine.

The flow diagram for this routine (Subroutine A) is shown in Figure 7.7.

Firstly, the required interrupt interval is entered together with the

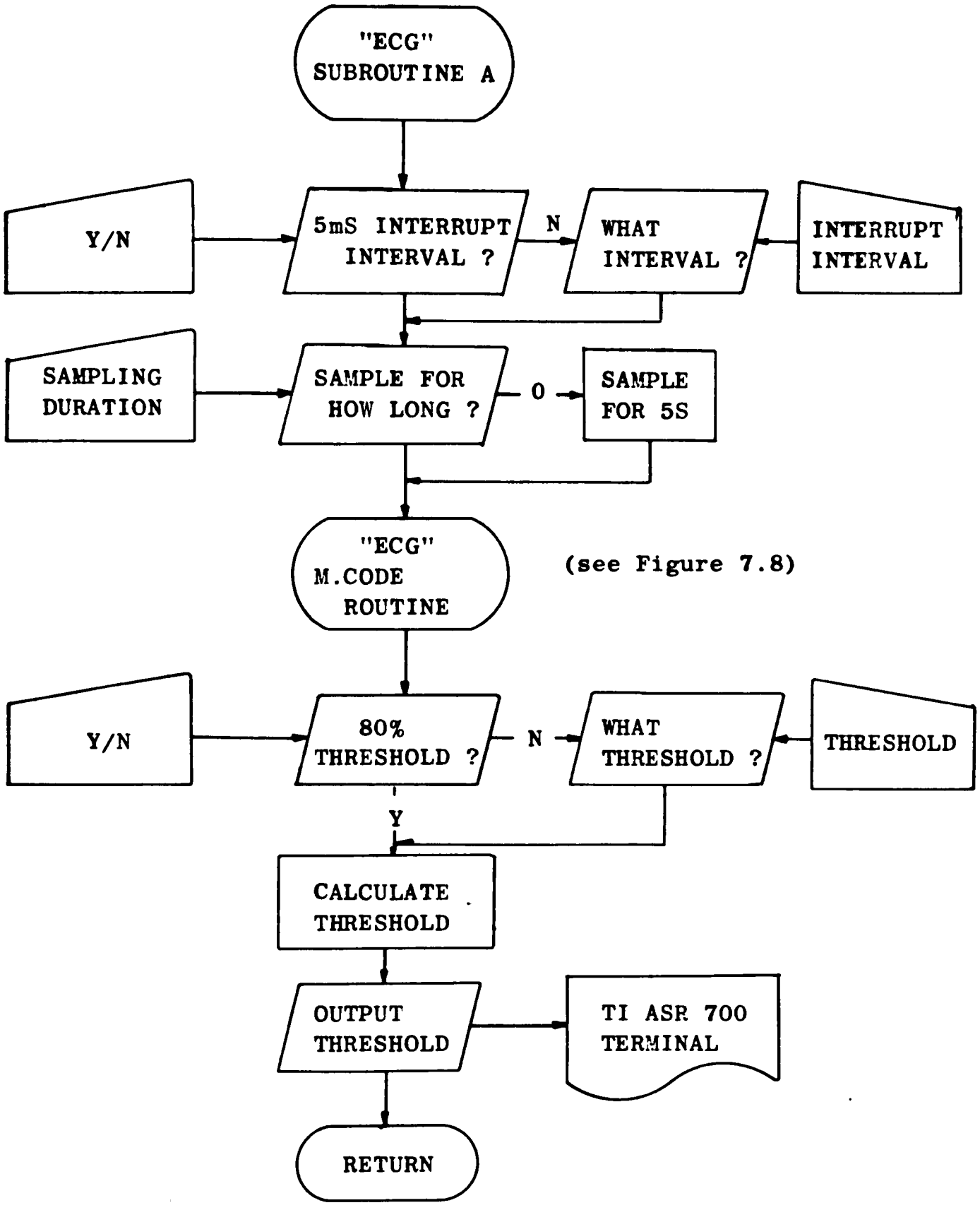

Figure 7.7 Flow diagram of "ECG" BASIC subroutine.

duration of ECG sampling. The default interrupt interval is approximately 5ms giving a PPG sampling rate of 200Hz, with a default sampling time of 5 secs. The values are required for the machine code routine which is then executed (see below). On exit a "threshold" value

is calculated as a chosen percentage (with a default value of 80%) of the difference between the maximum and minimum recorded levels of the ECG. This "threshold" value printed at the terminal for validation, and subsequently used in the R-wave detection algorithm (see Section 7.5.6.1).

7.5.4.3 "ECG" Machine Code Routine.

The ECG is continuously sampled approximately every 30 µs, and the sample value stored if it is either the highest or lowest signal level yet sampled.

The duration of sampling is timed using interrupts (whose rate is set in the BASIC subroutine), which when they occur cause a counter to be decremented. Sampling continues until this counter has reached zero, that is after a period (the sampling duration) given by the product of the interrupt interval and the initial value of the counter. The flow diagram for this routine is given in Figure 7.8.

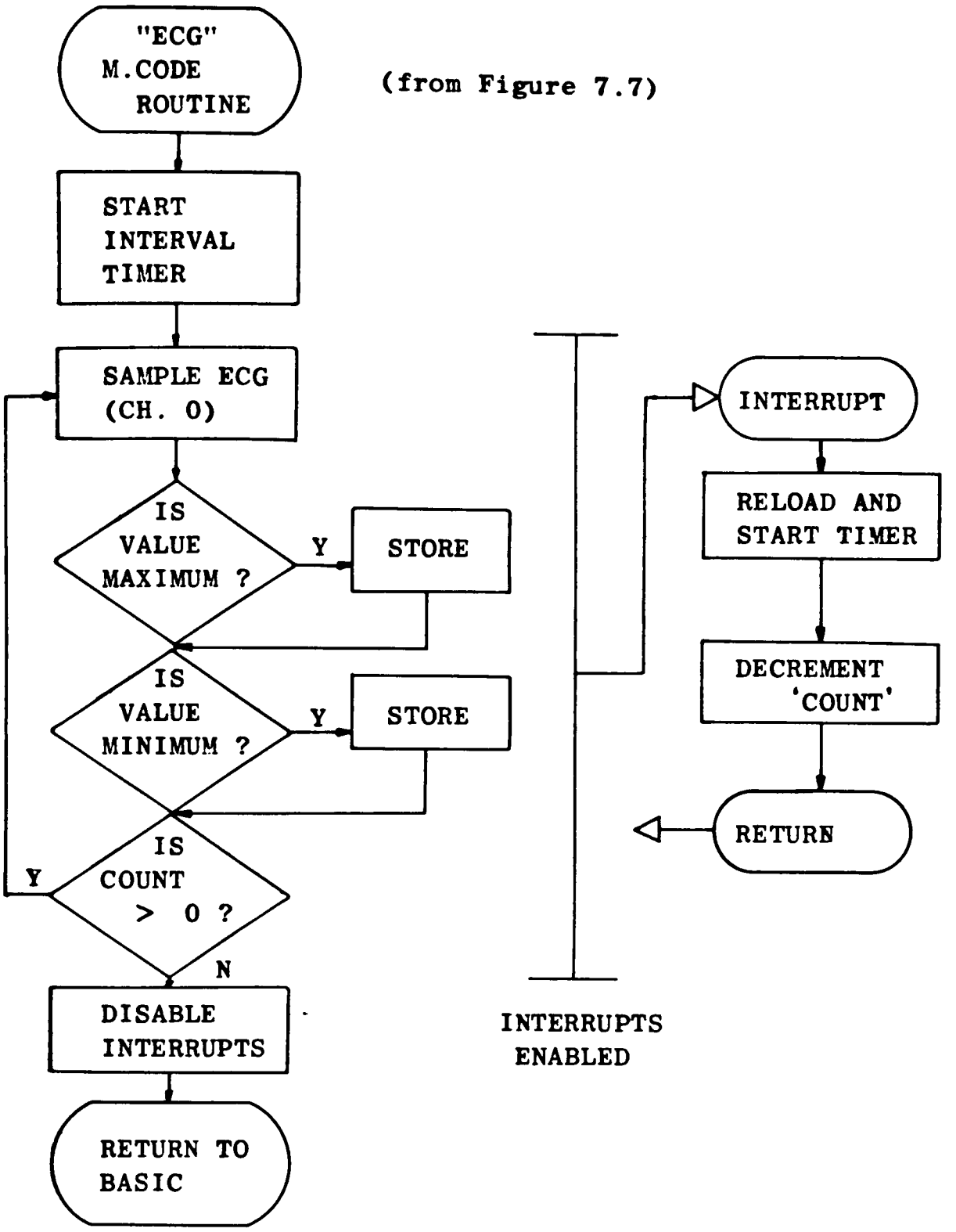

Figure 7.8 Flow diagram of "ECG" machine code routine, including the interuppt service routine.

7.5.5 User Selection of Programme Options.

There are two points in the programme. (Nodes 1 and 2 in Figure 7.5) where the user must choose the next operation (eg plot or sample) rather

than simply the value for a parameter. The first is Node 1, where the next operation must be chosen, the second Node 2 where the action concerning the hardcopy output is decided.

Node 1: "What Next?"

Option : E Execute "ECG" subroutine again.

S Sample and store incoming PPG.

R Restart.

P Obtain graphical output.

X End program.

Node 2: "What Type of Plot?"

Option: 1 "raw" AC-coupled plot.

2 Normalised "transmittance" plot.

3 Normalised "absorbance" plot.

4 Plot graph only, no axes or labels.

No ordinate autoscaling

5 Plot graph, axes and labels.

Autoscaling on.

6 Choose new pen speed and colours.

7 Change ordinate scaling.

8 Change abscissa scaling.

The functions for options 4-8 are of the same type of those used in the scanning spectrophotometer routine (Section 3.5.6.6).

7.5.6 "PPG" Subroutine.

The "PPG" subroutine controls the sampling, summation and storage of the PPG, it also contains the R-wave pulse detection algorithm used to initiate summation. Because parameters used during peak detection can be altered interactively in BASIC the peak detection algorithm (which is implemented in machine code) is described first followed by the BASIC and finally the machine code routines.

7.5.6.1 R-Wave Peak Detection.

The peak of the ECG's R-wave is used to initiate summation of the sampled PPGs (see Figure 7.6). The peak is found by detecting the change of slope (from positive-to-negative) at the top of the wave. This is accomplished by taking pairs of consecutive samples from the ECG and checking whether their difference is positive or negative.

A basic form of noise suppression is provided by the ability to select the number of pairs of points indicating a negative slope before peak detection is accepted. A consequence of this is that for a clean signal triggering will be delayed by t us given by:

$$t = 2\,(N-1) \,/\, f \qquad 7.5$$

where N is the number of pairs of samples used and f is the ECG sampling rate in μs.
However, in practice f is so large that any error introduced is negligible.

The above method will detect any slope change (and hence peak) and therefore some means of prohibiting false triggering from the P and S complexes of the ECG is required. This is provided by the use of the "threshold" value computed in the ECG subroutine (Section 7.5.4.2). Basically the slope change algorithm is implemented only when the ECG

signal level is above the "threshold" value and therefore above the level of the P and S complexes. (The R-Wave peak detection algorithm is written in assembly language, shown in Figure 7.10 and described in Section 7.5.6.3).

Once an R-wave peak has been detected the search for the next one is delayed for a specified time to allow the ECG signal to fall below the threshold level, and hence prevents immediate implementation of the peak search algorithm.

7.5.6.2 'PPG' BASIC Subroutines.

The BASIC subroutine (Subroutine B) is used to allow the user to select certain parameters and to call the assembly language routines. The flow diagram is shown in Figure 7.9. The required number of PPGs to be sampled is the only parameter which must be entered for the programme to run, with the others taking default values.
However, two parameters used in the peak detection algorithm: namely the number of pairs of samples which are needed to indicate a negative slope and the number of samples taken before peak searching is resumed can be altered from the BASIC routine. (Default values are 6 and 50 respectively.)

Once the necessary input has been given the "bell" is sounded to indicate that sampling is to begin and the machine code routine called. Upon exit the time is recorded and subsequently used to annotate the graphical output. The user must also input the DC output voltage from the photodetector when requested which corresponds to the mean "dc" light intensity detected from the tissue. This is subsequently used for normalising the PPG for the "transmittance" and "absorbance" plots as described in Section 7.4.2.

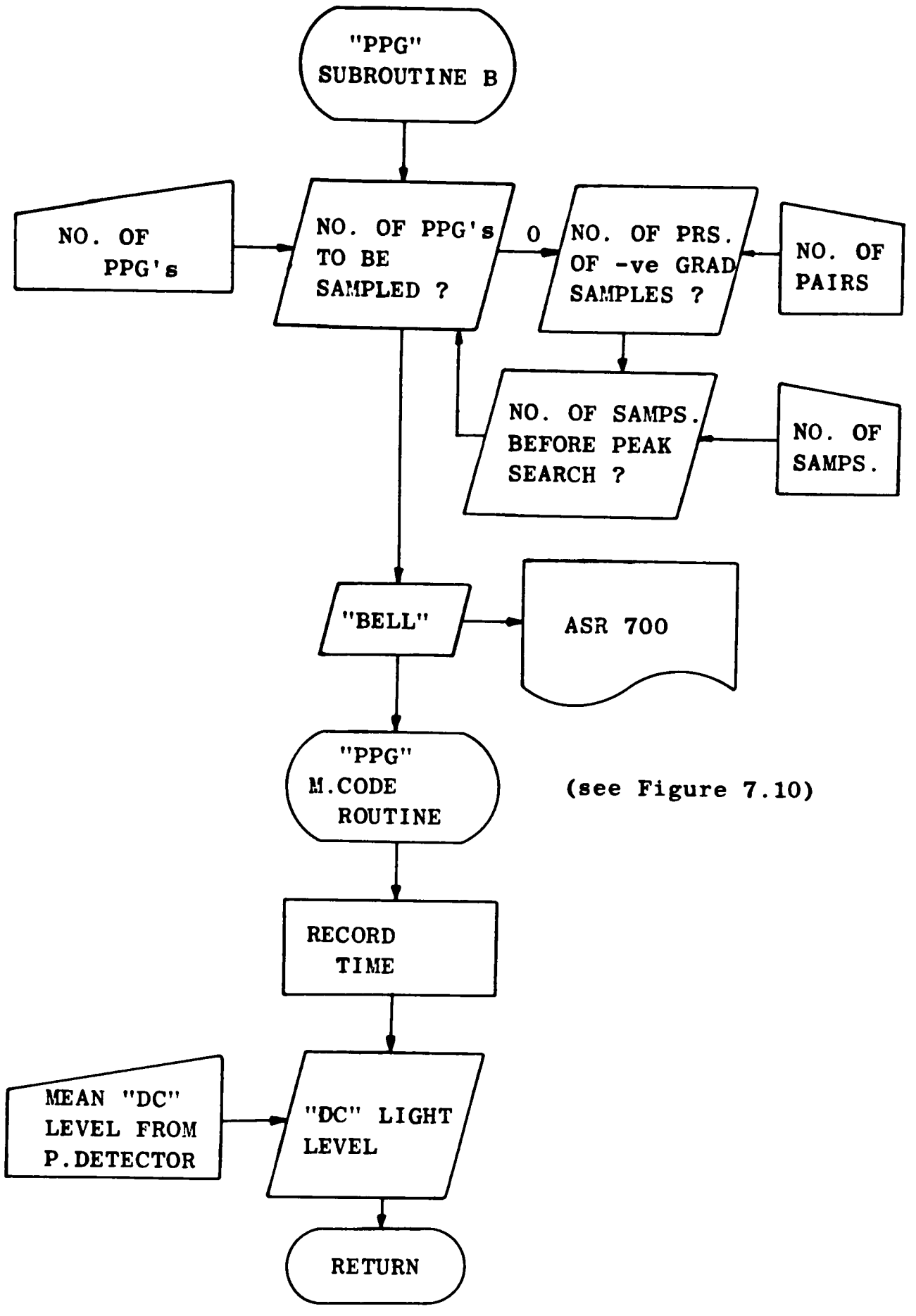

Figure 7.9 Flow diagram of "PPG" BASIC subroutine.

7.5.6.3 "PPG" Machine Code Routine.

This routine performs interrupt driven sampling of the PPG with the

summation of corresponding samples from consecutive PPGs being synchronised to the R-wave peak of the ECG. Once the required number of PPGs have been sampled and summed the data is stored together with other relevant parameters.

7.5.6.3.1 Peak Detection.

The flow diagram of the peak detection algorithm previously described in Section 4.3.1 is shown in Figure 7.10.
Before sampling of the PPG is begun (ie upon initially entering the routine) the interrupts are disabled and the ECG R-wave peak detection algoritm is executed uninterrupted.

However thereafter upon implementing the algorithm. interrupts will be enabled and the PPG sampled at the selected interrupt interval rate. This means the peak detection algorithm will be periodically left, the PPG sampled, and the algorithm returned to. However, due to the relatively short time that sampling takes the ECG and PPG appear to be sampled simultaneously. Because of the interrupts and the structure of the algorithm an exact value for the rate of ECG sampling cannot be given, although it is estimated to be about 30 μs.

7.5.6.3.2 Control of PPG Sampling.

This is shown in Figure 7.11.
Once the R-wave peak has been detected the countdown of the interrupt interval timer is started and the PPG sampled. If the PPG has already been sampled then if the number of samples taken is the minimum or maximum for this PPG then the value is recorded. (These values are subsequently used in the production of the output).

The number of PPGs sampled is then incremented and if equal to the

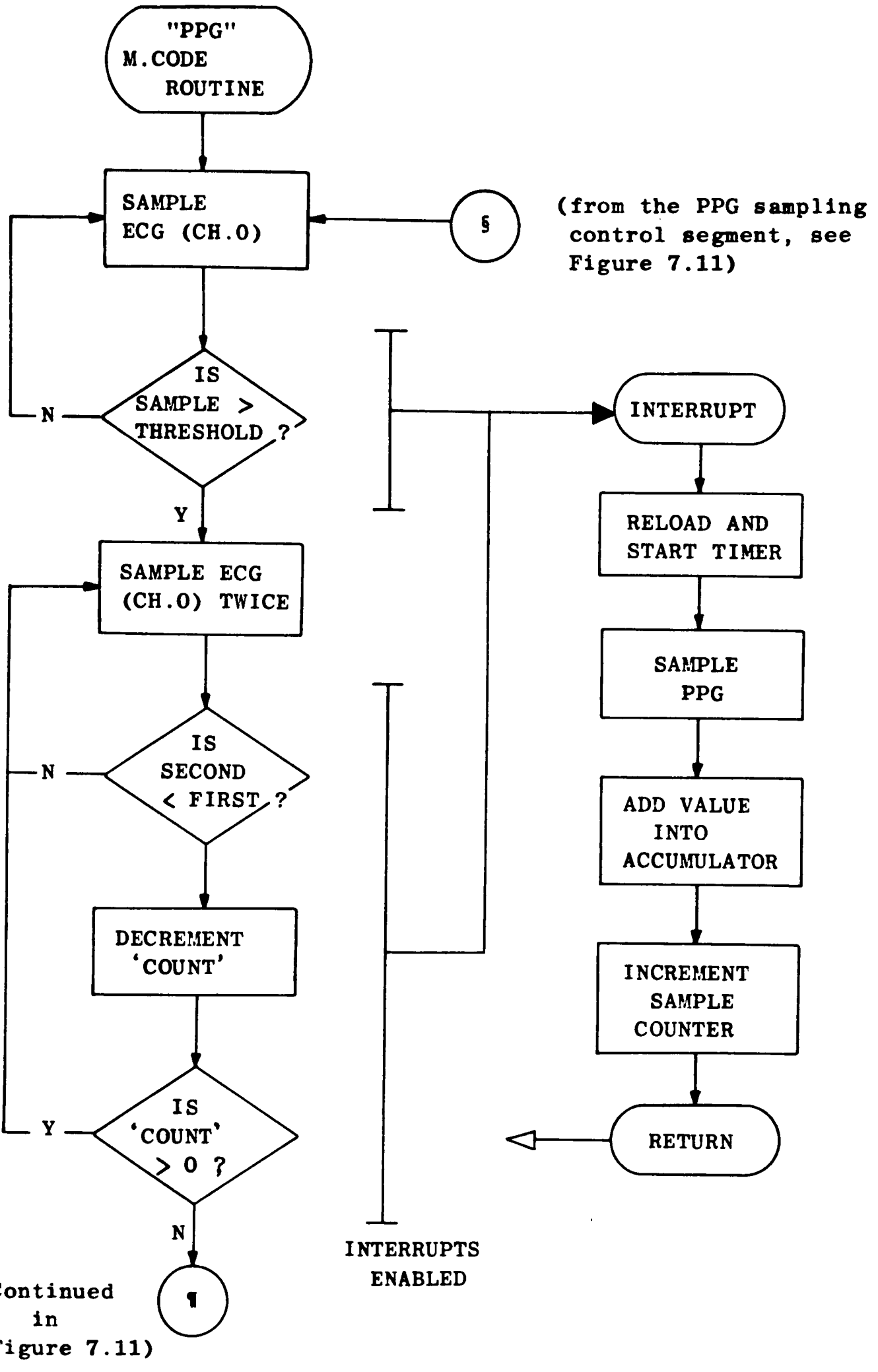

Figure 7.10 Flow diagram of the "PPG" machine code routine ("R-wave peak search segment"), and interrupt service routine. (See also Figure 7.11).

number requested from BASIC then the storage segment is entered (next

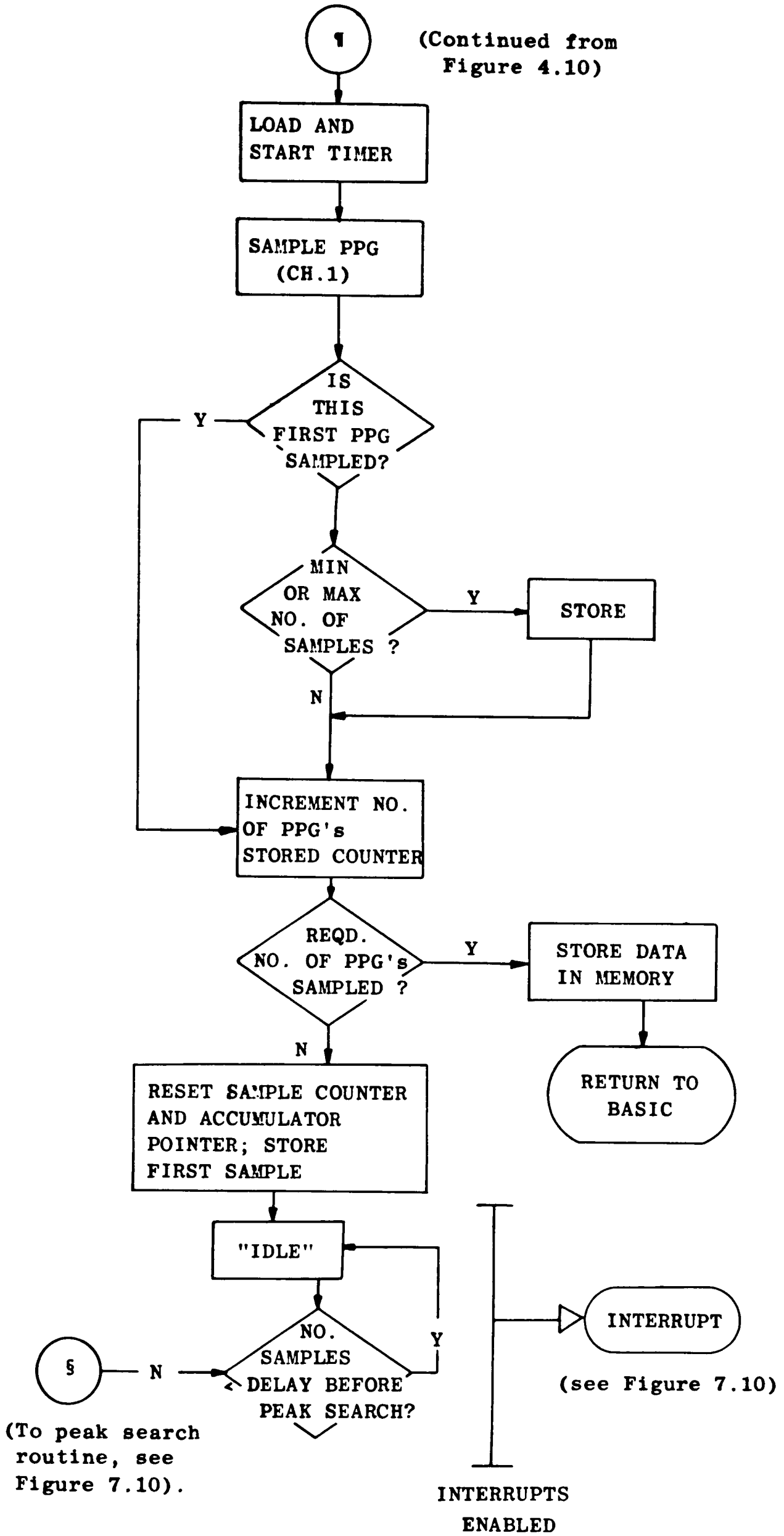

Figure 7.11 Flow diagram of the "PPG" machine code routine (PPG sampling and summation segment). See also Figure 7.10.

section). Otherwise, various counters and pointers used to control and monitor sampling and summation of the PPG are reset and the interrupts enabled.

The programme then waits at the IDLE command until an interrupt is received causing the PPG to be sampled. (This will be the second sample from the current PPG and all of the above will have been performed in approximately 70μs between the first and second samples, therefore not compromising the sampling rate.)

The programme then continues to cycle through sampling the PPG upon interrupt and waiting at the IDLE statement until the number of samples taken corresponds to the delay required for the ECG to fall below the threshold value necessary to prevent false triggering. Once sufficient samples have been taken for this purpose then the R-wave peak detection algorithm is re-entered and executed whilst the interrupt driven PPG sampling continues.

Because ECG sampling must be completed (on A/D channel 0) before the PPG can be sampled (on channel 1) the interrupts are disabled as marked in Figures 7.10 and 7.11. This introduces a time delay between interrupts because if an interrupt occurs whilst the ECG is being sampled it must wait to be serviced. That this is indeed the case could be seen by using a sensitive means of monitoring sampling period (see Appendix E),and comparing PPG sampling when performed alone (when cycling with the IDLE command) to that together with ECG sampling. In practice the time delays are too small to be significant. when considered in terms of the frequency spectrum of the PPG and the actual sampling rate of the PPG.

Upon peak detection, sampling of the PPG is halted (interrupts disabled) and the processes described in this section repeated again

commencing with reinitialisation of the interrupt timer and taking the first sample from the PPG after the R-wave peak. The sampling period of the PPG can be set in the "ECG" BASIC subroutine from 64μs to 16.32ms in steps of 64μs (see Section 7.5.4.1).

7.5.6.3.3 Storage segment.

When the required number of PPGs have been sampled and summed the storage segment of the programme is implemented. This reads the summed values (from the memory locations reserved for summation) to an area of memory set aside for data storage. The number of PPGs sampled, and the minimum and maximum number of samples recorded in any one PPG are also stored. There is enough memory space to store upto 10 PPGs of 400 samples each

7.5.7 Output Routines.

Three types of graphical output are available, the "raw" PPG as it appears at the AC-coupled output of the photodetector, or the PPG normalised with respect to the "dc" light level either as a "transmitance" or an "absorbance" plot.

The graph's ordinate represents time after R-wave peak detection and the abscissa the actual or normalised increase and decrease in light level detected. The number of points plotted is determined by the minimum number of samples taken for any one of the summed series of PPGs.

7.5.7.1 Processing of Stored Summed Sample Values.

Subroutine C performs this function and is entered when graphical output is requested at Node 2. The user must then input the storage number of the PPG which is to be plotted. The summed sample values of this PPG are then averaged and processed, and stored in a BASIC variable array ready for plotting. The other stored parameters are also read into BASIC variables and processed for use in controlling plotting and/or annotating the graph. The processing used is dependent upon the type of plot required.

7.5.7.1.1 "Raw" Plot.

This plots the PPG as it was input to the A/D converter, except that it will have been averaged, and therefore the ordinate represents voltage. The actual values plotted are simply the summed sample values divided by the number of PPGs sampled.

7.5.7.1.2 "Transmittance" Plot.

With this type of plot the voltage input to the A/D converter (ie

after AC-coupling or DC-offsetting) is normalised with respect to the mean "dc" voltage level input by the user. The ordinate represents the increase or decrease in light level as a percentage of the mean "dc" level (see Section 7.4.2).

7.5.7.1.3 "Absorbance" Plot.

The "absorbance" type plot is fundamentally the same as the "transmittance" type in that the input signal is normalised with respect to the "dc" voltage. The difference is that in this plot the ordinate represents an increase or decrease in (negative) absorbance.

7.5.7.2 Plotting the Graph.

Once the ordinate values of the sample points have been calculated by one of the methods just described then the plotting can be performed. If required scaling of the ordinate axis can be adjusted automatically by the "Autoscale" subroutine (Sub D) to ensure a satisfactory plot for the calculated values. The actual plotting on the HP7475A is performed by the "Plot" subroutine (Sub E).

In addition to plotting the requested PPG, the time at which the sampling finished is given, together with the number of PPGs sampled and summed, the sampling period and the minimum and maximum heart rates.

If required the frame, axis and labels can be omitted to enable several different PPGs to be overlaid (with the autoscale function overidden although this can be reversed whenever necessary). Plotting of the PPG can be aborted at any time.

7.5.7.3 Control of Output Format.

Three subroutines allow the follwing to be changed:

(i) X-axis scaling. (Sub H)

(ii) Y-axis scaling (which overides the autoscale facility)
(Sub G)

(iii) Pen Speed and colours for the frame, axis and labels
and graph. (Sub F)

7.6 Results and Discussion.

7.6.1 Introduction.

Upon using the instrument to study PPGs it soon became apparent that so many variables are involved that a comprehensive investigation could not be performed in the available time. However. some extremely interesting results were obtained (all from the same male caucasian subject) wnich may have some bearing on the use of the PPG in clinical instrumentation. and certainly serve as a guide to what future studies could be undertaken with the instrument.

The studies performed included looking at the following. Variations in the PPG from the finger in both reflection and transmission modes at different wavelengths. The effect of larger incident light levels on the PPG, and the amount of DC-blocking used to remove the "dc" photoplethysmogram. The use of different active diameter. and discrete. as against bifurcated fibre bundles.(ie transducer geometry) and finally attempts to record inverted PPGs.

A typical plot from the PPG recording instrument is shown in Figure 7.12. It is not of a PPG but the output from an ECG simulator, wnich was fed into both ECG and PPG input channels. The trace shows how the summing and averaging uses the peak of the R-wave as its trigger and illustrates the annotation given on a typical trace. "Raw" indicates no processing was performed on the incoming signal which was sampled at intervals of 4.992 ms (the closest to 5ms available), and averaged over 10 complete ECGs with a heart rate varability (calculated from the beat-to-beat interval) of 59-60bpm. The time and date of the record is shown in the top right hand corner. whilst no mean "dc" level of the incoming signal was entered for normalisation. Headings can be added as required

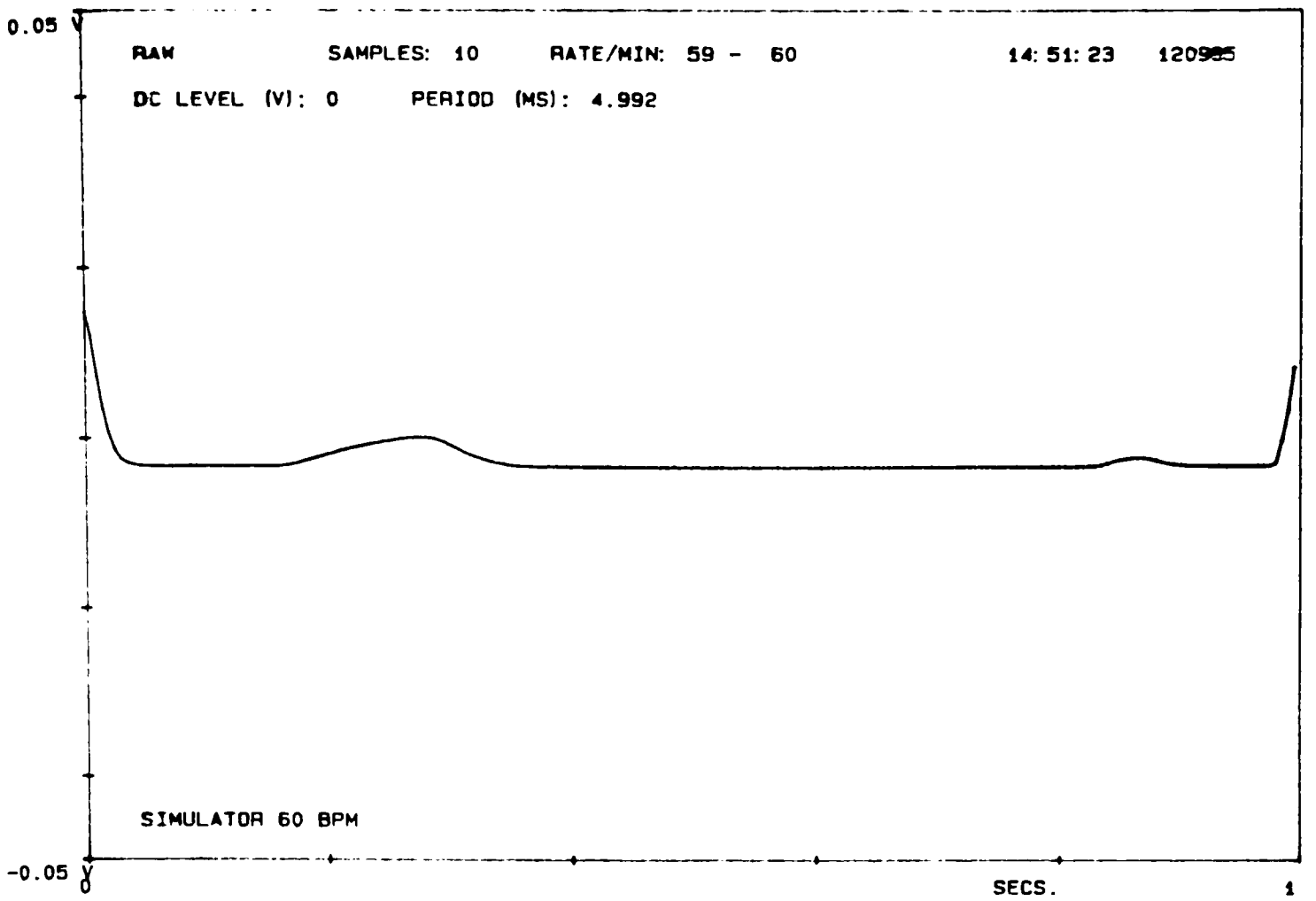

Figure 7.12 Typical graphical output from the PPG recording instrument showing the output from an ECG simulator.

and are printed at the bottom of the trace.

7.6.2 Basic Shape of the PPG and the effect of AC Coupling.

In Section 7.4.1 the intention to offset the "dc" pedestal and then record the PPG with no DC-blocking in these studies was described. In practice once the "dc" bias had been offset there was still sufficient "dc" fluctuation (ie "dc" photoplethysmogram) that after amplifying the signal its mean level was so unstable that some kind of DC-blocking was necessary. This was achieved using a simple high pass filter (see Section 7.5.2).

Because of the enforced use of this filter the opportunity was taken to investigate the extent to which this type of filtering affected the

shape of the PPG.

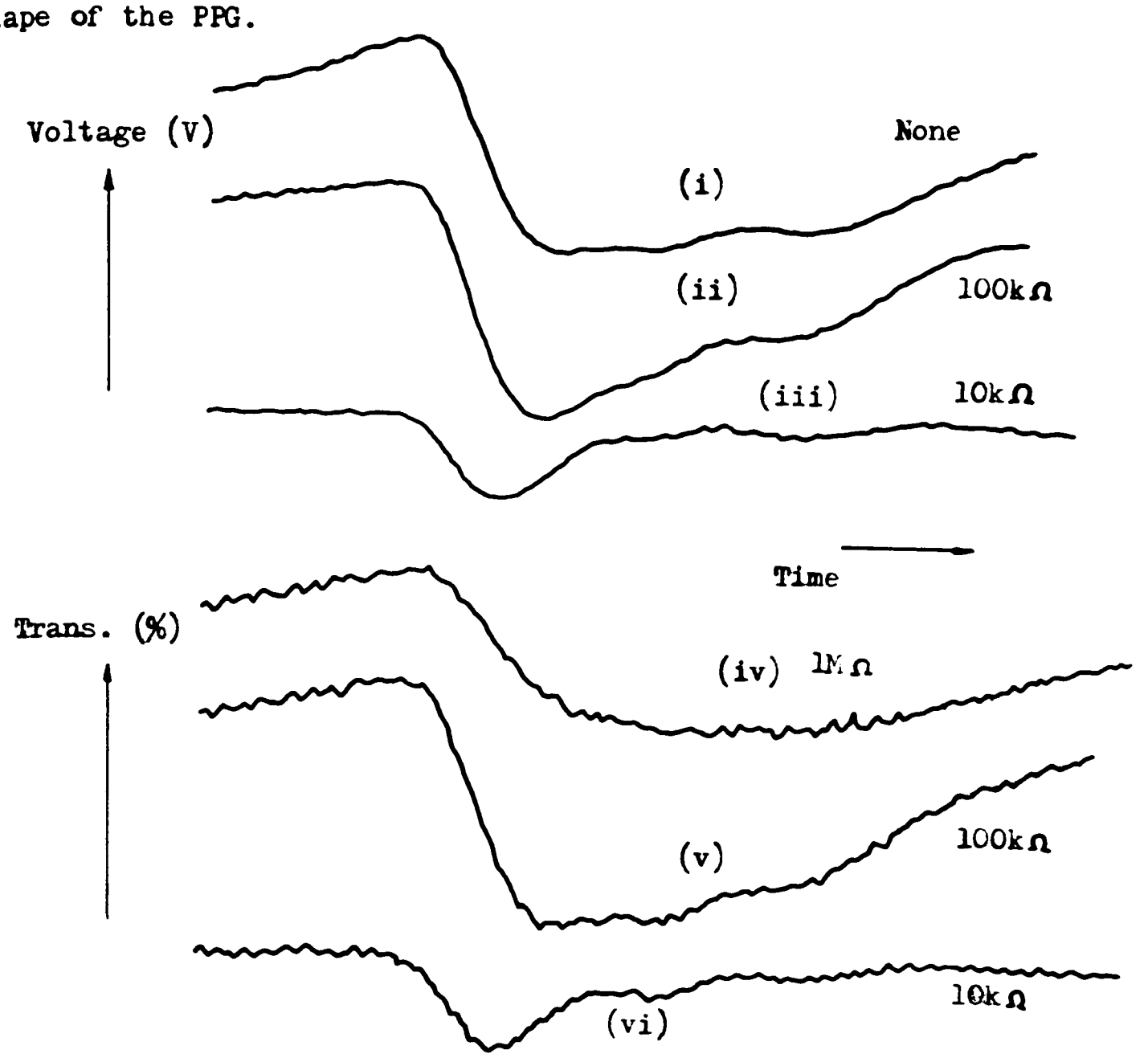

Figure 7.13 Effect of filtering on the PPG (as indicated) from: i)-iii) thumb using white light, large bifurcated fibre and photodiode ("Raw")
iv)-vi) finger using 600nm light, two small fibre budles and PMT. (transmission)

A capacitor of 3.3μF was used with resistors of 10kΩ, 100kΩ and 1MΩ (giving 3db down points of 5, 0.5 and 0.05 Hz). The effect of the filtering on the PPG was quite significant as demonstated in Figures 7.13 which snow PPGs obtained (with conditions given in the figures) using the different value resistors.

The traces show that as the DC-blocking (AC-coupling) increases with smaller value resistors used, so the PPG assumes the shape usually seen in the majority of publications. (This is because if the PPG is studied over a long period then a relatively large amount of DC-blocking is usually required to restrict the drift due to the "dc" photplethysmogram.

The pulse shape consists of two basic peaks seperated by a notch (the dichrotic notch), and is common to pulses associated with other variables such as those seen in traces of volume pulsations or obtained when using electrical impedance plethysmography or performing arterial pressure measurements.

With lesser amounts of "dc" blocking the pulse assumes a much less "angular" shape with three rather than two separate pulses visible (see further figures also) and a much longer sustained decrease in signal after the initial fall. (This is not surprising since it represents a rapid shift in the "dc" level whose lower frequency components would be removed by DC-blocking).

The two peaks of the filtered PPG separated by the dichrotic notch are generally considered to be due to the pulse wave generated by the rapid expulsion of blood from the heart followed by the closure of the aortic valve. Whether the three pulses observed in the unfiltered PPGs can be seen at all sites on the body or are peculiar to the finger is an area for further investigation, and may be linked to variations in the shape of PPGs obtained from different sites as discussed below.

Since PPG shape is likely to be related to the elasticity of the vessels it may provide information concerning the physical state of the vasculature.

The fundamental question behind the shape of the PPG is essentially what its frequency spectrum is, and for this reason frequency analysis would be of value.

Little information concerning the frequency range of instrumentation used for obtaining PPGs is available. In his review CHALLONER (1979) remarks that although the fundamental period of the PPG is approximately

1Hz (ie cardiac frequency) components up to 30Hz are present, later commenting that a low pass filter operating at 30Hz is used to remove extraneous noise from "mains interference". He also commented on the use of AC-coupling the input to prevent overloading from the large DC-offset (ie the filtering under investigation here) but gives no details of the filters employed, whilst in their study of the PPG TAMURA (1985) calculated the PSD over the range 0.1Hz to 10kHz.

In conclusion, further studies on the frequency spectrum of the PPG that would enable the effect of filtering to be predicted are considered to be warranted. This type of study is intrinsically linked with those concerning measurements at different sites and of the inverted PPG as described below.

7.6.3 PPGs From Sites Other Than the Finger.

The majority of the studies performed were on the finger, where it was noticed that it was easier to obtain noise free PPGs in the transmission rather than the reflection mode (which may be partly due to a greater susceptibility to movement artefacts in reflection mode).

Despite this a few PPGs were recorded in reflection mode from other sites such as the palm of the hand just below the thumb, the temple and radial artery. The results suggested that the PPG shape may depend upon position, and this aspect of the work merits further investigation. In transmission mode PPGs were obtained at near-IR wavelengths through the wrist, and examples are shown (at 760 and 830nm) in Figure 7.14. As can be seen from the traces 50 PPGs were averaged and less than 1% of the total transmitted light was pulsatile.

That PPGs obtained at different sites around the body may have fundamentally different shapes is known (see JENNINGS (1983)); and so

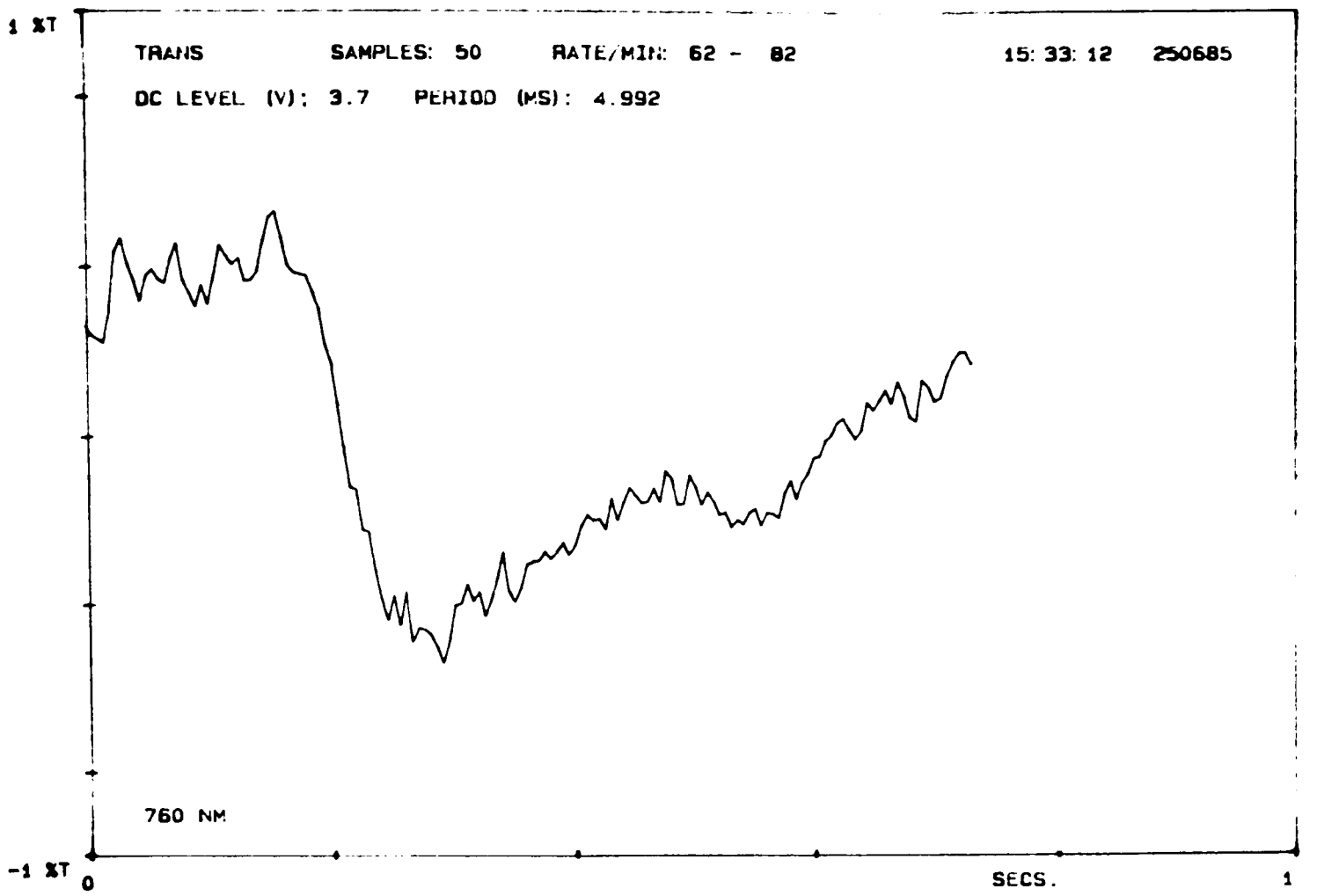

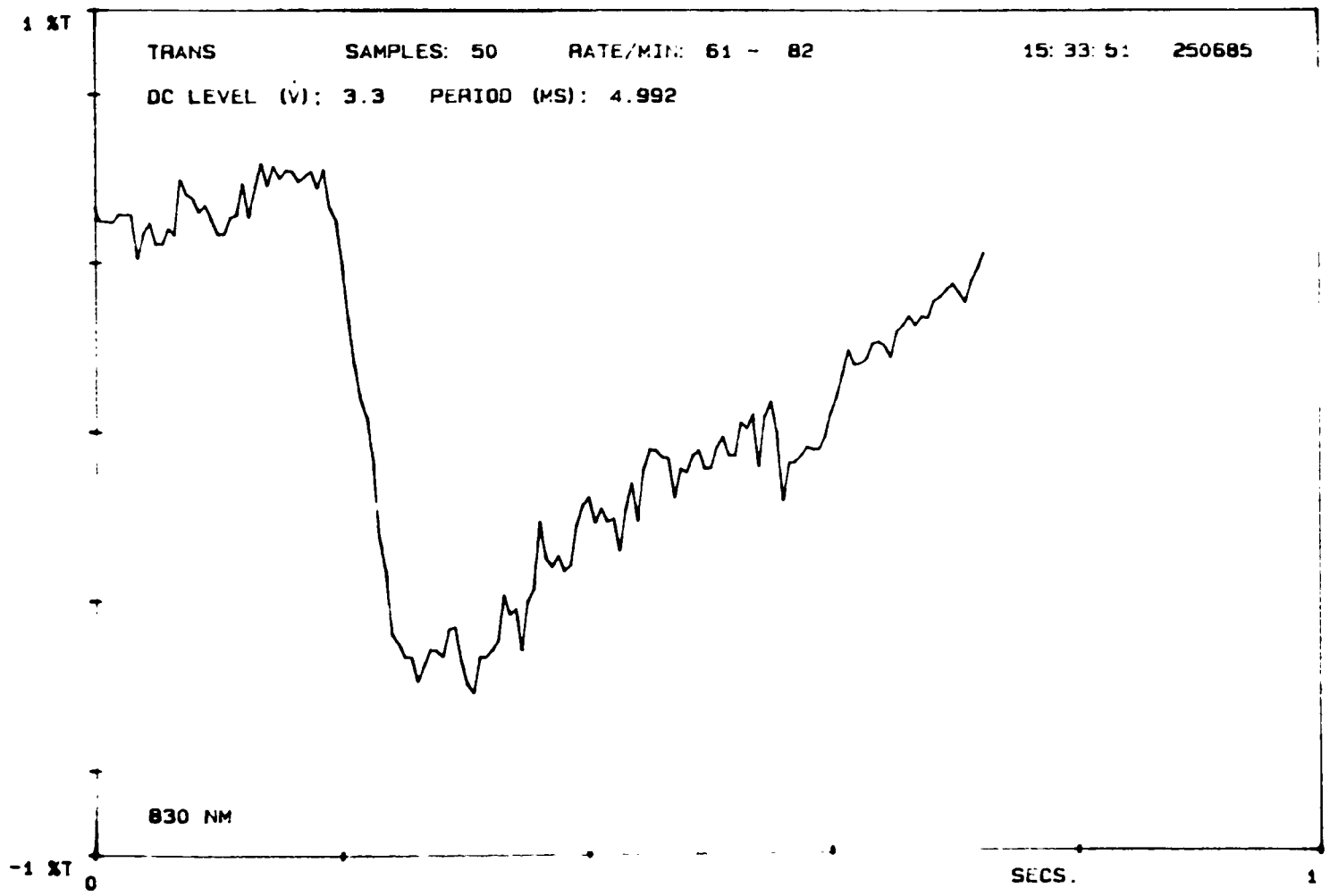

Figure 7.14 Reduced copies of PPGs obtained through the wrist at near-IR wavelengths using the PMT for detection.

these preliminary findings are of no surprise. Furthermore, as there are a

number of factors contributing to the PPG there may accordingly be several possible causes for a change in shape.

One effect that is known to affect the shape of the PPG is the time it takes the pulse to reach the measurement site after propagation from the heart (the PTT). This is because the different frequency components of the pulse travel at different speeds and consequently affect the shape as their phase relations alter. These phenomena are therefore related to the above section concerning the effect of filtering on the PPG.

7.6.4 Inverted PPGs.

Apart from the work of NIJBOER (1982) there have been no known thorough details of *in vivo* studies on the inverted PPG *in vivo*. For this reason efforts were made to obtain inverted PPGs from the finger using Nijboer's venous engorgement technique. However. inverted PPGs could not be reliably obtained, with the most likely cause of this failure being the lack of experience of the method, which once mastered would probably enable inverted PPGs to be readily observed.

Despite this failure, inverted PPGs were seen during the studies on the left wrist (above the radial artery). This is apparently an area where such PPGs can often be detected, depending upon the conditions such as transducer pressure. although the precise circumstances necessary are personally still unknown. The reason that inverted PPGs can regularly be obtained from this region is most likely associated with the presence of a large vessel close to the surface of the skin, and the interaction of the incident light with the vessel wall.

Traces of a normal and inverted PPG recorded during the same study on the skin surface above the left wrist's radial artery are shown in Figure 7.15. It is noticeable that the inverted PPG reaches its peak

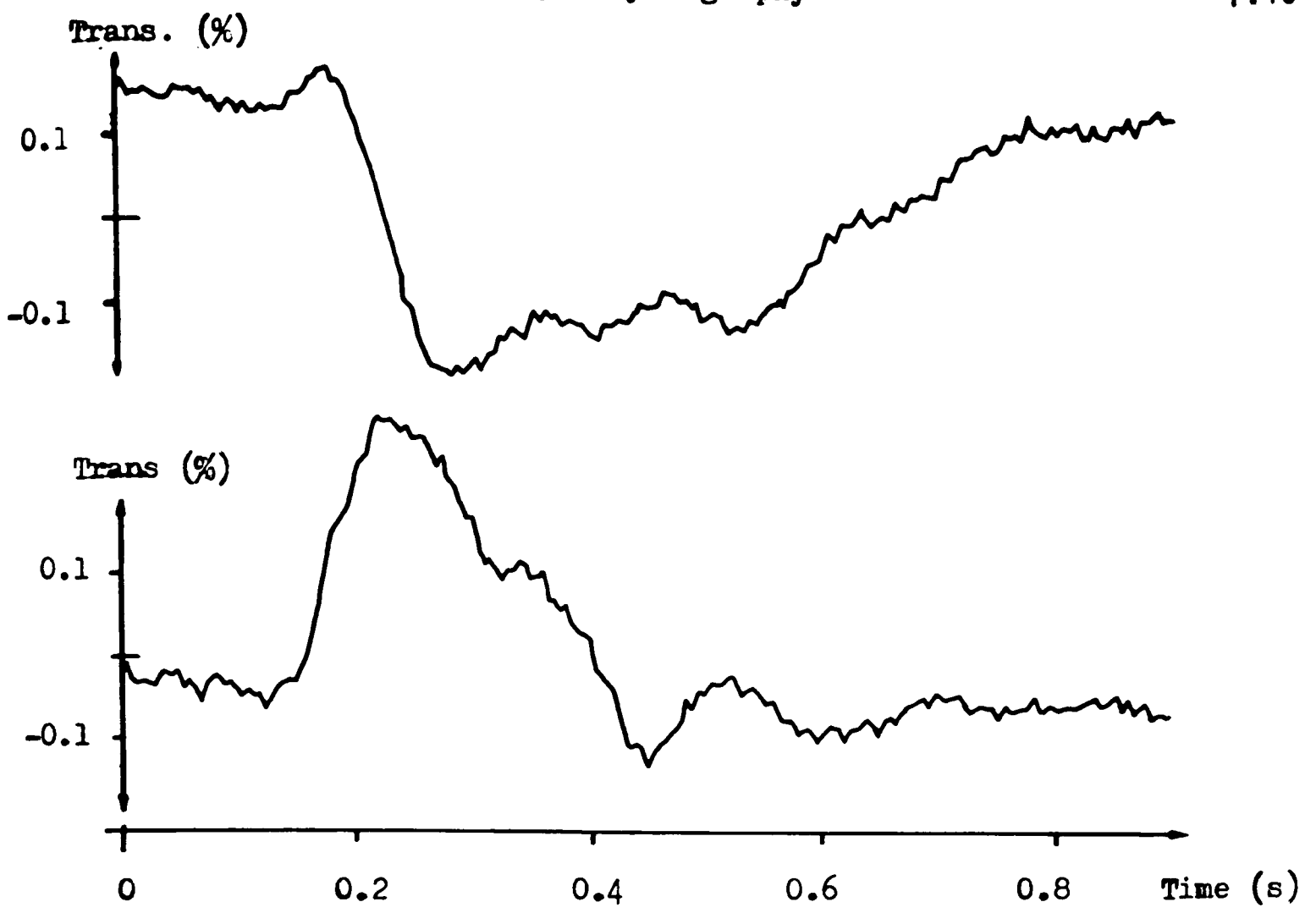

Figure 7.15 Examples of normal and "inverted" PPGs obtained from above the radial artery using white light and two small fibre bundles to "pipe" to and from the tissue.

(ie lowest light level) before the normal PPG, although insufficient data has been taken so far to conclude that this is always so. However, if this is the case it may provide information concerning the underlying differences between the two types of PPG. Further studies at a variety of wavelengths could also be useful as the wavelength dependency of the two types of PPG may differ.

7.6.5 Variations in the Magnitude of the PPG With Wavelength in Transmittance and Reflectance Modes.

The majority of PPG studies were performed on the finger in both reflection (using the large bifurcated fibre. the fabricated polymer bifurcated fibre and two 3mm bundles in close proximity) and transmission modes. Wavelength selection was by interference filter at the following

wavelengths: 440.550.590.600.760.810.830,840 and 905nm. However, after combining all of the results obtained using both the PMT and photodiode, from all of these preliminary studies some unexpected trends emerged.

These became evident after considering the amplitude of the "transmission" PPG (ie the percentage of the detected signal which was pulsatile as described in Sections 7.4.2 and 7.5.7.1.2) at the various wavelengths used (which were restricted by the available interference filters).

From the combined data it was found that in reflection mode, in the near-IR and down to 620nm, this amplitude was always below about 0.7%, wheras at 600nm and below the percentage "transmission" increased to levels of a few percent (ie typically 4-6%).

Although the limited number of filters in the region 400-600nm precluded further measurements and the data is not sufficient to come to any more definite conclusions, it is felt that these preliminary results show that at wavelengths below about 600nm the percentage of the reflected signal which is pulsatile is about an order of magnitude higher than it is at wavelengths above this value (over the range studied).

The significance of this variation is that it has similar characteristics as the absorbance of blood, a fact that is considered unlikely to be purely coincidental as discussed below. The amplitude of the PPG was also usually slightly larger at 550nm than 440nm.

Studies with the two small fibre bundles in close proximity (using the holder shown in Figure 6.1(iii)) showed a similar trend of a higher percentage of the signal being pulsatile below 600nm. although around 600nm in particular the limited data was very scattered. Nevertheless, the amplitudes were always higher than in the near-IR. where the data was

more closely grouped and had "transmittance" values of approximately 0.5-1.5%.

Finally. the results obtained of the amplitudes of the PPGs in transmission were even more scattered with no sign of a variation in amplitude of the "transmission" PPG with wavelength at all. although this could have been due to the limited data and insufficient sensitivity. However. from these preliminary results all that can be concluded is that in contrast to the reflection studies there is no obvious variation in amplitude with wavelength. with amplitudes of 2-10% most common at all wavelengths studied. (The highest values seen were from 590-620nm).

These results are potentially the most interesting to arise from these preliminary studies. They indicate that in reflectance mode using bifurcated fibre bundles (ie many "sources" and "detectors" very close to each otner) the amplitude of the PPG is inversely related to the absorbance of haemoglobin (although not linearly), whilst from the limited data no such clear observation could be made from the transmission mode studies, and the PPG appeared independent of wavelength, although the data was very scattered.

It is re-emphasised that the amplitude referred to is not the actual size of the pulsatile signal (ie the voltage, V, in equation 7.1) but rather the percentage of the detected light that was pulsatile, that is the value given by equation 7.2.

The studies with the two 3mm active diameter fibre bundles in close proximity gave results somewhere between those obatained in the reflection and transmission modes, suggesting a transition from a reflection to a transmission regime as was the case for the measurements described in Chapter 6.

Although preliminary these results (all on the finger of the same caucasion male) may be of some significance concerning certain uses of the PPG in clinical monitoring, in addition to suggesting further studies that may be of value in ascertaining the precise cause of the PPG.

Transmission pulse oximeters operate by assuming that absorbance measurements are performed solely on arterial blood which flows into the finger to produce the PPG (see Figure 1.28 in Section 1.5.1.3.3). Because of this it would have been expected that the amplitude of the PPG obtained in transmission mode would have followed a similar pattern to the absorbance spectra of haemoglobin. It is therefore interesting to note that no such relation was seen although a relation of this nature was observed in reflection mode over at least part of the spectrum. (It is noted that the respective amplitudes of the 440 and 550nm PPGs did not exhibit this dependence).

Certainly a thorough series of studies in reflection and transmission modes would be of interest to determine the precise variation in the amplitude of the normalised PPG with respect to wavelength (and at different sites, and of the inverted PPG).

Following such an investigation, if the expected trend was still not evident in transmission mode then this may mean that transmission pulse oximeters, which are certainly capable of monitoring oxygen saturation, may operate in a different manner than that described, which is based upon the Lambert-Beer law.

The simplest possible model of how the amplitude of the normalised transmission PPG (see section 7.4.2.2) obtained in transmission mode would vary with wavelength is shown in Figure 7.16. With light of intensity, I_o, incident upon the tissue, and intensity, I, transmitted,

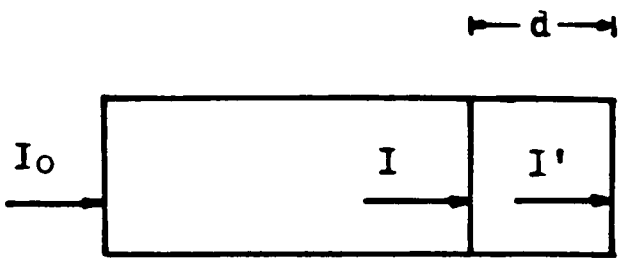

Non-pulsatile absorbance, A.

Pulsatile absorbance, A.

In both non- pulsatile and pulsatile compartments the absorption coefficient is α, and the concentration, C.

Magnitude of the pulsatile component as a percentage:

$$PPG\% = \frac{I-I'}{I}$$

$$= 1 - e^{-\Delta A} \qquad \text{to first order approximation}$$

$$\doteq \Delta A$$

$$\doteq \alpha Cd$$

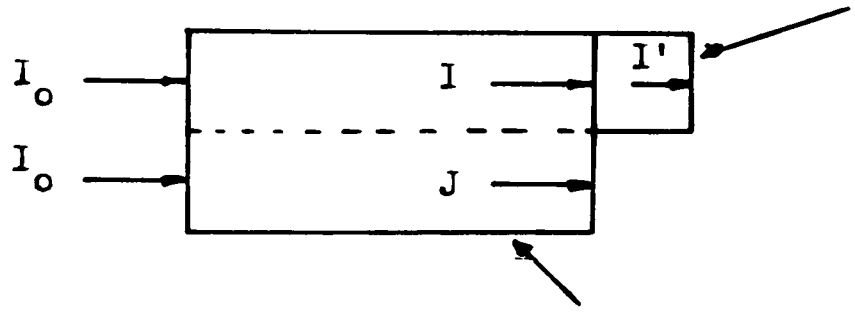

Light passing through this compartment is not affected by the pulsations and so only contributes to the mean "dc" level. This then complicates the expression for PPG%.

Figure 7.16 Simple absorption model of the photoplethysmogram, and a possible reason why the situation may be more complex in practice.

but then reduced to I' by the pulse (so producing the PPG), then the proportion of the tansmitted light which is pulsatile. PPG%, as shown in the figure is approximately equal to:

$$PPG\% = \alpha Cd \qquad 7.6$$

This model predicts that the size of the PPG will be directly proportional to the absorption of the pulsatile medium (ie the blood) which is the type of behaviour obtained, at least in part, in reflection mode.

A possible reason why this dependence may not have been seen in transmission mode, (apart from the possible lack of resolution and insufficient data) may be that not all of the "dc" light level received passes throught the pulsatile "compartment", as shown diagramatically in Figure 7.16. If this is so then the expression for the PPG becomes more complicated, and extra details of the absorbance of the sample must be known.

The reflection mode results which appear to fit the above simple theory may also explain the operation of pulse oximetry (MENDELSON (1983b,c). The technique is based upon the observation that the ratio of the absolute size of the PPG at red and near-IR wavelengths (ie PPG_{635nm}/PPG_{935nm}) decreases with increasing oxygen saturation.

This is in direct contrast to the relation found in fibre optic reflection oximetery (see Section 1.5.1.4) where the ratio of the detected light, RED_{660nm}/IR_{805}, increases with oxygen saturation. The catheter oximeter functions in this manner because at 660nm the reflectance of whole blood increased with oxygenation.

Considering the reflection pulse oximeter, the results presented here may explain how this operates, because since the absorbance of blood at 635nm decreases with oxygenation so too will the percentage of the reflected light that is pulsatile.

Although Mendelson used absolute rather than percentage (transmision) amplitudes, the use of the second near-IR wavelength may

peform this function since at this wavelength the variation in the absorption of blood with oxygenation state is relatively small.

An alternative explanation of the PPGs amplitude variation with wavelength may be due to the different penetration depths of light with wavelength (see Section 1.4.2.2) which has been used to study different depths of the vasculature (GILTVEDT (1984)). Indeed, in practice as made evident in the Introduction, as several effects contribute to the production of the PPG it would be expected that its precise nature will be dependent upon several factors.

Finally. concering the findings of TAMURA (1985) that the relative sizes of the PPG is more sensitive to cold/heat stress at 550nm than in the near-IR. Since a differenece between the two conditions will be the extent of skin blood flow it is likely that this will nave a larger effect on the PPG at 550nm than in the near-IR since the absorbance of blood at 550nm is much larger.

7.7 Summary.

From the preliminary studies performed it was apparent that many variables influence the nature of the recorded PPG, and therefore a comprehensive study would require much time and planning.

However. the preliminary results presented here demonstrate some interesting features of the normalised PPG and serve as a guide to those areas which would be of interest for further study.

In addition to the studies on the effect of AC-coupling, site of measurement and wavelength and search for inverted PPGs described above, a few initial studies were performed to investigate whether the level of the incident light affected the PPG. It was found that there was no evidence of non-linear effects.

One marked effect that was noticed was the position of the hand during measurements on the fingers due to the effect of hydrostatic pressure. For this reason all measurements were made with the hand resting on a bench at a level just below the heart.

7.7.1 Conclusions.

An instrument has been built which allows PPGs to be recorded and subsequently analysed under various conditions. Although only preliminary experiments have been performed, some interesting characteristics of the PPG have been found that merit further investigation, and which appear capable of explaining certain results of other workers.

Further studies of variation of the PPG with site, wavelength and transducer geometry are considered worth undertaking.

Chapter 8 : Summary and Conclusions.

The aim of this research was to investigate the use of optical methods for physiological and biochemical measurements. In particular, the feasibility of non-invasively monitoring the redox state of cytochrome oxidase, the terminal enzyme of the mammalian respiratory chain. was studied.

There are claims that this technique, pioneered by Prof F F Jobsis (Duke University, NC, USA). and now generally referred to as niroscopy (from near infra-red oxygen sufficiency scope), can be used to produce a metabolic monitor by indirectly monitoring oxygen sufficiency at its site of utilization (ie in the mitochondria).

If this is so then niroscopy would potentially be of tremendous use in several areas of research and clinical medicine, particularly in view of the possibilities of such an instrument being marketed at relatively low cost, easy to operate and "portable".

This would be no more so than in paediatrics where brain haemorrhage in preterm babies is a common and still incompletely understood occurence, with niroscopy appearing to offer a means of not only discovering more about the aetiology of haemorrhage, but also of monitoring infants at risk. Hence the interest in this technique.

Although niroscopy was primarily the optical method of interest, it is clear that all such methods have much in common (as has the use of light for treatment as well as diagnosis). Therefore certain areas of the thesis are also applicable to other uses of light in medicine such as oximetry which itself exists in many forms, and whose use compared to niroscopy was considered within this thesis.

The use of visible and near-IR wavelengths (ie light) in biological and clinical applications for both diagnosis and treatment is steadily increasing, with all modes of interactions of light and matter being exploited. As mentioned above, there are many similarities, and much data in common between these areas which if appreciated can greatly enhance the understanding and development of optical based instrumentation.

However, at present (and partly due to the wide range of applications) much of this fundamentally related material is spread throughout the literature. For this reason the Introduction, Chapter 1. not only contains information directly relevant to the remainder of the thesis, but also brief details of other work, albeit indirectly related. This is justified since it supplements the underlying theme of the thesis, and may be of considerable use as a starting point for further research into the use of optical methods or for undertaking some of the suggestions for further work.

To investigate monitoring the redox state of cytochrome oxidase in vivo it was felt that there were two possible approaches. Firstly a Niroscope could have been constructed using published details as a guide, and then employed to perform measurements. Secondly in view of some of the questions concerning the technique a more fundamental approach could have been chosen in which basic studies on the enzyme would be made, followed by work on yeast cells, then going on to more complex systems (eg blood free/perfused, excised/exposed, in situ/non-invasive in situ organs) and eventually finally studies equivalent to those which would be performed in a clinical setting.

Some preliminary work involving construction of a Niroscope was performed, which was taken over at an early stage and continued to a

currently operational instrument by Mr. Y.A.B.D. Wickramasinghe (Appendix A)

All of the work presented in this thesis comes from adopting the second approach. Experiments were performed on purified enzyme and then yeast cells using a mixture of commercial and personally constructed instrumentation. The results demonstrate the nature of the kinetics of the enzyme in vitro, and played a large part in arriving at the summary and conclusions now given.

It is felt that niroscopy has the potential to become an invaluable clinical and research tool. However, there are certainly unanswered questions remaining concerning its precise operation. The major one is that of the ability of the current means of processing to successfully obtain artefact free signals relating solely to changes in cytochrome oxidase redox state. oxygen saturation and blood volume in the region under investigation. The problems with performing this kind of processing were highlighted in the analysis of the methods generally used by Jobsis and what is theoretically required for a simple system.

This question of specificity raises an interesting point about the clinical use of niroscopy. Since most physiological changes liable to affect the redox state will also affect oxygen saturation and blood volume. and as oxygen saturation is as strongly linked to oxygen tension as the redox state of cyt oxidase. then perhaps a near-IR monitor to follow changes in oxygen saturation and blood volume alone would be as much use clinically as an instrument monitoring all three. Therefore as the major instrument problem would appear to be that of resolving a cytochrome oxidase signal, perhaps the development of a "simpler" whole organ oximeter is potentally a more fruitful path to explore, particularly as a commercially available Niroscope is not yet a reality

despite publication of results 4 years ago from what was assumed to be a prototype of such an instrument.

This relationship between cytochrome oxidase redox state and oxygen saturation, which are both functions of oxygen tension is in part reliant upon the affinity of cytochrome oxidase for oxygen *in vivo*, which is itself a controversial area of cytochrome oxidase monitoring, and is directly relevant to the clinical application of the technique.

A possible explanation for the apparent lowering of the affinity of the enzyme for oxygen *in vivo* compared to *in vitro* is presented in the thesis which is based on physical considerations. This theory is in line with the ideas of workers involved in measuring tissue oxygenation levels using microelectrodes and requires no intrinsic change in affinity of the enzyme, unlike some theories which have been proposed as a result of extensive studies monitoring cytochrome oxidase redox state *in vivo*.

In developing this theory, a mathematical model of the variation of absorbance of the enzyme and the oxygen tension was produced which appears to fit *in vitro* experiments, and suggests that the redox state of the enzyme (and hence absorbance) can be considered to be directly linked to oxygen consumption.

The key points in the theory concerning the apparent change in affinity are the presence of distinctively shaped pO_2-histograms in tissue and the (perhaps surprisingly) low pO_2s recorded.

The significance of the first point is that if the theory is true it suggests that any disturbance of the pO_2-histogram may result in a different apparent affinity and so compromise the use of the technique for reliable and reproducible monitoring. This would be of particular relevance since it is known that some anaesthetics do have such an effect

on the pO_2-histogram.

The second point, of the extremely low oxygen tensions found in tissue, may have a profound significance concerning brain haemorrhage, plus some other disease states which inflict preterm infants (eg retinopathy of prematurity (ROP)), that may be due to cellular oxidative damage. Such damage is caused by the destructive action of free radicals, a source of which is the univalent reduction of oxygen. It is possible that the premature infant is not fully adapted to a transfer from a low oxygen tension intrauterine to a high oxygen tension extrauterine existence, and so the high oxygen tension necessarily produced by oxygen administration to prevent brain damage is actually responsible for oxidative damage which may ultimately result in brain haemorrhage. Treatment of this problem may be possible using antioxidant compounds such as Vitamin E, whose beneficial use has done much to support the oxidative damage hypothesis.

It is interesting to note, and one of the reason for the interest in oxidative damage, that the cytochrome oxidase which may perhaps be monitored to discover more about brain haemorrhage, is the substance which consumes most of the oxygen in the body as the final part of oxidative metabolism, and thus reduces the risk of oxidative damage.

Further research along the gradual approach towards a Niroscope in which an understanding of any problems is obtained on each increasingly complex system is continuing within the Bioengineering Unit, as is the aforementioned development of a clinically applicable Niroscope.

In addition to the work specific to monitoring cytochrome oxidase redox state, studies of the overall "reflection" and "transmission" properties of tissue were also performed. This information is relevant

to any *in vivo* optical method and it is therefore somewhat surprising that some data is scarce, particularly that of transmission spectra (due to the high attenuation) which is what is required concerning the application of niroscopy to the neonatal brain.

Some experiments were performed using an image intensifier, although these were restricted by the limited availability of the device. However, they demonstrated that such an instrument would be extremely useful for investigating the optical characteristics of tissue, complementing the standard measurements (see below) because of the ability of such devices to make simultaneous intensity and spatially resolved measurements simply because it is an imaging device.

Preliminary single wavelength meaurements were made using narrow pass band filters and a white light source, and compared to those from a laser diode system. However, results showed that for a comprehensive understanding of the optical properties of tissue *in vivo* then whole spectra are really necessary.

Consequently a computer controlled scanning spectrophotometer was constructed based around a continuously scanning monochromator. This was then used for extensive *in vivo* visible and near-IR reflection and transmission measurements using photomultipliers and photodiode detectors. The results match previous data and also show some features such as water and lipid absorption not commonly shown. Tney also demonstrate generally the problem of observing a small change in absorption on top of a large background attenuation. It is these kind of studies in conjunction with the known spectra of compounds that should be used to determine the most suitable wavelengths for performing analytical meaurements *in vivo*.

The instrument could also be used for other spectroscopic studies (eg obtaining spectral properties of materials or investigative work into fibre optic sensors), and in addition for further studies on the optical characteristics of tissue both *in vivo* (where the limits of the optical components of the instrument are in fact being approached) or *in vitro* where there are many valuable experiments which could be performed.

Finally, a computer based instrument was constructed to analyse the cardiac synchronous variations in reflected and transmitted light intensity (the photoplethysmogram (PPG)) which are often observed on top of the "steady" component measured in the above studies. Preliminary studies of the PPG with respect to site, electronic filtering and wavelength were performed. These latter studies are of particular interest and show that in reflection mode the percentage of the overall reflected signal which is pulsatile is strongly related to the absorption coefficient of blood, which does not appear to be the case in transmission mode. The results also raise some interesting points concerning the use of both reflection and transmission pulse oximeters.

The instrument could now be used to investigate more fully many aspects of the PPG which may lead to the refinement of existing or even the development of new devices. Such studies should also assist in determining what the fundamental processes which produce the PPG in its varied forms actually are.

Chapter 9 : Addendum.

9.1 Introduction.

The experimental results presented in Section 4.6 and Chapter 6 are representative of the reproducible and conclusive observations, which were obtained from spectrophotometric studies of yeast cell suspensions and *in vivo* reflection and transmission measurements from adult volunteers.

However, as briefly described in the relevant sections, these results were only obtained after extensive preliminary studies. It was the information and experience gained from these studies, in terms of sample preparation, actually performing experiments, optimising instrument performance and interpreting results, that led to the production of the results already presented.

Examples of results from these preliminary studies are given in this chapter. These show the difficulties in performing such measurements, illustrate the progress made towards obtaining the final results and also demonstrate additional interesting but as yet inconclusive effects which were observed.

In addition, using all results obtained as a guide, suggestions for further work are made that may lead to both the successful completion of studies already attempted and to a greater understanding in the field as a whole.

9.2.1 Spectrophotometric Studies of Yeast Cell Suspensions.

As described in Section 4.6.4 the reason for choosing to experiment on yeast cell suspensions was that it would provide experience of optically monitoring the redox state of cytochrome oxidase, and interpreting such results, on a more complex system than the purified enzyme, but a simpler one than excised organs.

It was anticipated that by artificially oxidising and reducing such suspensions and using a split beam spectrophotometer, difference spectra as presented by other authors would be readily obtained in the visible region. This procedure would then be repeated in the near-IR and the results and experience gained used to construct an instrument capable of monitoring the "metabolism" of yeast cells under various conditions as the first in a line of developmental "Niroscopes".

However, as described in Section 4.6.4 obtaining such spectra proved to be far more difficult than expected, with no results at all produced until a dual beam (Aminco DW2) spectrophotometer was used.

In the early experiments on the dual beam machine the light brown colour of the growth medium and additional colouring of the artificial oxidising agent had a clearly detrimental effect on the results which meant that the cells had to be thoroughly washed and resuspended in buffer. Following this the cells actually looked "white" suggesting that the presence of any cytochromes (regardless of redox state) was having little effect on the spectral properties of light either reflected from or transmitted through the suspension. (In direct contrast to the light emerging from a suspension of red blood cells for example).

Furthermore as there was no visible evidence of the presence of any cytochromes (as a colouring of the suspension), then observing a slight variation in the absorption spectra of the cytochromes when reduced and oxidised (ie the difference spectra, analogous to the difference in absorbance between oxygenated and deoxygenated haemoglobin) was clearly

going to be a difficult task. This was in marked contrast to the studies on purified cytochrome oxidase which could be seen to change from a brown to green colour upon becoming reduced.

At this point it should be noted that in the results presented in Chapter 4, absorbance units were used to indicate both the level of, and size of changes in, transmitted light intensity. This is strictly incorrect since all samples used were turbid to some degree and therefore both absorption and scattering processes were responsible for the attenuation of light. Absorbance units were used because the spectrophotometers' output readings were in these units, which express the attenuation as the logarithm of the ratio of incident and transmitted (as detected by the instruments optics) light levels.

Because of the small size of the change in absorbance due to a change in redox state compared to the overall attenuation of the sample it was not surprising that using split beam mode was unsuccessful. Only a slight variation in cell density, for instance, between the sample and reference would produce a difference in attenuation far greater than the absorbance change caused by a shift in redox state and therefore swamp the difference spectra.

It was for these reasons that the first successful studies were performed in dual beam mode, and hence on a single cell suspension, on the Soret band, which exhibits the largest absorbance change, and in kinetic mode, so that the cells became reduced after consuming the dissolved oxygen (see Section 4.6.5.2).

As previously described such kinetic experiments with reduction caused by the consumption of dissolved oxygen were of particular use because the suspensions were not irreversibly oxidised and reduced. Therefore dual beam kinetic studies could always be repeated at any time to check the scaling for another study or simply ensure the cells were still viable. The main disadvantage was that although a greater cell

density meant a greater concentration of cytochromes, it also increased the oxygen consumption rate and therefore the cells remained oxidised for a shorter period of time.

Following the success of the kinetic dual beam study on the Soret band similar experiments were then performed on the α and β bands of the cytochromes and also repeated in single wavelength mode (see Figures 4.28 and 4.29). As expected the latter results were more noisy as there was no longer any compensation made for non-specific changes in attenuation caused, for example, by changes in the amount of scattering. However, despite this the instrument was capable of monitoring the very small change in absorbance related to redox state on top of the large background attenuation.

After these sucessful kinetic studies the next step was to attempt to obtain difference spectra, of reduced and oxidised cytochromes, from the yeast cells. For this purpose the Aminco DW2 could be used in two conventional ways, either dual beam or split beam mode (see Section 3.4). In both of these modes a flat baseline, representing no or at least a constant difference in attenuation between the sample and reference had to be obtained manually.

The split beam difference spectra represents the difference in attenuation (ideally due to a difference in absorption by the cytochromes) between reduced and oxidised cells. The dual beam difference spectra is composed of the difference in attenuation between the sample and reference wavelength for oxidised cells. (The differences in attenuation between the sample and reference wavelength for reduced cells having been manually set to zero for all wavelengths).

An example of the results obtained using split beam mode over the range 400-490nm (the Soret bands) was shown in Figure 4.30. The procedure adopted was firstly to obtain (manually) a flat baseline representing a constant difference in attenuation between reduced cells

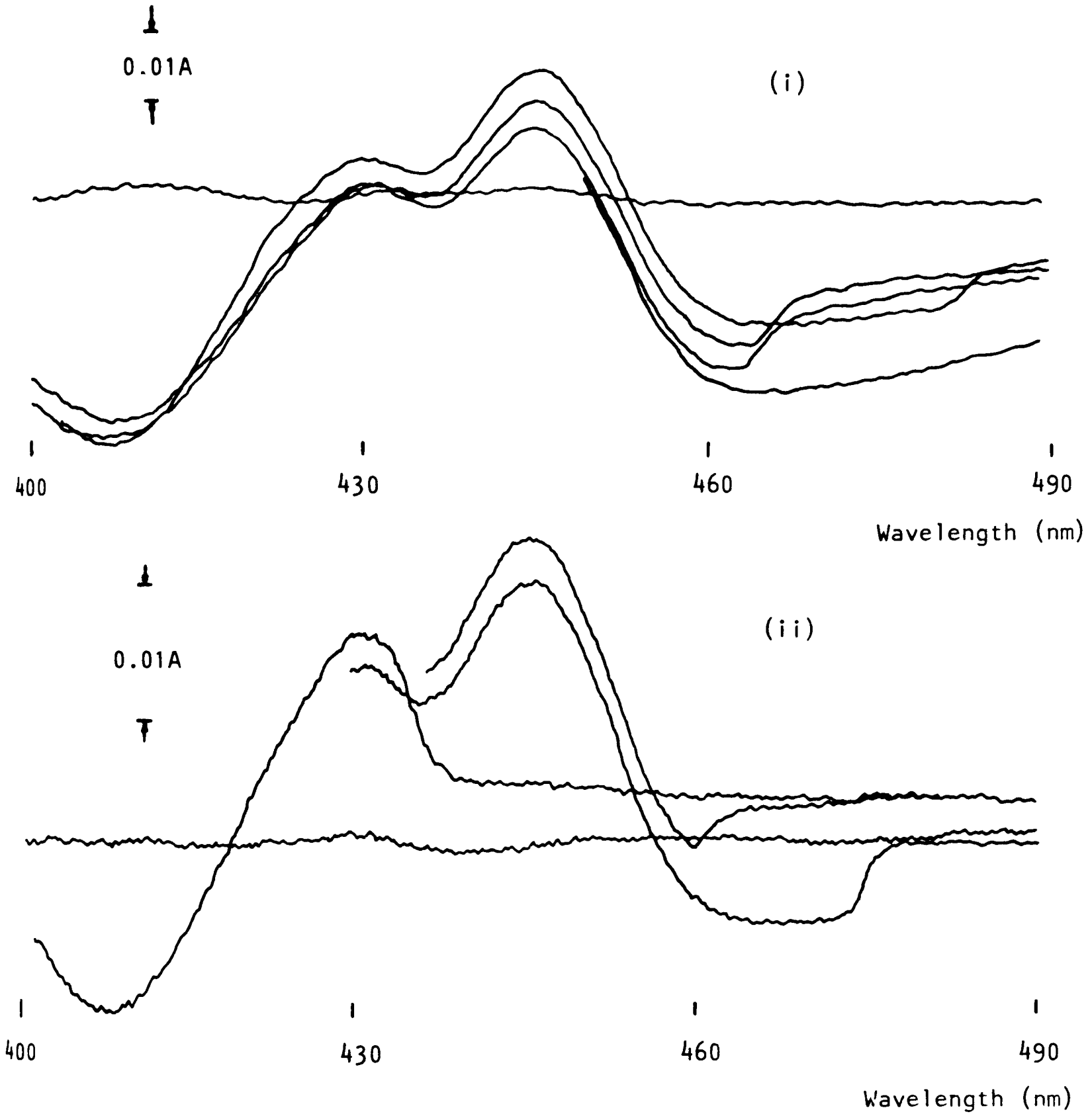

Figure 9.1 Two sets of difference spectra of reduced versus oxidised yeast cells obtained using split beam mode. (Baseline of reduced versus reduced cells). Discontinuities in the traces were produced by the oxidised reference sample consuming all available oxygen and so becoming reduced.

(i) Cell density: 3.8×10^8 cells ml^{-1}, Slit width: 3nm, scanning speed: 2nm s^{-1}

(ii) Cell density: 4.6×10^8 cells ml^{-1}, slit width: 3nm, scanning speed: 1nm s^{-1}

in both sample and reference cuvettes, and then shake the reference cuvette to oxidise the cells and so produce the difference spectra of reduced versus oxidised cells.

Further spectra, over the range 400-490nm, produced in this manner are shown in Figure 9.1. These both include the baseline, and then several traces corresponding to a oxidation of the reference cuvette. The disadvantage of this method of oxidation in producing only a limited period during which the difference spectra could be obtained, is evident by the discontinuities in most traces at higher wavelengths caused by a re-reduction of the cells in the reference cuvette. The spectra in this region was completed by beginning scanning towards the middle of the wavelength region. These traces also demonstrate the problems of shifting baselines (ie the reduced versus reduced cells attenuation), probably largely due to the settling out of cells, and changes in the relative magnitudes of absorption peaks, probably due to slightly differing redox states of the various cytochromes present.

Above the 400-490nm region manually flattening the baseline proved incresingly more difficult. The reason for this was that because of the sensitivity necessary for recording difference spectra (due to the lower absorption coefficients of the α and β bands) any non-specific changes in attenuation between the sample and reference (or measuring and reference wavelength for dual beam mode) caused a large change in the baseline position. Examples of difference spectra obtained in split beam mode and demonstrating this together with the general problem of drift, are shown in Figure 9.2 (see also Figure 4.31).

It was because of this difficulty in obtaining difference spectra in scanning mode that a means of "manual" scanning was devised which circumvented the need to set up a baseline. Rather a series of kinetic studies were performed a few nanometres apart, but with no time base. This resulted in a straight vertical line whose height was related to the

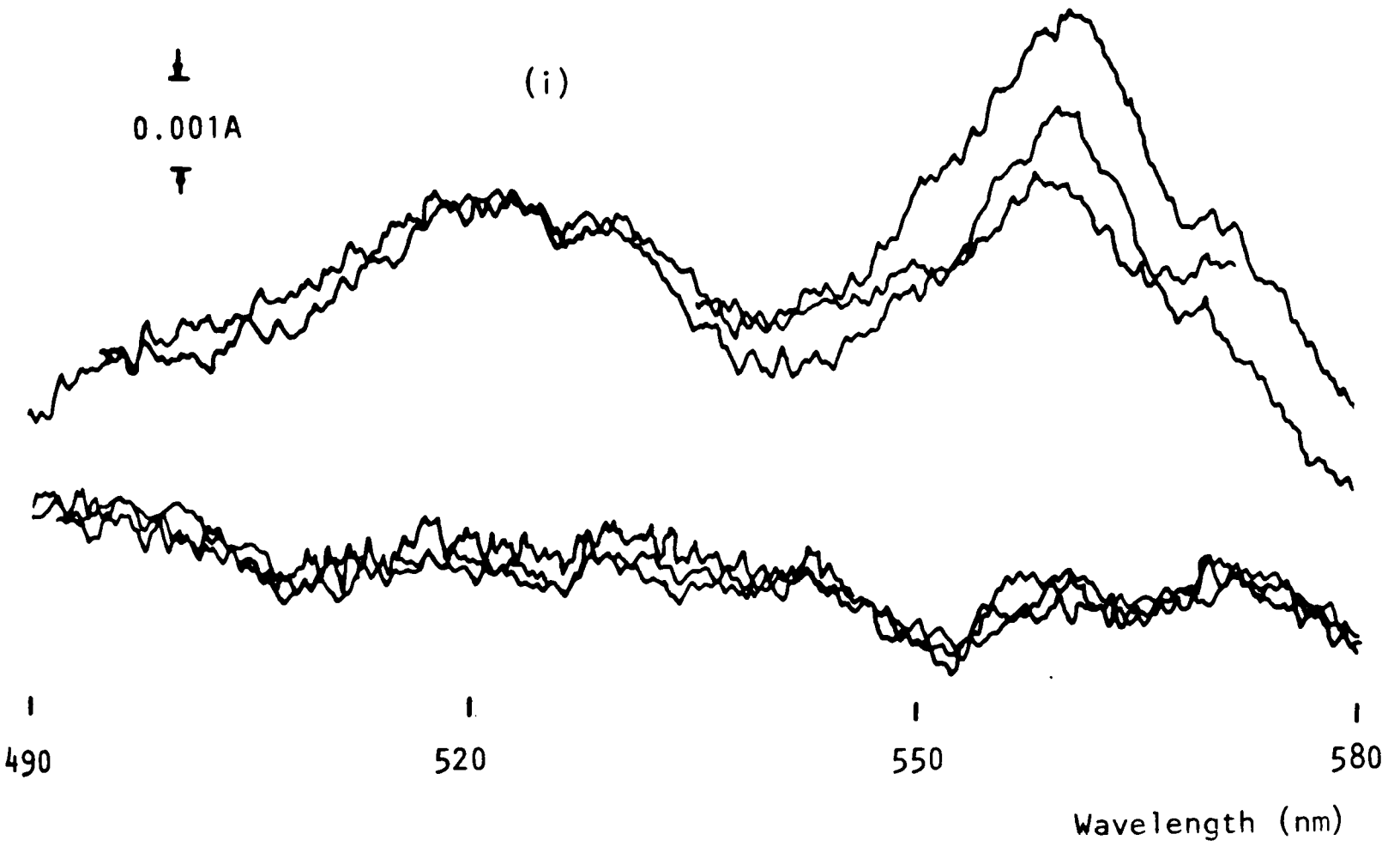

Figure 9.2 Difference spectra of reduced versus oxidised yeast cells obtained using split beam mode. Note the difficulty of obtaining a flat baseline of reduced versus reduced cells. After oxidising the cells in (i) the trace moved off scale and had to be moved back manually.

(i) Cell density 3.6×10^8 cells ml^{-1}, slit width 2nm, scanning speed 2nm s^{-1}.

(ii) Cell density 3.6×10^8 cells ml^{-1}, slit width 3nm, scanning speed 1nm s^{-1}.

change in attenuation, drawn at a position on the recorder corresponding to the measuring wavelength.

The technique could be used in both dual and split beam mode and examples of results obtained in this manner from 400-490nm are given in Figure 9.3 showing the same basic outline as the spectra in Figure 9.1.

Over the 400-490nm range "manual" scanning studies are not actually required since the spectra in Figure 9.1 are clear enough on ther own. However, for the 490-580nm region some conformation of the noisy spectra presented in Figure 9.2 would be of value, whilst at higher wavelengths no spectra at all, requiring manual flattening of the baseline, were successfully recorded.

In Figure 9.4 the dual beam spectra obtained in this manner over the range 500-620nm is shown which confirms the form of the spectra in Figure 9.2 and also shows the presence of the α band of cytochrome oxidase. Further recordings of this band are shown in Figure 9.5, (it was from traces such as this that the spectra presented in Figure 4.32 was drawn).

Although by some means difference spectra were recorded of all the cytochromes in the visible region no sucessful studies at all were performed in the near-IR, not even in kinetic mode (see Section 4.6.5.4). This was perhaps not too surprising in view of the quality of results at 605nm, on the α band of cytochrome oxidase, and considering that the change in absorbance at 830nm is approximately nine times less than at this wavelength. Figure 9.6 contains examples of kinetic traces at 830nm that demonstrate this fact, and which again show the necessity of removing second order spectra when using a monochromator to ensure erroneous results are not obtained.

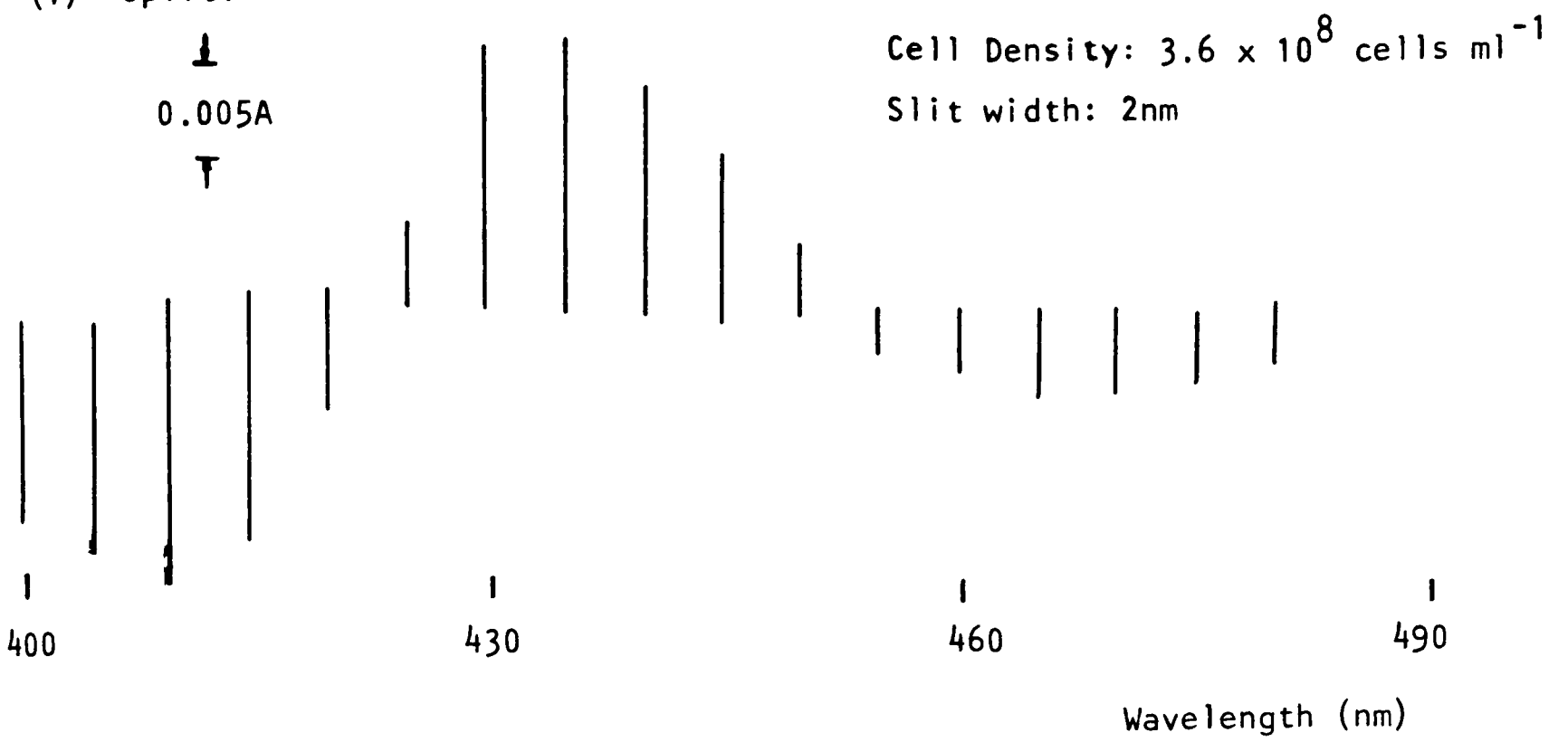

Figure 9.3 Difference spectra of the Soret bands obtained using: (i) "manual" split beam mode and (ii) "manual" dual beam mode v. 460nm.

These traces amount to performing a series of kinetic studies using no timebase, and with the result displayed at a position corresponding to the monitoring wavelength.

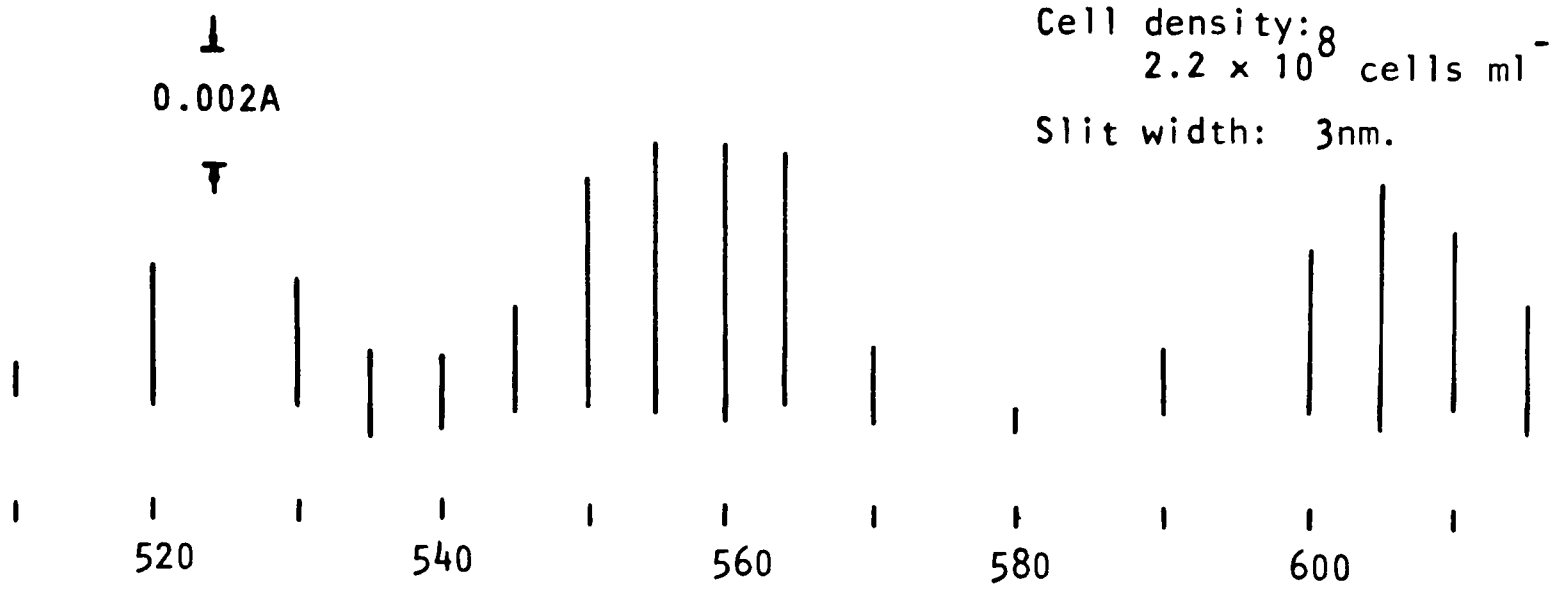

Figure 9.4 Difference spectra of the ∝ and β bands of the cytochromes, obtained using "manual" dual beam mode versus 575nm.

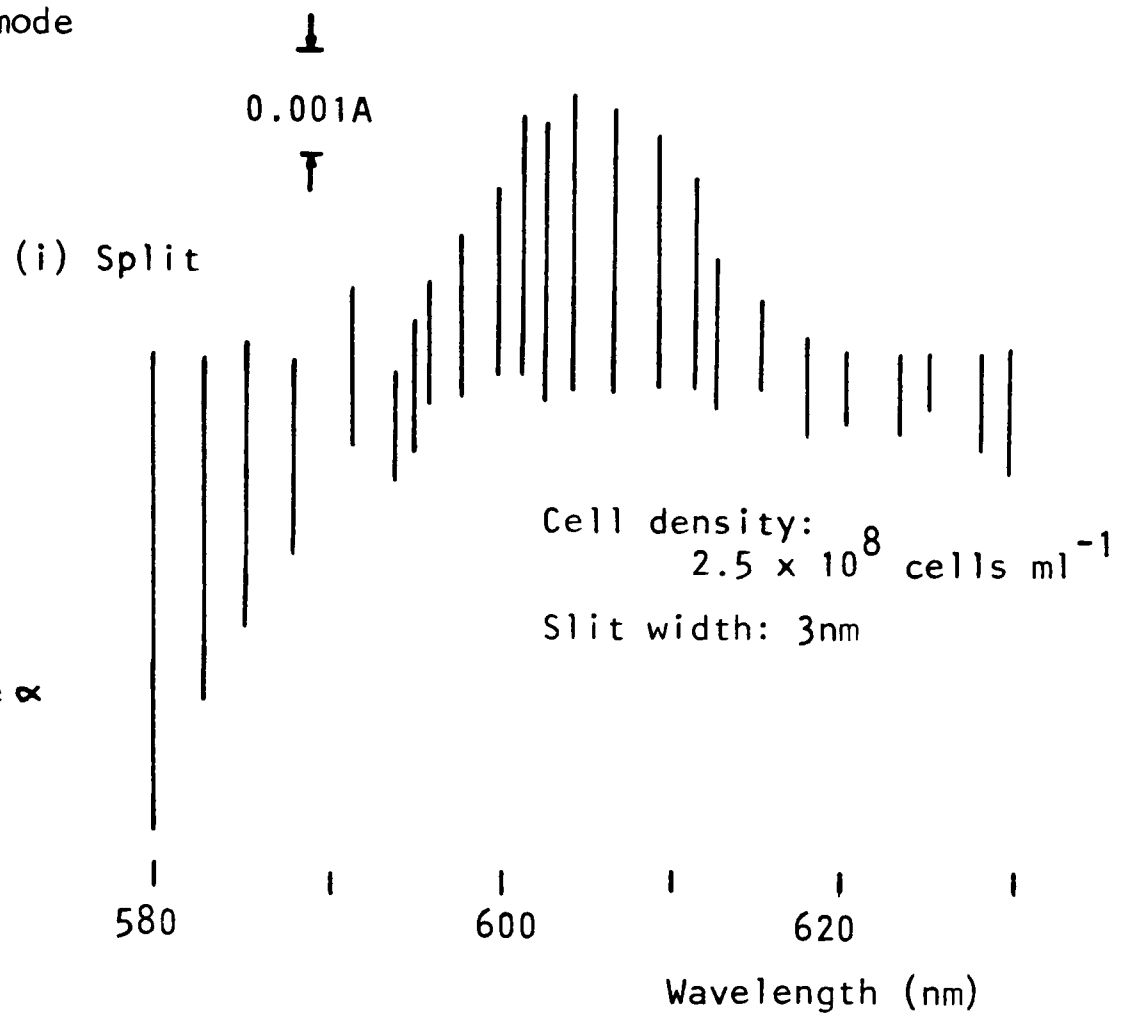

Figure 9.5
Difference spectra obtained using:
(i) "manual" split beam mode and
(ii) "manual" dual beam mode v. 630nm.

These show the form of the ∝ cytochrome oxidase band.

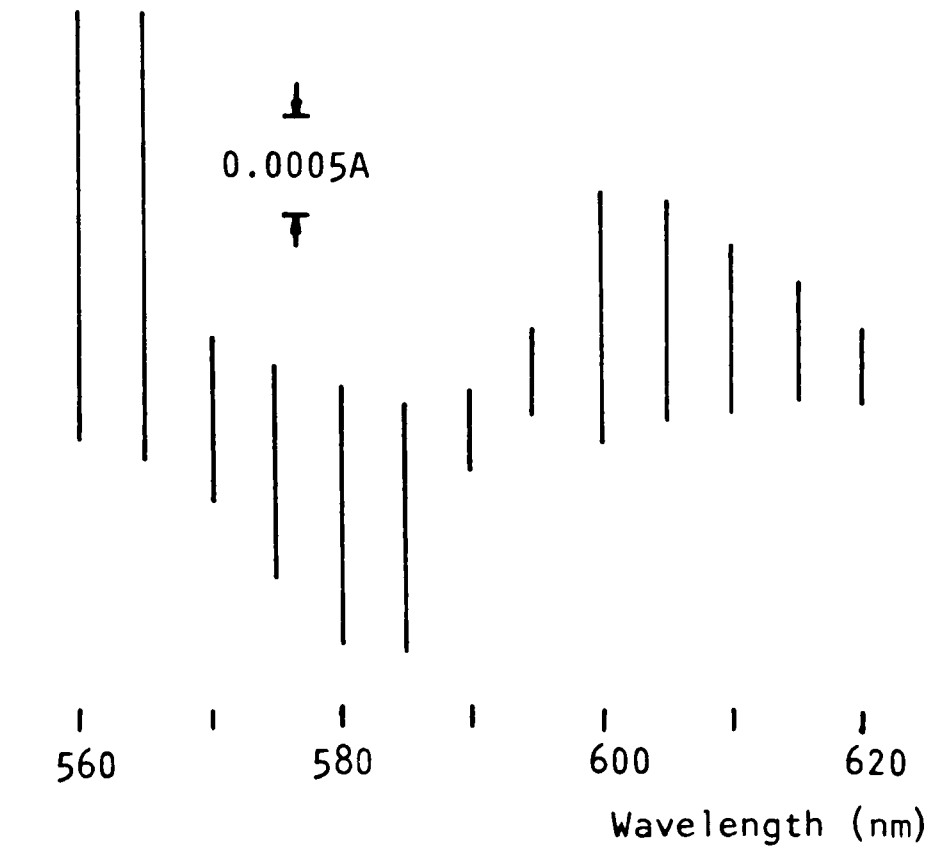

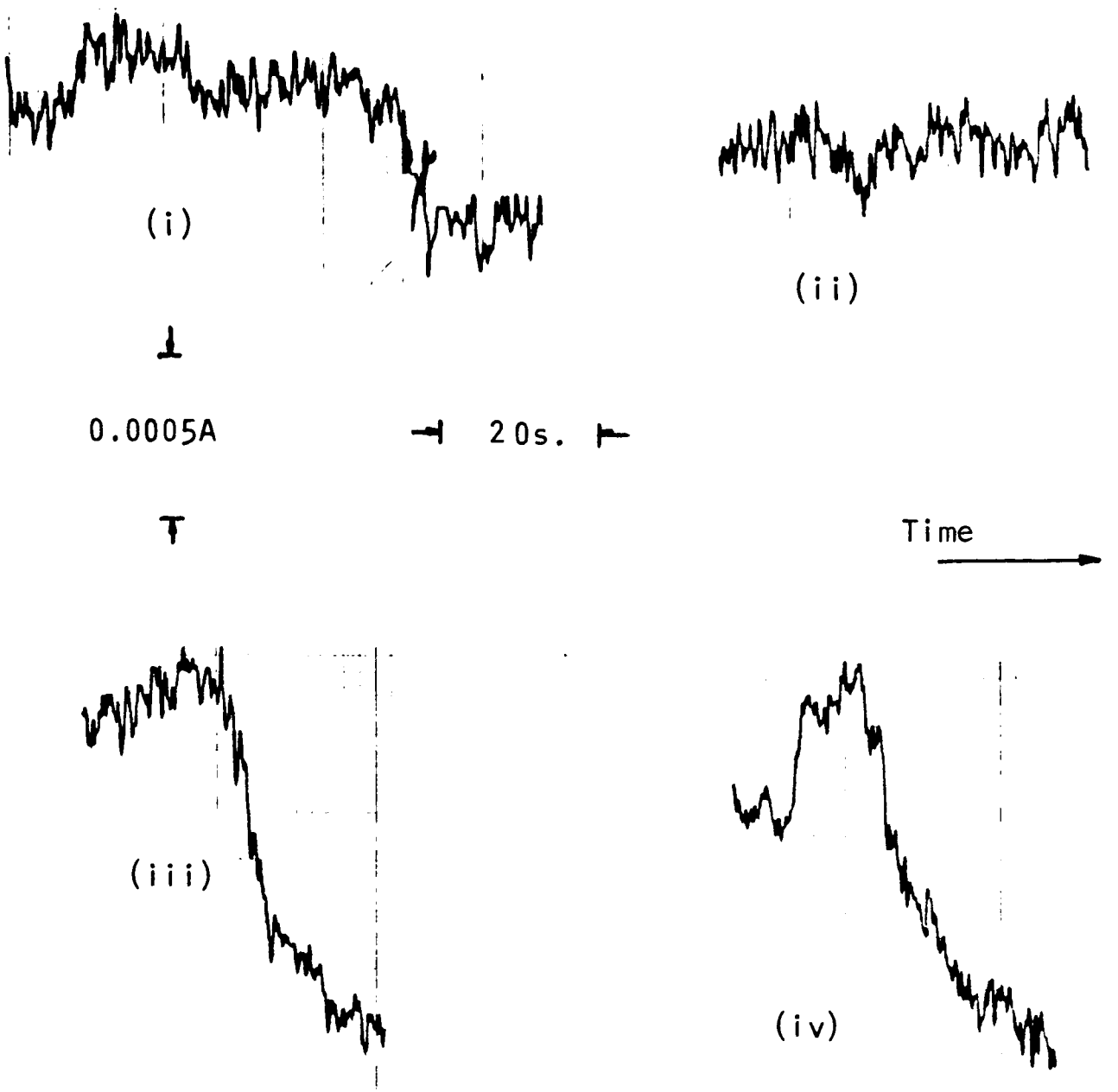

Figure 9.6 Recordings obtained using dual beam kinetic mode with wavelngths 825 v. 775nm and a slit width of 20nm.

Traces were begun after vigorously shaking the cuvette to oxidise the cells. (i) and (ii) (made using appropriate filtering) show that no successful recordings were made in the near-IR, whilst (iii) and (iv) demonstrate the need to use second order spectral filtering when using a monochromator in order to avoid artefacts.

The shifts in traces (iii) and (iv) is due to a change in the redox state at approximately 410nm (see Figure 9.1).

This was also the case for studies on yeast cell suspensions using personally constructed apparatus, since kinetic studies were sucessfully performed at 440, 550 and 600nm but not at 830nm. Shown in Figure 9.7 are two examples of traces obtained at 830nm together with the oxygen content of the solution. Further examples (to those in Figure 4.37) of results obtained at 440, 550 and 600nm are also given for comparison.

One source of the noise on these traces is due to the continual stirring of the cells, required to prevent oxygen depletion effects by the oxygen electrode. The variation in intensity caused by the cells motion was clearly visible and so would have been detected by the optical fibre in intimate contact with the sample chamber.

This problem could perhaps be overcome by detecting the light from a larger surface area of the chamber. In this way the local variations in light intensity (detected by the small fibre bundles) would be averaged out so only changes in intensity due to alterations in the optical properties of the bulk sample would be observed.

Because of the size of the change in detected light intensity during kinetic studies at 440nm attempts were made to obtain difference spectra using the scanning spectrophotometer described in Section 3.5. The spectra from an oxygenated cell suspension were continually stored (at appropriate intervals) until all the oxygen had been consumed, and then processed to hopefully produce a difference spectra. However, despite the large change in signal level observed during kinetic studies no difference spectra were obtained, and this is discussed in more detail in the following section. The scanning spectrophotometer, was however used to record the overall spectral characteristics of the light emerging from the cell suspension using a fabricated cuvette holder that fixes as close as possible to the input slit of the scanning monochromator.

These traces are shown in Figure 9.8 and since there are no large

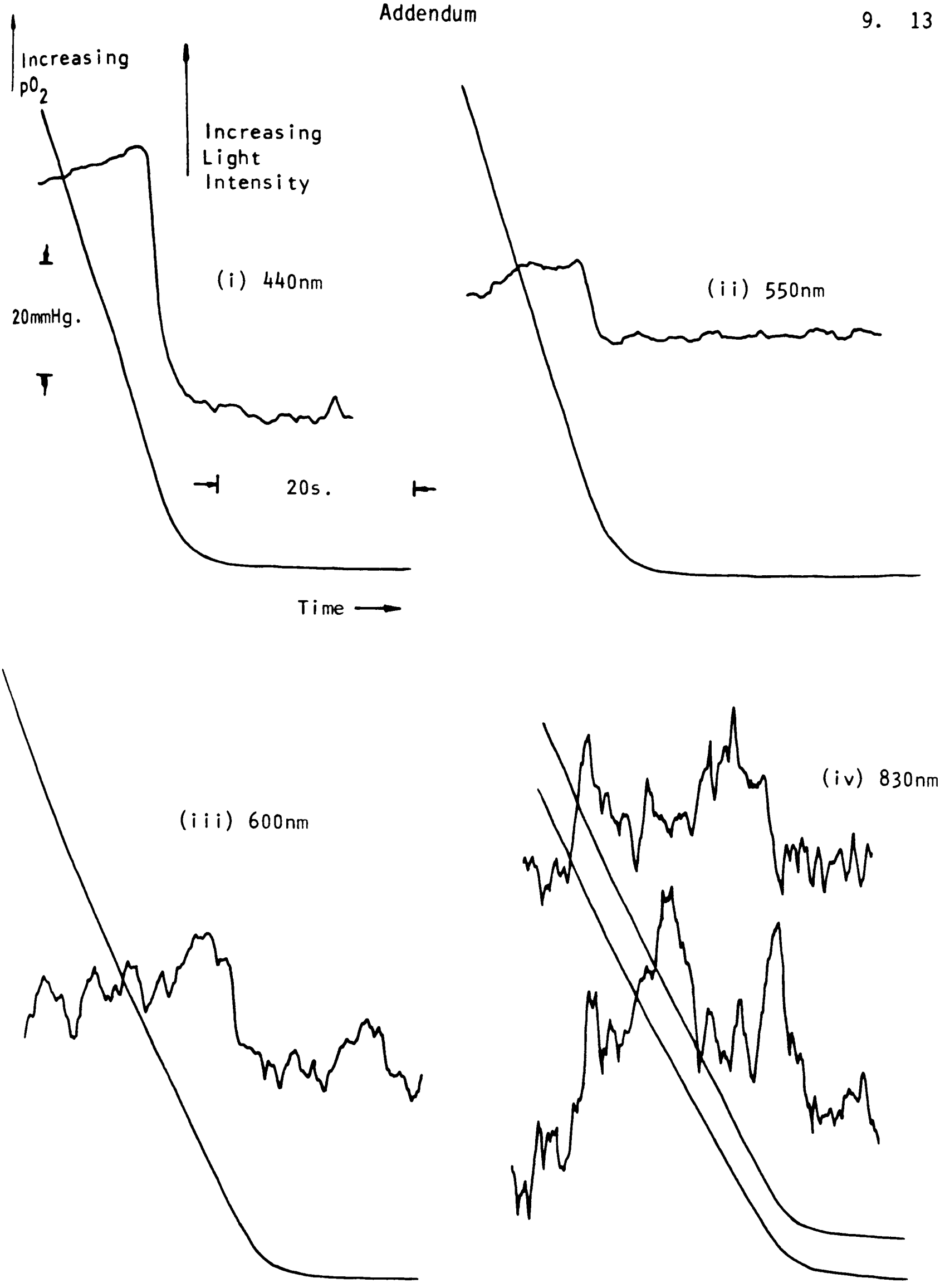

Figure 9.7 Change in the intensity of light transmitted through, and pO_2 of, a yeast cell suspension (density: 1.0×10^8 cells ml^{-1}, demonstrating the consumption of oxygen by the cells and consequent reduction of the cytochromes monitored at: (i) 440, (ii) 550 and (iii) 600 nm.
At 830nm (iv), no such distinctive change can be seen. (An increase in light level would be expected).
(Annotation for (ii)-(iv) as for (i)).

attenuation bands in the visible regions (nor any fine structure either) confirms the visual observations of "white" light being piped to the cuvette and then scattered out in all directions. Indeed, the only marked feature on top of the overall similar attenuation level is centred around 960nm and can be attributed to absorption by water.

That this is so is demonstrated in Figure 9.9 which shows the absorption spectra of water alone, recorded in the same way as the cells spectra, using the scanning spectrophotometer but with a container giving a greater path length and on a commercially available spectrophotometer. In the first two spectra the absorption band around 960nm is clearly visible with the smaller band at 760nm also noticable. The third spectra shows this band, which is of relevance to the in vivo studies considered in the following section in greater detail. (Because of the small absorption coefficient of water, particularily below about 800nm, and the optics of the scanning spectrophotometer precise quantification of the absorption coefficients was not possible. However, the purpose of these traces was rather to demonstrate the presence and position of absorption bands in water, and their relative size).

At this point it is appropriate to note that the wavelength scales on the traces in Chapter 6 from studies using the scanning spectrophotometer are slightly incorrect. This is because when designing the instrument it was wrongly assumed that the wavelength present at the output slit of the spectralyser was linearly related to the elapsed time from the trigger pulse (see Figure 3.21). This is not in fact so, and means at the higher wavelengths on these traces there is a maximum possible error of about 10nm. For future studies this non-linearity could be compensated for within the scanning spectrophotometer's processing routines.

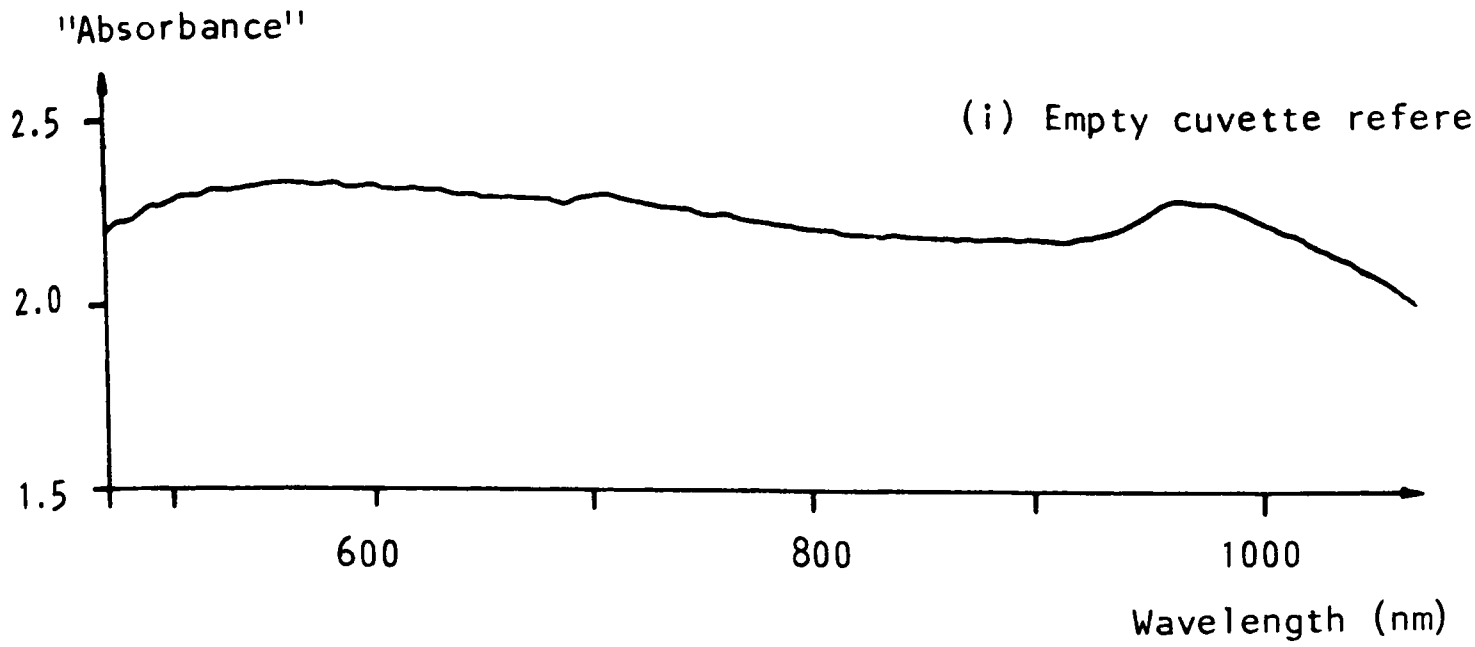

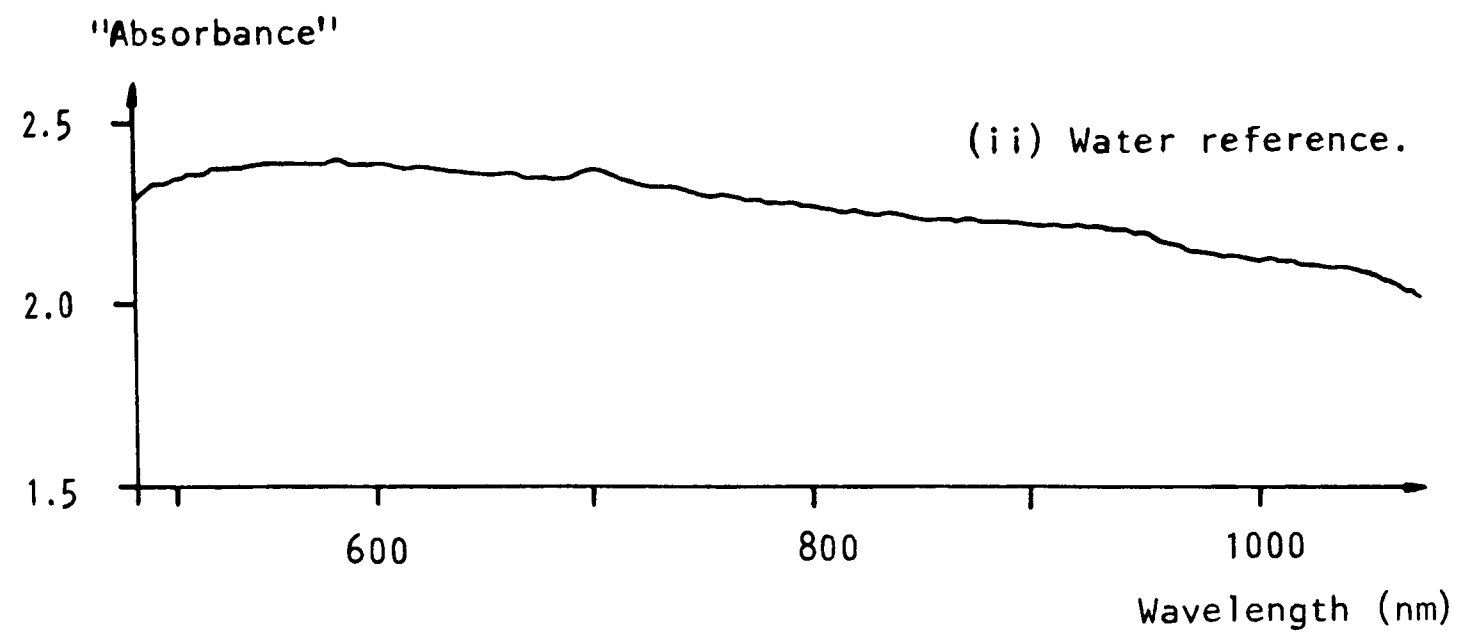

Figure 9.8 "Absorption" spectra from a yeast cell suspension (density 3.8×10^8 cells ml^{-1}) averaged over 300 spectral scans and with references of (i) an empty cuvette and (ii) water (averaged over 10 scans each).

(A slit width of 5nm was used, with light detection by photodiode).

The use of water as a reference removes the absorption band at around 960nm. The peak at around 700nm is an artefact due to the problem described in Section 3.5.8.

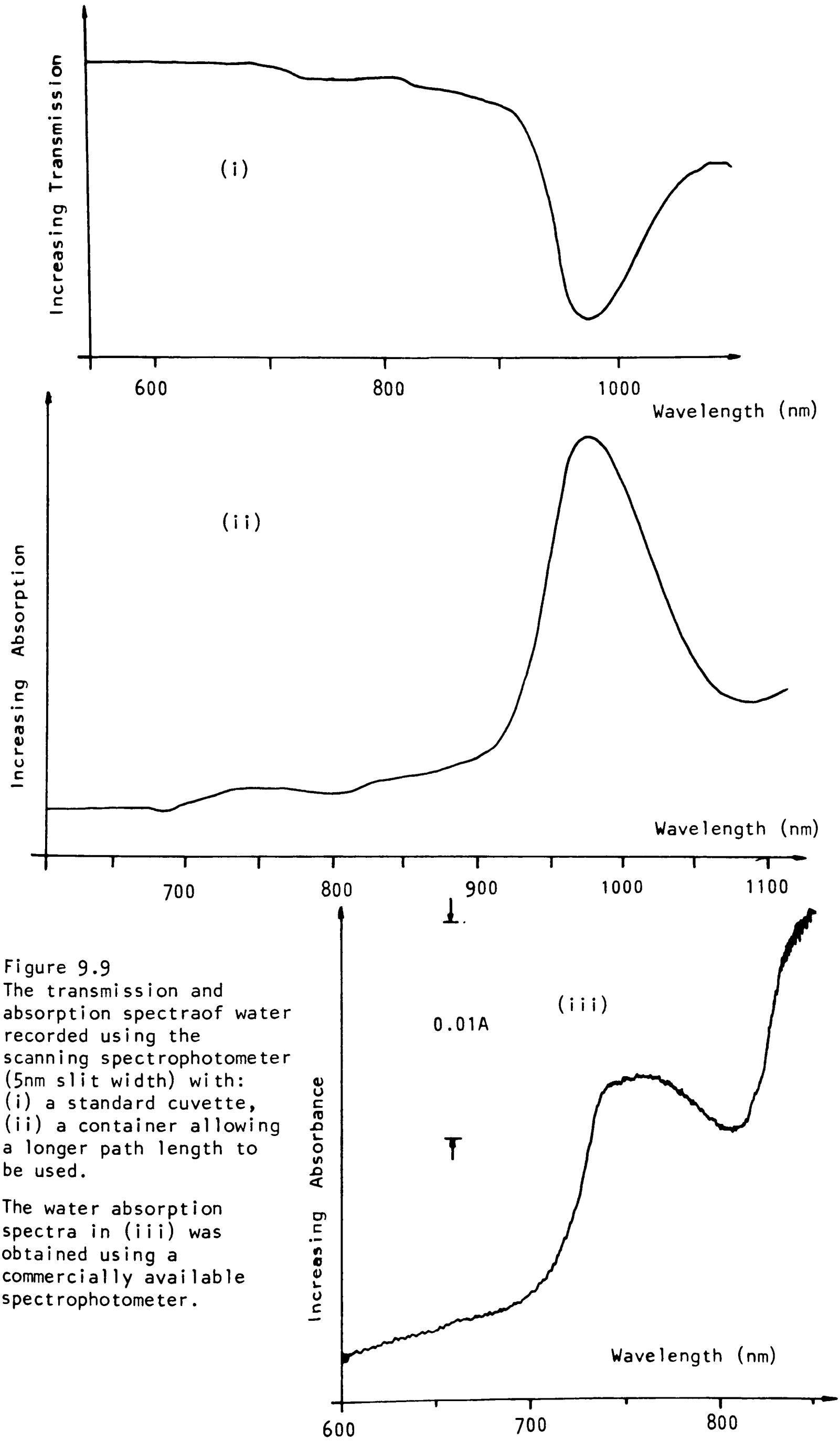

Figure 9.9
The transmission and absorption spectraof water recorded using the scanning spectrophotometer (5nm slit width) with:
(i) a standard cuvette,
(ii) a container allowing a longer path length to be used.

The water absorption spectra in (iii) was obtained using a commercially available spectrophotometer.

9.2.2 Suggestions for Further Studies on Yeast Cells.

Having described what was achieved and discovered from the studies on yeast cells it is appropriate to speculate on the nature of the results obtained, and suggest ways in which both unsucessfully attempted experiments may be completed and more may be learned about optically monitoring yeast cells.

Firstly though, from the experience gained from performing these studies the following advice can be given concerning their repetition. The yeast cells must be grown in sterile conditions, preferably on glycerol based media to promote aerobic metabolism and hence the production of cytochromes. Observation of the culture using a microscope is a useful cautionary measure to ensure that there is no contamination.

Once a clean culture has been grown then if possible the oxygen consumption of the cells should be monitored to ensure that the cells are respiring aerobically. (Consumption should be closely related to cell density, and linear down to very low oxygen tensions).

Before attempting any spectrophotometric studies the cells should be washed thoroughly and resuspended in buffer. Oxidation of the cells (initially at least) should be performed by vigorously shaking, and therefore aerating, the suspension. The cells will then consume the oxygen and hence become re-reduced.

It is suggested that the first studies should be performed kinetically on the Soret band, and in dual beam mode, then moving on to the α and β bands at higher wavelengths. Following the successful completion of these experiments it should then be possible to obtain difference spectra, again beginning in the region of the Soret band.

From the results in Chapter 4 and those above, perhaps the most surprising finding was the initial difficulty in obtaining any results whatsoever, particularly in view of the apparent ease with which similar measurements are made on excised and exposed organs and even non-invasively *in vivo*. In addition, whilst kinetic studies in the

visible could eventually be performed with relative ease this was never the case for obtaining difference spectra in all but the Soret region, and no studies in the near-IR were successfully completed.

The most obvious cause of these difficulties would be the use of inadequate instrumentation. However, considering the spectrophotometer used this is unlikely to be the sole reason even if a contributory factor. Future attempts to discover the true cause are considered of value since this is likely to not only provide information of fundamental interest concerning the use of optical methods for this type of measurement, but also allow completion of some of the unsuccessfully attempted experiments.

Whilst considering the apparent ease (and therefore the relatively large changes in signals obtained) of monitoring changes in the redox state of cytochrome oxidase in various other situations reported by other authors it is suggested that the following type of calculation may prove to be of use. That is to consider the head, for instance, on which optical studies have been performed, and assuming a simple Lambert-Beer Law type relationship estimate the total attenuation of light due to the absorption by the haemoglobin and cytochrome oxidase present (and perhaps water). The magnitude of changes in the spectra observed caused by the deoxygenation of haemoglobin and reduction of cytochrome oxidase could then also be predicted.

The values so calculated could then be compared with experimental results, and although it would be unlikely for there to be a close correlation (due to the simplicity of the model) if similar, (for either the total attenuation or more likely the predicted changes) this would suggest the substances used within the model are those that largely determine the attenuation, and therefore those that it may be possible to monitor.

If there was little correlation (for example it was predicted that a

slight change in oxygen saturation would overwhelm any effects due to the variation of the redox state of cytochrome oxidase) then this could mean one of several things. The model may be totally inappropriate (ie in its composition) or the model may be reasonably accurate but the experimental results inaccurate (due perhaps to the specificity problems discussed in Section 4.10). Alternatively, for studies where the oxygen tension was gradually changing then the interaction between the various components would have to be modelled. Therefore, both the model's composition may be appropriate and results valid, but the interaction between oxygen saturation, cytochrome oxidase redox state and oxygen tension, inappropriately modelled. (The possible relationships between these under various circumstances was discussed in Section 4.11). Consequently, whatever the outcome of such a model the results would appear to be of interest.

Returning to the yeast studies since the cells appear white, and as shown in Figure 9.8 the light emerging from a cell suspension has no distinct spectral properties, then there would appear to be neither any wavelength dependent scattering effects taking place or any strongly absorbing compounds being encountered. An explanation of these observations must be found in order that the optical characteristics of the cells can be understood and so the unsucessfully attempted experiments completed, and further studies performed.

The yeast cells themselves are single celled eukaryotic organisms of approximate size 7.5 x 5.5um and contain amongst their intracellular organelles mitochondria (approximate size 0.8 x 0.8um) which themselves house the cytochromes (ROSE (1969)).

The simplest explanation of the optical properties of a yeast cell suspension is that the cells are large enough to sustain normal reflection and refraction processes and therefore have scattering properties which are not preferential to any one wavelength and so appear

white (cf many granular and powdered substances). However, if this is the case then the cytochromes within the cells must have had very little effect on the overall spectral properties of the emergent light.

This absence of any characteristic attenuation due to the absorbance of light by the cytochromes could be for two reasons. Firstly the concentration of either cytochromes in mitochondria or the mitochondria themselves may be sufficiently low that their contribution to the overall attenuation is too small to be monitored. Alternatively the light may be entering the yeast cells but not the mitochondria so that their contents have a minimal effect on the properties of the emerging light.

This second possibility could also be applied to the yeast cells themselves, so that rather than the light entering the cells it could perhaps be being scattered from their outer walls. Consequently little light would enter the cells and therefore encounter the mitochondria. (An indication of the effect of a change in redox state on the detected light level compared to the overall attenuation can be gained from Figures 4.36 and 9.8 respectively)

A variety of methods could be used to discover more about the optical properties of yeast cells and so determine if any of the above ideas is correct. With this knowledge further experiments on the cells could perhaps be performed with a greater degree of sucess.

In the experiments so far the cell densities have been so large that multiple scattering will have occurred. By using lower cell densities then single scattering studies could be carried out and so enable the cells basic optical characteristics to be discovered (ie the absorption and scattering cross sections could be found in a similar manner to that used for red blood cells).

Whilst considering the cell densities used it was stated earlier that large densities would be expected to produce difference spectra of greater amplitude but that this advantage must be weighed against the

disadvantage of a greater oxygen consumption rate. An alternative means of producing larger signal changes is to use longer path lengths (a standard procedure for observing the absorption spectra of gases). The effect of this was seen during the kinetic studies on yeast cells as described in the results of Section 4.6.6. The effect of a change in redox state at 600nm was only observed using the oxygen measurement cell with its correspondingly longer effective path length than a standard cuvette.

Another means of discovering more about the cells' properties would be to use refractive index matching techniques (BARER (1984)). If the cells are supporting normal reflection and refraction processes then with this method it should be possible to match the suspension fluid's refractive index to that of the cytoplasm and so eliminate scattering. If this is so then it may be possible to observe the properties of the intracellular organelles including the mitochondria in intact cells.

Both of the above suggestions involve studying the whole cell. An alternative approach would be to selectively break down the cell and investigate the resultant components. This could be gradually achieved by firstly enzymatically removing the cell wall (using an enzyme such as glusulase) to produce spheroplasts. These cells without outer walls could then be studied to determine whether the light usually enters the cell itself or gets significantly scattered by the cell wall. Measurements made on the intact cells could also be repeated on the spheroplasts.

The cells could be further broken down by lysing the spheroplasts, with suitable isolation procedures then used to obtain mitochondrial suspensions. These could then be investigated in the same manner as the yeast cell suspensions, and would be expected to exhibit significant absorption properties due to the cytochromes contained within them. For this reason the production of difference spectra should be technically

much simpler than with the intact yeast cells. Following this the cytochromes themselves could be isolated and studied spectrophotometrically.

In conclusion, investigations of this type should enable much to be learnt of the optical properties of yeast cells and may suggest methods by which previously unsucessful experiments could be completed, and allow additional studies of interest to be performed.

In addition to the overall difficulties encountered during this work, one specific experiment which appeared possible in fact proved otherwise. This was the production of a difference spectrum in the Soret region using the scanning spectrophotometer, despite the results obtained from kinetic studies at 440nm using personally constructed apparatus and the fact that spectra in this region were obtained in split beam mode on the Aminco DW2.

The reason for this failure, was primarily felt to be because the output of the tungsten-halogen lamp decreases towards the shorter wavelength end of the spectrum (see Figure 3.1). Consequently, to obtain a change in light level that will cause a significant change in the output from the photomultiplier tube (PMT) (as was the case in the single wavelength kinetic studies), would mean that at higher wavelengths the PMT would be saturated and in danger of being permanently damaged.

To overcome this problem a band pass optical filter to restrict the wavelength range being monitored is what is required (or alternatively a supplementary lamp). With such a filter it should then be possible to obtain difference spectra similar to those from the Aminco DW2. However, with the scanning spectrophotometer the cells would have to be aerated, the overall spectra recorded and then another spectra taken when the cells had become reduced, with the two then used to produce the difference spectra.

A bonus of this is that because whole spectra are recorded, by

storing several spectra as the cells become reduced it may be possible to record the intermediate redox states of the cells as a whole as the various cytochromes go from their oxidised to reduced states one after the other.

There is no apparent reason why such studies should not be possible on the Soret bands, but the experience of using the Aminco DW2 to obtain difference spectra would suggest that this is unlikely to be the case at higher wavelengths if intact yeast cell suspensions are used.

However, besides any studies on non-intact cells (eg those with the walls removed) which may allow results to be obtained more easily, it is likely that the ability to monitor intact cells would still be of value (see below). Therefore, some means of allowing difference spectra to be obtained at higher wavelengths would be required. As described above a major cause of the problems encountered is drift in the detected signal, the main source of which is felt to be due to the movement of cells causing local variations in cell density.

One means of overcoming this problem is to compensate for non-specific changes in attenuation. With the scanning spectrophotometer this could be attempted by normalising all recorded spectra with respect to the signal obtained at one reference wavelength (in a similar way to the operation of a dual beam machine). Such a procedure could be readily accommodated into the processing programme of the instrument.

If the observed drift is indeed due to the motion of the cells, such as their settling out with time, then several possible methods of reducing this exist. Firstly if settling out of the cells is the main cause of the drift then taller cuvettes could be used so that by monitoring the cells at the centre of the cuvette it would take longer for the decrease in cell density, first seen at the top of the suspension, to affect the detected light level.

Alternatively the cells could be continually stirred, as in the

oxygen consumption measurement chamber, although this can introduce its own problems, which would need compensating for as described above.

A means of permanently restricting cell movement would be to use a more viscous suspension medium, although for non-artificially oxidised cells this may introduce problems of aeration. Another application of this method would be to study the kinetics of cytochrome oxidase since with cells suspended in this way oxygen tension gradients could be produced and so "averaged" redox state optical monitoring performed as suggested in Section 4.11.

In conclusion, by using the above suggestions it should be possible to obtain difference spectra and perform kinetic studies throughout the visible and near-IR regions of the spectrum. This would ideally be on intact yeast cells, but at the very least on suitably prepared cells or separated intracellular organelles.

A multiwavelength instrument could be constructed (eg the scanning spectrophotometer with a suitably modified programme) capable of simultaneously monitoring the redox state of all the cytochromes. Such an instrument would have the same technical requirements as a "Niroscope" since it woudld need to address the same kind of problems that must be overcome in a clinical instrument capable of simultaneously monitoring changes in the redox state of cytochrome oxidase, oxygen saturation and changes in blood volume.

With this instrument and a more controllable sample than tissue (in terms of its optical properties) then the relationship between qualitative and quantitative measurements obtained depending upon the sample being used (which could vary in complexity from isolated mitochondria to intact yeast cells) could be investigated. Once such an instrument capable of simultaneously monitoring the redox state of the cytochromes is constructed then an analogue of the <u>in vivo</u> situation in which haemoglobin plays a major part in determining the optical

properties could be produced by the addition of blood (firstly as a haemoglobin solution and then as red blood cells), with suitable algorithms developed to simultaneously monitor redox states and oxygen saturation, as required *in vivo*. In such studies as this in particular, it would be of use to also monitor the oxygen tension to investigate the relationships between these three variables and so study the levels of cytochrome oxidase.

Finally, in addition to its potential use in developing optical methods for non-invasive *in vivo* monitoring, an instrument capable of optically monitoring the concentration and redox states of the cytochromes may also be of value in the expanding area of biotechnology; where yeast cells are among those organisms that are being considered for use in the large scale biological production of a variety of proteins.

Reference.

Rose, A.H., and Harrison, J.S., (1969), The Yeasts, Vol.1, The Biology of Yeasts, Academic Press, London.

9.3 In vivo Reflection and Transmission Measurements.

As with the spectrophotometric studies on yeast cells, the *in vivo* reflection and transmission measurements presented in Chapter 6 represent the most conclusive and reproducible findings. Therefore, they do not convey fully the extent of work that was required to produce them, which included results that although less conclusive were nevertheless still of interest.

At the beginning of Chapter 6, a brief description of early *in vivo* single wavelength studies was given, and how it was the results from these that led to the decision that multiwavelength measurements were required to fully understand the processes involved in modulating the reflected and transmitted light levels with respect to time.

Examples of these early experimental results and the anomalies they produced are now given, together with a possible explanation of their cause. A theoretical analysis of this type of study is also presented, with suggestions for further experiments which should demonstrate whether such a model, although basic, is able to provide a reasonable description of experimental results.

Following this is a more detailed account of the *in vivo* reflection and transmission measurements which were made. This includes some of the interesting but less conclusive findings that were not presented in Chapter 6, and advice for repeating such studies.

Finally, suggestions for further work are given, based in part upon the results and experience gained. As described there is a need for the difficulties involved in producing quantitative results to be addressed and overcome, and more to be learnt of the optical characteristics of tissue to enable the field of transillumination imaging to be investigated further.

9.3.1 Single Wavelength Studies.

Single wavelength studies were performed using the tungsten-halogen light source, interference filters and either a photodiode or photomultiplier tube (PMT) (all described in Section 3.2). The first non-invasive *in vivo* studies were simply meant to determine whether the instrumentation was sufficiently sensitive to detect any light emerging from the hand or arm after transillumination. This was certainly found to be the case, particularly for near-IR light, as expected considering the many references to this effect and the visually observed redness of light after transillumination.

These observations were also in agreement with qualitative results obtained showing the wavelength dependence of the attenuation of light by neonatal skull and dura. These preliminary experiments were performed by placing the post-mortem samples of skull and dura over a small hole in an illuminated opaque sheet, with measurements then made of the transmitted light intensity at five wavelengths using a (small area) photodiode mounted above the hole. Reference measurements were made with no sample present, (to allow for spectral variations in the lamp's output and detector's response) to calculate the attenuation of the sample as an "absorbance" (as discussed above).

The aim of these experiments was simply to confirm that in general terms there is less attenuation of light in the near-IR by biological tissue. Samples of the skull and dura were chosen due to the long term goals of non-invasive neonatal cerebral monitoring.

The studies were not intended to be rigorously quantitative, with no attempt made to break the attenuation down into its absorption and scattering components. The results, shown in Figure 9.10, were taken with the detector approximatly 1cm from the surface of the sample and

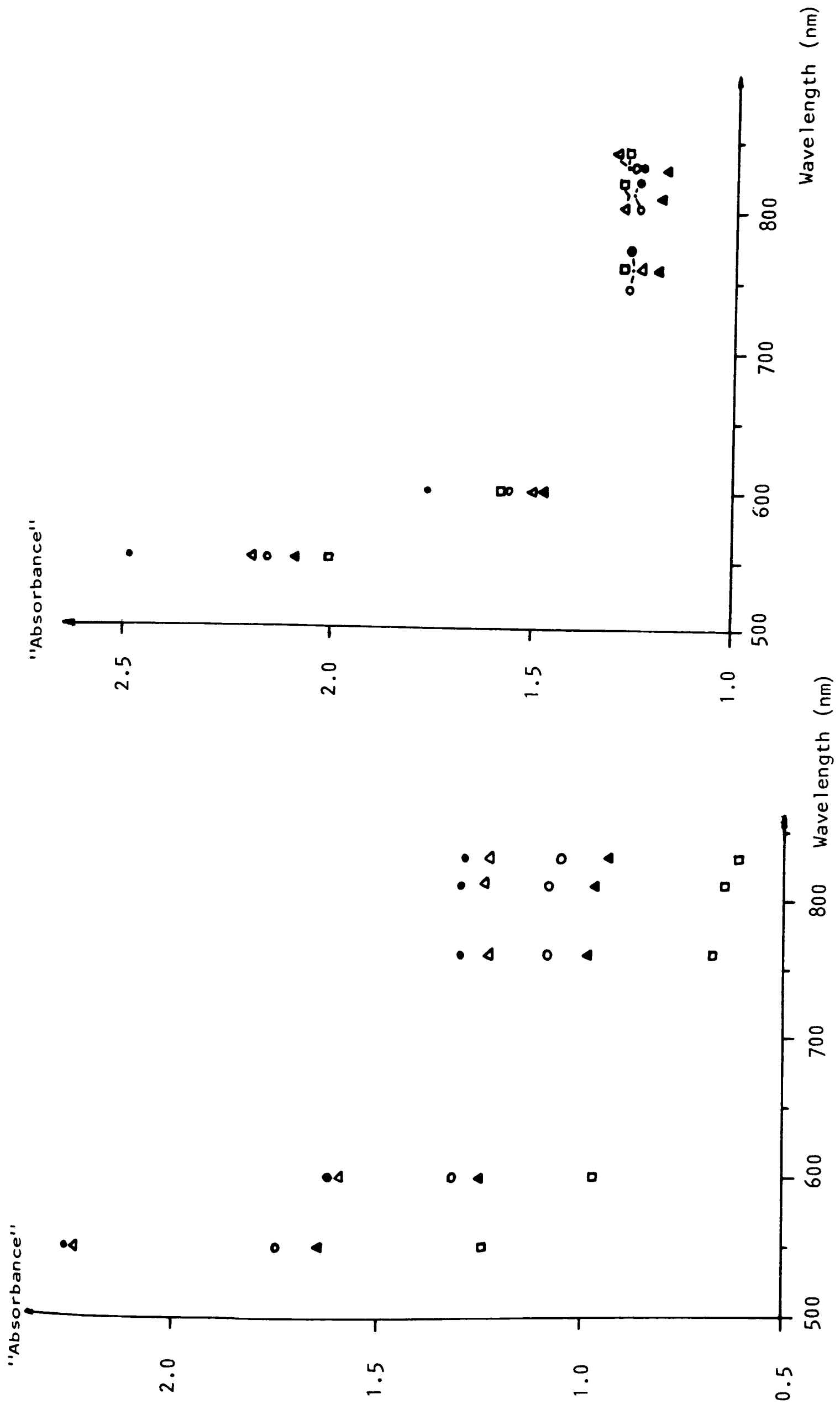

Figure 9.10 Qualitative assessment of the attenuation of neonatal (i) skull and (ii) dura measured at 5 sites (denoted by different symbols) on each sample, at 5 wavelengths (550, 600, 760, 810, 830nm). The traces show that the attenuation becomes less at near-IR wavelengths.

show that the attenuation does indeed decrease in the near-IR (similar results were later found from the hands and arms of adult volunteers as presented in chapter 6). As expected an increase in the distance of the detector from the sample resulted in a decrease in the detected light due to the divergence of the light (caused by scattering) from the sample.

Returning to the non-invasive *in vivo* studies, once it had been found that the detection of transilluminated light over a certain wavelength range was possible, the next aim was to investigate the effect of arterial and venous occlusion of the upper arm on the transmitted light level through the lower arm.

The reason for these studies was that it was felt that the absorption of light due to blood would be the largest variable factor in the attenuation of light by the arm or hand. If so then arterial occlusion would lead to a decrease in the oxygen saturation and so alter the absorbance at all but isobestic wavelengths, whereas venous occlusion would lead to an increase in the volume of blood in the lower arm and therefore cause an increase in absorbance at all wavelengths. Consequently, by knowing the monitoring wavelength the qualitative effects of occlusion and its subsequent release on the transmitted light level should have been predictable from the absorption spectra of haemoglobin. This was considered an appropriate starting point to begin to investigate non-invasive optical *in vivo* monitoring.

For these studies light was "piped" to and from the tissue using fibre optic bundles and held in place using holders similar to that shown in Figure 6.1 (ii). In some experiments lock-in amplification was used whereas in others the level of transmitted light was detected directly with the area under investigation shrouded from ambient light.

As anticipated the results show that venous occlusion always led to a decrease in the level of transmitted light, whereas the effect of arterial occlusion was wavelength dependent. Figure 9.11 shows traces

obtained at 550, 590, 760, 810, and 840nm which all exhibit the expected responses in view of the haemoglobin and oxyhaemoglobin absorption spectra. (The recording at 810nm shows an unexpected sharp increase in detected light intensity upon arterial occlusion, before the gradual increase as expected, followed by an equally rapid decrease upon removal of the cuff. This is discussed below). Also evident in these, as in all, traces are the marked effects of the rapid outflow of blood following venous occlusion and reactive hyperaemia after arterial occlusion.

In addition to these traces showing the expected effect of arterial occlusion, during many of the earlier arterial occlusion studies the level of light intensity actually decreased even though the absorbance of deoxyhaemoglobin was less than that of oxyhaemoglobin. This was obviously unexpected, and appeared to be dependent upon the method of monitoring. The reason for this was because although in all of the similar single wavelength studies performed in collaboration, with my colleague Mr. Y Wickramasinghe, using the laser diode based spectrophotometer, the effect of arterial occlusion was always as expected, upon performing simultaneous studies using the white light and laser diode based instruments on the same arm (although at different sites) markedly different results were produced as shown in Figure 9.12.

These observations of seemingly identical studies producing very different results presented a puzzling anomaly. After some consideration and subsequent experimentation, the significant factor was traced to the application pressure of the fibre optic bundles on either side of the sample (ie hand or arm). With the laser diode based system the fibres were always applied with a relative large pressure in order to obtain an adequate level of transmitted light. However, with the tungsten-halogen lamp based instrument results could be obtained with less pressure and so a wider range of application pressures were used, compressing the sample

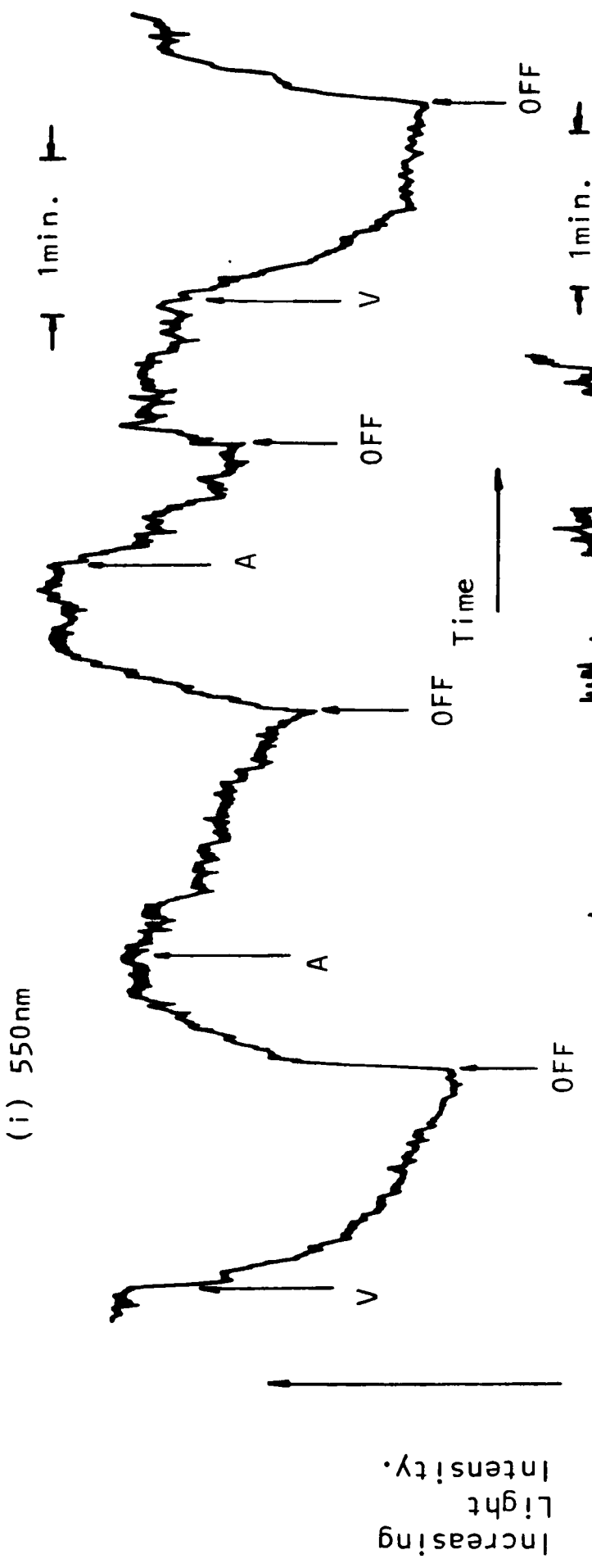

Figure 9.11 The effect of venous and arterial occlusion on the level of light transmitted through the hand at (i) 550nm and (ii) 590nm.

(figure continued on next page).

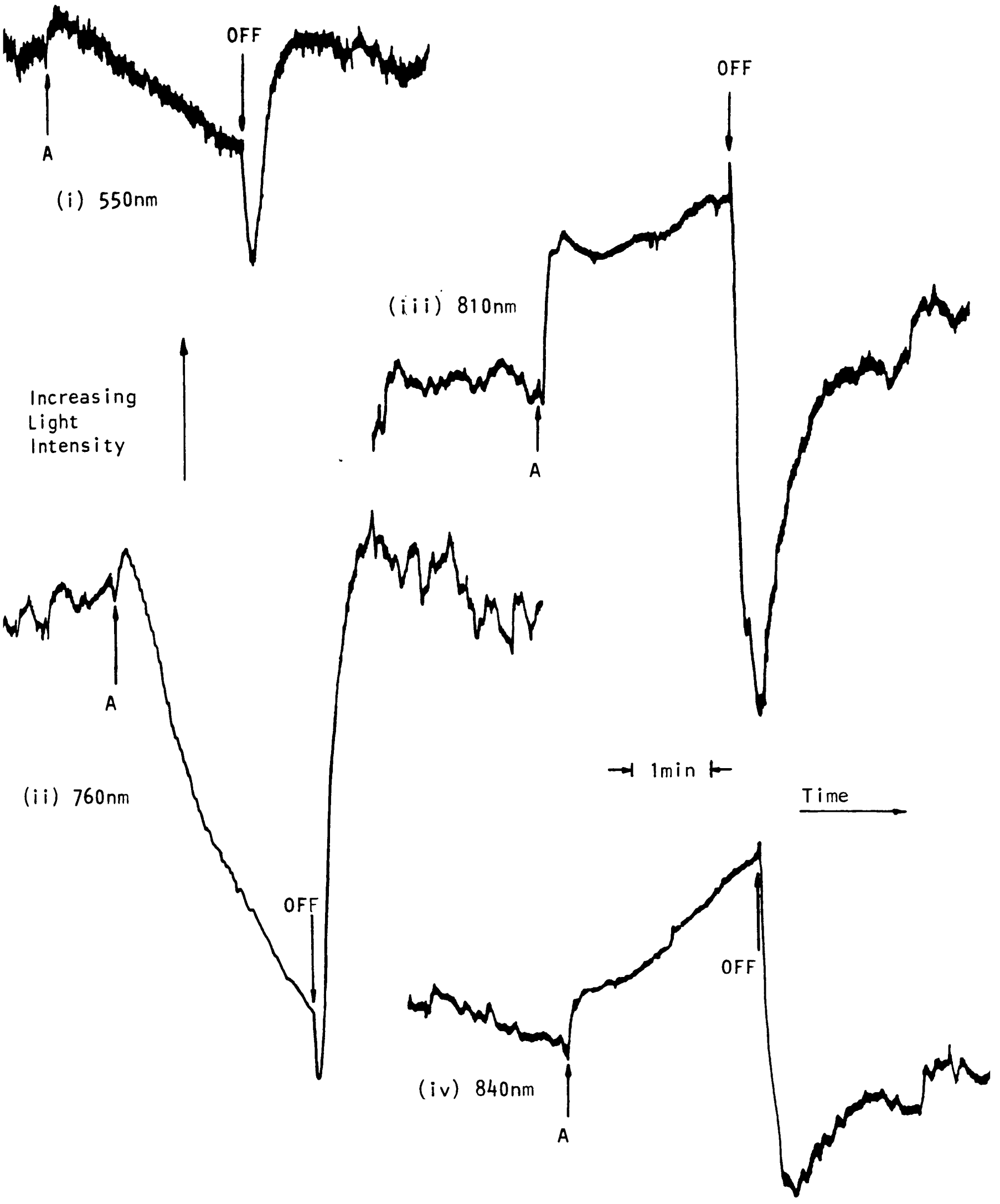

Figure 9.11 (cont.) Effect of arterial occlusion on the level of light transmitted through the wrist at: (i) 550, (ii) 760, (iii) 810 and 840nm.

to a greater or lesser degree.

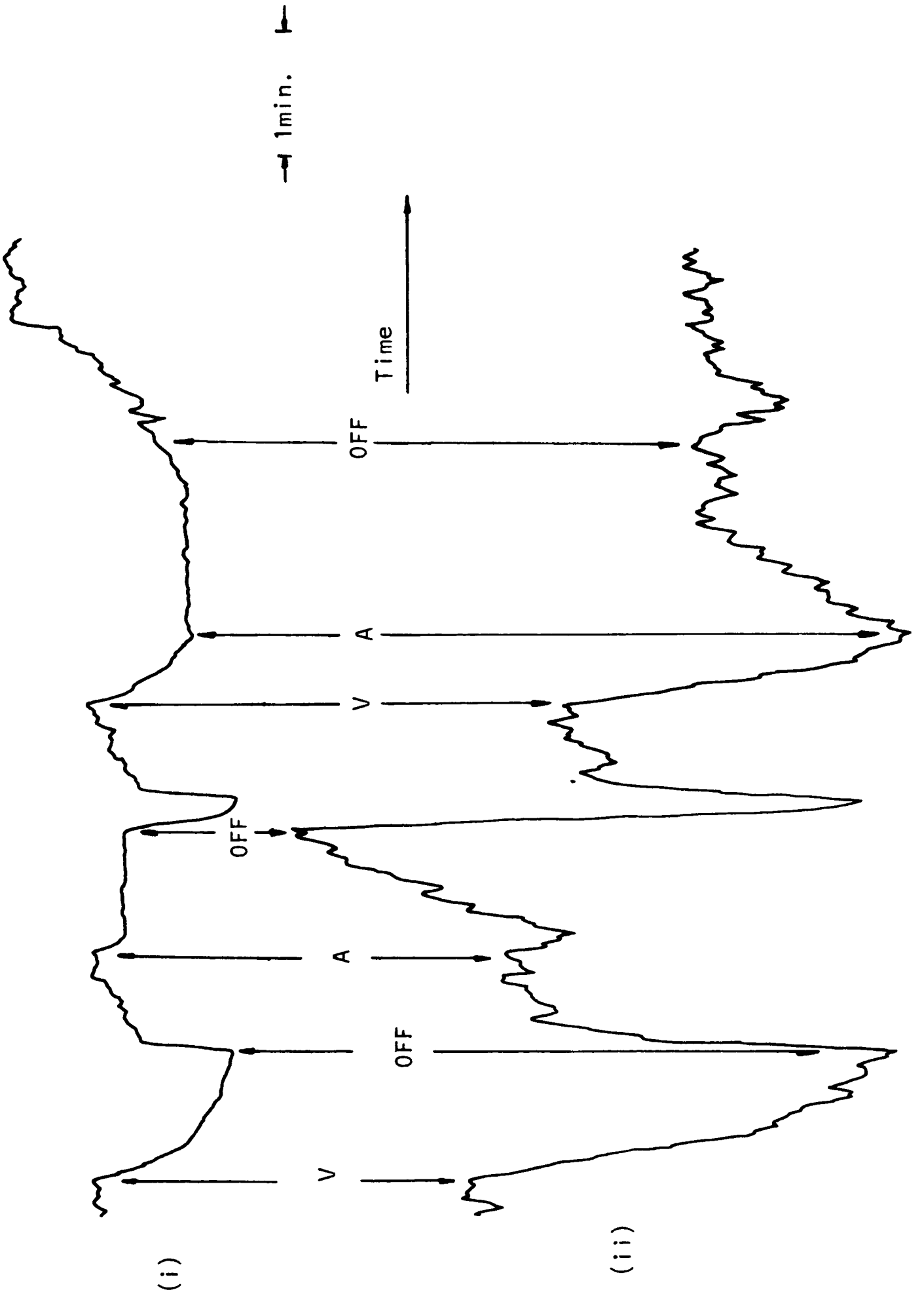

Figure 9.12 Variations in transmitted light intensity through the arm monitored simultaneously, and showing the different results obtained due to different fibre bundle application pressures, with the: (i) white light based intstrument operating at 840nm, and (ii) the laser diode spectrophotometer at 840nm.

That this was indeed the cause of the anomaly is illustrated in Figure 9.13 which shows the effect of arterial occlusion with the only difference between traces being the increase in the pressure of the fibre bundles on the tissue. (As would be expected this also produced a marked increase in the overall level of transmitted light).

A possible explanation for this unexpected effect is as follows. When the cuff is inflated (which was by hand and takes approximately 5-10 seconds) then its pressure on the arm will cause blood directly beneath the cuff to be expelled from this region and redistributed on either side of itself. Consequently upon the application of an arterial cuff, the volume of blood in the lower arm will increase slightly. The way in which this may explain the observed results concerns the re-distribution of this expelled blood within the lower arm. (In addition to the displacement of blood, because of the time taken to inflate the cuff there will also be some initial filling of the arm with blood since venous occlusion is effectively performed before the final arterial occlusion).

It is likely that of all the blood present in the arm, that which is in the regions of tissue directly beneath the light source and detector has the largest influence on the attenuation of light. Therefore, if the expelled blood from under the cuff enters this region it will have a profound effect on the detected light level. However at large fibre bundle application pressures, much of the blood from under the "source" and "detector" fibres will have already been expelled with no possibility of any further blood entering this region.

Consequently for small application pressures, expelled blood from under the cuff may enter the tissue under the source and detector and therefore cause a decrease in detected light level irrespective of wavelength. This hypothesis is supported by the fact that the decrease in light level is more rapid than would be expected for either

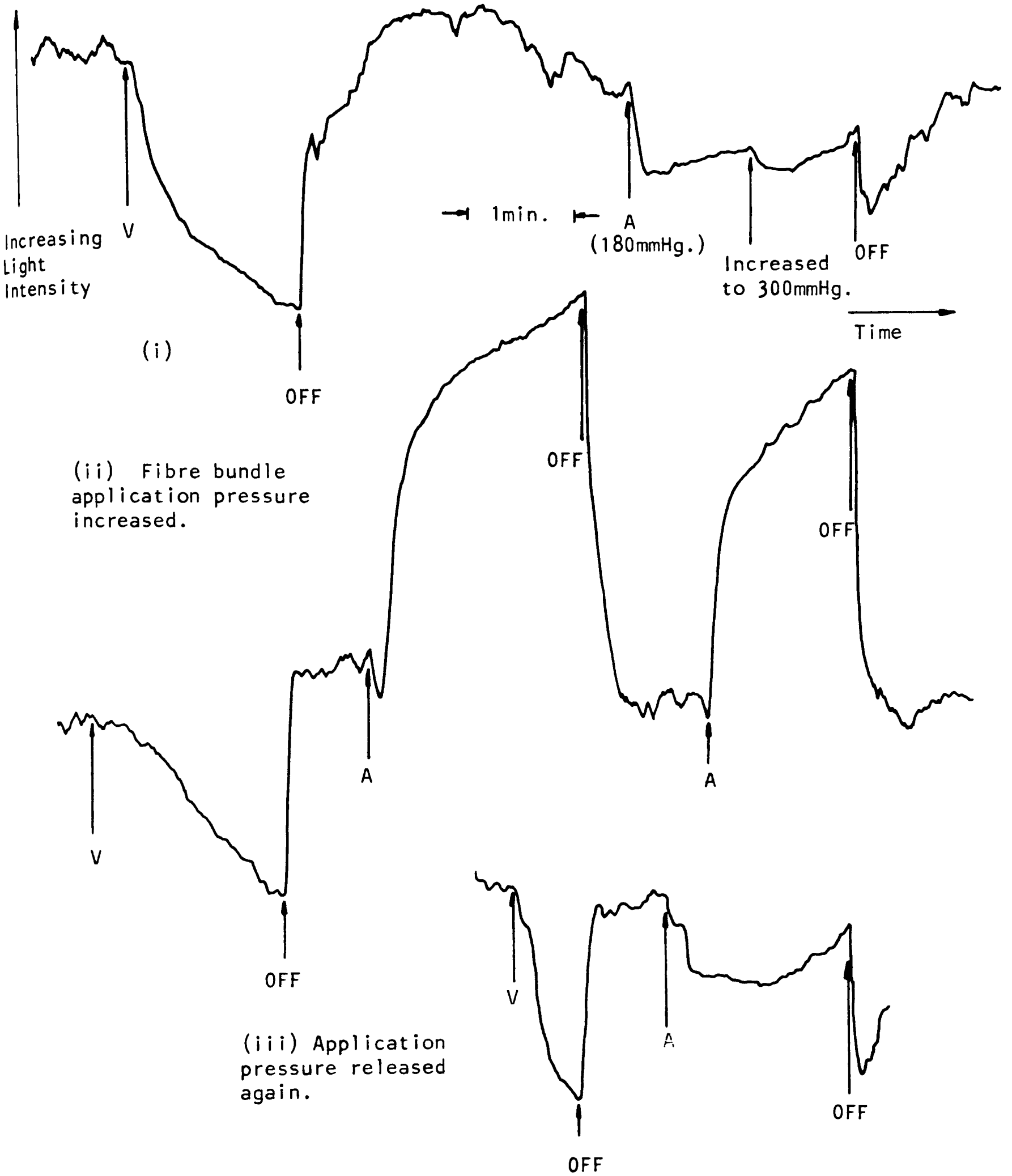

Figure 9.13 Recordings from three consecutive studies showing the effect of an increase (ii) and then decrease (iii) in fibre bundle application pressure on transmitted light intensity. Measurements were made at 830nm on the hand.

The incident light intensity was adjusted between studies to accomodate the higher overall transmitted intensity at the larger application pressure.

deoxygenation of blood or the filling of the arm with blood following venous occlusion (see Figures 9.12 and 9.13). In addition after the initial decrease, which is virtually simultaneous with cuff application, there is then some evidence of a slight increase in light level (at wavelengths above the 805nm isobestic point) which would be due to a decrease in the oxygen saturation of the blood.

At large fibre bundle application pressures no blood should enter the region directly beneath the bundles and so the major effect that is observed is the gradual increase in light intensity (for wavelengths above the isobestic) as the blood in the arm becomes deoxygenated. Despite this, before the increase in light intensity a slight decrease can be seen (see Figure 9.13) which is not totally unexpected since some of the expelled blood may still enter the lower arm, although not directly beneath the fibre bundles.

However, the trace is primarily influenced by the oxygen desaturation of blood, and in a far more marked manner than the barely observable effect at lower application pressures. Why this latter point is so is not obvious but it may be related to the fact that at lower application pressures there is probably a much smaller relative contribution to the overall attenuation from the blood directly beneath the fibres, compared to that which is somewhat deeper within the arm. In addition that the overall detected signal is less at lower application pressures may be of some significance, and not unrelated to the question of which regions play the major role in modulating the transmitted light level.

If the relative contributions from different regions of tissue is dependent upon fibre bundle application pressure then by using different cuff application pressures it may be possible to obtain proportionally more or less information from surface rather than deeper vessels and tissue. If this is so then such discrimination may be of some use as a

diagnostic tool.

Furthermore, if the dependence on fibre bundle application pressure is linked with the expulsion of blood from underlying tissue then it must also be related to the blood pressure within the occupying vessels. Consequently it may be that by using a range of application pressures and then monitoring the effects of both arterial and venous occlusion, the suitably analysed results would be of value for assessing the state of the vasculature. For these reasons further studies of this nature (probably using more than one wavelength as discussed below) are considered of value.

In concluding this discussion it should be noted that a further factor may also play a part. In the recording at 810nm in Figure 9.11, arterial occlusion led to a sharp increase in detected light level, rapidly returning to its former level upon cuff removal. This effect was also noticed around this wavelength range during multiwavelength studies described in the next section. A possible cause may be that for certain application pressures and/or measurement sites the slight filling of the arm with blood during arterial occlusion may actually cause a more efficient coupling of light into and out of the tissue so increasing, rather than decreasing, the detected light level. If this is so then it must be related to the fact that the distance between the fibre bundles is fixed and so any such effect should disappear if the two bundles were fixed directly and independently to either side of the sample.

Despite the interesting results from these preliminary studies, they clearly demonstrate the disadvantage of single wavelength measurements by showing that if more than one variable can effect the detected light intensity then it is not necessarily obvious what is the cause of any observed change.

The most effective way of determining whether, for instance, the light level at a particular wavelength has decreased due to a change in

oxygen saturation or blood volume is to perform multi-wavelength measurements. If monitoring is performed at two or more appropriate wavelengths then by considering the respective changes in detected light level it should be possible for the cause of the change to be determined.

However, this may be adequate for simple experiments (such as the above occlusion studies) where the absorption of the blood was considered of primary importance. For multicomponent systems, where several compounds may be absorbing light and the level of absorbance may depend on more than two parameters (ie oxygen saturation and blood volume), more wavelengths would be required.

The most complete solution is to use a scanning spectrophotometer to investigate changes in detected light level across the whole spectrum. Then not only could values at selected wavelengths be used for subsequent processing but variations in the shape of the whole spectra used to monitor any changes of the state or concentration of any compounds. For instance an increase in light level above 805nm could easily be attributed to either a decrease in blood volume or oxygen saturation by observing the shape of the overall spectrum. Furthermore, for research into novel optical methods, such measurements over the whole spectrum would be needed to confirm that wavelengths selected by theoretical considerations are indeed those most suitable for monitoring the state and concentration of specific compounds. For this reason it was decided to construct a scanning spectrophotometer and then attempt to repeat the above studies.

9.3.2 Multi Wavelength Studies.

As described above, because of the anomalous results obtained using single wavelength measurements it was decided that multi-wavelength studies were required to determine the reasons for the changes in the level of transilluminated light. For this reason the computer based scanning spectrophotometer described in Section 3.5 was constructed.

The intention was to use this instrument to repeat the occlusion experiments and so monitor the effect of changes in both oxygen saturation and blood volume on spectral shape, and determine whether the above hypothesis concerning the fibre bundle application pressure was correct.

Preliminary studies in both transmission and reflection modes were attempted and some of the results obtained are now described. In general the reflection studies were more successful because the level of reflected (back scattered) light from the surface of the skin is far greater than the level transmitted (ie scattered) through tissue.

(This is an appropriate point to clarify that the terms transmission and reflectance as used here respectively refer to the detection of light emerging from the sample in the same and opposite direction as the incident light. In Chapter 6, the term transmission was also used to describe one of the methods used for presenting the level of the normalised detected light intensity (with absorbance the other alternative). This was described in Section 3.5.6).

The initial reflectance studies were performed using a bifurcated fibre optic bundle which was fabricated using ten 0.5mm diameter unclad polymer fibres (Barr and Stroud). The ten fibres were randomly arranged at the non-bifurcated end with respect to the five fibres in each "leg". Later studies used the single glass fibre bundles and bifurcated glass fibre bundle described in Section 3.2.4.

Early studies were encouraging with distinct changes in spectral

shape observable upon cuff application and removal. The traces in Figure 9.14 were obtained using the bifurcated polymer fibre bundle with the PMT used for detection. They show the "raw" spectra (ie not normalised) and so are influenced not only by the optical characteristics of the sample but also of the source, detector and other optical components.

The reference spectra of light backscattered from a box of white tissues is shown in Figure 9.14(i), with the spectra from the forearm of a caucaesian male: under normal condidions, following venous and arterial occlusion and during reactive hyperaemia, in Figure 9.14(ii).

The effect of absorption by the polymer fibres is clearly evident, and the relatively rapid variations in light intensity this produces together with the drift problem of the spectrophotometer (see Section 3.5.8) meant that any calculated spectra were very noisy and unreliable in this region. This is demonstrated in the difference spectra of haemoglobin in Figure 9.14(iii) produced from the spectra recorded during reactive hyperaemia (oxyhaemoglobin) and arterial occlusion (deoxyhaemoglobin). Apart from these problems above about 700nm, the trace gives a good qualitative representation of the haemoglobin difference spectra.

It was during these early studies that the effect of light "coupling" into the skin was noted once intimate contact was made between the fibre bundle and the skin. The results of preliminary investigations into this effect using the bifurcated polymer bundle are shown in Figures 9.15 and 9.16. The former shows spectra obtained with the bundle at different heights from the skin and the second the effect of applying slight pressure to the bundle which expels surface blood and therefore leads to a decrease in absorption as described in Chapter 6.

Similar studies were conducted using two small (3mm active diameter) glass fibre bundles mounted side by side (see Chapter 6). These results are shown in Figure 9.17, and demonstrate several points. Firstly

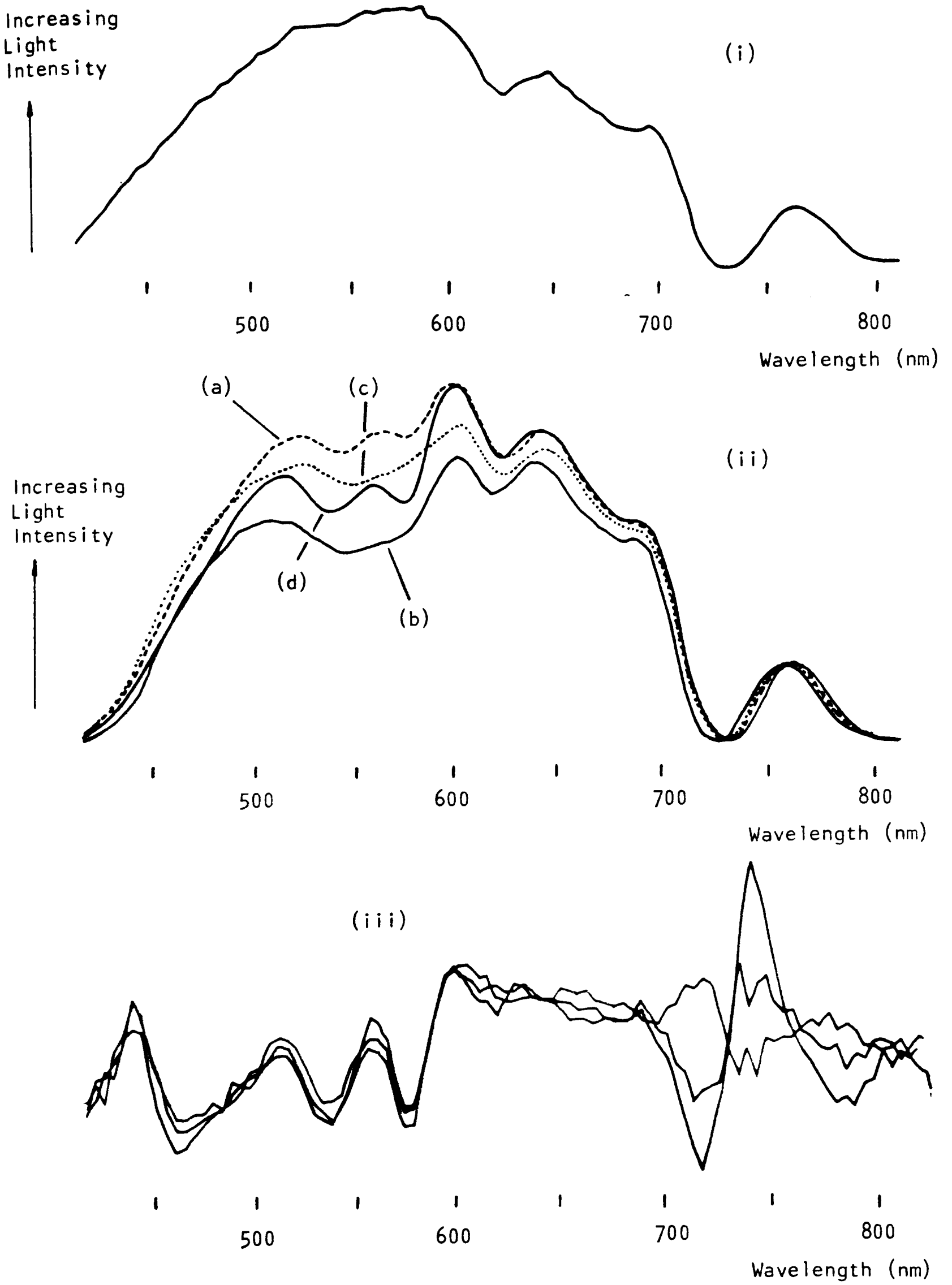

Figure 9.14 "Raw" (ie not normalised) spectra recorded using the bifurcated polymer fibre bundle from (i) white tissue paper (reference) and (ii) the forearm under: (a) normal conditions, following (b) venous and (c) arterial occlusion, and (d) during the reactive hyperaemic phase.

(iii) Qualitative difference spectra of haemoglobin produced using the spectra obtained duriing arterial occlusion and reactive hyperaemia (3 of each to produce 3 difference spectra).

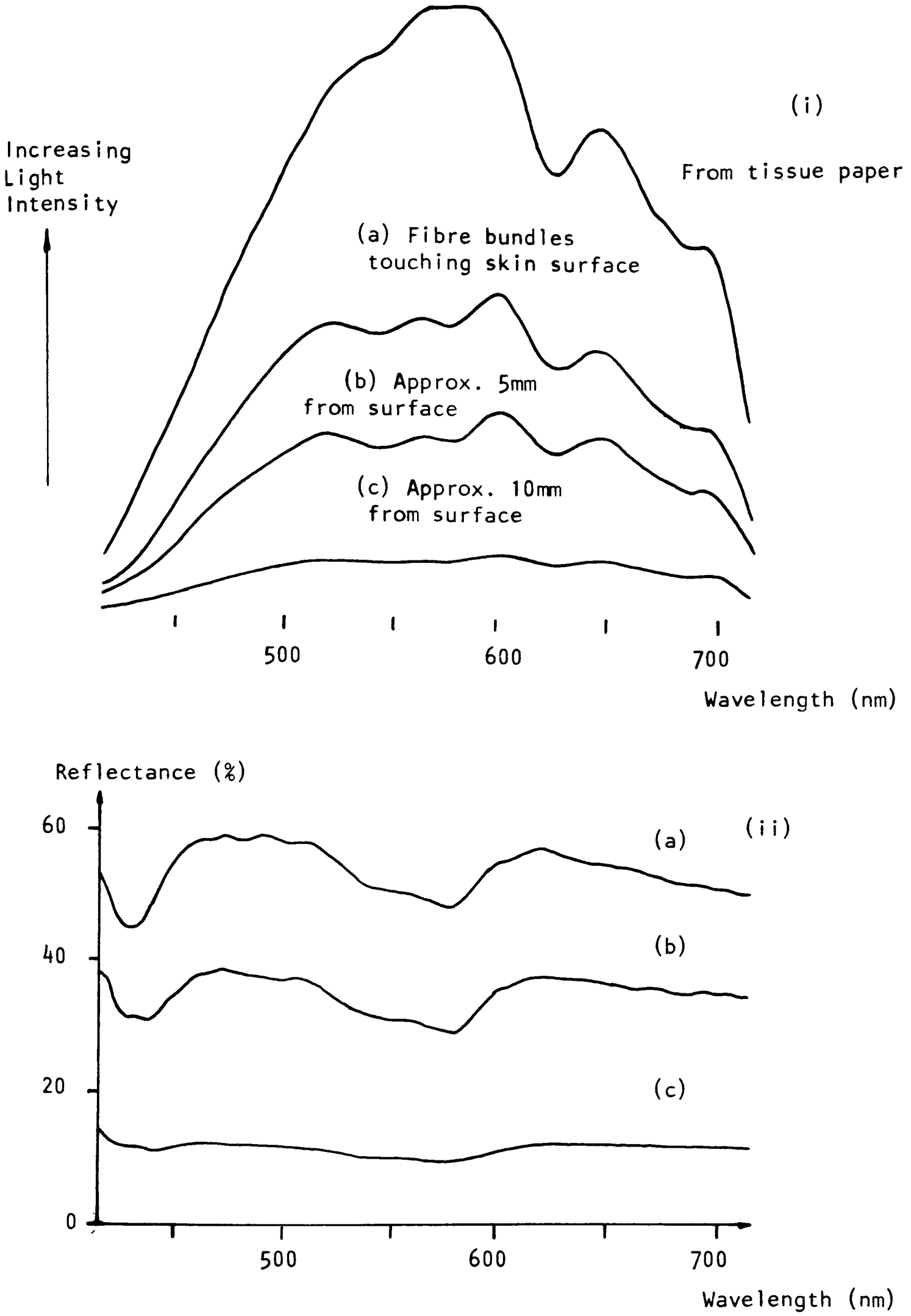

Figure 9.15 (i) "Raw" spectra recorded using the bifurcated polymer fibre bundle from: tissue paper (reference), and from the skin when touching, and at a distance of 5 and 10mm.

(ii) Reflectance spectra derived using the "raw" spectra in (i).

comparison of the reference spectra to those in Figures 9.14 and 9.15

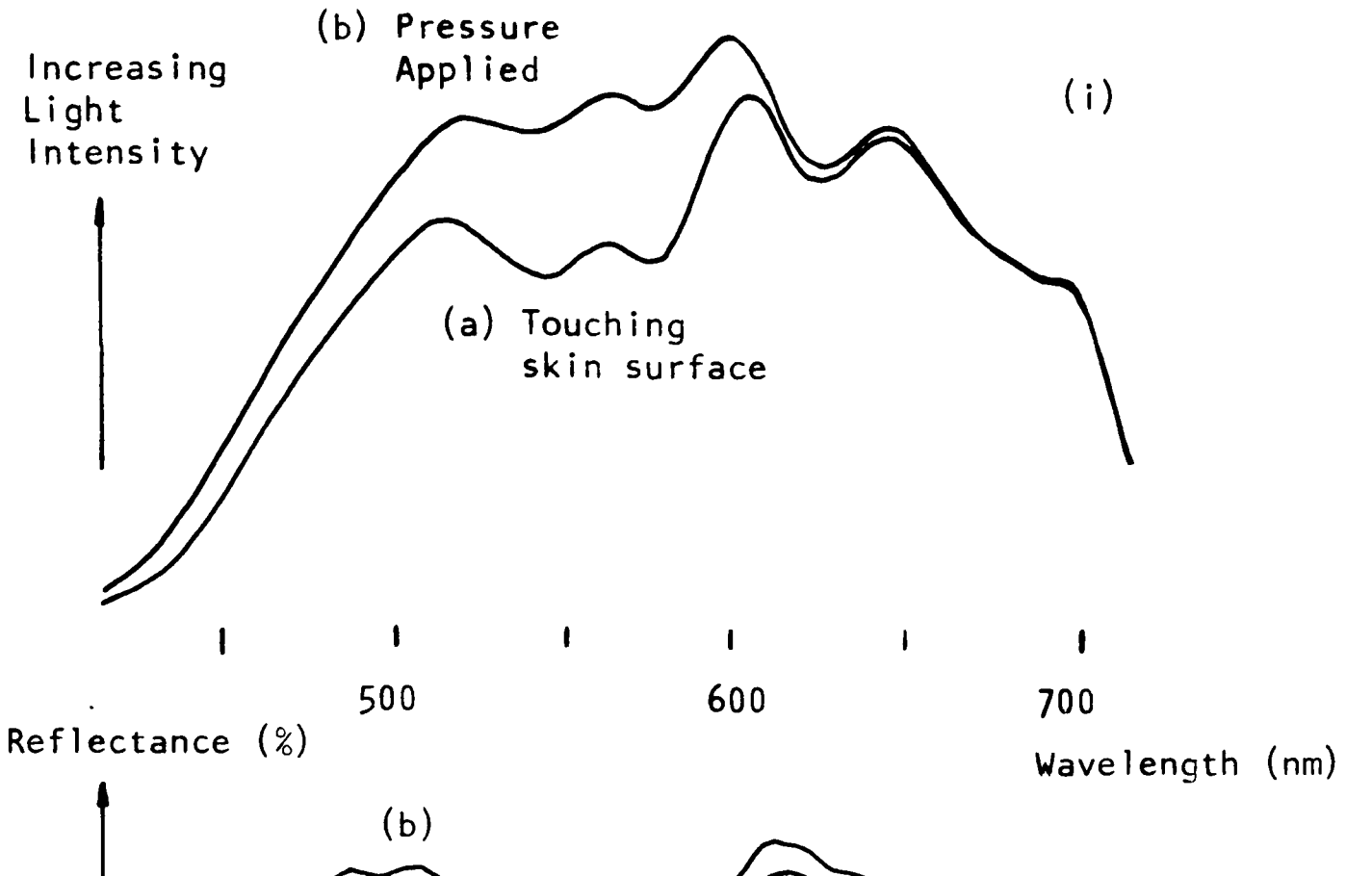

Figure 9.16 (i) "Raw" spectra of light reflected from the back of the hand of a caucasian subject, using the bifurcated polymer fibre bundle, (a) lightly touching the skin surface and (b) with slight pressure applied.

(ii) Reflectance spectra (using tissue paper as a reference) of the two above traces.

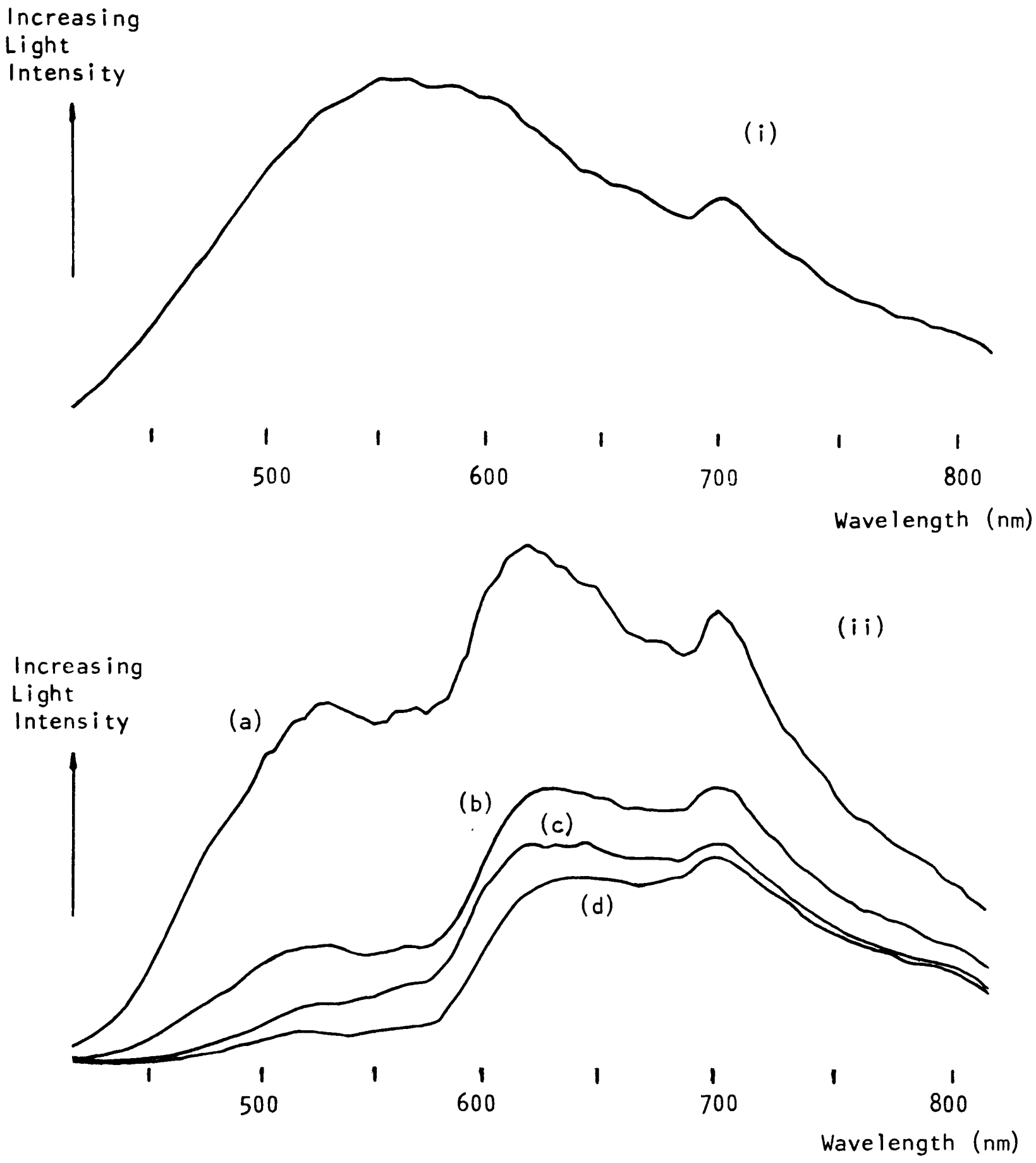

Figure 9.17 "Raw" spectra obtained using two 3mm active diameter glass fibre bundles. These show the spectral properties of light scattered from: (i) white tissue paper and (ii) the skin surface at distances of approximately (a) 10 and (b) 5mm, and when touching the skin surface (c) with and (d) without pressure applied.

shows the effect of the absorption by the polymer fibres.

The greater attenuation below about 600nm when using this transducer geometry is also evident due to the transition from a reflection to transmission type measurement as was described in Chapter 6. As with the bifurcated polymer fibre slight pressure on the bundle causes an increase in the detected signal. However, in contrast to the results in Figure 9.16 the signal decreased as the bundles were moved closer to the skin rather than increasing. This behaviour can be understood by considering the "cones" of light that emerge from, and the acceptance angles of the fibre optic bundles.

Following these reflection type studies, transmission measurements were attempted to try and repeat the single wavelength studies over a wide wavelength range. As expected no light below about 600nm could be detected or above 830nm, although this upper limit was largely due to the response of the PMT.

It was during these experiments that the relatively larger attenuation of light at around 760nm was noted for the hand compared to the finger. This is shown in Figure 9.18 which gives the "raw" transmission spectra together with a reference spectra. As discussed in Chapter 6 the likely candidates for this attenuation at around 760nm are deoxyhaemoglobin (due to the peak in its absorption spectrum at this point) or water.

The effect of venous occlusion on the transmission spectra of the hand is shown in Figure 9.19 and as expected leads to an overall decrease in the transmitted light level.

The effect of arterial occlusion and its release are shown in Figure 9.20. The traces are of the normal spectra and those obtained during and after arterial occlusion. The results were somewhat inconclusive with problems due to the low light levels detected and subsequent noise and necessity for long sampling periods. In addition shifts in the overall spectra often appeared to occur upon application of the cuff which are

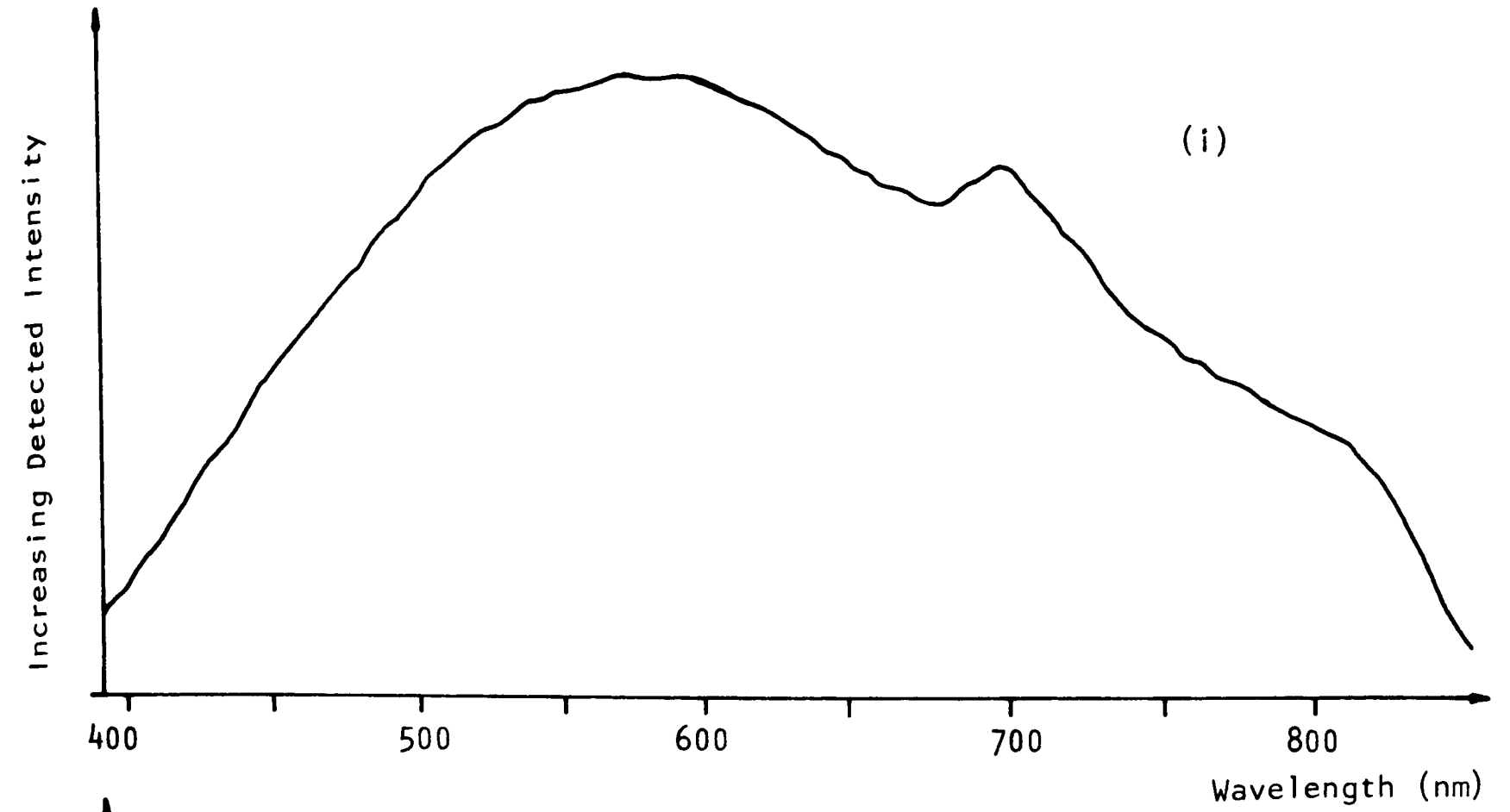

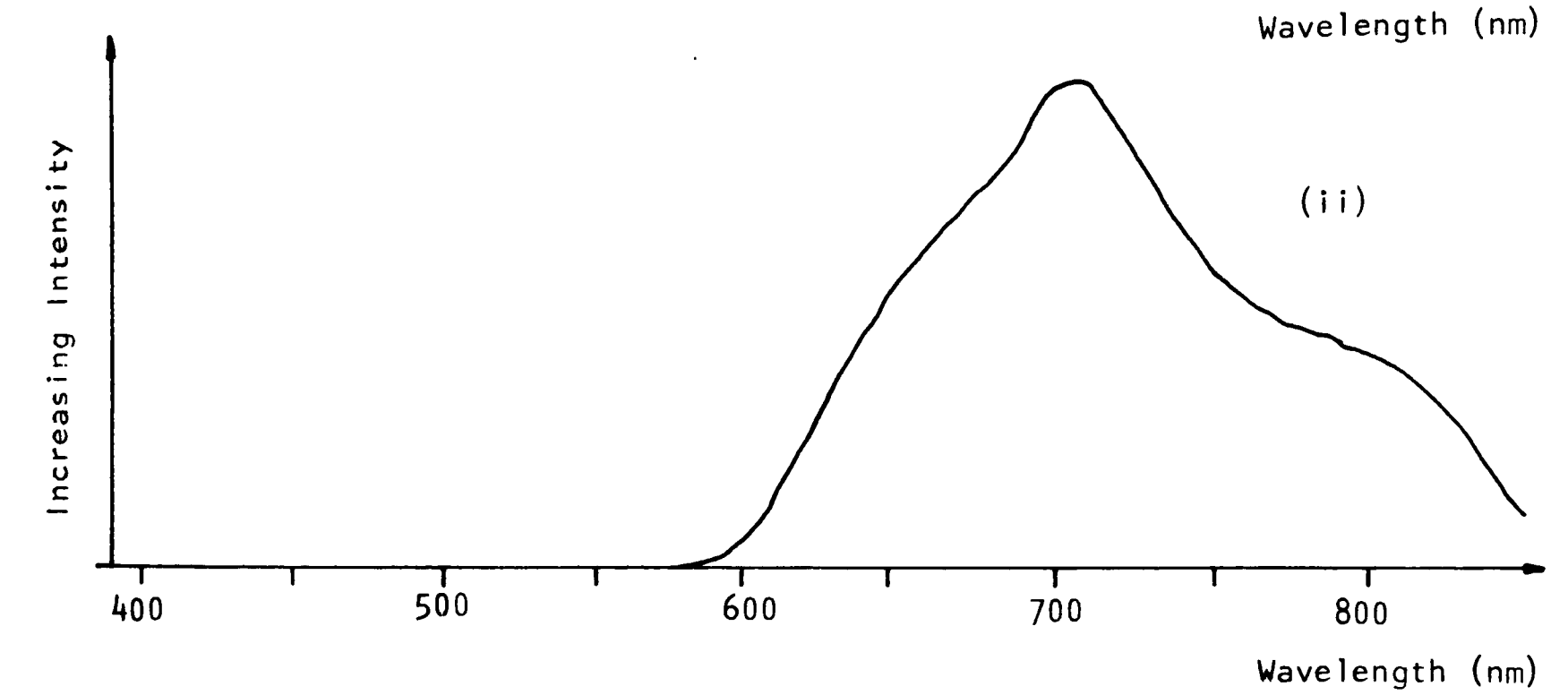

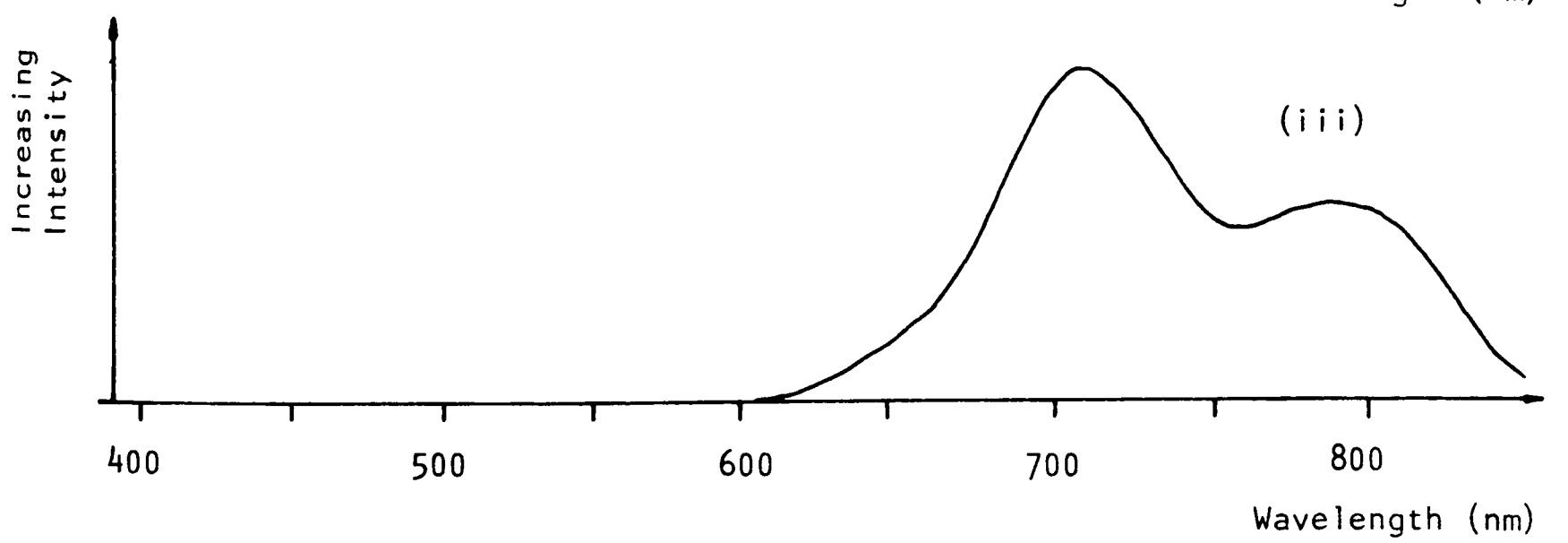

Figure 9.18 The "raw" (ie not normalised) spectra obtained: (i) as a reference and from the transillumination of (ii) a finger and (iii) a hand.

Note the increased attenuation in (iii) at about 760nm, and that no detectable light is transmitted in (ii) and (iii) below about 600nm.

(The ordinate axes have increasing sensitivity from (i) to (iii). Detection was by PMT and a slit width of 20nm was used).

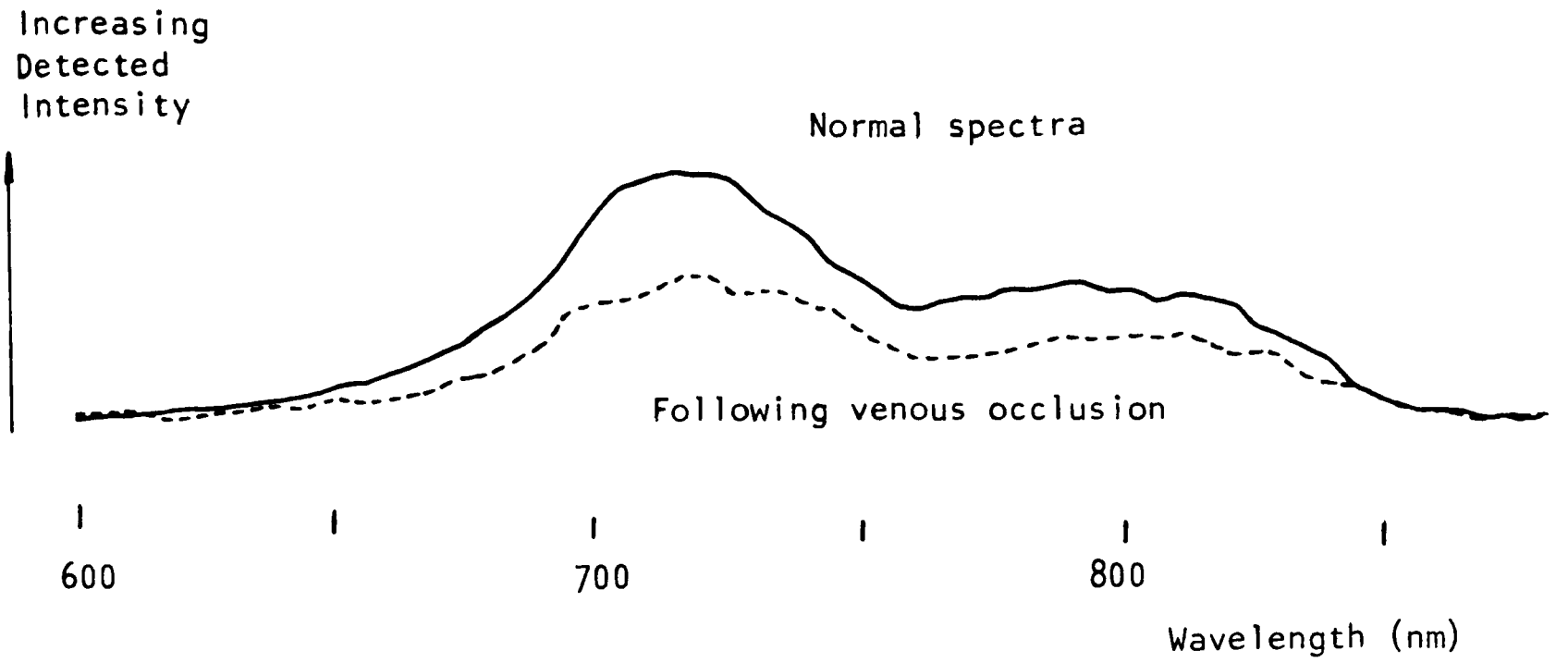

Figure 9.19 Raw spectra showing the effect of venous occlusion on the level of light transmitted through the hand (dashed trace).

(The spectra are the average from 1000 sampled spectral scans, with a slit width of 20nm and detection by PMT).

probably related to the observed effects during single wavelength studies described above.

Despite this general effects were evident. After arterial occlusion the signal level below about 760nm usually decreased whilst that above remained the same or increased slightly. This is probably due to the deoxygenation of haemoglobin, as can be seen by considering its absorption spectra, since the absorbance of oxyhaemoglobin and deoxyhaemoglobin become closer as the isobestic point is reached.

Upon release of the arterial cuff, below 760nm the light level generally increased back to or above the normal level whilst above 760nm the level decreased. Since reactive hyperaemia is associated with the inflow of oxygenated blood, the decrease in light level can be considered to be due to an increase in blood volume, whilst the increase is probably due to the fact that the incoming blood is highly oxygenated and therefore has an attenuation lower even than the blood present in a

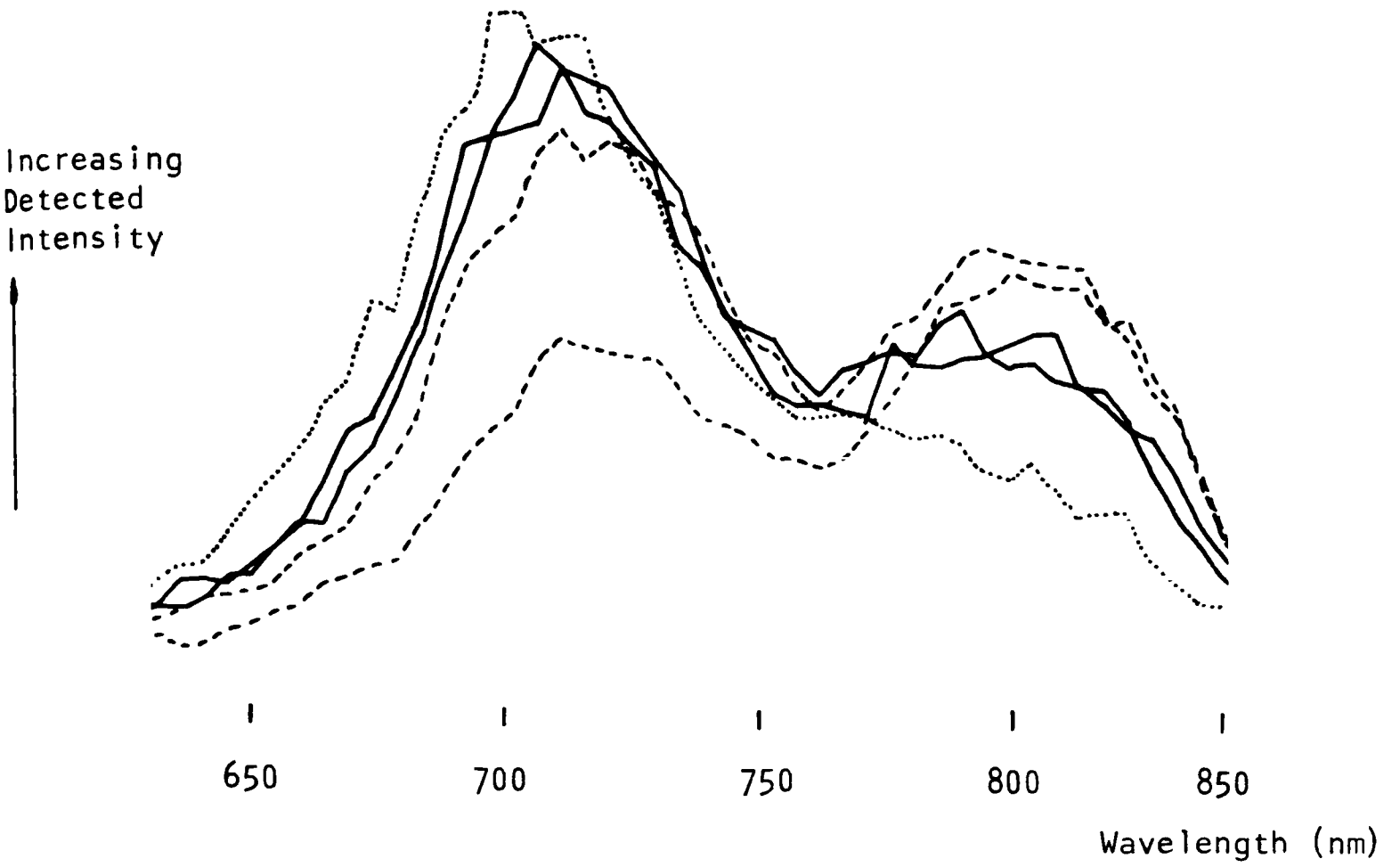

Figure 9.20 Two examples of "raw" spectra recorded showing the spectral properties of light transmitted through the hand under normal conditions (solid lines), following arterial occlusion (dashed lines) and afer the release of the cuff (reactive hyperaemic phase) (dotted lines).

(Detection was by PMT using a 20nm slit width on the spectrophotometer).

normal arm.

It would be of interest to repeat these studies with improved instrumentation to obtain more conclusive results, the validity of which could be ensured by resolving the absorption peak in the deoxyhaemoglobin spectra at 760nm. In addition, as discussed in the single wavelength section above the initial effects of occlusion on transmitted light levels warrant further investigation.

From the above studies it was evident that changes in reflectance and transmission spectra, could be seen in certain parts of the spectrum upon venous and arterial occlusion, with the effect of reactive hyperaemia and decrease in blood volume following the cessation of venous occlusion also visible. However, the difference spectra illustrating changes in oxygen saturation and blood volume obtained were by no means as clear and reproducible as was hoped, especially in the near-IR region which was of particular interest. The main cause of this being the technical limitations of the equipment which simply did not possess the required degree of sensitivity.

Also clear from these initial studies was the way in which the transducer geometry (ie position of the source and detector fibres) played a major role in determining the overall spectra obtained. This is of importance because it is slight fluctuations in these overall spectra that reflect changes in the variables such as oxygen saturation and total blood volume, and which must be followed for the purposes of non-invasive monitoring. In addition the nature of this overall attenuation is of relevance concerning the application of such methods since it may either preclude monitoring in certain regions of the spectrum using given transducer configurations, or alternatively suggest the most appropriate configuration in other instances.

It was because of this importance of the overall attenuation of tissue but scarcity of data concerning the <u>in vivo</u> reflectance properties

over about 700nm, and virtual lack of any data of the *in vivo* transmission characteristics that it was decided to perform a comprehensive series of experiments to determine these spectra. The results from these studies were presented in Chapter 6 and in addition to the overall reflectance and transmission spectra over the visible and near-IR regions include the spectra obtained using two 3mm fibre bundles side by side, and an example of the difference spectra obtained during the arterial occlusion study in reflectance mode in the visible.

From the experience gained, whilst performing the above *in vivo* optical experiments with the scanning spectrophotometer the following advice can be given concerning these type of studies

Because of the relative ease of reflection, compared to transmission measurements, it is advisable firstly to obtain some results in this mode to assess the equipment being used and gain experience of the problems involved during *in vivo* monitoring such as securing the fibre bundles to the tissue, and then keeping them steady. Ideally a random bifurcated optical fibre bundle (as large as is practical) should be used for these initial studies (this corresponding to what was termed the reflection mode above) so that an appropriate level of light will be detected below, as well as above, 600nm. With this set up in addition to the overall reflection spectra the effects of venous and arterial occlusion and their release upon the shape of the recorded spectra can also be observed. The use of optical fibre bundles to "pipe" light to and from the tissue is recommended over any other method because of their ease of use and the flexibility they allow in terms of measurement site and "source" and "detector" positioning.

With all other *in vivo* measurements beside those in reflection mode the problem of low detected light levels is likely to occur, therefore anything which is likely to increase the signal level is to be advised. This could include increasing the lamp's output, or using its light more

effeciently, and using large diameter fibre bundles with a sensitive detector intimately coupled to the detecting fibres. Below about 600nm the response of photodiodes begins to fall off and so it is advisable to use a PMT. Indeed in many ways the ideal detector is a PMT with a response that extends out to the near-IR, and which therefore can be used over the entire range under investigation.

A cautionary note should be added that care must be taken to ensure that the incident light level is never large enough to cause tissue damage or, although less importantly induce, physiological changes. For this reason heat blocking filters may be of some use.

Another means of increasing the detected light level (and which was used to obtain the results in transmission mode in Chapter 6) is to increase the slit width of the monochromator. The disadvantage of this is that the spectral resolution of the instrument is reduced, however although some of the results in Chapter 6 were made with a 20nm slit width the shapes of the absorption bands can still be recognized which demonstrates that this degree of resolution is adequate for preliminary studies at least after which the width can be developed as appropriate.

In conclusion, once an instrument capable of monitoring <u>in vivo</u> measurements has been constructed, then there is a wide range of studies that can be attempted because of the large number of variables (eg measurement site and transducer geometry) involved in producing the final results. It is for this reason that it is important to rigorously record the details of such studies for subsequent analysis, and comparison of results with those of other workers.

9.3.3 Conclusions and Suggestions for Further Work.

The results from the *in vivo* studies show that although the overall reflection and transmission characteristics were performed with some success, the small changes in detected light intensity due to physiological effects (such as changes in oxygen saturation or blood volume) were more difficult to obtain. Indeed the only reliably reproducible results of this nature were obtained in reflection mode in the visible region.

This is because the change in signal level which is being monitored is small, and comparable to the background noise, where this term is used to include any unwanted cause of a change in signal level in the same way that the term "drift" was used whilst discussing the yeast studies.

If attempts are made to obtain difference spectra then the noise problem is compounded since both a noisy signal and reference spectra will be used as both spectra will be the result of *in vivo* measurements. (This is not so when obtaining the overall reflectance and transmission properties since then even for low signal light levels the reference spectra will at least be stable).

The most straightforward solution to these problems is to build an improved scanning spectrophotometer with better optical characteristics, particularily in terms of its light throughput. Then higher light levels would be detected and so the signal-to-noise ratios of any spectra obtained would be improved. However, although this would undoubtedly improve results, problems would still be anticipated due to the equivalent of the drift problems in the yeast studies. That is non-specific changes in signal level, due for example to fibre bundle movement at the skin surface.

One solution to this particular problem is to ensure that no such movements can take place by fixing the fibre bundles to the skin in a more stable mechanical manner. However, whereas this approach may work for evaluation purposes, it is felt that in a clinical situation this aspect may prove quite a problem where monitoring over a period of tens of minutes or

even hours may be required.

The pulse oximeter overcomes these problems by only analysing the cardiac synchronous pulsatile component of the detected light, but although (see Chapter 7) such a component may be detected through thicker tissue samples than the finger the signal is very small. There is also the disadvantage that theoretically the pulse oximeter only monitors the oxygen saturation of the pulsatile blood (see Section 1.4.5) and so this approach would be of no value for monitoring the redox state of cytochrome oxidase present in tissue for example.

Another possiblity would be to use the same solution offered by the dual beam spectrophotometer. That is to employ one or more wavelengths for monitoring and thus allow for any non-specific changes. As described above, the scanning spectrophotometer could be suitably modified (via the BASIC control programme) to accomodate this.

The method is the same in principle as that used during dual wavelength spectrophotometeric monitoring (see Section 4.10) to follow the changes in the redox state of cytochrome oxidase whilst compensating for any changes in oxygen saturation, except that in this more general application all non-specific variations would hopefully be compensated for.

However, consideration of the way in which any such reference signal should be used demonstrates one of the major problems in the field of non-invasive optical monitoring. This was discussed in Section 4.10 in terms of the specificity of monitoring when using reference wavelengths in dual beam spectrophotometry and is linked to the overall problem that as yet there is no complete model that describes the way in which light interacts with tissue to dictate how any processing of the detected intensities at various wavelengths should proceed.

Within this thesis the effects of the wavelength dependence of lamp output and detector sensitivity have been accounted for by normalising the detected light levels to produce a value for the "transmission" or

"absorbance" with respect to some reference spectra. However, the results produced in this way only give details of the relative total attenuation of reflected or transmitted light at different wavelengths and offer no information on the relative contributions due to scattering and absorption processes.

As stated above this highlights a major problem with in vivo optical measurements. Although the overall reflection and transmission spectra obtained can be understood in a qualitative manner in terms of the major light absorbing chromophores present, the prediction of the exact form of these spectra in quantitative terms is far more difficult. Yet it is these spectra that are important since it is the slight changes in their shape that gives rise to the difference spectra whose variations may enable variables such as oxygen saturation and cytochrome oxidase redox state to be monitored.

Clearly, the prediction of the overall attenuation of a tissue sample in quantitative terms, or the quantification of the results obtained from optical measurements is an extremely complex problem. Tissue is in general highly heterogeneous in both macroscopic and microscopic terms with intense scattering and absorption processes both influencing the passage of photons through the body components with various individual optical properties likely to be encountered within any sample. This in itself presents many difficulties in producing a theoretical description of the attenuation of light by tissue, compounded by the fact that results obtained can vary depending upon the relative positioning (and characteristics) of the source and detector or at least the fibre bundles connected to them (ie the transducer geometry).

That this last point is so is shown by the results within this thesis and is probably because the paths the photons describe within the tissue (ie the body components encountered) is strongly affected by transducer geometry.

Factors such as this must be accounted for by any complete theory along with allowances for other variables such as the illumination and detection processes themselves. The fact that a larger proportion of light appears to be "coupled" into the tissue once the fibre bundle end is in intimate contact with the surface has been described, and such an effect would seem to suggest that matching of refractive indices may lead to a more efficient use of light. In addition the variation of detected signal with the distance of the transducer from the skin surface has been demonstrated, and shown to be dependent upon transducer geometry.

Concerning detector geometry, most authors performing in vivo measurements now use optical fibre bundles to collect the emerging light. This not only raises the question of "coupling" the light from the tissue into the detector, but also that of what fraction of the emerging light is actually collected.

Before fibre optic bundles became widely available integrating spheres were generally used for reflectance measurements, and it would be of value to know the relationship between their respective detection characteristics. SINGH (1982) has partly addressed this problem, whilst BASHFORD (1982) has suggested that his use of fibre optic bundles compared to other author's use of an integrating sphere may actually help to explain differences between results. It is for reasons such as this that further investigation into the characteristics of detectors and sources, and how they may be modelled is considered worthwhile.

In addition to, and more fundamental than, the instrumentation's characteristics, to address the quantification of in vivo optical measurements, further experimental and theoretical work on the optical characteristics of tissue are both required.

Experimentally, measurements must be made on excised body components of various degrees of complexity so that their absorption and scattering coefficients can be found. In addition measurements on whole tissue, such

as those described here, are required so that the effects of variations in transducer geometry and possible use of coupling compounds can be investigated as well as determining at what sites and over what wavelength ranges monitoring is feasible.

Observation of the spectral variation of the small changes in detected light intensity due to changes in oxygen saturation, cytochrome oxidase redox state and blood volume are also of value since it is these types of measurements which will eventually be used for monitoring and therefore hopefully quantified. Other studies on bloodless, blood perfused and blood substitute perfused organs could also be performed to investigate in more detail the precise contribution to optical characteristics made by blood.

Theoretically, any modelling must ideally take into account the scattering properties of tissue which is essentially a collection of randomly densely packed scattering centres. As described in Section 1.3, and in the introduction of ISHIMARU (1978) a variety of techniques can and have been used to approach this problem. However the majority of models employed so far assume a radiative transfer approach as described in Section 1.3.4 and only consider the major absorption and scattering processes, or indeed simply assume that one dominates the other.

One approach which appears to have been largely overlooked in the non-invasive monitoring field is diffuse reflectance spectroscopy. Although largely empirical this technique has found widespread use in the food industry for the analysis of powdered and other diffusely reflecting (ie back scattering) compounds (WETZEL (1983)). Indeed the work of CONWAY (1984) on the analysis of fat composition of tissue has its origins in this field.

One alternative theoretical approach is the Monte Carlo method (see Section 1.4.10) which would appear to be ideally suited to the problem because of its ability to readily accomadate regions of different optical characteristics. However, an inverse approach to this method would be

required for its use in diagnosis which is likely to be computationally diffcult to apply in practical terms.

Since a complete theoretical description of the characteristics of tissue is unlikely to be produced in the near future, it is likely that appropriate approximations will enable some linking of experimental and theoretical data. In fact approximations using the Lambert-Beer law are already used to provide the theoretical basis for oximeters (Section 1.5.1), whilst assumptions concerning the relative magnitude of absorption and scattering effects have been applied in the field of PDT and are also likely to be used in the area of optical transillumination imaging.

One of the most interesting results to arise from the transmission measurements presented above and in Chapter 6 was the disproportionately large attenuation, around 760nm, by the hand when compared to that of the finger. As discussed, the most likely contributors to this attenuation are deoxygenated haemoglobin and water. Judging by the relative absorption coefficients of the two in this region (and the lack of any appearance of an absorption band due to water in a solution of oxyhaemoglobin) then deoxygenated haemoglobin would appear to be the most likely candidate. However, the effect of the water absorption band at approximately 960nm is visible in both reflection and transmission spectra (see Chapter 6), whilst BOLIN (1984) also attributes the attenuation at 760nm in various bloodless tissue samples to water. In addition the definate existence of an absorption band at 760nm is clearly shown in Figure 9.9.

The relative contribution of these two compounds, (and possibly others), could be investigated by studying the transmission spectra of blood free, blood perfused and non-blood perfused tissues (as suggested above for studying the optical characteristics of tissue in general). Because of the apparent link between sample thickness (ie the finger and hand) and the manifestation of this attenuation then the studies should be made on samples of different thicknesses.

Such investigation is considered of particular importance because this attenuation is within the region of the near-IR which will be, and is already, used for non-invasive monitoring. At present no allowances are usually made for this attenuation which indeed may not be necessary for thin samples (eg the ear or finger), however, for larger samples this may not be a valid assumption.

Finally, on the subject of transillumination imaging JARRY (1983) has used a He-Ne laser and laser diodes to obtain images using a collimated source and detector from thin tissue samples. These type of studies could be repeated using the scanning spectrophotometer for wavelength selection to produce images throughout the visible and near-IR regions. The results may help to determine the optimum wavelengths for image clarity (due to reduced scattering) and the detection of certain structures (due to increased attenuation) for use on certain tissues. Such studies would be similar to those carried out with the image intensifier as described in Chapter 2 but with collimation. The intensifier itself could also be used for further studies, together with conventional photography as suggested at the end of that chapter. These would include the use of photography at discrete wavelengths to investigate whether structures under the skin may be imaged which should help determine the wavelength dependence of the back-scattered light from within the tissue to a photodetector on the surface. This would be expected to be linked to the penetration depths (those depths at which 37% of the light has not been attenuated) since if less photons reach a certain depth then fewer can be back scattered to the surface to be detected if a suitable scatterer is encountered.

Finally, the transillumination studies of the hand described in Chapter 2 may have a potential use in security applications. The preliminary results suggest that individuals have distinct venous patterns on the back of their hands, therefore transillumination imaging could be used together with pattern recognition techniques to determine a person's identity.

Reference.

Wetzel, D.L. (1983), Anal. Chem., 55, 1165A-1176A.

Acknowledgements.

Firstly I would like to thank Dr Peter Rolfe, for allowing me the oppurtunity to work within the Bioengineering Unit, his stimulating discussions and apparently unerring faith in my ability to complete this thesis.

Secondly I would like to express my gratitude to Dr Philip Rea who in addition to introducing me to the field of biochemistry, was a constant source of help and encouragement during the early part of my research.

I must also thank Dr B.Hill and his colleagues (Department of Biological Sciences, University of East Anglia) for supplying me with samples of purified cytochrome oxidase, and R.Emms and Dr P.Lund for allowing me access to their dual beam spectrophotometer (Metabolic Research Lab, Radcliffe Infirmary, Oxford), and their helpful discussions on the toxicity of free radicals.

Concerning the growth of yeast cells I am grateful to Dr A.J.Kingsman (Department of Biochemistry, University of Oxford) for the use of his facilities via his research assistant, my wife, Nicki.

It remains for me to express my appreciation to fellow members within the Bioengineering Unit. This includes my colleague Y.A.B.D.Wickramasinghe for his continued assistance and patience, P.J.Goddard, R.S.Wolton and P.J.Burton for their excellent technical support and advice, J.Dyer for introducing me to the Texas microcomputer system and M.Briers, M.Martin, C.and D.Murphy and T.Newson for their help and useful discussions.

Finally, I must thank the SERC (and Nicki) for financial support and partly funding an informative visit to Dr G.Jarry (Créteil Medical School, Créteil, Paris France), whose hospitality was greatly appreciated.

Appendix A.

OPTICAL METHOD ADAPTABLE FOR CEREBRAL MONITORING IN THE NEWBORN

Y.A.B.D. Wickramasinghe, J.A. Crowe and P. Rolfe

Bio-Engineering Unit, University of Oxford, John Radcliffe Hospital, Oxford, United Kingdo

NEED FOR CEREBRAL MONITORING

Although biological materials are mostly transparent to light in the near infra-red, oxygenated haemoglobin exhibits specific spectral absorption characteristics in this wave length range. Another substance in living tissues which exhibits oxygen dependent absorption is an enzyme called cytochrome aa_3.

It has been suggested that by observing their absorption characteristics, valuable information regarding the oxygen utilization and energy turnover of living tissue could be obtained. Jobsis and co-workers were the first to employ this method (1,2,3), which is non-invasive and allows the possibility of continuous monitoring. It provides the potential for application to sick neonates who are at risk of hypoxic/ischaemic brain injury and brain haemorrhage. Although the precise cause of brain haemorrhage is not clear, imperfect regulation of cerebral blood flow, together with fluctuations in blood gas levels, or blood pressure are felt to be contributory factors. A means of continuously monitoring cerebral blood volume, oxygen saturation and the redox state of cytochrome aa_3 may help to determine the underlying causes (4).

We have developed a laser-based instrument and have performed experiments on adult volunteer forearms in order to assess the potential of this method, so that it may be adapted for use on sick neonates.

METHOD: LIGHT SOURCE;

For in-vivo measurements, as the specimen (organ) thickness increases, the light level that emerges after absorption and scattering becomes extremely weak. There is the need to perform the studies in normal room lighting conditions, thus imposing restrictions on the use of light detecting devices which tend to saturate under such conditions. For our experiments on adult forearms, we have used single heterojunction laser diodes which emit light pulses of 200 ns duration and are operated at a frequency of 500 Hz. A high voltage regulator (figure 1) provides excellent stability against power supply fluctuations. The temperature of the laser diode also needs to be kept at about 20°C to ensure stability.

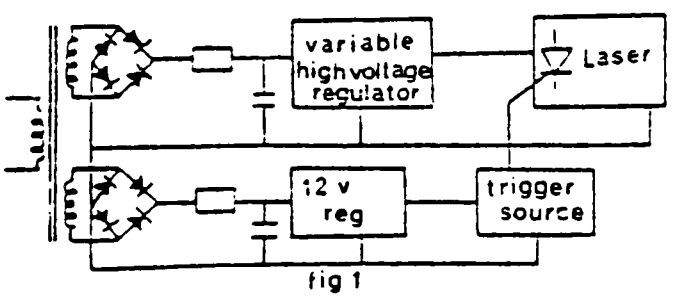

fig 1

Laser power supply

DETECTOR:

We have used a fast response silicon photo assembly to detect the light level, and we employ filtering and amplification (figure followed by gating, sampling and integratio

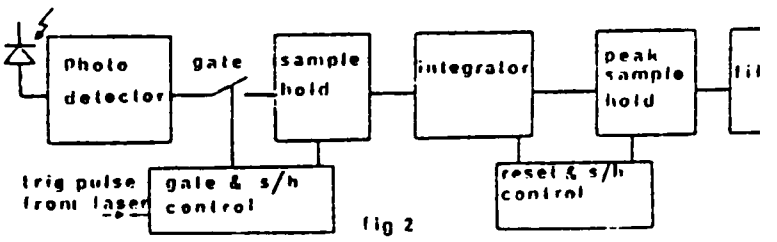

fig 2

Signal Processing

RESULTS

Figure 3 shows a study performed on a volu adult forearm using the laser diode system arterial cuff was applied around the upper When this was inflated to above systolic pressure, it produced a fall in PsO_2, a ris $PsCO_2$ and an increase in the detected ligh intensity when transilluminated by a laser 845 nm. The cuff pressure was held consta from A to B. Upon release of the cuff, th PsO_2 increased and $PsCO_2$ decreased, and a and rapid decrease in the transmitted ligh intensity was observed.

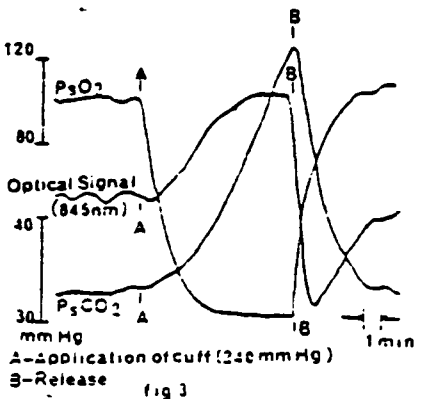

fig 3

Variations in optical signal. PsO_2 and $PsCO_2$ with application of arterial pres around the upper arm.

Figure 4 shows a similar study in which a laser Doppler system was used to monitor t cutaneous blood flow.

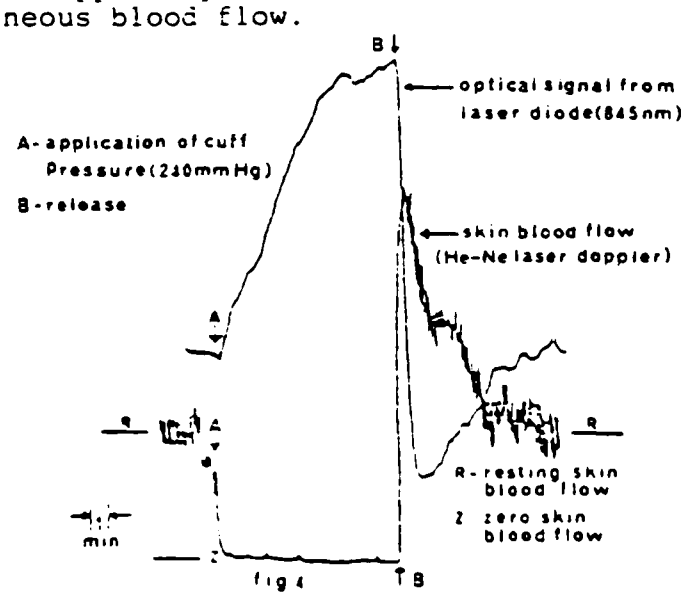

fig 4

Laser diode signal variations and ski blood flow with arterial cuff around the upper arm.

As the cuff pressure is increased to 240 mm Hg, the skin blood flow falls tozero quite rapidly and remains at zero until the cuff pressure is released. During this period of zero blood flow, the laser diode optical signal (845 nm) initially increases steadily and then tends to plateau. It may be assumed that from A to B, there is no blood flow into the forearm and therefore the blood volume remains constant. The changes in the 845 nm laser diode signal could be attributed to the conversion of oxyhaemoglobin to haemoglobin. Upon release of the cuff, the rapid decrease in the detected light (845 nm) seems to follow the anticipated increase in blood volume resulting from reactive hyperaemia.

DISCUSSION AND FUTURE STUDIES

With the instrument developed so far, we are not able to separate the influences of all of the variables known to be relevant, i.e. the blood volume changes, oxygen saturation and the redox state of cytochrome aa_3. Although cytochrome aa_3 exhibits oxygen dependent absorption at 845, our in-vivo results indicate that blood volume changes and oxygen saturation also have profound effects on the 845 nm signal. Blood volume and oxygen saturation can, of course, be estimated at two different wavelengths to 845 nm. We are at present developing a multiple wavelength laser diode system which could offer the possibility of determining the relative changes in each of the variables mentioned.

ACKNOWLEDGEMENTS

We acknowledge the support of the Wellcome Trust, the British Council and Unilever PLC for YABD; the SERC for JC and the Wolfson Foundation for the provision of facilities within the Bio-Engineering Unit.

REFERENCES

1. F.F.Jobsis et al. J. Appl. Physiol., 43, 858-872
2. F F Jobsis. Adv Neurol, 26, 299-318, 1979
3. E J Fox et al. Anesthesiology, 57 (Suppl), A 160, 1982.
4. J A Crowe et al. In Fetal and Neonatal Physiological Measurements, Vol 2. Guildford, Butterworths, 1985.

From Med. Biol. Eng. Comp., 23, Suppl. 1, 468-469, (1985)

```
140  GOSUB 20000
150  GOSUB 20000
160  GOSUB 20000
200  DIM SP[200],HED[10],LAB[4],AXS[25],T[22,3]
202  INPUT "INPUT TIME      HOURS    ";?202;H"        ";
203  INPUT "MINUTES    ";?203;M
204  TIME H,M,0
210  INPUT "INPUT DATE   ";?210;DAT
220  INPUT "SPECTRAL RANGE  A,B OR C   ";?220;$P"    ";
230  IF $P="A" THEN Q1=1:: Q2=140:: GOTO 260
240  IF $P="B" THEN Q1=31:: Q2=170:: GOTO 260
250  Q1=61:: Q2=200
260  XAX=139:: X1=Q1:: X2=Q2
270  BAUD 2,4:: UNIT 2
280  PRINT "IN; "
281  UNIT 1
282  FOR I=1 TO 19
283   READ AXS[I]
284  NEXT I
290  P1=1:: P2=2:: P3=3:: SPD=38.1:: PON=0
300  C=0:: B=0A48CH:: TST=0:: NSP=0:: Z3=1
350  INPUT "TIC-TOC ?   ";?350;$P
360  IF $P="Y" THEN GOTO 600
450  PRINT "SINGLE SPECTRA PROGRAMME    ";
460  GOSUB 1000   ! SAMPLE
470  INPUT "PLOT OR SAMPLE ";?470;$P"     ";
472  IF $P="X" THEN STOP
476  IF $P="R" THEN GOTO 290
480  IF $P="S" THEN GOTO 460
482  IF $P="P" THEN GOTO 490
485  IF $P="O" THEN GOTO 720
488  GOTO 470
490  INPUT "WHAT TYPE   ";?490;TYP"     ";
492  IF TYP=0 THEN GOTO 720
493  ON TYP THEN GOSUB 2000,2200,2800,3200
494  IF TYP<5 THEN GOTO 470
495  IF TYP=5 THEN PON=1:: TST=1
500  IF TYP=6 THEN PON=0:: TST=0
505  IF TYP=7 THEN TST=1
510  IF TYP=8 THEN TST=0
512  IF TYP=9 THEN NPT=1
513  IF TYP=10 THEN NPT=0
520  ON (TYP-10) THEN GOSUB 7000,7200,7400
525  IF TYP<21 THEN GOTO 490
530  IF TYP>26 THEN GOTO 490
540  PON=1:: TST=1:: P3=(TYP-20)
550  GOTO 490
600  INPUT "NO OF SPECTRA   ";?600;NSP"     ";
602  STO=0:: NSP=NSP+C
605  IF NSP>22 THEN PRINT "MAX 22";:: GOTO 600
610  IF NSP=0 THEN GOTO 450
615  INPUT "NO OF SAMPLES   ";?615;N"     ";
620  IF N=0 THEN PRINT "MIN OF 1";:: GOTO 615
625  INPUT "TIME BETWEEN SPECTRA    ";?625;T3P      ";
630  T1=2.4*N:: T2=25*TSP
635  IF T1<T2 THEN GOTO 650
640  PRINT "SAMPLE TIME MORE THEN TIME BETWEEN SPECTRA.
645  GOTO 615
650  PRINT :: PRINT "PRESS 0 TO START  SPEC NO: ";
665  IF NKY[051H] THEN GOTO 670
667  GOTO 665
```

```
670  PRINT C+1;
675  GOSUB 1000
680  T3=TI[0]
685  IF NSP=0 THEN GOTO 700
690  TT=TI[T3]:: IF TT>=T2-T1 THEN GOTO 670
695  IF NKY[05]H] THEN PRINT "RESTART":: C=0:: B=[illegible]
696  GOTO 690
700  T1=TT/2.5+0.5:: TT=INP[TT]:: TT=TT/10
720  INPUT "PLOT OR RESAMPLE ";?720;$P"    ";
721  IF $P="Q" THEN GOTO 470
722  IF $P="X" THEN STOP
723  IF $P="R" THEN GOTO 725
724  GOTO 740
725  INPUT "TOTAA RESTART ; SCRAP ALL SPECTRA ? ";[illegible]
727  IF $P="Y" THEN C=0:: B=0A480H:: GOTO 600
729  INPUT "KEEP OLD SPECS ; NEW PARAMETERS ? ";[illegible]
730  IF $P="Y" THEN GOTO 600
732  PRINT "TIMING ETC. AS BEFORE ";
734  NSP=NSP+C
735  IF NSP<23 THEN GOTO 650
736  PRINT "NOT ENOUGH SPACE LEFT  ";:: GOTO 720
740  INPUT "TYPE OF PLOT    ";?750;TYP"    ";
741  PON=0:: TST=0
745  IF TYP<1 THEN GOTO 720
747  IF TYP>7 THEN GOTO 720
750  IF TYP<5 THEN GOTO 765
755  ON (TYP-4) THEN GOSUB 7000,7200,7400
760  GOTO 740
765  INPUT "WHICH SPECS    ";?765;S"    ";T10"    ";
770  IF T10>22 THEN PRINT "SPECS < 22":: GOTO 765
772  INPUT "WHAT STEP, REF    ";?767;T11"    ";R"    ";
773  STO=0
775  ON TYP THEN GOSUB 2005,2210,2810,3010
780  PON=1:: TST=1
785  FOR S=(S+T11) TO T10 STEP T11
790   ON TYP THEN GOSUB 2005,2210,2810,3010
795  NEXT S
800  PON=0:: TST=0
805  GOTO 720
1000  C=C+1
1010  FOR K=2 TO 400 STEP 2
1020   MWD[0A300H+K]=0
1040  NEXT K
1050  A=B+6:: B=A+398
1060  MWD[0A008H]=A:: MWD[0A00AH]=B
1062  IF NSP<>0 THEN GOTO 1120
1065  PRINT
1070  PRINT "SPEC NO.   ";C"    ";
1080  INPUT "NO SAMPLES   ";?1080;N"    ";
1090  IF N=0 THEN STOP
1100  IF C<17 THEN GOTO 1120
1110  PRINT "NO DATA STORE LEFT
1115  INPUT "RESTART   ";?111;$P"    ";
1116  IF $P="Y" THEN POP :: GOTO 470
1117  POP :: GOTO 470
1120  MWD[0A00CH]=N
1125  PRINT "[illegible]";
1130  CALL [illegible]
1135  [illegible]
1140  RETURN
2000  INPUT "SPEC NO [illegible]
2002  IF [illegible] THEN RETURN
```

```
2003  IF S0>23 THEN RETURN
2005  K=-2:: YM=0:: S1=0A2FEH+(S*404)
2007  SNM=MWD[S1+400]:: RNM=MWD[S1+402]
2010  FOR J=1 TO 200
2020   K=K+2
2030   SP[J]=MWD[S1+K]/SNM
2040   IF SP[J]>YM THEN YM=SP[J]
2050  NEXT J
2055  IF TST=1 THEN GOTO 2075
2060  Z1=1:: Z2=8:: Z3=409.6:: NPT=0
2064  GOSUB 4000
2066  Y1=INP[Y1+0.5]
2070  $LAB[0]=" ABSOLUTE":: $L="V"
2075  $T[0,0]=$T[S,0]
2080  GOSUB 9000
2090  RETURN
2200  INPUT "REF + SIG SPEC  ";?2200;R" ";S" ";ST"    ";
2204  IF R<1 THEN RETURN
2205  IF R>17 THEN RETURN
2206  IF S<1 THEN RETURN
2207  IF S>17 THEN RETURN
2210  K=-2:: YM=0
2220  R1=0A2FEH+(R*404):: RNM=MWD[R1+400]
2230  S1=0A2FEH+(S*404):: SNM=MWD[S1+400]
2240  RAT=SNM/RNM
2250  FOR J=1 TO 200
2260   K=K+2
2270   IF MWD[R1+K]/RNM<3 THEN SP[J]=0:: GOTO 2310
2280     ELSE IF MWD[S1+K]/SNM<3 THEN SP[J]=0:: GOTO 2330
2290   X=MWD[R1+K]/MWD[S1+K]
2300    X=LOG[X*RAT]
2310    SP[J]=X/0.230259
2320    IF ABS[SP[J]]>YM THEN YM=ABS[SP[J]]
2330  NEXT J
2340  IF TST=1 THEN GOTO 2365
2350  Z1=10:: Z2=14:: Z3=10
2355  GOSUB 4000
2360  $LAB[0]=" ABSORBANCE":: $L="A"
2365  $T[STO,0]=$T[S,0]:: $T[0,0]=$T[STO,0]
2370  GOSUB 9000
2380  IF STO<>0 THEN GOSUB 6000
2390  RETURN
2800  INPUT "REF + SIG SPEC  ";?2800;R" ";S" ";ST"    ";
2804  IF R<1 THEN RETURN
2805  IF R>17 THEN RETURN
2806  IF S<1 THEN RETURN
2807  IF S>17 THEN RETURN
2810  K=-2:: YM=0
2820  R1=0A2FEH+(R*404):: RNM=MWD[R1+400]
2830  S1=0A2FEH+(S*404):: SNM=MWD[S1+400]
2840  RAT=SNM/RNM
2850  FOR J=1 TO 200
2860   K=K+2
2865   IF MWD[S1+K]>MWD[R1+K] THEN GOTO 2875
2870   IF MWD[R1+K]/RNM<3 THEN SP[J]=0:: GOTO 2910
2880     ELSE IF MWD[S1+K]/SNM<3 THEN SP[J]=0:: GOTO 2910
2890   X=MWD[R1+K]/MWD[S1+K]
2900   X=X*RAT
2910   SP[J]=1000/X
2920   IF SP[J]>YM THEN YM=SP[J]
2930  NEXT J
2940  NPT=0:: GOTO 2850
```

```
2925  K=-2:: YM=0
2926  FOR J=1 TO 200
2927   K=K+2
2928   IF MWD[R1+K]/RNM<3 THEN SP[J]=0:: GOTO 2936
2929     ELSE IF MWD[S1+K]/SNM<3 THEN SP[J]=0:: GOTO 2936
2930   X=MWD[R1+K]/MWD[S1+K]
2931   X=X*RAT
2932   SP[J]=(1000/X)-1000
2934   IF ABS[SP[J]]>YM THEN YM=ABS[SP[J]]
2936  NEXT J
2938  NP=1
2950  IF TST=1 THEN GOTO 2965
2952  Z1=16:: Z2=18:: Z3=10
2953  IF NP=0 THEN NPT=0
2954    ELSE NPT=1
2955  GOSUB 4000
2960  $LAB[0]=" TRANSMITTANCE":: $L="%"
2965  $T[STO,0]=$T[S,0]:: $T[0,0]=$T[STO,0]
2970  GOSUB 9000
2980  IF STO<>0 THEN GOSUB 6000
2990  RETURN
3200  INPUT "REF + SIG SPEC  ";#3200;R" ";S" ";"TO"    ";
3204  IF R<1 THEN RETURN
3205  IF R>17 THEN RETURN
3206  IF S<1 THEN RETURN
3207  IF S>17 THEN RETURN
3210  K=-2:: Y1=0
3220  R1=0A2FEH+(R*404):: RNM=MWD[R1+400]
3230  S1=0A2FEH+(S*404):: SNM=MWD[S1+400]
3240  IF R>16 THEN SNM=1:: RNM=1
3260  FOR J=1 TO 200
3270   K=K+2
3280   X=MWD[R1+K]*SNM-MWD[S1+K]*RNM
3290   SP[J]=X/(SNM*RNM)
3400   IF ABS[SP[J]]>YM THEN YM=ABS[SP[J]]
3410  NEXT J
3417  IF TST=1 THEN GOTO 3445
3420  Z1=1:: Z2=8:: Z3=409.6:: NPT=1
3430  GOSUB 4000
3440  $LAB[0]=" DIFFERENCE":: $L="%"
3445  $T[STO,0]=$T[S,0]:: $T[0,0]=$T[STO,0]
3450  GOSUB 9000
3460  IF STO<>0 THEN GOSUB 6000
3470  RETURN
4000  FOR I=Z1 TO Z2
4010   IF YM<AXS[I]*0.9 THEN Y1=AXS[I]:: Y11=Y1*Z3
4020     ELSE NEXT I
4030    ELSE Y1=AXS[I]:: Y11=Y1/Z3
4034  IF TYP<>2 THEN GOTO 4040
4036  IF NSP=0 THEN NPT=0
4038    ELSE NPT=1
4040  IF NPT=1 THEN Y2=-Y1:: Y21=-Y11
4050    ELSE Y2=0:: Y21=0
4060  RETURN
6000  IF STO<17 THEN GOTO 6002
6001  IF STO<23 THEN GOTO 6010
6002  PRINT "CAN'T STORE HERE  ";
6004  INPUT "STORE WHERE  ";#6004;STO
6006  GOTO 6000
6010  SOT=0A2FEH+(STO*404):: K=-2
6020  FOR J=1 TO 200
6030   K=K+2
```

```
6040    MWD[SOT+K]=SP[J]
6050   NEXT J
6060   MWD[SOT+400]=SNM
6070   MWD[SOT+402]=RNM
6080   RETURN
7000   INPUT "MIN + MAX PTS  ";?7000;X1"   ";X2"   ";
7001   IF X1<1 THEN GOTO 7008
7002   IF X1>200 THEN GOTO 7008
7003   IF X2<1 THEN GOTO 7008
7004   IF X2>200 THEN GOTO 7008
7006   IF X2<=X1 THEN GOTO 7009
7007   GOTO 7018
7008   PRINT "PTS BETWEEN 0-200 ONLY  ";:: GOTO 7000
7009   PRINT "MIN > MAX    ";:: GOTO 7000
7010   IF X2<>0 THEN GOTO 7030
7020   X1=01:: X2=02:: PRINT "ORIG SPEC RANGE  ";
7030   XAX=X2-X1
7040   RETURN
7200   INPUT "MIN + MAX Y-AXIS  ";?7200;Y21"   ";Y11"   ";
7210   IF Y21=Y11 THEN RETURN
7220   Y1=Y11*Z3:: Y2=Y21*Z3:: TST=1
7230   RETURN
7400   INPUT "PEN SPEED  ";?7400;SPD"    ";
7410   IF SPD<1 THEN SPD=38.1
7420     ELSE IF SPD>38.1 THEN SPD=38.1
7430   INPUT "PEN:  FRAME  ";?7430;P1"   ";
7440   INPUT "LABELS ";?7440;P2"   ";
7450   INPUT "PLOTS  ";?7450;P3"   ";
7460   RETURN
9000   IF PON=0 THEN INPUT "HEADING  ";?9000;$HED[0]     ";
9020   UNIT 2
9030   PRINT "VS";SPD;";  PU;"
9035   PRINT "IP 1400,1400,10244,7430;"
9037   IF PON=1 THEN GOTO 9120
9040   PRINT "SP";P1;";PA 1400,1400; EA 10244,7430;"
9050   PRINT "YT; PA 1400,2406; YT; PA 1400,3812; YT;"
9060   PRINT "PA 1418, 5000; YT; PA 1400, 6224; YT;"
9065   PRINT "PA 1400,7430; YT;"
9070   PRINT "SP";P2;";PA 920,1340; LB";Y21;" ";$L;"<03>;"
9075   PRINT "PA 760,7370; LB";Y11;" ";$L;"<03>;"
9080   PRINT "PA 1800,7080; LB";$LAB[0];"<03>;"
9081   IF TYP>1 THEN GOTO 9086
9083   IF SNM=1 THEN PRINT "LB       >2 RAW SPECS <03>;":: GOTO
9083   PRINT "LB       SAMPLES:";SNM;"<03>;"
9084   IF S>17 THEN PRINT "LB$+ ";RNM;"R <03>;"
9085   GOTO 9090
9086   IF S<17 THEN PRINT "LB       SAMPLES:";SNM;"S+ ";RNM;"R<0
9087   IF TYP=4 THEN PRINT "LB       >2 RAW SPECS <03 ;"\:: GOTO
9090   PRINT "PA 1800,6880; LB";$HED[0];"<03>;"
9100   PRINT "PA 8100,7080; LB";$TI0.0];"   ";DAT;"<03>;"
9102   IF NSP<>0 THEN PRINT "PA 8100,6880 ;LB ";T1*T1;"<03>;"
9105   PRINT "PA 10000,1230; LB";X2;"<03>"
9110   PRINT "PA 8000,1160; LBWAVELENGTH <03>"
9115   PRINT "PA 1370,1230; LB";X1;"<03>"
9120   PRINT "SP";P3;";SC 0,";XAX;Y2;Y1;"; PU; FR ";:SP1X1;"
9140   FOR X=X1 TO X2
9150    UNIT 1:: IF NKY(05)HD THEN UNIT 2:: GOTO 91
9160    UNIT 2
9170    PRINT "PA";X-X1;SH*Y1;
9180   NEXT X
9190   PRINT "<27><46><75>; IN; SP0;"
9200   UNIT 1
```

```
9210  RETURN
20000  READ LOC
20010  READ DI
20020  IF DI=0FFFFH THEN RETURN
20030  MWD[LOC]=DI:: LOC=LOC+2
20040  GOTO 20010
30000  DATA 0A040H
30010  DATA 0420H,0A0B0H,045BH,0,0,0,0,0,0A000H,0A100H - 0FFFFH
30020  DATA 0A100H
30030  DATA 0300H,0H,0201H,01H,0203H,0H,01000H,0300H
30040  DATA 0H,01000H,0207H,0A302H,01000H,0C800H,09C03H,0C800H
30050  DATA 09C0AH,0540H,09C00H,011FDH,0C0A0H,09C05H,0282H,0444H
30060  DATA 011F4H,0282H,0FFDH,015F3H,0C800H,09C04H,0F30H,09C0CH
30070  DATA 011FDH,0C0A0H,09C0EH,0282H,0444H,015F4H,01000H,01056
30075  DATA 0FFFFH
30080  DATA 0A100H
30090  DATA 0C801H,09C08H,0C800H,09C0AH,0287H,0A490H,01509H,0100
30100  DATA 01000H,01000H,01000H,0ADE0H,09C0EH,010F4H,01000H,010
30110  DATA 0583H,08183H,01305H,01000H,0460H,0A114H,01000H,01000
30120  DATA 0207H,0A302H,01000H,0CD37H,0814AH,01502H,010FDH,010C
30130  DATA 0CD03H,0C500H,01000H,0300H,04H,0380H,0FFFFH
30340  DATA 20.48,40.96,102.4,204.8,409.6,1024,2048,3172,4096
30350  DATA 5,10,15,20,25,30
30360  DATA 250,500,750,1000
```

```
FD00 0200 LI   R0,>0000
FD04 0201 LI   R1,>0001
FD08 0203 LI   R3,>0000
FD0C 1000 NOP
FD0E 0300 LIMI >0000
FD12 1000 NOP
FD14 0207 LI   R7,>A302
FD18 1000 NOP
FD1A C800 MOV  R0,@>8FF8
FD1E C800 MOV  R0,@>8FFA
FD22 056A INV  @>8FFC
FD26 11FD JLT  >FD22
FD28 C0A0 MOV  @>8FFE,R2
FD2C 0282 CI   R2,>0666
FD30 11F6 JLT  >FD1E
FD32 0282 CI   R2,>0FFD
FD36 15F3 JGT  >FD1E
FD38 C800 MOV  R0,@>8FFA
FD3C 0560 INV  @>8FFC
FD40 11FD JLT  >FD3C
FD42 C0A0 MOV  @>8FFE,R2
FD46 0282 CI   R2,>0666
FD4A 15F6 JGT  >FD38
FD4C 1000 NOP
FD4E 1058 JMP  >FE00
```

```
FE00 C801 MOV  R1,@>8FF
FE04 C800 MOV  R0,@>8FF
FE08 0287 CI   R7,>A490
FE0C 1509 JGT  >FE20
FE0E 1000 NOP
FE10 1000 NOP
FE12 1000 NOP
FE14 1000 NOP
FE16 AIE0 A    @>8FFE,*
FE1A 10F4 JMP  >FE04
FE1C 1000 NOP
FE1E 1000 NOP
FE20 0583 INC  R3
FE22 8183 C    R3,R6
FE24 1305 JEQ  >FE30
FE26 1000 NOP
FE28 0460 B    @>FD14
FE2C 1000 NOP
FE2E 1000 NOP
FE30 0207 LI   R7,>A302
FE34 1000 NOP
FE36 CD37 MOV  *R7+,*R4-
FE38 8144 C    R4,R5
FE3A 1502 JGT  >FE40
FE3C 10FC JMP  >FE36
FE3E 1000 NOP
FE40 CD03 MOV  R3,*R4+
FE42 C500 MOV  R0,*R4
FE44 1000 NOP
FE46 0300 LIMI >0004
FE4A 0380 RTWP
FE4C 1000 NOP
FE4E 1000 NOP
```

```
FD00=0200 0000 0201 0001  0203 0000 1000 0300
FD10=0000 1000 0207 A302  1000 C800 8FF8 C800
FD20=8FFA 0560 8FFC 11FD  C0A0 8FFE 0282 0666
FD30=11F6 0282 0FFD 15F3  C800 8FFA 0560 8FFC
FD40=11FD C0A0 8FFE 0282  0666 15F6 1000 1058

FE00=C801 8FF8 C800 8FFA  0287 A490 1509 1000
FE10=1000 1000 1000 AIE0  8FFE 10F4 1000 1000
FF20=0583 8183 1305 1000  0460 FD14 1000 1000
FE30=0207 A302 1000 CD37  8144 1502 10FC 1000
FE40=CD03 C500 1000 0300  0004 0380 1000 1000
```

.Appendix E.

METHOD FOR THE DETECTION OF SMALL CHANGES IN THE SAMPLING RATE OF A DATA ACQUISITION SYSTEM

Indexing terms: Signal processing, Data acquisition systems

A means of detecting small changes in either the sampling rate of a data acquisition system or the frequency of a sinusoidal signal is described. The method is based on the fact that when a sinusoidal signal is sampled at less than twice its frequency then 'aliasing' occurs.

Introduction: When a sinusoidal signal is sampled at a rate which is less than twice its frequency then 'aliasing' occurs,[1] and the fundamental frequency of the signal which is reconstructed from the samples is less than that of the original sampled signal.

Within this letter the relationship between this fundamental frequency (i.e. of the reconstructed signal) and the sampling period is derived. As would be expected the expression shows that, as the sampling period approaches an integer multiple of the original signal's period, then the fundamental frequency of the reconstructed signal goes to zero, with its period correspondingly approaching infinity.

In addition to this it is also shown that, for a given change in sampling period, the closer the sampling period is to an integer multiple of the original signal's period, the larger is the change in the period of the reconstructed signal. It is suggested that this property could be utilised as a method for monitoring, or measuring, small changes in either the sampling period of a data acquisition system or the frequency of a sinusoidal signal.

Theory: If a sinusoidal signal of frequency f Hz and period T seconds is sampled every Q seconds commencing at time $t = 0$ (as shown in Fig. 1), then the nth sample will be taken after t seconds, where

$$t = Qn \tag{1}$$

and will have the value $y(n)$ given by

$$y(n) = \sin 2\pi \frac{Qn}{T} \tag{2}$$

However, any sample period Q can be expressed as an integer multiple of the sampled signal's period T plus or minus some time increment S; that is

$$Q = KT + S \tag{3}$$

where K is a positive integer and $|S| < 0{\cdot}5T$ (see Fig. 1).

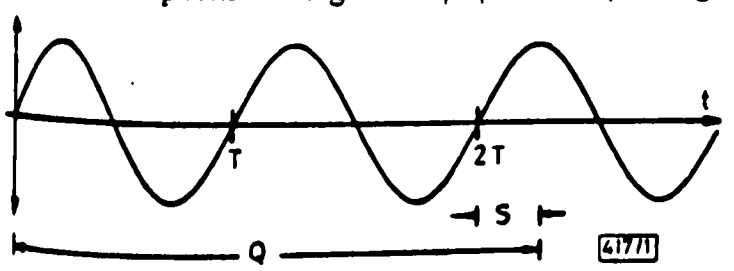

Fig. 1 *Sinusoidal wave of frequency f and period T, sampled every Q seconds*

Q is expressed as an integer number of periods KT plus a small increment S

Substituting this expression into eqn. 2, and simplifying using standard trigonometrical formulas, gives

$$y(n) = \sin 2\pi \frac{Sn}{T} \tag{4}$$

which again describes the sample values as in eqn. 2.

However, eqns. 1 and 3 can be used to rearrange eqn. 4 to give the graph obtained on reconstruction of the signal (in terms of t) as

$$y = \sin \frac{2\pi St}{(KT + S)T} \tag{5}$$

which is periodic, with period T' given as a function of the original signal's period T by

$$T' = (KT + S)T/S \tag{6}$$

with corresponding frequency $f' = 1/T'$.
(Note that the actual sample values are given by using values of t in eqn. 5 which are satisfied by eqn. 1.)

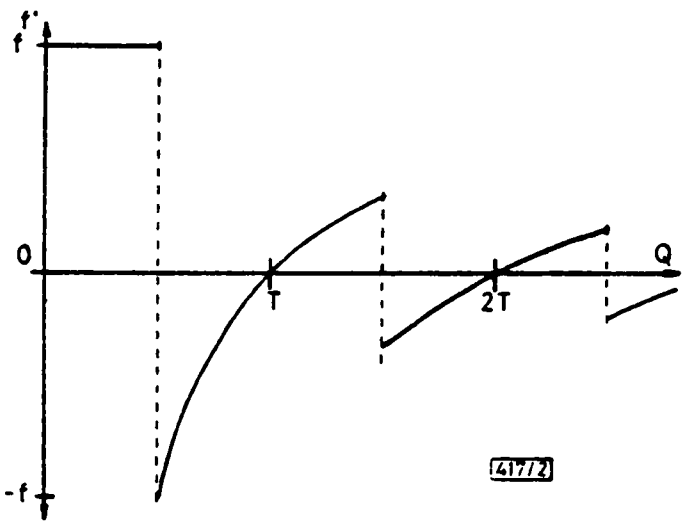

Fig. 2 *Fundamental frequency f' of reconstructed signal against sampling period Q*

The variations of the fundamental frequency f' and period T' of the reconstructed signal as functions of the sampling period Q are shown in Figs. 2 and 3. (A negative ordinate value in these graphs simply indicates that the first sample taken is negative.) For a sampling frequency of $2f$ or greater (i.e. $Q < T/2$), then $f' = f$ and no aliasing occurs (illustrating the 'sampling' theorem).[1] At lower sampling frequencies aliasing does occur with $f' < f$ and correspondingly $T' > T$.

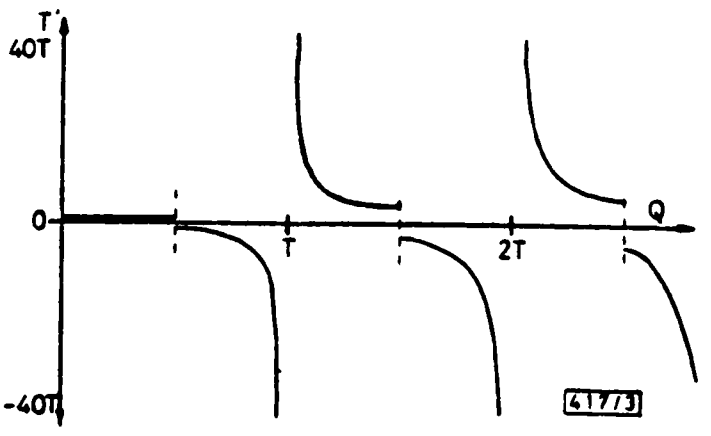

Fig. 3 *Fundamental period T' of reconstructed signal against sampling period Q*

Also evident is the fact that as Q approaches an integer multiple of T then f' approaches zero and T' rapidly goes to infinity. It is this last fact that the method is effectively based on, since a small change in sampling frequency (or alternatively the frequency of the sampled signal) will cause a very large change in T'.

Thus, if a stable signal with period T is sampled at intervals $Q \simeq KT$ (i.e. $S \ll T$) then T', the reconstructed signal period, will be very large. Moreover, a small change in sampling period (i.e. if S is slightly altered) will cause T' to change by a large amount. Hence by monitoring for variations in T', very small changes in S (and therefore Q) can be detected and measured.

Alternatively the same principle can be used to monitor small fluctuations in the period T of a sinusoidal signal by sampling at a constant interval of $Q \approx KT$.

The sensitivity of the method can be found by differentiating T' with respect to S:

$$\frac{dT'}{dS} = -\frac{KT^2}{S^2} \tag{7}$$

This shows that the sensitivity increases with increasing K (larger integer multiples of T), and decreasing S (so that Q approaches KT), both of which can be seen by examination of Fig. 3. The graph of dT'/dS against Q is shown in Fig. 4.

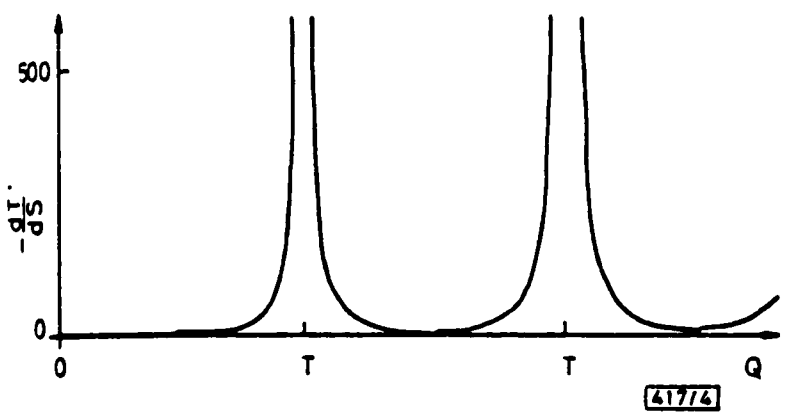

Fig. 4 *Rate of change of reconstructed signal period T' with respect to S, plotted as a function of Q*

Use of method: The following is a suggestion of a way in which the above principle may be used to monitor for either (i) the change in sampling period of a data acquisition system (although not on a sample-to-sample basis) or (ii) the change in period of a sinusoidal signal.

For (i) a stable sinusoidal signal is required which is then sampled by the data acquisition system under investigation, while for (ii) a data acquisition with constant sampling period must be used to sample the sinusoidal signal being monitored. In both cases the sampling rate would be chosen with the criteria given above in mind (that is with S and K, respectively, as small and as large as would be practically feasible).

For both (i) and (ii) the sinusoidal signal would initially be sampled by the data acquisition system. The sample values could then be used to determine how many samples N (each Q seconds apart) would be needed to describe one period T' of the reconstructed signal. These values can then be related by

$$T' = QN \tag{8}$$

For case (i) the sampling period can then be considered to change by ΔS to $(Q + \Delta S)$, which will cause the reconstructed signal's period to change to $(T' + \Delta T')$. Hence, this period will now be described by M samples each $(Q + \Delta S)$ apart, and so

$$T' + \Delta T' = (Q + \Delta S)M \tag{9}$$

However, T' and $(T' + \Delta T')$ can also be found from eqn. 6, and then equated with eqns. 8 and 9, from which the change in sampling period, ΔS, can be expressed as

$$\Delta S = T(N - M)/NM \tag{10}$$

(In applying this method in practice, K and T (the stable signal's period) would need to be known, with N and M then measured.)

For (ii) assume that the signal period changes by ΔT to $(T + \Delta T)$, causing the fundamental period of the reconstructed signal T' to become $(T' + \Delta T')$. In this case P samples, still Q seconds apart (as in this case the sampling period is constant), will be needed to describe a single period of $(T' + \Delta T')$, and so

$$T' + \Delta T' = QP \tag{11}$$

As for case (i) both T' and $(T' + \Delta T')$ can also be found from eqn. 6 when used in the form

(obtained by substituting for S from eqn. 3). These values can then be equated with eqns. 8 and 10 [as in case (i)] to finally give the change in signal period, ΔT, as

$$\Delta T = \frac{Q(P - N)}{(1 + PK)(1 + NK)} \tag{13}$$

(For this case K and Q would need to be known, with N and P measured.)

J. CROWE

University of Oxford
Bioengineering Unit, John Radcliffe Hospital
Oxford OX3 9DU, United Kingdom

10th February 1986

Reference

1 LYNNE, P. A.: 'An introduction of the analysis and processing of signals' (Macmillan, 1973), pp. 160–164

```
GOSUB 20000
DIM PPG[400],AXS[30],HED[10],LAB[4],TI[10,1],DC[10]
BASE 25
INPUT "INPUT TIME     HOURS    ";?200;H"      ";
INPUT "MINUTES    ";?210;M"    ";
TIME H,M,0
INPUT "INPUT DATE    ";?230;DAT"    "
BAUD 2,4:: UNIT 2
PRINT "IN; ":: UNIT 1
FOR I=1 TO 24
 READ AXS[I]
NEXT I
C=0:: B=0A61AH
P1=1:: P2=2:: P3=3:: SPD=38.1
TST=0:: PON=0
X11=0:: X21=1
GOSUB 9500  ! ECG THRESHOLD
INPUT "WHAT NEXT?    ";?710;$0"    ";
IF $0="P" THEN GOTO 750
IF $0="R" THEN GOTO 450
IF $0="X" THEN STOP
IF $0="E" THEN GOSUB 9500
IF $0="S" THEN GOSUB 10000
GOTO 710
INPUT "WHAT TYPE?    ";?750;TYP"    ";
IF TYP<=0 THEN GOTO 750
IF TYP<4 THEN GOSUB 2000
ON (TYP-3) THEN GOSUB 7000,7200,7400
IF TYP=7 THEN TST=1:: PON=1
IF TYP=8 THEN TST=0:: PON=0
IF TYP<4 THEN GOTO 710
GOTO 750
 INPUT "PPG NO.    ";?2000;S"    ";
 IF S>10 THEN PRINT "DOES NOT EXIST":: GOTO 2000
 IF S<1 THEN PRINT "DOES NOT EXIST":: GOTO 2000
 K=-2:: S1=0A2FCH+(S*806):: YM=0
 SNM=MWD[S1+800]:: SNM=SNM-1
 SMN=MWD[S1+802]:: SMX=MWD[S1+804]
 RMN=60*SMR/(SMN-1):: RMX=60*SMR/(SMX-1)
 RMN=INP[RMN]:: RMX=INP[RMX]
 DCU=DC[S]*204.8:: DCL=DC[S]
 ON TYP THEN GOTO 2050,2150,2250
 FOR J=1 TO SMN
  K=K+2
  PPG[J]=MWD[S1+K]/(SNM*100)
  IF ABS[PPG[J]]>YM THEN YM=ABS[PPG[J]]
 NEXT J
 GOTO 2350
 FOR J=1 TO SMN
  K=K+2
  PPG[J]=(DCU+(MWD[S1+K]/(SNM*100)))/DCU
  PPG[J]=(PPG[J]*1000)-1000
  IF ABS[PPG[J]]>YM THEN YM=ABS[PPG[J]]
 NEXT J
 GOTO 2350
 FOR J=1 TO SMN
  K=K+2
  PPG[J]=(DCU+(MWD[S1+K]/(SNM*100)))/DCU
  PPG[J]=LOG[PPG[J]]/0.0302579
  IF ABS[PPG[J]]>YM THEN YM=ABS[PPG[J]]
 NEXT J
```

```
2350  IF TST=1 THEN GOTO 2420
2360  ON TYP THEN GOTO 2370,2380,2390
2370  Z1=1:: Z2=8:: Z3=204.8
2375  $LAB[0]="RAW":: $L="V":: GOTO 2410
2380  Z1=10:: Z2=14:: Z3=100
2385  $LAB[0]="TRANS":: $L="%T":: GOTO 2410
2390  Z1=16:: Z2=24:: Z3=10
2395  $LAB[0]="ABS":: $L="A"
2410  GOSUB 4000
2420  IF TYP<>1 THEN GOTO 2430
2424  Y1=INP[Y1+0.5]:: Y2=INP[Y2+0.5]
2430  $T[0,0]=$T[S,0]
2450  IF X2<SMN THEN XMX=X2
2460    ELSE XMX=SMN
2470  GOSUB 9000
2480  RETURN
4000  FOR I=Z1 TO Z2
4010   IF YM<AXS[I]*0.8 THEN Y2=AXS[I]:: Y21=Y2/Z3
4020     ELSE NEXT I
4030    ELSE Y2=AXS[I]:: Y21=Y2/Z3
4040  Y1=-Y2:: Y11=-Y21
4050  RETURN
7000  INPUT "MIN+MAX FOR T-AXIS (SECS)    ";?7000;X11 "   ";X21"
7010  IF X11<0 THEN PRINT "MIN<0";:: GOTO 7000
7020  IF X11<X21 THEN GOTO 7040
7030  PRINT "MAX<MIN";:: GOTO 7000
7040  X1=X11*SMR:: X2=X21*SMR:: XAX=X2-X1:: PLX=X1-1
7050  IF X2<401 THEN GOTO 7080
7060  PRINT "MAX TOO BIG. WOULD NEED ";X2;"SAMPLES    ";
7070  GOTO 7000
7080  RETURN
7200  INPUT "MIN & MAX FOR Y-AXIS  ";?7200;Y11"   ";Y21"    ";
7210  Y1=Y11*Z3:: Y2=Y21*Z3:: TST=1
7220  RETURN
7400  INPUT "PEN SPEED   ";?7400;SPD     ";
7410  IF SPD<1 THEN SPD=38.1
7420    ELSE IF SPD>38.1 THEN SPD=38.1
7430  INPUT "PEN:  FRAME   ";?7430;P1"    ";
7440  INPUT "LABELS  ";?7440;P2"    ";
7450  INPUT "PLOTS  ";?7450;P3"    "
7460  RETURN
9000  INPUT "HEADING?  ";?9000;$HED[0]"    ";
9005  UNIT 2
9008  PRINT "VS";SPD;"; PU;"
9010  PRINT "IP 1400,1400,10244,7430;"
9015  IF PEN=1 THEN GOTO 9180
9020  PRINT "SP";P1;";PA 1400,1400; EA 10244,7430;"
9030  PRINT "YT; PA 1400,2008; YT; PA 1400,3209; YT;"
9040  PRINT "PA 1400,4415; YT; PA 1400,5621; YT;"
9050  PRINT "PA 1400,6827; YT; PA 1400,7430; YT;"
9052  PRINT "PA 1400,1400; XT; PA 3169,1400; XT;"
9054  PRINT "PA 4938,1400; XT; PA 6707,1400; XT;"
9056  PRINT "PA 8476,1400; XT; PA 10244,1400; XT;"
9060  PRINT "SP";P2;";PA 440,1260; LB";Y11;" ";$L;"<03>;"
9070  PRINT "PA 760,7290; LB";Y21;" ";$L;"<03>;"
9080  PRINT "PA 1800,7080; LB";$LAB[0];"<03>;"
9090  PRINT "PA 3212,7080;LBSAMPLES:";SNM;"<03>;"
9095  PRINT "PA 4820,7080; LBRATE/MIN:";RMX;" - ";RMN;"<03>;"
9100  PRINT "PA 8100,7080; LB";$T[0,0];"  ";DAT;"<03>;"
9105  PRINT "PA 1800,6760; LBDC LEVEL (V);";DCL;"<03>;"
9110  PRINT "PA 3812,6760; LBPERIOD (MS):";SPR;"<03>;"
9118  PRINT "PA 1240,1160; LB";X11;"<03>;"
```

```
9170  PRINT "PA 1800,1640; LB";$H-$DC02;"<03>;"
9150  PRINT "PA 8000,1640; LB$$EC9.<03>;"
9160  PRINT "PA 1000,1160; LB";X2;"<03>;"
9180  PRINT "SP ";P9;"; SC 0,";XMX;Y1;Y2;" PU;"
9190  PRINT "PA ";0;PPG[PLX];"; PD;"
9200  FOR X=(PLX+1) TO XMX
9210   UNIT 1:: IF KEY[051H] THEN UNIT 2:: GOTO 9250
9220   UNIT 2
9230   PRINT "PA ";X-PLX;PPG[X];
9240  NEXT X
9250  PRINT "<27><46><750; DF; SP0;"
9260  UNIT 1
9270  RETURN
9500  MWD[0A038H]=0   ! FLAG
9510  INPUT "ECG: SMP SAMP?  ";?9510;$P"    ";
9520  IF $P<>"N" THEN SMP=5:: GOTO 9540
9530  INPUT "SAMP PERIOD?  ";?9530;SMP"    ";
9540  PRD=INP[SMP*1000/64]
9545  IF PRD>255 THEN PRINT "TOO LONG    ";:: GOTO 9530
9550  MWD[0A044H]=PRD   ! TIMER
9555  SPR=INP[PRD]*0.064
9560  SMR=INP[1000/SMP]
9570  INPUT "HOW LONG?  ";?9570;T1"    ";
9575  IF T1=0 THEN T1=5
9580  T2=SMR*T1
9585  IF T2>32767 THEN PRINT "TOO LONG    ";:: GOTO 9570
9590  MWD[0A00EH]=T2   !  COUNTER
9595  CRB[3]=0
9600  CALL "SUB",0A0A0H
9610  TMN=MWD[0A03AH]:: TMX=MWD[0A03CH]
9615  CRB[3]=1
9618  INPUT "THRESH OF 80%?  ";?9618;$P"    ";
9620  IF $P<>"N" THEN TLL=0.8:: GOTO 9625
9621  INPUT "WHAT THRESH?    ";?9621;TLL
9622  IF TLL<0 THEN PRINT "TOO LOW";:: GOTO 9621
9623  IF TLL>100 THEN PRINT "TOO HIGH";:: GOTO 9621
9624  TLL=TLL/100
9625  THR=TMN+TLL*(TMX-TMN)
9630  THV=THR/204.8
9635  THV=THV*100
9638  THV=INP[THV]:: THV=THV/100
9640  PRINT "THRESH ";THV" V"
9650  X1=X11*SMR:: X2=X21*SMR:: XAX=X2-X1:: PLX=X1+1
9670  RETURN
10000  MWD[0A038H]=1   ! FLAG
10010  C=C+1:: A=B+8:: B=A+798
10020  FOR K=0 TO 798 STEP 2
10030   MWD[0A302H+K]=0
10040  NEXT K
10050  MWD[0A002H]=THR   ! THRESHOLD FOR ECG
10060  MWD[0A036H]=A:: MWD[0A006H]=B
10070  PRINT
10072  IF C<10 THEN GOTO 10080
10074  PRINT "NO DATA STORE LEFT"
10076  POP :: GOTO 710
10080  PRINT "PPG NO.  ";C"    ";
10090  INPUT "NO. SAMPS?    ";?10090;N"    ";
10100  IF N>0 THEN NEG=5:: PPS=50:: GOTO 10130
10110  INPUT "NO OF TIMES NEG IN ECG TRIGGER?  ";?10110;NEG
10112  IF NEG<1 THEN NEG=5
10114    ELSE IF NEG>20 THEN NEG=5
10120  INPUT "NO OF SAMPS BEFORE PEAK SEARCH?    ";?10120;PPS
```

```
10132   IF PKS<1 THEN PKS=50
10136     ELSE IF PKS>100 THEN PKS=50
10140   GOTO 10100
10180   MWD[0A014H]=NEG:: MWD[0A060H]=PKS
10200   MWB[0A03EH]=N
10250   PRINT "<07>";
10258   CRB[3]=0
10260   CALL "SUB",0A0A0H
10262   CRB[3]=1
10265   TIME $TIC,0
10267   INPUT "DC LEVEL?     ";?10267;DC[0]"    ";
10268   DC[0]=DC[0]*204.8
10270   RETURN
20000   READ LOC
20005   PRINT "A";
20010   READ DI
20030   IF DI=0FFFFH THEN RETURN
20040   MWB[LOC]=DI:: LOC=LOC+2
20050   GOTO 20010
30000   DATA 0A0A0H
30010   DATA 0420H,0A0A4H,045BH,0A030H,0A0ACH,01000H,[300H,0
30020   DATA 0200H,0,08004H,01502H,0460H,0A1B0H,0201H,[1H
30030   DATA 0205H,0,0206H,0,0209H,0FFFH,020AH,0
30035   DATA 04E0H,09D08H,0C820H,0A014H,0A000H,0300H,[0C800H
30040   DATA 09D0AH,0560H,09D0CH,011FDH,0D0A0H,09D0EH,[300H,04H
30045   DATA 0880ZH,0A002H,011F2H,01000H,01000H,01000H,01000H,0
30050   DATA 0H,0C800H,09D0AH,0540H,09D0CH,011FDH,0D0[H,09D0EH
30055   DATA 0C80CH,09D04H,0560H,09D0CH,011FDH,0C820H,[D0EH,0A0
30060   DATA 0300H,04H,080A0H,0A004H,01101H,010E9H,06[H,0A000H
30065   DATA 08020H,0A000H,015E4H,01000H,0300H,0H,042[H,0A1FDH
30070   DATA 0C801H,09D08H,0C800H,09D0AH,0540H,09D0C[H,011FDH,0C
30080   DATA 09D0EH,08006H,01306H,08246H,01501H,0C246[H,08286H,0
30085   DATA 0C286H,0505H,081C5H,0150EH,0204H,0,0208[H,24802H
30090   DATA 0AE02H,0300H,04H,0340H,08806H,0A060H,011F[H,010A8H
30091   DATA 01000H,01000H,020CH,0100H,01E04H,0300H,0,[208H
30094   DATA 0A302H,0CCF8H,08803H,0A006H,01503H,010FB[H,01000H,0
30096   DATA 0CCC5H,0CCC9H,0CCCAH,0300H,03H,0380H,010[H,01000H
30100   DATA 0A8A0H,0C804H,0A06AH,0205H,0FFFH,0206H,0,[300H
30110   DATA 09D08H,0420H,041FCH,0300H,04H,0C800H,09D[AH,0540H
30120   DATA 09D0CH,011FDH,0D0A0H,09D0EH,08140H,01501H[,0C142H,0
30130   DATA 01101H,0C182H,08020H,0A00FH,015F0H,020DH,[100H,01E
30140   DATA 0300H,03H,0380H,01000H,01000H,01000H,0A0[H,0A250H
30150   DATA 0300H,0,0420H,0A20DH,01004H,01000H,0A060H,0A250H
30170   DATA 01000H,08820H,0A038H,0A030H,01313H,01000H,02E0H,0A
30180   DATA 0C801H,09D08H,0C800H,09D0AH,0540H,09D0CH,[11FDH,0A
30190   DATA 09D0EH,0584H,0C800H,09D08H,02E0H,0A000H,[380H,0100
30200   DATA 0407H,0380H,01000H,01000H,01000H,01000H,[1000H,010
30260   DATA 020CH,080H,01D0DH,01E0EH,08205H,01D14H,[1DCH,0100H
30270   DATA 01F00H,01D04H,0380H,0FFFFH
30300   DATA 4.096,10.24,20.48,40.96,102.4,204.8,409.[,1024,204
30310   DATA 5,10,50,100,250,500
30320   DATA 1,2,5,10,15,20,25,30,35,40
```

```
A0A0 0420 BLWP @>A0A6
A0A4 045B RT
A0A6 A030 A     *P0+,P0
A0A8 A0AC A     @>1000(P12),P2
A0AC 0300 LIMI >0000
A0B0 0200 LI    P0,>0000
A0B4 8004 C     P4,P0
A0B6 1502 JGT   >A0BC
A0B8 0460 B     @>A1B0
A0BC 0201 LI    P1,>0001
A0C0 0205 LI    P5,>0000
A0C4 0206 LI    P6,>0000
A0C8 0209 LI    P3,>FFFE
A0CC 020A LI    P10,>0000
A0D0 04E0 CLR   @ 9C08
A0D4 C820 MOV   @>A014,@>A000
A0DA 0300 LIMI >0000
A0DE C800 MOV   P0,@>9C0A
A0E2 0560 INV   @>9C0C
A0E6 11FD JLT   >A0E2
A0E8 C0A0 MOV   @>9C0E,P2
A0EC 0300 LIMI >0004
A0F0 8802 C     P2,@>A002
A0F4 11F2 JLT   >A0DA
A0F6 1000 NOP
A0F8 1000 NOP
A0FA 1000 NOP
A0FC 1000 NOP
A0FE 0300 LIMI >0000
A102 C800 MOV   P0,@>9C0A
A106 0560 INV   @>9C0C
A10A 11FD JLT   >A106
A10C C0A0 MOV   @>9C0E,P2
A110 C800 MOV   P0,@>9C0A
A114 0560 INV   @>9C0C
A118 11FD JLT   >A114
A11A C820 MOV   @>9C0E,@>A004
A120 0300 LIMI >0004
A124 80A0 C     @>A004,P2
A128 1101 JLT   >A12C
A12A 10F9 JMP   >A0FE
A12C 0620 DEC   @>A000
A130 8020 C     @>A000,P0
A134 15E4 JGT   >A0FE
A136 1000 NOP
A138 0300 LIMI >0000
A13C 0420 BLWP @>A1FC
A140 C801 MOV   P1,@>9C08
A144 C800 MOV   P0,@>9C0A
A148 0560 INV   @>9C0C
A14C 11FD JLT   >A148
A14E C0A0 MOV   @>9C0E,P2
A152 8006 C     P6,P0
A154 1306 JEQ   >A162
A156 8246 C     P6,P9
A158 1501 JGT   >A15C
A15A C246 MOV   P6,P9
A15C 8286 C     P6,P10
A15E 1101 JLT   >A162
A160 C286 MOV   P6,P10
A162 0585 INC   P5
A164 81C5 C     P5,P7
A166 150E JGT   >A184
A168 0206 LI    P6,>0000
A16C 0208 LI    P8,>A302
A170 AE02 A     P2,*P8+
A172 0300 LIMI >0004
A176 0340 IDLE
A178 8806 C     P6,@>A060
A17C 11FC JLT   >A176
A17E 10A8 JMP   >A0D0
A180 1000 NOP
A182 1000 NOP
A184 020C LI    P12,>0100
A188 1E04 SBZ   4
A18A 0300 LIMI >0000
A18E 0208 LI    P8,>A302
A192 CCF8 MOV   *P8+,*P3+
A194 8803 C     P3,@>A006
A198 1503 JGT   >A1A0
A19A 10FB JMP   >A192
A19C 1000 NOP
A19E 1000 NOP
A1A0 CCC5 MOV   P5,*P3+
A1A2 CCC9 MOV   P9,*P3+
A1A4 CCCA MOV   P10,*P3+
A1A6 0300 LIMI >0003
A1AA 0380 RTWP
A1AC 1000 NOP
A1AE 1000 NOP
A1B0 0A8A SLA   P10,8
A1B2 C80A MOV   P10,@>A06A
A1B6 0205 LI    P5,>0FFF
A1BA 0206 LI    P6,>0000
A1BE C800 MOV   P0,@>9C08
A1C2 0420 BLWP @>A1FC
A1C6 0300 LIMI >0004
A1CA C800 MOV   P0,@>9C0A
A1CE 0560 INV   @>9C0C
A1D2 11FD JLT   >A1CE
A1D4 C0A0 MOV   @>9C0E,P2
A1D8 8142 C     P2,P5
A1DA 1501 JGT   >A1DE
A1DC C142 MOV   P2,P5
A1DE 8182 C     P2,P6
A1E0 1101 JLT   >A1E4
A1E2 C182 MOV   P2,P6
A1E4 8020 C     @>A00E,P0
A1E8 15F0 JGT   >A1CA
A1EA 020C LI    P12,>0100
A1EE 1E04 SBZ   4
A1F0 0300 LIMI >0003
A1F4 0380 RTWP
A1F6 1000 NOP
A1F8 1000 NOP
A1FA 1000 NOP
A1FC A060 A     @>A250,P1
```

```
A200 0300 LIMI >0000
A204 0420 BLWP @>A20C
A208 1004 JMP  >A212
A20A 1000 NOP
A20C A060 A    @>A250,R1
A210 1000 NOP
A212 8820 C    @>A038,@>A030
A218 1313 JEQ  >A240
A21A 1000 NOP
A21C 02E0 LWPI >A030
A220 C801 MOV  R1,@>9C08
A224 C800 MOV  R0,@>9C0A
A228 0560 INV  @>9C0C
A22C 11FD JLT  >A228
A22E AE20 A    @>9C0E,*R8+
A232 0586 INC  R6
A234 C800 MOV  R0,@>9C08
A238 02E0 LWPI >A000
A23C 0380 RTWP
A23E 1000 NOP
A240 0607 DEC  R7
A242 0380 RTWP
A244 1000 NOP
A246 1000 NOP
A248 1000 NOP
A24A 1000 NOP
A24C 1000 NOP
A24E 1000 NOP
A250 020C LI   R12,>0080
A254 1D0D SBO  13
A256 1E0E SBZ  14
A258 3205 LDCR R5,8
A25A 1D14 SBO  20
A25C 020C LI   R12,>0100
A260 1E00 SBZ  0
A262 1D04 SBO  4
A264 0380 RTWP
A266 1000 NOP
A268 1000 NOP
A26A 1000 NOP
A26C 1000 NOP
A26E 1000 NOP
```

```
A0A0=0420 A0A6 045B A030  A0AC 1000 0300 0000
A0B0=0200 0000 8004 1502  0460 A1B0 0201 0001
A0C0=0205 0000 0206 0000  0209 FFFE 020A 0000
A0D0=04E0 9C08 C820 A014  A000 0300 0000 C800
A0E0=9C0A 0560 9C0C 11FD  C0A0 9C0E 0300 0004
A0F0=8802 A002 11F2 1000  1000 1000 1000 0300
A100=0000 C800 9C0A 0560  9C0C 11FD C0A0 9C0E
A110=C800 9C0A 0560 9C0C  11FD C820 9C0E A004
A120=0300 0004 80A0 A004  1101 10E9 0620 A000
A130=8020 A000 15E4 1000  0300 0000 0420 A1FC
A140=C801 9C08 C800 9C0A  0560 9C0C 11FD C0A0
A150=9C0E 8006 1306 8246  1501 C246 8286 1101
A160=C286 0585 81C5 150E  0206 0000 0208 A302
A170=AE02 0300 0004 0340  8806 A060 11FC 10A8
A180=1000 1000 020C 0100  1E04 0300 0000 0208
A190=A302 CCF8 8803 A006  1503 10FB 1000 1000
A1A0=CCC5 CCC9 CCCA 0300  0003 0380 1000 1000
A1B0=0A8A C80A A06A 0205  0FFF 0206 0000 C800
A1C0=9C08 0420 A1FC 0300  0004 C800 9C0A 0560
A1D0=9C0C 11FD C0A0 9C0E  8142 1501 C142 8182
A1E0=1101 C182 8020 A00E  15F0 020C 0100 1E04
A1F0=0300 0003 0380 1000  1000 1000 A060 A250
A200=0300 0000 0420 A20C  1004 1000 A060 A250
A210=1000 8820 A038 A030  1313 1000 02E0 A030
A220=C801 9C08 C800 9C0A  0560 9C0C 11FD AE20
A230=9C0E 0586 C800 9C08  02E0 A000 0380 1000
A240=0607 0380 1000 1000  1000 1000 1000 1000
A250=020C 0080 1D0D 1E0E  3205 1D14 020C 0100
A260=1E00 1D04 0380 1000  1000 1000 1000 1000
```

Afromowitz. M.A., Heimbach. D.M. and Burns. M.W. (1979) Electro-Optic Burn Depth Indicator. In Proceedings of XII Int.Conf.Med.Biol.Eng and V Int.Conf.Med.Phys., Aug.19-24. Jerusalem. Israel. 10.1.

Afromowitz. M.A. (1983) Techniques for Early Characterization of Burn Injuries. In Proceedings 36th ACEMB, Sept.12-14. Columbus. Ohio. USA. 12.6.

Ahmann. P.A., Lazzara. A. and Dykes, F.D. (1980) Intracranial Haemorrhage in the High-risk Preterm Infant: Incidence and Outcome. Annals of Neur., 7. 118-124.

Amazon, K., Soloni. F. and Rywlin, A.M. (1981) Separation of Bilirubin from Hemoglobin by Recording Derivative Spectrophotometry. Am.J.Clin.Path., 75, 521-525.

Anders. A. and Aufmuth. P. (1982) Lasers in Photomedicine. In Optoelectronics in Medicine. Ed Waidelich, W., Springer-Verlag.

Anderson. N.M. and Sekelj. P. (1965) Studies on the Light Transmission of Nonhemolyzed Whole Blood. Determination of Oxygen Saturation. J.Lab.Clin.Med., 65, 153-166.

Anderson. N.M. and Sekelj. P. (1967a) Light-absorbing and Scattering Properties of Non-haemolysed Blood. Phys.Med.Biol., 12, 173-184.

Anderson. N.M. and Sekelj. P. (1967b) Reflection and Transmission of Light by thin films of Nonhaemolysed Blood. Phys.Med.Biol., 12, 185-192.

Anderson. R.R., Hu, J. and Parrish. J.A. (1980) Optical Radiation Transfer in the Human Skin and Applications in in vivo Remittance Spectroscopy. In Bioengineering and the Skin, Chapt.28

Anderson. R.R. and Parrish, J.A. (1981) The Optics of Human Skin. J.Invest.Dermat., 77. 13-19.

Arai. T., Tomita. Y., Kikuchi. M. and Negishi. N. (1985) Transcutaneous Detection for Blood Glucose Change by Measurement fo Effusion Fluid using Suction ATR Method. In XIV ICMBE and VII ICMP. Espoo. Finland, 303-304.

Arndt, K.A., Noe. J.M. and Rosen. S. Eds. (1983) Cutaneous Laser Therapy: Principles and Methods, Wiley.

Atkins. P.W. (1978) Physical Chemistry. Oxford Univ.Press. Oxford.

Babior. M.B. (1978) Oxygen-dependent Microbial Killing of Phagocytes. N.Eng.J.Med., 298, 659-680.

Balaban, R.S. and Sylvia. A.S. (1981) Spectrophotometric Monitoring of O2 Delivery to the Exposed Rat Kidney. Am.J.Physiol., 241, F257-F262.

Barbenel. J.C., Turnbull. F.W. and Nisbet, R.M. (1979) Backscattering of Light by Red Cell Suspensions. Med.Biol.Eng.Comp., **17**, 763-768.

Barber. D.C. and Brown, B.H. (1984) Applied Potential Tomography. J.Phys.E.(Sci.Inst.), **17**, 723-733.

Barer. R. and Joseph, S. (1954) Refractometry of Living Cells. Part 1. Basic Principles. Quat.J.Microscop.Sci., **95**, 399-423.

Barlow. R.B. and Polanyi, M.L. (1962) Absorption Measurements for Oxygenated and Reduced Hemoglobin in The Range 0.6-1.88 microns. Clin.Chem., **8**, 67-71.

Bashford, C.L., Barlow, C.H., Chance, B. and Haselgrove, J. (1980) The Oxidation - Reduction State of Cytochrome Oxidase in Freeze Trapped Gerbil Brains. FEBS Letters, **113**, 78-80.

Bashford, C.L., Barlow, C.H., Chance, B., Haselgrove, J. and Sorge, J. (1982) Optical Measurements of Oxygen Delovery and Consumption in Gerbil Cerebral Cortex. Am.J.Physiol., **242**, C265-C271.

Belmont. A., Zietz, S. and Nicolini, C. (1982) Theory of Differential Light Scattering by Chromatin. **In** Proceedings of the 35th ACEMB, Sept.22-24. Philadelphia. 34.4.

Berne. B.J. and Pecora. R. (1976) Dynamic Light Scattering with Applications to Chemistry, Biology and Physics. Wiley Interscience, New York.

Bloomfield, V.A. (1981) Quasi-Elastic Light Scattering Applications in Biochemistry and Biology. Ann.Rev.Biophys.Bioeng., **10**, 421-450.

Boggett. D., Blond, P. and Rolfe. P. (1985) Laser Doppler Measurements of Blood Flow in Skin Tissue. J.Biomed.Eng., **7**, 225-232.

Bolin, F.P., Preuss, L.E. and Cain, B.W. (1984) A Comparison of Spectral Transmittance for Several Mammalian Tissues: Effects of PRT Frequencies. **In** Porphyrin Localisation and Treatment of Tumours, 211-225. Liss, A.R., New York.

Bourgelais, D.B.C. and Itzkan, I. (1983) The Physics of Lasers. **In** Cutaneous Laser Therapy, Arndt, K.A. **Ed.** Wiley, Chapt.2.

Brazy. J.E., Lewis, D.V., Mitnick, M.H. and Jobsis, F.F. (1985) Noninvasive Monitoring of Cerebral Oxygenation in Preterm Infants: Preliminary Observations. Pediatrics, **75**, 217-225.

Budde. W. (1983) Physical Detectors of Optical Radiation. Vol.4. Academic Press. London.

Bulkley, G.B. (1983) The role of oxygen free radicals in human disease processes. Surgery, **94**, 407-411.

Burton. G.W., Ingold, K.U. (1984) β-carotene: An unusual type of lipid antioxidant. Science, 224, 560-573.

Cambern, A.M. and Shurtleff. D.B. (1961) Photography of Transilluminated Intracranial Lesions in Infants. Med.Radiog.Photog., 37, 8-11.27.

Cartwright, C.H. (1930) Infra-red Transmission of the Flesh. J.Opt.Soc.Am., 20, 81-84.

Challoner. A.V.J. (1979) Photoelectric Plethysmography for Estimating Cutaneous Blood Flow. In Non-Invasive Physiological Measurements, Vol.1. Ed Rolfe. P., Chapter 6. Academic Press, London.

Chance. B. (1951a) Rapid and Sensitive Spectrophotometry I. Rev.Sci.Inst.. 22, 619-627.

Chance, B. (1951b) Rapid and Sensitive Spectrophotometry II. Rev.Sci.Inst., 22, 627-634.

Chance, B. (1951c) Rapid and Sensitive Spectrophotometry III. A Double Apparatus. Rev.Sci.Inst., 22, 634-638.

Chance. B. (1952) Spectrophotometry and Reaction Kinetics of Respiratory Pigments of Homogenised and Intact Cells. Nature. 169, 215-221.

Chance, B. (1954) Spectrophotometry of Intracellular Respiratory Pigments. Science, 120, 767-775.

Chance, B. and William. G.R. (1956) The Respiratory Chain and Oxidative Phosphorylation. Adv.Enz., 65-134.

Chance. B. (1959) Phosphorylation Efficiency of the Intact Cell. II. Crossover Phenomena in Baker's Yeast. J.Biol.Chem., 234,3036-3043.

Chance, B., Mayer, D. and Legallais, V. (1971) A Dual-Wavelength Spectrophotometer and Fluorometer Using Interference Filters. Anal.Biochem., 42, 494-504.

Chang, R. (1971) Basic Principles of Spectroscopy. McGraw Hill, New York.

Cheung, P.W., Takatini, S. and Ernst. E.A. (1977) Multiple Wavelength Reflectance Oximetry in Peripheral Tissues. Adv.Exp.Med.Biol., 94, 63-67.

Chiswick, M.L., Johnson. M., Woodhall. C., Gowland, M., Davies, J., Toner. N. and Sims, D.G. (1983) Protective effect of vitamin E (DL-alpha-tocopherol) against intraventricular haemorrhage in premature babies. Br.Med.J., 287, 81-84.

Chitra. T., Srinivasan, T.M. and Singh, M. (19) In vivo tissue characterization through He-Ne Laser Reflectance Studies. Biomed.Eng. II, 389-392. Pergamon-Press.

Cochrane. T., Sheriff. S.B., Boulton. A.J.M., Ward, J.D. and ana Atkins. R.M. (1986) Laser Doppler Flowmetry: in the Assessment of Peripheral Vascular Disorders? A Preliminary Evaluation. Clin.Phys.Physiol.Meas., 7. 31-42.

Cohen. A and Longini, R.L. (1971) Theoretical Determination of the Blood's Relative Oxygen Saturation in vivo. Med.Biol.Eng.Comp., 9, 61-69.

Cohen. A. and Wadsworth. N. (1972) A Light Emitting Diode Skin Reflectance Oximeter. Med.Biol.Eng.Comp., 10, 385-391.

Colacino. J.M., Grubb, B. and Jobsis, F.F. (1981) Infra-red Technique for Cerebral Blood Flow: Comparison with 133Xe Clearance. Neurol.Res., 3, 17-31.

Colver. G.B., Cherry, G.W.. Dawber. R.P.R. and Ryan T.J. (1985) Tattoo Removal Using Infra-red Coagulation. Brit.J.Derm., 112, 481-485.

Colver. G.B., Cherry, G.W., Dawber. R.P.R and Ryan, T.J. (1986) The Treatment of Cutaneous Vascular Lesions with the Infra-red Coagulator: A Prelimnary Report. Brit.J.Plas.Surg., 39, 131-135.

Conway, J.M., Norris, K.H. and Bodwell. C.E. (1984) A New Approach for the Estimation of Body Composition: Infrared Interactance. Am.J.Clin.Nutr., 40, 1123-1130.

Cope. M. (1985) Near Infra-red Spectroscopy for Non-invasive Blood and Tissue Oxygenation Monitoring. In Optical Sensors and Optical Sensing Techniques in Biology and Medicine. BES Transducers Group Meeting, UCL. 22 May 1985.

Corcuff. P., De Rigal, J. and Leveque. J.L. (1982) Image Analysis fo the Cutaneous Microrelief. Bioeng.and the Skin, 4, 16-31.

Crowe, J., Rea. P.A. and Rolfe. P. (1986) Retinopathy of Prematurity, Intraventricular Haemorrhage and Oxidative Damage (Letter). Peds., 77. 129-130.

Cummins, H.Z. and Swinney, H.L. (1970) Light Beating Spectroscopy. In Progress in Optics, 8, Ed Wolf. E.. 135-200.

D'Agrosa. L.S. and Hertzman, A.B. (1967) Opacity Pulse of Individual Minute Arteries. J.Appl.Physiol., 23, 613-620.

Danforth. R.S. (1930) The Penetration of Living Tissues by Ordinary Radient Energy. Proc.Soc.Exp.Biol.Med., 27, 283-285.

Dawson. J.B., Barker, D.J., Ellis, D.J., Grassam, E., Cotterill. J.A., Fisher. G.W. and Feather. J.W. (1980) A Theoretical and Experimental Study of Light Absorption and Scattering by in vivo skin. Phys.Med.Biol., 25, 695-709.

Del Maestro. R.F. (1980) An Approach to free radicals in medicine and biology. Acta.Physiol.Scand., **Suppl.492**, 153-168.

Delori. F.C., Rogers, F.J., Bursell, S.E. and Parker, J.S. (1982) A System for Non-invasive Oximetry of Retinal Vessels. **In** Proc. IEEE Frontiers of Eng. in Health Care. 296-299.

Demopoulos, H.B., Flamm. E.S., Pietronigro, D.D. and Seligman, M.L. (1980) The free radical pathology and the microcirculation in the major central nervous system disorders. Acta.Physiol.Scand., **Suppl. 492**, 91-119.

Diffey, B.L. (1983) A Mathematical Model for Ultraviolet Optics in Skin. Phy.Med.Biol., **28**, 647-657.

Dillard, C.J., Dumelin, E.E., Tappel, A.L. (1977) Effect of dietary vitamin E on expiration of pentane and ethane by the rat. Lipids, **12**, 109-114.

Dixon, M. and Webb, E.C. (1979) Enzymes (3rd ed.). Longman, London.

Doiron. D.R., Svaasand, L.O. and Profio, A.E. (1983) Light Dosimetry in Tissue: Application to Photoradiation Therapy. Adv.Exp.Med.Biol., **160**, 63-77.

Dormandy. T.L. (1983) An approach to free radicals. The Lancet, Oct 29.

Duckrow, R.B., LaManna. J.C. and Rosenthal, M. (1982) Sensitive and Inexpensive Dual-Wavelength Reflection Spectrophotometry using Interference Filters. Anal.Biochem.. **125**, 13-23.

Duling, B.R., Damon, D.N., Donaldson. S.R. and Pittman, R.N. (1983) A Computerized System for Densitometric Analysis of the Microcirculation. J.Appl.Physiol., **55**, 642-651.

Edwards, E.A. and Duntley, S.Q. (1939) The Pigments and Color of Living Human Skin. Am.J.Anat.. **65**, 1-32.

Eichler. J. and Lenz, H. (1977) Measurements on the Depth of Penetration of Light (0.35-1.0 um) in Tissue. Rad.Environm.Biophys., **14**, 239-242.

Eisberg, R.M. (1961) Fundamentals of Modern Physics. Wiley, London.

Elam, J.O., Neville, J.F., Sleator. W. and Elam. W.N. (1949) Sources of Error in Oximetry. Ann.Surg., **130**, 755-773.

Engel, R.R. (1982) Nuances or Nuisances for Cutaneous Bilirubinometry? Pediatrics, **69**, 126-127.

Enson, Y., Briscoe. W.A., Polayni, M.L. and Cournand, A. (1962) In vivo Studies with an Intravascular and Intracardiac Reflection Oximeter. J.Appl.Physiol., **17**, 552-558.

Epstein, F.H., Balaban, R.S. and Ross, B.D. (1982) Redox State of Cytochrome aa3 in Isolated Perfused Rat Kidney. Am.J.Pnysiol., 243, F356-F363.

Fabel, H. and Lubbers, D.W. (1965) Measurements of Reflection Spectra of the Beating Rabbit Heart in situ. Biochem.Zeit., 341, 351-356.

Fairs, S.L.E., De Trafford, J.C., Potter. C. and Roberts, V.C. (1985) Skin Blood Flow Measurement. A Comparison Between Photoplethysmography and Laser Doppler Flowmetry. In Proc.XIV ICMBE and VII ICMP, Espoo. Finland, 1101-1102.

Feather. J.W., Dawson. J.B., Barker. D.J. and Cotterill. J.A. (1980) A Theoretical and Experimental Study of the Optical Properties of in vivo skin. In Bioengineering and the Skin, Chapt.30.

Ferrari. M., Giannini, I., Amilcare. C. and Fasella, P. (1982a) Near I.R. Spectroscopy in Non Invasive Monitoring of Cerebral Function. In Proceedings World Cong.Med.Phys.Biomed.Eng., Hamburg, 22.17.

Ferrari. M., Giannini, I., Carpi, A., Fasella, P., Fieschi. C. and Zanette. E. (1982b) Non-Invasive Infrared Monitoring of Tissue Oxygenation and Circulatory Parameters. Angiology: New Developments. 299-303. Plenum, New York.

Ferrari. M., Giannini, Carpi, A. and Fasella, P. (1983) Non-Invasive Near Infrared Spectroscopy of Brain in Fluorocarbon Exchange-Transfused Rats. Phys.Chem.Phys.Med.NMR., 15, 107-113.

Feuk, T. (1971) The Wavelength Dependence of Scattered Light Intensity in Rabbit Cornea. IEEE Trans.Biomed.Eng., 18, 92.

Figulla, H.R., Hoffman, J. and Lubbers, D.W. (1983) Coronary Conductivity and Tissue Oxygenation as Measured by the Myoglobin Oxygen Saturation and the Cytochrome Oxidase Redox State in the Langendorff Guinea Pig Heart Preparation. Adv.Exp.Med.Biol., 159, 579-585.

Figulla, H.R., Hoffman. J. and Lubbers, D.W. (1984) Evaluation of Reflection Spectra of the Isolated Heart by Multicomponent Spectra Analysis in Comparison to Other Evaluating Methods. Adv.Exp.Med.Biol., 169, 821-829.

Finar. I.L. (1976) Organic Chemistry (Vol.1. The Fundamental Principles). Longman, London.

Fine, I., Loewinger. E., Weinreb, A. and Weinberger. D. (1985) Optical Properties of the Sclera. Phys.Med.Biol., 30, 565-571.

Fleschi and Zanette. E. (1980) Non-Invasive Infrared Monitoring of Tissue Oxygenation and Circulatory Parameters. In XII World Congress of Angiology. 663.

Fox, E.J., Harmel, M.H., Mitnick, M.H. and Jobsis. F.F. (1982) Non-Invasive Monitoring of Cerebral Oxygen Sufficiency During General Anesthesia. Anaesthesiology. 57, Suppl. A160.

Fox, E.J. (1983) The Monitor of the Future? (Editorial) Anaesthesia, **38**, 433-434.

Frank, K.H., Schubert. A., Friedl, A., Brunner. M., Hoper. J., Kerl, G., and Kessler. M. (1984) Correlation Between Tissue pO2 and Intracapillary Hb Spectra. Adv.Exp.Med.Biol., **169**, 811-820.

Frank, L. and Groseclose. E.E. (1984) Preparation for birth into an O_2-rich enviroment: the antioxidant enzymes in the developing rabbit lung. Ped.Res., **18**, 240-244.

Fridovich, I. (1978) The biology of oxygen radicals. Science, **201**, 875-880.

Gamble, W.J., Hugenholtz, P.G., Monroe, R.G., Polanyi and Nadas, A.S. (1965) The Use Of Fibreoptics in Clinical Cardiac Catheterization. I. Intracardiac Oximetry. Circulation, **31**, 328-343.

Geiser. G., Reuter. P., Korn, A., Lukas, D. and Schulte, W. (1982) Colorimetric Determination of the Inflammation of the Gingiva Propria. In Proceedings of World Cong.Med.Phys.Biomed.Eng., Hamburg, 22.24.

Giannini, I., Ferrari. M., Carpi, A. and Fasella, P. (1982) Rat Brain Monitoring by Near-infrared Spectroscopy: An Assessment of Possible Clinical Significance. Physiol.Chem.Phys., **14**, 295-305.

Giannini, I., Ferrari. M., De Marchis, C., Di Nicola, A., Palermo, D. and Bucci, G. (1985) Neonatal Brain Monitoring by Near Infrared Spectroscopy. In Proc.XIV ICMBE and VII ICMP, Espoo. Finland.

Gibson. H.L. (1945) Infrared Photography of Patients. Rad.Clin.Photog., **21**, 72-86.

Gibson, H.L. (1961) Postprandial Intensification of Venous Pattern. An Example Demonstrated by Infrared Photography. Med.Radiog.Photog., **37**. 16-18.

Gibson, H.L. (1964) Diffuse Lighting for Clinical Infrared Photography. Med.Radiog.Photog., **40**, 38-40.

Giltvedt, J., Sira. A. and Helme, P. (1984) Pulsed Multifrequency Photoplethysmograph. Med.Biol.Eng.Comp., **22**, 212-215.

Gordy, E. and Drabkin, D.L. (1957) Spectrophotometric Studies. XVI. Determination of the Oxygen Saturation of Blood by a Simplified Technique, Applicable to Standard Equipment. J.Biol.Chem., **227**, 285-299.

Gough, D.A. (1982) The Composition and Optical Rotatory Dispersion of Bovine Aqueous Humor. Diabetes.Care., **5**, 266-270.

Granger, D.N. and Parks, D.A. (1982) Role of oxygen radicals in the pathogenesis of intestinal ischaemia. The Physiologist, **26**, 159-164.

Greguss. P. (1984) Low Level Laser Therapy - Reality or Myth. Opt.Las.Tech., **16**, 81-85.

Griffiths, D.E. and Wharton. D.C. (1961) Studies of the Electron Tansport System. J.Biol.Chem., **236**. 1850-1856.

Gros. C., Quenneville, Y. and Hummel, Y. (1972) Diaphanologie Mammaire (French). J.Radiol.Electrol., **53**, 297-306.

Gush, R.J., King, T.A. and Jayson. M.I.V. (1984) Aspects of Laser Light Scattering from Skin Tissue with Applications to Laser Doppler Blood Flow Measurements. Phys.Med.Biol., **29**, 1463-1476.

Haase, T. (1980) Method and Apparatus for in vivo Measurement of Blood Gas Partial Pressures, Blood Pressure and Blood Pulse. US Patent, No. 4.201.222. (Filed 1977).

Hannemann. R.E., DeWitt. D.P. and Wiechel, J.F. (1978) Neonatal Serum Bilirubin from Skin Reflectance. Pediat.Res., **12**, 207-210.

Hannemann. R.E., Dewitt. D.P., Hanley. E.J., Schreiner. R.L. and Bonderman. P. (1979) Determination of Serum Bilirubin by Skin Reflectance: Effect of Pigmentation. Pediat.Res., **13**, 1326-1329.

Hannemann. R.E. (1982) Evaluation of the Minolta Bilirubin Meter as a Screening Device in White and Black Infants (Letter). Pediatrics, **69**, 107-109.

Harcke, H.T., Naeye, R.L. and Storch, A. (1972) Perinatal Cerebral Intraventricular Haemorrhage. J.Paeds., **80**, 37-42.

Hardy, J.D., Hammel, H.T. and Murgatroyd, D. (1956) Spectral Transmittance and Reflectance of Excised Human Skin. J.Appl.Physiol., **9**, 257-264.

Hargens, C.W. (1980) The Surface Translucence Meter: Its Use in Studying Human Skin. **In** Bioengineering and the Skin, Chapt.35.

Hassinen, I. and Jasma, T. (1982) A Reflectance Spectrophotometer-Surface Fluorometer Suitable for Monitoring Changes in Hemprotein Spectra and Fluorescence of Flavins and Nicotinamide Nucleotides in Intact Tissues. Anal.Biochem., **120**, 365-372.

Hatefi. Y. (1985) The Mitochondrial Electron Transport and Oxidative Phosphorylation System. Ann.Rev.Biochem., **54**, 1015-1069.

Hayashi. T., Saito. M. and Utsunomiya, T. (1979) Measurements of Peripheral Circulation with Photo-Plethysmography. XII Int.Conf.Med.Biol.Eng., Jerusalem, Israel, Aug.19-24. **69.3**.

Hecht, E. and Zajac, A. (1974) Optics. Addison-Wesley, London.

Hecht, H.G. (1983) A Comparison of the Kubelka-Munk, Rozenberg, and Pitts-Giovanelli Methods of Analysis of Diffuse Reflectance for Several Model Systems. Appl.Spect., **37**, 348-353.

Heeke, G. (1982) A Measurment System for Otoscopic Spectroscopy in vivo. In Springer Series in Optical Sciences, 31, Ed von Balley, E., 176-180. Springer-Verlag.

Hegyi, T., Hiatt. I.M. and Indyk, L. (1981a) Transcutaneous Bilirubinometry I. Correlations in Term Infants. J.Peds., 98, 454-457.

Hegyi, T., Hiatt. I.M., Gertner. I. and Indyk, L. (1981b) Transcutaneous Bilirubinometry. The Cephacaudal Progression of Dermal Icterus. Am.J.Dis.Child., 135, 547-549.

Heinrich, U., Hoffman, J. and Lubbers, D.W. (1983) Quantitative Analysis of Reflection Spectra on the Perfused Brain in Different States of Oxygen Supply. Adv.Exp.Med.Biol., 159, 119-127.

Hickham. J.B., Frayser. R. and Ross, J.C. (1963) A Study of Retinal Venous Blood Oxygen Saturation in Human Subjects by Photographic Means. Circulation, 27, 375-386.

Higgins, J.L. and Franck, A. (1986) Photoplethysmographic Evaluation of the Relation Between Skin Reflectance and Skin Blood Volume. J.Biomed.Eng., 8, 130-136.

Hirko, R.J., Fretterd, R.J. and Longini, R.L. (1975) Application of the Diffusion Dipole to Modelling the Optical Characteristics of Blood. Med.Biol.Eng.Comp., 13, 192-195.

Hittner. H.M., Speer. M.E., Rudolph. A.J., Blifeld, C., Chadda, P., Holbein, M.E.B., Godio, L.B. and Kretzer F.L. (1984) Retrolental fibroplasia and vitamin E in the preterm infant - Comparison of oral versus intramuscular:oral administration. Pediatrics, 73, 238-249.

Hoffman. J., Wodick, R., Hannebauer. F. and Lubbers, D.W. (1984) Quantitative Analysis of Reflection Spectra of the Surface of the Guinea Pig Brain. Adv.Exp.Med.Biol., 169, 831-839.

Ishimaru (1978) Wave Propogation and Scattering in Random Media, Vol.2. Academic Press. New York.

Jacquez, J.A., Kuppenheim. H.F., Dimitroff. J.M., McKeehan. W., and Huss, J. (1955a) Spectral Reflectance of Human Skin in the Region 235-700 mu. J.Appl.Physiol., 8, 212-214.

Jacquez, J.A., Huss. J., McKeehan. W., Dimitroff. J.M. and Kuppenheim. H.F. (1955b) Spectral Reflectance of Human Skin in the Region 0.7-2.6 u. J.Appl.Physiol., 8, 297-299.

Janssen. F.J. (1972) The Principle Design and Features of a New Hb-Oximeter. Med.Biol.Eng.Comp., 10, 9-22.

Jarry, G., Ghesquire. S., Maarek, J.M., Fraysse. F., Debray. S. Mong Hung, B. and Laurent. D. (1984) Imaging Mammalian Tissues and Organs Using Laser Collimated Transillumination. J.Biomed.Eng., 6, 70-74.

Jarry, G., Marzouki, L., Crowe, J., Ghesquire, S., Debray, S., Maarek, J.M., Mong Hung, B. and Laurent, D. (1985) Spectrophotometer Using Optical Fibers. Bioengineering, 1, MELENCON '85. 203-205.

Jarry, G., Marzouki, L., Debray, S., Ghesquire, S., Besson, B., Mong Hung, B. and Laurent. D. (1986) Scanning Spectrophotometry for the Dynamic Study of Tissue Respiration in Intact Organs. J.Biomed.Eng., 8, 166-170.

Jennings, J.R. and Choi, S. (1983) An Arterial to Peripheral Pulse Wave Velocity Measure. Physchophysiology. 20, 410-418.

Jobsis, F.F. (1972) Oxidative Metabolism at Low pO2. Fed.Proc., 31, 1404-1413.

Jobsis, F.F., Keizer, J.H., LaManna, J.C. and Rosenthal, M. (1977a) Reflectance Spectrophotometry of Cytochrome aa3 in vivo. J.Appl.Physiol., 43, 858-872.

Jobsis, F.F. (1977b) Non-Invasive, Infra-Red Monitoring of Cerebral O2 Sufficiency, Bloodvolume, HbO2-Hb Shifts and Bloodflow. Acta.Neurol.Scand., Suppl. 56 (64), 24.20-24.21.

Jobsis, F.F. (1977c) Noninvasive, Infrared Monitoring of Cerebral and Myocardial Oxygen Sufficiency and Circulatory Parameters. Science, 198, 1264-1267.

Jobsis, F.F. (1977d) Method and Apparatus for Monitoring Metabolism in Body Organs. US Patent. 4.281.645. Granted 1981.

Jobsis, F.F. (1978) Spectrophotometric Monitoring of Cerebral O2 Sufficiency and Circulatory Parameters. Fronts.Biol.Energ., 2, 1457-1466.

Jobsis, F.F. (1979a) Oxidative Metabolic Effects of Cerebral Hypoxia. Adv.Neurol., 26, 299-318.

Jobsis, F.F. (1979b) Method and Apparatus for Monitoring Metabolism in Body Organs in vivo. US Patent. 4.223.680. Granted 1980.

Jobsis, F.F. (1981) Apparatus for Monitoring Metabolism in Body Organs. US Patent. 4.380.240. Granted 1983.

Johnson, C.C. (1970a) Optical Diffusion in Blood. IEEE Trans.Biomed.Eng., 17. 129-133.

Johnson, C.C. (1970b) Near Infrared Propogation in Blood. J.Assoc.Adv.Med.Inst., 4, 22-27.

Johnson. C.C., Palm, R.D., Stewart. D.C. and Martin, W.M. (1971) A Solid State Fibreoptics Oximeter. J.Assoc.Adv.Med.Inst., 5, 77-83.

Johnson. C.C. (1974) Fibreoptic Probe for Oxygen Saturation and Dye Concentration Monitoring. ISA BM 14310. 45-48.

Johnson. L., Abbasi, S., Grous, M., Dalin., C. (1984) The need for a micro platelet malondialdehyde (MDA) assay. Ped.Res., **18**, (4), 241A, **875**.

Jones. D.P., Smith, A.T., Sturrock, G.D. and Wright. P. (1979) Opthalmic Fluorophotometry: An Improved Slit-Lamp Fluorophotometer. Med.Biol.Eng.Comp., **17**. 365-370.

Kaiser, N. (1979) Laser Absorption Spectroscopy with an ATR Prism - Noninvasive in vivo Determination of Glucose. Horm.Met.Res., **Suppl.8**, **Eds** Hepp et al, 30-33.

Kariman. K., Hempel, F.G. and Jobsis, F.F. (1983a) In vivo Comparison of Cytochrome aa3 Redox State and Tissue pO2 in Transient Anoxia. J.Appl.Physiol., **55**, 1057-1063.

Kariman, K., Jobsis, F.F. and Saltzman, H.A. (1983b) Early indicator of Metabolic Recovery from Hemorrhagic Shock in Rats. J.Clin.Invest., **72**, 180-191.

Kariman, K. and Burkhart. D.S. (1985) Non-invasive In Vivo Spectrophotometric Monitoring of Brain Cytochrome Oxidase Revisited. Brain.Res., **360**, 203-213.

Kaye, P.H., Ludlow, I.K. and Milburn, M.R. (1982) Categorization of Microparticles and Biological Cells by Laser Diffractometry. Springer Series in Optical Science, **31**, **Ed** von Balley, G, 167-171. Springer-Verlag.

Kilkson. R., Bickel, W.S., Jeter, W.S. and Stafford, M.E. (1979) Influence of Absorption on Polarization Effects in Light Scattering from Human Red Blood Cells. BBA, **584**, 175-179.

Kimura, R.E., Thulin, G.E., Wender. D. and Warshaw, J.B. (1983) Decreased oxidative metabolism in neonatal rat lung exposed to hyperoxia. J.Appl.Physiol., **55**, 1501-1505.

Kinsey, J.H. and Cortese, D.A. (1980) Examination and Electronic Detection of Fluorescence. Rev.Sci.Inst., **51**, 1403-1406.

Kobayashi. S., Yoshimura, M., Suzaki, T., Shibahara. T. and Miyake, T. (1979) A Scanning Spectrophotometer for Monitoring of the Redox State of Living Organs. XII Int.Conf.Med.Biol.Eng., Jerusalem, Israel, Aug 19-24. **24.3**.

Kodak (1977) Applied Infrared Photography. Eastman Kodak, New York.

Konishi, M. (1976) Photoelectric Oximeter. US Patent 3.998,550. (Filed 1975).

Kontos, H.A., Wei, E.P., Christman. C.W., Levasseur, J.E., Porlishock, J.T. and Ellis, E.F. (1982) Free oxygen radicals in cerebral vascular responses. The Physiologist, **26**, 165-169.

Kopans, D.B., Meyer, J.E. and Sadowsky, N. (1984) Breast Imaging. New.Eng.J.Med., **310**, 960-967.

Kramer. K., Elam, J.O.. Saxton, G.A. and Elam, W.N. (1950) Influence of Oxygen Saturation. Erythrocyte Concentration and Optical Depth Upon the Red and Near-Infrared Light Transmittance of Whole Blood. Am.J.Physiol., **165**, 229-246.

Kramer. R.S. and Pearlstein, R.D. (1979) Cerebral Cortical Microfluorometry at Isosbestic Wavelengths for Correction of Vascular Artifact. Science, **205**, 693-696.

Krauss, A.N., Post. P.W., Waldman, S. and Auld, P.A.M. (1976) Skin Reflectance in the Newborn Infant. Pediat.Res., **10**, 776-778.

Kreismman, N.R., Sick, T.J., LaManna. J.C. and Rosenthal, M. (1981) Local Tissue Oxygen Tension - Cytochrome aa3 Redox Relationships in Rat Cerebral Cortex in vivo. Brain Res., **218**, 161-174.

Kreismman. N.R., Rosenthal, M., LaManna. J.C. and Sick, T.J. (1983) Cerebral Oxygenation During Recurrent Seizures. Adv.Neurol., **34**, 231-239.

Kretzer, F.L., Mehta. R.S., Johnson. A.T., Hunter. D.G., Brown, E.S. and Hittner. H.M. (1984) Vitamin E protects against retinopathy of prematurity through action on spindle cells. Nature. **309**, 793-795.

Kubelka, P. (1948) New Contributions to the Optics of Intensely Light-Scattering Materials. Part I. J.Opt.Soc.Am., **38**, 448-457.

Kubelka, P. (1954) New Contributions to the Optics of Intensely Light-Scattering Materials. Part II: Nonhomogenous Layers. J.Opt.Soc.Am., **44**, 330-335.

Kuppenheim. H.F., Dimitroff. J.M., Melotti. P.M., Graham. I.C. and Swanson. D.W. (1956) Spectral Reflectance of the Skin of Chester White Pigs in the Ranges 235-700 mu and 0.707-2.6 u. J.Appl.Physiol., **9**, 75-78.

La Manna. J., Watkins, G. and Rosenthal, M. (1975) Relationship of Inspired Oxygen, Redox Level of Cytochrome a and ECoG in Cats. The Physiologist, **18**, 284.

La Manna. J.C., Rosenthal, M., Novack, R., Moffett. D.F., and Jobsis F.F. (1980) Temperature Coefficients for the Oxidative Metabolic Responses to Electrical Stimulation in Cerebral Cortex. J.Neurochem., **34**, 203-209.

La Manna. J.C. Pikarsky. S.M., Sick, T.J. and Rosenthal, M. (1985) A Rapid-Scanning Spectrophotometer Designed for Biological Tissues in vitro or in vivo. Anal.Biochem., **144**, 483-393.

Laing, R.A., Danisch, L.A. and Young, L.R. (1975) The Choiroidal Eye Oximeter: An Instrument for Measuring Oxygen Saturation of Choiroidal Blood in vivo. IEEE Trans.Biomed.Eng., **22**, 183-195.

Lee, K-S. and Gartner. L.M. (1976) Spectrophotometric Characteristics of Bilirubin. Pediat. Res., **10**, 782-788.

Lehninger. A.L. (1977) Biochemistry (2nd ed.). New York, Worth.

Letokhov, V.S. (1985) Laser Biology and Medicine. Nature. **316**, 325-329.

Levene. M.I., Wigglesworth. J.S. and Dubowitz. V. (1980) Cerebral Structure and Intraventricular Haemorrhage in the Neonate: A Real-time Ultrasound Study. Arch.Dis.Child., **56**, 416-424.

Lin, J.C. (1974) A Note on the Optical Scattering Characteristics of Whole Blood. IEEE Trans.Biomed.Eng., **21**, 43-45.

Loewinger. E., Gordon. A., Weinreb, A. and Gross, J. (1964) Analysis of a Micromethod for Transmission Oximetry of Whole Blood. J.Appl.Physiol., **19**, 1179-1184.

Longini, R.L. and Zdrojkowski. R. (1968) A Note on the Theory of Backscattering of Light by Living Tissue. IEEE Trans.Biomed.Eng., **15**, 4-10.

Lothian. G.F. Lewis, P.C. (1956) Spectrophotometry of Granulated Materials with Particular Reference to Blood Corpuscles. Nature. **178**, 1342-1343.

Lubbers, D.W. and Wodick, R. (1969) The Examination of Multicomponent Systems in Biological Materials by Means of a Rapid Scanning Photometer. Appl.Opt., **8**, 1055-1062.

Lubbers, D.W. and Wodick, R. (1973) Advances in Spectrophotometric Methods as Applied to Living Tissue. **In** Modern Techniques in Physiological Sciences, **Ed** Gross. J.F. et al, 163-180. Academic Press. London.

Lubbers, D.W. and Wodick, R. (1975) Absolute Reflection Photometry Applied to the Measurement of Capillary Oxyhaemoglobin Saturation of the Skin in Man. **In** Oxygen Measurements in Biology and Medicine. **Eds** Payne and Hill. Chapter 7. 85-110.

Lubbers, D.W. and Starlinger. H. (1975) Anoxia and Critical Oxygen Tension in Brain Tissue. **In** Cerebral Circulation and Metabolism. **Ed** Longfitt. T.W. et al, Springer-Verlag, NY, 177-179.

Lubbers, D.W., Figulla, H.H., Hoffman, J. and Wodick, R. (1983) The Effect of Hypoxic and Histotoxic Hypoxia on Contractility and Blood Flow of the Langendorff Guinea Pig Heart Preparation. Adv.Exp.Med.Biol., **159**, 225-230.

Lucey, J.F. and Dangman. B. (1984) A reexamination of the role of oxygen in retrolental fibroplasia. Pediatrics, **73**, 82-96.

M.D.W. (1986) Near-Infrared Spectrometry in Clinical Analysis. ("Focus" Article). Anal.Chem., **58**, 874A-876A.

Maarek, J.M., Jarry, G., De Cosnac, B. and Mong Hung, B. (1982) Simulation of Transillumination through Blood and Tissues. In Proceedings of World Cong.Med.Phys.Biomed.Eng., Hamburg, 22.30.

Maarek, J.M., Jarry, G., Cosnac, B. de and Mong Hung, B. (1984) A Simulation Method for the Study of Laser Transillumination of Biological Tissues. Ann.Biomed.Eng., 12, 281-304.

Maarek, J.M., Jarry, G., Crowe, J., Mong Hung, B. and Laurent, D. (1986) Simulation of Laser Tomoscopy in a Heterogeneous Biological Medium. Med.Biol.Eng.Comp., 24, 407-414.

Malenfant, A.L. and Brown, L.J. (1979) An Instrument to Simultaneously Measure Total Hb, %O2Hb, % COHB, % MetHb and O2 Content in Whole Blood. In Proc. XII Int.Conf.Med.Biol.Eng. and V Int.Conf.Med.Phys., Aug.19-24. Jerusalem, Israel, 24.5.

Mandel, L.J., Moffett, D.F. and Jobsis, F.F. (1975) Redox State of Respiratory Chain Enzymes and Potassium Transport in Silkworm Mid-Gut. B.B.A., 408, 123-134.

March, W.F., Rabinovitch, B. and Adams, R.L. (1982) Noninvasive Glucose Monitoring of the Aqueous Humor of the Eye: Part II. Animal Studies and the Scleral Lens. Diabetes Care, 5, 259-265.

Marshall, R.J. and Marks, R. (1982) A Photographic Method for the Measurement of Skin Surface Textures. Bioeng.and the Skin, 4, 7-15.

Mavelli, I., Rigo, A., Federico R., Ciricolo M.R. and Rotilio G. (1982) Superoxide dismutase, glutathione peroxidase and catalase in developing rat brain. Biochem.J., 204, 535-540.

Mayevsky, A. (1984) Brain NADH Redox State Monitored In Vivo by Fiber Optic Surface Fluorometry. Brain.Res.Rev., 7, 49-68.

McConnell, M.L. (1981) Particle Size Determination by Quasielastic Light Scattering. Anal.Chem., 53, 1007A-1018A.

McCord, J.M. (1982) The biochemistry and pathophysiology of superoxide. The Physiologist, 26, 156-158.

McCracken, D.D. (1955) The Monte Carlo Method. Sci.Am., 192, 90-96.

McDonagh, A.F., Palma, L.A. and Lightner, D.A. (1980) Blue Light and Bilirubin Excretion. Science, 208, 145-151.

McKenzie, A.L. and Carruth, J.A.S. (1984) Lasers in Surgery and Medicine. Phys.Med.Biol., 29, 619-641.

Medgyesi, S. (1973) Photoelectric Oscillometry. Scand.J.Plast.Reconstr. Surg., 7, 29-34.

Mendelson. Y., Cheung, P.W. and Neuman, M.R. (1983a) Tissue Model for Transcutaneous Reflectance Oximetry. In Proceedings of the 36th ACEMB, Sept.12-14. Columbus, Ohio, 19.2.

Mendelson. Y., Cheung, P.W. and Neuman, M.R. (1983b) Instrumentation Development for Noninvasive Arterial OS. 36th ACEMB, Columbus, Ohio, Sept 12-14, 19.3.

Mendelson. Y., Cheung, P.W., Neuman, M.R., Fleming, D.G. and Cahn, S.D. (1983c) Spectrophotometric Investigation of Pulsatile Blood Flow for Transcutaneous Reflectance Oximetry. Adv.Exp.Med.Biol., 159, 93-102.

Merrick, E.B. and Hayes, T.J. (1976) Continuous Non-Invasive Measurements of Arterial Blood Oxygen Levels. Hewlett Packard Jnl., 28, 2-9.

Milgrom, L. (1984) Vampires, Plants and Crazy Kings. New.Sci., Apr 26. 9-13.

Mills, E. and Jobsis, F.F. (1970) Simultaneous Measurement of Cytochrome aa3 Reduction and Chemoreceptor Afferent Activity in the Carotid Body. Nature, 225, 1147-1148.

Mitnick, M.H. and Jobsis, F.F. (1976) Pyrenebutyric Acid as an Optical Oxygen Probe in the Intact Cerebral Cortex. J.Appl.Physiol., 41, 593-596.

Mohapatra. S.N. and Smith, C.W. (1975) Infrared Isobestic Region for Whole Blood. (Technical Note). Med.Biol.Eng.Comp., 38, 929-931.

Mook, G.A., Osypka, P., Sturm. R.E. and Wood E.H. (1968) Fibre Optic Reflection Photometry on Blood. Cardiovasc.Res., 2, 199-209.

Mook, G.A., Assendelft, O.W., Zijlstra. W.G. (1969) Wavelength Dependency of the Spectrophotometric Determination of Blood Oxygen Saturation. Clin.Chim.Acta., 26, 170-173.

Mook, P.H., Proctor, H.J., Jobsis, F. and Wildevuur, Ch.R.H. (1984) Assessment of Brain Oxygenation: A Comparison Between an Oxygen Electrode and Near-Infrared Spectrophotometry. Adv.Exp.Med.Biol., 169, 841-847.

Muhl, T., Blazek, V. and Wienert. V. (1985) LRR: An Optical System for the Measurement and Recording of Blood Pressure Variations in the Dermal Vessel Plexus. Bioeng.Skin, 1, 25-33.

Mul, F.F.M. de, Spijker, J. von, Plas, D. van der, Greve, J., Aardnouse, J.G. and Smits, T.M. (1984) Mini Laser-doppler (blood) Flow Monitor with Laser Source and Detection Integrated into the Probe. Appl.Opt., 23, 2970-2973.

Mullaney, P.F. and Dean, P.N. (1970) The Small Angle Light Scattering of Biological Cells. Theoretical Considerations. Biophys.J., 10, 764-772.

Muller, A. (1979) In vivo Measurement of Glucose Concentration with Lasers. Horm.Met.Res., **Suppl.8, Ed** Hepp et al. 33-35.

Murrell, J.N., Kettle, S.F.A. and Tedder, J.M.. (1978) The Chemical Bond. Wiley, Chichester.

Nijboer. J.A., Dorlas, J.C. and Mahieu, H.F. (1981) Photoelectric Plethysmography - Some Fundamental Aspects of the Reflection and Transmission Method. Clin.Phys.Physiol.Meas., 3, 205-215.

Nijboer. J.A. and Dorlas, J.C. (1982) The Origin of Inverted Waveforms in the Reflection Plethysmogram. Br.J.Anaesth., **54**, 1289-1293.

Nilsson. G.E., Tenland, T. and Oberg, P.A. (1980) Evaluation of a Laser Doppler Flowmeter for Measurement of Tissue Blood Flow. IEEE Trans.Biomed.Eng., **27**, 597-604.

Nilsson. N.J. (1960) Oximetry. Physiol.Rev., **40**, 1-26.

Niwa, M., Sakamoto. K. and Kanai. H. (1982) Angular Distribution of Reflected Light from Flowing Blood. In Proc. World Cong.Med.Phys and Biomed.Eng., Hamburg, 22.29.

Nyalander. C., Liedberg, B. and Lind, T. (1982/3) Gas Detection by Means of Surface Plasmon Resonance. Sens.Actuators., 3, 79-88.

Nyalander. C. (1985) Chemical and Biological Sensors. J.Phys.E.(Sci.Inst.), **18**, 736-750.

Obrist, P.A., Light, K.C., McCubbin, J.A., Hutcheson, J.S. and Hoffer, J.L. (1979) Pulse Transit Time: Relationship to Blood Pressure and Myocardial Performance. Physchophysiology. **16**, 292-301.

Ochoa, W. and Ohara. I. (1980) The Effect of Hematocrit on Photoelectric Plethysmogram. Tohoku.J.Exp.Med., **132**, 413-419.

Ohyama. M. (1982) Reflectance Spectrophotometeric Studies on Mucosal Pathology of the Upper Airways. Laryngoscope. **92**, 1168-1172.

Palladino. W.G., Proctor. H.J. and Jobsis. F.F. (1983) Effect of Hypothermia during Hypoxic Hypotension on Cerebral Metabolism. J.Surg.Res., **34**, 388-393.

Pape. K.E. and Wigglesworth, J.S. (1979) **In** Haemorrhage, Ischaemia and the Perinatal Brain, Heinemann. London. for Spastics International Publications.

Parrish, J.A. (1983) Photobiologic Considerations in Photoradiation Therapy. Adv.Exp.Med.Biol., **160**, 91-107.

Parrish, J.A. (1982) Therapeutic in vivo Photochemistry: Photochemical Toxicity in Humans. JNCI, **69**, 273-277.

Payne, J.P. and Hill, D.W. **Eds.** (1975) Oxygen Measurements in Biology and Medicine. Butterworths.

Pecora, R. (1972) Quasi-Elastic Light Scattering from Macromolecules. Ann.Rev.Biophys.Bioeng., 257-276.

Peterson, J.I. and Vurek, G.G. (1984) Fiber-Optic Sensors for Biomedical Applications. Science, **224**, 123-127.

Phelps, D.L. (1984) Vitamin E and CNS haemorrhage. (Commentary). Pediatrics, **74**, 1113-1116.

Phelps, D.L. (1984) E-Ferol: What happened and what now? (Commentary) Pediatrics, **74**, 1114-1116.

Philip, G.S. (1982) Non-Invasive Diagnosstic Techniques in Newborn Infants. **In** The Paediatric Clinics of North America, The Newborn, 1275-1298.

Piantadosi, C.A., Sylvia, A.L. and Jobsis, F.F. (1983) Cyanide-Induced Cytochrome aa3 Oxidation-Reduction Responses in Rat Brain in vivo. J.Clin.Invest., **72**, 1224-1233.

Piantadosi, C.A. and Sylvia, A.L. (1984) Cerebral Cytochrome aa3 Inhibition by Cyanide in Bloodless Rats. Toxicology, **33**, 67-69.

Pikarsky, S.M., LaManna, J.C, Sick, T.J. and Rosenthal, M. (1985) A Computer-Assisted Rapid-Scanning Spectrophotometer with Applications to Tissues in vitro and in vivo. Comps.Biomed.Res., **18**, 408-421.

Pittman, R.N. and Duling, B.R. (1975a) A New Method for the Measurement of Percent Oxyhemoglobin. J.Appl.Physiol., **38**, 315-320.

Pittman, R.N. and Duling, B.R. (1975b) Measurement of Percent Oxyhemoglobin in the Microvasculature. J.Appl.Physiol., **38**, 321-327.

Polanyi, M.L. and Hehir, R.M. (1960) New Reflection Oximeter. Rev.Sci.Inst., **31**, 401-403.

Polanyi, M.L. and Hehir, R.M. (1962) In vivo Oximeter with Fast Dynamic Response. Rev.Sci.Inst., **33**, 1050-1055.

Polanyi, M.L. (1972) Fibreoptics in Cardiac Catheterization. I. Theoretical Considerations. **In** Dye Curves: The Theory and Practice of Indicator Dilution, **Ed** Bloomfield, D.A., HM and M Pubs, Aylesbury, Chapt.15.

Polanyi, M.L. (1975) Recent Developments in Fibre Optics Oximetry. **In** Oxygen Measurements in Biology and Medicine, **Ed** Payne and Hill, Chapt.24.

Pollak, V. (1979) Optical Measurements on Scattering Media for Biomedical Applications. Med.Biol.Eng.Comp., **17**, 230-238.

Profio, A.E. and Doiron, D.R. (1981) Dosimetry Considerations in Phototherapy. Med.Phys., **8**, 190-196.

Preuss, L.E., Cartland, B.W., and Bolin, F.P. (1983) Measurment of Photodynamic Light in Mammalian Tissues. In Proceedings of the 36th ACEMB, Sept.12-14. Colombus, Ohio, 15.3.

Proctor, H.J., Sylvia, A.L. and Jobsis, F. (1982) Failure of Brain Cytochrome aa3 Redox Recovery After Hypoxic Hypotension as Determined by in vivo Reflectance Spectrophotometry. Stroke, 13, 89-92.

Proctor, H.J., Palladino, G.S., Cairns, C. and Jobsis, F.F. (1983) An Evaluation of Perfluorochemical Resuscitation after Hypoxic Hypotension. J.Trauma, 23, 79-83.

Pugliese, P.T. and Milligan, A.J. (1980) Ellipsometric Measurement of Skin Refractive Index in vivo. In Bioengineering and the Skin, Chapt 32. MTP Press, London.

Rabinovitch, B., March, W.F. and Adams, R.L. (1982) Noninvasive Glucose Monitoring of the Aqueous Humor of the Eye. Part I. Measurement of Very Small Optical Rotations. Diabetes Care. 5, 254-258.

Reichert, W.J. (1966) The Theory and Construction of Oximeters. Int.Anaest.Clinics, 4, No.1. Little, Brown and Co., Boston.

Reid, C. The Design of Fibre-Optic Oximeters. In Oxygen Measurements in Biology and Medicine, Ed Payne and Hill. Chapt.23.

Renault, G., Raynal, E., Sinet, M., Berthier, J.P, Godard, B. and Cornillault, J. (1982) A Laser Fluorimeter for Direct Cardiac Metabolism Investigation. Opt.Laser.Tech., 14, 143-148.

Renault, G., Raynal, E., Sinet, M., Muffat-Joly, M., Berthier, J-P, Cornillault, J., Godard, B. and Pocidalo, J-J. (1984) In Situ double-beam NADH Laser Fluorimetry: Choice of Reference Wavelength. Am.J.Physiol., 246, H491-499.

Reynolds, L.O. and Sanchez, R. (1983a) Radiative Transport Solution for Microparticulate Sizing. In Proceedings of 36th ACEMB, Sept.12-14. Columbus, Ohio, USA, 15.1.

Reynolds, L.O. and Drumm, G.W. (1983b) Optical Scattering Technique for Detection of Blood Plasma pH. In Proceedings of the 36th ACEMB, Sept.12-14. Colombus, Ohio, 15.4.

Richterich, R. and Colombo, J.P. (1981) Clinical Chemistry. Wiley, Chichester.

Roberts, V.C. (1982) Photoplethysmography - Fundamental Aspects of the Optical Properties of Blood in Motion. Trans.Int.M.C., 4, 101-106.

Rochkind, S., Razon, N. and Bortal, A. (1986) HeNe Low Energy Laser, Is it Completely Harmless. J.Biomed.Eng., 8, 77.

Rodrigo, F.A. (1953) The Determination of the Oxygenation of Blood in vitro by using Reflected Light. Am.Heart.J., **45**, 809-824.

Rosenbloom, M.A. (1953) Infrared Photography of the Female Breast. Obstet.Gyne., **2**, 603-610.

Rosenfeld, W., Evans, H., Concepcion, L., Jhaveri. R., Schaeffer. H. and Friedman, A. (1984) Prevention of bronchopulmonary dysplasia by administration of bovine superoxide dismutase in preterm infants with respiratory distress syndrome. J. Peds., **105**, 781-785.

Rosenthal, M., LaManna, J.C., Jobsis, F.F., Levasseur, J.E., Kontos, H.A., and Patterson. J.L. (1976) Effects of Respiratory Gases on Cytochrome a in Intact Cerebral Cortex: Is There a Critical pO2 ? Brain Res., **108**, 143-154.

Rosenthal, M., Adams, M.R. and LaManna. J.C. (1981) Nitrous Oxide Alters Oxidative Metabolic Activities of Rat Neocortex in situ. Brain Res., **213**, 405-414.

Ross, I. and Mbano. A. (1985) Optical Monitoring of Glucose Concentrations. Opt.Las.Tech., **17**, 31-35.

Rossotti. H. (1983) Colour. Penguin Books, New York.

Samueloff, S., Miday, R., Wasserman, D., Behrens, V., Hornung, R., Asburry, W., Doyle, T., Dukes-Dobos, F. and Badger, D. (1981) A Peripheral Vascular Insufficiency Test Using Photocell Plethysmography. J.Occ.Med., **23**, 643-646.

Sato. N., Kamada, T., Shichiri, M., Kawano. S., Abe, H., and Hagihara, B. (1979a) Measurement of Hemoperfusion and Oxygen Suficiency in Gastric Mucosa in vivo. Gastroenterology, **76**, 814-819.

Sato. N., Shichiri. M., Hayashi, N., Kamada, T., Abe, H. and Hagihara, B. (1979b) Behavior of Cytochrome Oxidase in Living Liver Tissue: Direct Analysis of Turnover of Cytochrome aa3 in Liver in situ by Reflectance Spectrophotometry. **In** Cytochrome Oxidase, Eds.King, T.E.et al, Elsevier 819-829.

Sato. N., Matsumura, T., Shichiri, M., Kamada, T., Abe, H. and Hagihara, B. (1981a) Hemoperfusion, Rate of Oxygen Consumption and Redox Levels of Mitochondrial Cytochrome c(+c1) in Liver in situ of Anaesthetized Rat Measured by Reflectance Spectrophotometry. B.B.A., **634**, 1-10.

Sato. N., Hayashi, N., Meren, H., Shichiri. M., Kamada, T., Abe, H., Nishioka, K., Nishihara. T., Hagihara, B., Ono, K. and Yoshida, K. (1981b) Transcutaneous PO2 Monitoring and Hepatic Hemodynamics as Assessed by Reflectance Spectrophotometry of the Liver in Patients with Hepatitis or Cirrhosis. (1981b) **In** Continuous Transcutaneous Blood Gas Monitoring, Eds.Huch, H. and Huch, R., 813-822.

Sattelle, D.B., Palmer, G.R., Griffin, M.C.A. and Holder, R.E.D. (1982) Spectrometer for Laser-light Scattering Measurements of Macromolecular and Subcellular Particle Motions. Med.Biol.Eng.Comp., **20**, 37-43.

Saugstad, O.D., Hallman, M., Abraham, J.L., Epstein, B., Cochrane. C. and Gluck, L. (1984) Hypoxanthine and oxygen induced lung injury: A possible basic mechanism of tissue damage? Ped.Res., **18**, 501-504.

Schwab, H. and Sies, H. (1978) A New Organ Spectrophotometer for Sensitive Dual-Wavelength Absorbance Measurement and Spectral Scanning of Intact Perfused Organs. Hoppe-Seylers Z.Physiol.Chem., 385-392.

Seeds, J.W., Cefalo, R.C., Proctor, H.J. and Jobsis, F.F. (1984) The Relationship of Intracranial Infrared Light Absorbance to Fetal Oxygenation. Am.J.Obs.Gyn., **149**, 679-684.

Sekelj, P., Johnson, A.L., Hoff, H.E. and Schuerch, M.P. (1951) A Photoelectric Method for the Determination of Arterial Oxygen Saturation in Man. Am.Heart.J., **42**, 826-848.

Seyfried, M. and Fukshansky, L. (1983) Light Gradients in Plant Tissue. Appl.Opt., **22**, 1402-1408.

Shankar, T.M.R. and Webster. J.G. (1985) Contribution of Different Sized Vessels in the Extremeties to the Arterial Pulse Waveform as Recorded by Electrical Impedance and Volume Plethysmography. Med.Biol.Eng.Comp., **23**, 155-164.

Shimada, Y., Yoshiya, I., Oka, N. and Hamaguri, K. (1984) Effects of Multiple Scattering and Peripheral Circulation on Arterial Oxygen Saturation Measured with a Pulse Type Oximeter. Med.Biol.Eng.Comp., **22**, 475-478.

Shimazu, H., Fukuoka, M., Ito, H. and Yamakoshi, K. (1985) Non-Invasive Measurement of Beat-to-beat Vascular Viscoelastic Properties in Human Fingers and Forearms. Med.Biol.Eng.Comp., **23**, 43-47.

Sick, T.J., Lutz, P.L., LaManna. J.C. and Rosenthal, M. (1982) Comparative Brain Oxygenation and Mitochondrial Redox Activity in Turtles and Rats. J.Appl.Physiol., **53**, 1354-1359.

Silver, I.A. (1985) Fluorescence Measurements in Biomedical Monitoring. **In** Optical Sensors and Optical Sensing Techniques in Biology and Medicine, BES Transducers Group Meeting, UCL, 22 May 1985.

Silverman, W.A. (1980) Retrolental Fibroplasia: A Modern Parable. Grune and Stratton, New York.

Singh, M. (1981) Helium-Neon Laser Screening of Human Body. Med.Biol.Eng.Comp., **19**, 175-178.

Singh, M. (1982) Development of an Optical Fibre Technique for He-Ne Laser Screening of (Technical Note). Human Body and its Comparison with the Integrating Sphere Method. Med.Biol.Eng.Comp., 20, 111-112.

Singh, M. and Periasamy, A. (1984) Determination of Safe Exposure Levels of HeNe Laser Light to the Human Body by Means of Erythrocyte Irradiation Studies. Med.Biol.Eng.Comp., 22, 147-150.

Sliney, D. and Wolbarsht, M. (1980) Safety with Lasers and Other Optical Sources: A Comprehensive Handbook. Plenum Press, New York.

Smith, G.D. (1978) Numerical Solutions of Partial Differential Equations; Finite Difference Methods (2nd ed.). Oxford Univ.Press, Oxford.

Smith, K.C. Ed. (1977) The Science of Photobiology. Plenum Press, NY and London.

Snow, T.R., Kleinmann, L.H., LaManna, J.C., Wechsler, A.S. and Jobsis, F.F. (1981) Response of Cyt aa3 in the in situ Canine Heart to Transient Ischemic Episodes. Basic.Res.Cardiol., 76, 289-304.

Sokol, R.J. (1984) Vitamin E toxicity. (Letter) Pediatrics, 74, 564-565.

Speer, M.E., Blifield, C., Rudolph, A.J., Chadda, P., Holbein, M.E.B. and Hittner, H. (1984) Intraventricular haemorrhage and vitamin E in the very low-birth weight infant: Evidence for efficacy of early intramuscular vitamin E administration. Pediatrics, 74, 1107-1112.

Spiegel, H.U., Hauss, J., Schwarze, H. and Schonleben, K. (1986) The Influence of Different Anaesthetics on the Local Oxygen Supply. Microvasc.Res., in Press.

Stimson, A. and Fee, E. (1953) Color and Reflectance of Human Flesh. J.SMPTE. 60, 553-558.

Sutterer, W.F. (1967) Optical Artifacts in Whole Blood Densitometry (Review). Pediat.Res., 1, 66-75.

Sutterer, W.F. and Bloomfield, D.A. (1972) Dye Densitometers. In Dye Curves, Ed Bloomfield, D.A., HM and M Pubs., Aylesbury, Chapt.19.

Svaasand, L.O. and Ellingsen, R. (1983a) Optical Properties of Human Brain. Photochem.Photobiol., 38, 293-299.

Svaasand, L.O. and Doiron, D.R. (1983b) Thermal Distribution During Photoradiation Therapy. Adv.Exp.Med.Biol., 160, 77-90.

Svaasand, L.O. and Ellingsen, R. (1985) Optical Peneteration in Human Intracranial Tumours. Photochem.Photobiol., 41, 73-76.

Swick, H.M., Cunningham, M.D. and Shield, L.K. (1976) Transillumination of the Skull in Premature Infants. Pediatrics, 58, 658-664.

Sylvia. A.L., Proctor. H.J., Goldsmith, M.M. and Jobsis, F.F. (1982) Exchange Transfusion with Fluosol 43: In vivo Assessment of Cerebral Cytochrome c Oxidase Redox State. J.Trauma, 22, 815-819.

Takatini, S. (1978) On the Theory and Development of a Non-Invasive Tissue Reflectance Oximeter. D.Phil. Thesis, Case Western Reserve Univ., USA.

Takatini, S. and Graham. M.D. (1979) Theoretical Analysis of Diffuse Reflectance from a Two-Layer Tissue Model. IEEE Trans.Biomed.Eng., 26, 656-664.

Takatini, S., Cheung, P.W. and Ernst. E.A. (1980) A Noninvasive Tissue Reflectance Oximeter. An Instrument for Measurment of Tissue Hemoglobin Oxygen Saturation in vivo. Ann.Biomed.Eng., 8, 1-15.

Tamarkin, L., Baird, C.J. and Almeida, O.F.X. (1985) Melatonin: A Coordinating Signal for Mammalian Reproduction? Science, 227, 714-715.

Tamura, T., Salerud, E.G. and Oberg, P.A. (1985) Evaluation of Fiber Optic Plethysmography. In Proc.XIV ICMBE and VII ICMP. Espoo, Finland, 1001-1002.

Tanaka, T., Riva, C. and Ben-Sira. I. (1974) Blood Velocity Measurements in Human Retinal Vesssels. Science, 186, 830-831.

Tang, S. and Wan, S. (1983) The Spectrophotometer and Measurement of Skin Color. In Cutaneous Laser Therapy: Principles and Methods, Chapt.3. Wiley, Ed Arndt, K.A. et al.

Tanswell. A.K. and Freeman, B.A. (1984) Pulmonary antioxidant enzyme maturation in the fetal and neonatal rat. I. Developmental profiles. Ped.Res., 18, 584-587.

Taylor, A.E. and Martin. D. (1982) Oxygen radicals and the microcirculation. The Physiologist, 26, 152-155.

Trafford, J. de and Lefferty, K. (1984) What does Photoplethysmography Measure? (Letter). Med.Biol.Eng.Comp., 22, 479-480.

Tromberg, B.J., Eastham. J.F. and Sepaniak, M.J. (1984) Optical Fiber Fluoroprobes for Biological Measurments. Appl.Spect., 38, 38-42.

Tzagaloff, A. (1982) Mitochondria. Plenum Press, New York.

Uretzky, G. and Palti, Y. (1971) A Method for Comparing Transmitted and Reflected Light Photoelectric Plethysmogaphy. J.Appl.Physiol., 31, 132-135.

Waffarn, F., Lee, N., Weinberg, L., Jilek, J. and Hon, E.H. (1983) The Cutaneous R-Pulse Interval: Its Application as a Clinical Measure of Neonatal Cardiovascular Function. Crit.Care.Med., 11, 921-925.

Wan, S., Anderson, R.R. and Parrish, J.A. (1981a) Analytical Modeling for the Optical Properties of the Skin with in vitro and in vivo Applications. Photochem.Photobiol., 34, 493-499.

Wan, S., Parrish, J.A, Anderson. R.R. and Madden, M. (1981b) Transmittance of Nonionizing Radiation in Human Tissues. Photochem.Photobiol., 34, 679-681.

Ware. P.F., Polanyi, M.L., Hehir. R.M., Stapleton. J.F., Sanders, J.I., and Kocot. S.L. (1960) A New Reflection Oximeter. J.Thor.Cardiovasc.Surg., 42, 580-588.

Watmough, D.J. (1983) Diaphonography. In Imaging with Non-Ionizing Radiation: Progress in Medical and Enviromental Physics, Vol.2. Jackson. D. Ed. Chapt.6.

Weale, R.A. (1966) Fundus Reflectivity. J.Phys., 186, 175.

Weinman, J., Hayat, A. and Raviv. G. (1977) Reflection Photoplethysmography of Arterial-Blood-Volume Pulses. Med.Biol.Eng.Comp., 15, 22-31.

Wiernsperger. N., Sylvia. A.L. and Jobsis. F.F. (1981) Incomplete Transient Ischaemia: A Non-Destructive Evaluation of in vivo Cerebral Metabolism and Hemodynamics in Rat Brain. Stroke, 12, 864-868.

Wiernsperger, N. and Gygax, P. (1983) Incomplete Cerebral Ischemia in the Rat: Vascular and Metabolic Changes as Measured by Infrared Transillumination in vivo. Adv.Exp.Med.Biol., 159, 5-15.

Wilber, S.A. (1983) Blood Constituent Measuring Device and Method. US Patent No. 4.407.290. (Filed 1981).

Wilkinson. A.R., Phibbs, R.H. and Gregory, G.A. (1979) Continuous in vivo Oxygen Saturation on Newborn Infants with Pulmonary Disease. Crit.Care.Monit., 7, 232-236.

Wilksch, P.A., Jacka, F. and Blake, A.J. (1984) Studies of Light Propagation through Tissue. In Porphyrin Localisation and Treatment of Tumours, 149-161. Liss, A.R., New York.

Williams, D.H. and Fleming, I. (1973) Spectroscopic Methods in Organic Chemistry. McGraw Hill. UK.

Wilson, B.C. and Adams, G. (1983) A Monte Carlo Model for the Absorption and Flux Distributions of Light in Tissue. Med.Phys., 10, 824-830.

Wilson, B.C., Jeeves, W.P., Lowe, D.M. and Adam, G. (1984) Light Propagation in Animal Tissues in the Wavelength Range 375-825nm. In Porphyrin Localisation and Treatment of Tumours, Eds. Doiron, D.R. and Gomar, C.J., 115-132. Pub.Liss, A.R.

Wilson. B.C., Patterson. M.S.. Jeeves, W.P., Flock, S.L. and Lowe, D.M. (1985) Light Propagation in Tissue as applied to Radiation Dosimetry for Photodynamic Therapy. In Proc. XIV ICMBE and VII ICMP. Espoo. Finland, 1203-1204.

Wilson. D.F., Owen, C.S. and Erecinska, M. (1979) Quantitative Dependence of Mitochondrial Oxidative Phosphorylation on Oxygen Concentration: A Mathematical Model. Arch.Biochem.Biophys., 195, 494-504.

Wood, E.H. and Geraci, J.E. (1949) Photoelectric Determination of Arterial Oxygen Saturation in Man. J.Lab.Clin.Med., 34, 387-401.

Yamada, S.. Sanders, D.C. and Maeda, G. (1981) Oxidative Metabolism During and Following Iscahemia of Cat Spinal Cord. Neurol.Res., 3, 1-16.

Yamakoshi, K., Kaworda, A., Kamiya, A., Shimazu, H. and Hito. H. (1985) Long Term Ambulatory Monitoring of Indirect Arterial Pressure Using a Volume Oscillometric Method. Med.Biol.Eng.Comp., 23, 459-465.

Yamanouchi, I., Yamauchi, Y and Igarashi, I. (1980) Transcutaneous Bilirubinometry: Preliminary Studies of Noninvasive Transcutaneous Bilirubin Meter in the Okayama National Hospital. Pediatrics, 65, 195-202.

Yamanouchi, I (1983) Minolta Transcutaneous Bilirunin Meter. In Non-Invasive Fetal and Neonatal Physiological Measurements 2. Ed Rolfe, P.

Yang, C. and Legallais, V. (1954) A Rapid and Sensitive Recording Spectrophotometer for the Visible and Ultraviolet Region I. Description and Performance. Rev.Sci.Inst., 25, 801-807.

Yelderman. M. and New, W. (1983) Evaluation of Pusle Oximetry. Anesthesiology, 59, 349-352.

Yoshiya, I., Shimada, Y. and Tanaka, K. (1980) Spectrophotometric Monitoring of Arterial Oxygen Saturation in the Fingertip. Med.Biol.Eng.Comp., 18, 27-32.

Yoshiya, I and Shimada, Y. (1983) Non-Invasive Spectrophotometric Estimation of Arterial Oxygen Saturation. In Non-Invasive Fetal and Neonatal Physiological Measurments 2. Cnapt. 7. Rolfe, P. Ed. Academic Press, London.

Zdrojkowski, R.J. and Longini, R.L. (1969) Optical Transmission through Whole Blood Illuminated with Highly Collimated Light. J.Opt.Soc.Am., 59, 898-903.

Zdrojkowski, R.J. and Pisharoty, N.R. (1970) Optical Transmission and Reflection by Blood. IEEE Trans.Biomed.Eng., 17, 122-128.

Zijlstra. W.G. (1953) Fundamentals and Applications of Clinical Oximetry. 2nd Ed, Van Gorcum, Assen.

Zijlstra. W.G., Buursma, A. and Zwart. A. (1983) Molar Absorptivities of Human Hemoglobin in the Visible Spectral Range. J.Appl.Physiol., 54, 1287-1291.

Appendix D

Memory Map Configuration of TMS 990 as used.